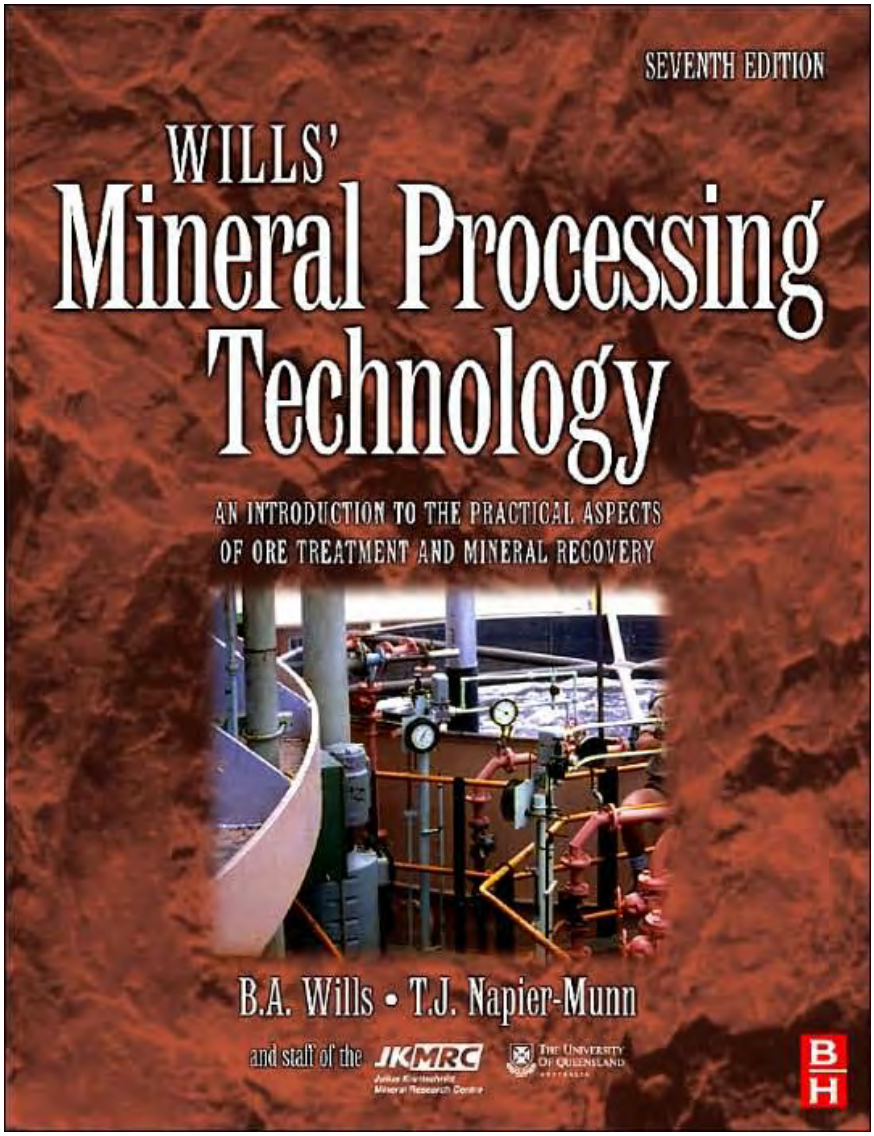
Mineral Processing Technology

An Introduction to the Practical Aspects of Ore Treatment and Mineral Recovery, *by* *Barry A. Wills*, *Tim Napier-Munn*



- ISBN: 0750644508
- Publisher: Elsevier Science & Technology Books
- Pub. Date: October 2006

Preface to 7th Edition

Although mining is a conservative industry, economic drivers continue to encourage innovation and technological change. In mineral processing, equipment vendors, researchers and the operations themselves work to develop technologies that are more efficient, of lower cost and more sustainable than their predecessors. The results are apparent in new equipment and new operating practice. Any textbook needs to reflect these changes, and Barry Wills' classic is no exception.

It is nearly 30 years since *Mineral Processing Technology* was first published, and it has become the most widely used English-language textbook of its kind. The sixth edition appeared in 1997 and Barry and his publishers felt that it was again time to bring the text up to date. They approached the Julius Kruttschnitt Mineral Research Centre at the University of Queensland to take on the challenging task. My colleagues and I agreed to do so with some trepidation. The book's well-deserved reputation and utility were at stake, and the magnitude of the task was clear. Revising someone else's text is not an easy thing to do successfully, and there was a real danger of throwing the baby out with the bath water.

The value of *Mineral Processing Technology* lies in its clear exposition of the principles and practice of mineral processing, with examples taken from practice. It has found favour with students of mineral processing, those trained in other disciplines who have converted to mineral processing, and as a reference to current equipment and practice. It was important that its appeal to these different communities be preserved and if possible enhanced. We therefore adopted the following guidelines in revising the book.

The 7th edition is indeed a revision, not a complete re-write. This decision was based on the view that "if it ain't broke, don't fix it". Each diagram, flowsheet, reference or passage of text was considered as follows. If it reflected current knowledge and practice, it was left unchanged (or modestly updated where necessary). If it had been entirely superseded, it was removed unless some useful principle or piece of history was being illustrated. Where the introduction of new knowledge or practice was thought to be important to preserve the book's currency, this was done. As a consequence, some chapters remain relatively unscathed whereas others have experienced substantial changes.

A particular problem arose with the extensive references to particular machines, concentrators and flowsheets. Where the point being illustrated remained valid, these were generally retained in the interest of minimising changes to the structure of the book. Where they were clearly out of date in a misleading sense and/or where alternative developments had attained the status of current practice, new material was added.

It is perhaps a measure of Barry Wills' original achievement that it has taken more than a dozen people to prepare this latest edition. I would like to acknowledge my gratitude to my colleagues at the JKMRC and elsewhere, listed below, for subscribing their knowledge, experience and valuable time to this good cause; doing so has not been easy. Each chapter was handled by a particular individual with expertise in the topic (several individuals in the case of the larger chapters). I must also thank the editorial staff at Elsevier, especially Miranda Turner and Helen Eaton, for their support and patience, and Barry Wills for his encouragement of the enterprise. My job was to contribute some of the chapters, to restrain some of the more idiosyncratic stylistic extravagancies, and to help make the whole thing happen. To misquote the great comic genius Spike Milligan: the last time I edited a book I swore I would never do another one. This is it.

Tim Napier-Munn
December 2005

Contributors

Chapters 1, 4, 9, 11, 14	Prof. Tim Napier-Munn (JKMRC)
Chapters 2 and 16	Dr Glen Corder (JKTech)
Chapter 3	Dr Rob Morrison (JKMRC) and Dr Michael Dunglison (JKTech)
Chapters 5 and 6	Dr Toni Kojovic (JKMRC)
Chapter 7	Dr Frank Shi (JKMRC)
Chapter 8	Marko Hilden (JKMRC) and Dean David (GRD Minproc, formerly with JKTech)
Chapters 10, 13 and 15	Dr Peter Holtham (JKMRC)
Chapter 12	Dr Dan Alexander (JKTech), Dr Emmy Manlapig (JKMRC), Dr Dee Bradshaw (Dept. Chemical Engineering, University of Cape Town) and Dr Greg Harbort (JKTech)
Appendix III	Dr Michael Dunglison (JKTech)

Acknowledgements

Secretarial assistance	Vynette Holliday and Libby Hill (JKMRC)
Other acknowledgements	Prof. J-P Franzidis (JKMRC) and Evie Franzidis for their work on an earlier incarnation of this project. Dr Andrew Thornton and Bob Yench of Mipac for help with aspects of process control. The Julius Kruttschnitt Mineral Research Centre, The University of Queensland, for administrative support. The logos of the University and the JKMRC are published by permission of The University of Queensland, the Director, JKMRC.

Table of Contents

1	Introduction	1
2	Ore handling	30
3	Metallurgical accounting, control and simulation	39
4	Particle size analysis	90
5	Comminution	108
6	Crushers	118
7	Grinding mills	146
8	Industrial screening	186
9	Classification	203
10	Gravity concentration	225
11	Dense medium separation (DMS)	246
12	Froth flotation	267
13	Magnetic and electrical separation	353
14	Ore sorting	373
15	Dewatering	378
16	Tailings disposal	400

App. 1 Metallic ore minerals 409

App. 2 Common non-metallic ores 421

App. 3 Excel spreadsheets for formulae in chapter 3

1 Introduction

Minerals and ores

Minerals

The forms in which metals are found in the crust of the earth and as sea-bed deposits depend on their reactivity with their environment, particularly with oxygen, sulphur, and carbon dioxide. Gold and platinum metals are found principally in the *native* or metallic form. Silver, copper, and mercury are found native as well as in the form of sulphides, carbonates, and chlorides. The more reactive metals are always in compound form, such as the oxides and sulphides of iron and the oxides and silicates of aluminium and beryllium. The naturally occurring compounds are known as *minerals*, most of which have been given names according to their composition (e.g. galena – lead sulphide, PbS; sphalerite – zinc sulphide, ZnS; cassiterite – tin oxide, SnO_2).

Minerals by definition are natural inorganic substances possessing definite chemical compositions and atomic structures. Some flexibility, however, is allowed in this definition. Many minerals exhibit *isomorphism*, where substitution of atoms within the crystal structure by similar atoms takes place without affecting the atomic structure. The mineral olivine, for example, has the chemical composition $(Mg, Fe)_2\ SiO_4$, but the ratio of Mg atoms to Fe atoms varies in different olivines. The total number of Mg and Fe atoms in all olivines, however, has the same ratio to that of the Si and O atoms. Minerals can also exhibit *polymorphism*, different minerals having the same chemical composition, but markedly different physical properties due to a difference in crystal structure. Thus, the two minerals graphite and diamond have exactly the same composition, being composed entirely of carbon atoms, but have widely different properties due to the arrangement of the carbon atoms within the crystal lattice. The term "mineral" is often used in a much more extended sense to include anything of economic value which is extracted from the earth. Thus, coal, chalk, clay, and granite do not come within the definition of a mineral, although details of their production are usually included in national figures for mineral production. Such materials are, in fact, *rocks*, which are not homogeneous in chemical and physical composition, as are minerals, but generally consist of a variety of minerals and form large parts of the earth's crust. For instance, granite, which is one of the most abundant *igneous* rocks, i.e. a rock formed by cooling of molten material, or *magma*, within the earth's crust, is composed of three main mineral constituents, feldspar, quartz, and mica. These three homogeneous mineral components occur in varying proportions in different parts of the same granite mass.

Coals are not minerals in the geological sense, but a group of bedded rocks formed by the accumulation of vegetable matter. Most coal-seams were formed over 300 million years ago by the decomposition of vegetable matter from the dense tropical forests which covered certain areas of the earth. During the early formation of the coal-seams, the rotting vegetation formed thick beds of *peat*, an unconsolidated product of the decomposition of vegetation, found in marshes and bogs. This later became overlain with shales, sandstones, mud, and silt, and under the action of the increasing pressure and temperature and time, the peat-beds became altered, or *metamorphosed*, to produce the sedimentary rock known as coal. The degree of alteration is known as the *rank* of the coal, the lowest ranks (lignite or brown coal) showing little alteration, while the highest rank (anthracite) is almost pure graphite (carbon).

Metallic ore processing

Metals

The enormous growth of industrialisation from the eighteenth century onward led to dramatic increases in the annual output of most mineral commodities, particularly metals. Copper output grew by a factor of 27 in the twentieth century alone, and aluminium by an astonishing factor of 3800 in the same period. Figure 1.1 shows the world production of aluminium, copper and zinc for the period 1900–2002 (data from USGS, 2005).

All these metals suffered to a greater or lesser extent when the Organisation of Petroleum Exporting Countries (OPEC) quadrupled the price of oil in 1973–74, ending the great postwar industrial boom. The situation worsened in 1979–81, when the Iranian revolution and then the Iran–Iraq war forced the price of oil up from $13 to nearly $40 a barrel, plunging the world into another and deeper recession, while early in 1986 a glut in the world's oil supply cut the price from $26 a barrel in December 1985 to below $15 in 1986. Iraq's invasion of Kuwait in 1990 pushed the price up again, from $16 in July to a peak of $42 in October, although by then 20% of the world's energy was being provided by natural gas.

In 1999, overproduction and the Asian economic crisis depressed oil prices to as low as $10 a barrel from where it has climbed steadily to a record figure of over $60 a barrel in 2005, driven largely by demand especially from the emerging Asian economies, particularly China.

These large fluctuations in oil prices have had a significant impact on metalliferous ore mining, due to their influence both on the world economy and thus the demand for metals, and directly on the energy costs of mining and processing. It has been estimated that the energy cost in copper production is about 35% of the selling price of the metal (Dahlstrom, 1986).

The price of metals is governed mainly by supply and demand. Supply includes both newly mined and recycled metal, and recycling is now a significant component of the lifecycle of some metals – about 60% of lead supply comes from recycled sources. There have been many prophets of doom over the years pessimistically predicting the imminent exhaustion of mineral supplies, the most extreme perhaps being the notorious "Limits to Growth" report to the Club of Rome in 1972, which forecast that gold would run out in 1981, zinc in 1990, and oil by 1992 (Meadows et al., 1972).

In fact major advances in productivity and technology throughout the twentieth century greatly increased both the resource and the supply of newly mined metals, through geological discovery and reductions in the cost of production. This actually drove down metal prices in real terms, which reduced the profitability of mining companies and had a damaging effect on economies heavily dependent on mining, particularly those in Africa and South America. This in turn drove further improvements in productivity and technology. Clearly mineral resources are finite, but supply and demand will generally balance in such

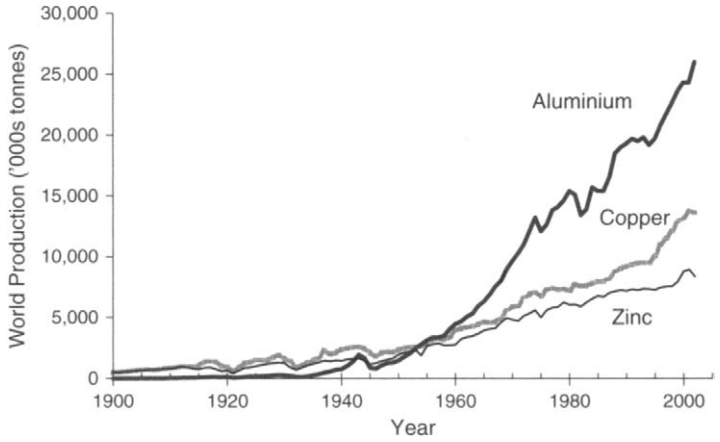


Figure 1.1 World production of aluminium, copper and zinc for the period 1900–2002

a way that if supplies decline or demand increases, the price will increase, which will motivate the search for new deposits, or technology to render marginal deposits economic, or even substitution by other materials.

Interestingly gold is an exception, its price having not changed much in real terms since the sixteenth century, due mainly to its use as a monetary instrument and a store of wealth (Humphreys, 1999).

Estimates of the crustal abundances of metals are given in Table 1.1 (Taylor, 1964), together with the actual amounts of some of the most useful metals, to a depth of 3.5 km (Chi-Lung, 1970).

The abundance of metals in the oceans is related to some extent to the crustal abundances, since they have come from the weathering of the crustal rocks, but superimposed upon this are the effects of acid rain-waters on mineral leaching processes; thus the metal availability from sea-water shown in Table 1.2 (Chi-Lung, 1970) does not follow precisely that of the crustal abundance. The sea-bed may become a viable source of minerals in the future. Manganese nodules have been known since the beginning of the nineteenth century (Mukherjee et al., 2004), and recently mineral-rich hydrothermal vents have been discovered and plans are being made to mine them (Scott, 2001).

It can be seen from Table 1.1 that eight elements account for over 99% of the earth's crust; 74.6% is silicon and oxygen, and only three of the industrially important metals (aluminium, iron, and magnesium) are present in amounts above 2%. All the other useful metals occur in amounts below 0.1%; copper, for example, which is the most important non-ferrous metal, occurring only to the extent of 0.0055%. It is interesting to note that the so-called common metals, zinc and lead, are less plentiful than the rare-earth metals (cerium, thorium, etc.).

It is immediately apparent that if the minerals containing the important metals were uniformly distributed throughout the earth, they would be so thinly dispersed that their economic extraction would be impossible. However, the occurrence of minerals in nature is regulated by the geological

Table 1.2 Abundance of metal in the oceans

Element	*Abundance in sea-water* (tonnes)	*Element*	*Abundance in sea-water* (tonnes)
Magnesium	10^{15}–10^{16}	Vanadium	10^{9}–10^{10}
Silicon	10^{12}–10^{13}	Titanium	
Aluminium		Cobalt	
Iron	10^{10}–10^{11}	Silver	10^{12}–10^{13}
Molybdenum		Tungsten	
Zinc		Chromium	
Tin		Gold	$<10^{8}$
Uranium		Zirconium	
Copper	10^{9}–10^{10}	Platinum	
Nickel			

Table 1.1 Abundance of metal in the oceans

Element	*Abundance* (%)	*Amount in* 3.5 km *of crust* (tonnes)	*Element*	*Abundance* (%)	*Amount in* 3.5 km *of crust* (tonnes)
(Oxygen)	46.4		Vanadium	0.014	10^{14}–10^{15}
Silicon	28.2		Chromium	0.010	
Aluminium	8.2	10^{16}–10^{18}	Nickel	0.0075	
Iron	5.6		Zinc	0.0070	
Calcium	4.1		Copper	0.0055	10^{13}–10^{14}
Sodium	2.4		Cobalt	0.0025	
Magnesium	2.3	10^{16}–10^{18}	Lead	0.0013	
Potassium	2.1		Uranium	0.00027	
Titanium	0.57		Tin	0.00020	
Manganese	0.095	10^{15}–10^{16}	Tungsten	0.00015	10^{11}–10^{13}
Barium	0.043		Mercury	8×10^{-6}	
Strontium	0.038		Silver	7×10^{-6}	
Rare earths	0.023		Gold	$<5 \times 10^{-6}$	
Zirconium	0.017	10^{14}–10^{16}	Platinum metals	$<5 \times 10^{-6}$	$<10^{11}$

conditions throughout the life of the mineral. A particular mineral may be found mainly in association with one rock type, e.g. cassiterite mainly associates with granite rocks, or may be found associated with both igneous and *sedimentary* rocks (i.e. those produced by the deposition of material arising from the mechanical and chemical weathering of earlier rocks by water, ice, and chemical decay). Thus, when granite is weathered, cassiterite may be transported and re-deposited as an *alluvial* deposit.

Due to the action of these many natural agencies, mineral deposits are frequently found in sufficient concentrations to enable the metals to be profitably recovered. It is these concentrating agencies and the development of demand as a result of research and discovery which convert a mineral deposit into an *ore*. Most ores are mixtures of extractable minerals and extraneous rocky material described as *gangue*. They are frequently classed according to the nature of the valuable mineral. Thus, in *native* ores the metal is present in the elementary form; *sulphide* ores contain the metal as sulphides, and in *oxidised* ores the valuable mineral may be present as oxide, sulphate, silicate, carbonate, or some hydrated form of these. *Complex* ores are those containing profitable amounts of more than one valuable mineral. Metallic minerals are often found in certain associations within which they may occur as mixtures of a wide range of particle sizes or as single-phase solid solutions or compounds. Galena and sphalerite, for example, associate themselves commonly, as do copper sulphide minerals and sphalerite to a lesser extent. Pyrite (FeS_2) is very often associated with these minerals.

Ores are also classified by the nature of their gangues, such as *calcareous* or *basic* (lime rich) and *siliceous* or *acidic* (silica rich). An ore can be described as an accumulation of mineral in sufficient quantity so as to be capable of economic extraction. The minimum metal content (grade) required for a deposit to qualify as an ore varies from metal to metal. Many non-ferrous ores contain, as mined, as little as 1% metal, and often much less.

Gold may be recovered profitably in ores containing only 1 part per million (ppm) of the metal, whereas iron ores containing less than about 45% metal are regarded as of low grade. Every tonne of material in the deposit has a certain *contained value* which is dependent on the metal content and current price of the contained metal. For instance, at a copper price of £2000/t and a molybdenum price of £18/kg, a deposit containing 1% copper and 0.015% molybdenum has a contained value of more than £22/t. The deposit will be economic to work, and can be classified as an ore deposit if:

Contained value per tonne > (total processing costs + losses + other costs) per tonne

A major cost is mining, and this can vary enormously, from only a few pence per tonne of ore to well over £50/t. High-tonnage operations are cheaper in terms of operating costs but have higher initial capital costs. These capital costs are paid off over a number of years, so that high-tonnage operations can only be justified for the treatment of deposits large enough to allow this. Small ore bodies are worked on a smaller scale, to reduce overall capital costs, but capital and operating costs *per tonne* are correspondingly higher (Ottley, 1991).

Alluvial mining is the cheapest method and, if on a large scale, can be used to mine ores of very low contained value due to low grade or low metal price, or both. For instance, in S.E. Asia, tin ores containing as little as 0.01% Sn are mined by alluvial methods. These ores had a contained value of less than £1/t, but very low processing costs allowed them to be economically worked.

High-tonnage open-pit and underground block-caving methods are also used to treat ores of low contained value, such as low-grade copper ores. Where the ore must be mined selectively, however, as is the case with underground vein-type deposits, mining methods become very expensive, and can only be justified on ores of high contained value. An underground selective mining cost of £30/t would obviously be hopelessly uneconomic on a tin ore of alluvial grade, but may be economic on a hard-rock ore containing 1.5% tin, with a contained value of around £50/t.

In order to produce metals, the ore minerals must be broken down by the action of heat (pyrometallurgy), solvents (hydrometallurgy) or electricity (electrometallurgy), either alone or in combination, the most common method being the pyrometallurgical process of smelting. These chemical methods

consume vast quantities of energy. Treatment of 1 t of copper ore, for instance, consumes in the region of 1500–2000 kW h of electrical energy, which at a cost of say 5 p/kW h is around £85/t, well above the contained value of all current copper ores.

Smelters are often remote from the mine site, being centred in areas where energy is relatively cheap, and where access to roads, rail or sea-links is available for shipment of fuel and supplies to, and products from, the smelter. The cost of transportation of mined ore to remote smelters could in many cases be greater than the contained value of the ore.

Mineral processing is usually carried out at the mine site, the plant being referred to as a *mill* or *concentrator*. The essential purpose is to reduce the bulk of the ore which must be transported to and processed by the smelter, by using relatively cheap, low-energy physical methods to separate the valuable minerals from the waste (gangue) minerals. This enrichment process considerably increases the contained value of the ore to allow economic transportation and smelting.

Compared with chemical methods, the physical methods used in mineral processing consume relatively small amounts of energy. For instance, to upgrade a copper ore from 1 to 25% metal would use in the region of 20–50 kW h t^{-1}. The corresponding reduction in weight of around 25:1 proportionally lowers transport costs and reduces smelter energy consumption to around 60–80 kW h in relation to the weight of mined ore. It is important to realise that, although the physical methods are relatively low energy users, the reduction in bulk lowers smelter energy consumption to the order of that used in mineral processing, and it is significant that as ore grades decline, the energy used in mineral processing becomes an important factor in deciding whether the deposit is viable to work or not.

Mineral processing reduces not only smelter energy costs but also smelter metal losses, due to the production of less metal-bearing slag. Although technically possible, the smelting of extremely low-grade ores, apart from being economically unjustifiable, would be very difficult due to the need to produce high-grade metal products free from deleterious impurities. These impurities are found in the gangue minerals and it is the purpose of mineral processing to reject them into the discard (tailings), as smelters often impose penalties according to their level. For instance, it is necessary to remove arsenopyrite from tin concentrates, as it is difficult to remove the contained arsenic in smelting and the process produces a low-quality tin metal.

Against the economic advantages of mineral processing, the losses occurred during milling and the cost of milling operations must be charged. The latter can vary over a wide range, depending on the method of treatment used, and especially on the scale of the operation. As with mining, large-scale operations have higher capital but lower operating costs (particularly labour and energy) than small-scale operations. As labour costs per tonne are most affected by the size of the operation, so, as capacity increases, the energy costs per tonne become proportionally more significant, and these can be more than 25% of the total milling costs in a 10,000 t d^{-1} concentrator.

Losses to tailings are one of the most important factors in deciding whether a deposit is viable or not. Losses will depend very much on the ore mineralogy and dissemination, and on the technology available to achieve efficient concentration. Thus, the development of froth flotation allowed the exploitation of vast low-grade copper deposits which were previously uneconomic to treat. Similarly, the introduction of solvent extraction enabled Nchanga Consolidated Copper Mines in Zambia to treat 9 Mt/yr of flotation tailings, to produce 80,000 t of finished copper from what was previously regarded as waste (Anon., 1979).

In many cases not only is it necessary to separate valuable from gangue minerals, but it is also required to separate valuable minerals from each other. For instance, porphyry copper ores are an important source of molybdenum and the minerals of these metals must be separated for separate smelting. Similarly, complex sulphide ores containing economic amounts of copper, lead and zinc usually require separate concentrates of the minerals of each of these metals. The provision of clean concentrates, with little or no contamination with associated metals, is not always economically feasible, and this leads to another source of loss other than direct tailing loss. A metal which reports to the "wrong" concentrate may be difficult, or economically impossible, to recover, and never achieves its potential valuation. Lead, for example, is essentially irrecoverable in copper concentrates and is often penalized as an impurity by the copper

smelter. The treatment of such polymetallic base metal ores, therefore, presents one of the great challenges to the mineral processor.

Mineral processing operations are often a compromise between improvements in metallurgical efficiency and milling costs. This is particularly true with ores of low contained value, where low milling costs are essential and cheap unit processes are necessary, particularly in the early stages, where the volume of material treated is relatively high. With such low-value ores, improvements in metallurgical efficiency by the use of more expensive methods or reagents cannot always be justified. Conversely high metallurgical efficiency is usually of most importance with ores of high contained value and expensive high-efficiency processes can often be justified on these ores.

Apart from processing costs and losses, other costs which must be taken into account are indirect costs such as ancillary services – power supply, water, roads, tailings disposal – which will depend much on the size and location of the deposit, as well as taxes, royalty payments, investment requirements, research and development, medical and safety costs, etc.

Non-metallic ores

Ores of economic value can be classed as metallic or non-metallic, according to the use of the mineral. Certain minerals may be mined and processed for more than one purpose. In one category the mineral may be a metal ore, i.e. when it is used to prepare the metal, as when bauxite (hydrated aluminium oxide) is used to make aluminium. The alternative is for the compound to be classified as a non-metallic ore, i.e. when bauxite or natural aluminium oxide is used to make material for refractory bricks or abrasives.

Many non-metallic ore minerals associate with metallic ore minerals (Appendix II) and are mined and processed together, e.g. galena, the main source of lead, sometimes associates with fluorite (CaF_2) and barytes ($BaSO_4$), both important non-metallic minerals.

Diamond ores have the lowest grade of all mined ores. The richest mine in terms of diamond content (Argyle in Western Australia) enjoyed grades as high as 2 ppm in its early life. The lowest grade deposits mined in Africa have been as low as 0.01 ppm. Diamond deposits are mined mainly for their gem quality stones which have the highest value, with the low-value industrial quality stones being essentially a by-product; most industrial diamond is now produced synthetically.

Tailings retreatment

Mill tailings which still contain valuable components constitute a potential future resource. New or improved technologies can allow the value contained in tailings, which was lost in earlier processing, to be recovered, or commodities considered waste in the past can become valuable in a new economic order. Reducing or eliminating tailings dumps or dams by retreating them also reduces the environmental impact of the waste.

The cost of tailings retreatment is sometimes lower than that of processing the original ore, because much of the expense has already been met, particularly in mining and comminution. There are many tailings retreatment plants in a variety of applications around the world. The East Rand Gold and Uranium Company (ERGO) closed its operations in 2005 after 28 years of retreating over 870 Mt of the iconic gold dumps of Johannesburg, significantly modifying the skyline of the Golden City and producing 250 t of gold in the process. Also in 2005 underground mining in Kimberley closed, leaving a tailings dump retreatment operation as the only source of diamond production in the Diamond City. Some platinum producers in South Africa now operate tailings retreatment plants for the recovery of platinum group metals (PGMs), and also chromite as a by-product from the chrome-rich UG2 Reef.

Although these products, particularly gold, tend to dominate the list of tailings retreatment operations because of the value of the product, there are others, both operating and being considered as potential major sources of particular commodities. For example coal has been recovered from tailings in Australia (Clark, 1997), uranium is recovered from copper tailings by the Uranium Corporation of India, and copper has been recovered from the Bwana Mkubwa tailings in Zambia, using solvent extraction and electrowinning. The Kolwezi Tailings project in the DRC which proposes to recover oxide copper and cobalt from the tailings of 50 years of copper mining is expected to be the largest source of cobalt in the world.

The re-processing of industrial scrap and domestic waste is also a growing economic activity, especially in Europe. It is essentially a branch of mineral processing with a different feedstock, though operation is generally dry rather than wet (Hoberg, 1993; Furuyama et al., 2003).

Mineral processing methods

"As-mined" or "run-of-mine" ore consists of valuable minerals and gangue. Mineral processing, sometimes called *ore dressing*, *mineral dressing* or *milling*, follows mining and prepares the ore for extraction of the valuable metal in the case of metallic ores, and produces a commercial end product of products such as iron ore and coal. Apart from regulating the size of the ore, it is a process of physically separating the grains of valuable minerals from the gangue minerals, to produce an enriched portion, or *concentrate*, containing most of the valuable minerals, and a discard, or *tailing*, containing predominantly the gangue minerals. The importance of mineral processing is today taken for granted, but it is interesting to reflect that less than a century ago, ore concentration was often a fairly crude operation, involving relatively simple gravity and hand-sorting techniques performed by the mining engineers. The twentieth century saw the development of mineral processing as a serious and important professional discipline in its own right, and without physical separation, the concentration of many ores, and particularly the metalliferous ores, would be hopelessly uneconomic (Wills and Atkinson, 1991).

It has been predicted, however, that the importance of mineral processing of metallic ores may decline as the physical processes utilised are replaced by the hydro and pyrometallurgical routes used by the extractive metallurgist (Gilchrist, 1989), because higher recoveries are obtained by some chemical methods. This may certainly apply when the useful mineral is very finely disseminated in the ore and adequate liberation from the gangue is not possible, in which case a combination of chemical and mineral processing techniques may be advantageous, as is the case with some highly complex ores containing economic amounts of copper, lead, zinc and precious metals (Gray, 1984; Barbery, 1986). Also new technologies such as direct reduction may allow direct smelting of some ores. However, in the majority of cases the energy consumed in direct smelting or leaching of low-grade ores would be so enormous as to make the cost prohibitive. Compared with these processes, mineral processing methods are inexpensive, and their use is readily justified on economic grounds.

If the ore contains worthwhile amounts of more than one valuable mineral, it is usually the object of mineral processing to separate them; similarly if undesirable minerals, which may interfere with subsequent refining processes, are present, it may be necessary to remove these minerals at the separation stage.

There are two fundamental operations in mineral processing: namely the release, or *liberation*, of the valuable minerals from their waste gangue minerals, and separation of these values from the gangue, this latter process being known as *concentration*.

Liberation of the valuable minerals from the gangue is accomplished by *comminution*, which involves crushing, and, if necessary, grinding, to such a particle size that the product is a mixture of relatively clean particles of mineral and gangue. Grinding is often the greatest energy consumer, accounting for up to 50% of a concentrator's energy consumption. As it is this process which achieves liberation of values from gangue, it is also the process which is essential for efficient separation of the minerals, and it is often said to be the key to good mineral processing. In order to produce clean concentrates with little contamination with gangue minerals, it is necessary to grind the ore finely enough to liberate the associated metals. Fine grinding, however, increases energy costs, and can lead to the production of very fine untreatable "slime" particles which may be lost into the tailings. Grinding therefore becomes a compromise between clean (high-grade) concentrates, operating costs and losses of fine minerals. If the ore is low grade, and the minerals have very small grain size and are disseminated through the rock, then grinding energy costs and fines losses can be high, unless the nature of the minerals is such that a pronounced difference in some property between the minerals and the gangue is available.

An intimate knowledge of the mineralogical assembly of the ore is essential if efficient processing is to be carried out. A knowledge not

only of the nature of the valuable and gangue minerals but also of the ore "texture" is required.

The texture refers to the size, dissemination, association and shape of the minerals within the ore. The processing of minerals should always be considered in the context of the mineralogy of the ore in order to predict grinding and concentration requirements, feasible concentrate grades and potential difficulties of separation (Hausen, 1991; Guerney et al., 2003; Baum et al., 2004). Microscopic analysis of concentrate and tailings products can also yield much valuable information regarding the efficiency of the liberation and concentration processes (see Figures 1.2a–i for examples). It is particularly useful in troubleshooting problems which arise from inadequate liberation. Conventional optical microscopes can be used for the examination of thin and polished sections of mineral samples, and in mineral sands applications the simple binocular microscope is a practical tool. However, it is becoming increasingly common to utilise the new technologies of automated mineral analysis using scanning electron microscopy, such as the Mineral Liberation Analyser (MLA) (Gu, 2003) and the QEMSCAN (Gottlieb et al., 2000).

The most important physical methods which are used to concentrate ores are:

(1) Separation based on optical and other properties. This is often called *sorting*, which used

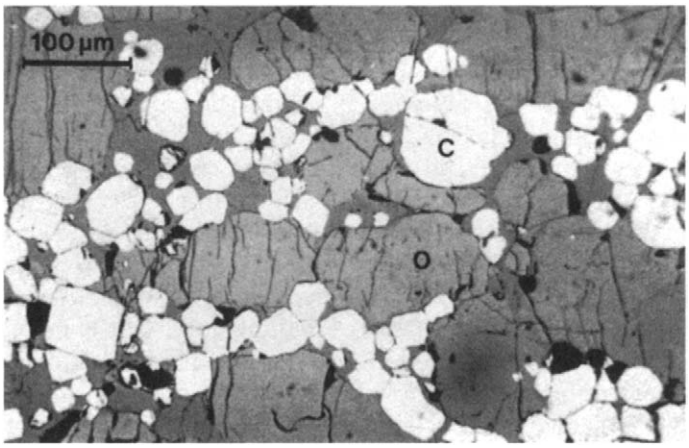


Figure 1.2a Chromite ore. Relatively coarse grain size, and compact morphology of chromite (C) grains makes liberation from olivine (O) gangue fairly straightforward

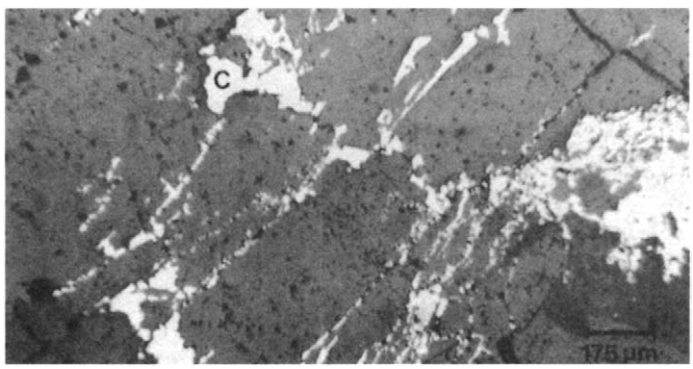


Figure 1.2b North American porphyry copper ore. Chalcopyrite (C) precipitated along fractures in quartz. Liberation of chalcopyrite is fairly difficult due to "chain-like" distribution. Fracture is, however, likely to occur preferentially along the sealed fractures, producing particles with a surface coating of chalcopyrite, which can be effectively recovered into a low-grade concentrate by froth flotation

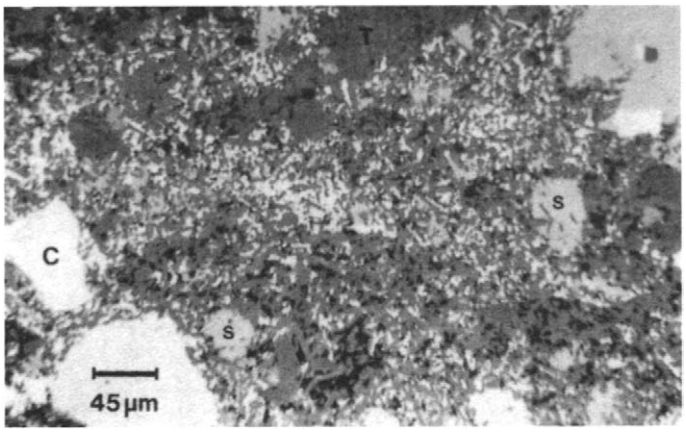


Figure 1.2c Mixed sulphide ore, Wheal Jane, Cornwall. Chalcopyrite (C) and sphalerite (S), much of which is extremely finely disseminated in tourmaline (T), making a high degree of liberation impracticable

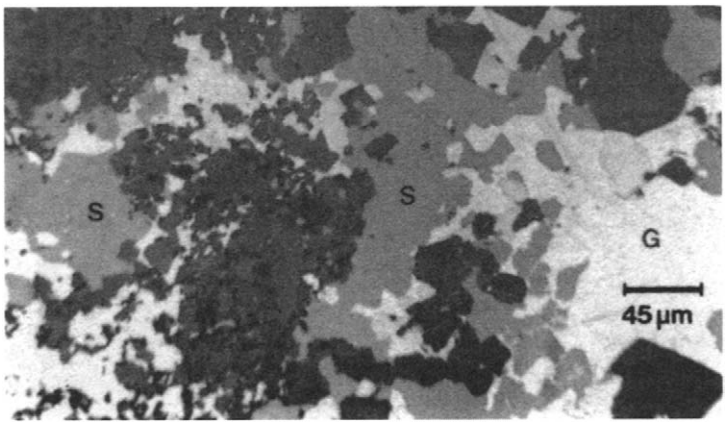


Figure 1.2d Hilton lead–zinc ore body, Australia. Galena (G) and sphalerite (S) intergrown. Separate "clean" concentrates of lead and zinc will be difficult to produce, and contamination of concentrates with other metal is likely

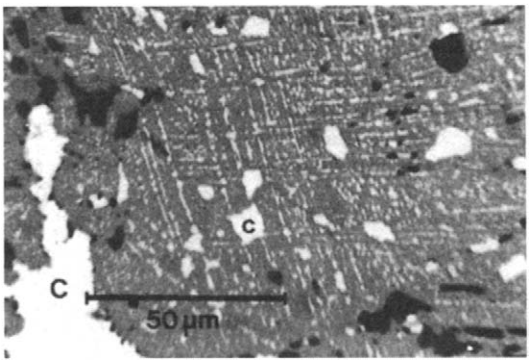


Figure 1.2e Copper–zinc ore. Grain of sphalerite with many minute inclusions of chalcopyrite (C) along cleavage planes. Fracturing during comminution takes place preferentially along the low coherence cleavage planes, producing a veneer of chalcopyrite on the sphalerite surface, making depression of the latter difficult in flotation

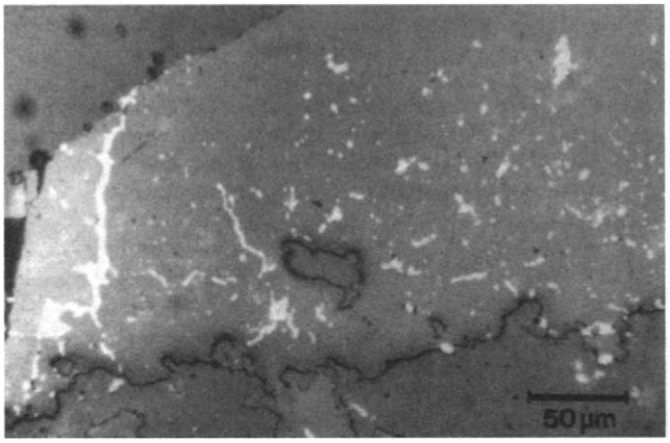


Figure 1.2f Lead–zinc ore. Fine grained native silver in vein networks and inclusions in carbonate host rock. Rejection of this material by heavy medium separation could lead to high silver loss

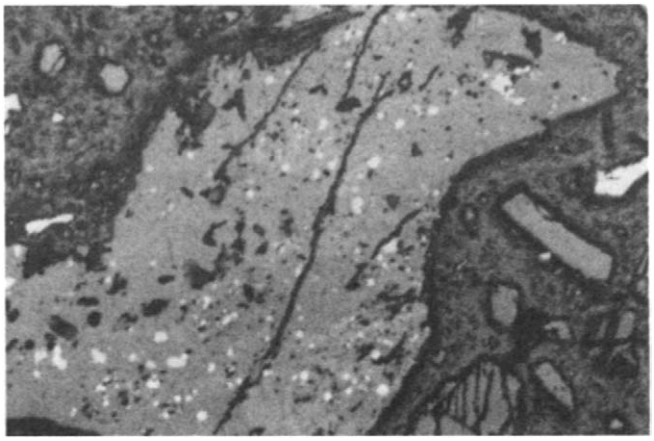


Figure 1.2g Flotation tailings, Palabora Copper Mine, South Africa. Finely disseminated grains of chalcopyrite enclosed in a grain of gangue, and irrecoverable by flotation. Maximum grain size of chalcopyrite is about 20 microns, so attempts to liberate by further grinding would be impracticable

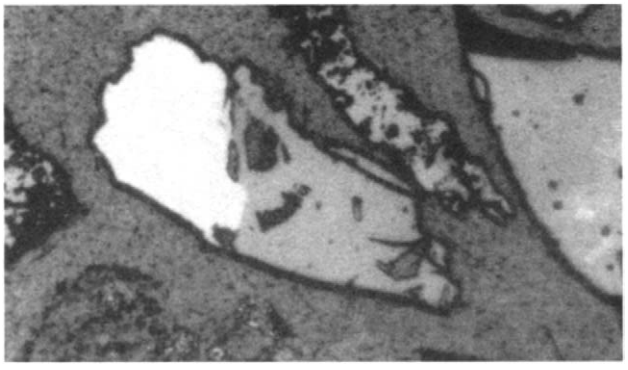


Figure 1.2h Gravity circuit tailings, tin concentrator. Cassiterite (light grey) locked with gangue (darker grey), mainly quartz. The composite particle is very fine (less than 20 µm), and has reported to tailings, rather than middlings, due to the inefficiency of gravity separation at this size. Loss of such particles to tailings is a major cause of poor recovery in gravity concentration. In this case, the composite tailings particles could be recovered by froth flotation into a low-grade concentrate

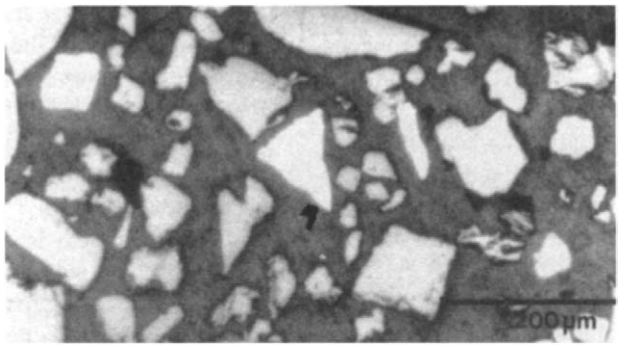


Figure 1.2i Tin concentrate, assaying about 60% tin. Although there is some limited locking of the cassiterite (light grey) with gangue (darker grey), the main contaminant is arsenopyrite (white), which, being a heavy mineral (S.G. 6), has partitioned with the cassiterite (S.G. 7) into the gravity concentrate. The arsenopyrite particles are essentially liberated, and can easily be removed by froth flotation, thereby increasing the tin grade of the concentrate and avoiding smelter penalties due to high arsenic levels

to be done by hand but is now mostly accomplished by machine (see Chapter 14).

(2) Separation based on differences in density between the minerals. *Gravity concentration*, a technology with its roots in antiquity, is based on the differential movement of mineral particles in water due to their different hydraulic properties. The method has recently enjoyed a new lease of life with the development of a range of enhanced gravity concentrating devices. In *dense medium separation* particles sink or float in a dense liquid or (more usually) an artificial dense suspension; it is widely used in coal beneficiation, iron ore and diamond processing, and in the preconcentration of metalliferous ores.

(3) Separation utilising the different surface properties of the minerals. *Froth flotation*, which is one of the most important methods of concentration, is effected by the attachment of the mineral particles to air bubbles within the agitated pulp. By adjusting the "climate" of the pulp by various reagents, it is possible to make the valuable minerals air-avid (*aerophilic*) and the gangue minerals water-avid (*aerophobic*). This results in separation by transfer of the valuable minerals to the air bubbles which form the froth floating on the surface of the pulp.

(4) Separation dependent on magnetic properties. Low intensity magnetic separators can be used to concentrate ferromagnetic minerals such as magnetite (Fe_3O_4), while high-intensity separators are used to separate paramagnetic minerals from their gangue. Magnetic separation is an important process in the beneficiation of iron ores, and finds application in the treatment of paramagnetic non-ferrous minerals. It is used to remove paramagnetic wolframite ((Fe, Mn) WO_4) and hematite (Fe_2O_3) from tin ores, and has found considerable application in the processing of non-metallic minerals, such as those found in mineral sand deposits.

(5) Separation dependent on electrical conductivity properties. *High-tension separation* can be used to separate conducting minerals from non-conducting minerals. This method is interesting, since theoretically it represents the "universal" concentrating method; almost all minerals show some difference in conductivity and it should be possible to separate almost any two by this process. However, the method has fairly limited application, and its greatest use is in separating some of the minerals found in heavy sands from beach or stream placers. Minerals must be completely dry and the humidity of the surrounding air must be regulated, since most of the electron movement in dielectrics takes place on the surface and a film of moisture can change the behaviour completely. The biggest disadvantage of the method is that the capacity of economically sized units is low.

In many cases, a combination of two or more of the above techniques is necessary to concentrate an ore economically. Gravity separation, for instance, is often used to reject a major portion of the gangue, as it is a relatively cheap process. It may not, however, have the selectivity or efficiency to produce the final clean concentrate. Gravity concentrates therefore often need further upgrading by more expensive techniques, such as froth flotation.

Ores which are very difficult to treat (*refractory*), due to fine dissemination of the minerals, complex mineralogy, or both, respond very poorly to the above methods.

A classic example is the huge zinc–lead–silver deposit at McArthur River, in Australia. Discovered in 1955, it is one of the world's largest zinc–lead deposits comprising measured, indicated and inferred resources totalling 124 Mt with up to 13% Zn, 6% Pb and 60 g/t Ag (in 2003). For 35 years it resisted attempts to find an economic processing route due to the very fine grained texture of the ore. However, the development of the proprietary IsaMill fine grinding technology (Pease, 2005) by the mine's owners Mount Isa Mines (now Xstrata), together with an appropriate flotation circuit, allowed the ore to be successfully processed and the mine was finally opened in 1995. The concentrator makes a bulk lead–zinc concentrate with a very fine product size of 80% smaller than 7 μm. There are many stages of flotation cleaning to achieve the necessary product grades with sufficient rejection of silica. McArthur River is a good example of how developments in technology can render previously uneconomic ore deposits viable. Process evolution for McArthur River continues, with the proprietary Albion atmospheric leaching process being considered for the direct treatment of concentrates (Anon., 2002).

Chemical methods, such as pyrometallurgy or hydrometallurgy, can be used to alter mineralogy, allowing the low cost mineral processing methods to be applied to refractory ores (Iwasaki and Prasad, 1989). For instance, non-magnetic iron oxides can be roasted in a weakly reducing atmosphere to produce ferromagnetic magnetite. It has also been suggested (Parsonage, 1988) that the magnetic response could be increased without chemically altering the minerals, by the adsorption of fine magnetite particles onto the surfaces of non-magnetic minerals in the slurry.

Some refractory copper ores containing sulphide and oxidised minerals have been pre-treated hydrometallurgically to enhance flotation performance. In the Leach-Precipitation-Flotation process, developed in the years 1929–34 by the Miami Copper Co., USA, the oxidised minerals are dissolved in sulphuric acid, after which the copper in solution is precipitated as *cement copper* by the addition of metallic iron. The cement copper and acid-insoluble sulphide minerals are then recovered by froth flotation. This process, with several variations, has been used at a number of American copper concentrators, but a more widely used method of enhancing the flotation performance of oxidised ores is to allow the surface to react with sodium sulphide. This "sulphidisation" process modifies the flotation response of the mineral causing it to behave, in effect, as a pseudo-sulphide. Such chemical conditioning of mineral surfaces is widely used in froth flotation (see Chapter 12); sphalerite, for example, can be made to respond in a similar way to chalcopyrite, by allowing the surface to react with copper sulphate.

Recent developments in biotechnology are currently being exploited in hydrometallurgical operations, particularly in the bacterial oxidation of sulphide gold ores and concentrates (Brierley and Brierley, 2001; Hansford and Vargas, 2001). The bacterium *Acidithiobacillus ferrooxidans* is mainly used to enhance the rate of oxidation, by breaking down the sulphide lattice and thus liberating the occluded gold for subsequent removal by cyanide leaching (Lazer et al., 1986). There is good evidence to suggest that certain microorganisms could be used to enhance the performance of conventional mineral processing techniques (Smith et al., 1991). It has been established that some bacteria will act as pyrite depressants in coal flotation, and preliminary work has shown that certain organisms can aid flotation in other ways, with potential profound changes to future industrial froth flotation practice.

Extremely fine mineral dissemination leads to high energy costs in comminution and high losses to tailings due to the generation of difficult-to-treat fine particles. Much research effort has

been directed at minimizing fines losses in recent years, either by developing methods of enhancing mineral liberation, thus minimizing the amount of comminution needed, or by increasing the efficiency of conventional physical separation processes, by the use of innovative machines or by optimising the performance of existing ones. Several methods have been researched and developed to attempt to increase the apparent size of fine particles, by causing them to come together and agglomerate. *Selective flocculation* of certain minerals in suspension, followed by separation of the aggregates from the dispersion, has been successfully achieved on a variety of ore-types at laboratory scale, but plant application is limited (see Chapter 15).

Ultra-fine particles in a suspension can be agglomerated under high shear conditions if the particle surfaces are hydrophobic (water-repellent). A shear field, caused by vigorous agitation, of sufficient magnitude to overcome the energy barrier separating the particles is necessary to bring them together for hydrophobic association. Although the phenomenon of *shear flocculation* is well known it has not, as yet, been exploited commercially (Bilgen and Wills, 1991).

Selective agglomeration of fine particles by oil is a promising method, and has been developed to a commercial scale for the treatment of fine coal (Capes, 1989; Huettenhain, 1991). In the *oil agglomeration* process an immiscible liquid (e.g. a hydrocarbon) is added to the suspension. On agitation, the oil is distributed over oleophilic/hydrophobic surfaces and particle impact allows inter-particle liquid bridges to form, causing agglomeration. The oleophilicity of specific minerals can be controlled, for example, by adding froth flotation reagents. As yet, the oil agglomeration process has not been used to treat ultra-fine minerals outside the laboratory (House and Veal, 1989).

The flowsheet

The flowsheet shows diagrammatically the sequence of operations in the plant. In its simplest form it can be presented as a block diagram in which all operations of similar character are grouped (Figure 1.3). In this case comminution deals with all crushing, grinding and initial

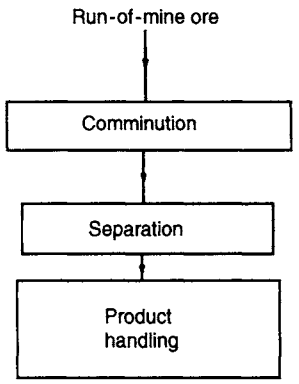


Figure 1.3 Simple block flowsheet

rejection. The next block, "separation", groups the various treatments incident to production of concentrate and tailing. The third, "product handling", covers the disposal of the products.

The simple line flowsheet (Figure 1.4) is for most purposes sufficient, and can include details of machines, settings, rates, etc.

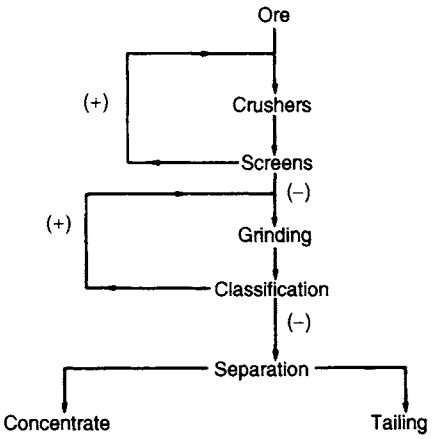


Figure 1.4 Line flowsheet. (+) indicates oversized material returned for further treatment and (−) undersized material, which is allowed to proceed to the next stage

Milling costs

It has been shown that the balance between milling costs and metal losses is crucial, particularly with low-grade ores, and because of this, most mills keep detailed accounts of operating and maintenance costs, broken down into various sub-divisions, such

as labour, supplies, energy, etc. for the various areas of the plant. This type of analysis is very useful in identifying high-cost areas where improvements in performances would be most beneficial. It is impossible to give typical operating costs for milling operations, as these vary enormously from mine to mine, and particularly from country to country, depending on local costs of energy, labour, water, supplies, etc., but Table 1.3 is a simplified example of such a breakdown of costs for a 100,000 t/d copper concentrator. Note the dominance of grinding, due mainly to power requirements.

Table 1.3 Costs per metric tonne milled for a 100,000 t/d copper concentrator

Item	*Cost – US$ per tonne*	*Percent cost*
Crushing	0.088	2.8
Grinding	1.482	47.0
Flotation	0.510	16.2
Thickening	0.111	3.5
Filtration	0.089	2.8
Tailings	0.161	5.1
Reagents	0.016	0.5
Pipeline	0.045	1.4
Water	0.252	8.0
Laboratory	0.048	1.5
Maintenance support	0.026	0.8
Management support	0.052	1.6
Administration	0.020	0.6
Other expenses	0.254	8.1
Total	3.154	100

Efficiency of mineral processing operations

Liberation

One of the major objectives of comminution is the liberation, or release, of the valuable minerals from the associated gangue minerals at the coarsest possible particle size. If such an aim is achieved, then not only is energy saved by the reduction of the amount of fines produced, but any subsequent separation stages become easier and cheaper to operate. If high-grade solid products are required, then good liberation is essential; however, for subsequent hydrometallurgical processes, such as leaching, it may only be necessary to *expose* the required mineral.

In practice, complete liberation is seldom achieved, even if the ore is ground down to the grain size of the desired mineral particles. This is illustrated by Figure 1.5, which shows a lump of ore which has been reduced to a number of cubes of identical volume and of a size below that of the grains of mineral observed in the original ore sample. It can be seen that each particle produced containing mineral also contains a portion of gangue; complete liberation has not been attained; the bulk of the major mineral – the gangue – has, however, been liberated from the minor mineral – the value.

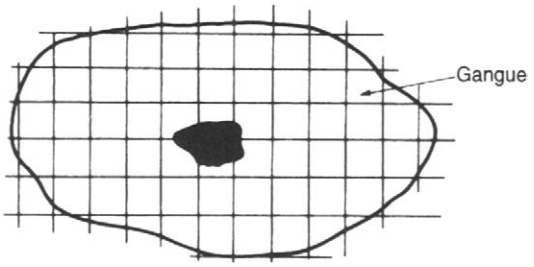


Figure 1.5 "Locking" of mineral and gangue

The particles of "locked" mineral and gangue are known as *middlings*, and further liberation from this fraction can only be achieved by further comminution.

The "degree of liberation" refers to the percentage of the mineral occurring as free particles in the ore in relation to the total content. This can be high if there are weak boundaries between mineral and gangue particles, which is often the case with ores composed mainly of rock-forming minerals, particularly sedimentary minerals. Usually, however, the adhesion between mineral and gangue is strong and, during comminution, the various constituents are cleft across. This produces much middlings and a low degree of liberation. New approaches to increasing the degree of liberation involve directing the breaking stresses at the mineral crystal boundaries, so that the rock can be broken without breaking the mineral grains (Wills and Atkinson, 1993).

Many researchers have tried to quantify degree of liberation with a view to predicting the behaviour

of particles in a separation process (Barbery, 1991). The first attempt at the development of a model for the calculation of liberation was made by Gaudin (1939); King (1982) developed an exact expression for the fraction of particles of a certain size that contained less than a prescribed fraction of any particular mineral. These models, however, suffered from many unrealistic assumptions that must be made with respect to the grain structure of the minerals in the ore, in particular that liberation is preferential, and in 1988 Austin and Luckie concluded that "there is no adequate model of liberation of binary systems suitable for incorporation into a mill model". For this reason liberation models have not found much practical application. However, some fresh approaches by Gay, allowing multi-mineral systems to be modelled (not just binary systems) free of the assumptions of preferential breakage, have recently demonstrated that there may yet be a useful role for such models (Gay, 2004a,b). The quantification of liberation is now routinely possible using the dedicated scanning electron microscope MLA and QEMSCAN systems mentioned earlier, and concentrators are increasingly using such systems to monitor the degree of liberation in their processes.

It should also be noted that a high degree of liberation is not necessary in certain processes, and, indeed, may be undesirable. For instance, it is possible to achieve a high recovery of values by gravity and magnetic separation even though the valuable minerals are completely enclosed by gangue, and hence the degree of liberation of the values is zero. As long as a pronounced density or magnetic susceptibility difference is apparent between the locked particles and the free gangue particles, the separation is possible. A high degree of liberation may only be possible by intensive fine grinding, which may reduce the particles to such a fine size that separation becomes very inefficient. On the other hand, froth flotation requires as much of the valuable mineral *surface* as possible to be exposed, whereas in a chemical leaching process, a portion of the surface must be exposed to provide a channel to the bulk of the mineral.

In practice, ores are ground to an *optimum* grind size, determined by laboratory and pilot scale testwork, to produce an economic degree of liberation. The concentration process is then designed to produce a concentrate consisting predominantly of valuable mineral, with an accepted degree of locking with the gangue minerals, and a middlings fraction, which may require further grinding to promote optimum release of the minerals. The tailings should be mainly composed of gangue minerals.

Figure 1.6 is a cross-section through a typical ore particle, and illustrates effectively the liberation dilemma often facing the mineral processor. Regions A represent valuable mineral, and region AA is rich in valuable mineral but is highly *intergrown* with the gangue mineral. Comminution produces a range of fragments, ranging from fully liberated mineral and gangue particles, to those illustrated. Particles of type 1 are rich in mineral, and are classed as concentrate as they have an acceptable degree of locking with the gangue, which limits the concentrate grade. Particles of type 4 would likewise be classed as tailings, the small amount of mineral present reducing the recovery of mineral into the concentrate. Particles of types 2 and 3, however, would probably be classed as middlings, although the degree of regrinding needed to promote economic liberation of mineral from particle 3 would be greater than in particle 2.

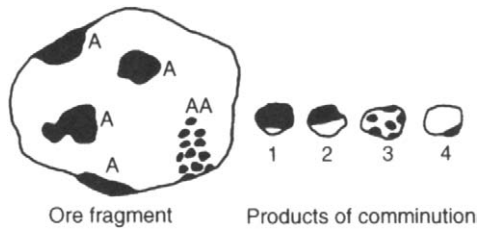


Figure 1.6 Cross-sections of ore particles

During the grinding of a low-grade ore the bulk of the gangue minerals is often liberated at a relatively coarse size (see Figure 1.5). In certain circumstances it may be economic to grind to a size much coarser than the optimum in order to produce in the subsequent concentration process a large middlings fraction and a tailings which can be discarded at a coarse grain size. The middlings fraction can then be reground to produce a feed to the final concentration process (Figure 1.7).

This method discards most of the coarse gangue early in the process, thus considerably reducing

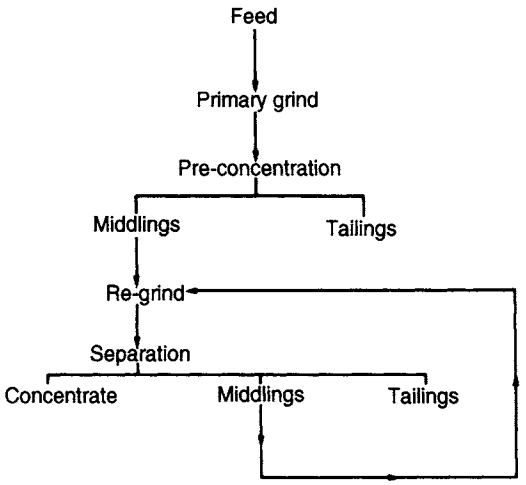


Figure 1.7 Flowsheet for process utilising two-stage separation

grinding costs, as needless comminution of liberated gangue is avoided. It is often used on minerals which can easily be separated from the free gangue, even though they are themselves locked to some extent with gangue. It is the basis of the dense medium process of preconcentration (Chapter 11).

Concentration

The object of mineral processing, regardless of the methods used, is always the same, i.e. to separate the minerals into two or more products with the values in the concentrates, the gangue in the tailings, and the "locked" particles in the middlings. Such separations are, of course, never perfect, so that much of the middlings produced are, in fact, *misplaced* particles, i.e. those particles which ideally should have reported to the concentrate or the tailings. This is often particularly serious when treating ultra-fine particles, where the efficiency of separation is usually low. In such cases, fine liberated valuable mineral particles often report in the middlings and tailings. The technology for treating fine-sized minerals is, as yet, poorly developed, and, in some cases, very large amounts of fines are discarded. For instance, it is common practice to remove material less than 10 μm in size from tin concentrator feeds and direct this material to the tailings, and, in the early 1970s, 50% of the tin mined in Bolivia, 30% of the phosphate mined in Florida, and 20% of the world's tungsten were lost as fines. Significant amounts of copper, uranium, fluorspar, bauxite, zinc, and iron were also similarly lost (Somasundaran, 1986).

Figure 1.8 shows the general size range applicability of unit concentration processes (Mills, 1978). It is evident that most mineral processing techniques fail in the ultra-fine size range. Gravity concentration techniques, especially, become unacceptably inefficient. Flotation, one of the most important of the concentrating techniques, is now practised successfully below 10 μm but not below 1 μm

It should be pointed out that the process is also limited by the mineralogical nature of the ore. For example, in an ore containing native copper it is theoretically possible to produce a concentrate

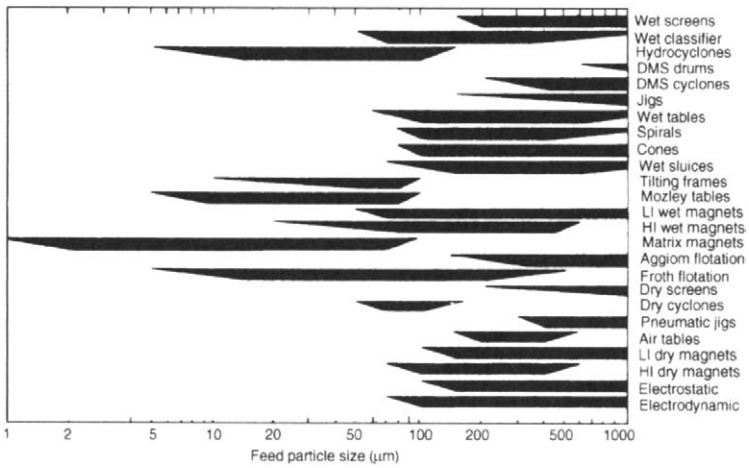


Figure 1.8 Effective range of application of conventional mineral processing techniques

containing 100% Cu, but, if the ore mineral was chalcopyrite ($CuFeS_2$), the best concentrate would contain only 34.5% Cu.

The *recovery*, in the case of the concentration of a metallic ore, is the percentage of the total metal contained in the ore that is recovered from the concentrate; a recovery of 90% means that 90% of the metal in the ore is recovered in the concentrate and 10% is lost in the tailings. The recovery, when dealing with non-metallic ores, refers to the percentage of the total mineral contained in the ore that is recovered into the concentrate, i.e. recovery is usually expressed in terms of the valuable *end* product.

The *ratio of concentration* is the ratio of the weight of the feed (or *heads*) to the weight of the concentrates. It is a measure of the efficiency of the concentration process, and it is closely related to the *grade* or *assay* of the concentrate; the value of the ratio of concentration will generally increase with the grade of concentrate.

The grade, or assay, usually refers to the content of the marketable end product in the material. Thus, in metallic ores, the per cent metal is often quoted, although in the case of very low-grade ores, such as gold, metal content may be expressed as parts per million (ppm), or its equivalent grams per tonne (gt^{-1}). Some metals are sold in oxide form, and hence the grade may be quoted in terms of the marketable oxide content, e.g. $\%WO_3$, $\%U_3O_8$, etc. In non-metallic operations, grade usually refers to the mineral content, e.g. $\%CaF_2$ in fluorite ores; diamond ores are usually graded in *carats* per 100 tonnes (t), where 1 carat is 0.2 g. Coal is graded according to its *ash* content, i.e. the amount of incombustible mineral present within the coal. Most coal burned in power stations ("steaming coal") has an ash content between 15 and 20%, whereas "coking coal" used in steel making generally has an ash content of less than 10% together with appropriate coking properties.

The *enrichment ratio* is the ratio of the grade of the concentrate to the grade of the feed, and again is related to the efficiency of the process.

Ratio of concentration and recovery are essentially independent of each other, and in order to evaluate a given operation it is necessary to know both. For example, it is possible to obtain a very high grade of concentrate and ratio of concentration by simply picking a few lumps of pure galena from a lead ore, but the recovery would be very low. On the other hand, a concentrating process might show a recovery of 99% of the metal, but it might also put 60% of the gangue minerals in the concentrate. It is, of course, possible to obtain 100% recovery by not concentrating the ore at all.

There is an approximately inverse relationship between the recovery and grade of concentrate in all concentrating processes. If an attempt is made to attain a very high-grade concentrate, the tailings assays are higher and the recovery is low. If high recovery of metal is aimed for, there will be more gangue in the concentrate and the grade of concentrate and ratio of concentration will both decrease. It is impossible to give figures for representative values of recoveries and ratios of concentration. A concentration ratio of 2 to 1 might be satisfactory for certain high-grade non-metallic ores, but a ratio of 50 to 1 might be considered too low for a low-grade copper ore; ratios of concentration of several million to one are common with diamond ores. The aim of milling operations is to maintain the values of ratio of concentration and recovery as high as possible, all factors being considered.

Since concentrate grade and recovery are metallurgical factors, the *metallurgical efficiency* of any concentration operation can be expressed by a curve showing the recovery attainable for any value of concentrate grade. Figure 1.9 is a typical *recovery-grade curve* showing the characteristic inverse relationship between recovery and concentrate grade. Mineral processes generally move *along* a recovery-grade curve, with a trade-off between grade and recovery. The mineral processor's challenge is to move the whole curve to a *higher* point so that both grade and recovery are maximised.

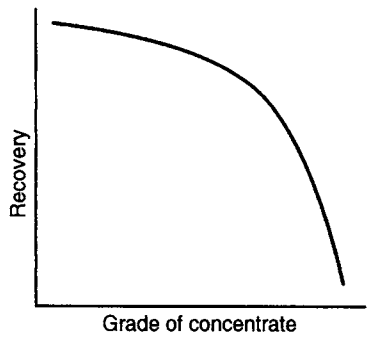


Figure 1.9 Typical recovery-grade curve

Concentrate grade and recovery, used simultaneously, are the most widely accepted measures of assessing metallurgical (not economic) performance. However, there is a problem in quantitatively assessing the technical performance of a concentration process whenever the results of two similar test runs are compared. If both the grade and recovery are greater for one case than the other, then the choice of process is simple, but if the results of one test show a higher grade but a lower recovery than the other, then the choice is no longer obvious. There have been many attempts to combine recovery and concentrate grade into a single index defining the metallurgical efficiency of the separation. These have been reviewed by Schulz (1970), who proposed the following definition:

$$\text{Separation efficiency (S.E.)} = Rm - Rg \quad (1.1)$$

where Rm = % recovery of the valuable mineral,
Rg = % recovery of the gangue into the concentrate.

Suppose the feed material, assaying f% metal, separates into a concentrate assaying c% metal, and a tailing assaying t% metal, and that C is the fraction of the total feed weight that reports to the concentrate, then:

$$Rm = \frac{100Cc}{f} \quad (1.2)$$

i.e. recovery of valuable mineral to the concentrate is equal to metal recovery, assuming that all the valuable metal is contained in the same mineral.

The gangue content of the concentrate $= 100 - (100c/m)$%, where m is the percentage metal content of the valuable mineral,

$$\text{i.e. gangue content} = \frac{100(m-c)}{m}$$

Therefore, $Rg = C\times$ gangue content of concentrate/gangue content of feed:

$$= \frac{100C(m-c)}{(m-f)}$$

$$\text{Therefore, } Rm - Rg = \frac{100Cc}{f} - \left\{\frac{100C(m-c)}{(m-f)}\right\}$$

$$= \frac{100Cm(c-f)}{(m-f)f} \quad (1.3)$$

Example 1.1

A tin concentrator treats a feed containing 1% tin, and three possible combinations of concentrate grade and recovery are:

High grade	63% tin at 62% recovery
Medium grade	42% tin at 72% recovery
Low grade	21% tin at 78% recovery

Determine which of these combinations of grade and recovery produce the highest separation efficiency.

Solution

Assuming that the tin is totally contained in the mineral cassiterite (SnO_2), which, when pure, contains 78.6% tin, and since mineral recovery (Equation 1.2) is $100 \times C\times$ concentrate grade/feed grade, for the high-grade concentrate:

$$62 = C \times 63 \times \frac{100}{1}, \text{ and so } C = 9.841 \times 10^{-3}$$

Therefore,

$$\text{(S.E.) (Equation 1.3)} = \frac{0.984 \times 78.6 \times (63-1)}{(78.6-1)\times 1}$$

$$= 61.8\%$$

Similarly, for the medium-grade concentrate, from Equation 1.2:

$$72 = 100 \times C \times 42/1$$

Therefore,

$$C = 1.714 \times 10^{-2},$$

and S.E. (Equation 1.3) = 71.2%.

For the low-grade concentrate, from Equation 1.2:

$$78 = 100 \times C \times 21/1$$

Therefore, $C = 3.714 \times 10^{-2}$, and S.E. (Equation 1.3) = 75.2%.

Therefore, the highest separation efficiency is achieved by the production of a low-grade (21% tin) concentrate at high (78%) recovery.

Although the value of separation efficiency can be useful in comparing the performance of different

operating conditions on selectivity, it takes no account of economic factors, and, as will become apparent, a high value of separation efficiency does not necessarily lead to the most economic return.

Since the purpose of mineral processing is to increase the economic value of the ore, the importance of the recovery-grade relationship is in determining the most *economic* combination of recovery and grade which will produce the greatest financial return per tonne of ore treated in the plant. This will depend primarily on the current price of the valuable product, transportation costs to the smelter, refinery, or other further treatment plant, and the cost of such further treatment, the latter being very dependent on the grade of concentrate supplied. A high grade concentrate will incur lower smelting costs, but the lower recovery means lower returns of final product. A low grade concentrate may achieve greater recovery of the values, but incur greater smelting and transportation costs due to the included gangue minerals. Also of importance are impurities in the concentrate which may be penalized by the smelter, although precious metals may produce a bonus.

The net return from the smelter (NSR) can be calculated for any recovery-grade combination from:

NSR = Payment for contained metal
− (Smelter charges + Transport costs)

This is summarised in Figure 1.10, which shows that the highest value of NSR is produced at an optimum concentrate grade. It is essential that the mill achieves a concentrate grade which is as close as possible to this target grade. Although the effect of moving slightly away from the optimum may only be of the order of a few pence per tonnes treated, this can amount to very large financial losses, particularly on high-capacity plants treating thousands of tonnes per day. Changes in metal price, smelter terms, etc. obviously affect the NSR–concentrate grade curve, and the value of the optimum concentrate grade. For instance, if the metal price increases, then the optimum grade will be lower, allowing higher recoveries to be attained (Figure 1.11).

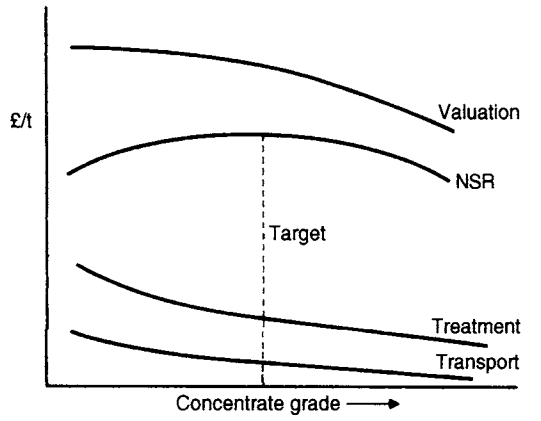


Figure 1.10 Variation of payments and charges with concentrate grade

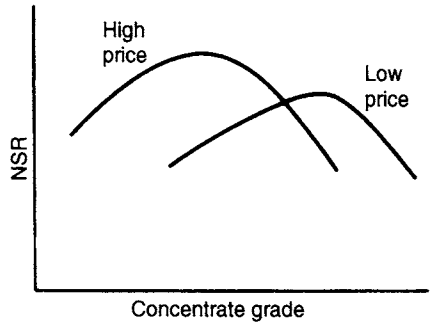


Figure 1.11 Effect of metal price on NSR-grade relationship

It is evident that the terms agreed between the concentrator and smelter are of paramount importance in the economics of mining and milling operations. Such *smelter contracts* are usually fairly complex. Concentrates are sold under contract to "custom smelters" at prices based on quotations on metal markets such as the London Metal Exchange (LME). The smelter, having processed the concentrates, disposes of the finished metal to the consumers. The proportion of the "free market" price of the metal received by the mine is determined by the terms of the contract negotiated between mine and smelter, and these terms can vary considerably. Table 1.4 summarises a typical low-grade smelter contract for the purchase of tin concentrates. As is usual in many contracts, one assay unit is deducted from the concentrate assay in assessing the value of the concentrates, and arsenic present in the concentrate is penalised. The concentrate assay is of prime importance in determining the valuation, and the value of the assay is usually agreed on the result of independent sampling and assaying performed by the mine and smelter. The

Table 1.4 Simplified tin smelter contract

Material	Tin concentrates, assaying no less than 15% Sn, to be free from deleterious impurities not stated, and to contain sufficient moisture as to evolve no dust when unloaded at our works.
Quantity	Total production of concentrates.
Valuation	Tin, less 1 unit per dry tonne of concentrates, at the lowest of the official London Metal Exchange prices.
Pricing	On the 7th market day after completion of arrival of each sampling lot into our works.
Treatment charge	£385 per dry tonne of concentrates.
Moisture	£24 per tonne of moisture.
Penalties	Arsenic £40 per unit per tonne.
Lot charge	£175 per lot sampled of less than 17 tonnes.
Delivery	Free to our works in regular quantities, loose on a tipping lorry or in any other manner acceptable to both parties.

assays are compared, and if the difference is no more than an agreed value, the mean of the two results may be taken as the agreed assay. In the case of a greater difference, an "umpire" sample is assayed at an independent laboratory. This umpire assay may be used as the agreed assay, or the mean of this assay and that of the party which is nearer to the umpire assay may be chosen.

The use of smelter contracts, and the importance of the by-products and changing metal prices, can be seen by briefly examining the economics of processing two base metals – tin and copper – whose fortunes have fluctuated over the years for markedly different reasons.

Economics of tin processing

Tin constitutes an interesting case study in the vagaries of commodity prices and how they impact on the mineral industry and its technologies. Almost a half of the world's supply of tin in the mid-nineteenth century was mined in south-west England, but by the end of the 1870s Britain's premium position was lost, with the emergence of Malaysia as the leading producer and the discovery of rich deposits in Australia. By the end of the century, only nine mines of any consequence remained in Britain, where 300 had flourished 30 years earlier. From alluvial or secondary deposits, principally from South-East Asia, comes 80% of mined tin.

Unlike copper, zinc and lead, production of tin has not risen dramatically over the years and has rarely exceeded 250,000 t/yr.

The real price of tin spent most of the first half of the twentieth century in a relatively narrow band between US$10 and US$15/t (1998$), with some excursions (Figure 1.12; USGS, 2005). From 1956 its price was regulated by a series of international agreements between producers and consumers under the auspices of the International Tin Council (ITC), which mirrored the highly successful policy of De Beers in controlling the gem diamond trade. Price stability was sought through selling from the ITC's huge stockpiles when the price rose and buying into the stockpile when the price fell.

From the mid-1970s, however, the price of tin was driven artificially higher at a time of world recession, expanding production and falling consumption, the latter due mainly to the increasing use of aluminium, rather than tin-plated steel, cans. Although the ITC imposed restrictions on

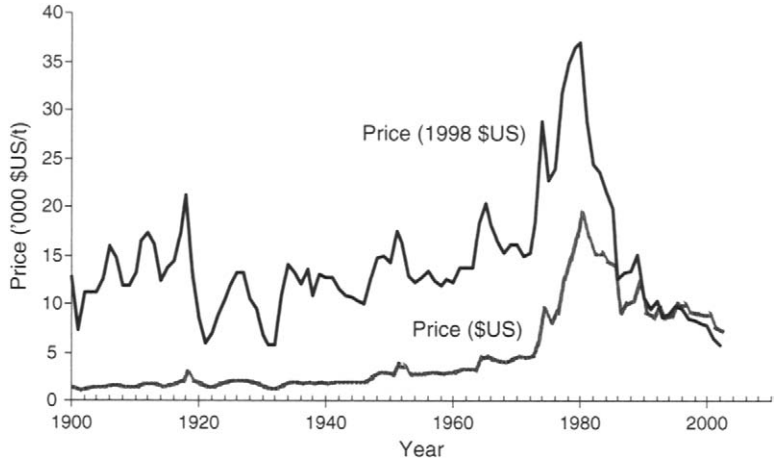


Figure 1.12 Tin prices 1900–2002

the amount of tin that could be produced by its member countries, the reason for the inflating tin price was that the price of tin was fixed by the Malaysian dollar, while the buffer stock manager's dealings on the LME were financed in sterling. The Malaysian dollar was tied to the American dollar, which strengthened markedly between 1982 and 1984, having the effect of increasing the price of tin in London simply because of the exchange rate. However, the American dollar began to weaken in early 1985, taking the Malaysian dollar with it, and effectively reducing the LME tin price from its historic peak. In October 1985, the buffer stock manager announced that the ITC could no longer finance the purchase of tin to prop up the price, as it had run out of funds, owing millions of pounds to the LME traders. This announcement caused near panic, the tin price fell to £8140/t and the LME halted all further dealings. In 1986 many of the world's tin mines were forced to close down due to the depressed tin price, and prices continued to fall in subsequent years. The following discussion therefore relates to tin processing prior to the collapse, including prices and costs. The same principles can be applied to the prices and costs of any particular period including the present day.

It is fairly easy to produce concentrates containing over 70% tin (i.e. over 90% cassiterite) from alluvial ores, such as those worked in South-East Asia. Such concentrates present little problem in smelting and hence treatment charges are relatively low. Production of high-grade concentrates also incurs relatively low freight charges, which is important if the smelter is remote.

For these reasons it has been traditional in the past for hard-rock, lode tin concentrators to produce high-grade concentrates, but high tin prices and the development of profitable low-grade smelting processes changed the policy of many mines towards the production of lower-grade concentrates. The advantage of this is that the recovery of tin into the concentrate is increased, thus increasing smelter payments. However, the treatment of low-grade concentrates produces much greater problems for the smelter, and hence the treatment charges at "low-grade smelters" are normally much higher than those at the high-grade smelters. Freight charges are also correspondingly higher.

Suppose that a tin concentrator treats a feed containing 1% tin, and that three possible combinations of concentrate grade and recovery are (as in Example 1.1):

High grade	63% tin at 62% recovery
Medium grade	42% tin at 72% recovery
Low grade	21% tin at 78% recovery

Assuming that the concentrates are free of arsenic, and that the cost of transportation to the smelter is £20/t of dry concentrate, then the return on each tonne of ore treated can be simply

calculated, using the low-grade smelter terms set out in the contract in Table 1.4.

For instance, at a grade of 42% tin and 72% recovery, the weight of concentrate produced from 1 t of ore is 17.14 kg (from Example 1.1).

The smelter payment for tin in this concentrate is

$$P \times 17.14 \times (42 - 1)/100{,}000$$

where P = tin price in £/t

Assuming a tin price of £8500/t, then the net smelter payment is £59.73.

The smelter treatment charge is £385 × concentrate weight = £6.59, and the transportation cost is £0.34.

The net smelter return for the processing of 1 t of concentrator feed is thus £59.73 − (6.59 + 0.34) = £52.80. Therefore, although the ore contains, at free market price, £85 worth of tin per tonne, the mine realises only 62% of the ore value in payments received.

Production of a lower-grade concentrate incurs higher smelter and freight charges, but increases the payment for contained metal, due to the higher recovery. Similar calculations show that at a grade of 21% tin and 78% recovery, the payment for tin is increased to £63.14, but the total deductions also increase to £15.04, producing a net smelter return of £48.10/t of ore treated.

Clearly, lowering the concentrate grade to 21% tin, in order to increase recovery, has increased the separating efficiency (Example 1.1), but has adversely affected the economic return from the smelter, the increased charges being more important than the increase in revenue from the metal.

Increasing the grade to 63% tin can obviously reduce charges even further, particularly if the concentrate can be sent to a higher-grade smelter with lower treatment charges.

Assuming a treatment charge of £50/t of concentrate, and identical payments and freight charges, the payment for metal in such a concentrate would be only £51.86, but the charges are reduced to £0.69/t. The NSR per tonne of ore treated is thus £51.17. In this case, therefore, the return is highest from the low-grade smelter treating a medium-grade concentrate. This situation may change, however, if the metal price changes markedly. If the tin price falls and the terms of the smelter contracts remain the same, then the mine profits will suffer due to the reduction in payments. Rarely does a smelter share the risks of changing metal price, as it performs a service role, changes in smelter terms being made more on the basis of changing smelter costs rather than metal price. The mine does, however, reap the benefits of increasing metal price.

At a tin price of £6500/t, the NSR per tonne of ore from the low-grade smelter treating the 42% tin concentrate is £38.75, while the return from the high-grade smelter, treating a 63% Sn concentrate, is £38.96. Although this is a difference of only 21/t of ore, to a small 500 t d^{-1} tin concentrator this change in policy from relatively low- to high-grade concentrate, together with the subsequent change in concentrate market, would expect to increase the revenue by £0.21 × 500 × 365 = £38,325 per annum. The concentrator management must always be prepared to change its policies, both metallurgical and marketing, in this way if maximum returns are to be made, although production of a reliable grade–recovery relationship is often difficult due to the complexity of operation of lode tin concentrators and variations in feed characteristics.

It is, of course, necessary to deduct the costs of mining and processing from the NSR in order to deduce the profit achieved by the mine. Some of these costs will be indirect, such as salaries, administration, research and development, medical and safety, as well as direct costs, such as operating and maintenance, supplies and energy. The breakdown of milling costs varies enormously from mine to mine, depending very much on the size and complexity of the operations. Mines with very large ore reserves tend to have very high throughputs, and so although the capital outlay is higher, the operating and labour costs tend to be much lower than those on smaller plants, such as those treating lode tin ores. Mining costs also vary enormously, and are very much higher for underground than for open-pit operations.

If mining and milling costs of £40 and £8 respectively per tonne of ore are typical of underground tin operations, then it can be seen that at a tin price of £8500 the mine, producing a concentrate of 42% tin, which is sold to a low-grade smelter, makes a profit of £52.80 − 48 = £4.80/t of ore, which at a throughput of 500 t d^{-1} corresponds to a gross annual profit of £867,000. It is also clear

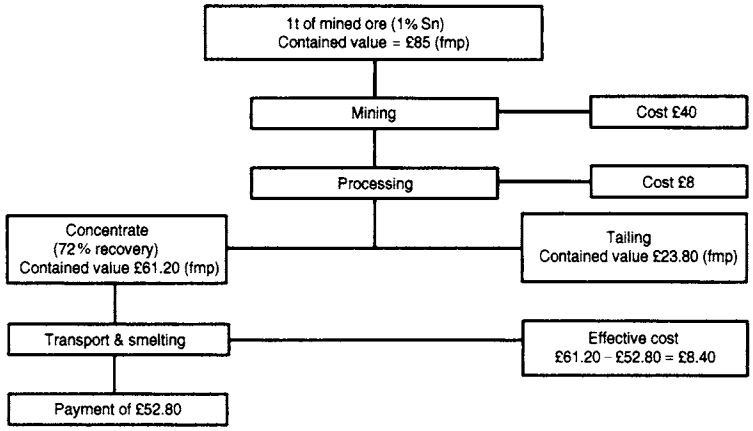


Figure 1.13 Breakdown of costs and revenues for treatment of lode tin ore (fmp = free market price)

that if the tin price falls to £6500/t, the mine loses £48 − 38.96 = £9.04 for every tonne of ore treated.

The breakdown of revenue and costs at a tin price of £8500/t is summarised in Figure 1.13. The mine profit per tonne of ore treated can be summarised as:

$$\text{Contained value of ore} - (\text{costs} + \text{losses})$$

$$= £(85 - (40 + 8 + 23.80 + 8.40)) = 4.80/\text{t}$$

Since 1 t of ore produces 0.0072 t of tin in concentrates, and the free market value of this contained metal is £61.20, the total effective cost of producing 1 t of tin in concentrates is £(61.20 − 4.80)/0.0072 = £7833.

The importance of metal losses in tailings is shown clearly in Figure 1.13. With ore of relatively high contained value, the recovery is often more important than the cost of promoting that recovery. Hence relatively high-cost unit processes can be justified if significant improvements in recovery are possible, and efforts to improve recoveries should always be made. For instance, suppose the concentrator, maintaining a concentrate grade of 42% tin, improves the recovery by 1% to 73% with no change in actual operating costs. The NSR will be £53.53/t and after deducting mining and milling costs, the profit realised by the mine is £5.53/t of ore. Since 1 t of ore now produces 0.0073 t of tin, having a contained value of £62.05, the cost of producing 1 t of tin in concentrates is thereby reduced to £(62.05 − 5.53)/0.0073 = £7742.

Due to the high processing costs and losses, hard-rock tin mines, such as those in Cornwall and Bolivia, had the highest production costs, being above £7500/t in 1985. Alluvial operations, such as those in Malaysia, Thailand and Indonesia, have lower production costs (around £6000/t in 1985). Although these ores have much lower contained values (only about £1 − 2/t), mining and processing costs, particularly on the large dredging operations, are extremely low, as are smelting costs and losses, due to the high concentrate grades and recoveries produced. In 1985 the alluvial mines in Brazil produced the world's cheapest tin, having production costs of only about £2200/t (Anon., 1985a).

Economics of copper processing

In 1835, the United Kingdom was the world's largest copper producer, mining around 15,000 t/y, just below half the world production. This leading position was held until the mid-1860s when the copper mines of Devon and Cornwall became exhausted and the great flood of American copper began to make itself felt. The United States produced about 10,000 t in 1867, but by 1900 was producing over 250,000 t/yr. This output had increased to 1,000,000 t/yr in the mid-1950s, by which time Chile and Zambia had also become major producers. World annual production was approaching 15,000,000 t at the beginning of the twenty-first century (see Figure 1.1).

Figure 1.14 shows that the price of copper in real terms grew steadily from about 1930 until the period of the oil shocks of the mid-1970s

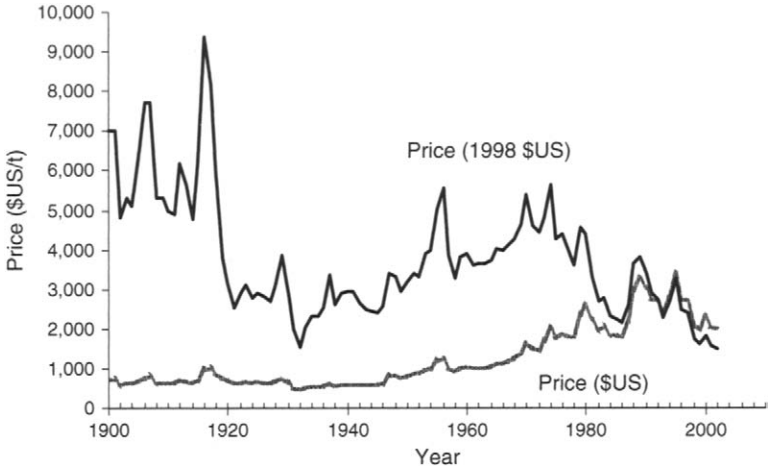


Figure 1.14 Copper prices 1900–2002

and then declined steeply until the early twenty-first century, the average real price in 2002 being lower than that any time in the twentieth century. The pressure on costs was correspondingly high, and the lower cost operators such as those in Chile had more capacity to survive than the high cost producers such as some of those in the USA. However, world demand, particularly from emerging economies such as China, has driven the price strongly since 2002 and in mid-2005 it had recovered to about US$3500/t (in dollars of the day).

The move to large-scale operations (Chile's Minerara Escondida's two concentrators had a total capacity of 230,000 t/d in 2003), improvements in technology and operating efficiencies have kept the major companies in the copper-producing business. In some cases by-products are important revenue earners. BHP Billiton's Olympic Dam produces gold and silver as well as its main products of copper and uranium, and Rio Tinto's Kennecott Utah Copper is also a significant molybdenum producer.

A typical smelter contract for copper concentrates is summarised in Table 1.5. As in the case of the tin example, the principles illustrated can be applied to current prices and costs.

Consider a porphyry copper mine treating an ore containing 0.6% Cu to produce a concentrate containing 25% Cu, at 85% recovery. This is a concentrate production of 20.4 kg t^{-1} of ore treated. Therefore, at a copper price of £980/t:

Table 1.5 Simplified copper smelter contract

Payments	
Copper:	Deduct from the agreed copper assay 1 unit, and pay for the remainder at the LME price for higher-grade copper.
Silver:	If over 30 g t^{-1} pay for the agreed silver content at 90% of the LME silver price.
Gold:	If over 1 g t^{-1} pay for the agreed gold content at 95% of the LME gold price.
Deductions	
Treatment charge: £30 per dry tonne of concentrates	
Refining charge: £115 per tonne of payable copper	

$$\text{Payment for copper} = £20.4 \times 0.24 \times \frac{980}{1000}$$
$$= £4.80$$
$$\text{Treatment charge} = £30 \times \frac{20.4}{1000} = £0.61$$
$$\text{Refining charge} = £115 \times 20.4 \times \frac{0.24}{1000}$$
$$= £0.56$$

Assuming a freight cost of £20/t of concentrate, the total deductions are £(0.61 + 0.56 + 0.41) = £1.58, and the NSR per tonne of ore treated is thus £(4.80 − 1.58) = £3.22.

As mining, milling and other costs must be deducted from this figure, it is apparent that only those mines with very low operating costs can have

any hope of profiting from such low-grade operations. Assuming a typical large open-pit mining cost of £1.25/t of ore, a milling cost of £2/t and indirect costs of £2/t, the mine will lose £2.03 for every tonne of ore treated. The breakdown of costs and revenue is summarised in Figure 1.15.

As each tonne of ore produces 0.0051 t of copper in concentrates, with a free market value of £5.00, the total effective production costs are £(5.00 + 2.03)/0.0051 = £1378/t of copper in concentrates.

However, if the ore contains appreciable by-products, the effective production costs are reduced. Assuming the concentrate contains $25\,g\,t^{-1}$ of gold and $70\,g\,t^{-1}$ of silver, then the payment for gold, at a LME price of £230/troy oz (1 troy oz = 31.1035 g),

$$= \frac{20.4}{1000} \times \frac{25}{31.1035} \times 0.95 \times 230 = £3.58$$

and the payment for silver at a LME price of £4.5/troy oz

$$= \frac{20.4}{1000} \times \frac{70}{31.1035} \times 0.9 \times 4.5 = £0.19$$

The net smelter return is thus increased to £6.99/t of ore, and the mine makes a profit of £1.74/t of ore treated. The effective cost of producing 1 t of copper is thus reduced to £(5.00 − 1.74)/0.0051 = £639.22.

By-products are thus extremely important in the economics of copper production, particularly for very low-grade operations. In this example, 42% of the mine's revenue is from gold, copper contributing 56%. This compares with the contributions to revenue realised at Bougainville Copper Ltd (Sassos, 1983).

Table 1.6 lists estimated effective costs per tonne of copper processed in 1985 at some of the world's major copper mines, at a copper price of £980/t (Anon., 1985b).

It is evident that, apart from Bougainville, which had a high gold content, and Palabora, a large open-pit operation with numerous heavy mineral by-products, the only economic copper mines in 1985 were the large South American porphyries. The mines profited due to relatively low actual operating costs, by-product molybdenum production, and higher average grades (1.2% Cu) than the North American porphyries, which averaged only 0.6% Cu. Relatively high-grade deposits such as that at Nchanga failed to profit due partly to high operating costs, but mainly due to the lack of by-products. It is evident that if a large copper mine is to be brought into production in such an economic climate, then initial capitalization on high-grade secondary ore and by-products must be made, as at Ok Tedi in Papua New Guinea, which commenced production in 1984, initially mining and processing the high-grade gold ore in the leached capping ore.

Table 1.6 Effective costs at world's leading copper mines in 1985

Mine	*Country*	*Effective cost £/t of processed copper*
Chuquicamata	Chile	589
El Teniente	Chile	622
Bougainville	Papua New Guinea	664
Palabora	South Africa	725
Andina	Chile	755
Cuajone	Peru	876
El Salvador	Chile	906
Toquepala	Peru	1012
Inspiration	USA	1148
San Manuel	USA	1163
Morenci	USA	1193
Twin Buttes	USA	1208
Utah/Bingham	USA	1329
Nchanga	Zambia	1374
Gecamines	Zaire	1374

Since the profit margin involved in the processing of modern copper ores is usually only small, continual efforts must be made to try to reduce milling costs and metal losses. Even relatively small increases in return per tonne can have a significant effect, due to the very large tonnages that are often treated. There is, therefore, a constant search for improved flowsheets and flotation reagents.

Figure 1.15 shows that in the example quoted, the contained value in the flotation tailings is £0.88/t of treated ore. The concentrate contains copper to the value of £5.00, but the smelter payment is £3.22. Therefore, the mine realises only 64.4% of the free market value of copper in the concentrate. On this basis, the actual metal loss into the tailings is only about £0.57/t of ore. This is relatively small compared with milling costs, and an increase in recovery of 0.5% would raise the net smelter return by only £0.01. Nevertheless, this

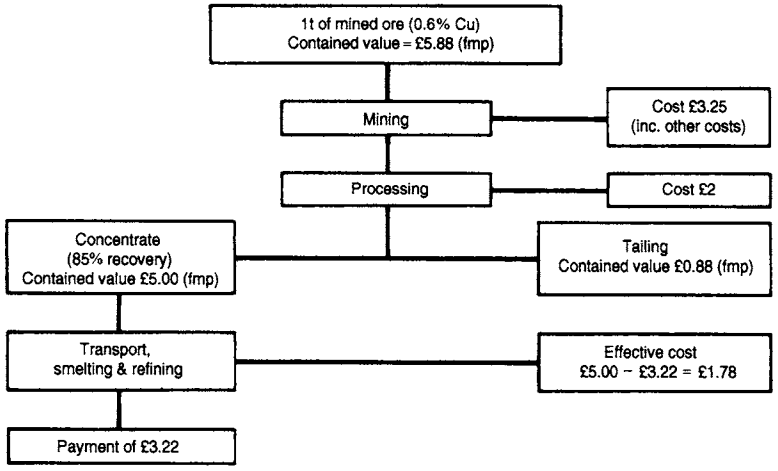


Figure 1.15 Breakdown of costs and revenues for treatment of typical porphyry copper ore (fmp = free market price)

can be significant; to a mine treating 50,000 t d^{-1}, this is an increase in revenue of £500/d, which is extra profit, providing that it is not offset by any increased milling costs. For example, improved recovery may be possible by the use of a more effective reagent or by increasing the dosage of an existing reagent, but if the increased reagent cost is greater that the increase in smelter return, then the action is not justified.

This balance between milling cost and metallurgical efficiency is very critical on a concentrator treating an ore of low contained value, where it is crucial that milling costs be as low as possible. Reagent costs are typically around 10% of the milling costs on a large copper mine, but energy costs may contribute well over 25% of these costs. Grinding is by far the greatest energy consumer and this process undoubtedly has the greatest influence on metallurgical efficiency. Grinding is essential for the liberation of the minerals in the assembly, but it should not be carried out any finer than is justified economically. Not only is fine grinding energy intensive, but it also leads to increased media costs. Grinding steel often contributes as much as, if not more than, the total mill energy cost, and the quality of grinding medium used often warrants special study. Figure 1.16 shows the effect of fineness of grind on NSR and grinding costs for a typical low-grade copper ore. Although flotation recovery, and hence NSR, increases with fineness of grind, it is evident that there is no economic benefit in grinding finer than 105 microns. Even this fineness will probably be beyond the economic limit because of the additional capital cost of the grinding equipment required to achieve it.

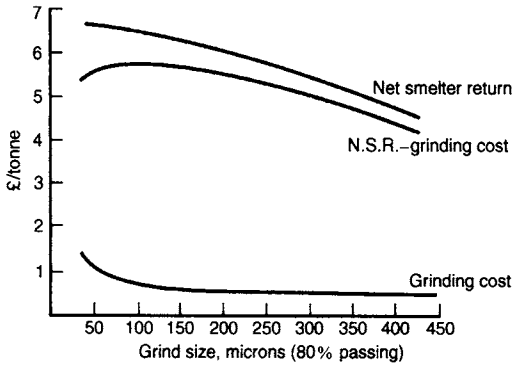


Figure 1.16 Effect of fineness of grind on net smelter return and grinding costs

Economic efficiency

It is evident from the foregoing that the metallurgical significance of grade and recovery is of less importance than the economic consideration. It is apparent that a certain combination of grade and recovery produces the highest economic return under certain conditions of metal price, smelter terms, etc. However, this metallurgical efficiency combination may not promote the highest return if those conditions change. *Economic efficiency* compares the *actual* NSR per tonne of ore milled with the *theoretical* return, thus taking into account

all the financial implications. The theoretical return is the maximum possible return that could be achieved, assuming "perfect milling", i.e. complete separation of the valuable mineral into the concentrate, with all the gangue reporting to tailings. Using economic efficiency, plant efficiencies can be compared even during periods of fluctuating market conditions.

Example 1.2

Calculate the economic efficiency of a tin concentrator, treating an ore grading 1% tin producing a concentrate grading 42% tin at 72% recovery, under the conditions of the smelter contract shown in Table 1.4. The cost of transportation to the smelter is £20/t of concentrate. Assume a tin price of £8500/t.

Solution

It was shown in the section on tin processing that this concentrate would realize a net smelter return of £52.80.

Assuming perfect milling, 100% recovery of the tin would be achieved, into a concentrate grading 78.6% tin (i.e. pure cassiterite).

The weight of concentrate produced from 1 tonne of feed = 12.72 kg.

$$\text{Therefore, transport cost} = £12.71 \times \frac{20}{1000}$$

$$= £0.25$$

$$\text{Treatment charge} = £385 \times \frac{12.72}{1000}$$

$$= £4.90$$

$$\text{Valuation} = £12.72 \times (78.6 - 1) \times \frac{8500}{100{,}000} = £83.90$$

Therefore, net smelter return $= £(83.90 - 4.90 - 0.25) = £78.75$, and economic efficiency $= 100 \times 52.80/78.75 = 67.0\%$.

In recent years, attempts have been made to optimize the performance of some concentrators by controlling plant conditions to achieve maximum economic efficiency (see Chapters 3 and 12). A dilemma often facing the metallurgist on a complex flotation circuit producing more than one concentrate is: how much contamination of one concentrate by the mineral that should report to the other concentrate can be tolerated? For instance, on a plant producing separate copper and zinc concentrates, copper is always present in the zinc concentrate, as is zinc in the copper concentrate. Metals misplaced into the wrong concentrate are rarely paid for by the specialist smelter, and are sometimes penalised. There is, therefore, an optimum "degree of contamination" that can be tolerated. The most important reagent controlling this factor is often the depressant, which inhibits flotation of the zinc minerals. Increase in the addition of this reagent not only produces a cleaner copper concentrate but also reduces copper recovery into this concentrate, as it also has a lesser depressing effect on the copper minerals. The depressed copper minerals are likely to report to the zinc concentrate, so the addition rate of depressant needs to be carefully monitored and controlled to produce an optimum compromise. This should occur when the economic efficiency is maximised.

Example 1.3

The following assay data was collected from a copper–zinc concentrator:

Feed	0.7% copper,	1.94% zinc
Cu concentrate	24.6% copper,	3.40% zinc
Zn concentrate	0.4% copper,	49.7% zinc

Mass flow measurement showed that 2.6% of the feed weight reported to the copper concentrate, and 3.5% to the zinc concentrate.

Calculate the overall economic efficiency under the following simplified smelter terms:

Copper:
Copper price: £1000/t
Smelter payment: 90% of Cu content
Smelter treatment charge: £30/t of concentrate
Transport cost: £20/t of concentrate

Zinc:
Zinc price: £400/t
Smelter payment: 85% of zinc content
Smelter treatment charge: £100/t of concentrate
Transport cost: £20/t of concentrate

Solution

1. Assuming *Perfect milling*

   (a) *Copper*
   Assuming that all the copper is contained in the mineral chalcopyrite, then maximum copper grade is 34.6% Cu (pure chalcopyrite).

   If C is weight of copper concentrate per 1000 kg of feed, then for 100% recovery of copper into this concentrate:

$$100 = \frac{34.6 \times C \times 100}{0.7 \times 1000} \quad \text{and}$$

$$C = 20.2\,\text{kg}$$

$$\text{Transport cost} = £20 \times 20.2/1000 = £0.40$$

$$\text{Treatment cost} = £30 \times 20.2/1000 = £0.61$$

$$\text{Revenue} = £20.2 \times 0.346 \times 1000 \times 0.9/1000 = £6.29$$

   Therefore, NSR for copper concentrate = £5.28/t of ore.

   (b) *Zinc*
   Assuming that all the zinc is contained in the mineral sphalerite, maximum zinc grade is 67.1% (pure sphalerite).

   If Z is weight of zinc concentrate per 1000 kg of feed, then for 100% recovery of zinc into this concentrate:

$$100 = \frac{67.1 \times Z \times 100}{1000 \times 1.94} \quad \text{and}$$

$$Z = 28.9\,\text{kg}$$

$$\text{Transport cost} = £20 \times 28.9/1000 = £0.58$$

$$\text{Treatment cost} = £100 \times 28.9/1000 = £2.89$$

$$\text{Revenue} = £28.9 \times 0.671 \times 0.85 \times 400/1000 = £6.59$$

   Therefore, NSR for zinc concentrate = £3.12/t of ore.

   Total NSR for perfect milling = £(5.28 + 3.12) = £8.40/t.

2. *Actual milling*
   Similar calculations give:

   Net copper smelter return = £4.46/t of ore

   Net zinc smelter return = £1.71/t of ore

   Total net smelter return = £6.17/t

   Therefore, overall economic efficiency = $100 \times 6.17/8.40 = 73.5\%$.

References

Anon. (1979). Nchanga Consolidated Copper Mines, *Engng. Min. J.*, **180**(Nov.), 150.

Anon. (1985a). Tin-paying the price, *Min. J.* (Dec. 27), 477.

Anon. (1985b). Room for improvement at Chuquicamata, *Min. J.* (Sept. 27), 249.

Anon. (1992). Mining activity in the Western World, *Mining Mag.*, **166**, 34.

Anon. (2002). Albion process progress, *Min. J.* (Nov. 8th), 324.

Austin, L.G. and Luckie, P.T. (1988). Problems of quantifying mineral liberation: A review, *Particle & Particle Systems Characterisation*, **5(3)**, Sep., 122–129.

Barbery, G. (1986). Complex sulphide ores-processing options, in *Mineral Processing at a Crossroads-problems and prospects*, ed. B.A. Wills and R.W. Barley, Martinus Nijhoff, Dordrecht, 157.

Barbery, G. (1991). *Mineral Liberation*, Les Editions GB, Quebec.

Baum, W., Lotter, N.O., and Whittaker, P.J. (2004). Process mineralogy – A new generation for ore characterisation and plant optimisation, *2003 SME Annual Meeting* (Feb.), Denver, Preprint 04–12.

Bilgen, S. and Wills, B.A. (1991). Shear flocculation – a review. *Minerals Engng.*, **4(3–4)**, 483.

Brierley, J.A. and Brierley, C.L. (2001). Present and future commercial applications of biohydrometallurgy, *Hydrometallurgy*, **59(2–3)**, Feb., 233–239.

Buchanan, D.T. (1984). The McArthur river deposit. *The Aus. IMM Conference* Darwin, N.T., 49.

Capes, C.E. (1989). Liquid phase agglomeration: Process opportunities for economic and environmental challenges, in *Challenges in Mineral Processing*, ed. K.V.S. Sastry and M.C. Fuerstenau (eds), SME, Inc., Littleton, 237.

Clark, K. (1997). The business of fine coal tailings recovery, *The Australian Coal Review* (Jul.), 24–27.

Dahlstrom, D.A. (1986). Impact of changing energy economics on mineral processing, *Mining Engng.*, **38**(Jan.), 45.

Down, C.G. and Stocks, J. (1977). Positive uses of mill tailings, *Min. Mag.* (Sept.), 213.

EIA. (2005). http://www.eia.doe.gov/emeu/cabs/chron.html (accessed Aug. 2005).

Furuyama, T., et al. (2003). Development of a processing system of shredded automobile residues, in *Proc. XXII Int. Miner. Proc. Cong.*, ed. Lorenzen and Bradshaw, SAIMM, Cape Town, 1805–1813.

Gaudin, A.M. (1939). *Principles of Mineral Dressing*, McGraw-Hill, London.

Gay, S.L. (2004a). A liberation model for comminution based on probability theory, *Minerals Engng.*, **17(4)**, Apr., 525–534.

Gay, S.L., (2004b). Simple texture-based liberation modelling of ores, *Minerals Engng.*, **17(11–12)**, Nov./Dec., 1209–1216.

Gilchrist, J.D. (1989). *Extraction Metallurgy*, 3rd edn, Pergamon Press, Oxford.

Gottlieb, P., Wilkie, G., Sutherland, D., Ho-Tun, E., Suthers, S., Perera, K., Jenkins, B., Spencer, S., Butcher, A., and Rayner, J. (2000). Using quantitative electron microscopy for process mineral applications, *Journal of Minerals Metals & Materials Soc.*, **52(4)**, 24–25.

Gray, P.M.J. (1984). Metallurgy of the complex sulphide ores, *Mining Mag.* (Oct.), 315.

Gu, Y. (2003). Automated scanning electron microscope based mineral liberation analysis – an introduction to JKMRC/FEI Mineral Liberation Analyser, *Journal of Minerals & Materials Characterisation & Engineering*, **2(1)**, 33–41.

Guerney, P.J., Laplante, A.R., and O'Leary, S. (2003). Gravity recoverable gold and the Mineral Liberation Analyser, *Proc. 35th Annual Meeting of the Canadian Mineral Processors*, CMP, CIMMP, Ontario (Jan.), 401–416.

Hansford, G.S. and Vargas, T. (2001). Chemical and electrochemical basis of bioleaching processes, *Hydrometallurgy*, **59(2–3)**, Feb., 135–145.

Hausen, D.M. (1991). The role of mineralogy in mineral beneficiation, in *Evaluation and Optimization of Metallurgical Performance*, ed. D. Malhotra et al., SME Inc., Chapter 17.

Hoberg, H. (1993). Applications of mineral processing in waste treatment and scrap recycling, *XVIII IMPC, Sydney*, Vol. 1, AusIMM. 27.

House, C.I. and Veal, C.J. (1989). Selective recovery of chalcopyrite by spherical agglomeration, *Minerals Engng.*, **2(2)**, 171.

Huettenhain, H. (1991). Advanced physical fine coal cleaning "spherical agglomeration", *Proc. 16th Int. Conf. on Coal and Slurry Tech.*, 335.

Humphreys, D.S.C. (1999). What future for the mining industry? *Minerals Industry International*, IMM, London (Jul.), 191–196.

Iwasaki, I. and Prasad, M.S. (1989). Processing techniques for difficult-to-treat ores by combining chemical metallurgy and mineral processing, *Mineral Processing and Extractive Metallurgy Review*, **4**, 241.

King, R.P. (1982). The prediction of mineral liberation from mineralogical textures, *XIVth International Mineral Process Congress*, paper VII-1, CIM, Toronto, Canada.

Lazer, M.T., et al. (1986). The release of refractory gold from sulphide minerals during bacterial leaching. in *Gold 100, Proc. Of the Int. Conf. on Gold*, Vol. 2, S.A.I.M.M., Johannesburg, 235.

Lee Tan Yaa Chi-Lung, (1970). Abundance of the chemical elements in the Earth's crust, *Int. Geology Rev.*, **12**, 778.

Meadows, D.H., et al. (1972). *The Limits to Growth*, Universal Books, New York.

Mills, C. (1978). Process design, scale-up and plant design for gravity concentration, in *Mineral Processing Plant Design*, ed. A.L. Mular and R.B. Bhappu, AIMME, New York.

Mukherjee, A., Raichur, A.M., Natarajan, K.A., and Modak, J.M. (2004). Recent developments in processing ocean manganese nodules – A critical review. *Mineral Processing and Extractive Metallurgy Review*, **25(2)**, Apr./Jun., 91–127.

Ottley, D.J. (1991). Small capacity processing plants, *Mining Mag.*, **165**(Nov.), 316.

Parsonage, P. (1988). Principles of mineral separation by selective magnetic coating, *Int. J. Min. Proc.*, **24**(Nov.), 269.

Pease, J. (2005). Fine grinding as enabling technology – The IsaMill. *6th Annual Crushing and Grinding Conference*, Mar., Perth (IIR: www.iir.com.au).

Schulz, N.F. (1970). Separation efficiency, *Trans. SME-AIME*, **247**(Mar.), 56.

Scott, S.D. (2001). Deep ocean mining. *Geoscience Canada*, **28(2)**, Jun., 87–96.

Smith, R.W., et al. (1991). Mineral bioprocessing and the future, *Minerals Engng.* **4(7–11)**, 1127.

Somasundaran, P. (1986). An overview of the ultrafine problem, in *Mineral Processing at a Crossroads-problems and prospects*, ed. B.A. Wills and R.W. Barley, Martinus Nijhoff Publishers, Dordrecht, 1.

Sutherland, D.N. and Gottlieb, P. (1991). Application of automated quantitative mineralogy in mineral processing, *Minerals Engng.*, **4(7–11)**, 753.

Sutherland, D., et al. (1991). Assessment of ore processing characteristics using automated mineralogy, *Proc. XVII IMPC* Dresden, Vol. III, Bergakademie Freiberg, 353.

Sutherland, D., et al. (1993). The measurement of liberation in section, *XVIII IMPC, Sydney*, Vol. 2, AusIMM, 471.

Taylor, S.R. (1964). Abundance of chemical elements in the continental crust, *Geochim. Cosmochim. Acta.*, **28**, 1280.

USGS (2005) – http://minerals.usgs.gov/minerals/pubs/of01-006/ (accessed Augu. 2005).

Warner, N.A. (1989). Advanced technology for smelting McArthur River ore, *Minerals Engng.*, **2(1)**, 3.

Wills, B.A. and Atkinson, K. (1991). The development of minerals engineering in the 20th century, *Minerals Engng.*, **4(7–11)**, 643.

Wills, B.A. and Atkinson, K. (1993). Some observations on the fracture and liberation of mineral assemblies, *Minerals Engng.*, **6(7)**, 697.

2

Ore handling

Introduction

Ore handling, which may account for 30–60% of the total delivered price of raw materials, covers the processes of transportation, storage, feeding, and washing of the ore *en route* to, or during, its various stages of treatment in the mill.

Since the physical state of ores *in situ* may range from friable, or even sandy material, to monolithic deposits with the hardness of granite, the methods of mining and provisions for the handling of freshly excavated material will vary extremely widely. Ore that has been well broken can be transported by trucks, belts, or even by sluicing, but large lumps of hard ore may need individual blasting. Modern developments in microsecond delay fuses and plastic explosive have resulted in more controllable primary breakage and easier demolition of occasional very large lumps. At the same time, crushers have become larger and lumps up to 2 m in size can now be fed into some primary units.

Open-pit ore tends to be very heterogeneous, the largest lumps often being over 1.5 m in diameter. The broken ore from the pit, after blasting, is loaded directly into trucks, holding up to 200 t of ore in some cases, and is transported directly to the primary crushers. Storage of such ore is not always practicable, due to its "long-ranged" particle size which causes segregation during storage, the fines working their way down through the voids between the larger particles; extremely coarse ore is sometimes difficult to start moving once it has been stopped. Sophisticated storage and feed mechanisms are therefore often dispensed with, the trucks depositing their loads directly into the mouth of the primary crusher.

The operating cycle on an underground mine is complex. Drilling and blasting are often performed on one shift, the ore broken in this time being hoisted to the surface during the other two shifts of the working day. The ore is transported through the passes via chutes and tramways and is loaded into skips, holding as much as 30 t of ore, to be hoisted to the surface. Large rocks are often crushed underground by primary breakers in order to facilitate loading and handling at this stage. The ore, on arrival at the surface, having undergone some initial crushing, is easier to handle than that from an open pit mine and storage and feeding is usually easier, and indeed essential, due to the intermittent arrival of skips at the surface.

The removal of harmful materials

Ore entering the mill from the mine (*run-of-mine ore*) normally contains a small proportion of material which is potentially harmful to the mill equipment and processes. For instance, large pieces of iron and steel broken off from mine machinery can jam in the crushers. Wood is a major problem in many mills as this is ground into a fine pulp and causes choking or blocking of screens, etc. It can also choke flotation cell ports, consume flotation reagents by absorption and decompose to give depressants, which render valuable minerals unfloatable.

Clays and slimes adhering to the ore are also harmful as they hinder screening, filtration, and thickening, and again consume valuable flotation reagents.

All these must be removed as far as possible at an early stage in treatment.

Hand sorting from conveyor belts has declined in importance with the development of mechanised methods of dealing with large tonnages, but it is still used when plentiful cheap labour is available.

Crushers can be protected from large pieces of "tramp" iron and steel by electromagnets suspended over conveyor belts (Figure 2.1). These powerful electromagnets can pick up large pieces of iron and

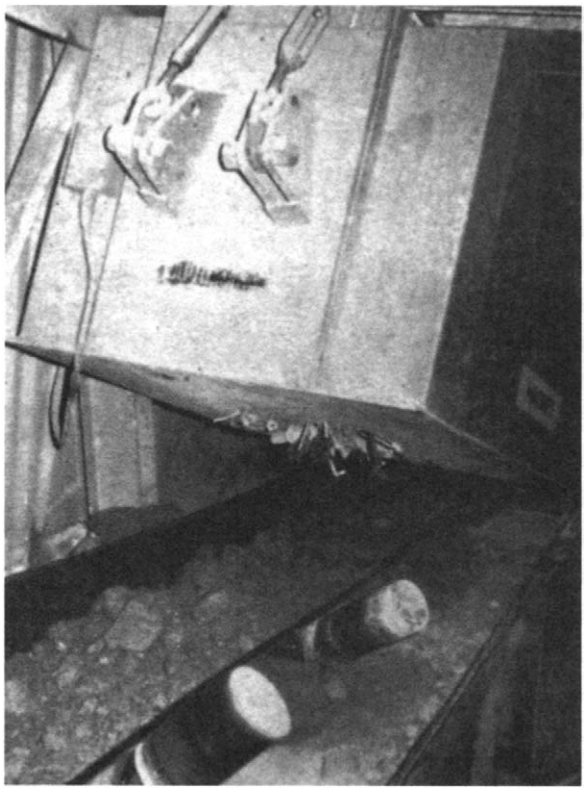


Figure 2.1 Conveyor guard magnet

steel travelling over the belt and, at intervals, can be swung away from the belt and unloaded. Guard magnets, however, cannot be used to remove tramp iron from magnetic ores, such as those containing magnetite, nor will they remove non-ferrous metals or non-magnetic steels from the ore. Metal detectors, which measure the electrical conductivity of the material being conveyed, can be fitted over or around conveyor belts. The electrical conductivity of ores is much lower than that of metals and fluctuations in electrical conductivity in the conveyed material can be detected by measuring the change that tramp metal causes in a given electromagnetic field.

When a metal object causes an alarm, the belt automatically stops and the object can be removed. It is advantageous with non-magnetic ores to precede the metal detector with a heavy guard magnet which will remove the ferromagnetic tramp metals and thus minimise belt stoppages.

Large pieces of wood which have been "flattened out" by passage through a primary crusher can be removed by passing the ore feed over a vibrating scalping screen. Here the apertures of the screen are slightly larger than the maximum size of particle in the crusher discharge, allowing the ore to fall through the apertures and the flattened wood particles to ride over the screen and be collected separately.

Wood can be further removed from the pulp discharge from the grinding mills by passing the pulp through a fine screen. Again, while the ore particles pass through the apertures, the wood collects on top of the screen and can be periodically removed.

Washing of run-of-mine ore can be carried out to facilitate sorting by removing obscuring dirt from the surfaces of the ore particles. However, washing to remove very fine material, or *slimes*, of little or no value, is more important.

Washing is normally performed after primary crushing as the ore is then of a suitable size to be passed over washing screens. It should always precede secondary crushing as slimes severely interfere with this stage.

The ore is passed through high-pressure jets of water on mechanically vibrated screens. The screen apertures are usually of similar size to the particles in the feed to the grinding mills, the reason for which will become apparent.

In the circuit shown in Figure 2.2 material passing over the screen, i.e. washed ore, is transported to the secondary crushers. Material passing through the screens is classified into coarse and fine fractions by a mechanical classifier or hydrocyclone (Chapter 9) or both. It may be beneficial to classify initially in a mechanical classifier as this is more able to smooth out fluctuations in flow than is the hydrocyclone and it is better suited to handling coarse material.

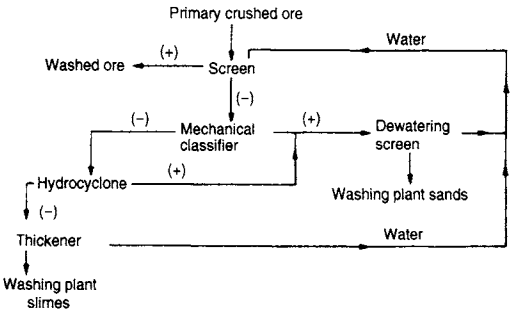


Figure 2.2 Typical washing plant flowsheet

The coarse product from the classifier, designated "washing plant sands", is either routed direct to the grinding mills or is dewatered over vibrating screens before being sent to mill storage. A considerable load, therefore, is taken off the dry crushing section.

The fine product from classification, i.e. the "slimes", may be partially dewatered in shallow large diameter settling tanks known as *thickeners* (Chapter 15) and the thickened pulp is either pumped to tailings disposal or, if containing values, pumped direct to the concentration process, thus removing load from the grinding section. In the circuit shown, the thickener overflows are used to feed the high-pressure washing sprays. Water conservation in this manner is practised in most mills.

Wood pulp may again be a problem in the above circuit, as it will tend to float in the thickener, and will choke the water spray nozzles unless it is removed by retention on a fine screen.

Ore transportation

In a mineral processing plant, operating at the rate of $400{,}000\,t\,d^{-1}$, this is equivalent to about 28 t of solid per minute, requiring up to $75\,m^3\,min^{-1}$ of water. It is therefore important to operate with the minimum upward or horizontal movement and with the maximum practicable pulp density in all of those stages subsequent to the addition of water to the system. The basic philosophy requires maximum use of gravity and continuous movement over the shortest possible distances between processing units.

Dry ore can be moved through chutes, provided they are of sufficient slope to allow easy sliding, and sharp turns are avoided. Clean solids slide easily on a 15–25° steel-faced slope, but for most ores, a 45–55° working slope is used. The ore may be difficult to control if the slope is too steep.

The belt conveyor is the most widely used method of handling loose bulk materials. Belts now in use are with capacities up to $20{,}000\,t\,h^{-1}$ and single flight lengths exceeding 15,000 m ("Bulk Materials Handling", 2005), with feasible speeds of up to $10\,m\,s^{-1}$.

The standard rubber conveyor belt has a foundation of sufficient strength to withstand the driving tension and loading strains. This foundation, which may be of cotton, nylon, or steel cord, is bound together with a rubber matrix and completely covered with a layer of vulcanised rubber.

The carrying capacity of the belt is increased by passing it over troughing idlers. These are support rollers set normal to the travel of the belt and inclined upward from the centre so as to raise the edges and give it a trough-like profile. There may be three or five in a set and they will be rubber-coated under a loading point, so as to reduce the wear and damage from impact. Spacing along the belt is at the maximum interval which avoids excessive sag. The return belt is supported by horizontal straight idlers which overlap the belt by a few inches at each side.

To induce motion without slipping requires good contact between the belt and drive pulley. This may not be possible with a single 180° turn over a pulley and some form of "snubbed pulley" drive or "tandem" drive arrangement may be more effective (Figure 2.3).

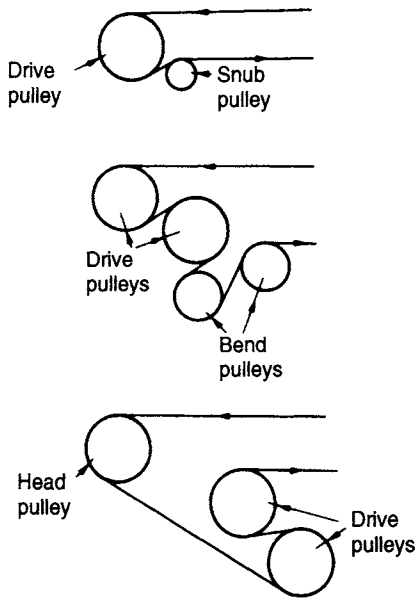


Figure 2.3 Conveyor-belt drive arrangements

The belt system must incorporate some form of tensioning device to adjust the belt for stretch and shrinkage and thus prevent undue sag between idlers, and slip at the drive pulley. In most mills, gravity-operated arrangements are used which adjust the tension continuously (Figure 2.4). Hydraulics have also been used extensively, and

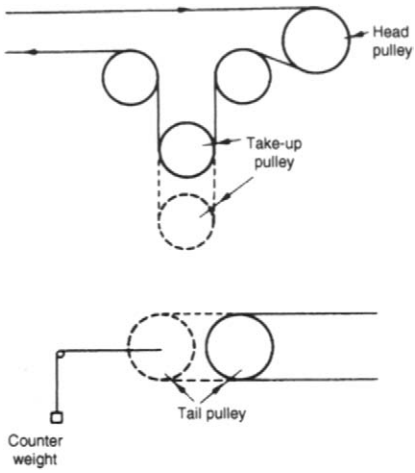


Figure 2.4 Conveyor-belt tensioning systems

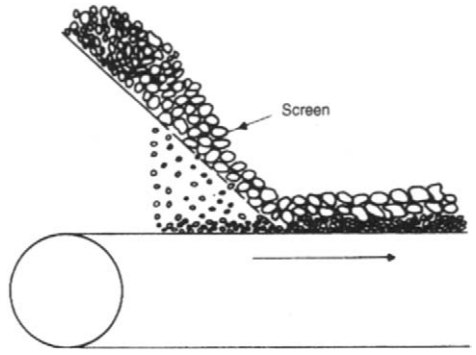


Figure 2.5 Belt-loading system

when more refined belt-tension control is required, especially in starting and stopping long conveyors, load-cell-controlled electrical tensioning devices are used.

The reliability of belt systems has been enhanced by advances in control technology, making possible a high degree of fail-safe automation. A series of belts should incorporate an interlock system such that failure of any particular belt will automatically stop preceding belts. Interlock with devices being fed by the belt is important for the same reasons. It should not be possible to shut down any machine in the system without arresting the feed to the machine at the same time and, similarly, motor failure should lead to the automatic tripping of all preceding belts and machines. Sophisticated electrical, pneumatic and hydraulic circuits have been widely employed to replace all but a few manual operations.

Several methods can be used to minimise loading shock on the belt. A typical arrangement is shown in Figure 2.5 where the fines are screened on to the belt first and provide a cushion for the larger pieces of rock.

Feed chutes must be designed to deliver the bulk of the material to the centre of the belt and at a velocity close to that of the belt. Ideally it should be the same, but in practice this condition is seldom obtained, particularly with wet sand or sticky materials. Where conditions will allow, the angle of the chute should be as great as possible, thereby allowing it to be gradually placed at lesser angles to the belt until the correct speed of flow is obtained. The material, particularly if it is heavy, or lumpy, should never be allowed to strike the belt vertically. Baffles in transfer chutes, to guide material flow, are now often remotely controlled by hydraulic cylinders.

The conveyor may discharge at the head pulley, or the load may be removed before the head pulley is reached. The most satisfactory device for achieving this is a tripper. This is an arrangement of pulleys by which the belt is raised and doubled back so as to give it a localised discharge point. It is usually mounted on wheels, running on tracks, so that the load can be delivered at several points, over a long bin or into several bins. The discharge chute on the tripper can deliver to one or both sides of the belt. The tripper may be moved by hand, by head and tail ropes from a reversible hoisting drum, or by a motor. It may be automatic, moving backwards and forwards under power from the belt drive.

Shuttle belts are reversible self-contained conveyor units mounted on carriages, which permit them to be moved lengthwise to discharge to either side of the feed point. The range of distribution is approximately twice the length of the conveyor. They are often preferred to trippers for permanent storage systems because they require less head room and, being without reverse bends, are much easier on the belt.

Where space limitation does not permit the installation of a belt conveyor, gravity bucket elevators can be used (Figure 2.6). These provide only low handling rates with both horizontal conveying and elevating of the material. The elevator consists of a continuous line of buckets attached by pins to two endless roller chains running on tracks and driven by sprockets. The buckets are pivoted so that they always remain in an upright position and

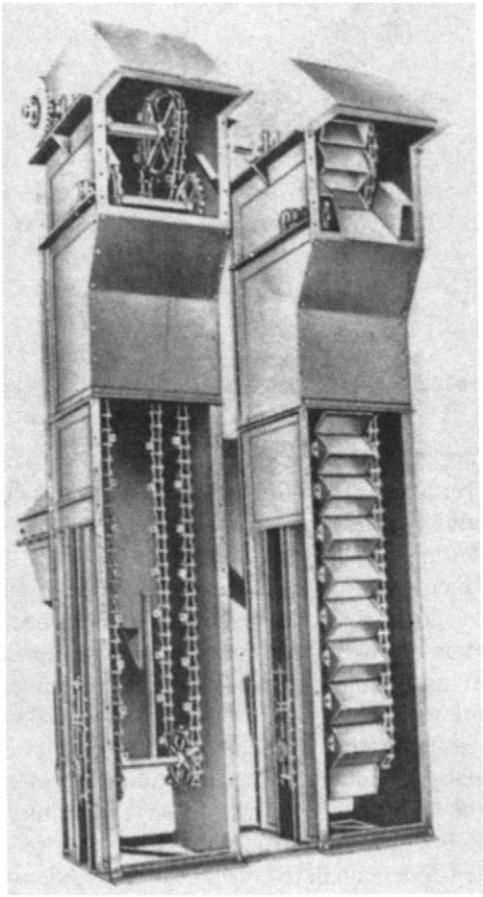


Figure 2.6 Gravity bucket elevator

are dumped by means of a ramp placed to engage a shoe on the bucket, thus turning it into the dumping position.

Sandwich conveyor systems can be used to transport solids at steep inclines from 30 to 90°. The material being transported is "sandwiched" between two belts which hold the material in position and prevent it from sliding back down the conveyor even after the conveyor has stopped or tripped. As pressure is applied to material to hold it in place, it is important the material has a reasonable internal friction angle. The advantage of sandwich belt conveyors is that they can transport material at steep angles at similar speeds to conventional belt conveyors ("Sandwich Conveyors", 2005).

Screw conveyors are another means of transporting dry or damp particles or solids. The material is pushed along a trough by the rotation of a helix, which is mounted on a central shaft. The action of the screw conveyor allows for virtually any degree of mixing of different materials and allows for the transportation of material on any incline from the horizontal to vertical. The main limitation of screw conveyors is their capacity, which has a maximum rate of about $300\,m^3/h$ (Perry and Green, 1997).

Hydraulic transport of the ore stream normally takes over from dry transportation at the grinding stage in most modern mills. Pulp may be made to flow through open launders by gravity in some cases. Launders are gently sloping troughs of rectangular, triangular or semicircular section, in which the solid is carried in suspension, or by sliding or rolling. The slope must increase with particle size, with the solid content of the suspension, and with specific gravity of the solid. The effect of depth of water is complex; if the particles are carried in suspension, a deep launder is advantageous because the rate of solid transport is increased. If the particles are carried by rolling, a deep flow may be disadvantageous.

In plants of any size, the pulp is moved through piping via centrifugal pumps. Pipelines should be as straight as possible to prevent abrasion at bends. The use of oversize pipe is dangerous whenever slow motion might allow the solids to settle and hence choke the pipe. The factors involved in pipeline design and installation are complex and include the solid–liquid ratio, the average pulp density, the density of the solid constituents, the size analysis and particle shape, and the fluid viscosity (Loretto and Laker, 1978).

Centrifugal pumps are cheap in capital cost and maintenance, and occupy little space (Wilson, 1981; Pearse, 1985). Single-stage pumps are normally used, lifting up to 30 m and in extreme cases 100 m. Their main disadvantage is the high velocity produced within the impeller chamber, which may result in serious wear of the impeller and chamber itself, especially when a coarse sand is being pumped.

Ore storage

The necessity for storage arises from the fact that different parts of the operation of mining and milling are performed at different rates, some being intermittent and some continuous, some being subject to frequent interruption for repair, and others being essentially batch processes. Thus,

unless reservoirs for material are provided between the different steps, the whole operation is rendered spasmodic and, consequently, uneconomical.

The amount of storage necessary depends on the equipment of the plant as a whole, its method of operation, and the frequency and duration of regular and unexpected shutdowns of individual units.

For various reasons, at most mines, ore is hoisted for only a part of each day. On the other hand, grinding and concentration circuits are most efficient when running continuously. Mine operations are more subject to unexpected interruption than mill operations, and coarse-crushing machines are more subject to clogging and breakage than fine crushers, grinding mills and concentration equipment. Consequently, both the mine and the coarse-ore plant should have a greater hourly capacity than the fine crushing and grinding plants, and storage reservoirs should be provided between them. Ordinary mine shutdowns, expected or unexpected will not generally exceed a 24 h duration, and ordinary coarse-crushing plant repairs can be made within an equal period if a good supply of spare parts is kept on hand. Therefore, if a 24 h supply of ore that has passed the coarse-crushing plant is kept in reserve ahead of the mill proper, the mill can be kept running independent of shutdowns of less than a 24 h duration in mine and coarse-crushing plant. It is wise to provide for a similar mill shutdown and, in order to do this, the reservoir between coarse-crushing plant and mill must contain at all times unfilled space capable of holding a day's tonnage from the mine. This is not economically possible, however, with many of the modern very large mills; there is a trend now to design such mills with smaller storage reservoirs, often supplying less than a two-shift supply of ore, the philosophy being that storage does not *do* anything to the ore, and can, in some cases, have an adverse effect by allowing the ore to oxidise. Unstable sulphides must be treated with minimum delay, and wet ore cannot be exposed to extreme cold as it will freeze and be difficult to move.

Storage has the advantage of allowing blending of different ores so as to provide a consistent feed to the mill. Both tripper and shuttle conveyors can be used to blend the material into the storage reservoir. If the units shuttle back and forth along the pile, the materials are layered and mix when reclaimed. If the units form separate piles for each quality of ore, a blend can be achieved by combining the flow from selected feeders onto a reclaim conveyor.

Depending on the nature of the material treated, storage is accomplished in stockpiles, bins, or tanks.

Stockpiles are often used to store coarse ore of low value outdoors. In designing stockpiles, it is merely necessary to know the angle of repose of the ore, the volume occupied by the broken ore and the tonnage.

Although material can be reclaimed from stockpiles by front-end loaders or by bucket-wheel reclaimers, the most economical method is by the reclaim tunnel system, since it requires a minimum of manpower to operate (Dietiker, 1978). It is especially suited for blending by feeding from any combination of openings. Conical stockpiles can be reclaimed by a tunnel running through the centre, with one or more feed openings discharging via gates, or feeders, onto the reclaim belt. The amount of reclaimable material, or the *live storage*, is about 20–25% of the total (Figure 2.7). Elongated stockpiles are reclaimed in a similar manner, the live storage being 30–35% of the total (Figure 2.8).

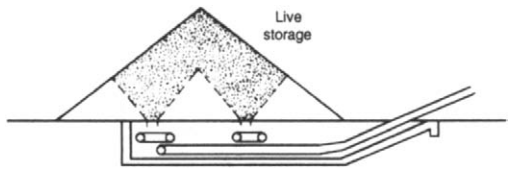


Figure 2.7 Reclamation from conical stock pile

For continuous feeding of crushed ore to the grinding section, feed bins are used for transfer of the coarse material from belts and rail and road trucks. They are made of wood, concrete, or steel. They must be easy to fill and must allow a steady fall of the ore through to the discharge gates with no "hanging up" of material or opportunity for it to segregate into coarse and fine fractions. The discharge must be adequate and drawn from several alternative points if the bin is large. Flat-bottom bins cannot be emptied completely and must retain a substantial tonnage of dead rock. This, however, provides a cushion to protect the bottom from wear, and such bins are easy to construct. This type of bin, however, should not be used with easily oxidised ore which might age dangerously and mix with the

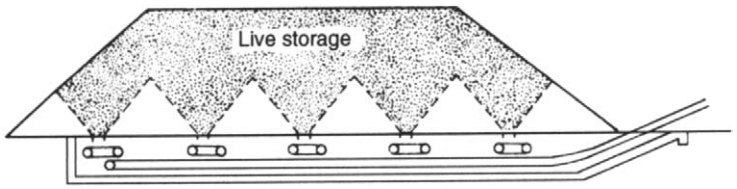


Figure 2.8 Reclamation from elongated stock pile

fresh ore supply. Bins with sloping bottoms are better in such cases.

Pulp storage on a large scale is not as easy as dry ore storage. Conditioning tanks are used for storing suspensions of fine particles to provide time for chemical reactions to proceed. These tanks must be agitated continuously, not only to provide mixing but also to prevent settlement and choking up. Surge tanks are placed in the pulp flow-line when it is necessary to smooth out small operating variations of feed rate. Their content can be agitated by stirring, by blowing in air, or by circulation through a pump.

Feeding

Feeders are necessary whenever it is desired to deliver a uniform stream of dry or moist ore, since such ore will not flow evenly from a storage reservoir of any kind through a gate, except when regulated by some type of mechanism.

Feeding is essentially a conveying operation in which the distance travelled is short and in which close regulation of the rate of passage is required. Where succeeding operations are at the same rate, it is unnecessary to interpose feeders. Where, however, principal operations are interrupted by a storage step, it is necessary to provide a feeder.

A typical feeder consists of a small bin, which may be an integral part of a large bin, with a gate and a suitable conveyor. Feeders of many types have been designed, notably apron, belt, chain, roller, rotary, revolving disc, and vibrating feeders.

In the primary crushing stage, the ore is normally crushed as soon as possible after its arrival at the surface. Skips, lorries, trucks, and other handling vehicles are intermittent in arrival whereas the crushing section, once started, calls for steady feed. Surge bins provide a convenient holding arrangement able to receive all the intermittent loads and to feed them steadily through gates at controllable rates. The chain-feeder (Figure 2.9) is sometimes used for smooth control of bin discharge.

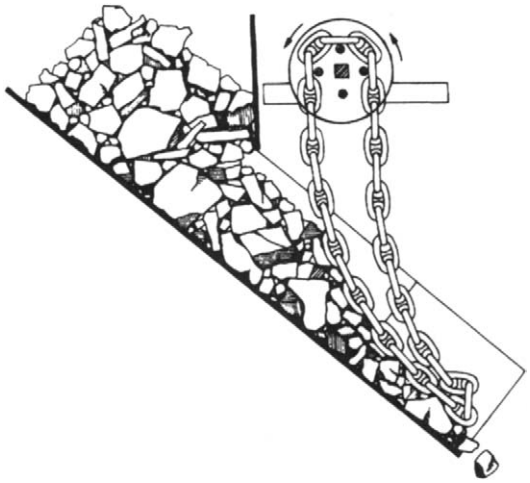


Figure 2.9 Chain-feeder

This consists of a curtain of heavy loops of chain, lying on the ore at the outfall of the bin at approximately the angle of repose. The rate of feed is controlled automatically or manually by the chain sprocket drive such that when the loops of chain move, the ore on which they rest begins to slide.

Primary crushers depend for normal operation on the fact that broken rock contains a certain amount of voidage. If all the feed goes to a jaw crusher without a preliminary removal of fines, there can be danger when there has been segregation of coarse and fine material in the bin. Such fines could pass through the upper zones of the crusher and drop into the finalising zone so as to fill the voids. Should the bulk arriving at any level exceed that departing, it is as though an attempt is being made to compress solid rock. This so-called "packing of the crushing chamber" is just as serious as tramp

iron in the crusher and can cause major damage. It is common practice, therefore, to "scalp" the feed to the crusher, heavy-duty screens known as *grizzlies* normally preceding the crushers and removing fines and undersize.

Primary crusher feeds, which scalp and feed in one operation, have been developed, such as the vibrating grizzly feeder. The elliptical bar feeder (Figure 2.10) consists of elliptical bars of steel which form the bottom of a receiving hopper and are set with the long axes of the ellipses in alternate vertical and horizontal positions. Material is dumped directly onto the bars which rotate in the same direction, all at the same time, so that the spacing remains constant. As one turns down, the succeeding one turns up, imparting a rocking, tumbling motion to the load. This works loose the fines, which sift through the load directly on to a conveyor belt, while the oversize is moved forward to deliver to the crusher. This type of feeder is probably better suited to handling high clay or wet materials such as laterite, rather than hard, abrasive ores.

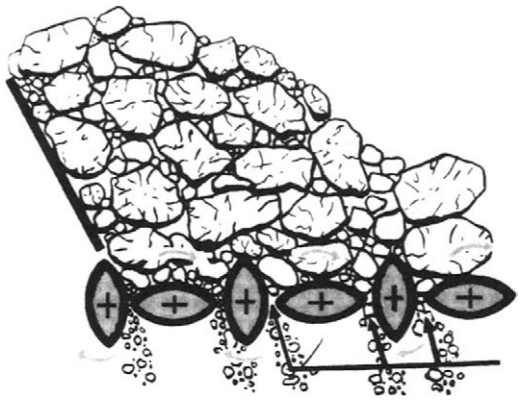


Figure 2.10 Cross-section of elliptical bar feeder

The apron feeder (Figure 2.11) is one of the most widely used feeders for handling coarse ore, especially jaw crusher feed. It is ruggedly constructed, consisting of a series of high carbon or manganese steel pans, bolted to strands of heavy-duty chain, which run on steel sprockets. The rate of discharge is controlled by varying the speed or by varying the height of the ribbon of ore by means of an adjustable gate.

Apron feeders are often preferred to reciprocating plate feeders which push forward the ore lying at the bottom of the bin with strokes at a controllable rate and amplitude, as they require less driving power and provide a steadier, more uniform feed.

Belt feeders are essentially short belt conveyors, used to control the discharge of material from inclined chutes. They frequently replace apron feeders for fine ore and are increasingly being used to handle coarse, primary crushed ore. They require less installation height, cost substantially less, and can be operated at higher speeds than apron feeders.

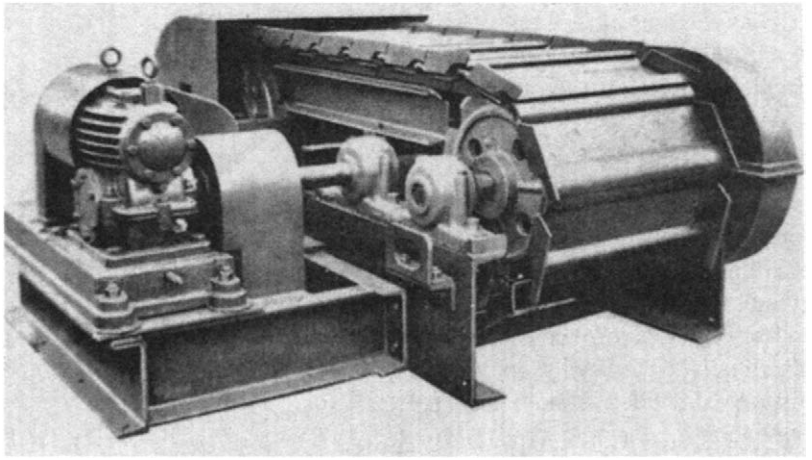


Figure 2.11 Apron feeder

References

"Bulk Materials Handling" (2005), viewed 27 July 2005, http://www.bateman-bulk.com/.

Dietiker, F.D. (1978). Belt conveyor selection and stockpiling and reclaiming applications, in *Mineral Processing Plant Design*, ed. A.L. Mular and R.B. Bhappu, AIMME, New York.

Loretto, J.C. and Laker, E.T. (1978). Process piping and slurry transportation, in *Mineral Processing Plant Design*, ed. A.L. Mular and R.B. Bhappu, AIMME, New York.

Pearse, G. (1985). Pumps for the minerals industry, *Min. Mag.* (Apr.), 299.

Perry, R.H. and Green, D.W. (eds) (1997). *Perry's Chemical Engineers' Handbook*, 7th edn, pp. 21–7 McGraw-Hill International Edition, New York.

"Sandwich Conveyors" (2005), viewed 15 July 2005, http://www.ckit.co.za/.

White, L. (1976). Processing responding to new demands, *Engng. Min. J.* (Jun.), 219.

Wilson, G. (1981). Selecting centrifugal slurry pumps to resist abrasive wear, *Mining Engng.*, **33**(Sept.), 1323.

3

Metallurgical accounting, control and simulation

Introduction

Metallurgical accounting is an essential feature of all efficient metallurgical operations. Not only is it used to determine the distribution of the various products of a concentrator, and the values contained in them, but it is also used to make decisions about the operation since the values of recovery and grade obtained from the accounting procedure are indications of process efficiency. To perform successful metallurgical accounting it is necessary to collect reliable data from the process. This chapter deals with the collection, analysis, and use of process data.

The essential requirements of a good accounting and control system are efficient and representative sampling of the process streams, upon which accurate analyses of the value components can be undertaken, and reliable and accurate measurement of the mass flow rate of important flowstreams.

Computer control of mineral processing plants requires continuous measurement of such parameters, and the development of real-time on-line sensors, such as magnetic flowmeters, nuclear density gauges and chemical and particle size analysers has made important contributions to the rapid developments in this field since the early 1970s, as has the increasing availability and reliability of cheap microprocessors.

Computer simulation is increasingly being used to aid circuit design and optimisation, and is likely to be a major future use of the computer in mineral processing.

A balanced approach to decision-making requires commercial data in addition to technical data. While a detailed discussion of commercial data collection is beyond the scope of this book, it is worth noting that matching cost reporting areas to process areas and equipment will greatly assist in matching technical and commercial data. A reasonably close match makes it much easier to estimate the potential costs and benefits of process changes.

Sampling and weighing the ore

Ideally, weighing and sampling should be carried out before the material is subject to losses in the mill. For this to be absolutely the case, these operations must be carried out on run-of-mine ore entering the primary crusher stage. Weighing can be carried out satisfactorily, but accurate sampling is not possible on account of the wide range of particle size and heterogeneity of the material being handled. This difficulty applies particularly to the preparation of a moisture sample, an essential requirement, since all calculations are carried out on the basis of dry weights of material. Run-of-mine, and coarsely crushed ore, tends to segregate, and it is very likely that the fines are of a different grade and moisture content from the coarse material. It will probably be necessary to take at least 5% of the total weight of ore as a primary sample

if the required degree of accuracy is to be obtained. This must be reduced in size by successive stages, the bulk being reduced by a sample division or "cut" between each stage.

For this reason, and also because of the high capital cost of a sample plant designed to operate on coarse feed, accurate sampling and weighing of coarse rock is confined usually to those cases where two ores must be accounted for separately, and it is not possible to operate parallel crushing sections. Weighing and sampling are, therefore, wherever possible, undertaken when the ore is in its most finely divided state.

Moisture sampling

While all metallurgical accounting requires accurate knowledge of the dry weights of solids handled, actual materials may contain moisture to varying degrees and samples must be taken for this constituent to be measured accurately. Ideally, the moisture sample and the assay sample should be prepared from the same quantity of material, both being taken from a point near to the weighing equipment. With proper handling the errors due to subsequent wetting or drying can be reduced to very low levels. In practice, it is common to find that some form of *grab sampling* is used for moisture determination. This is the least accurate of the common sampling methods, but the cheapest and most rapid. By this method, small quantities of material are chosen at random from different spots in the large bulk, and these are mixed together to form the base for the final sample. Grab sampling ensures that the sample can be quickly collected and placed in sealed containers, the assumption being that error due to crudeness of method is less than the error introduced by longer exposure of material during more elaborate sampling.

Grab samples for moisture determination are frequently taken from the end of a conveyor belt after material has passed over the weighing device. The samples are immediately weighed wet, dried at a suitable temperature until all hygroscopic water is driven off, and then weighed again. The difference in weight represents moisture and is expressed as:

$$\%\ \text{moisture} = \frac{\text{wet weight} - \text{dry weight}}{\text{wet weight}} \times 100 \tag{3.1}$$

The drying temperature should not be so high that breakdown of the minerals, either physically or chemically, occurs. Sulphide minerals are particularly prone to lose sulphur dioxide if overheated; samples should not be dried at temperatures above 105 °C.

Assay sampling

Sampling is the means whereby a small amount of material is taken from the main bulk in such a manner that it is representative of that larger amount. Great responsibility rests on a very small sample, so it is essential that samples are truly representative of the bulk (Holmes, 1991, 2001).

Wherever possible samples should be taken of the material when it has been reduced to the smallest particle size consistent with the process. For instance, the ground ore pulp will be easier to sample, and will give more accurate results than the feed to the primary crusher.

In practice, the most satisfactory method of minimising variables in the feed stream, such as particle size variation in belt loading, settling out of particles in the pulp due to velocity change, surges, etc., is to sample the material while it is in motion at a point of free fall discharge, making a cut at right angles to the stream. Since there may be segregation or changed composition within the stream, good practice demands a sample of all the stream. When a sample cutter moves continuously across the stream at a uniform speed, the sample taken represents a small portion of the entire stream. If the cutter moves through the stream at regular intervals it produces incremental samples that are considered representative of the stream at the time the sample was taken.

Sampling is dependent on probability, and the more frequently the incremental sample is taken the more accurate the final sample will be. The sampling method devised by Gy (1979) and Smith (2001) is often used to calculate the size of sample necessary to give the required degree of accuracy. The method takes into account the particle size of the material, the content and degree of liberation of the minerals, and the particle shape.

Gy's basic sample equation can be written as:

$$\frac{ML}{L - M} = \frac{Cd^3}{s^2} \tag{3.2}$$

where M is the minimum weight of sample required (g), L is the gross weight of material to be sampled (g), C is the sampling constant for the material to be sampled ($g\,cm^{-3}$), d is the dimension of the largest pieces in the material to be sampled (cm), and s is the measure of the statistical error committed by sampling. In most cases, M is small in relation to L, and Equation 3.2 approximates to:

$$M = \frac{Cd^3}{s^2} \tag{3.3}$$

The term s is used to obtain a measure of confidence in the results of the sampling procedure. The *relative* standard deviation of a normal distribution curve representing the random assay-frequency data for a large number of samples taken from the ore is s and the relative variance is s^2 (Gy, 1979).

Assuming normal distribution, 67 out of 100 assays of samples would lie within $\pm s$ of the true assay; 95 out of 100 assays would be within $\pm 2s$ of the true assay, and 99 out of 100 would be within $\pm 3s$ of the true assay. As sampling is a statistical problem, there can never be complete confidence in the result of a sampling exercise, and for most practical purposes, a 95 times in 100 chance of being within prescribed limits is an acceptable level. Table 3.1 shows the results of a computer simulation of a random unbiased sampling exercise on an ore containing exactly 50% valuable material. It is apparent that it can never be guaranteed that the assay result will lie within the prescribed limits, but that the more sample is taken, the greater is the confidence. The effect of undersampling is, however, clearly illustrated.

The actual variance determined by Gy's equation may differ from that obtained in practice because it is usually necessary to carry out a number of sampling steps in order to obtain the assay sample, and there are also errors in assaying. The practical variance (or total variance) would therefore be the sum of all other variances, i.e.

$$S_t^2 = s^2 + S_s^2 + S_a^2$$

The values of S_s (sampling) and S_a (assay) would normally be small, but could be determined by assaying a large number of portions of the same sample (at least 50) to give S_a^2 and by cutting a similar number of samples in an identical manner and assaying each one to give $(S_a^2 + S_s^2)$. However, for routine plant sampling, s^2 can be assumed to equal S_t^2, and wherever possible, or practical, two to three times the minimum weight of sample should be taken to allow for the many unknowns, although, of course, over-sampling has to be avoided to preclude problems in handling and preparation.

The sampling constant C is specific to the material being sampled, taking into account the mineral content, and its degree of liberation,

$$C = f\,glm$$

where f is a shape factor, which is taken as 0.5, except for gold ores, where it is 0.2; g is a factor which is dependent on the particle size range. If approximately 95% of the sample weight contains

Table 3.1 Results of sampling a hypothetical ore containing 50% value. The ore was sampled 100 times at each sample weight, and the value content of each sample assessed. The number of "assays" within 5% of the true value content is shown, as is the maximum assay error encountered, and the mean assay of the 100 samples taken

Sample weight (g)	*Mean assay* (%)	*Number of assays within 5%*	*Maximum error* (%)
10	46.70	14	88.55
100	49.70	24	45.60
500	50.35	37	18.38
1000	50.08	74	14.80
2500	50.18	86	9.94
3500	49.82	93	7.09
5000	50.12	98	5.10
10 000	49.97	99	5.01

particles of size less than d cm, and 95% of size greater than d' cm, then if:

$$d/d' > 4 \qquad g = 0.25$$
$$d/d' \text{ is } 2-4 \qquad g = 0.5$$
$$d/d' < 2 \qquad g = 0.75$$
$$d/d' = 1 \qquad g = 1$$

l is a liberation factor, which has values between 0 for completely homogeneous material and 1.0 for completely homogeneous material. Gy devised a table (shown below) based on d, the dimension of the largest pieces in the ore to be sampled, which can be taken as the screen aperture which passes 90–95% of the material, and L, the size in centimetres at which, for practical purposes, the mineral is essentially liberated. This can be estimated microscopically. Values of l can be estimated from the table below, from corresponding values of d/L, or can be calculated from the expression:

$$l = \left(\frac{L}{d}\right)^{1/2}$$

d/L	<1	1–4	4–10	10–40	40–100	100–400	>400
l	1	0.8	0.4	0.2	0.1	0.05	0.02

m is a mineralogical composition factor which can be calculated from the expression

$$m = \frac{1-a}{a}[(1-a)r + at]$$

where r and t are the mean densities of the valuable mineral and gangue minerals respectively, and a is the fractional average mineral content of the material being sampled. This value could be determined by assaying a number of samples of the material. Modern electron microscopes can measure most of these properties directly. For a more detailed description of the sampling constant, see Lyman (1998).

Gy's equation assumes that samples are taken at random, and without bias, and is most applicable to streams of ore transported on conveyors or in pulp streams rather than heap deposits which are partly inaccessible to the sampler.

The equation gives the minimum theoretical weight of sample which must be taken, but does not state how the sample is to be taken. The size of each increment taken, in the case of stream sampling, and the increment between successive cuts must be such that sufficient weight is recovered to be representative.

Gy's equation can be used to illustrate the benefits of sampling material when it is in its most finely divided state. Consider, for instance, a lead ore, assaying about 5% Pb, which must be routinely sampled for assay to a confidence level of ±0.1% Pb, 95 times out of 100. The galena is essentially liberated from the quartz gangue at a particle size of 150 μm.

If sampling is undertaken during crushing, when the top size of the ore is 25 mm, then

$$d = 2.5\,\text{cm}$$
$$2s = \frac{0.1}{5} = 0.02$$

Therefore $s = 0.01$.

$$l = \left(\frac{0.015}{2.5}\right)^{1/2} 0.077$$

Assuming the galena is stoichiometrically PbS, then the ore is composed of 5.8% PbS.

Therefore $a = 0.058$, $r = 7.5$, $t = 2.65$.

Therefore $m = 117.8\,\text{g cm}^{-3}$

$$C = f\,g\,l\,m = 0.5 \times 0.25 \times 0.077 \times 117.8$$
$$= 1.13\,\text{g cm}^{-3}$$
$$M = Cd^3/s^2 = 176.6\,\text{kg}$$

In practice, therefore, about 350 kg of ore would have to be sampled in order to give the required degree of confidence, and to allow for assay and mechanical sampling errors. No account has been taken here of further sample divisions required prior to assay.

If, however, the sampling takes place from the pulp stream after grinding to the liberation size of the ore, then $d = 0.015$ cm, and assuming that classification has given fairly close sizing,

$$C = 0.5 \times 0.5 \times 1 \times 117.8$$
$$= 29.46\,\text{g cm}^{-3}$$

Therefore $M = 1$ g

Such a small weight of sample could not, however, be cut for assay from a pulp stream, as it makes no provision for segregation within the stream, variations in assay, particle size, etc., with

time. It may, however, be used as a guide for the increment to be cut at each passage of the cutter, the interval between cuts being decided from the fluctuations in the quality of the pulp stream.

Sampling systems

Most automatic samplers operate by moving a collecting device through the material as it falls from a conveyor or a pipe. It is important that:

(1) The face of the collecting device or cutter is presented at right angles to the stream.
(2) The cutter covers the whole stream.
(3) The cutter moves at constant speed.
(4) The cutter is large enough to pass the sample.

The width of the cutter w will be chosen to give an acceptable weight of sample, but must not be made so small that the biggest particles have difficulty in entering. Particles that strike the edges of the receiver are likely to bounce out and not be collected, so that the effective width is $(w - d)$, where d is the diameter of the particles. The effective width is therefore greater for small particles than for large ones. To reduce this error to a reasonable level, the ratio of cutter width to the diameter of the largest particle should be made as large as possible, with a minimum value of 20:1.

All sampling systems require a primary sampling device or cutter, and a system to convey the collected material to a convenient location for crushing and further sample division (Figure 3.1).

There are many different types of sample cutter; the *Vezin* type sampler (Figure 3.2) is widely used to sample a falling ore stream. This consists of a revolving cutter in the shape of a circular sector

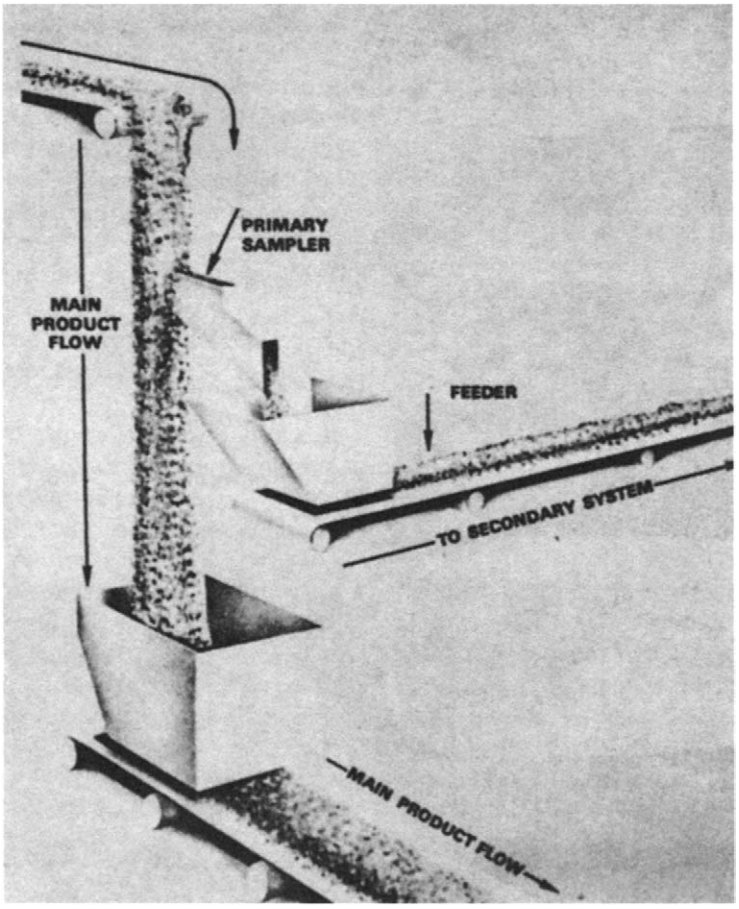


Figure 3.1 Typical sampling system

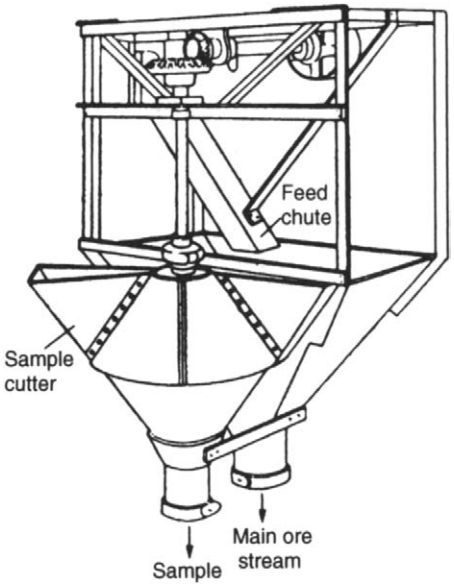


Figure 3.2 Vezin sampler

of such dimensions as to cut the whole stream of ore, and divert the sample into a separate sample chute. Figure 3.3 shows four types of Outokumpu slurry sampler which are commonly used to deliver samples to on-line analysis systems.

Automatic samplers known as *poppet valves* are used in some plants (Carson, 1973). They consist essentially of a pneumatically operated piston immersed directly into the pipeline, usually a rising main, carrying the pulp stream, the piston in the "open" position allowing the transfer of a sample from the pulp stream, and in the "closed" position preventing the passage of pulp to the sample line. The cycle of opening and closing is controlled by an automatic timer, sample level controller, or other means, depending on the circumstances, the volume of sample taken at each cut being determined by the time elapsed with the valve raised from its seat.

In recent years mineral processing plants have increased substantially in size. During the 1970s, 10 to 20 grinding lines were required to process

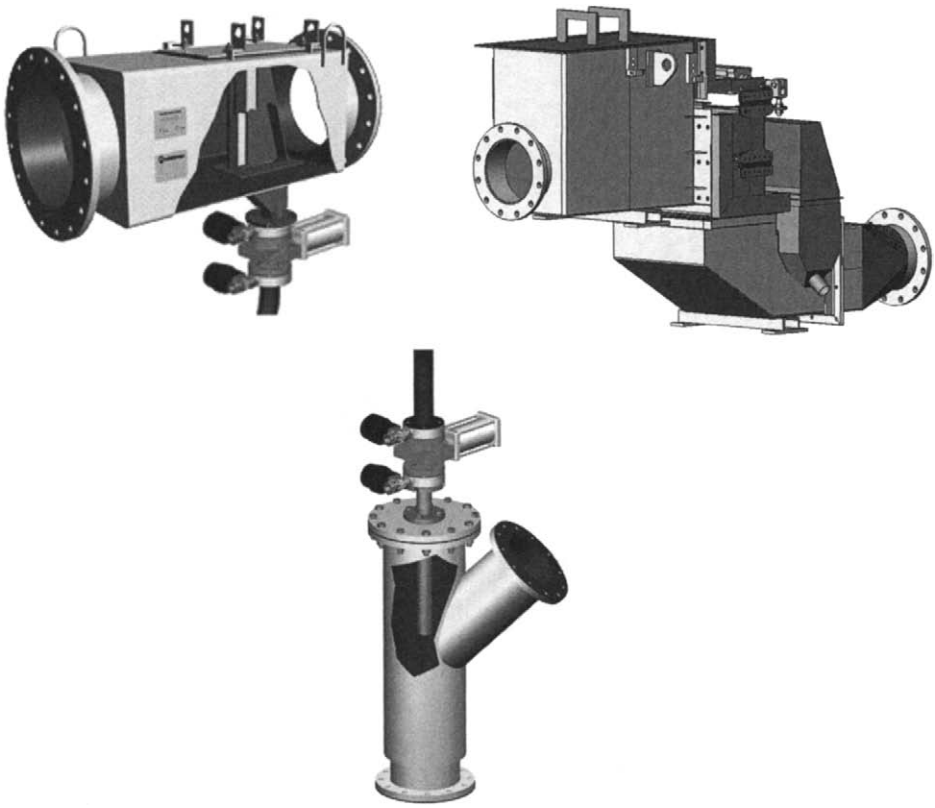


Figure 3.3 Outokumpu automatic single- and multi-stage sample cutters and pipe sampler (Courtesy Outokumou Technology Minerals Oy)

100,000 t of ore per day. In the late 1990s single processing lines treating as many, or more, tonnes per day became quite common.

The slurry streams to be sampled flow at 5000 t/h or more and are essentially impossible to hand cut. Equipment is available for the sampling of very large flows using either stationary or moving cutters.

For large flows on conveyors some steps can be taken to reduce the labour for size sampling by simply counting large particles until a suitable level of accuracy is reached. The variance of a sample of n particles is simply n. Therefore to achieve a relative standard deviation of 10%, about 100 particles in that size range are required. For a detailed description of this technique, see Napier-Munn et al. (1996), Chapter 5. This reference offers many helpful suggestions for sampling comminution circuits.

The bulk sample requires thorough drying and mixing before further division to produce a reasonable size for assay. The principles involved in reducing the material down to the assay sample are the same as those discussed when considering the collection of the gross sample. To obtain the best results, the bulk sample should be made as homogeneous as possible. If complete homogeneity of the material is achieved, then every increment obtained by the sampling method will be representative of the material. Ores and concentrates containing coarse particles are less homogeneous than those containing fine particles, and it is always necessary to take a larger sample of coarse material in order for it to representative. Wherever possible a sampling step is preceded by a reduction in particle size, the number of steps being dependent on the size of the original sample and the equipment available for crushing. The weight of sample required at each stage in sample division can be determined using Gy's formula for the "fundamental error", which is a function of the number of particles and thus particle size for a given mass. For example, consider the sampling of the lead ore discussed earlier, from the crushing circuit, at a top size of 25 mm.

Each incremental sample taken, representative of the ore at the time of sampling, is conveyed to the secondary sample system for further division and sampling, either automatically or manually.

Assuming that the sample is crushed in three stages, to 5 mm, 1 mm, and, finally, for assay, to 40 μm, and is sampled after each stage, then there are in total four sampling stages, and the square of the total error produced in sampling is the sum of the squares of the errors incurred at each stage, i.e.

$$S_t^2 = S_1^2 + S_2^2 + S_3^2 + S_4^2$$

If an equal error is assumed at each stage, then

$$S_t^2 = 4S_1^2$$

Therefore $\dfrac{S_1^2 = S_2^2 = S_3^2 = S_4^2 = S_t^2}{4}$.

Since a confidence level in assaying of 5% ± 0.1% Pb, 95 times out of 100 is to be achieved:

$$S_t = 0.01$$

Therefore $S_1^2 = S_2^2 = S_3^2 = S_4^2 = 0.25 \times 10^{-4}$.
For the primary sampling stage at 25 mm top size:

$$M = \frac{1.13 \times (2.5)^3}{0.25 \times 10^{-4}} = 706.3\,\text{kg}$$

For the second sampling stage at 5 mm:

$$M = 12.8\,\text{kg}$$

For the third sampling stage at 1 mm:

$$M = 228.2\,\text{g}$$

For the fourth stage, at 40 μm:

$$M = 0.04\,\text{g}$$

The sampling system could be designed from this information. For instance, the following weights might be taken to allow for assay and other errors: 1.5 t of ore per shift is taken from the crushed ore stream, is crushed to 5 mm, and a 25 kg sample taken. This sample is further crushed to 1 mm and a 500 g sample taken, which is finely ground to 40 microns, from which a sample of about 0.5 g is cut for assay.

The sample weights calculated above assume equal statistical errors at each sampling stage. The primary sample weight required can, however, be reduced by taking more than the calculated requirement of the finer sizes. For instance, in the above example, 0.5 g of sample is taken for final assay, which is well above the sample requirement calculated from Gy's formula. This means that the statistical error at this stage is relatively low, allowing larger errors (smaller sample weights) in the early

sample stages, since $S_t^2 = S_1^2 + S_2^2 + S_3^2 + S_4^2$. An Excel spreadsheet "GY" has been prepared to calculate the required sample mass for a given fundamental error, particle size (sample stage) and other conditions, or conversely the error obtained for a completed sampling exercise. Details can be found in Appendix III. Table 3.2 shows the effect of increasing the weight of the finer sized samples on the amount of primary sample required (safety factor of 2 applied).

Table 3.2

	Stage 1 (kg)	*Stage 2* (kg)	*Stage 3* (g)	*Stage 4* (g)
Equal sampling error at each stage	1412.6	25.6	456.4	0.08
Fixed weight at stages 2, 3, and 4	570.1	50.0	500.0	1.0

Sample division methods

Some of the common methods of sample division are given below.

Coning and quartering

This is an old Cornish method which is often used in dividing samples of material. It consists of pouring the material into a conical heap and relying on its radial symmetry to give four identical samples when the heap is flattened and divided by a cross-shaped metal cutter. Two opposite corners are taken as the sample, the other two corners being discarded. The portion chosen as the sample may again be coned and quartered, and the process continued until a sample of the required size is produced. Although accuracy is increased by crushing the sample between each division, the method is very dependent on the skill of the operator and should not be used for accurate sampling.

The Jones riffle

This splitter (Figure 3.4) is an open V-shaped box in which a series of chutes is mounted at right angles to the long axis to give a series of rectangular slots of equal area alternatively feeding two trays placed on either side of the trough. The laboratory sample is poured into the chute and split into equal portions by the slots, until after repeated cycles a sample of the desired size is obtained.

A much more robust approach is to use a vibratory feeder to distribute the bulk sample into a number of wedge shaped containers as shown in Figure 3.5. This device is sometimes called a "spinning riffle" or "rotating sampler" and is the most accurate method of extracting representative samples from dry granular or powdered material.

The ore or concentrate sample must now be analysed, or assayed, so that the exact chemical composition of the material is obtained. Assays are of great importance, as they are used to control operations, calculate throughput and reserves, and to calculate profitability. Modern methods of assaying are very sophisticated and accurate, and are beyond the scope of this book. They include chemical methods, X-ray fluorescence, atomic absorption spectrometry (Strasham and Steele, 1978), and neutron activation.

On-line analysis

The benefits of continuous analysis of process streams in mineral processing plants led to the development in the early 1960s of devices for X-ray fluorescence (XRF) analysis of flowing slurry streams. On-line analysis enables a change of quality to be detected and corrected rapidly and continuously, obviating the delays involved in off-line laboratory testing. This method also frees skilled staff for more productive work than testing of routine samples. The whole field of on-line chemical analysis applied to concentrator automation has been comprehensively reviewed elsewhere (Lyman, 1981; Cooper, 1984; Kawatra and Cooper, 1986; Braden et al., 2002).

The principle of on-line chemical analysis is shown in Figure 3.6. Basically it consists of a source of radiation which is absorbed by the sample and causes it to give off fluorescent response radiation characteristic of each element. This enters a detector which generates a quantitative output signal as a result of measuring the characteristic radiation of one element from the sample. The detector output signal is generally used to obtain an assay value which can be used for process control.

Two practical methods of on-line X-ray fluorescence analysis are centralised X-ray (on-stream)

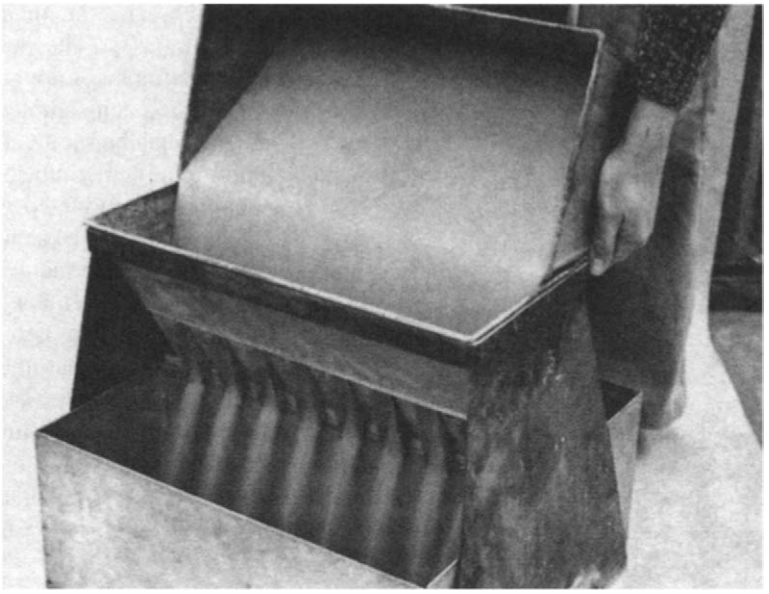


Figure 3.4 Jones riffle sampler

and in-stream probe systems. Centralised, on-stream analysis employs a single high-energy excitation source for analysis of several slurry samples delivered to a central location where the complete equipment is installed. In-stream analysis employs sensors installed in, or near, the slurry stream, and sample excitation is carried out with convenient low-energy sources, usually radioactive isotopes (Bergeron and Lee, 1983; Toop et al., 1984). This overcomes the problem of transporting representative samples of slurry to the analyser. The excitation sources are packaged with a detector in a compact device called a probe.

Centralised analysis is usually installed in large plants, requiring continuous monitoring of many different pulp streams, whereas smaller plants with fewer streams may incorporate probes on the basis of lower capital investment.

One of the major problems in on-stream X-ray analysis is ensuring that the samples presented to the radiation are representative of the bulk, and that the response radiation is obtained from a representative fraction of this sample. The exciting radiation interacts with the slurry by first passing through a thin plastic film window and then penetrating the sample which is in contact with this window. Response radiation takes the opposite path back to the detector. Most of the radiation is absorbed in a few millimetres depth of the sample, so that the layer of slurry in immediate contact with the window has the greatest influence on the assays produced. Accuracy and reliability depend on this very thin layer being representative of the bulk material. Segregation in the slurry can take place at the window due to flow patterns resulting from the presence of the window surface. This can be eliminated by the use of high turbulence flow cells in the centralised X-ray analyser. Operating costs and design complexities of sampling and pumping can be largely avoided with the probe-measuring devices positioned near the bulk stream to be assayed, noting the requirement for turbulent flow of representative slurry sample at the measurement interface of the probe.

There are many different types of sampling systems available for on-stream analysis. A typical one was developed by Outokumpu for use with the Courier 300 analysis system (Leskinen et al., 1973; Lundan, 1982), the oldest and perhaps most widely known process analyser. In this system a continuous sample flow is taken from each process slurry to be analysed. The final sample flow is obtained by abstractions from two or three parts depending on the volume of the process flow. Each slurry flows through a separate cell in the analyser, where fluorescence intensities are measured through thin

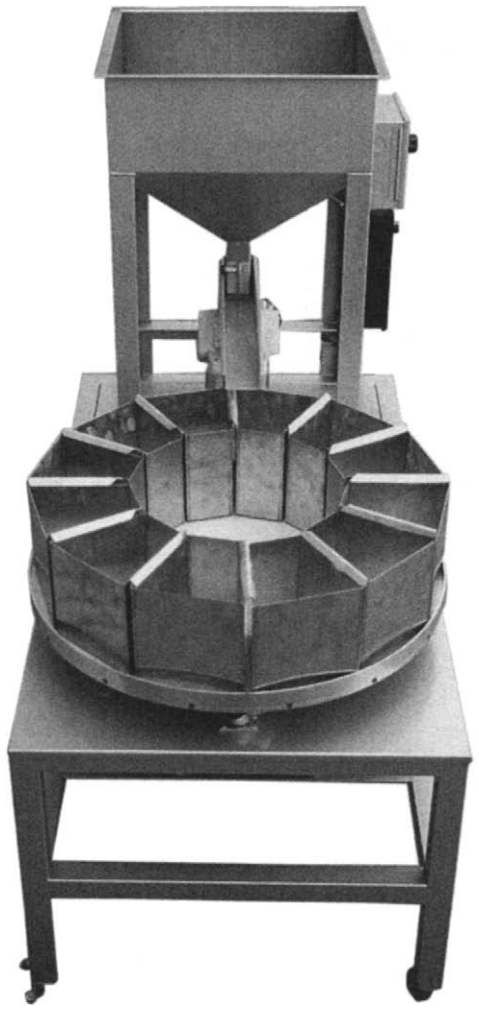


Figure 3.5 Sepor rotary sample splitter (Courtesy Sepor Inc.)

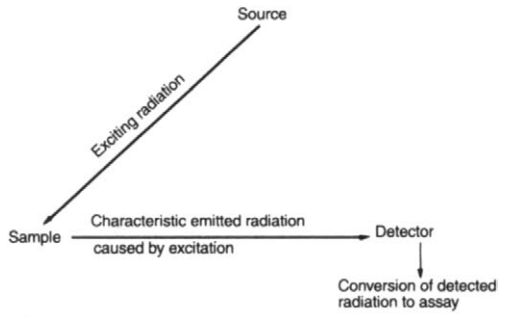


Figure 3.6 Principle of on-line chemical analysis

windows in the cells, the measurement time for each slurry being 20 s. The system comprises up to 14 sampling circuits, although by duplexing two slurry streams into each sample cell, a sequence of up to 28 samples can be set up. The XRF measuring head containing the X-ray tube and the crystal spectrometer channels is mounted on a trolley, which travels along the bank of 14 sample cells, analysing each slurry sample in sequence (Figure 3.7). The unit analyses up to 7 elements plus a reading of the slurry density, and completion of one full cycle takes 7 min, meaning that the analysis of each sample is updated every 7 or 14 min, depending on the system version (14 or 28 lines).

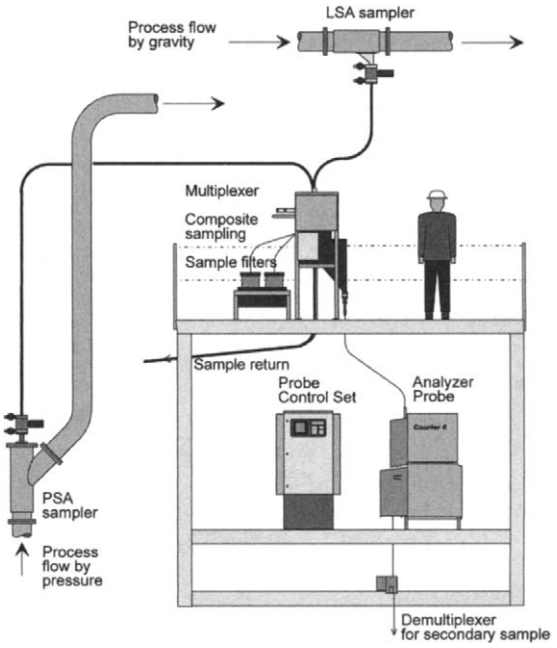


Figure 3.7 Outokumpu's Courier 6 SL on-stream analyser, showing a pressure pipe sampler (PSA) and a vertical cutter sampler (LSA) (Courtesy Outokumou Technology Minerals Oy)

The Courier 300 has now been superseded by the Courier 6 SL (Figure 3.7) which can handle up to 24 sample streams, with typical installations handling 12–18 streams. The primary sampler (see also Figure 3.3) directs a part of the process stream to the multiplexer for secondary sampling. The probe combines high-performance wavelength and energy dispersive X-ray fluorescence methods and has an automatic reference measurement

for instrument stability and self-diagnostics. The built-in calibration sampler helps the operator to take a representative and repeatable sample from the measured slurry for comparative laboratory assays.

The measurement sequence is fully programmable. Critical streams can be measured more frequently and more measurement time can be used for tailings streams. The switching time between samples is used for internal reference measurements, which are used for monitoring and automatic drift compensation.

An alternative approach is to place a probe which uses an isotope as an X-ray source into the slurry stream. These probes can be single element or multi-element (up to 8, plus percent solids). Accuracy is improved by using a well-stirred tank of slurry (an analysis zone). Combined with solid state cryogenic (liquid N_2) detectors these probes are competitive in accuracy with traditional X-ray generator systems and can be multi-plexed to analyse more than one sample stream. Such devices were pioneered by AMDEL and are now marketed by Thermo Gamma-Metrics. Figure 3.8 shows the TGM in-stream "AnStat" system – a dedicated analyser with sampling system (Boyd, 2005).

On-stream ash analysis

On-stream monitoring of the ash content of coals is being increasingly used in coal preparation plants to automatically control the constituents which make up a constant ash blend (Bernatowicz et al., 1984). The operating principle of the monitor is based on the concept that when a material is subjected to irradiation by X-rays, a portion of this radiation is absorbed, with the remainder being reflected. The radiation absorbed by elements of low atomic number (carbon and hydrogen) is lower than that absorbed by elements of high atomic number (silicon, aluminium, iron), which form the ash in coal, so the variation of absorption coefficient with atomic number can be directly applied to the ash determination.

A number of analysers have been designed, and a typical one is shown in Figure 3.9.

A representative sample of coal is collected and crushed, and fed as a continuous stream into the presentation unit of the monitor, where it is

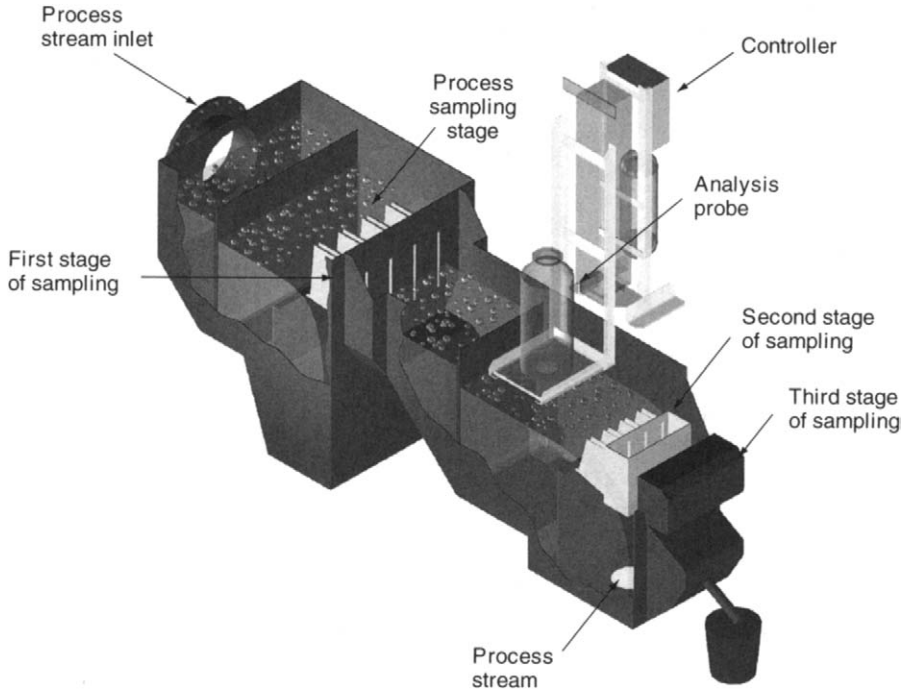


Figure 3.8 The Thermo Gamma-Metrics AnStat in-stream analysis probe and sampler (Courtesy Thermo Electron Corporation)

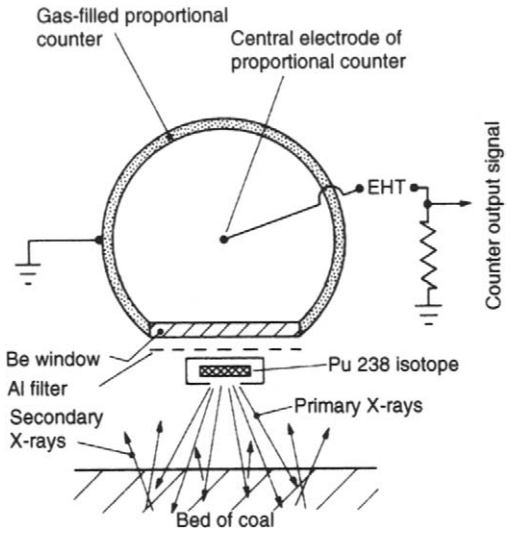


Figure 3.9 Sensor system of ash monitor

compressed into a compact uniform bed of coal, with a smooth surface and uniform density. The surface is irradiated with X-rays from a plutonium 238 isotope and the radiation is absorbed or back-scattered in proportion to the elemental composition of the sample, the back-scattered radiation being measured by a proportional counter. At the low-energy level of the plutonium 238 isotope (15–17 keV), the iron is excited to produce fluorescent X-rays that can be filtered, counted, and compensated. The proportional counter simultaneously detects the back-scattered and fluorescent X-rays after they have passed through an aluminium filter. This absorbs the fluorescent X-rays preferentially, its thickness preselected to suit the iron content and its variation. The proportional counter converts the radiation to electrical pulses that are then amplified and counted in the electronic unit. The count-rate of these pulses is converted to a voltage which is displayed and is also available for process control.

A key sensor required for the development of an effective method of controlling coal flotation is one which can measure the ash content of coal slurries. Production units have recently been manufactured and installed in coal preparation plants (Jenkinson, 1985; Kawatra, 1985), and due to the development of on-line ash monitors, coupled with an improved knowledge of process behaviour, control strategies for coal flotation have been developed (Herbst and Bascur, 1985; Salama et al., 1985; Clarkson, 1986).

On-line size analysis

Measuring the size of coarse ore particles on conveyor belts or fine particles in slurries can now be done on-line with appropriate instrumentation. This is covered more fully in Chapter 4.

Weighing the ore

Many schemes are used for determination of the tonnage of ore delivered to or passing through different sections of a mill. The general trend is towards weighing materials on the move. The predominant advantage of continuous weighing over batch weighing is its ability to handle large tonnages without interrupting the material flow. The accuracy and reliability of continuous-weighing equipment have improved greatly over recent years. However, static weighing equipment is still used for many applications because of its greater accuracy.

Belt scales, or *weightometers*, are the most common type of continuous-weighing devices and consist of one or more conveyor idlers mounted on a weighbridge. The belt load is transmitted from the weighbridge either direct or via a lever system to a load-sensing device, which can be either electrically, mechanically, hydraulically, or pneumatically activated. The signal from the load-sensing device is usually combined with another signal representing belt speed. The combined output from the load and belt-speed sensors provides the flow rate of the material passing over the scale. A totaliser can integrate the flow-rate signal with time, and the total tonnage carried over the belt scale can be registered on a digital read-out. Accuracy is normally 1–2% of the full-scale capacity.

Periodic testing of the weightometer can be made either by passing known weights over it or by causing a length of heavy roller chain to trail from an anchorage over the suspended section while the empty belt is running.

Most simple concentrators use one master weight only, and in the case of a weightometer this will probably be located at some convenient point between the crushing and the grinding sections. The conveyor feeding the fine-ore bins is often selected, as this normally contains the total ore feed of the plant.

Weighing the concentrates is usually carried out after dewatering, before the material leaves the

plant. Weighbridges can be used for material in wagons, trucks, or ore cars. They may require the services of an operator, who balances the load on the scale beam and notes the weight on a suitable form. After tipping the load, the tare (empty) weight of the truck must be determined. This method gives results within 0.5% error, assuming that the operator has balanced the load carefully and noted the result accurately. With recording scales, the operator merely balances the load, then turns a screw which automatically punches a card and records the weight. Modern scales weigh a train of ore automatically as it passes over the platform, which removes the chance of human error entirely except for occasional standardisation. Sampling, of course, must be carried out at the same time for moisture determination. Assay samples should be taken, whenever possible, from the moving stream of material, as described earlier, before loading the material into the truck.

Sampling is very unsatisfactory from a wagon or container because of the severe segregation that occurs during filling and in motion. Sampling should be performed to a pre-set pattern by *augering* the loaded truck. This is achieved by pushing in a sample probe which extracts the sample in the form of a cylinder extending the full depth of the load. This avoids selective removal of particles which slide down the surface and avoids the surface layer in which extreme segregation will probably have occurred due to vibration.

Tailings weights are rarely, if ever, measured. They are calculated from the difference in feed and concentrate weights. Accurate sampling of tailings is essential, and is easy to carry out accurately with the use of automatic sample cutters.

Slurry streams

From the grinding stage onwards, most mineral processing operations are carried out on slurry streams, the water and solids mixture being transported through the circuit via pumps and pipelines.

As far as the mineral processor is concerned, the water is acting as a transport medium, such that the *weight* of slurry flowing through the plant is of little consequence. What is of importance is the *volume* of slurry flowing, as this will affect residence times in unit processes. For the purposes of metallurgical accounting, the weight of dry solids contained within the slurry is important.

If the volumetric flow rate is not excessive, it can be measured by diverting the stream of pulp into a suitable container for a measured period of time. The ratio of volume collected to time gives the flow rate of pulp. This method is ideal for most laboratory and pilot scale operations, but is impractical for large-scale operations, where it is usually necessary to measure the flow rate by on-line instrumentation.

Volumetric flow rate is important in calculating retention times in processes. For instance, if $120\,m^3/h$ of slurry is fed to a flotation conditioning tank of volume $20\,m^3$, then, *on average*, the retention time of particles in the tank will be:

$$\text{Tank volume/flow rate} = 20 \times \frac{60}{120} = 10 \text{ min}$$

Slurry, or pulp, density is most easily measured in terms of weight of pulp per unit volume (kg/m^3). As before, on flowstreams of significant size, this is usually measured continuously by on-line instrumentation.

Small flowstreams can be diverted into a container of known volume, which is then weighed to give slurry density directly. This is probably the most common method for routine assessment of plant performance, and is facilitated by using a density can of known volume which, when filled, is weighed on a specially graduated balance giving direct reading of pulp density.

The composition of a slurry is often quoted as the % solids by weight (100–% moisture), and can be determined by sampling the slurry, weighing, drying and reweighing, and comparing wet and dry weights (Equation 3.1). This is time-consuming, however, and most routine methods for computation of % solids require knowledge of the density of the solids in the slurry. There are a number of methods used to measure this, each method having its relative merits and demerits. For most purposes the use of a standard density bottle has been found to be a cheap and, if used with care, accurate method. A 25- or 50-ml bottle can be used, and the following procedure adopted:

(1) Wash the density bottle with acetone to remove traces of grease.
(2) Dry at about 40 °C.
(3) After cooling, weigh the bottle and stopper on a precision analytical balance, and record the weight, $M1$.

(4) Thoroughly dry the sample to remove all moisture.
(5) Add approximately 5–10 g of sample to the bottle and reweigh. Record the weight, $M2$.
(6) Add double distilled water to the bottle until half-full. If appreciable "slimes" (minus 45 micron particles) are present in the sample, there may be a problem in wetting the mineral surfaces. This may also occur with certain hydrophobic mineral species, and can lead to false low density readings. The effect may be reduced by adding one drop of wetting agent, which is insufficient to significantly affect the density of water. For solids with extreme wettability problems, an organic liquid such as toluene can be substituted for water.
(7) Place the density bottle in a desiccator to remove air entrained within the sample. This stage is essential to prevent a low reading. Evacuate the vessel for at least 2 min.
(8) Remove the density bottle from the desiccator, and top up with double distilled water (do not insert stopper at this stage).
(9) When close to the balance, insert the stopper and allow it to fall into the neck of the bottle under its own weight. Check that water has been displaced through the stopper, and wipe off excess water from the bottle. Record the weight, $M3$.
(10) Wash the sample out of the bottle.
(11) Refill the bottle with double distilled water, and repeat procedure 9. Record the weight, $M4$.
(12) Record the temperature of the water used, as temperature correction is essential for accurate results.

The density of the solids (s) is given by:

$$s = \frac{M2 - M1}{(M4 - M1) - (M3 - M2)} \times Df \text{ kg/m}^3 \quad (3.4)$$

where Df = density of fluid used.

Knowing the densities of the pulp and dry solids, the % solids by weight can be calculated. Since the total pulp volume is equal to the volume of the solids plus the volume of water, then for 1 m^3 of pulp:

$$1 = \frac{xD}{100s} + (100 - x)\frac{D}{100w} \quad (3.5)$$

where x = % solids by weight, D = pulp density (kg/m^3), s = density of solids (kg/m^3), w = density of water.

Assigning a value of 1000 kg/m^3 to the density of water, which is sufficiently accurate for most purposes, Equation 3.5 gives:

$$x = \frac{100s(D - 1000)}{D(s - 1000)} \quad (3.6)$$

Having measured the volumetric flow rate (F m^3/h), the pulp density (D kg/m^3), and the density of solids (s kg/m^3), the weight of slurry can now be calculated (FD kg/h), and, of more importance, the mass flow rate of dry solids in the slurry, M kg/h:

$$M = FDx/100 \quad (3.7)$$

or combining Equations 3.6 and 3.7:

$$M = \frac{Fs(D - 1000)}{(s - 1000)} \text{ kg/h} \quad (3.8)$$

Example 3.1

A slurry stream containing quartz is diverted into a 1-litre density can. The time taken to fill the can is measured as 7 sec. The pulp density is measured by means of a calibrated balance, and is found to be 1400 kg/m^3. Calculate the % solids by weight, and the mass flow rate of quartz within the slurry.

Solution

The density of quartz is 2650 kg/m^3. Therefore, from Equation 3.6,

% solids by weight,

$$x = \frac{100 \times 2650 \times (1400 - 1000)}{1400 \times (2650 - 1000)}$$
$$= 45.9\%$$

The volumetric flow rate,

$$F = \frac{1}{7} \text{ litres/s}$$
$$= \frac{3600}{7000} \text{ m}^3/\text{h}$$
$$= 0.51 \text{ m}^3/\text{h}$$

Therefore, mass flow rate

$$M = \frac{0.51 \times 1400 \times 45.9}{100}$$
$$= 330.5\,\text{kg/h}$$

Example 3.2

A pump is fed by two slurry streams. One stream has a flow rate of $5.0\,m^3/h$ and contains 40% solids by weight. The other stream has a flow rate of $3.4\,m^3/h$ and contains 55% solids. Calculate the tonnage of dry solids pumped per hour. (Density of solids is $3000\,kg/m^3$.)

Solution

Slurry stream 1 has a flow rate of $5.0\,m^3/h$ and contains 40% solids. Therefore, from Equation 3.6:

$$D = \frac{1000 \times 100s}{s(100 - x) + 1000x} \qquad (3.9)$$

or

$$D = \frac{1000 \times 100 \times 3000}{(3000 \times 60) + (1000 \times 40)}$$
$$= 1364\,\text{kg/m}^3$$

Therefore, from Equation 3.8, the mass flow rate of solids in slurry stream 1

$$= \frac{5.0 \times 3000 \times (1364 - 1000)}{(3000 - 1000)}\,\text{kg/h}$$
$$= 2.73\,\text{t/h}$$

Slurry stream 2 has a flow rate of $3.4\,m^3/h$ and contains 55% solids. From Equation 3.9, the pulp density of the stream $= 1579\,kg/m^3$. Therefore, from Equation 3.8, the mass flow rate of solids in slurry stream $2 = 1.82\,t/h$. The tonnage of dry solids pumped is thus:

$$1.82 + 2.73 = 4.55\,\text{t/h}$$

In some cases it is necessary to know the % solids by volume. This is a parameter sometimes used in mathematical models of unit processes.

$$\%\ \text{solids by volume} = \frac{xD}{s} \qquad (3.10)$$

Also of use in milling calculations is the ratio of the weight of water to the weight of solids in the slurry, or the *dilution ratio*. This is defined as:

$$\text{Dilution ratio} = \frac{100 - x}{x} \qquad (3.11)$$

This is particularly important as the product of dilution ratio and weight of solids in the pulp is equal to the weight of water in the pulp.

Example 3.3

A flotation plant treats 500 t of solids per hour. The feed pulp, containing 40% solids by weight, is conditioned for 5 min with reagents before being pumped to flotation. Calculate the volume of conditioning tank required. (Density of solids is $2700\,kg/m^3$.)

Solution

The volumetric flow rate of *solids* in the slurry stream

$$= \text{mass flow rate/density}$$
$$= 500 \times 1000/2700 = 185.2\,m^3/h$$

The mass flow rate of water in the slurry stream

$$= \text{mass flow rate of solids} \times \text{dilution ratio}$$
$$= 500 \times (100 - 40)/40$$
$$= 750\,t/h$$

Therefore, volumetric flow rate of water $= 750\,m^3/h$.

Volumetric flow rate of slurry $= 750 + 182.2 = 935.2\,m^3/h$.

Therefore, for a nominal retention time of 5 min, the conditioning tank should have a volume of $935.2 \times 5/60 = 77.9\,m^3$.

Example 3.4

Calculate the % solids content of the slurry pumped from the sump in Example 3.2.

Solution

The mass flow rate of solids in slurry stream 1 is 2.73 t/h. The slurry contains 40% solids, hence the mass flow rate of water

$$= 2.73 \times 60/40 = 4.10\,\text{t/h}$$

Similarly, the mass flow rate of water in slurry stream 2

$$= 1.82 \times 45/55 = 1.49\,\text{t/h}$$

Total slurry weight pumped

$$= 2.73 + 4.10 + 1.82 + 1.49 = 10.14\,\text{t/h}$$

Therefore, % solids by weight

$$= 4.55 \times 100/10.14 = 44.9\%$$

On-line instrumentation for mass flow measurement

Many modern plants now use *mass-flow integration* to obtain a continuous recording of dry tonnage of material from pulp streams.

The mass-flow unit consists essentially of an electromagnetic flowmeter and a radioactive source density gauge fitted to the vertical pipeline carrying the upward-flowing ore stream.

The fundamental operating principle of the magnetic flowmeter (Figure 3.10) is based on Faraday's law of electromagnetic induction, which states that the voltage induced in any conductor as it moves across a magnetic field is proportional to the velocity of the conductor. Thus, providing the pulp completely fills the pipeline, its velocity will be directly proportional to the flow rate. Generally, most aqueous solutions are adequately conductive for the unit and, as the liquid flows through the metering tube and cuts through the magnetic field, an emf is induced in the liquid and is detected by two small measuring electrodes fitted virtually flush with the bore of the tube, the flow rate then being recorded on a chart or continuously on an integrator. The coil windings are excited by a single-phase AC mains supply and are arranged around the tube to provide a uniform magnetic field across the bore. The unit has many advantages over conventional flow-measuring devices, notable ones being that there is no obstruction to flow; pulps and aggressive liquids can be handled; and it is immune to variations in density, viscosity, pH, pressure, or temperature.

A further development is the DC magnetic flowmeter which uses a pulsed or square excitation for better stability and reduced zero error.

Two types of ultrasonic flowmeters are also in common use. The first relies on reflection of an ultrasonic signal by discontinuities (particles or bubbles) into a transmitter/receiver ultrasonic transducer. The reflected signal exhibits a change in frequency due to the Doppler effect which is

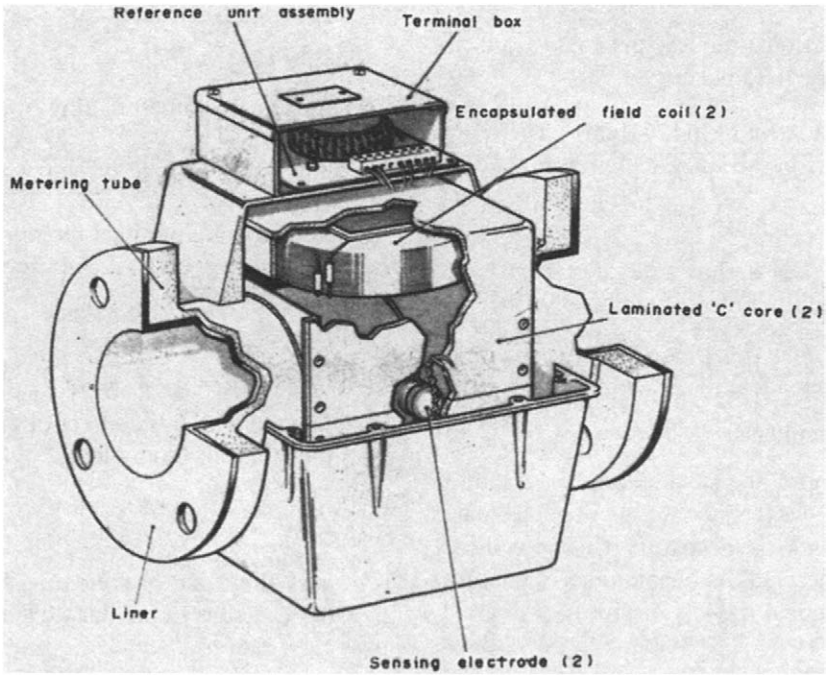


Figure 3.10 Magnetic flowmeter

proportional to the flow velocity; these instruments are commonly called "Doppler flow meters". As the transducer can be attached to the outside of a suitable pipe section, these meters can be portable.

The other type of meter uses timed pulses across a diagonal path. These meters depend only on geometry and timing accuracy. Hence they can offer high precision with minimal calibration.

The density of the slurry is measured automatically and continuously in the nucleonic density gauge (Figure 3.11) by using a radioactive source. The gamma rays produced by this source pass through the pipe walls and the slurry at an intensity that is inversely proportional to the pulp density. The rays are detected by a high-efficiency ionisation chamber and the electrical signal output is recorded directly as pulp density. Fully digital gauges using scintillation detectors are also now in common use. The instrument must be calibrated initially "on-stream" using conventional laboratory methods of density analysis from samples withdrawn from the line.

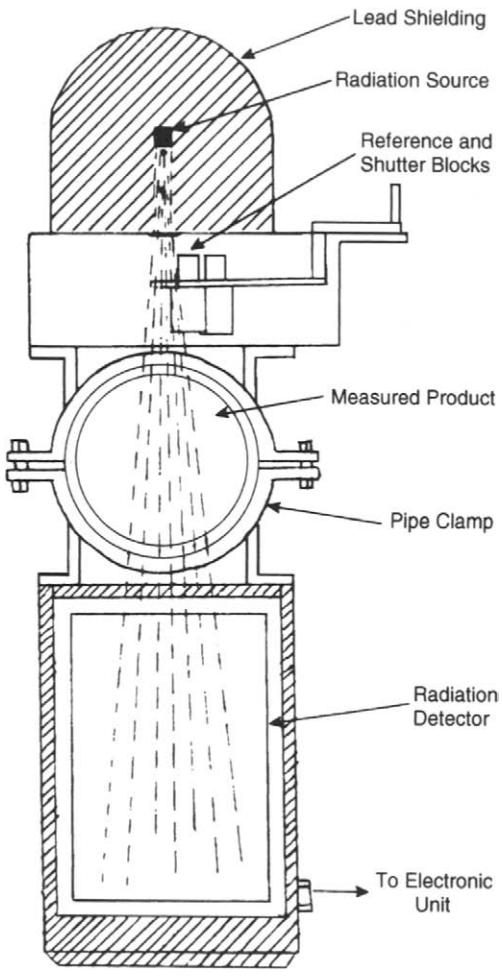


Figure 3.11 Nucleonic density gauge

The mass-flow unit integrates the rate of flow provided by the magnetic flowmeter and the pulp density to provide a continuous record of tonnage of dry solids passing through the pipeline, providing that the specific gravity of the solids comprising the ore stream is known. The method offers a reliable, accurate means of weighing the ore stream and entirely removes any chance of operator error and errors due to moisture sampling. Another advantage is that accurate sampling points, such as poppet valves, can be incorporated at the same location as the mass-flow unit. Mass-flow integrators are less practicable, however, with concentrate pulps, especially after flotation, as the pulp contains many air bubbles, which lead to erroneous values of flow rate and density.

Automatic control in mineral processing

Important advances have been made since the early 1970s in the field of automatic control of mineral processing operations, particularly in grinding and flotation. The main reasons for this rapid development are:

(i) The development of reliable instrumentation for process control systems. On-line sensors such as flowmeters, density gauges, and chemical composition analysers are of greatest importance, and on-line particle size analysers (Chapter 4) have been successfully utilised in grinding circuit control.

Other important sensors are pH meters, and level and pressure transducers, all of which provide a signal relating to the measurement of the particular process variable. This allows the final control elements, such as servo valves, variable speed motors, and pumps, to manipulate the process variable based on a signal from the controllers. These sensors and final control elements are used in many industries besides the minerals industry, and are described elsewhere (Considine, 1974; Anon., 1979; Edwards et al., 2002).

(ii) The availability of sophisticated digital computers at very low cost. During the 1970s the real cost of computing virtually halved each year, and the development of the microprocessor allowed very powerful computer hardware to be housed in increasingly smaller units. The development of high-level languages allowed relatively easy access to software, providing a more flexible approach to changes in control strategy within a particular circuit.

(iii) A more thorough knowledge of process behaviour, which has led to more reliable mathematical models of various important unit processes being developed (Mular, 1989; Napier-Munn and Lynch, 1992). Many of the mathematical models which have been developed theoretically, or "off-line", have had limited value in automatic control, the most successful models having been developed "on-line" by empirical means. Often the improved knowledge of the process gained during the development of the model has led to improved techniques for the control of the system.

(iv) The increasing use of very large grinding mills and flotation cells has facilitated control, and reduced the amount of instrumentation required.

Financial models have been developed for the calculation of costs and benefits of the installation of automatic control systems (Purvis and Erickson, 1982), and benefits reported include significant energy savings, increased metallurgical efficiency and throughput, and decreased consumption of reagents, as well as increased process stability (Chang and Bruno, 1983; Flintoff et al., 1991).

The concepts, terminology, and practice of process control in mineral processing have been comprehensively reviewed by Ulsoy and Sastry (1981) and Edwards et al. (2002), and will be briefly reviewed here and in the relevant later chapters.

The basic function of a control system is to stabilise the process performance at a desired level, by preventing or compensating for disturbances to the system. Ultimately the objective is not only stabilisation but also optimisation of the process performance based on economic considerations (Mular, 1979a).

In order to achieve these objectives, there are various "levels" of control used to make up a "distributed hierarchial computer system". At the lowest level – regulatory control – the process variables are controlled at defined "set-points" by the various individual control loops.

A simple feed-back control loop, which can be used to control the level of slurry in a pump, is shown in Figure 3.12.

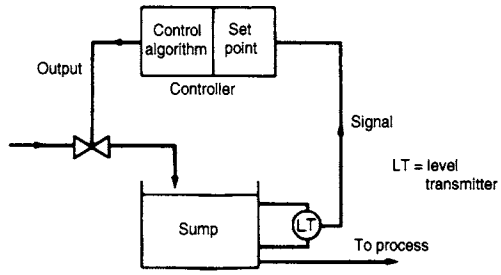


Figure 3.12 Simple feed-back control loop

Feedback, or "closed-loop", control is by far the most widely used in practice. The signal from the level transmitter is fed to the controller where the measured value is compared with the desired value or set-point. The controller then transmits a signal which adjusts the opening of the feed valve according to the difference between the measured and desired value. The output signal is controlled by a standard control algorithm which is most commonly a proportional plus integral plus derivative (PID) algorithm. The PID, or "three-term" controller, carries out signal processing according to the following equation:

$$m = K_c[e + 1/T_i \int e\mathrm{d}t + T_d \mathrm{d}e/\mathrm{d}t]$$

where m = controller output; K_c = proportional sensitivity (gain); e = deviation of measured variable from set-point; T_i = integral time constant; T_d = derivative time constant; t = time.

The three-term controller generates an output that is intended to drive the process so that the deviation from set-point (e) decreases to zero. The proportional action ($K_c e$) provides an action which is directly proportional to the deviation, with the constant of proportionality, or "gain", equal to K_c. It is a feature of proportional controllers that they can produce an exact correction only for one load condition. With all other load conditions there must be some deviation of corrected output from set-point, and this is called "offset".

Offset can be eliminated by the second term in the equation, $K_c/T_i \int e\,dt$, which is *integral*, or "reset" control. This changes the value of the manipulated variable (m) at a *rate* which is proportional to the deviation of the measured variable from the set-point. Thus, if the deviation is double its previous value, the final control element (i.e. the valve, feeder, or pump) responds twice as fast. When the measured value is at its set-point, i.e. $e = 0$, only then does the final control element remain stationary. The integral time, T_i, is the time of change of manipulated variable caused by unit change of deviation, and is usually expressed as "reset-rate" (inverse of integral time in minutes per repeat), defined as the number of times per minute that the proportional part of the response is duplicated.

Problems can occur with integral control if large, sustained load changes occur, where the measured variable deviates from the set-point for long periods. This can occur, for example, under automatic start-up of the process, where integral action results in large overshooting above the set-point by the control variable. At start-up the measured variable is zero, so the controller output is at a maximum as there is maximum deviation from measured value and set-point. The control element, therefore, does not close until the variable crosses the set-point. *Derivative* action reduces the controller output proportional to the rate of change of the deviation with time, and helps avoid overshooting the set-point. However, integral and derivative modes interact when operating successively on a signal and most commercial controllers provide only proportional and integral terms, and are known as "PI controllers".

The constants K_c and T_i (and T_d) can be adjusted on controllers to suit process conditions, and such adjustment is known as "tuning", the objective being to determine values for the parameters such that the deviation between set-point and the actual value of the process output is most efficiently corrected. For instance, if the controller has a low value of gain (K_c), then the control action will be small and the time for stabilisation of the process will be relatively long. However, above a certain value for the gain, the system becomes unstable. A high value of gain, which should cause the output to track the set-point better, causes the controller to adjust the control action by a greater amount than is actually necessary. When the output responds, it overshoots the set-point and goes so far that the deviation is not only reversed, but is even larger than it was originally. The control action is thus reversed, again by too much, and after a delay due to the transient nature of the system, the output reverses its magnitude by an amount even greater than before. The optimum gain is usually at the point where oscillations start. In most systems the integral time (T_i) is of the same order, or slightly less than the period of the oscillation. Empirical rules for establishing the optimum values of the controller parameters have evolved from the original work of Ziegler and Nichols (1942).

An alternative form more appropriate for implementation using a digital computer is

$$m_i = K_1 e_i + K_2 \sum_i e_i \Delta t + K_3 \left(\frac{e_{i-1} - e_i}{\Delta t} \right)$$

where the subscript, i, refers to a time step Δt which is small compared with the process response time; K_1 is the controller gain as before; K_2 the inverse of the integral time constant; and K_3 is the derivation time constant.

Although the various processes may be controlled by separate analogue controllers, it is now more common to control the variables at their set-points by a process computer. The requirement of such *direct digital control* is that the analogue signals from the measuring devices are converted into digital pulses by an analogue-digital converter, and that the digital signals from the computer are converted to analogue form and transmitted to the transducers which convert the analogue signals to mechanical form in order to operate the control devices.

Although set-points may be adjusted manually, it is preferable to control them automatically by other computers in the hierarchy. Such *supervisory*, or *cascade*, control may use *feed-back* loops, such as in the regulation of reagent feed to a flotation process in response to the metal content of the flotation tailing (Figure 3.13).

A change in the metal content of the tailing is acted upon by the supervisory computer which, by means of a process algorithm, modifies the set-point used by the process computer in the regulatory control loop. The greatest problem found, which has never been fully overcome in flotation control, is in developing algorithms which accommodate changes in ore type and which can define

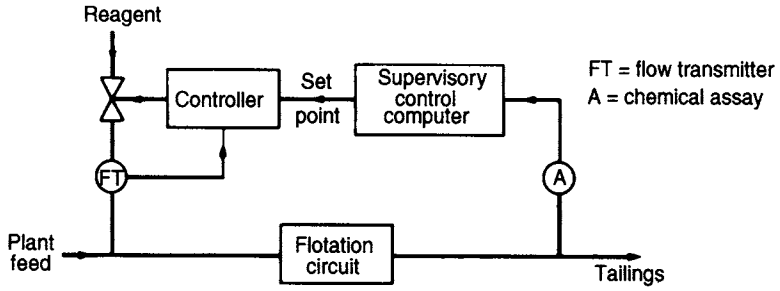


Figure 3.13 Feed-back loop with supervisory control

flexible limits to the maximum and minimum amounts of reagent added.

The disadvantage of feed-back control loops is that they compensate for disturbances in the system only after the disturbances have occurred, and the effect of the control system on the manipulated variables is not observed until after a time delay roughly equivalent to the residence time of the process flow between the control device and the measuring device.

Feed-forward control loops do not suffer from this disadvantage, and they are sometimes used in flotation processes to control the addition of a specific reagent to the process feed. Such a control loop is shown in Figure 3.14.

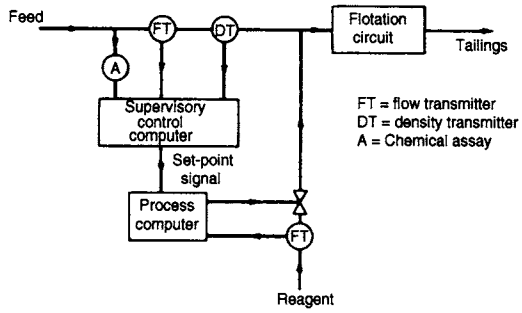


Figure 3.14 Feed-forward control loop

The flow rate of slurry and slurry density are continuously measured by means of a magnetic flowmeter and density gauge respectively, the two signals being computed to mass flow rate of dry solids. The chemical analysis signal is incorporated to obtain the mass flow rate of valuable metal to the process, the resultant value being used to calculate the required reagent flow rate in order to maintain constant reagent addition per unit weight of metal. The new set-point is then compared with the measured value of reagent flow rate and adjustments made as before. The success of such control loops depends upon a consistent and predictable relationship between the controlled variable, i.e. the reagent flow, and the measured variable (the metal flow rate to the plant), and they often fail when significant changes occur in the nature of the plant feed. Since it is really *mineral* content which controls reagent requirements, and this can only be inferred from the metal content, changes in mineralogy or concentration of recycled reagents can cause unmeasured disturbances, which cannot be compensated for in such pure feed-forward loops, and hence some form of feed-back trim is sometimes incorporated (Gault et al., 1979), often only with limited success.

Figure 3.15 shows a simple feed-forward/feed-back system which has been used to control the reagent addition to maintain an optimum tailings assay.

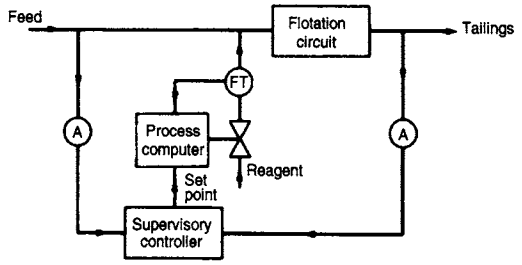


Figure 3.15 Feed-forward/feed-back system

The optimum tailings assay is calculated using the assay of the feed to the process and a feed-forward algorithm. The reagent addition is controlled at the set-point, which is adjusted according to the difference between the calculated

and actual tailings assays. The disadvantage of this system, as with the simple feed-back loop, is the time lag between changes in head grade and tailings grade response.

Although single-variable control, with PI or PID-type controllers, is the approach used for the majority of process control applications, it does have certain limitations. One such limitation is in the overall control of processes that show severe interaction, or "coupling behaviour", between loops. Normal decoupling techniques, which may involve "detuning", i.e. slowing the response, of one controller, only partially eliminate the interactions, and a solution may be some form of multi-variable control (Owens, 1981; Barker, 1984), where the interactions are specifically accommodated in the design of the control system.

PI control alone also has considerable limitations because of the long time delays of many mineral processes; unless the controller is detuned, the controller output will be such as to cause process oscillations. A detuned PI controller provides very slow response, which can be unsuitable for many processes where input disturbances result in process upsets, and so dynamic compensation is added to the PI controller in cases of long time delays.

The problem of PI controller tuning is compounded by the non-linear nature of most mineral processing operations, and variability of process response is frequently encountered in mineral control systems, this often being caused by changes in the nature of the ore. Some of these disturbances, such as ore hardness, slurry viscosity, and liberation characteristics, are difficult or impossible to measure. The necessary controller gain settings are not fixed in such situations, and imposition of fixed gains to suit the average dynamic behaviour of the process frequently results in poor controller performance. In order to overcome these deficiencies, a range of "modern" model-based control techniques is being developed, which can not only tune the controller automatically but also optimise and control its set-point.

The development of reliable on-line models has led to "adaptive" control methods, which overcome some of the weaknesses of classical PI control techniques (Hodouin and Najim, 1992). It is now possible for a microprocessor-based controller to review the performance of the control loop, and to modify the controller parameters to suit the current dynamic process responses. This type of "self-tuning" control adapts not only to load-dependent dynamic changes, but also to time-related and/or random dynamic characteristic changes (Rajamani and Hales, 1987).

The ultimate aim of control is not only to stabilise the process, but also to optimise the process performance and hence increase the economic efficiency. This higher level of control has been attempted in a few concentrators with somewhat limited success, as optimisation can only be achieved when reliable supervisory stabilisation of the plant has been fully effective. The *evolutionary optimisation* (EVOP) approach is based on control action to either continue or reverse the direction of movement of a process efficiency by manipulating the set-point of the controller in order to achieve some higher level of performance. The efficiency of the process is determined by a suitable economic criterion which in the case of a concentrator can be the economic efficiency attained (Chapter 1). The controlled variables are altered according to a predetermined strategy, and the effect on the process efficiency is computed on-line. If the efficiency is increased as a result of the change, then the next change is made in the same direction, otherwise the direction is reversed; eventually the efficiency should converge to the optimum (Krstev and Golomeov, 1998).

A logic flow diagram for the control of reagent to a flotation circuit is shown in Figure 3.16 (King, 1973).

The system incorporates an alarm to alert the process operator when the computer's efforts fail to halt a falling efficiency. Action can then be initiated to adjust process variables not influenced by the control strategy. In searching for peaks in efficiency, the controller is beginning to act in an intelligent manner. It is seeking a performance peak in a similar way as do operators, by reacting according to changes in process conditions.

The EVOP approach is fairly simple, requiring no process mathematical model. However, it is realised that some form of process model which is capable of providing more accurate predictions of process behaviour is really essential for effective optimisation, and it is for this reason that most optimising control systems are now model-based strategies (Herbst and Bascur, 1984; McKee and Thornton, 1986, Hodouin et al., 2001).

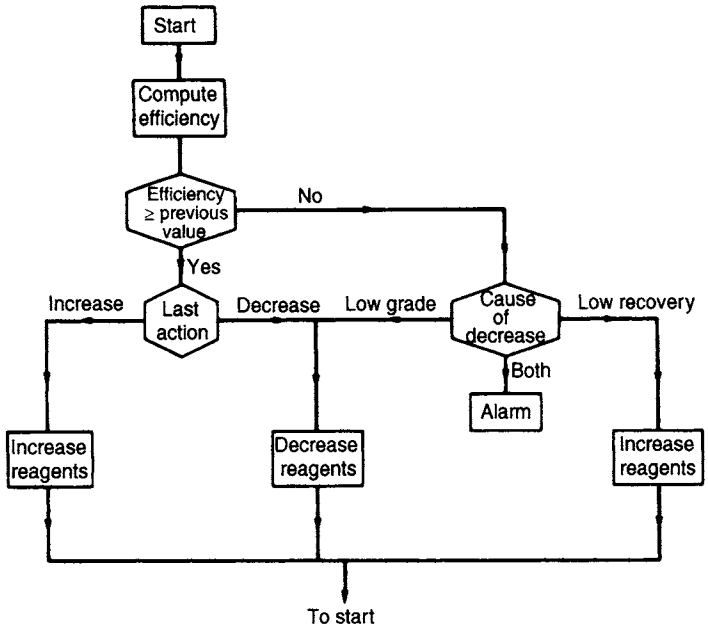


Figure 3.16 Optimisation control logic

The application of model-based control systems is summarised in Figure 3.17 (Herbst and Rajamani, 1982).

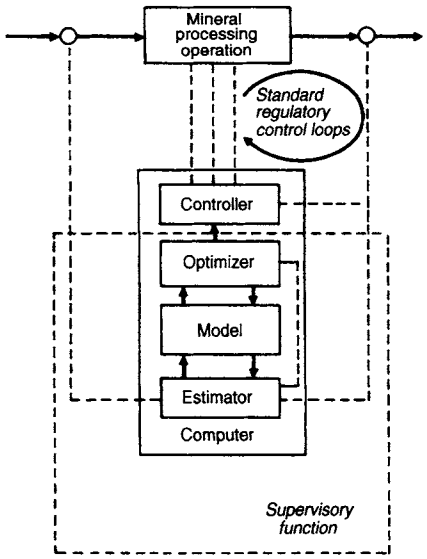


Figure 3.17 Components of a model-based control system (after Herbst and Rajamani, 1982)

The function of the estimator is to combine both model predictions and process measurements to define the state of the system. The optimiser selects a set of control actions which are calculated to maximise or minimise an objective function. Set-points for standard PI controllers are calculated in the optimisation procedure. In the estimator a model of the process is run in parallel with the actual process, and the inputs to the process are also fed to the model. The measurements coming from the actual process are compared to the measurements predicted by the model, and the difference is used as the basis for the correction to the model. This correction alters the parameters and states in the model so as to make its predictions match those of the actual process better. The basis of parameter estimation is "recursive estimation", or *Kalman filtering* (Bozic, 1979), where the estimator updates its estimates continuously with time as each input arrives, rather than collecting all the information together and processing in a single batch (Figure 3.18).

A simple recursive least-squares algorithm is most commonly used to update the model parameters:

$$y(t+1) = a_1 y(t) + \cdots a_n y(t-n+1) + b_0 u(t) + \cdots b_n u(t-n+1) + z(t) \qquad (3.12)$$

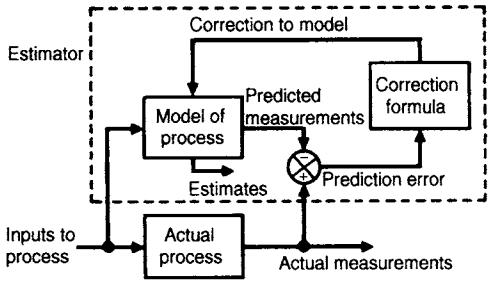


Figure 3.18 Schematic diagram of the operation of recursive estimation (after Barker, 1984)

where $y(t)$ = process output at time t; $u(t)$ = process input at time t; $z(t)$ = output noise at time t; a_1–a_n, b_1–b_n are model parameters.

Since the model parameters $a_1 \ldots a_n$ and $b_1 \ldots b_n$ are being updated continuously, then Equation 3.12 should give a reasonably accurate prediction of the dynamic behaviour of the process. The model parameters can then be used to calculate controller parameters. With this technique a control law is used which is always suitably tuned for the current process characteristics (McKee and Thornton, 1986).

In addition to the process and supervisory control computers, a general purpose computer may be incorporated in the hierarchy. This computer is generally housed in the central control room (Figure 3.19) and coordinates the activities of the supervisory computers, as well as performing such tasks as logging and evaluation of plant data, preparation and printing of shift, daily and monthly reports, and supervision of shut-down and start-up. The computer can allow the operator to input information such as changes in metal prices, smelter terms, reagent costs, etc., which can aid optimisation of the set-points of the supervisory controllers.

Better access to on-line data and more powerful computers provides opportunities to optimise product value on line. A good example was reported by Holdsworth et al. (2002) for the Greens Creek silver–lead–zinc mine in Alaska. The highly instrumented concentrator carried out frequent on-line mass balances based on the last 2 h of operation. The balanced data was used to calibrate a simple flotation model. The operator could then assess strategies for "moving" metal between low-value bulk concentrate and high-value lead or zinc concentrates with the aid of a simple on-line smelter contract model.

Statistical process control is a methodology involving simple graphical techniques such as control charts and cumulative sum (cusum) charts to plot process data as a time series, together with statistical methods to determine whether the process is out of control as judged by some performance criterion, i.e. low recovery or concentrate grade (Ipek et al., 1999). These methods can

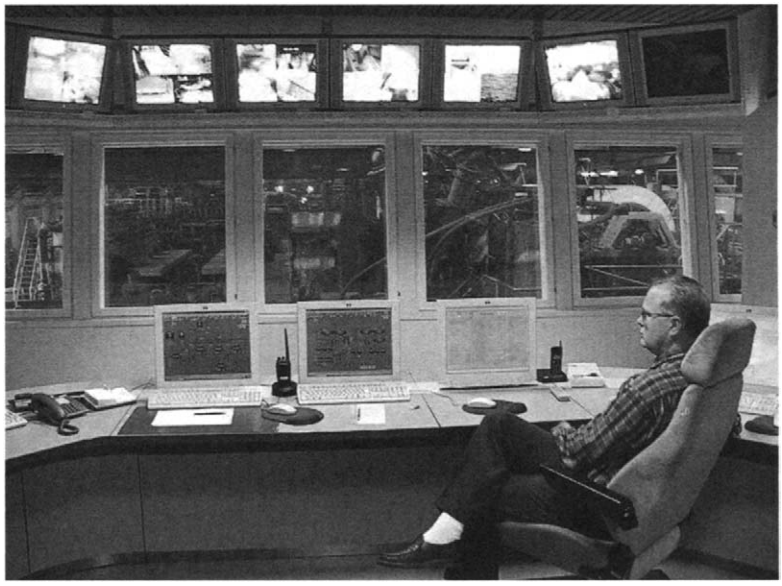


Figure 3.19 Outokumpu's Pyhasalmi concentrator control room (Courtesy Outokumou Technology Minerals Oy)

be used as decision-making tools or in the analysis of historical data.

Control systems based on rules with fuzzy logic support have steadily become more ambitious. Van der Spuy et al. (2003) propose an "on-line expert" which will provide both operator training and assistance. Expert systems have also proven to be very useful for selecting which advanced control method might be appropriate, based on a set of rules related to the current operating conditions (Flintoff, 2002).

Expert systems are in common use for control of autogenous and semi-autogenous mills (Hales and Ynchausti, 1997). Expert systems find favour with many operators because of their "English language"-like rules. These rules are self-documenting to some degree.

Neural networks

Neural networks are based on a simple conceptual model of a neuron, or brain cell. The neuron has a number of inputs and at least one output. When the sum of the inputs, each multiplied by a chosen weight, reaches a certain value the neuron "fires" and contributes an output signal, which can be an input signal to a further layer of neurons, i.e. a network.

A typical practical system will have about three layers, as shown in Figure 3.20. The network is "trained" by applying a known set of inputs and adjusting the weights until the desired output is achieved.

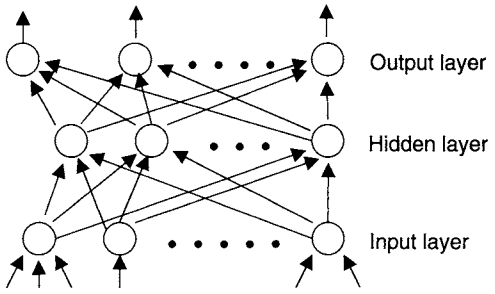


Figure 3.20 Artificial neural network, with an input layer of process elements or neurons (the circles), a single hidden layer, and an output layer (after Hales and Ynchausti, 1992)

Neural networks have had good success in pattern recognition such as optical character recognition. Training a network should use a full, rigorous experimental design for adjustment of key variables. A disadvantage is that while neural nets can mimic operations they provide no insight to the human users. If the training process is continued for too long, the network will model the noise in the data. Hence it is necessary to test performance against another set of data.

Expert systems

Expert systems are developed from research into artificial intelligence and are computer programs that simulate the reasoning component of human expertise in a narrowly focused domain (Laguitton and Leung, 1989; Bearman and Milne, 1992). Essentially they are computer systems that achieve high levels of performance in tasks for which humans would require years of special education, training, or experience. Their main application has to date been in process diagnosis, operator support, and training (off-line systems).

However, it may be that the highly mathematical approach needed for modern adaptive control methods may lead to the increasing use of expert systems for on-line control. Many plants and processes are operated effectively by experienced operators without elaborate control schemes and, in many cases, automatic controllers are often overridden by plant personnel. This suggests that a less rigorous approach to computer control, particularly for operations such as flotation, may be more appropriate.

Human operators often make "rule-of-thumb" educated guesses that have come to be known as *heuristics*. *Fuzzy-logic* theory involves the development of an ordered set of *fuzzy* conditional statements, which provide an approximate description of a control strategy, such that modification and refinement of the controller can be performed without the need for special technical skills. These statements are of the form – If A then B, where A and B represent linguistic expressions such as grade is "high" and increase reagent "a lot". All the conditional rules taken together constitute a fuzzy decisional algorithm for controlling the plant. Harris and Meech (1987) have presented an excellent introduction to Fuzzy Control, showing how this has been applied to a simulation model of a secondary crushing plant. The simplicity of the method allows for its application to other systems

such as grinding circuits, flotation plants, and de-watering circuits (Meech and Jordan, 1993).

Circuit design and optimisation by computer simulation

Computer simulation has become a very powerful tool in the design and optimisation of mineral processing plants. The capital and operating costs of mineral processing circuits are high and in order to reduce them to a minimum consistent with desired metallurgical performance, the design engineer must be able to predict accurately the metallurgical performances of every circuit which is to be considered for final design, relate performance to costs, and make a choice for detailed design based on these data. Simulation techniques are suitable for this purpose provided that the unit models are valid, and considerable progress has been made in this area recently.

Computer simulation is intimately associated with mathematical modelling and realistic simulation relies heavily on the availability of accurate and physical meaningful models. A model is an equation, or set of equations, that relates responses (independent variables) of interest to controllable independent variables. They are of three types – theoretical, empirical and phenomenological.

Theoretical models are the most effective as they are valid over a complete range, being developed from basic scientific principles, necessitating a sound understanding of the process. Mineral processing models are rarely of this type, however, due to the complexities of the physico-chemical processes involved.

Empirical models are the simplest, and are generated from data acquired around the process unit. They are less expensive to produce than the theoretical models, where first principles and much experimentation may be involved (Mular, 1989). Empirical models often express process performance in terms of process variables by making use of simple linear regression methods, and as such are valid only for that particular process and within the operating bounds of the data collected. A simple, but commonly used, empirical model is the partition curve, which is used to assess the efficiency of classification and other separation processes (see Chapters 9 and 11). Although often rejected as legitimate models by the purists, empirical models are useful in that they can be produced relatively easily and cheaply, and their development often leads to a better understanding of the process, which can aid production of more general models.

Normally models are a combination of theoretical with empirical. These *phenomenological* models are developed from a mechanistic description of the process in conjunction with physically meaningful process parameters determined from experiments rather than from basic science (Sastry and Lofftus, 1989; Sastry, 1990). An example of such a model is the population balance approach, commonly used to simulate comminution processes (see Chapter 5). These models are more realistic representations of the process than are empirical models, and are capable of extrapolation. Their effectiveness can be extended by correlation of calculated parameter values and operational variables of the process.

Mathematical models can be either *dynamic* (involving time) or *steady state*. The latter predominate at present, although it is expected that dynamic models will become more prevalent in future, particularly for control systems, as time-variations of the process variables play an important role in the operating performances of process units (Hodouin, 1988).

King (2001) provides a good review of modelling and simulation methods. Comminution and classification models are well developed and in routine use for design and optimisation (Napier-Munn et al., 1996). Kinetic models of flotation have also been used for this purpose for many years (Lynch et al., 1981) and new, more powerful approaches to modelling flotation are now available for practical use (Alexander et al., 2005). Models of gravity and dense medium processes are available though are not as widely used (Napier-Munn and Lynch, 1992), and the modelling of liberation has progressed though is not yet routine (Gay, 2004).

Several commercial simulators for mineral processing are now available: examples are JKSimMet (Morrison and Richardson, 2002), USimPac (Brochot et al., 2002), Modsim (King, 2001), and Plant Designer (Hedvall and Nordin, 2002). The first two simulators also provide powerful data analysis and model calibration capabilities. Limn (Leroux and Hardie, 2003) is a flowsheet solution package implemented as a layer on top of Microsoft Excel with simulation capability.

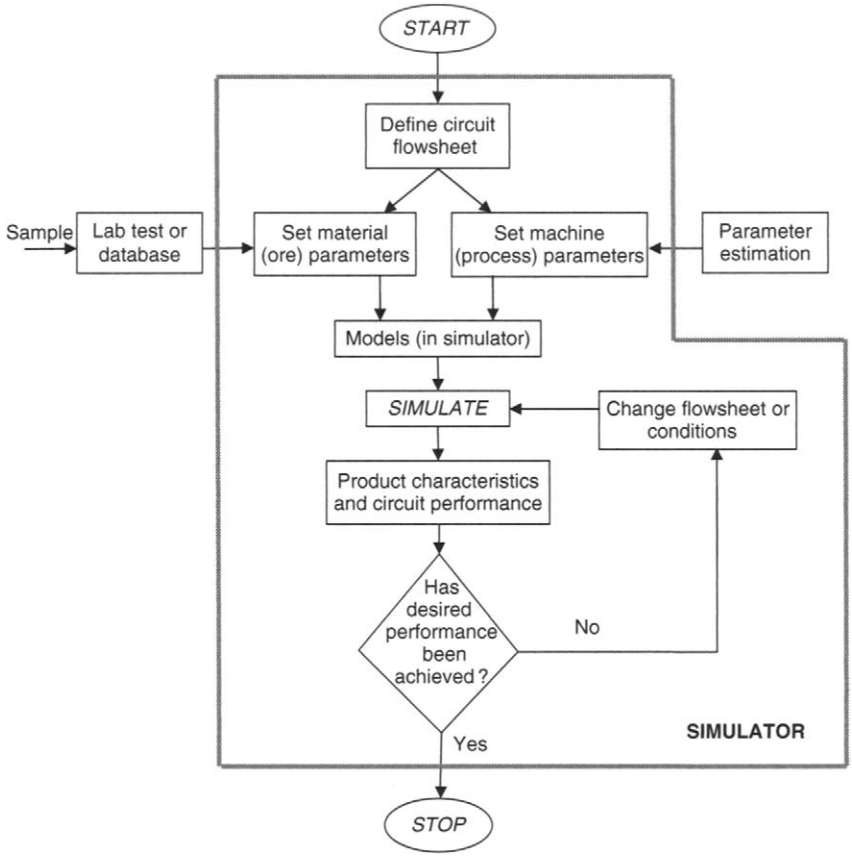


Figure 3.21 Procedure for simulation to optimise design or performance (from Napier-Munn et al., 1996; Courtesy JKMRC, The University of Queensland)

Figure 3.21 illustrates the procedure for using simulation to predict process performance for process design or process optimisation. The key inputs are the material characteristics (e.g. grindability or floatability) and the parameters of the process models. The latter are obtained by estimation from operating data (preferred) or from a parameter library.

Computer simulation offers clear advantages in terms of the accurate predictions of the metallurgical performances of alternative circuits, which can be used to optimise design, and the flow rates of process streams, which can be used to size pumps and pipelines, largely eliminating the need for laborious and expensive plant trials. However, the dangers of computer simulation come from its great computational power and relative ease of use. It is always necessary to bear in mind the realistic operating range over which the models are used, as well as the realistic limits which must be placed on equipment operation, such as pumping capacity. Also it is worth remembering that good simulation models combined with poor data or poor model parameter estimates can produce highly plausible looking nonsense. This is an example of the GIGO effect (garbage in–garbage out) which is quite often true of computer programs. Simulation studies are a powerful and useful tool, complementary to sound metallurgical judgement and familiarity with the circuit being simulated and its metallurgical objectives.

Mass balancing methods

In order to assess plant performance, and to control the operation using the evaluated results, it is necessary to account for the products in terms of material and contained component weights. Mass balancing

is particularly important in accounting for valuable mineral or metal distributions, and the *two-product formula* is of great use in this respect.

If the weights of the feed, concentrate, and tailings are F, C, and T respectively, and their corresponding assays f, c, and t, then

$$F = C + T \tag{3.13}$$

i.e. material input = material output

$$\text{and } Ff = Cc + Tt \tag{3.14}$$

i.e. the valuable metal (or mineral) is balanced.

$$\text{Therefore, } Ff = Cc + (F - C)t$$

$$\text{which gives } F/C = (c - t)/(f - t) \tag{3.15}$$

where F/C represents the *ratio of concentration*.

The plant *recovery* is $(Cc/Ff) \times 100\%$

$$\text{or Recovery} = 100c(f - t)/f(c - t)\% \tag{3.16}$$

As values of recovery, ratio of concentration and *enrichment ratio* (c/f) can be determined from the assay results alone, the two-product formula method is often used to provide information for plant control, although this will be retrospective, dependent on the time taken to receive and process the assay results. Direct control can be achieved by the use of on-stream analysis systems, where values of c, f, and t can be continuously computed to provide up-to-date values of metallurgical performance.

Example 3.5

The feed to a flotation plant assays 0.8% copper. The concentrate produced assays 25% Cu, and the tailings 0.15% Cu. Calculate the recovery of copper to the concentrate, the ratio of concentration, and the enrichment ratio.

Solution

The concentrator recovery (Equation 3.16) is:

$$\frac{100 \times 25(0.8 - 0.15)}{0.8(25 - 0.15)}\% = 81.7\%$$

The ratio of concentration (Equation 3.15) is:

$$\frac{25 - 0.15}{0.8 - 0.15} = 38.2.$$

The enrichment ratio (c/f) is:

$$25/0.8 = 31.3.$$

Metallurgical accounting

There are many methods used to account for a plant's production. Most concentrators produce a metallurgical balance showing the performance of each shift, the shift results being cumulated over a longer period (daily, monthly, annually) to show the overall performance.

Although concentrates can be weighed accurately prior to loading into rail cars or lorries, it is improbable that concentrate weighed in this way during a particular shift will correspond with the amount actually produced, as there is often a variable inventory of material between the concentrator and the final disposal area. This inventory may consist of stockpiled material, and concentrates in thickeners, filters, agitators, etc. For shift accounting, the feed tonnage to the concentrator is usually accurately measured, this providing the basis for the calculation of product stream weights. Samples are also taken periodically of the feed, concentrates, and tailings streams, the composite samples being collected and assayed at the end of the shift. Equation 3.15 can be used to calculate the concentrate weight produced, allowing a metallurgical balance to be prepared. Suppose, for instance, that a plant treats 210.0 t of material during a shift, assaying 2.5% metal, to produce a concentrate of 40% metal, and a tailing of 0.20% metal.

From Equation 3.15:

$$\frac{F}{C} = \frac{(40 - 0.20)}{(2.5 - 0.2)}.$$

Hence $C = 12.1$ t.

The tailing weight is thus $210.0 - 12.1 = 197.9$ t.

The metallurgical balance for the shift is tabulated in Table 3.3.

Table 3.3 Shift 1 performance

Item	*Weight* t	*Assay %*	*Weight metal* t	*Distribution metal %*
Feed	210.0	2.5	5.25	100.0
Concentrate	12.1	40.0	4.84	92.2
Tails	197.9	0.20	0.40	7.8

The distribution of the metal into the concentrate (i.e. recovery) is $4.84 \times 100/5.25 = 92.2\%$, this value corresponding to that obtained from Equation 3.16. Suppose that on the next shift 305 t of material are treated, assaying 2.1% metal, and that a concentrate of 35.0% metal is produced, leaving a tailing of 0.15% metal. The metallurgical balance for the shift is shown in Table 3.4. The composite balance for the two shifts can be produced by adding all material and metal weights, and then weighting the assays and distributions accordingly (Table 3.5).

Table 3.4 Shift 2 performance

Item	*Weight* t	*Assay %*	*Weight metal* t	*Distribution metal %*
Feed	305.0	2.1	6.41	100.0
Concentrate	17.1	35.0	5.99	93.45
Tails	287.9	0.15	0.42	6.55

Table 3.5 Combined performance

Item	*Weight* t	*Assay %*	*Weight metal* t	*Distribution metal %*
Feed	515.0	2.3	11.66	100.0
Concentrate	29.2	37.1	10.83	92.9
Tails	485.8	0.17	0.83	7.1

Similarly, the shift balances can be cumulated over a weekly, monthly, or annual period, in order to obtain the true feed weight and the weighted average assays of the streams. It is apparent that the calculated weights of concentrate and tailings are those which "fit" the available assay values, and a "perfect" balance is always produced by this method, as the two-product equation is consistent with the available data, i.e.

$$Ff - Cc - Tt = 0$$

A more realistic assessment can be made by accurately weighing one more stream, and comparing this with the calculated value (*check in–check out* method). For instance, if, in the previous example, the concentrate produced in the two shifts is accurately weighed, and is 28.8 t, then it is possible to obtain values for theoretical and actual plant recovery. The balance is shown in Table 3.6.

Table 3.6

Item	*Weight* t	*Assay %*	*Weight metal* t	*Distribution metal %*
Feed	515.0	2.3	11.66	100.0
Concentrate	28.8	37.1	10.68	91.6
Uncounted loss	–	–	0.15	1.3
Tails	486.2	0.17	0.83	7.1

The *actual* recovery (91.6%) is declared, and any discrepancy in metal weight is regarded as an *unaccounted loss* (11.3%). The weights of material are accepted and it is assumed that there are no *closure errors* in the material balance, i.e. $F - C - T = 0$. Physical losses will, of course, occur on any plant and it should always be endeavoured to keep these as low as possible. If the third weight is also accurately known (which it rarely is), then any closure error can also be reported as an unaccounted loss (or gain) of material.

As was mentioned earlier, it is not easy, particularly in a large plant, to obtain accurate concentrate production weights over a short period because of the inventory between the concentrator and the concentrates disposal area or smelter, where weighing is undertaken.

If over a monthly accounting period, for example, the change in inventory can be quantified by assessing at the beginning of each month the amount of concentrate retained in the plant in thickeners, filters, etc., and in trucks or other containers in transit between mill and smelter, then this inventory change can be used to adjust the smelter receipts to calculate the production figure.

For example, suppose that a smelter's monthly receipts from a mill are 3102 t of concentrates assaying 41.5% metal. The inventory of concentrates in the products disposal section is determined at the beginning and the end of the month and is as shown in Table 3.7.

Table 3.7

	Weight t	*% metal*	*Weight metal* t
(a) *Beginning of month*			
Thickeners	210	44.1	92.6
Agitators & filters	15	43.9	6.6
In transit to smelter	207	46.9	97.1
Total inventory	432	45.4	196.3
(b) *End of month*			
Thickeners	199	39.6	78.8
Agitators & filters	25	40.8	10.2
In transit to smelter	262	39.3	103.0
Total inventory	486	39.5	192.0

The monthly concentrate production can now be calculated thus:

	Weight t	*Assay (%)*	*Weight metal* t
Concentrate received	3102	41.5	1287.3
Inventory change	+54	–	−4.3
Production	3156	40.7	1283.0

Note that in this case there has been an increase in the inventory of material, which obviously increases the production, but a decrease in the inventory of metal, which lowers the metal production.

Although the metal content of the inventory can be assessed to some degree by sampling and assaying stockpiles and truck loads, it may be more accurate to rely on the weighted concentrate assay produced from the shift balances, rather than to adjust the value as above.

Example 3.6

From cumulative shift balances, the total monthly feed to a copper flotation plant was 28,760 dry tonnes at a grade of 1.1% copper. The weighted of concentrate and tailings assays were 24.9% and 0.12% Cu respectively. The weight of concentrate received at the smelter during the month was 1090.7 t, assaying 24.7% Cu.

At the beginning of the month, 257 t of concentrate were in transit to the smelter, and 210 t were in transit at the month end. Tabulate a metallurgical balance for the month's production, showing unaccounted losses of copper and compare actual and theoretical recoveries.

Solution

Inventory change during month $= 210 - 257 = -47$ t. Therefore, concentrate production is:

$$1090.7 - 47 = 1043.7\text{ t}.$$

Metallurgical balance:

	Weight t	*Assay % Cu*	*Weight Cu* t	*Distn % Cu*
Feed	28,760.0	1.1	316.4	100.0
Concentrate	1043.7	24.9	259.9	82.1
Unaccounted loss	–	–	23.2	7.3
Tails	27,716.3	0.12	33.3	10.5

The actual recovery is 82.1%, and the theoretical recovery is $82.1\% + 7.3\% = 89.4\%$. Clearly there is a large discrepancy, which could indicate poor sampling, assaying, or weighing of flowstreams.

Note that many "unaccounted losses" are a consequence of measurement accuracy or precision (or lack thereof) and within suitably defined bounds should not be cause for concern.

As there is essentially no excess ("redundant") data, it is difficult to identify the likely source of error. Analysis with redundant or excess data is an important method of improving mass flow estimates and is considered in "Reconciliation of Excess Data" below.

The use of size analyses in mass balancing

Many unit process machines, such as hydrocyclones and certain gravity separators, produce a good degree of particle size separation, and size analysis data can often be effectively used in the two-product formula.

Example 3.7

In the circuit shown in Figure 3.22, the rod mill is fed at the rate of 20 t/h of dry solids (density 2900 kg/m^3). The cyclone feed contains 35% solids by weight, and size analyses on the rod mill discharge, ball mill discharge, and cyclone feed gave:

Rod mill discharge 26.9% + 250 μm
Ball mill discharge 4.9% + 250 μm
Cyclone feed 13.8% + 250 μm

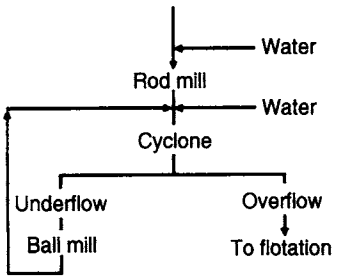


Figure 3.22 Rod mill – ball mill – cyclone circuit

Calculate the volumetric flow rate of feed to the cyclone.

Solution

A material balance on the cyclone feed junction gives:

$$F = 20 + B$$

where F = cyclone feed, and B = ball mill discharge.

Therefore $F = 20 + (F - 20)$, and a balance of +250 μm material gives:

$$13.8F = (26.9 \times 20) + (F - 20) \times 4.9$$

from which $F = 49.4$ t/h.

Volumetric flow rate of solids $= 49.4 \times 1000/2900$

$$= 17.0 \text{ m}^3/\text{h}$$

Volumetric flow rate of water $= 49.4 \times 65/35$

$$= 91.7 \text{ m}^3/\text{h}$$

Therefore, flow rate of feed to the cyclone

$$= 17.0 + 91.7$$

$$= 108.7 \text{ m}^3/\text{h}$$

The use of dilution ratios in mass balancing

Water plays a very important role in mineral processing operations. Not only is it used as a transportation medium for the solids in the circuit, but it is also the medium in which most of the mineral separations take place. Individual processes require different optimum water contents. Ball mills, for instance, rarely operate below about 65% solids by weight, and the discharge may need diluting before being fed to hydrocyclones. Most flotation operations are performed at between 25 and 40% solids by weight, and some gravity concentration devices, such as Reichert cones, operate most efficiently on slurries containing 55–70% solids. A mineral processing plant is a large consumer of water. In a plant treating 10,000 t/d of ore, about 20 m^3/min of water is required, which is expensive if some form of conservation is not practised. If the slurry must be dewatered before feeding to a unit process, then the water should be used to dilute the feed as required elsewhere in the circuit. For optimum performance, therefore, there is a water requirement which produces optimum slurry composition in all parts of the circuit. The two-product formula is of great use in assessing water balances.

Consider a hydrocyclone fed with a slurry containing f% solids by weight, and producing two products – an underflow containing u% solids and an overflow containing v% solids. If the weight of solids per unit time in the feed, underflow, and overflow are F, U, and V respectively, then, providing the cyclone is operating under equilibrium conditions:

$$F = U + V \qquad (3.17)$$

The dilution ratio of the feed slurry $= (100 - f)/f = f'$. Similarly, the dilution ratio of the underflow $= (100 - u)/u = u'$ and dilution ratio of overflow $= (100 - v)/v = v'$.

Since the weight of water entering the cyclone must equal the weight leaving in the two products, the water balance is:

$$Ff' = Uu' + Vv' \qquad (3.18)$$

Combining Equations 3.17 and 3.18:

$$U/F = (f' - v')/(u' - v') \qquad (3.19)$$

Example 3.8

A cyclone is fed at the rate of 20 t/h of dry solids. The cyclone feed contains 30% solids, the underflow 50% solids, and the overflow 15% solids by weight. Calculate the tonnage of solids per hour in the underflow.

Solution

Dilution ratio of feed slurry $= 70/30 = 2.33$
Dilution ratio of underflow $= 50/50 = 1.00$
Dilution ratio of overflow $= 85/15 = 5.67$

A material balance on the cyclone gives:

$$20 = U + V$$

where U = tonnes of dry solids per hour in underflow; V = tonnes of dry solids per hour in overflow.

Since the weight of water entering the cyclone equals the weight of water leaving:

$$20 \times 2.33 = 1.00U + 5.67V$$

or

$$46.6 = U + 5.67(20 - U)$$

which gives

$$U = 14.3\,\text{t/h}$$

Example 3.9

A laboratory hydrocyclone is fed with a slurry of quartz (density 2650 kg/m^3) at a pulp density of 1130 kg/m^3. The underflow has a pulp density of 1280 kg/m^3 and the overflow 1040 kg/m^3.

A 2-litre sample of underflow was taken in 3.1 s. Calculate the mass flow rate of feed to the cyclone.

Solution

% solids content of feed (Equation 3.6)

$$= \frac{100 \times 2650 \times 130}{1130 \times 1650} = 18.5\%$$

Similarly:

% solids content of underflow $= 35.1\%$

% solids content of overflow $= 6.2\%$

Therefore, dilution ratios of feed, underflow, and overflow are 4.4, 1.8, and 15.1 respectively.

Volumetric flow rate of underflow $= 2/3.1$ litres/s

$$= \frac{2 \times 3600}{3.1 \times 1000}\,\text{m}^3/\text{h} = 2.32\,\text{m}^3/\text{h}$$

Therefore, mass flow rate of underflow (Equation 3.7)

$$= 2.32 \times 1280 \times 35.1/100 = 1.04\,\text{t/h}$$

Therefore, from a water balance on the cyclone:

$$4.4F = 1.04 \times 1.8 + (F - 1.04) \times 15.1$$

which gives mass flow rate of feed $(F) = 1.29$ t/h

In the example shown above, a two-product balance can be performed using pulp densities alone, obviating the need to convert to % solids and dilution ratios. The density of solids, therefore, need not be measured (assuming that this is the same in all three streams).

Since a material balance on the cyclone gives:

$$F = U + V$$

a balance of *slurry* weights gives:

$$\frac{F}{\%\text{ solids in feed}} = \frac{U}{\%\text{ solids in underflow}} + \frac{V}{\%\text{ solids in overflow}}$$

If f, u, and v are the pulp densities of feed, underflow, and overflow respectively, then from Equation 3.6:

$$\frac{Ff(s-1000)}{100s(f-1000)} = \frac{Uu(s-1000)}{100s(u-1000)} + \frac{Vv(s-1000)}{100s(v-1000)}$$

or

$$\frac{Ff}{f-1000} = \frac{Uu}{u-1000} + \frac{(F-U)v}{v-1000}$$

which gives

$$\frac{U}{F} = \frac{(f-v)(u-1000)}{(u-v)(f-1000)} \qquad (3.20)$$

Therefore, in Example 3.9,

$$\frac{U}{F} = \frac{(1130-1040)(1280-1000)}{(1280-1040)(1130-1000)}$$

$$= 0.81.$$

Water balances can be used to calculate circuit water requirements, and to determine the value of circulating loads.

Example 3.10

The flowsheet shown in Figure 3.23 illustrates a conventional closed circuit grinding operation.

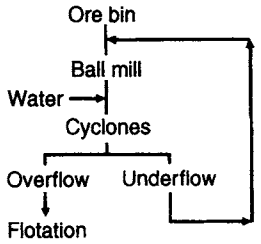


Figure 3.23 Closed circuit grinding flowsheet

The cyclone overflow line is instrumented with a magnetic flowmeter and nuclear density gauge, and the mass of dry ore fed to flotation is 25 t/h.

The feed from the fine ore bins is sampled, and is found to contain 5% moisture.

The cyclone feed contains 33% solids, the cyclone underflow 65% solids, and the overflow 15% solids.

Calculate the circulating load on the circuit and the amount of water required to dilute the ball mill discharge.

Solution

A water balance on the cyclone gives:

$$\frac{67F}{33} = \frac{85}{15} \times 25 + \frac{35U}{65}$$

where, F = cyclone feed (dry t/h); U = cyclone underflow (dry t/h).

The mass flow rate of feed from the ore bin = 25t/h (since input to circuit = output).

$$\text{Therefore, } F = 25 + U$$

and

$$(25 + U)\frac{67}{33} = 25 \times \frac{85}{15} + \frac{35U}{65}$$

from which $U = 61.0$ dry t/h.

The circulating load is therefore 61.0 t/h, and the circulating load ratio is $61.0/25 = 2.44$.

The ball mill feed = ore from bin + circulating load

Water in ball mill feed $= 25 \times 5/95 + 61.0 \times 35/65 = 34.2\,m^3/h$

Water in cyclone feed $= (25 + 61.0)67/33 = 174.6\,m^3/h$

Therefore, water requirement at cyclone feed
$= 174.6 - 34.2$
$= 140.4\,m^3/h$

Example 3.11

Calculate the circulating load in the grinding circuit shown in Figure 3.19 and the amounts of water added to the rod mill and cyclone feed.

Feed to rod mill = 55 t of dry ore per hour
Rod mill discharge = 62% solids
Cyclone feed = 48% solids
Cyclone overflow = 31% solids
Cyclone underflow = 74% solids

Solution

Since input to circuit = output, the cyclone overflow contains 55 t/h of solids.

A water balance on the cyclone gives:

$$(U + 55)\frac{52}{48} = \frac{26U}{74} + \frac{69}{31} \times 55$$

which gives $U = 85.8$ t/h.

The circulating load ratio is thus $85.8/55 = 1.56$.

Water in rod mill discharge $= 55 \times 38/62 = 33.7$ t/h

Therefore, water addition to rod mill is $33.7\,m^3/h$

Water in ball mill discharge $= 85.8 \times 26/74 = 30.1$ t/h

Water in cyclone feed $= (55 + 85.8) \times 52/48 = 152.5$ t/h

Therefore, water requirement to cyclone feed
$= 152.5 - (33.7 + 30.1) = 88.7$ t/h
$= 88.7\,m^3/h$

Example 3.12

The flowsheet shown in Figure 3.24 is that of a tin concentrator treating 30 dry tonnes per hour of ore.

The ore, containing 10% moisture, is fed into a rod mill which discharges a pulp containing 65% solids by weight. The rod mill discharge is diluted

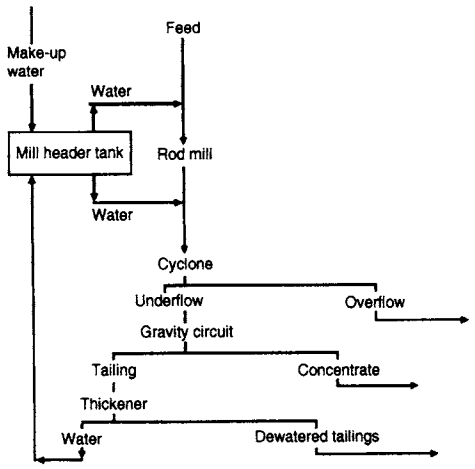


Figure 3.24 Tin concentrator circuit

to 30% solids before being pumped to cyclones. The cyclone overflows, at 15% solids, are pumped to the slimes treatment plant.

The cyclone underflows, at 40% solids, and containing 0.9% tin, are fed to a gravity concentration circuit, which produces a tin concentrate containing 45% tin, and a tailing containing 0.2% tin.

The tailing slurry, containing 30% solids by weight, is dewatered to 65% solids in a thickener, the overflow being routed to the mill header tank, which supplies water to the rod mill feed and rod mill discharge.

Calculate the flow rate of make-up water required for the header tank, and the water addition needed to the rod mill feed and discharge.

Solution

Water content of plant feed $= 30 \times 10/90 = 3.33$ t/h

Water content of rod mill feed $= 30 \times 35/65 = 16.2$ t/h

Therefore, water addition to rod mill feed

$$= 16.2 - 3.33 = 12.9 \text{ m}^3/\text{h}$$

Water content of cyclone feed $= 30 \times 70/30 = 70$ t/h

Therefore, water addition to cyclone feed

$$= 70 - 16.2 = 53.8 \text{ m}^3/\text{h}$$

A water balance on the cyclone gives:

$$30 \times 70/30 = (U \times 60/40) + (30 - U)85/15$$

which gives $U = 24.0$ t/h

The feed to the gravity concentrator is thus 24.0 t/h, containing 0.9% tin.

A mass balance on the gravity concentrator gives:

$$24.0 = C + T$$

where C = concentrate weight (t/h); T = tailings weight (t/h).

Since the weight of tin entering the plant equals the weight leaving:

$$24.0 \times 0.9/100 = [(24.0 - T) \times 45.0/100] + [T \times 0.2/100],$$

which gives $T = 23.6$ t/h.

Water in thickener feed $= 23.6 \times 70/30 = 55.1 \text{ m}^3/\text{h}$. Assuming no solids are lost in the thickener overflow, water in thickener underflow $= 23.6 \times 35/65 = 12.7 \text{ m}^3/\text{h}$. Therefore, water in thickener overflow

$$= 55.1 - 12.7 = 42.4 \text{ m}^3/\text{h}.$$

Therefore, make-up water required to header tank

$$= 53.8 + 12.9 - 42.4$$

$$= 24.3 \text{ m}^3/\text{h}.$$

Limitations of the two-product formula

Although of great use, the two-product formula does have limitations in plant accounting and control. The equations assume steady-state conditions, the fundamental assumption being that input is equal to output. While this may be true over a fairly long period, and so may be acceptable for daily, or shift, accounting, such dynamic equilibrium may not exist over a shorter period, such as the interval between successive onstream analyses of products.

Sensitivity of the recovery equation

Equation 3.16, defining recovery of a unit operation, is very sensitive to the value of t, as the equation represents the ratio of the two expressions c/f and $(c - t)/(f - t)$, which differ only by the presence of t in the latter. Equation 3.16 can be

partially differentiated with respect to f, c, and t to give:

$$\frac{\partial R}{\partial f} = \frac{100ct}{f^2(c-t)}$$

$$\frac{\partial R}{\partial c} = \frac{-100t(f-t)}{f(c-t)^2}$$

$$\frac{\partial R}{\partial t} = \frac{-100c(c-f)}{f(c-t)^2}$$

Since the variance of a function can be found from its derivatives:

$$V_{F(x)} = \sum_i \left(\frac{\partial F}{\partial x_i}\right)^2 V_{x_i} \qquad (3.21)$$

$$V_R = (\partial R/\partial f)^2\ V_f + (\partial R/\partial c)^2\ V_c + (\partial R/\partial t)^2\ V_t$$

where V_R, V_f, V_c, and V_t are the variances in R, f, c, and t respectively.

Therefore:

$$V_R = \frac{100^2}{f^2(c-t)^2}\left[\frac{c^2t^2}{f^2}\ V_f + \frac{(f-t)^2t^2}{(c-t)^2}V_c + \frac{c^2(c-f)^2}{(c-t)^2}V_t\right] \qquad (3.22)$$

Equation 3.22 is useful in assessing the error that can be expected in the calculated value of recovery due to errors in the measurement of f, c, and t.

For instance, in a concentrator which treats a feed containing 2.0% metal to produce a concentrate grading 40% metal and a tailing of 0.3% metal, the calculated value of recovery (Equation 3.16) is 85.6%, and:

$$V_R = 57.1V_f + 0.0003V_c + 2325.2V_t \qquad (3.23)$$

It is immediately apparent that the calculated value of recovery is most sensitive to the variance of the tailings assay, and is extremely insensitive to the variance of the concentrate assay.

If it is assumed that all the streams can be assayed to a relative standard deviation of 5%, then the standard deviations of feed, concentrate, and tailings streams are 0.1, 2, and 0.015% respectively, and, from Equation 3.23, $V_R = 1.1$, or the standard deviation of R is 1.05. This means that, to within 95% confidence limits, the recovery is $85.6 \pm 2.1\%$. (However it is worth remembering that constant relative error implies that smaller assays are better defined than large ones. This is often not true – see example 3.13.)

It is interesting to compare the expected error in the calculation of recovery from data in which little separation of the component values takes place. Suppose the feed, of 2.0% metal, separates into a concentrate of 2.2% metal and a tailing of 1.3% metal. The calculated recovery is, as before, 85.6%, and:

$$V_R = 6311V_f + 3155V_c + 738V_t$$

the value of recovery, in this case, being more dependent on the accuracy of the feed and concentrate assays than on the tailings assay. However, a relative standard deviation of 5% on each of the assay values produces a standard deviation in the recovery of 10.2%. The degree of accuracy obtained using the two-product formula is therefore dependent on the *extent* of the separation process and there must always be a significant difference between the component values (in this case assays) if reliable results are to be obtained.

Example 3.13

A copper concentrator has installed an on-stream analysis system on its process streams. The accuracy of the system is estimated to be:

% Cu	*Relative standard deviation (%)*
0.05–2.0	6–12
2.0–10.0	4–10
>10	2–5

The feed to a rougher bank is measured as 3.5% Cu, the concentrate as 18% Cu, and the tailing as 1% Cu. Calculate the recovery, and the uncertainty in its value.

Solution

Assuming relative standard deviations on feed, concentrate, and tailings assays of 4, 2, and 8% respectively, then the standard deviations are:

Feed	$4 \times 3.5/100 = 0.14\%$
Concentrate	$18 \times 2/100 = 0.36\%$
Tailings	$1 \times 8/100 = 0.08\%$

The calculated value of recovery (Equation 3.16) is 75.6%, and the variance in this value (Equation 3.22) is 5.7. Therefore, standard deviation on recovery is 2.4%, and, to a 95% confidence level, the uncertainty in the calculation of recovery is $\pm 2 \times 2.4 = \pm 4.8\%$.

(An Excel Spreadsheet – RECVAR – for such calculations is described in Appendix 3.)

Sensitivity of the mass equation

Equation 3.15 can be used to calculate the concentrate weight as a fraction or percentage (C) of the feed weight:

$$C = 100(f - t)/(c - t) \qquad (3.24)$$

Although expression 3.24 is very useful in material balancing, it is, like the recovery equation, prone to considerable error if the component values are not well separated. For example, a hydrocyclone is a separator which produces good separation in terms of contained water content, and of certain size fractions, but not necessarily in terms of contained metal values. When all such data is available, the problem is often deciding which component will produce the most accurate material balance.

If Equation 3.24 is partially differentiated with respect to f, c, and t respectively, then:

$$\partial C/\partial f = 100/(c - t)$$

$$\partial C/\partial c = -100(f - t)/(c - t)^2$$

$$\partial C/\partial t = -100(c - f)/(c - t)^2$$

From Equation 3.21, the variance in C, V_C can be determined from

$$V_C = (\partial C/\partial f)^2 V_f + (\partial C/\partial c)^2 V_c + (\partial C/\partial t)^2 V_t$$

$$= \left[\frac{100}{c - t}\right]^2 V_f + 100^2 \left[\frac{f - t}{(c - t)^2}\right]^2 V_c + 100^2 \left[\frac{(c - f)}{(c - t)^2}\right]^2 V_t \qquad (3.25)$$

This equation is called the "Propagation of Variance" and is a useful general rule. As all of the key terms are differences, the measurements with the largest differences will usually provide the best definition. The best defined separation will usually be the mineral (or metal) of commercial interest balanced across the entire concentrator. These ideas can also be extended to include process models within the balancing or accounting process (Richardson and Morrison, 2003).

Example 3.14

A unit spiral concentrator in a grinding circuit was sampled, and tin assays on feed and products were:

Feed	$0.92\% \pm 0.02\%$ Sn
Concentrate	$0.99\% \pm 0.02\%$ Sn
Tailings	$0.69\% \pm 0.02\%$ Sn

Pulp densities were also measured, and water–solid ratios were:

Feed	4.87 ± 0.05
Concentrate	1.77 ± 0.05
Tailings	15.73 ± 0.05

By means of sensitivity analysis, calculate the percentage of feed material reporting to the concentrate and the uncertainty in this value. Which component should be chosen for subsequent routine evaluations?

Solution

Assuming 95% confidence limits, the standard deviation in the tin assays is 0.01, and the variance is thus 1×10^{-4}. The value of C determined from tin assays (Equation 3.24) is 76.7%, and, from Equation 3.25, $V_c = 18.2$. The standard deviation, s, is thus 4.3, and the relative standard deviation in the mass calculation (s/C) is 0.06.

The standard deviation on measurement of water–solids ratio is 0.025, and the variance is 6.25×10^{-4}. The value of C calculated from water–solids ratio is 77.8%, and V_c is 0.05; therefore, s is 0.23. Relative standard deviation (s/C) is thus 0.003, this being lower than that obtained using tin assays. Water–solids ratio is therefore chosen for subsequent evaluations, being the less sensitive component.

Using water–solids ratio,

$C = 77.8\% \pm 0.46\%$ to 95% confidence limits.

(An Excel spreadsheet – MASSVAR – for such calculations is described in Appendix 3.)

Maximising the accuracy of two-product recovery computations

It has been shown that the recovery Equation (3.16) is very sensitive to the accuracy of the component values, and to the degree of separation that has taken place. Equation 3.16 can also be written as:

$$R = Cc/f \tag{3.26}$$

where

$$C = 100(f - t)/(c - t) \tag{3.24}$$

C represents the percentage of the total feed weight which reports to the concentrate. This value can often be calculated by using components other than the component whose recovery is being determined (Wills, 1985).

For instance, in a flotation concentrator treating a copper–gold ore, the recovery of gold into the concentrate may have to be assessed. If the gold assays are low (particularly the tailings assay), and not well separated, then the recovery from Equation 3.16 is prone to much uncertainty. However, if the copper assays are used to determine the value of C, then only the assays of gold in the concentrate and feed are required, the recovery being evaluated from Equation 3.26. The choice of "mass-fraction" component can be determined by sensitivity analysis. Equation 3.24 can be written as:

$$M = 100(a - d)/(b - d) \tag{3.27}$$

where a, b, and d are the mass-fraction components in feed, concentrate, and tailings respectively, these components being independent of f, c, and t, and M is the value of C calculated from these components. Hence:

$$R = Mc/f \tag{3.28}$$

From Equation 3.25:

$$V_M = \frac{100^2}{(b-d)^2}\left[V_a + \left(\frac{a-d}{b-d}\right)^2 V_b + \left(\frac{b-a}{b-d}\right)^2 V_d\right] \tag{3.29}$$

Providing that estimates of component variance are known, then V_M can be calculated. If a number of components (e.g. a complete size analysis) are available, Equation 3.29 can be used to select the least sensitive component as the mass-fraction component. The component will be that which produces the lowest value of relative standard deviation (RSD) in the mass calculations:

$$\text{RSD}(M) = V_M^{1/2}/M \tag{3.30}$$

Having chosen the mass-fraction component, the value of required component recovery can be calculated from:

$$R = 100c(a - d)/[f(b - d)] \tag{3.31}$$

The variance in calculation of recovery can be found from Equation 3.28, i.e.:

$$V_R = (\partial R/\partial M)^2 V_M + (\partial R/\partial c)^2 V_c + (\partial R/\partial f)^2 V_f$$

Therefore:

$$V_R = (c/f)^2 V_M + (M/f)^2 V_c + (Mc/f^2)^2 V_f \tag{3.32}$$

providing that c and f are independent of b and a.

Combining Equations 3.29 and 3.32:

$$V_R = \frac{100^2 c^2}{(b-d)^2 f^2}\left[V_a + \left(\frac{a-d}{b-d}\right)^2 V_b + \left(\frac{b-a}{b-d}\right)^2 V_d + \left(\frac{a-d}{c}\right)^2 V_c + \left(\frac{a-d}{f}\right)^2 V_f\right] \tag{3.33}$$

Should the mass-fraction component correspond to the recovery component, then Equation 3.22 must be used to express recovery variance.

Example 3.15

Calculate the recovery of tin into the concentrate of the spiral described in Example 3.14. Show how the accuracy of the recovery calculation is improved by using water–solids ratio as the mass-fraction component.

Solution

Using tin assays, the recovery of tin into the concentrate (Equation 3.16) is 82.5%, and, from Equation 3.22, V_R is 11.6. The standard deviation is thus 3.16, and:

Recovery $= 82.5 \pm 6.8\%$ to 95% confidence limits.

Since it was shown in Example 3.15 that the relative standard deviation in the mass calculation is lower when using water–solids ratio rather than

tin assays, water–solids ratio is chosen as the mass-fraction component, and, from Equation 3.28, $R = 83.7\%$, and, from Equation 3.33, $V_R = 1.60$, and standard deviation is 1.27. Therefore, recovery = $83.7 \pm 2.5\%$ to 95% confidence limits.

This method of maximising two-product recovery calculations is useful for assessment of unit operations, as once a preliminary survey has been made on the separator to determine the most suitable mass-fraction component, then this component can be routinely assessed for further evaluations with a high degree of confidence.

Introduction to mass balances on complex circuits

A concentrator, no matter how complex, can be broken down into a series of unit operations, each of which can be assessed by a two-product balance. For instance, in a complex flotation process, such a unit operation might be the composite feed to the roughing circuit, which splits into a rougher concentrate (cleaner feed) and rougher tailings (scavenger feed).

Example 3.16

25 t/h of ore containing 5% lead is fed to a bank of flotation cells.

A high-grade concentrate is produced, assaying 45% lead. The high-grade tailings assay 0.7% lead, and feed the low-grade cells, which produce a concentrate grading 7% lead. The low-grade tailings contain 0.2% lead. Calculate the weight of high- and low-grade concentrates produced per hour, and the recovery of lead produced in the bank of cells.

Solution

(a) *Balance on high-grade circuit*
From Equation 3.15:

$$C/25 = \frac{5 - 0.7}{45 - 0.7}$$

from which, $C = 2.43$ t/h.

Mass flow rate of high-grade tailings

$$= 25 - 2.43 = 22.57 \text{ t/h}$$

(b) *Balance on low-grade circuit*
From Equation 3.15:

$$\frac{C}{22.57} = \frac{0.7 - 0.2}{7 - 0.2}$$

from which, $C = 1.66$ t/h.

Weight of lead in concentrates

$$= \frac{2.43 \times 45}{100} + \frac{1.66 \times 7}{100}$$
$$= 1.21 \text{ t/h}.$$

Therefore, recovery of lead to concentrates

$$\frac{1.21 \times 100 \times 100}{25 \times 5} = 96.8\%$$

In this simple example it is not difficult to assess the number of streams which must be sampled in order to produce data for a unique set of equations for the system. However, in order to calculate a steady-state mass balance for an entire complex circuit, a more analytical method of generating n linear equations for n unknowns is required. Any plant flowsheet can be reduced to a series of *nodes*, where process streams either join or separate. *Simple nodes* have either one input and two outputs (a *separator*) or two inputs and one output (a *junction*) (Figure 3.25).



Figure 3.25 Simple nodes: (a) separator, (b) junction

It has been shown (Smith and Frew, 1983) that, providing the mass flow of a reference stream (usually the feed) is known, the minimum number of streams which must be sampled to ensure production of a complete circuit mass balance is

$$N = 2(F + S) - 1 \qquad (3.34)$$

where F = number of feed streams; S = number of simple separators.

The flowsheet described in Example 3.16 can be reduced to node form (Figure 3.26).

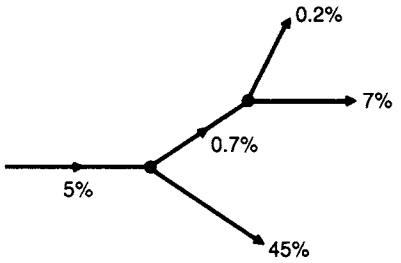


Figure 3.26 Simple node flowsheet

The circuit contains two simple separator nodes, and hence the minimum number of streams that must be sampled is:

$$2(1+2)-1=5$$

i.e. all streams must be sampled in order to produce a balance.

Separators which produce more than two products, or junctions which are fed by more than two streams, can be cascaded into simple nodes by connecting them with streams which have no physical existence. For instance, the flotation bank shown in Figure 3.27a can be reduced to node form (Figure 3.27b) and cascaded into simple nodes (Figure 3.27c).

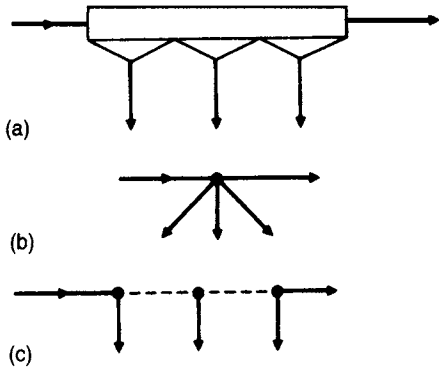


Figure 3.27 Flotation bank: (a) flowsheet, (b) in node form, (c) in simple nodes

The minimum number of streams that must be sampled is thus:

$$2(1+3)-1=7$$

and since only five streams can be sampled, two more weights are required to supplement the reference weight.

It can be seen from Figures 3.27b and 3.27c that a node producing two products can be cascaded to three simple separator nodes, and, in general, if a separator produces n products, then this can be cascaded to $n-1$ simple nodes. This is useful, as reducing a very complex plant to simple nodes, cascaded with non-existent streams, can lead to confusion and error. A procedure has been developed by Frew (1983) which allows easy automation and provides a check on the count-up of nodes from the flow diagram.

The method involves the use of the *connection-matrix C* (Cutting, 1976), where each element in the matrix is

$$C_{ij}=\begin{cases}+1 \text{ for stream } j \text{ flowing into the ith node}\\ -1 \text{ for stream } j \text{ flowing out of the ith node}\\ 0 \text{ for stream } j \text{ not appearing at the ith node}\end{cases}$$

The following examples illustrate the use of the method:

Consider the flowsheet shown in Fig 3.28a This can be reduced to the node flowsheet shown in Figure 3.28b.

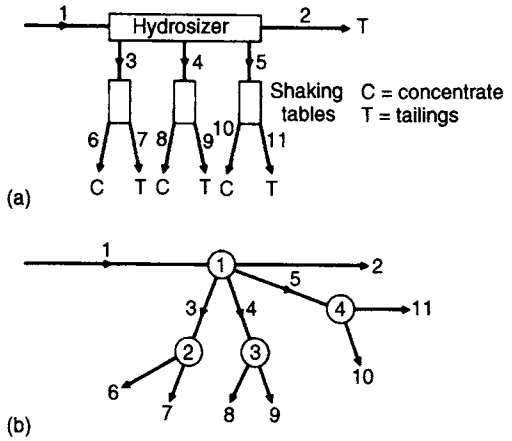


Figure 3.28 (a) Circuit flowsheet, (b) flowsheet in node form

There are eleven flowstreams and four nodes. The connection-matrix thus has eleven columns and four rows as shown below:

$$C=\begin{matrix}1 & -1 & -1 & -1 & -1 & 0 & 0 & 0 & 0 & 0 & 0\\ 0 & 0 & 1 & 0 & 0 & -1 & -1 & 0 & 0 & 0 & 0\\ 0 & 0 & 0 & 1 & 0 & 0 & 0 & -1 & -1 & 0 & 0\\ 0 & 0 & 0 & 0 & 1 & 0 & 0 & 0 & 0 & -1 & -1\end{matrix}$$

The contents of each column represent the individual streams, and when summed must equal

$+1, -1$, or 0, any other result indicating an error in the input of data,

$$\text{i.e. Column sum} = \begin{cases} +1 - \text{stream is a feed} \\ -1 - \text{stream is a product} \\ 0 - \text{stream is internal stream} \end{cases}$$

Therefore, summation of columns shows that stream 1 is a feed, streams 2, 6, 7, 8, 9, 10, and 11 are products, and streams 3, 4, and 5 are internal streams.

The elements of each row represent the individual nodes, and if the number of "+1" entries (n_p) and the number of "−1" entries (n_n) are counted, then n_p and n_n can be used to assess the number of simple nodes:

Number of simple junctions $(J) = n_p - 1$

Number of simple separators $(S) = n_n - 1$.

The nodes can now be classified as below:

Node	n_p	n_n	J	S
1	1	4	0	3
2	1	2	0	1
3	1	2	0	1
4	1	2	0	1
			0	6

There are thus six simple separators, and no junctions, and the minimum number of streams that must be sampled is:

$$2(1+6) - 1 = 13$$

Since there are only eleven available streams, two additional mass flows are required to supplement the reference stream in order to produce a balance. It is important that when additional mass flow measurements are required, no subset of flow measurements includes all streams at a node or group of nodes. Mass measurements on flowstreams 6 and 7, for example, will provide complete mass data for node 2 and a unique balance will not be produced.

Consider the circuit shown in Figure 3.29a. The circuit has been reduced to node form in Figure 3.29b. Note that the ball mill has been left out of this circuit, as it is an *abnormal node* where no separation takes place, and so there is no change in the overall assay or flow rate at steady state. Note that there will be a change in size distribution at this abnormal node, so size analysis data should not be used as the balancing components between nodes linked by this stream. Only components that are conserved at nodes can be used.

There are eleven flowstreams and six nodes, which can be represented by the connection-matrix:

$$C = \begin{matrix} 1 & 0 & 0 & 0 & 0 & 0 & 0 & 1 & 0 & 0 & -1 \\ 0 & -1 & -1 & 0 & 0 & 0 & 0 & 0 & 0 & 0 & 1 \\ 0 & 0 & 1 & 1 & -1 & 0 & 0 & 0 & 0 & 0 & 0 \\ 0 & 0 & 0 & 0 & 1 & -1 & 0 & 0 & -1 & 0 & 0 \\ 0 & 1 & 0 & 0 & 0 & 0 & -1 & 0 & 0 & -1 & 0 \\ 0 & 0 & 0 & 0 & 0 & 1 & 1 & -1 & 0 & 0 & 0 \end{matrix}$$

The column identifies streams 1 and 4 as feeds, streams 9 and 10 as products, and the other streams as internal flows.

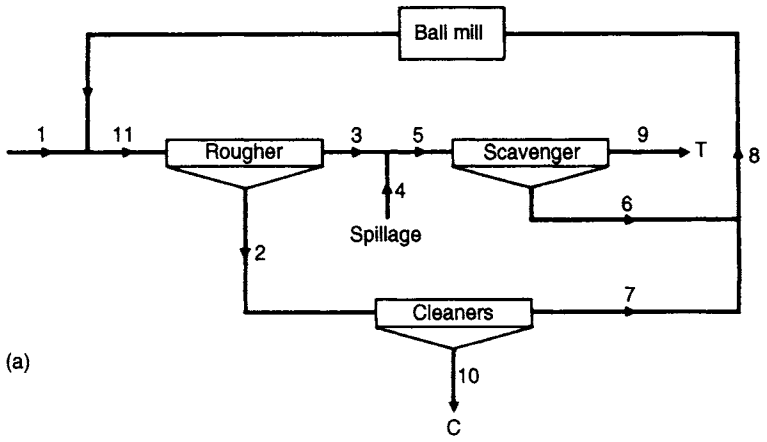


Figure 3.29 (a) Flotation flowsheet, (b) flotation circuit in node form

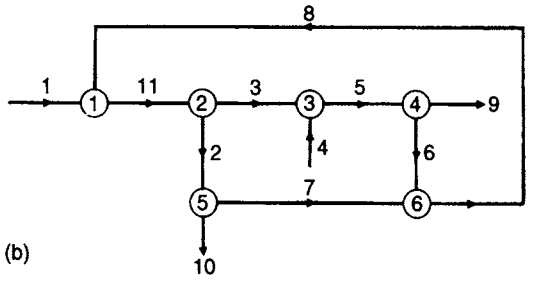


Figure 3.29 (*Continued*)

The node classification is:

Node	n_p	n_n	J	S
1	2	1	1	0
2	1	2	0	1
3	2	1	1	0
4	1	2	0	1
5	1	2	0	1
6	2	1	1	0
			3	3

The system thus consists of three simple junctions and three simple separators, and $N = 2(2 + 3) - 1 = 9$. Therefore, although there are eleven available streams, only nine need be sampled to produce a balance. In choosing the nine streams, all feeds and products should be part of the set and the connection matrix can be used to determine the choice of the remaining streams. If, in this example, stream 1 is the reference stream, then streams 2 to 11 are of unknown weight. Ten independent linear equations are therefore required to determine the mass flows of each stream relative to stream 1. A material balance can be performed on each node, giving six equations, and a component balance on the plant feeds and products provides an extra equation. Three component balances are thus required on the circuit nodes. It is apparent that if streams 3 and 7 are not sampled, then component balances are not possible on nodes which include either of these streams, i.e. nodes 2, 3, 5, and 6. Only two nodes are available for component balances, and insufficient independent equations are available. If, however, streams 3 and 5 are not sampled, then component balances are possible on nodes 1, 5, and 6, and a consistent set of equations is produced. It is also apparent that if sampling of only stream 3 is omitted, then ten linear equations can be produced from the six separate nodes, and the feed and product component balance becomes redundant. If the experimental data were entirely free of error, then the choice, if it exists, of the set of nine streams required would be of no consequence, as each complete set would yield an identical balance. Since experimental error does exist, the choice of flowstreams required to produce the balance is important, as certain streams may increase the sensitivity to error. For instance, a balance at a junction where little component separation takes place is prone to error. Smith and Frew (1983) have developed a sensitivity analysis technique which indicates which equations should be used in a minimum variance mass balance to obtain least sensitivity to data error. The procedures used also show that, where possible, measurement of mass flow should be performed, as this reduces sensitivity to experimental error. Each additional mass flow measurement reduces N by one, providing that, as stated earlier, the location for mass flow measurement is not chosen such that all the mass flows at any node are known, i.e. mass flows should not produce data which can be calculated from the available component measurements. In this respect, a concentrator can be reduced to a single separator node, such that if the feed mass flow rate is known, measurement of the concentrate mass flow rate enables the tailings mass flow rate to be directly calculated, so that although this information may be of use, it cannot be used in the overall balance.

It has been indicated that the connection matrix can be used to provide the set of linear equations that must be solved in order to produce the stream mass flow rates.

A material matrix, M, can be defined, where each element in the matrix is

$$M_{ij} = C_{ij}B_j$$

where B_j represents the mass flow rate of solids in stream j.

Using the flotation circuit (Figure 3.26) connection matrix as an example, each row in the matrix generates a linear equation representing a material balance. For instance, row 2 is:

$$C_{2j} = 0 - 1 - 100000001$$

and the material matrix M_{2j} at node 2 is thus:

$$-B_2 - B_3 + B_{11} = 0$$

A component matrix, A, can also be defined, where each matrix element is

$$A_{ij} = C_{ij}B_j a_j = M_{ij}a_j$$

a_j representing the component value (assay, % in size fraction, dilution ratio, etc.) in stream j, which gives at node 2:

$$-B_2a_2 - B_3a_3 + B_{11}a_{11} = 0$$

At any particular node, it is important that the same component is used to assess each stream, and the component should be chosen so as to produce an equation with least sensitivity to error. The component can be selected by sensitivity analysis, and providing that the same component is used at any particular node, other components can be used to balance other nodes in the circuit. This means that in a complex circuit balance, components such as metal content, dilution ratios, and size analyses may be utilised in various parts of the circuit (Wills, 1986).

Combining M_{ij} and A_{ij} into one matrix produces:

$$\begin{matrix} M_{11}M_{12} \cdots\cdots M_{1s} \\ M_{21}M_{22} \cdots\cdots M_{2s} \\ \cdot \\ \cdot \\ M_{n1}M_{n2} \cdots\cdots M_{ns} \\ A_{11}A_{12} \cdots\cdots A_{1s} \\ \cdot \\ \cdot \\ A_{n1}A_{n2} \cdots\cdots A_{ns} \end{matrix}$$

where $s =$ number of streams and $n =$ number of nodes.

If stream s is the reference stream (preferably a feed), and $B_s = 1$, then B_j represents the fraction of the reference stream reporting to stream j. Since $B_s = 1$, $M_{1s} = C_{1s}$, and $A_{1s} = C_{1s}a_s$.

Hence, in matrix form, the set of linear equations that must be solved is:

$$\begin{bmatrix} C_{11}.....C_{1(s-1)} \\ C_{21}.....C_{2(s-1)} \\ \cdot \\ \cdot \\ C_{n1}.....C_{n(s-1)} \\ C_{11}a_1.....C_{1(s-1)}a_{(s-1)} \\ C_{21}a_1.....C_{2(s-1)}a_{(s-1)} \\ \cdot \\ \cdot \\ C_{n1}a_1.....C_{n(s-1)}a_{(s-1)} \end{bmatrix} \begin{bmatrix} B_1 \\ B_2 \\ \cdot \\ \cdot \\ \cdot \\ \cdot \\ \cdot \\ \cdot \\ \cdot \\ B_{(s-1)} \end{bmatrix} = \begin{bmatrix} -C_{1s} \\ -C_{2s} \\ \cdot \\ \cdot \\ -C_{ns} \\ -C_{1s}a_s \\ -C_{2s}a_s \\ \cdot \\ \cdot \\ -C_{ns}a_s \end{bmatrix}$$

A further equation can be included in the set. The plant can be represented as a single node, such that the weight of contained component in the feed is equal to the component weight in the products. This equation should be used if possible, as there is usually very good component separation at this node. The material balance on this node cannot, however, be included in the set, as it is not independent of the set of material balance equations on the internal nodes.

Example 3.19

The circuit shown in Figure 3.30 is sampled, and the following results obtained:

Stream	*Assay % metal*
1	not sampled
2	0.51
3	0.12
4	16.1
5	4.2
6	25.0
7	not sampled
8	2.1
9	1.5

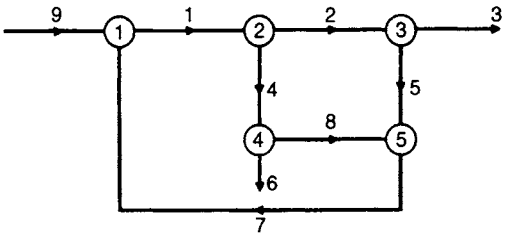


Figure 3.30 Flotation circuit in node form

Confirm by the use of the connection matrix that sufficient data has been obtained to calculate all the mass flow rates, and use the connection matrix to calculate the flows.

Solution

The connection matrix is:

−1	0	0	0	0	0	1	0	1
1	−1	0	−1	0	0	0	0	0
0	1	−1	0	−1	0	0	0	0
0	0	0	1	0	−1	0	−1	0
0	0	0	0	1	0	−1	1	0

The matrix confirms stream 9 as a feed, streams 3 and 6 as products, and the remaining streams as internal streams. The number of simple separators is equal to three, and so the minimum number of streams to be sampled (Equation 3.34) is

$$2(3+1)-1=7$$

Assuming stream $B_9=1$, then the material matrix (from the connection matrix) is:

$$\begin{matrix} -B_1 & 0 & 0 & 0 & 0 & 0 & B_7 & 0 & 1 \\ B_1 & -B_2 & 0 & -B_4 & 0 & 0 & 0 & 0 & 0 \\ 0 & B_2 & -B_3 & 0 & -B_5 & 0 & 0 & 0 & 0 \\ 0 & 0 & 0 & B_4 & 0 & -B_6 & 0 & -B_8 & 0 \\ 0 & 0 & 0 & 0 & B_5 & 0 & -B_7 & B_8 & 0 \end{matrix}$$

Since streams 1 and 7 were not sampled, component balances on nodes containing these streams cannot be performed. The component matrix (from nodes 3 and 4) is thus:

$$\begin{matrix} 0 & 0.51B_1 & -0.12B_3 & 0 & -4.2B_5 & 0 & 0 & 0 & 0 \\ 0 & 0 & 0 & 16.1B_4 & 0 & -25.0B_6 & 0 & -2.1B_8 & 0 \end{matrix}$$

In order to produce a square matrix, one further equation is required. If the whole circuit is considered as a simple node, then a component balance gives:

$$0.12B_3+25.0B_6-1.5=0.$$

Thus the streams sampled provide sufficient data, and the matrix which must now be solved is:

$$\begin{bmatrix} -1 & 0 & 0 & 0 & 0 & 0 & 1 & 0 \\ 1 & -1 & 0 & -1 & 0 & 0 & 0 & 0 \\ 0 & 1 & -1 & 0 & -1 & 0 & 0 & 0 \\ 0 & 0 & 0 & 1 & 0 & -1 & 0 & -1 \\ 0 & 0 & 0 & 0 & 1 & 0 & -1 & 1 \\ 0 & 0.51 & -0.12 & 0 & -4.2 & 0 & 0 & 0 \\ 0 & 0 & 0 & 16.1 & 0 & -25.0 & 0 & -2.1 \\ 0 & 0 & -0.12 & 0 & 0 & -25.0 & 0 & 0 \end{bmatrix} \begin{bmatrix} B_1 \\ B_2 \\ B_3 \\ B_4 \\ B_5 \\ B_6 \\ B_7 \\ B_8 \end{bmatrix} = \begin{bmatrix} -1 \\ 0 \\ 0 \\ 0 \\ 0 \\ 0 \\ 0 \\ -1.5 \end{bmatrix}$$

This matrix can be solved by Gaussian elimination and back-substitution to give:

$B_1=1.14$
$B_2=1.04$
$B_3=0.94$
$B_4=0.09$
$B_5=0.10$
$B_6=0.06$
$B_7=0.14$
$B_8=0.04$

The above example illustrates clearly the advantage of using the connection matrix to produce the necessary set of linear equations to evaluate the circuit. The seven streams sampled produced sufficient data for the evaluation. If, however, streams 2 and 8 had not been sampled, then component balances on nodes 2, 3, 4, and 5 would not have been possible, and insufficient linear equations would have been available.

The connection matrix is the basis for generalised computer packages for mass balancing which have been produced in recent years (Reid et al., 1982).

Software is now available for mass balancing such as Matbal, Bilmat (Hodouin et al., 1981), and JKMBal which allows the user to draw the flowsheet (Morrison and Richardson, 1991). More comprehensive packages have also been developed which use mass balancing as a step on the road to full metallurgical accounting and reconciliation, such as JKMetAccount (Morrison and Dunglison, 2005) and Sigmafine.

As suggested by the above analysis, quite general matrix–based solutions have been developed (Ramagnoli and Sanchez, 2000). Very complex hierarchical balance solutions have been developed to consider balancing of assays within each size fraction (Laguitton, 1985). Given the very large increase in the collection of mineral liberation data using automated mineralogical instruments, techniques are also being developed to carry out liberation balances.

Reconciliation of excess data

It has been shown that it is common practice in mass balancing computations to reduce the circuit to simple nodes, and to calculate relative mass flow rates by means of measured components. In many cases an excess of data is available at each node, such as multi-component size analyses, dilution rations, metal assays, etc., so that it is possible to calculate C (Equation 3.24) by a variety of routes, each route being independent of the others, and of apparently equal validity. The problem thus arising is which of these components should be used in order to produce a component balance, and hence which of the components becomes redundant. The approach which has become increasingly adopted is to use all the available data to compute a best estimate of C,

and to adjust the data to make the component values consistent with this estimate. These methods are complex when applied to circuits of arbitrary configuration, and require powerful computational facilities (Smith and Ichiyen, 1973; Hodouin and Everell, 1980; Hodouin et al., 1981; Reid et al., 1982). For simplicity, therefore, the techniques will be described in relation to simple nodes, as the computer programs required can readily be accommodated by a personal computer. It is worth noting that these techniques can be extended to reconciling (or balancing) from mine to product (Morrison et al., 2002). They need not be confined to the concentrator.

Two basic methods have commonly been adopted, both of which use a least-squares approach, and they can be broadly classified as:

(a) Minimisation of the sum of squares of the residuals in the component closure equations.
(b) Minimisation of the sum of squares of the component adjustments.

Minimisation of the sum of the squares of the closure residuals

In this method, the best-fit values of mass flow rates are calculated from the experimental data, after which the data is adjusted to accommodate these estimates (Finch and Matwijenko, 1977; Lynch, 1977; Tipman et al., 1978; Klimpel, 1979). If the simple separator streams are each sampled, and assayed for n components, then:

$$f_k - Cc_k - (1 - C)t_k = r_k \qquad (3.35)$$

for $k = 1$ to n, and where f_k represents the value of component k in the feed stream; c_k represents the value of component k in the concentrate stream; t_k represents component k in the tailings stream; r_k is the residual in the closure equation generated by experimental errors in the measurements of component k.

Equation 3.35 can be written as:

$$(f_k - t_k) - C(c_k - t_k) = r_k \qquad (3.36)$$

The objective of this method is to choose a value of C which minimises the sum of the squares of the closure errors; i.e. to minimise S, where:

$$S = \sum_{k=1}^{n} (r_k)^2 \qquad (3.37)$$

and by substitution from Equation 3.36:

$$S = \sum_{k=1}^{n} (f_k - t_k)^2 + C^2 \sum_{k=1}^{n} (c_k - t_k)^2 - 2C \sum_{k=1}^{n} (f_k - t_k)(c_k - t_k) \qquad (3.38)$$

The value of S cannot be zero at any value of C unless the data is consistent. However, it has a minimum value when $dS/dC = 0$ (Figure 3.31), i.e. when:

$$2\hat{C} \sum_{k=1}^{n} (c_k - t_k)^2 - 2 \sum_{k=1}^{n} (f_k - t_k)(c_k - t_k) = 0$$

where $\hat{C}$ = best-fit estimate of C.

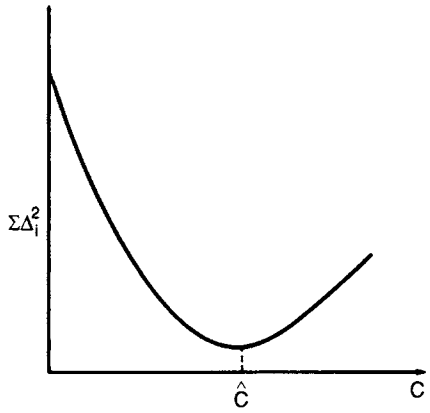


Figure 3.31 Plot of the sum of the squares of the component errors versus values of C

Therefore:

$$\hat{C} = \frac{\sum_{k=1}^{n} (f_k - t_k)(c_k - t_k)}{\sum_{k=1}^{n} (c_k - t_k)^2} \qquad (3.39)$$

this value being most influenced by the values of the components which are most altered by the separation process.

Having determined $\hat{C}$, the next stage is to adjust the component values to make them consistent with the calculated flow rates. The closure errors (Equation 3.35 must be distributed between the component values such that:

$$\hat{f}_k - \hat{C}\hat{c}_k - (1 - \hat{C})\hat{t}_k = 0 \qquad (3.40)$$

where $\hat{f}_k$, $\hat{c}_k$, and $\hat{t}_k$ are the best-fit values of component k in the three streams, i.e.

$$(f_k - f_{ka}) - \hat{C}(c_k - c_{ka}) - (1 - \hat{C})(t_k - t_{ka}) = 0 \quad (3.41)$$

where f_{ka}, c_{ka}, and t_{ka} are the adjustments to the kth component values in the three streams.

The closure Equation (3.35) can be written as:

$$f_k - \hat{C}c_k - (1 - \hat{C})t_k = r_k \quad (3.42)$$

and subtracting Equation 3.41 from this gives:

$$r_k = f_{ka} - \hat{C}c_{ka} - (1 - \hat{C})t_{ka}. \quad (3.43)$$

Using a least-squares approach, the sum of squares to be minimised is S_a, where:

$$S_a = \sum_{k=1}^{n}(f_{ka}^2 + c_{ka}^2 + t_{ka}^2) \quad (3.44)$$

subject to the constraint of Equation 3.43

This minimisation problem can be most conveniently solved by the method of Lagrangian multipliers. In this method, the constraints are expressed in such a way that they equal zero; i.e. Equation 3.43 becomes:

$$r_k - f_{ka} + \hat{C}c_{ka} + (1 - \hat{C})t_{ka} = 0 \quad (3.45)$$

The minimisation problem requires all the adjustments to be as small as possible, and the Lagrangian technique involves minimisation of the "Lagrangian L" defined as:

$$L = \sum_{k=1}^{n}(f_{ka}^2 + c_{ka}^2 + t_{ka}^2) + 2\sum_{k=1}^{n}\lambda_k(\text{constraint } k) \quad (3.46)$$

where $2\lambda_k$ is the Lagrangian multiplier for the constraint Equation k.

Thus:

$$L = S_a + 2\sum_{k=1}^{n}\lambda_k(r_k - f_{ka} + \hat{C}c_{ka} + (1 - \hat{C})t_{ka}) \quad (3.47)$$

L is differentiated with respect to each of the unknowns (adjustments and multipliers), and the derivatives are set to zero.

Hence, $\partial L/\partial f_{ka} = 2f_{ka} - 2\lambda_k = 0$

$$\text{i.e } f_{ka} = \lambda_k \quad (3.48)$$

$$\partial L/\partial c_{ka} = 2c_{ka} + 2\lambda_k\hat{C} = 0$$

$$\text{i.e } c_{ka} = -\lambda_k\hat{C} \quad (3.49)$$

$$\partial L/\partial t_{ka} = 2t_{ka} + 2\lambda_k(1 - \hat{C}) = 0$$

$$\text{i.e. } t_{ka} = -\lambda_k(1 - \hat{C}) \quad (3.50)$$

$$\partial L/\partial\lambda_k = 2(r_k - f_{ka} + \hat{C}c_{ka} + (1 - \hat{C})t_{ka} = 0$$

and substituting for f_{ka}, c_{ka}, and t_{ka}:

$$r_k = \lambda_k(1 + \hat{C}^2 + (1 - \hat{C})^2) = h\lambda_k,$$

$$\text{where } h = 1 + \hat{C}^2 + (1 - \hat{C})^2. \quad (3.51)$$

Hence:

$$f_{ka} = r_k/h \quad (3.52)$$

$$c_{ka} = -\hat{C}r_k/h \quad (3.53)$$

$$t_{ka} = -(1 - \hat{C})r_k/h. \quad (3.54)$$

Therefore, once $\hat{C}$ has been determined, h can be calculated from Equation 3.51, and r_k from Equation 3.42. The appropriate component value adjustments can then be calculated from Equations 3.52–3.54. The results of a six-component separation on a single node are presented in Table 3.8, together with adjusted data values, and a best-fit estimate of C.

Experimental and adjusted size analysis data on the streams from a hydrocyclone are tabulated in Table 3.9, U representing the proportion of the feed mass reporting to the cyclone underflow. The best estimate of U from the available data is 84.6%.

It is interesting to compare the results that are obtained if the data are presented in cumulative form rather than as a fractional distribution. Table 3.10 expresses the size analyses as cumulative oversize. It can be seen that the adjusted data differ slightly from the non-cumulative data, and the best-fit estimate of U is 85.2%. Identical results to those shown in Table 3.10 are produced by using cumulative undersize data. This clearly illustrates that the mass balance results obtained depend not only on the method which is used to deal with the

Table 3.8 Separator evaluation using minimisation of closure errors

Component	*Actual assay %*			*(C%)*	*Adjusted assay %*		
	Feed	*Conc.*	*Tails*		*Feed*	*Conc.*	*Tails*
Tin	21.90	43.00	6.77	41.76	20.78	43.41	7.47
Iron	3.46	5.50	1.76	45.45	3.25	5.58	1.89
Silica	58.00	25.10	75.30	34.46	57.16	25.41	75.83
Sulphur	0.11	0.12	0.09	66.67	0.10	0.12	0.09
Arsenic	0.36	0.38	0.34	50.00	0.36	0.38	0.34
TiO_2	4.91	9.24	2.07	39.61	4.79	9.28	2.15

Best-fit value of $C(\hat{C}) = 37.03\%$.

Table 3.9 Hydrocyclone stream analyses weight % in each fraction

Size range microns	*Experimental data*			*U(%)*	*Adjusted data*		
	Feed	*U/flow*	*O/flow*		*Feed*	*U/flow*	*O/flow*
+425	3.6	2.4	13.3	88.99	3.88	2.17	13.26
355–425	3.2	2.0	13.4	89.47	3.52	1.73	13.35
300–355	3.9	2.1	11.1	80.00	3.66	2.30	11.14
250–300	3.5	2.1	10.4	83.13	3.43	2.16	10.41
212–250	5.5	3.4	18.7	86.27	5.65	3.28	18.68
180–212	5.3	3.3	12.9	79.17	5.00	3.55	12.95
150–180	6.6	5.9	12.9	90.00	6.82	5.72	12.87
125–150	7.9	8.0	7.1	88.89	7.88	8.02	7.10
106–125	10.2	11.0	0.1	92.66	9.69	11.43	0.18
−106	50.3	59.8	0.1	84.09	50.48	59.65	0.07

Best estimate of $U(\%) = 84.60$.

Table 3.10 Hydrocyclone stream analyses cumulative oversize %

Size microns	*Experimental data*			*U(%)*	*Adjusted data*		
	Feed	*U/flow*	*O/flow*		*Feed*	*U/flow*	*O/flow*
425	3.6	2.4	13.3	88.99	3.84	2.20	13.27
355	6.8	4.4	26.7	89.24	7.32	3.96	26.62
300	10.7	6.5	37.8	86.58	10.95	6.29	37.76
250	14.2	8.6	48.2	85.86	14.35	8.47	48.18
212	19.7	12.0	66.9	85.97	19.94	11.79	66.86
180	25.0	15.3	79.8	84.96	24.91	15.38	79.81
150	31.6	21.2	92.7	85.45	31.70	21.11	92.68
125	39.5	29.2	99.8	85.41	39.59	29.13	99.79
106	49.7	40.2	99.9	84.09	49.32	40.52	99.96
−106	50.3	59.8	0.1	84.09	50.68	59.48	0.04

Best estimate of $U(\%) = 85.20$.

data, but also on the manner in which the information is presented. This is due to the difference in error structure in non-cumulative and cumulative data. On a cumulative basis, the errors are added and biases are introduced into the data, and because of this it is preferable to use non-cumulative data (Klimpel, 1979).

Minimisation of the sum of squares of the component adjustments

In this method, a residual is defined in each measured component, so that the calculated component values are consistent with estimated values of C (Mular, 1979b). The residuals are squared and summed, and the best-fit value of C is that which minimises this sum of squares. The objective, therefore, is to minimise S, where:

$$S = \sum_{i=1}^{3} \sum_{k=1}^{n} (x_{ik} - \hat{x}_{ik})^2 \qquad (3.55)$$

where n = number of component assays on each stream; x_{ik} = measured value of component k in stream i; $\hat{x}_{ik}$ = adjusted value of component k in stream i.

C is chosen iteratively such that Equation 3.40 is satisfied. The data adjustments which must be made in order to satisfy this condition can be calculated from Equations 3.42 and 3.51–3.54, and are used to calculate S. The method searches for a value of C which minimises the value of S.

Some workers (Wiegel, 1972; Cutting, 1979) solve this minimisation problem directly, by differentiating the Lagrangian equation (Equation 3.47) not only with respect to f_{ka}, c_{ka}, t_{ka}, and λ_{ka}, but also with respect to $\hat{C}$, which is not separately calculated from the raw data. The results obtained are identical to those achieved by iteration, but the direct method has computational advantages over iteration, particularly when assessing complex circuits. Combining Equations 3.42 and 3.47:

$$L = S_a + 2\sum_{k=1}^{n} \lambda_k [f_k - t_k - f_{ka} + t_{ka} - \hat{C}(c_k - t_k - c_{ka} + t_{ka})] \qquad (3.56)$$

Differentiating with respect to $\hat{C}$, and substituting for C_{ka} and t_{ka} (from Equations 3.53 and 3.54):

$$\partial L/\partial \hat{C} = -2\sum_{k=1}^{n} \lambda_k [c_k - t_k + (\hat{C} r_k/h) - \{(1-\hat{C}) r_k/h\}]$$

Setting this derivative to zero

$$\sum_{k=1}^{n} \lambda_k (c_k - t_k) + \left[\hat{C} \sum_{k=1}^{n} \lambda_k r_k/h\right] - \left[(1-\hat{C}) \sum_{k=1}^{n} \lambda_k r_k/h\right] = 0$$

and since $\lambda_k = r_k/h$:

$$\sum_{k=1}^{n} r_k (c_k - t_k)/h + \hat{C} \sum_{k=1}^{n} (r_k/h)^2 - (1-\hat{C}) \sum_{k=1}^{n} (r_k/h)^2 = 0 \qquad (3.57)$$

where $r_k = (f_k - t_k) - \hat{C}(c_k - t_k)$ (Equation 3.36)

and $h = 1 + \hat{C}^2 + (1-\hat{C})^2$ (Equation 3.51)

Equation 3.57 can be expanded and reduced to a quadratic equation, which can be written as:

$$\hat{C}^2(X - 2Z) + 2\hat{C}(Y - Z) + (2Z - Y) = 0 \qquad (3.58)$$

where

$$X = \sum_{k=1}^{n} (c_k - t_k)^2 \qquad (3.59)$$

$$Y = \sum_{k=1}^{n} (f_k - t_k)^2 \qquad (3.60)$$

$$Z = \sum_{k=1}^{n} (c_k - t_k)(f_k - t_k) \qquad (3.61)$$

This can be solved by applying the general solution to a quadratic:

$$C = \frac{-2(Y-Z) \pm \{[2(Y-Z)]^2 - 4(X-2Z)(2Z-Y)\}^{1/2}}{2(X-2Z)} \qquad (3.62)$$

Equation 3.62 has two roots, the +ve fraction being the true result. Once C is found, the data adjustment proceeds as before, according to Equations 3.52–3.54.

The two methods described have been compared by Wills and Manser (1985), who conclude that for most practical purposes the results achieved by both methods are essentially the same.

Weighting the adjustments

It is evident from the results of the six-component separation (Table 3.8) that $\hat{C}$ is biased towards the silica assay data, i.e. towards the assay values which are relatively high, but not necessarily most effectively separated. This is due to the assumption that the total absolute error in the experimental data is distributed equally to each assay value, or in other words that each assay value contains the same absolute error, which is highly unlikely in practice. It is more likely that the absolute error in each value is proportional to the assay itself (i.e. the *relative* error is constant), and where multi-component assays are used, as in the example discussed, each component may have a different relative error, which may also be dependent on the assay value. It is therefore preferable to weight the component adjustments such that good data is adjusted relatively less than poor data. The weighting factor which is most used is the inverse of the estimated component variance, such that Equation 3.55 becomes:

$$S = \sum_{i=1}^{3} \sum_{k=1}^{n} (x_{ik} - \hat{x}_{ik})^2 / V_{ik} \qquad (3.63)$$

where V_{ik} is the variance in the measurement of component k in stream i.

Similarly, the Lagrangian equation (Equation 3.56) becomes:

$$\begin{aligned} L = & \sum_{k=1}^{n} [(f_{ka}^2/V_{fk}) + (c_{ka}^2/V_{ck}) + (t_{ka}^2/V_{tk})] \\ & + 2 \sum_{k=1}^{n} \lambda_k [f_k - t_k - f_{ka} + t_{ka} \\ & - \hat{C}(c_k - t_k - c_{ka} + t_{ka})] \end{aligned} \qquad (3.64)$$

which can be solved by partial differentiation and reducing to a quadratic, as before.

If the variance is assumed proportional to the value of the assay, then Equation 3.63 becomes:

$$S = \sum_{i=1}^{3} \sum_{k=1}^{n} \left[\frac{x_{ik} - \hat{x}_{ik}}{e_k x_{ik}} \right]^2 \qquad (3.65)$$

where e_k = relative error in measurement of component k.

In the minimisation of closure residuals method, Equation 3.37 is weighted with the variances in the closure errors (V_{rk}):

$$S = \sum_{k=1}^{n} \frac{(r_k)^2}{V_{rk}} \qquad (3.66)$$

and since the variance of a function can be found from its derivatives (Equation 3.21), then for random changes (i.e. measurement errors) in f_k, c_k, and t_k:

$$V_{rk} = (\partial r_k/\partial f_k)^2 V_{fk} + (\partial r_k/\partial c_k)^2 V_{ck} + (\partial r_k/\partial t_k)^2 V_{tk}$$

so from Equation 3.42, as shown by Lynch (1977):

$$V_{rk} = V_{fk} + \hat{C}^2 V_{ck} + (1 - \hat{C})^2 V_{tk} \qquad (3.67)$$

where V_{fk}, V_{ck}, and V_{tk} are the variances in measurement of f, c, and t respectively for component k.

Equation 3.39 becomes:

$$\hat{C} = \frac{\dfrac{\sum_{k=1}^{n} (f_k - t_k)(c_k - t_k)}{V_{rk}}}{\dfrac{\sum_{k=1}^{n} (c_k - t_k)^2}{V_{rk}}} \qquad (3.68)$$

The expression for V_{rk} (Equation 3.67) contains $\hat{C}$, so the calculation must be performed iteratively. An estimated value of $\hat{C}$ is introduced into Equation 3.68, and a new value of $\hat{C}$ calculated. This value is used in the calculation until the estimated and calculated values converge, which is usually after only a few iterations. Once $\hat{C}$ has been determined, the data is adjusted as before, according to the following equations:

$$f_{ka} = \frac{r_k V_{fk}}{h_k} \qquad (3.69)$$

$$c_{ka} = \frac{-\hat{C} r_k V_{ck}}{h_k} \qquad (3.70)$$

$$t_{ka} = \frac{-(1 - \hat{C}) r_k V_{tk}}{h_k} \qquad (3.71)$$

where

$$h_k = V_{fk} + \hat{C}^2 V_{ck} + (1 - \hat{C})^2 V_{tk} \qquad (3.72)$$

Equations 3.69–3.72 being the weighted equivalents of Equations 3.51–3.54. Analysis of the six-component separation, assuming equal relative error on all assay data, produces very similar results using the methods of direct data adjustment and the closure residual minimisation method (Table 3.11), although this is not a general observation (Wills and Manser, 1985). It is evident, however, that

Table 3.11 Separation evaluation assuming equal relative error on assay values

Component	*Actual assay %*			*(C%)*	*Adjusted assay %*		
	Feed	*Conc.*	*Tails*		*Feed*	*Conc.*	*Tails*
Tin	21.90	43.00	6.77	41.76	21.80	43.16	6.78
Iron	3.46	5.50	1.76	45.45	3.36	5.61	1.78
Silica	58.00	25.10	75.30	34.46	55.87	25.26	77.41
Sulphur	0.11	0.12	0.09	66.67	0.10	0.12	0.09
Arsenic	0.36	0.38	0.34	50.00	0.36	0.38	0.34
TiO_2	4.91	9.24	2.07	39.61	4.98	9.13	2.06

Best-fit value of $C(\hat{C}) = 41.30\%$.

the bias towards the high value components (silica assays) has now been removed (see Appendix 3 for Excel spreadsheet – WEGHTRE – which reconciles excess data by a weighted least-squares method).

It has been proposed by Wills and Manser (1985) that a more significant estimate of $\hat{C}$ can be obtained by weighting the mean of the component calculations of C by the standard deviation in the calculation of each value of C, according to the equation:

$$\hat{C} = \frac{\sum_{k=1}^{n} \dfrac{(f_k - t_k)}{(c_k - t_k)(V_{ck})^{1/2}}}{\sum_{k=1}^{n} (1/V_{ck})^{1/2}}$$

where

$$V_{ck} = \frac{V_{fk}}{(c_k - t_k)^2} + \left[\frac{f_k - t_k}{(c_k - t_k)^2}\right]^2 V_{ck} + \left[\frac{c_k - f_k}{(c_k - t_k)^2}\right]^2 V_{tk}$$

Once $\hat{C}$ has been determined, the data values are adjusted as before, using Equations 3.69–3.72. An Excel spreadsheet (WILMAN) which reconciles excess data in this manner is described in Appendix 3, together with an evaluation of the six-component separation.

Design of experiments and plant trials

Successful process analysis and metallurgical accounting depends not only on collecting accurate data and analysing it properly, but on doing so according to appropriate statistical protocols. Much has been written about the design and analysis of experiments (Mason et al., 1989), and the classical statistical methods are eminently applicable to mineral processing and should be applied both in the laboratory and in the concentrator itself.

A common form of experiment is the plant trial, often conducted to compare some new condition such as a new flotation reagent or piece of equipment against the current arrangement to determine whether a process improvement can be achieved. It is essential that the correct protocol be followed in such cases. If not, the result will often be excessive time and costs in reaching a decision, or the wrong decision, or more often than not no decision at all. Several procedures are available for the conduct and analysis of plant trials (Cavender, 1993; Napier-Munn, 1995, 1998; Bruey and Briggs, 1997).

References

Alexander D.J., Bilney, T., and Schwarz, S. (2005). Flotation performance improvement at Placer Dome Kanowna Belle Gold Mine, *Proc. 37th Annual Meeting of the Canadian Mineral Processors*, CIM, Ottawa (Jan.), 171–201.

Anon. (1979). Instrumentation and process control, *Chemical Engng.* (Deskbook Issue), **86**(Oct. 15).

Atasoy, Y., Brunton, I., Tapia-Vergara, F., and Kanchibotla, S. (1998). Implementation of split to estimate the size distribution of rocks in mining and milling operations, *Proc. Mine to Mill Conf.*, AusIMM, Brisbane (Oct.), 227–234.

Barker, I.J. (1984). Advanced control techniques, *School on Measurement and Process Control in the Minerals Industry*, South Afr. IMM, Joburg (Jul.).

Bearman, R.A. and Milne, R. (1992). Expert systems: Opportunities in the minerals industries, *Min. Engng.*, **5**, 10–12.

Bergeron, A. and Lee, D.J. (1983). A practical approach to on-stream analysis, *Min. Mag.* (Oct.), 257.

Bernatowicz, et al. (1984). On-line coal analysis for control of coal preparation plants, in *Coal Prep. '84*, Industrial Presentations Ltd., Houston, 347.

Boyd, R. (2005). An innovative and practical approach to sampling of slurries for metallurgical accounting, *Proc. EMMES Conf.*, SAIMM Johannesburg (Nov.).

Bozic, S.M. (1979). *Digital and Kalman Filtering*, Edward Arnold, London.

Braden, T.F., Kongas, M., and Saloheimo, K. (2002). *Mineral Processing Plant Design, Practice and Control*, ed. A.L. Mular, D. Halbe, and D.J. Barrett, 2020–2047, SME, Littleton, Colorado.

Brochot, S., Villeneuve, J., Guillaneau, J.C., Durance, M.V., and Bourgeois, F. (2002). USIM PAC 3: Design of mineral processing plants from crushing to refining, *Proc. Mineral. Processing. Plant Design, Practice and Control*, SME, Vancouver, 479–494.

Bruey, F. and Briggs, D. (1997). The REFDIST method for design and analysis of plant trials, *Proc. 6th Mill Ops. Conf.*, AusIMM, Madang (Oct.), 205–207.

Carson, R. and Acornley, D. (1973). Sampling of pulp streams by means of a pneumatically operated poppet valve, *Trans. IMM* Sec. C, **82**(Mar.), 46.

Cavender, B.W. (1993). Review of statistical methods for the analysis of comparative experiments, *SME Annual Meeting*, Reno (Feb.), Preprint 93–182, 9.

Chang, J.W. and Bruno, S.J. (1983). Process control systems in the mining industry, *World Mining* (May), 37.

Clarkson, C.J. (1986). The potential for automation and process control in coal preparation, in *Automation for Mineral Resource Development – Proc. 1st IFAC Symposium*, Pergamon Press, Oxford, 247.

Considine, D.M. (ed.) (1974). *Process Instruments and Control Handbook*, McGraw-Hill Book Co., New York.

Cooper, H.R. (1984). Recent developments in on-line composition analysis of process streams, in *Control '84 Minerals/Metallurgical Processing*, ed. J.A. Herbst, AIMME, New York, 29.

Cutting, G.W. (1976). Estimation of interlocking mass-balances on complex mineral beneficiation plants, *Int. J. Min. Proc.*, **3**, 207.

Cutting, G.W. (1979). Material balances in metallurgical studies: Current use at Warren Spring Laboratory, *AIME Annual Meeting*, New Orleans, Paper 79–3.

Edwards, R., Vien, A., and Perry, R. (2002). Strategies for instrumentation and control of grinding circuits, in *Mineral Processing Plant Design, Practice and Control*, ed. A.L. Mular, D. Halbe, and D.J. Barrett, SME, 2130–2151.

Finch, J. and Matwijenko, O. (1977). Individual mineral behaviour in a closed-grinding circuit, *AIME Annual Meeting*, Atlanta, Paper 77–B–62 (Mar.).

Flintoff, B. (2002). Introduction to process control, *Mineral Processing Plant Design, Practice and Control*, ed. A.L. Mular, D. Halbe, and D.J. Barrett, SME, 2051–2065.

Flintoff, B.C., et al. (1991). Justifying control projects, *Plant Operators*, ed. D.N. Halbe et al., 45, SME Inc., Littleton.

Frew, J.A. (1983). Computer-aided design of sampling systems, *Int. J. Min. Proc.*, **11**, 255.

Gault, G.A., et al. (1979). Automatic control of flotation circuits, theory and operation, *World Mining* (Dec.), 54.

Gay S.L. (2004). Simple texture-based liberation modelling of ores. *Minerals. Engng.*, **17(11–12)**, Nov./Dec., 1209–1216.

Girdner, K., Kemeny, J., Srikant, A., and McGill, R. (1996). The Split system for analyzing the size distribution of fragmented rock, *Proc. FRAGBLAST-5 Workshop on Measurement of Blast Fragmentation*, ed. J. Franklin, and T. Katsabanis, Montreal, Quebec, Canada, 101–108.

Gy, P.M. (1979). *Sampling of Particulate Materials: Theory and Practice*, Elsevier Scientific Publishing Co., Amsterdam.

Hales, L. and Ynchausti, R. (1992). Neural networks and their use in prediction of SAG mill power, in *Comminution Theory and Practice*, ed. Kawatra, SME, 495–504.

Hales, L. and Ynchausti, R. (1997). Expert systems in comminution – Case studies, *Comminution Practices*, ed. S.K. Kawatra, SME, 57–68.

Harris, C.A. and Meech, J.A. (1987). Fuzzy logic: A potential control technique for mineral processing, *CIM Bull.*, **80**(Sept.), 51.

Hedvall, P. and Nordin, M. (2002). Plant designer: A crushing and screening modeling tool, *Proc. Mineral Processing Plant Design, Practice and Control*, SME, Vancouver, Canada, 421–441.

Herbst, J.A. and Rajamani, K. (1982). The application of modern control theory to mineral processing operation, in *Proc. 12th CMMI Cong.*, ed. H.W. Glenn, S. Afr., IMM, Joburg, 779.

Herbst, J.A. and Bascur, O.A. (1984). Mineral processing control in the 1980s – realities and dreams, in *Control '84 Mineral/Metallurgical Processing*, ed. J.A. Herbst et al., SME, New York, 197.

Herbst, J.A. and Bascur, O.A. (1985). Alternative control strategies for coal flotation, *Minerals and Metallurgical Processing*, **2**(Feb.), 1.

Hodouin, D. (1988). Dynamic simulators for the mineral processing industry, *Computer Applications in the Mineral Industry*, ed. K. Fytas et al. and A.A. Balkema, Rotterdam, 219.

Hodouin, D. and Everell, M.D. (1980). A hierarchical procedure for adjustment and material balancing of mineral processes data, *Int. J. Min. Proc.*, **7**, 91.

Hodouin, D. and Najim, K. (1992). Adaptive control in mineral processing. *CIM Bull.*, **85**, 70.

Hodouin, D., Kasongo, T., Kouame, E., and Everell, M.D. (1981). An algorithm for material balancing mineral processing circuits, *CIM Bull.*, **74**(Sept.), 123.

Hodouin, D., Jamsa-Jounela, S.-L., Carvalho, M.T., and Bergh, L. (2001). *Control Engineering Practice*, **9(9)**, Sept., 995–1005.

Holdsworth, M., Sadler, M., and Sawyer, R. (2002). Optimising concentrate production at the Green's Creek Mine. Preprint 02-62, SME Annual Meeting, Phoenix, 10.

Holmes, R.J. (1991). Sampling methods: Problems and solutions, in *Evaluation and Optimization of Metallurgical Performance*, ed. D. Malhotra et al., SME Inc., Littleton, Chapter 16.

Holmes, R. (2002). Sampling and measurement – the foundation of accurate metallurgical accounting, *Proc. Value Tracking Symp.*, AusIMM, Brisbane.

Ipek, H., Ankara, H., and Ozdag, H. (1999). The application of statistical process control, *Minerals. Engng.*, **12(7)**, 827–835.

Jenkinson, D.E. (1985). Coal preparation into the 1990s, *Colliery Guardian*, **223**(Jul.), 301.

Kawatra, S.K. (1985). The development and plant trials of an ash analyser for control of a coal flotation circuit, in *Proc. XV Int. Min. Proc. Cong.*, Cannes, **3**, 176.

Kawatra, S.K. and Cooper, H.R. (1986). On-stream composition analysis of mineral slurries, in *Design and Installation of Concentration and Dewatering Circuits*, ed. A.L. Mular and M.A. Anderson, SME Inc., Littleton, 641.

King, R.P. (1973). Computer controlled flotation plants in Canada and Finland, *NIM Report No. 1517*, South Africa.

King, R.P. (2001). *Modeling and Simulation of Mineral Processing Systems*, Butterworth-Heinemann, 403.

Klimpel, A. (1979). Estimation of weight ratios given component make-up analyses of streams, Paper 79–24, *AIME Annual Meeting*, New Orleans.

Krstev, B., and Golomeov, B. (1998). Use of evolutionary planning for optimisation of the galena flotation process, 27th APCOM, London, *Inst. Min. Met.*, Apr., 487–492.

Laguitton, D. (ed.) (1985). *The SPOC Manual Simulated Processing of Ore and Coal*, CANMET EMR, Canada.

Laguitton, D. and Leung, J. (1989). Advances in expert system applications in mineral processing, *Processing of Complex Ores*, ed. G.S. Dobby and S.R. Rao, Pergamon Press, New York, 565.

Leroux, D. and Hardie, C. (2003). Simulation of Closed Circuit Mineral Processing Operations using LimnR Flowsheet Processing Software, *Proc. CMP 2003 (Canadian Mineral Processor's 35th Annual Operator's Conference)*, CIM, Quebec (Jan.).

Leskinen, T., et al. (1973). Performance of on-stream analysers at Outokumpu concentrators, Finland, *CIM Bull.*, **66**(Feb.), 37.

Lundan, A. (1982). On-stream analysers improve the control of the mineral concentrator process, *ACIT '82 Convention*, Sydney, Australia (Nov.).

Lyman, G.J. (1981). On-stream analysis in mineral processing, in *Mineral and Coal Flotation Circuits*, ed. A.J. Lynch, et al., Elsevier Scientific Publishing Co., Amsterdam.

Lyman, G.J. (1986). Application of Gy's sampling theory to coal: A simplified explanation and illustration of some basic aspects, *Int. J. Min. Proc.*, **17**, 1–22.

Lyman, G.J. (1998). The influence of segregation of particulates on sampling variance-the question of distributional heterogeneity, *Int. J. Min. Proc.*, **55(2)**, 95–102.

Lynch, A.J. (1977). *Mineral Crushing and Grinding Circuits: Their Simulation, Optimisation, Design and Control*, Elsevier, 340.

Lynch, A.J., Johnson, N.W., Manlapig, E.V., and Thorne C.G. (1981). *Mineral and Coal Flotation Circuits*, Elsevier.

Mason, R.L, Gunst, R.F., and Hess, J.L. (1989). *Statistical Design and Analysis of Experiments*. Wiley, 692.

McKee, D.J. and Thornton, A.J. (1986). Emerging automatic control approaches in mineral processing, in *Mineral Processing at a Crossroads – Problems and Prospects*, ed. B.A. Wills and R.W. Barley, 117, Martinus Nijhoff, Dordrecht.

Meech, J.A. and Jordan, L.A. (1993). Development of a self-tuning fuzzy logic controller. *Minerals Engng.*, **6(2)**, 119.

Morrison, R.D. and Richardson, J.M. (1991). JKMBal – The mass balancing system. *Proc. Second Canadian Conference on Computer Applications for the Mineral Industry*, **1**, Vancouver, 275–286.

Morrison, R.D. and Richardson, J.M., (2002). JKSimMet – a simulator for analysis, optimisation and design of comminution circuits, *Proc. Mineral Processing Plant Design, Practice and Control*, SME, Vancouver, 442–460.

Morrison, R.D., Gu, Y., and McCallum, W. (2002). Metal balancing from concentrator to multiple sources. *Proc. Value Tracking Symp.*, AusIMM, Brisbane, 141–148.

Morrison, R.D. and Dunglison, M. (2005). Improving operational efficiency through corporate data reconciliation, *Proc. Proc. Systems '05*, Minerals Eng., Cape Town (Nov.).

Mular, A.L. (1979a). Process optimisation, in *Computer Methods for the 80s*, ed. A. Weiss, AIMME, New York.

Mular, A.L. (1979b). Data and adjustment procedures for mass balances, in *Computer Methods for the 80's in the Minerals Industry*, ed. A. Weiss, AIMME, New York.

Mular, A.L. (1989). Modelling, simulation and optimization of mineral processing circuits, in *Challenges in Mineral Processing*, ed. K.V.S. Sastry and M.C. Fuerstenau, SME, Inc., Littleton, 323.

Napier-Munn, T.J. (1995). Detecting performance improvements in trials with time-varying mineral processes, *Minerals Engng.*, **8(8)**, 843–858.

Napier-Munn, T.J. (1998). Analysing plant trials by comparing recovery-grade regression lines, *Minerals. Engng.*, **11(10)**, 949–958.

Napier-Munn, T.J. and Lynch, A.J. (1992). The modelling and computer simulation of mineral treatment processes – current status and future trends. *Minerals Engng.*, **5(2)**, 143.

Napier-Munn, T.J., Morrell, S., Morrison, R.D. and Kojovic, T. (1996). *Mineral Comminution Circuits: Their Operation and Optimisation*, JKMRC, University of Queensland, Brisbane, 413.

Owens, D.H. (1981). *Multivariable and Optimal Systems*, Academic Press, London.

Purvis, J.R. and Erickson, I. (1982). Financial models for justifying computer systems, *INTECH* (Nov.), 45.

Rajamani, K. and Hales, L.B. (1987). Developments in adaptive control and its potential in the minerals industry. *Minerals and Metallurgical Processing*, **4**(Feb.), 18.

Ramagnoli, J.A. and Sanchez, M.C. (2000). *Data Processing and Reconciliation for Chemical Process Operations*, Academic Press, 270.

Reid, K.J., et al. (1982). A survey of material balance computer packages in the mineral industry, in *Proc. 17th APCOM Symposium*, ed. T.B. Johnson and R.J. Barnes, AIME, New York, 41.

Richardson, J.M. and Morrison, R.D. (2003). Metallurgical balances and efficiency, in *Principles of Mineral Processing*, ed. M.C. Fuerstenau, and K.N.E. Han, SME, 363–389.

Salama, A.I.A., et al. (1985). Coal preparation process control, *CIM Bull.*, **78**(Sept.), 59.

Sastry, K.V.S. and Lofftus, K.D. (1989). Challenges and opportunities in modelling and simulation of mineral processing systems, in *Challenges in Mineral Processing*, ed. K.V.S. Sastry and M.C. Fuerstenau, SME, Inc., Littleton, 369.

Sastry, K.V.S. (1990). Principles and methodology of mineral process modelling, in *Control '90 – Mineral and Metallurgical Processing*, ed. R.K. Rajamani and J.A. Herbst, SME Inc., Littleton, 3.

Smith, P.L. (2001). A primer for sampling Solids, liquids, and gases: Based on the seven sampling errors of Pierre Gy, *Asa-Siam Series on Statistics and Applied Probability, Soc for Industrial & Applied Maths*, 96.

Smith, H.W. and Ichiyen, H.W. (1973). Computer adjustment of metallurgical balances, *CIM Bull.* (Sept.), 97.

Smith, H.W. and Frew, J.A. (1983). Design and analysis of sampling experiments – a sensitivity approach, *Int. J. Min. Proc.*, **11**, 267.

Strasham, A. and Steele, T.W. (1978). *Analytical Chemistry in the Exploration, Mining and Processing of Materials*, Pergamon Press, Oxford.

Tipman, R., Burnett, T.C., and Edwards, C.R. (1978). Mass balances in mill metallurgical operations, *10th Annual Meeting of the Canadian Mineral Processors*, CANMET, Ottawa.

Toop, A., et al. (1984). Advances in in-stream analysis, in *Mineral Processing and Extractive Metallurgy*, ed. M.J. Jones and P. Gill, IMM, London, 187.

Ulsoy, A.G. and Sastry, K.V.S. (1981). Principal developments in the automatic control of mineral processing systems, *CIM Bull.*, **74**(Dec.), 43.

Van der Spuy, D.V., Hulbert, D.G., Oosthuizen, D.J., and Muller, B. (2003). An on-line expert for mineral processing plants, *XXII IMPC*, SAIMM, Cape Town, Paper 368.

Wiegel, R.L. (1972). Advances in mineral processing material balances, *Can. Metall. Q.*, **11(2)**, 413.

Wills, B.A. (1985). Maximising accuracy of two-product recovery calculations, *Trans. Inst. Min. Metall.*, **94**(Jun.), C101.

Wills, B.A. (1986). Complex circuit mass balancing – a simple, practical, sensitivity analysis method, *Int. J. Min. Proc.*, **16**, 245.

Wills, B.A. and Manser, R.J. (1985). Reconciliation of simple node excess data, *Trans. Inst. Min. Metall.*, **94**(Dec.), C209.

Ziegler, J.G. and Nichols, N.B. (1942). Optimum settings for automatic controllers, *Trans. AIMME*, **64**, 759.

4

Particle size analysis

Introduction

Size analysis of the various products of a concentrator constitutes a fundamental part of laboratory testing procedure. It is of great importance in determining the quality of grinding and in establishing the degree of liberation of the values from the gangue at various particle sizes. In the separation stage, size analysis of the products is used to determine the optimum size of the feed to the process for maximum efficiency and to determine the size range at which any losses are occurring in the plant, so that they may be reduced.

It is essential, therefore, that methods of size analysis must be accurate and reliable, as important changes in plant operation may be made on the results of the laboratory tests. Since only relatively small amounts of material are used in the sizing tests, it is essential that the sample is representative of the bulk material and the same care should be taken over sampling for size analysis as for assay (Chapter 3).

Barbery (1972) derived an expression for the sample size necessary to meet the requirements of Gy's fundamental error in sampling (described also in Napier-Munn et al., 1996).

Particle size and shape

The primary function of precision particle analysis is to obtain quantitative data about the size and size distribution of particles in the material (Bernhardt, 1994; Allen, 1997). However, the exact size of an irregular particle cannot be measured. The terms "length", "breadth", "thickness", or "diameter" have little meaning because so many different values of these quantities can be determined. The size of a spherical particle is uniquely defined by its diameter. For a cube, the length along one edge is characteristic, and for other regular shapes there are equally appropriate dimensions.

For irregular particles, it is desirable to quote the size of a particle in terms of a single quantity, and the expression most often used is the "equivalent diameter". This refers to the diameter of a sphere that would behave in the same manner as the particle when submitted to some specified operation.

The assigned equivalent diameter usually depends on the method of measurement, hence the *particle-sizing technique should, wherever possible, duplicate the process one wishes to control.*

Several equivalent diameters are commonly encountered. For example, the *Stokes' diameter* is measured by sedimentation and elutriation techniques; the *projected area diameter* is measured microscopically and the *sieve-aperture diameter* is measured by means of sieving. The latter refers to the diameter of a sphere equal to the width of the aperture through which the particle just passes. If the particles under test are not true spheres, and they rarely are in practice, this equivalent diameter refers only to their second largest dimension.

Recorded data from any size analysis should, where possible, be accompanied by some remarks which indicate the approximate shape of the particles. Descriptions such as "granular" or "acicular" are usually quite adequate to convey the approximate shape of the particle in question.

Some of these terms are given below:

Acicular	needle-shaped
Angular	sharp-edged or having roughly polyhedral shape
Crystalline	freely developed in a fluid medium of geometric shape
Dendritic	having a branched crystalline shape
Fibrous	regular or irregularly thread-like
Flaky	plate-like
Granular	having approximately an equidimensional irregular shape
Irregular	lacking any symmetry
Modular	having rounded, irregular shape
Spherical	global shape

There is a wide range of instrumental and other methods of particle size analysis available. A short list of some of the more common methods is given in Table 4.1, together with their effective size ranges (these can vary greatly depending on the technology used), whether they can be used wet or dry and whether fractionated samples are available for later analysis.

Test sieving is the most widely used method for particle size analysis. It covers a very wide range of particle size, this range being the one of most industrial importance. So common is test sieving as a method of size analysis that particles finer than about 75 μm are often referred to as being in the "subsieve" range, although modern sieving methods allow sizing to be carried out down to about 5 μm. In recent years laser diffraction methods have also become common.

Table 4.1 Some methods of particle size analysis

Method	*Wet or dry*	*Fractionated sample?*	*Approx. useful size range* (microns)*
Test sieving	Both	Yes	5–100,000
Laser diffraction	Both	No	0.1–2,000
Optical microscopy	Dry	No	0.2–50
Electron microscopy	Dry	No	0.005–100
Elutriation (cyclosizer)	Wet	Yes	5–45
Sedimentation (gravity)	Wet	Yes	1–40
Sedimentation (centrifuge)	Wet	Yes	0.05–5

* A micron (μm) is 10^{-6} m

Sieve analysis

Sieve analysis is one of the oldest methods of size analysis and is accomplished by passing a known weight of sample material successively through finer sieves and weighing the amount collected on each sieve to determine the percentage weight in each size fraction. Sieving is carried out with wet or dry materials and the sieves are usually agitated to expose all the particles to the openings.

Sieving, when applied to irregularly shaped particles, is complicated by the fact that a particle with a size near that of the nominal aperture of the test sieve may pass only when presented in a favourable position. As there is inevitably a variation in the size of sieve apertures, due to irregularity of weaving, prolonged sieving will cause the larger apertures to exert an unduly large effect on the sieve analysis. Given time, every particle small enough could find its way through a very few such holes. The procedure is also complicated in many cases by the presence of "near-size" particles which cause "blinding", or obstruction of the sieve apertures, and reduce the effective area of the sieving medium. Blinding is most serious with test sieves of very small aperture size.

The process of sieving may be divided into two stages: first, the elimination of particles considerably smaller than the screen apertures, which should occur fairly rapidly and, second, the separation of the so-called "near-size" particles, which is a gradual process rarely reaching final completion. Both stages require the sieve to be manipulated in such a way that all particles have opportunities for passing the apertures, and so that any which blind an aperture may be removed from it. Ideally, each particle should be presented individually to an aperture, as is permitted for the largest aperture sizes, but for most sizes this is impractical.

The effectiveness of a sieving test depends on the amount of material put on the sieve (the "charge") and the type of movement imparted to the sieve.

A comprehensive account of sampling techniques for sieving is given in BS 1017–1 (Anon.,

1989a). Basically, if the charge is too large, the bed of material will be too deep to allow each one a chance to meet an aperture in the most favourable position for sieving in a reasonable time. The charge, therefore, is limited by a requirement for the maximum amount of material retained at the end of sieving appropriate to the aperture size. On the other hand, the sample must contain enough particles to be representative of the bulk, so a minimum size of sample is specified. In some cases, the sample will have to be subdivided into a number of charges if the requirements for preventing overloading of the sieves are to be satisfied.

Test sieves

Test sieves are designated by the nominal aperture size, which is the nominal central separation of opposite sides of a square aperture or the nominal diameter of a round aperture. A variety of sieve aperture ranges are currently used, the most popular being the German Standard, DIN 4188; ASTM standard, E11; the American Tyler series; the French series, AFNOR; and the British Standard, BS 1796.

Woven-wire sieves were originally designated by a mesh number, which referred to the number of wires per inch, which is the same as the number of square apertures per square inch. This has the serious disadvantage that the same mesh number on the various standard ranges corresponds to different aperture sizes, depending on the thickness of wire used in the woven-wire cloth. Sieves are now designated by aperture size, which gives the user directly the information needed.

Since some workers and the older literature still refer to sieve sizes in terms of mesh number, Table 4.2 lists mesh numbers for the British Standards series against nominal aperture size. A fuller comparison of several standards is given in Napier-Munn et al. (1996).

Wire-cloth screens are woven to produce nominally uniform square apertures within required tolerances (Anon., 2000a). Wire cloth in sieves with a nominal aperture of 75 μm and greater are plain woven, while those in cloths with apertures below 63 μm may be twilled (Figure 4.1).

Standard test sieves are not available with aperture sizes smaller than about 20 μm. Micromesh sieves are available in aperture sizes from 2 μm to 150 μm, and are made by electroforming nickel in square and circular mesh. Another popular type is the "micro-plate sieve", which is fabricated by electroetching a nickel plate. The apertures are in the form of truncated cones with the small circle uppermost (Figure 4.2). This reduces not only blinding but also the percentage open area, i.e. the

Table 4.2 BSS 1796 wire-mesh sieves

Mesh number	*Nominal aperture size* (μm)	*Mesh number*	*Nominal aperture size* (μm)
3	5600	36	425
3.5	4750	44	355
4	4000	52	300
5	3350	60	250
6	2800	72	212
7	2360	85	180
8	2000	100	150
10	1700	120	125
12	1400	150	106
14	1180	170	90
16	1000	200	75
18	850	240	63
22	710	300	53
25	600	350	45
30	500	400	38

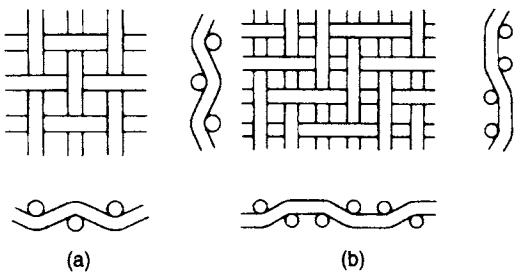


Figure 4.1 Weaves of wire cloth: (a) plain weave, (b) twilled weave

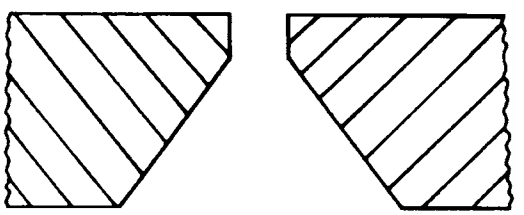


Figure 4.2 Cross-section of a micro-plate aperture

percentage of the total area of the sieving medium occupied by the apertures.

Micro-sieves are used for wet or dry sieving where a very high degree of accuracy is required in particle size analysis down to the very fine size range (Finch and Leroux, 1982). The tolerances in these sieves are much better than those for woven-wire sieves, the aperture being guaranteed to within 2 μm of nominal size.

For aperture sizes above about 1 mm, perforated plate sieves are often used, with round or square holes (Figure 4.3). Square holes are arranged in line with the centre points at the vertices of squares, while round holes are arranged with the centres at the apices of equilateral triangles (Anon., 2000b).

Choice of sieve sizes

In each of the standard series, the apertures of consecutive sieves bear a constant relationship to each other.

It has long been realised that a useful sieve scale is one in which the ratio of the aperture widths of adjacent sieves is the square root of $2(\sqrt{2}=1.414)$. The advantage of such a scale is that the aperture areas double at each sieve, facilitating graphical presentation of results.

Most modern sieve series are based on a fourth root of 2 ratio ($\sqrt[4]{2}=1.189$) or, on the metric scale, a tenth root of 10 ($\sqrt[10]{10}=1.259$), which makes possible much closer sizing of particles.

For most size analyses it is usually impracticable and unnecessary to use all the sieves in a particular series. For most purposes, alternative sieves, i.e. a $\sqrt{2}$ series, are quite adequate, whereas over certain size ranges of particular interest, or for accurate work, consecutive sieves, i.e. a $\sqrt[4]{2}$ series, may be used. Intermediate sieves should never be chosen at random, as the data obtained will be difficult to interpret.

In general, the sieve range should be chosen such that no more than about 5% of the sample is retained on the coarsest sieve, or passes the finest sieve. These limits, of course, may be lowered for more accurate work.

Testing methods

The general procedures for test sieving are comprehensively covered in BS 1796 (Anon., 1989b).

Machine sieving is almost universally used, as hand sieving is long and tedious, and its accuracy and precision depends to a large extent on the operator.

Sieves can be procured in a range of diameters, depending on the particle size and mass of material to be sieved. A common diameter for laboratory sieves is 200 mm.

The sieves chosen for the test are arranged in a stack, or *nest*, with the coarsest sieve on the top and the finest at the bottom. A tight-fitting pan or receiver is placed below the bottom sieve to receive the final undersize, and a lid is placed on top of the coarsest sieve to prevent escape of the sample.

The material to be tested is placed in the uppermost, coarsest sieve, and the nest is then placed in a sieve shaker which vibrates the material in a vertical plane (Figure 4.4), and, on some models, a horizontal plane. The duration of screening can be controlled by an automatic timer. During the shaking, the undersize material falls through successive sieves until it is retained on a sieve

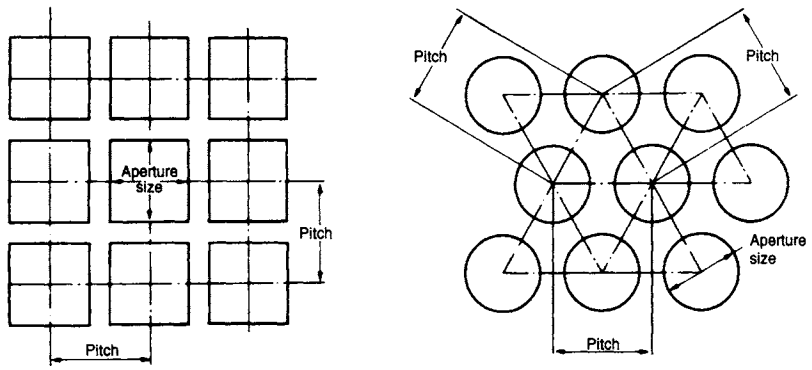


Figure 4.3 Arrangement of square and round holes in perforated plate sieves



Figure 4.4 Vibrating sieve shaker

having apertures which are slightly smaller than the diameter of the particles. In this way the sample is separated into size fractions.

After the required time, the nest is taken apart and the amount of material retained on each sieve weighed. Most of the near-mesh particles, which block the openings, can be removed by inverting the sieve and tapping the frame gently. Failing this, the underside of the gauze may be brushed gently with a soft brass wire or nylon brush. Blinding becomes more of a problem the finer the aperture, and brushing, even with a soft hair brush, of sieves finer than about 150 μm aperture tends to distort the individual meshes.

Wet sieving can be used on material already in the form of a slurry, or it may be necessary for powders which form aggregates when dry-sieved. A full description of the techniques is given in BS 1796 (Anon., 1989b).

Water is the liquid most frequently used in wet sieving, although for materials which are water-repellent, such as coal or sulphide ores, a wetting agent may be necessary.

The test sample may be washed down through a nest of sieves, with the finest sieve at the bottom. At the completion of the test the sieves, together with the retained oversize material, are dried at a suitable low temperature and weighed.

Presentation of results

There are several ways in which the results of a sieve test can be tabulated. The three most convenient methods are shown in Table 4.3 (Anon., 1989b). Table 4.3 shows:

(1) The sieve size ranges used in the test.
(2) The weight of material in each size range, e.g. 1.32 g of material passed through the 250 μm sieve, but was retained on the 180 μm sieve: the material therefore is in the size range −250 to +180 μm.

Table 4.3 Results of typical sieve test

(1) *Sieve size range* (μm)	(2) *Sieve fractions*	(3)	(4) *Nominal aperture size* (μm)	(5) *Cumulative %*	(6)
	wt (g)	*wt %*		*undersize*	*oversize*
+250	0.02	0.1	250	99.9	0.1
−250 to +180	1.32	2.9	180	97.0	3.0
−180 to +125	4.23	9.5	125	87.5	12.5
−125 to +90	9.44	21.2	90	66.3	33.7
−90 to +63	13.10	29.4	63	36.9	63.1
−63 to +45	11.56	26.0	45	10.9	89.1
−45	4.87	10.9			

(3) The weight of material in each size range expressed as a percentage of the total weight.
(4) The nominal aperture sizes of the sieves used in the test.
(5) The cumulative percentage of material passing through the sieves, e.g. 87.5% of the material is less than 125 μm in size.
(6) The cumulative percentage of material retained on the sieves.

The results of a sieving test should always be plotted graphically in order to assess their full significance (Napier-Munn et al., 1996).

There are many different ways of recording the results, the most common being that of plotting cumulative undersize (or oversize) against particle size. Although arithmetic graph paper can be used, it suffers from the disadvantage that points in the region of the finer aperture sizes tend to become congested. A semi-logarithmic plot avoids this, with a linear ordinate for percentage oversize or undersize and a logarithmic abscissa for particle size. Figure 4.5 shows graphically the results of the sieve test tabulated in Table 4.3.

It is not necessary to plot both cumulative oversize and undersize curves as they are mirror images of each other. A valuable quantity which can be determined from such curves is the "median size"

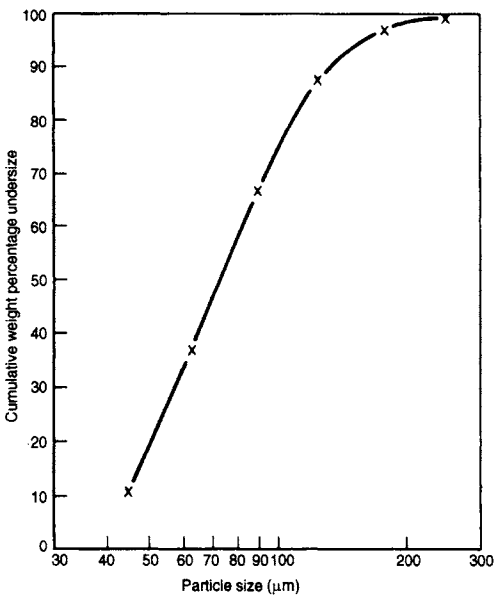


Figure 4.5 Screen analysis graph (Table 4.3)

of the sample. This refers to the mid-point in the size distribution –50% of the particles are smaller than this size and 50% are larger.

Size analysis is very important in assessing the performance of grinding circuits. The product size is usually quoted in terms of one point on the cumulative undersize curve, this often being the 80% passing size. Although this does not show on the overall size *distribution* of the material, it does facilitate routine control of the grinding circuit. For instance, if the target size is 80%–250 μm, then, for routine control, the operator needs only screen a fraction of the mill product at one size. If it is found that, say, 50% of the sample is –250 μm, then the product is too coarse, and control steps to remedy this can swiftly be made.

Many curves of cumulative oversize or undersize against particle size are S-shaped, leading to congested plots at the extremities of the graph. More than a dozen methods of plotting in order to proportion the ordinate are known. The two most common methods, which are often applied to comminution studies, where non-uniform size distributions are obtained, are the Gates-Gaudin-Schuhmann (Schuhmann, 1940) and the Rosin–Rammler (Rosin and Rammler, 1933–34) methods. Both methods are derived from attempts to represent particle size distribution curves by means of equations, which results in scales which, relative to a linear scale, are expanded in some regions and contracted in others.

In the Gates-Gaudin-Schuhmann method, cumulative undersize data are plotted against sieve aperture on log–log graph paper. As with most log–log plots, this very frequently leads to a straight line, over a wide range size, particularly over the finer sizes. Interpolation is much easier from a straight line than it is from a curve. Thus, if it known that data obtained from the material usually yield a straight-line plot, the burden of routine analysis can be greatly relieved, as relatively few sieves will be needed to check essential features of the size distribution.

Plotting on a log–log scale considerably expands the region below 50% in the cumulative undersize curve, especially that below 25%. It does, however, severely contract the region above 50%, and especially above 75%, which is a major disadvantage of the method (Figure 4.6).

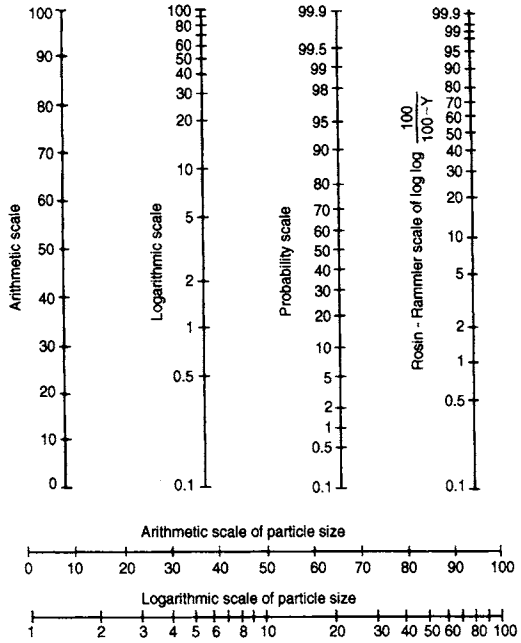


Figure 4.6 Comparison of scales

The Rosin–Rammler method is often used for representing the results of sieve analyses performed on material which has been ground in ball mills. Such products have been found to obey the following relationship:

$$100 - P = 100\exp(bd^n) \qquad (4.1)$$

where P is the cumulative undersize in per cent, b is a constant, d is the particle size, and n is a constant.

This can be rewritten as

$$\log\left[\ln\frac{100}{100-P}\right] = \log b + n\log d \qquad (4.2)$$

Thus, a plot of $\ln[100/(100-P)]$ versus d on log–log axes gives a line of slope n.

In comparison with the log–log method, the Rosin–Rammler plot expands the regions below 25% and above 75% cumulative undersize (Figure 4.6) and it contracts the 30–60% region. It has been shown, however, that this contraction is insufficient to cause adverse effects (Harris, 1971). The method is tedious to plot manually unless charts having the axes divided proportionally to $\log[\ln(100/(100-P))]$ and $\log d$ are used. However, it can easily be plotted in a spreadsheet.

The Gates-Gaudin-Schuhmann plot is often preferred to the Rosin–Rammler method in mineral processing applications, the latter being more often used in coal-preparation studies, for which it was originally developed. The two methods have been assessed by Harris (1971), who suggests that the Rosin–Rammler is in fact the better method for mineral processing applications. It is useful for monitoring grinding operations for highly skewed distributions, but, as noted by Allen (1997), it should be used with caution, since the method of taking logs always apparently reduces scatter, hence taking logs twice is not to be recommended.

Although cumulative size curves are used almost exclusively, the particle size distribution curve itself is sometimes more informative. Ideally, this is derived by differentiating the cumulative undersize curve and plotting the gradient of the curve obtained against particle size. In practice, the size distribution curve is obtained by plotting the retained fraction of the sieves against size. The points on the frequency curve may be plotted in between two sieve sizes. For example, material which passes through a 250 μm sieve, but is retained on a 180 μm sieve, may be regarded as having a mean particle size of 215 μm for the purpose of plotting. If the distribution is represented on a histogram, then the horizontals on the columns of the histogram join the various adjacent sieves used in the test. Unless each size increment is of equal width, however, the histogram has little value. Figure 4.7 shows the size distribution of the material in Table 4.3 represented on a frequency curve and a histogram.

Fractional curves or histograms are useful and rapid ways of visualising the relative frequency of occurrence of the various sizes present in the material. The only numerical parameter that can be obtained from these methods is the "mode" of the distribution, i.e. the most commonly occurring size.

For assessment of the metal losses in the tailings of a plant, or for preliminary evaluation of ores, assaying must be carried out on the various screen fractions. It is important, therefore, that the bulk sample satisfies the minimum sample weight requirement given by Gy's equation for the fundamental error (3.3).

Table 4.4 shows the results of a screen analysis performed on an alluvial tin deposit for preliminary evaluation of its suitability for treatment by gravity

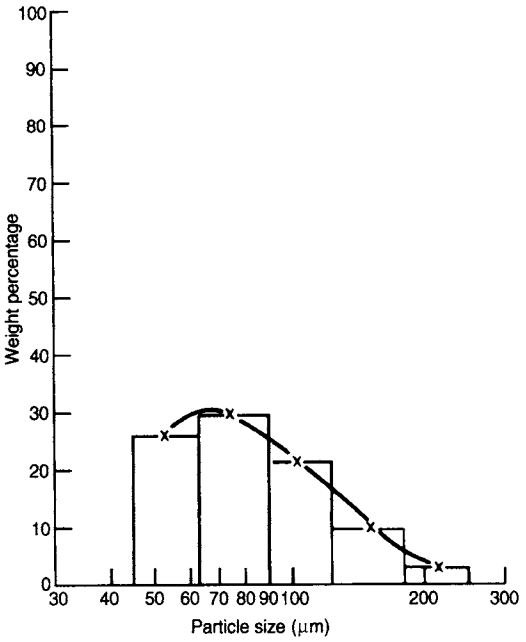


Figure 4.7 Fractional representation of screen analysis data

concentration. Columns 1, 2, and 3 show the results of the sieve test and assays, which are evaluated in the other columns. It can be seen that the calculated overall assay for the material is 0.21% Sn, but that the bulk of the tin is present within the finer fractions. The results show that, for instance, if the material was initially screened at 210 μm and the coarse fraction discarded, then the bulk required for further processing would be reduced by 24.9%, with a loss of only 4.6% Sn. This may be acceptable if mineralogical analysis shows that the tin is finely disseminated in this coarse fraction, which would necessitate extensive grinding to give reasonable liberation. Heavy liquid analysis (Chapter 11) on the −210 μm fraction would determine the theoretical grades and recoveries possible, but the screen analysis results also show that much of the tin (22.7%) is present in the −75 μm fraction, which constitutes only 1.9% of the total bulk of the material. This indicates that there may be difficulty in processing this material, as gravity separation techniques are not very efficient at such fine sizes.

Sub-sieve techniques

Sieving is rarely carried out on a routine basis below 38 μm; below this size the operation is referred to as *sub-sieving*. The most widely used methods are sedimentation, elutriation, microscopy, and laser diffraction, although many other techniques are available.

There are many concepts in use for designating particle size within the sub-sieve range, and it is important to be aware of them, particularly when combining size distributions determined by different methods. It is preferable to cover the range of a single distribution with a single method, but this is not always possible.

Conversion factors between methods will vary with sample characteristics and conditions, and with size where the distributions are not parallel. For spheres, many methods will give essentially the same result (Napier-Munn, 1985), but for irregular particles this is not so. Some approximate factors for a given characteristic size (e.g. P80) are

Table 4.4 Results of screen analysis to evaluate the suitability for treatment by gravity concentration

(1) *Size range* (μm)	*(2)* *Weight* (%)	*(3)* *Assay* (% *Sn*)	*Distribution* (% *Sn*)	*Size* (microns)	*Cumulative oversize* (%)	*Cumulative distribution* (% *Sn*)
+422	9.7	0.02	0.9	422	9.7	0.9
−422 + 300	4.9	0.05	1.2	300	14.6	2.1
−300 + 210	10.3	0.05	2.5	210	24.9	4.6
−210 + 150	23.2	0.06	6.7	150	48.1	11.3
−150 + 124	16.4	0.12	9.5	124	64.5	20.8
−124 + 75	33.6	0.35	56.5	75	98.1	77.3
−75	1.9	2.50	22.7			
	100.0	0.21	100.00			

given below (Austin and Shah, 1985; Napier-Munn, 1985; Anon., 1989b) – these should be used with caution:

Conversion	*Multiplying factor*
Sieve size to Stokes' diameter (sedimentation, elutriation)	0.94
Sieve size to projected area diameter (microscopy)	1.4
Sieve size to laser diffraction	1.5
Square mesh sieves to roundhole sieves	1.2

Stokes' equivalent diameter

In sedimentation techniques, the material to be sized is dispersed in a fluid and allowed to settle under carefully controlled conditions; in elutriation techniques, samples are sized by allowing the dispersed material to settle against a rising fluid velocity. Both techniques separate the particles on the basis of resistance to motion in a fluid. This resistance to motion determines the terminal velocity which the particle attains as it is allowed to fall in a fluid under the influence of gravity.

For particles within the sub-sieve range, the terminal velocity is given by the equation derived by Stokes (1891), namely:

$$v = \frac{d^2 g(D_s - D_f)}{18\,\eta} \tag{4.3}$$

where v is the terminal velocity of the particle ($m\,s^{-1}$), d is the particle diameter (m), g is the acceleration due to gravity ($m\,s^{-2}$), D_s is the particle density ($kg\,m^{-3}$), D_f is the fluid density ($kg\,m^{-3}$), and η is the fluid viscosity ($N\,s\,m^{-2}$); ($\eta = 0.001\,N\,s\,m^{-2}$ for water at 20 °C).

Stokes' law is derived for spherical particles; non-spherical particles will also attain a terminal velocity, but this velocity will be influenced by the shape of the particles. Nevertheless, this velocity can be substituted in the Stokes' equation to give a value of d, which can be used to characterise the particle. This value of d is referred to as the "Stokes' equivalent spherical diameter". It is also known as the "Stokes' diameter" or the "sedimentation diameter".

Stokes' law is only valid in the region of laminar flow (Chapter 9), which sets an upper size limit to the particles which can be tested by sedimentation and elutriation methods in a given liquid. The limit is determined by the particle Reynolds' number, a dimensionless quantity defined by

$$R = \frac{vdD_f}{\eta} \tag{4.4}$$

The Reynolds' number should not exceed 0.2 if the error in using Stokes' law is not to exceed 5% (Anon., 2001a). In general, Stokes' law will hold for all particles below 40 μm dispersed in water; particles above this size should be removed by sieving beforehand. The lower limit may be taken as 1 μm, below which the settling times are too long, and also the effects of unintentional disturbances, such as may be caused by convection currents, are far more likely to produce serious errors.

Sedimentation methods

Sedimentation methods are based on the measurement of the rate of settling of the powder particles uniformly dispersed in a fluid and the principle is well illustrated by the common laboratory method of "beaker decantation".

The material under test is uniformly dispersed in low concentration in water contained in a beaker or similar parallel-sided vessel. A wetting agent may need to be added to ensure complete dispersion of the particles. A syphon tube is immersed into the water to a depth of h below the water level, corresponding to about 90% of the liquid depth L.

The terminal velocity v is calculated from Stokes' law for the various sizes of particle in the material, say 35, 25, 15, and 10 μm. For an ore, it is usual to fix D_s for particles which are most abundant in the sample.

The time required for a 10 μm particle to settle from the water level to the bottom of the syphon tube, distance h, is calculated ($t = h/v$). The pulp is gently stirred to disperse the particles through the whole volume of water and then it is allowed to stand for the calculated time. The water above the end of the tube is syphoned off and all particles in this water are assumed to be smaller than 10 μm diameter (Figure 4.8). However, a fraction of the −10 μm material, which commenced settling

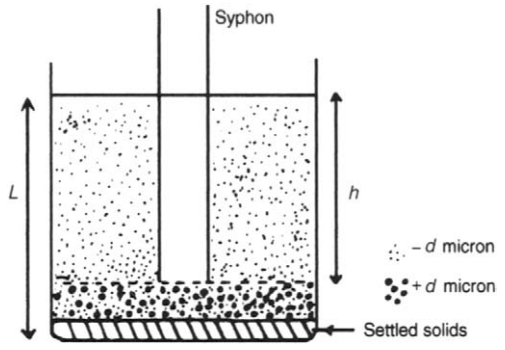


Figure 4.8 Beaker decantation

from various levels below the water level, will also be present in the material below the syphon level. In order to recover these particles, the pulp remaining must be diluted with water to the original level, and the procedure repeated until the decant liquor is essentially clear. In theory, this requires an infinite number of decantations, but in practice at least five treatments are needed, depending on the accuracy required. The settled material can be treated in a similar manner at larger separating sizes, i.e. at shorter decanting times, until a sufficient number of fractions is obtained.

The method is simple and cheap, and has the advantage over many other sub-sieve techniques in that it produces a true fractional size analysis, i.e. reasonable quantities of material in specific size ranges are collected, which can be analysed chemically and mineralogically.

This method is, however, extremely tedious, as long settling times are required for very fine particles, and separate tests must be performed for each particle size. For instance, a 25 μm particle of quartz has a settling velocity of $0.056\,\text{cm}\,\text{s}^{-1}$, and therefore takes about $3\frac{1}{2}$ min to settle 12 cm, a typical immersion depth for the syphon tube. Five separate tests to ensure a reasonably clear decant therefore require a total settling time of about 18 min. A 5 μm particle, however, has a settling velocity of $0.0022\,\text{cm}\,\text{s}^{-1}$, and therefore takes about $1\frac{1}{2}$ h to settle 12 cm. The total time for evaluation of such material is thus about 8 h. A complete analysis may therefore take an operator several days.

Another problem is the large quantity of water which dilutes the undersize material, due to repeated decantation. Theoretically an infinite number of decantations are required to produce a 100% efficient separation into oversize and undersize fractions, and the number of practical decantations must be chosen according to the accuracy required and the width of the size range required in each of the fractions.

In the system shown in Figure 4.8, after time t, all particles larger than size d have fallen to a depth below the level h.

All particles of a size d_1, where $d_1 < d$, will have fallen below a level h_1 below the water level, where $h_1 < h$.

The efficiency of removal of particles of size d_1 into the decant is thus:

$$\frac{h - h_1}{L}$$

since at time $t = 0$ the particles were uniformly distributed over the whole volume of liquid, corresponding to depth L, and the fraction removed into the decant is the volume above the syphon level, $h - h_1$.

Now, since $t = h/v$, and $v \propto d^2$,

$$\frac{h}{d^2} = \frac{h_1}{d_1^2}$$

Therefore the efficiency of removal of particles of size d_1

$$= \frac{h - h(d_1/d)^2}{L} = \frac{h[1 - (d_1/d)^2]}{L}$$
$$= a[1 - (d_1/d)^2] = E$$

where $a = h/L$.

If a second decantation step is performed, the amount of $-d_1$ material in the dispersed suspension is $1 - E$, and the efficiency of removal of $-d_1$ particles after two decantations is thus

$$E + (1 - E)E = 2E - E^2 = 1 - [1 - E]^2$$

In general, for n decantation steps, the efficiency of removal of particles of size d_1, at a separation size of d, is

$$= 1 - [1 - E]^n$$

$$\text{or efficiency} = 1 - \{1 - a[1 - (d_1/d)^2]\}^n \quad (4.5)$$

Table 4.5 shows the number of decantation steps required for different efficiencies of removal of various sizes of particle expressed relative to d, the separating size, where the value of $a = 0.9$. It can be shown (Heywood, 1953) that the value

Table 4.5 Number of decantations required for required efficiency of removal of fine particles

Relative particle size d_1/d	*Number of decantations*		
	90% *Efficiency*	95% *Efficiency*	99% *Efficiency*
0.95	25	33	50
0.9	12	16	25
0.8	6	8	12
0.5	2	3	4
0.1	1	1	2

of a has relatively little effect; therefore there is nothing to be gained by attempting to remove the suspension adjacent to the settled particles, thus risking disturbance and re-entrainment.

Table 4.5 shows that a large number of decantations are necessary for effective removal of particles close to the separation size, but that relatively small particles are quickly eliminated. For most purposes, unless very narrow size ranges are required, no more than about twelve decantations are necessary for the test.

A much quicker and less-tedious method of sedimentation analysis is the *Andreasen pipette technique* (Anon., 2001b).

The apparatus (Figure 4.9) consists of a half-litre graduated cylindrical flask and a pipette connected to a 10 ml reservoir by means of a two-way stopcock. The tip of the pipette is in the plane of the zero mark when the ground glass stopper is properly seated.

A 3–5% suspension of the sample, dispersed in the sedimentation fluid, usually water, is added to the flask. The pipette is introduced and the suspension agitated by inversion. The suspension is then allowed to settle, and at given intervals of time, samples are withdrawn by applying suction to the top of the reservoir, manipulating the two-way cock so that the sample is drawn up as far as the calibration mark on the tube above the 10 ml reservoir. The cock is then reversed, allowing the sample to drain into the collecting dish. After each sample is taken, the new liquid level is noted.

The samples are then dried and weighed, and the weights compared with the weight of material in the same volume of the original suspension.

There is a definite particle size, D, corresponding to each settling distance h and time t, and this

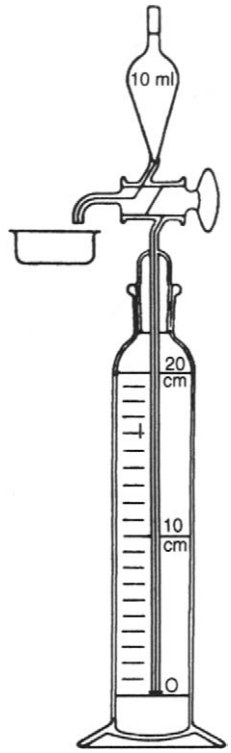


Figure 4.9 Andreasen pipette

represents the size of the largest particle that can still be present in the sample. These particle sizes are calculated from Stokes' law for the various sampling times. The weight of solids collected, g, compared with the corresponding original weight, g_o, i.e. g/g_o then represents the fraction of the original material having a particle size smaller than D, which can be plotted on the size-analysis graph.

The method is much quicker than beaker decantation, as samples are taken off successively throughout the test for increasingly finer particle sizes. For example, although 5 μm particles of quartz will take about $2\frac{1}{2}$ h to settle 20 cm, once this sample is collected, all the coarser particle-size samples will have been taken, and so the complete analysis, in terms of settling times, is only as long as the settling time for the finest particles.

The disadvantage of the method is that the samples taken are each representative of the particles smaller than a particular size, which is not as valuable, for mineralogical and chemical analysis, as samples of various size *ranges*, as are produced by beaker decantation.

Sedimentation techniques tend to be very tedious, due to the long settling times required for fine particles (up to 5 h for 3 μm particles) and the time required to dry and weigh the samples. The main difficulty, however, lies in completely dispersing the material within the suspending liquid, such that no agglomeration of particles occurs. Combinations of suitable suspending liquids and dispersing agents for various metals are given in BS ISO 13317–1 (Anon., 2001a).

Although the Andreasen pipette is perhaps the most widely used method of sizing by sedimentation, various other techniques have been developed, which attempt to speed up testing. Examples of these methods, which are comprehensively reviewed by Allen (1997), are the photo-sedimentometer, which combines gravitational settling with photo-electric measurement, and the sedimentation balance, in which the weight of material settling out onto a balance pan is recorded against time, to produce a cumulative sedimentation size analysis.

Elutriation techniques

Elutriation is a process of sizing particles by means of an upward current of fluid, usually water or air. The process is the reverse of gravity sedimentation, and Stokes' law applies.

All elutriators consist of one or more "sorting columns" (Figure 4.10) in which the fluid is rising at a constant velocity. Feed particles introduced into the sorting column will be separated into two fractions, according to their terminal velocities, calculated from Stokes' law.

Those particles having a terminal velocity less than that of the velocity of the fluid will report to the overflow, while those particles having a greater terminal velocity than the fluid velocity will sink to the underflow. Elutriation is carried out until there are no visible signs of further classification taking place or the rate of change in weights of the products is negligible.

This involves the use of much water, involving dilution of the undersize fraction, but it can be shown that this is not as serious as in beaker decantation. Consider a sorting column of depth h, sorting material at a separating size of d. If the upward velocity of water flow is v, then by Stokes' law, $v \propto d^2$.

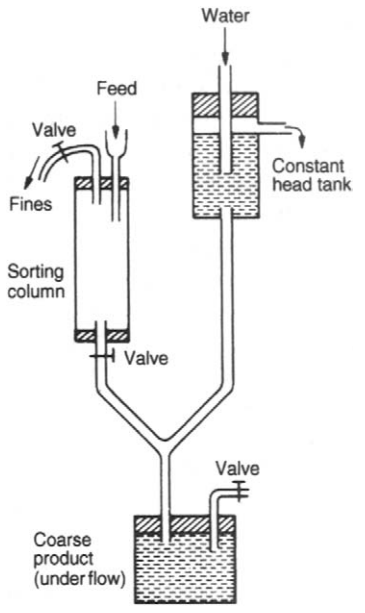


Figure 4.10 Simple elutriator

Particles smaller than the separating size d will move upwards in the water flow at a velocity dependent on their size.

Thus, particles of size d_1, where $d_1 < d$, will move upwards in the sorting column at a velocity v_1, where $v_1 \propto (d^2 - d_1^2)$.

The time required for a complete volume change in the sorting column is h/v, and the time required for particles of size d_1 to move from the bottom to the top of the sorting column is h/v_1.

Therefore the number of volume changes required to remove all particles of size d_1 from the sorting column

$$= \frac{h/v_1}{h/v} = \frac{d^2}{d^2 - d_1^2} = \frac{1}{1 - (d_1/d)^2}$$

The number of volume changes required for various values of d_1/d are:

d_1/d	*Number of volume changes required*
0.95	10.3
0.9	5.3
0.8	2.8
0.5	1.3
0.1	1.0

Comparing these figures with those in Table 4.1, it can be seen that the number of volume changes required is far less with elutriation than it is with decantation. It is also possible to achieve complete separation by elutriation, whereas this can only be achieved in beaker decantation by an infinite number of volume changes.

Elutriation thus appears more attractive than decantation, and has certain practical advantages in that the volume changes need no operator attention. It suffers from the disadvantage, however, that the fluid velocity is not constant across the sorting column, being a minimum at the walls of the column, and a maximum at the centre. The separation size is calculated from the mean volume flow, so that some coarse particles are misplaced in the overflow, and some fines are misplaced into the coarse overflow. The fractions thus have a considerable overlap in particle size and are not sharply separated. Although the decantation method never attains 100% efficiency of separation, the lack of sharpness of the division into fractions is much less than that due to velocity variation in elutriation (Heywood, 1953).

Elutriation is limited at the coarsest end by the validity of Stokes' law, but most materials in the sub-sieve range exhibit laminar flow. At the fine end of the scale, separations become impracticable below about 10 μm, as the material tends to agglomerate, or extremely long separating times are required. Separating times can be considerably decreased by utilisation of centrifugal forces, and one of the most widely used methods of sub-sieve sizing in modern mineral processing laboratories is the Warman cyclosizer (Finch and Leroux, 1982), which is extensively used for routine testing and plant control in the size range 8–50 μm for materials of specific gravity similar to quartz (sp. gr. 2.7), and down to 4 μm for particles of high specific gravity, such as galena (sp. gr. 7.5).

The cyclosizer unit consists of five cyclones (see Chapter 9 for a full description of the principle of the hydrocyclone), arranged in series such that the overflow of one unit is the feed to the next unit (Figure 4.11).

The individual units are inverted in relation to conventional cyclone arrangements, and at the apex of each, a chamber is situated so that the discharge is effectively closed (Figure 4.12).

Water is pumped through the units at a controlled rate, and a weighed sample of solids is introduced ahead of the cyclones.

The tangential entry into the cyclones induces the liquid to spin, resulting in a portion of the liquid, together with the faster-settling particles, reporting to the apex opening, while the remainder of the liquid, together with the slower settling particles, is discharged through the vortex outlet and into the next cyclone in the series. There is a successive decrease in the inlet area and vortex outlet diameter of each cyclone in the direction of the flow, resulting in a corresponding increase in inlet velocity and an increase in the centrifugal forces within the cyclone, resulting in a successive decrease in the limiting particle-separation size of the cyclones.

The cyclosizer is manufactured to have definite limiting separation sizes at standard values of

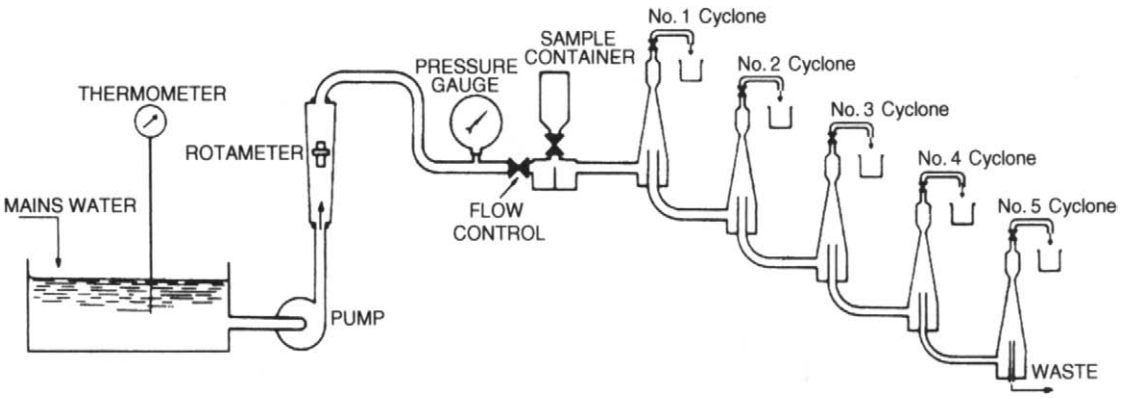


Figure 4.11 Warman cyclosizer

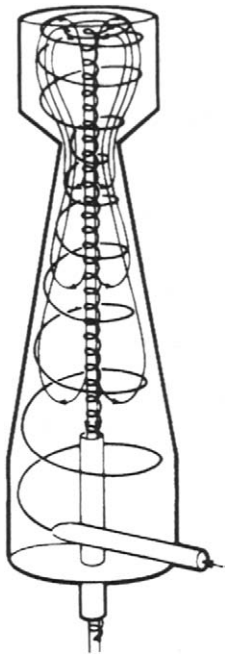


Figure 4.12 Flow pattern inside a cyclosizer cyclone unit

the operating variables, viz. water flow rate, water temperature, particle density, and elutriation time. To correct for practical operation at other levels of these variables, a set of correction graphs is provided.

Complete elutriation normally takes place after about 20 min, after which the sized fractions are collected by discharging the contents of each apex chamber into separate beakers.

Microscopic sizing and image analysis

Microscopy can be used as an absolute method of particle size analysis since it is the only method in which individual mineral particles are observed and measured (Anon., 1993; Allen, 1997). The image of a particle seen in a microscope is two-dimensional and from this image an estimate of particle size must be made. Microscopic sizing involves comparing the projected area of a particle with the areas of reference circles, or *graticules*, of known sizes, and it is essential for meaningful results that the mean projected areas of the particles are representative of the particle size. This requires a random orientation in three dimensions of the particle on the microscope slide, which is unlikely in most cases.

The optical microscope method is applicable to particles in the size range 0.8–150 μm, and down to 0.001 μm using electron microscopy.

Basically, all microscopy methods are carried out on extremely small laboratory samples, which must be collected with great care in order that they may be truly representative.

In manual optical microscopy, the dispersed particles are viewed by transmission, and the areas of the magnified images are compared with the areas of circles of known sizes inscribed on a graticule.

The relative numbers of particles are determined in each of a series of size classes. These represent the size distribution by number, from which it is possible to calculate the distribution by volume and, if all the particles have the same density, the distribution by weight.

Manual analysis of microscope slides is tedious and error prone; semi-automatic and automatic systems have been developed which speed up analyses and reduce the tedium of manual methods (Allen, 1997).

The development of quantitative image analysis has made possible the rapid sizing of fine particles using small laboratory samples. Image analysers accept samples in a variety of forms – photographs, electron micrographs, and direct viewing – and are often integrated in system software. Figure 4.13 shows the grayscale electron backscatter image of a group of mineral particles obtained with a scanning electron microscope; grains of chalcopyrite (Ch), quartz (Qtz), and epidote (Epd) are identified in the image. On the right are plotted the size distributions of the "grains" of the mineral chalcopyrite (i.e, the pieces of chalcopyrite identified by the instrument, whether liberated or not) and the "particles" in which the chalcopyrite is present. The plots are based on the analysis of several hundred thousand particles in the original sample, and are delivered automatically by the system software. Image analysis of this kind is available in many forms for the calculation of many quantities (such as size, surface area, boundary lengths) for most imaging methods, e.g. optical, electron.

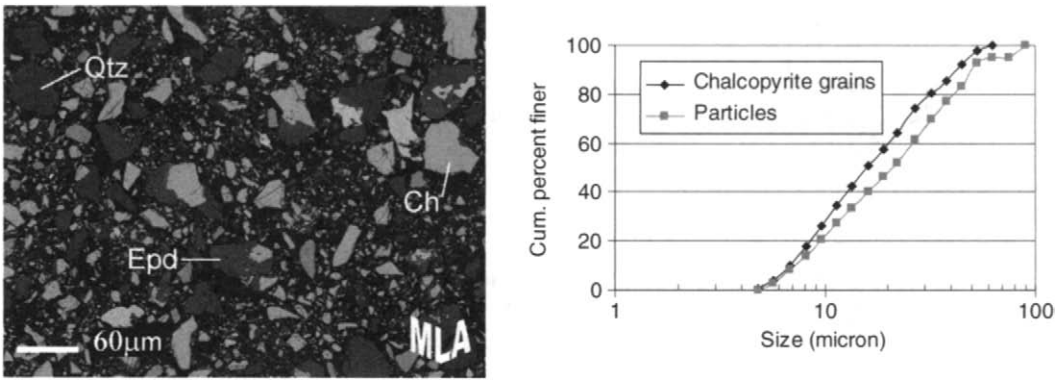


Figure 4.13 Using image analysis to estimate the size distributions of particle and mineral grains (Courtesy JKMRC and JKTech Pty Ltd)

Electrical impedance method

The Beckman Coulter Counter makes use of current changes in an electrical circuit reduced by the presence of a particle.

The measuring system of a *Coulter Counter* is shown in Figure 4.14.

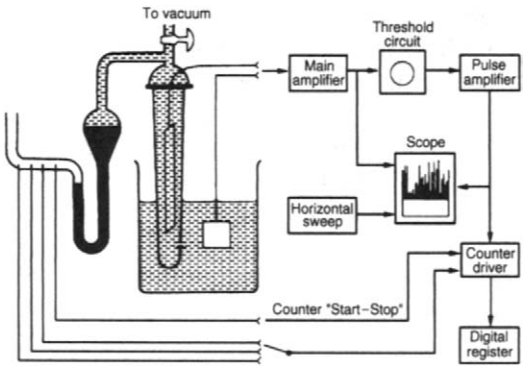


Figure 4.14 Principle of the Coulter Counter

The particles, suspended in a known volume of electrically conductive liquid, flow through a small aperture having an immersed electrode on either side; the particle concentration is such that the particles traverse the aperture substantially one at a time.

Each particle passage displaces electrolyte within the aperture, momentarily changing the resistance between the electrodes and producing a voltage pulse of magnitude proportional to particle volume. The resultant series of pulses is electronically amplified, scaled, and counted.

The amplified pulses are fed to a threshold circuit having an adjustable screen-out voltage level, and those pulses which reach or exceed this level are counted, this count representing the number of particles larger than some determinable volume proportional to the appropriate threshold setting. By taking a series of counts at various amplification and threshold settings, data is directly obtained for determining number frequency against volume, which can be used to determine the size distribution.

As the instrument measures particle volume, the equivalent diameter is calculated from that of a sphere of the same volume, which can be a more relevant size measure than some alternatives. The instrument is applicable in the range 0.4–1200 μm.

Laser diffraction instruments

In recent years, several instruments based on the diffraction of laser light by fine particles have become available, including the Malvern Master-Sizer and the Microtrac. The principle is illustrated in Figure 4.15. Laser light is passed through a dilute suspension of the particles which circulate through an optical cell. The light is scattered by the particles, and is detected by a solid state detector which measures light intensity over a range of angles. A theory of light scattering is used to calculate the particle size distribution from the light distribution pattern, finer particles inducing more scatter than coarse. The early instruments used Fraunhofer theory, which is suitable for coarser particles in the approximate range 1–2000 μm (the upper limit

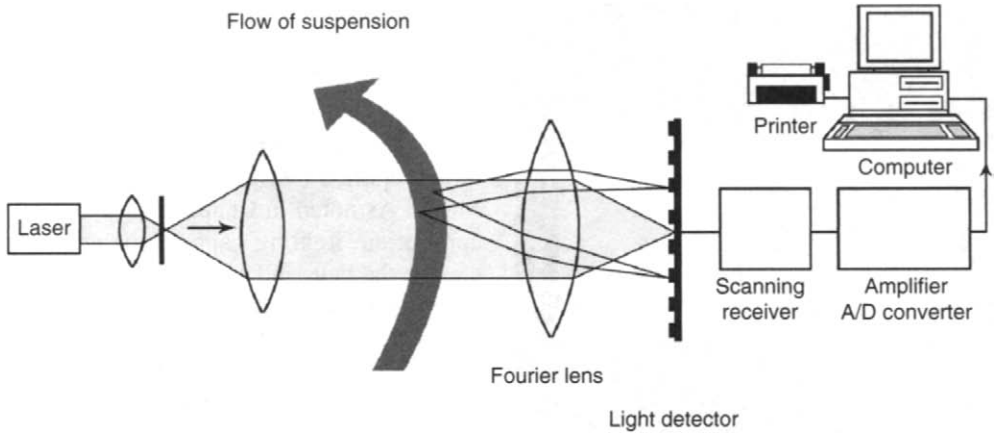


Figure 4.15 The laser diffraction instrument principle (from Napier-Munn et al., 1996; Courtesy JKMRC, The University of Queensland)

being imposed mainly by mechanical constraints). More recently Mie theory has been used to extend the capability down to 0.1 μm and below. Some modern instruments offer both options, or a combination, to cover a wide size range.

Laser diffraction instruments are fast, easy to use, and give very reproducible results. However, light scattering theory does not give a definition of size that is compatible with other methods, such as sieving. In most mineral processing applications, for example, laser diffraction size distributions tend to appear coarser than those of other methods. Austin and Shah (1983) have suggested a procedure for inter-conversion of laser diffraction and sieve-size distributions, and a simple conversion can be developed by regression for materials of consistent characteristics. In addition, the results can depend on the relative refractive indices of the solid particles and liquid medium (usually, though not necessarily, water), and even particle shape. Most instruments claim to compensate for these effects, or offer calibration inputs to the user.

For these reasons, laser diffraction size analysers should be used with caution. For routine high volume analyses in a fixed environment in which only *changes* in size distribution need to be detected, they probably have no peer. For comparison across several environments or materials, or with data obtained by other methods, caution should be used in interpreting the data. These instruments do not of course provide fractionated samples for subsequent analysis.

On-line particle size analysis

Continuous measurement of particle size in slurries has been available since 1971, the PSM system produced then by Armco Autometrics (subsequently by Svedala and now by Thermo GammaMetrics) having been installed in a number of mineral processing plants (Hathaway and Guthnals, 1976).

The PSM system consists of three sections: the air eliminator, the sensor section, and the electronics section. The air eliminator draws a sample from the process stream and removes entrained air bubbles. The de-aerated pulp then passes between the sensors. Measurement depends on the varying absorption of ultrasonic waves in suspensions of different particle sizes. Since solids concentration also affects the absorption of ultrasonic radiation, two pairs of transmitters and receivers, operating at different frequencies, are employed to measure particle size and solids concentration of the pulp, the processing of this information being performed by the electronics.

The current version of the PSM, Thermo GammaMetrics' PSM-400MPX (Figure 4.16) handles slurries up to 60% solids w/w and outputs five size fractions simultaneously.

Other measurement principles are now available in commercial form for slurries. The Outokumpu PSI 200 system measures the size of individual particles in a slurry stream directly using a reciprocating caliper sensor which converts position (and thus size) into an electrical signal (Saloheimo and

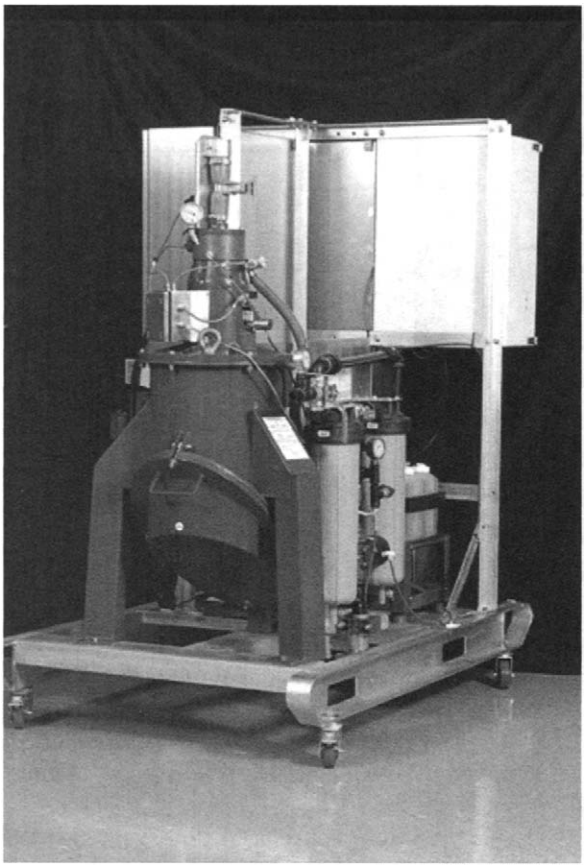


Figure 4.16 The Thermo GammaMetrics PSM-400MPX on-line particle size analyser (Courtesy Thermo Electron Corporation)

Antilla, 1994). Outokumpu has also developed an on-line version of the laser diffraction principle – the PSI 500 (Kongas et al., 2003).

Image analysis is commonly used in sizing rocks on conveyor belts. Systems available include those supplied by Split Engineering, WipFrag, and Metso. As noted in Chapter 3, a fixed camera with appropriate lighting captures images of the particles on the belt, and software segments the images, carries out appropriate corrections, and calculates the particle size distribution. Figure 4.17 shows the original camera views and the segmented images for a crusher feed and product, together with the calculated size distributions. Common problems with imaging systems are the inability to "see" particles under the top layer, and the difficulty of detecting fines, for which correction algorithms can be used. However, they are useful in detecting size changes in crusher circuits, and are increasingly used in measuring the feed to SAG mills for use in mill control.

There are other on-line systems available or under trial. For example, the CSIRO has developed a version of the ultrasonic attenuation principle, in which velocity spectrometry and gamma-ray transmission are incorporated to produce a more robust measurement in the range 0.1–1000 μm (Coghill et al., 2002).

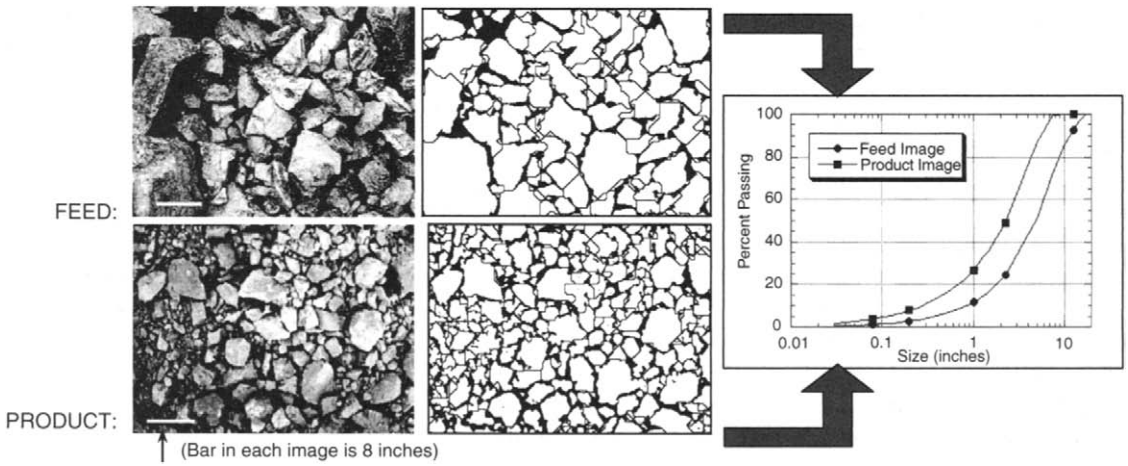


Figure 4.17 The original and segmented images of crusher feed and product, with the final estimated size distributions (Split Engineering's Split-Online system) (Courtesy Split Engineering)

References

Allen, T. (1997). *Particle Size Measurement*, Vol. 1., Chapman and Hall, London (5th edn).

Anon. (1989a). British Standard 1017-1: 1989. Sampling of coal and coke. Methods for sampling of coal.

Anon. (1989b). British Standard 1796-1: 1989, ISO 2591-1: 1988. Test sieving. Methods using test sieves of woven wire cloth and perforated metal plate.

Anon. (1993). British Standard 3406-4: 1993. Methods for the determination of particle size distribution. Guide to microscope and image analysis methods.

Anon. (2000a). British Standard 410-1: 2000, ISO 3310-1: 2000. Test sieves. Technical requirements and testing. Test sieves of metal wire cloth.

Anon. (2000b). British Standard 410-2: 2000, ISO 3310-2: 2000. Test sieves. Technical requirements and testing. Test sieves of perforated metal plate.

Anon. (2001a). British Standard ISO 13317-1: 2001. Determination of particle size distribution by gravitational liquid sedimentation methods. General principles and guidelines.

Anon. (2001b). British Standard ISO 13317-2: 2001. Determination of particle size distribution by gravitational liquid sedimentation methods. Fixed pipette method.

Austin, L.G. and Shah, I. (1983). A method for interconversion of microtrac and sieve size distributions, *Powder Tech.*, **35**, 271–278.

Barbery, G. (1972). Derivation of a formula to estimate the mass of a sample for size analysis, *Trans. Inst. Min. Metall.*, **81 (784)**, Mar., C49–C51.

Bernhardt, C. (1994). *Particle Size Analysis*, Chapman & Hall, London.

Coghill, P.J., Millen, M.J. and Sowerby, B.D. (2002). On-line measurement of particle size in mineral slurries, *Minerals Engng.*, **15(1–2)**, Jan., 83–90.

Finch, J.A. and Leroux, M. (1982). Fine sizing by cyclosizer and micro-sieve, *CIM Bull.*, **75**(Mar.), 235.

Harris, C.C. (1971). Graphical presentation of size distribution data: An assessment of current practice, *Trans. IMM* Sec. C, **80**(Sept.), 133.

Hathaway, R.E. and Guthnals, D.L. (1976). The continuous measurement of particle size in fine slurry processes, *CIM Bull.*, **766**(Feb.), 64.

Heywood, H. (1953). Fundamental principles of subsieve particle size measurement, in *Recent Developments in Mineral Dressing*, IMM, London.

Kongas, M., Saloheimo, K., Pekkarinen, H. and Turunen, J. (2003). New particle size analysis system for mineral slurries. IFAC Workshop on new Technologies for Automation of the Metallurgical Industry, Shanghai (Oct.), preprints, 384–389.

Napier-Munn, T.J. (1985). Determination of the size distribution of ferrosilicon powders, *Powder Tech.*, **42**, 273–276.

Napier-Munn, T.J., Morrell, S., Morrison, R.D. and Kojovic, T. (1996). *Mineral Comminution Circuits – Their Operation and Optimisation* (Appendix 3), JKMRC, The University of Queensland, Brisbane, 413.

Plitt, L.R. and Kawatra, S.K. (1979). Estimating the cut (d_{50}) size of classifiers without product particle size measurement, *Int. J. Min. Proc.*, **5**, 369.

Putman, R.E.J. (1973). Optimising grinding-mill loading by particle-size analysis, *Min. Cong. J.* (Sept.), 68.

Rosin, P. and Rammler, E. (1933–34). The laws governing the fineness of powdered coal, *J. Inst. Fuel*, **7**, 29.

Saloheimo, K. and Antilla, K. (1994). *Utlisation of Particle Size Measurement in Flotation Processes.* ExpoMin, Santiago.

Schuhmann, R., Jr. (1940). Principles of comminution, 1 – Size distribution and surface calculation, *Tech. Publs. AIME*, no. 1189, 11.

Stokes, Sir G.G. (1891). *Mathematical and Physical Paper III*, Cambridge University Press.

5

Comminution

Introduction

Because most minerals are finely disseminated and intimately associated with the gangue, they must be initially "unlocked" or "liberated" before separation can be undertaken. This is achieved by *comminution* in which the particle size of the ore is progressively reduced until the clean particles of mineral can be separated by such methods as are available. Comminution in its earliest stages is carried out in order to make the freshly excavated material easier to handle by scrapers, conveyors, and ore carriers, and in the case of quarry products to produce material of controlled particle size.

Explosives are used in mining to remove ores from their natural beds, and blasting can be regarded as the first stage in comminution. Comminution in the mineral processing plant, or "mill", takes place as a sequence of crushing and grinding processes. Crushing reduces the particle size of run-of-mine ore to such a level that grinding can be carried out until the mineral and gangue are substantially produced as separate particles.

Crushing is accomplished by compression of the ore against rigid surfaces, or by impact against surfaces in a rigidly constrained motion path. This is contrasted with grinding which is accomplished by abrasion and impact of the ore by the free motion of unconnected media such as rods, balls, or pebbles.

Crushing is usually a dry process, and is performed in several stages, *reduction ratios* being small, ranging from three to six in each stage. The reduction ratio of a crushing stage can be defined as the ratio of maximum particle size entering to maximum particle size leaving the crusher, although other definitions are sometimes used.

Tumbling mills with either steel rods or balls, or sized ore as the grinding media, are used in the last stages of comminution. Grinding is usually performed "wet" to provide a slurry feed to the concentration process, although dry grinding has limited applications. There is an overlapping size area where it is possible to crush or grind the ore. From a number of case studies, it appears that at the fine end of crushing operations equivalent reduction can be achieved for roughly half the energy and costs required by tumbling mills (Flavel, 1978).

Stirred mills are now commonly used in mineral processing, though they have been present in other industries for many years (Stehr and Schwedes, 1983). They represent the broad category of mills which use a stirrer to provide motion to the steel, ceramic, or rock media. Both vertical and horizontal configurations exist, and since they can operate with smaller media sizes, they are far more suitable for fine grinding applications than ball mills. Stirred mills are claimed to be more energy efficient (by up to 50%) than conventional ball mills (Stief et al., 1987). This is thought to be the result of having a narrower range of applied energy.

A relatively new comminution device, the high pressure grinding rolls (HPGR), utilises compression breakage of a particle bed, in which energy efficient inter-particle breakage occurs (Schönert, 1988). The reduction ratio obtained in a single pass through the HPGR is substantially higher than that obtained in conventional rolls crushers. Some evidence has also been reported for downstream benefits such as reduced grinding strength and improved leachability due to microcracking (Knecht, 1994). The HPGR offers a realistic potential to markedly reduce the comminution energy requirements needed by tumbling mills. Reports have suggested the HPGR to be between 20 and 50% more efficient than conventional crushers and mills (Esna-Ashari and Kellerwessel, 1988).

Principles of comminution

Most minerals are crystalline materials in which the atoms are regularly arranged in three-dimensional arrays. The configuration of atoms is determined by the size and types of physical and chemical bonds holding them together. In the crystalline lattice of minerals, these inter-atomic bonds are effective only over small distances, and can be broken if extended by a tensile stress. Such stresses may be generated by tensile or compressive loading (Figure 5.1).

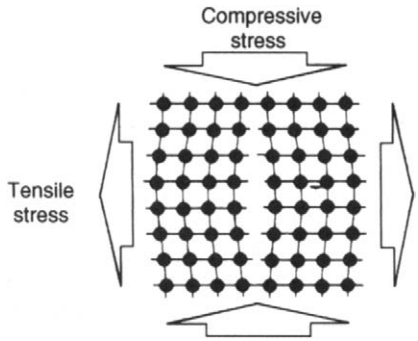


Figure 5.1 Strain of a crystal lattice resulting from tensile or compressive stresses

Even when rocks are uniformly loaded, the internal stresses are not evenly distributed, as the rock consists of a variety of minerals dispersed as grains of various sizes. The distribution of stress depends upon the mechanical properties of the individual minerals, but more importantly upon the presence of cracks or flaws in the matrix, which act as sites for stress concentration (Figure 5.2).

It has been shown (Inglis, 1913) that the increase in stress at such a site is proportional to the square root of the crack length perpendicular to the stress direction. Therefore, there is a critical value for the crack length at any particular level of stress at which the increased stress level at the crack tip is sufficient to break the atomic bond at that point. Such rupture of the bond will increase the crack length, thus increasing the stress concentration and causing a rapid propagation of the crack through the matrix, thus causing fracture.

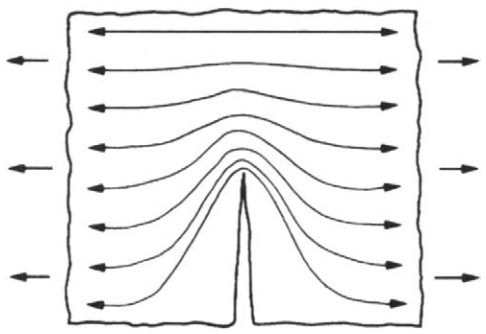


Figure 5.2 Stress concentration at a crack tip

Although the theories of comminution assume that the material is brittle, crystals can, in fact, store energy without breaking, and release this energy when the stress is removed. Such behaviour is known as *elastic*. When fracture does occur, some of the stored energy is transformed into free surface energy, which is the potential energy of atoms at the newly produced surfaces. Due to this increase in surface energy, newly formed surfaces are often more chemically active, and are more amenable to the action of flotation reagents, etc., as well as oxidising more readily.

Griffith (1921) showed that materials fail by crack propagation when this is energetically feasible, i.e. when the energy released by relaxing the strain energy is greater than the energy of the new surface produced. Brittle materials relieve the strain energy mainly by crack propagation, whereas "tough" materials can relax strain energy without crack propagation by the mechanism of plastic flow, where the atoms or molecules slide over each other and energy is consumed in distorting the shape of the material. Crack propagation can also be inhibited by encounters with other cracks or by meeting crystal boundaries. Fine-grained rocks, such as taconites, are therefore usually tougher than coarse-grained rocks.

The energy required for comminution is reduced in the presence of water, and can be further reduced by chemical additives which adsorb onto the solid (Hartley et al., 1978). This may be due to the lowering of the surface energy on adsorption providing that the surfactant can penetrate into a crack and reduce the bond strength at the crack tip before rupture.

Real particles are irregularly shaped, and loading is not uniform but is achieved through points, or small areas, of contact. Breakage is achieved mainly by crushing, impact, and attrition, and all three modes of fracture (compressive, tensile, and shear) can be discerned depending on the rock mechanics and the type of loading.

When an irregular particle is broken by compression, or crushing, the products fall into two distinct size ranges – coarse particles resulting from the induced tensile failure, and fines from compressive failure near the points of loading, or by shear at projections (Figure 5.3). The amount of fines produced can be reduced by minimising the area of loading and this is often done in compressive crushing machines by using corrugated crushing surfaces (Partridge, 1978).

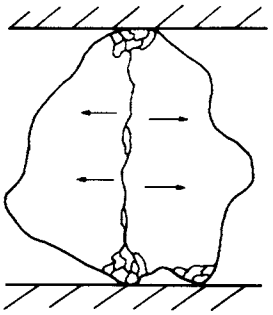


Figure 5.3 Fracture by crushing

In impact breaking, due to the rapid loading, a particle experiences a higher average stress while undergoing strain than is necessary to achieve simple fracture, and tends to break apart rapidly, mainly by tensile failure. The products are often very similar in size and shape.

Attrition (shear failure) produces much fine material, and may be undesirable depending on the comminution stage and industry sector. Attrition occurs mainly in practice due to particle–particle interaction (inter-particle comminution), which may occur if a crusher is fed too fast, contacting particles thus increasing the degree of compressive stress and hence shear failure.

Comminution theory

Comminution theory is concerned with the relationship between energy input and the particle size made from a given feed size. Various theories have been expounded, none of which is entirely satisfactory (Wills and Atkinson, 1993).

The greatest problem lies in the fact that most of the energy input to a crushing or grinding machine is absorbed by the machine itself, and only a small fraction of the total energy is available for breaking the material. It is to be expected that there is a relationship between the energy required to break the material and the new surface produced in the process, but this relationship can only be made manifest if the energy consumed in creating new surface can be separately measured.

In a ball mill, for instance, it has been shown that less than 1% of the total energy input is available for actual size reduction, the bulk of the energy being utilised in the production of heat.

Another factor is that a material which is plastic will consume energy in changing shape, a shape which it will retain without creating significant new surface. All the theories of comminution assume that the material is brittle, so that no energy is adsorbed in processes such as elongation or contraction which is not finally utilised in breakage.

The oldest theory is that of Von Rittinger (1867), which states that the energy consumed in the size reduction is proportional to the area of new surface produced. The surface area of a known weight of particles of uniform diameter is inversely proportional to the diameter, hence Rittinger's law equates to

$$E = K\left(\frac{1}{D_2} - \frac{1}{D_1}\right) \tag{5.1}$$

where E is the energy input, D_1 is the initial particle size, D_2 is the final particle size, and K is a constant.

The second theory is that of Kick (1885). He stated that the work required is proportional to the reduction in volume of the particles concerned. Where f is the diameter of the feed particles and p the diameter of the product particles, the reduction ratio R is f/p. According to Kick's law, the energy required for comminution is proportional to $\log R/\log 2$.

Bond (1952) developed an equation which is based on the theory that the work input is proportional to the new crack tip length produced in particle breakage, and equals the work represented by the product minus that represented by the feed. In particles of similar shape, the surface area of unit volume of material is inversely proportional to the diameter. The crack length in unit volume is considered to be proportional to one side of that area and therefore inversely proportional to the square root of the diameter.

For practical calculations the size in microns which 80% passes is selected as the criterion of

particle size. The diameter in microns which 80% of the product passes is designated as P, the size which 80% of the feed passes is designated as F, and the work input in kilowatt hours per short ton is W. Bond's third theory equation is

$$W = \frac{10W_i}{\sqrt{P}} - \frac{10W_i}{\sqrt{F}} \qquad (5.2)$$

where W_i is the *work index*. The work index is the comminution parameter which expresses the resistance of the material to crushing and grinding; numerically it is the kilowatt hours per short ton required to reduce the material from theoretically infinite feed size to 80% passing 100 μm.

Various attempts have been made to show that the relationships of Rittinger, Kick, and Bond are interpretations of single general equations. Hukki (1975) suggests that the relationship between energy and particle size is a composite form of the three laws. The probability of breakage in comminution is high for large particles, and rapidly diminishes for fine sizes. He shows that Kick's law is reasonably accurate in the crushing range above about 1 cm in diameter; Bond's theory applies reasonably in the range of conventional rod-mill and ball-mill grinding, and Rittinger's law applies fairly well in the fine grinding range of 10–1000 μm.

On the basis of Hukki's evaluation, Morrell (2004) has proposed a modification to Bond's equation that sees the exponent of P and F in Equation 5.2 varying with size as:

$$W = \frac{KM_i}{P^{f(P)}} - \frac{KM_i}{F^{f(F)}}$$

where M_i is the *material index* related to the breakage property of the ore and K is a constant chosen to balance the units of the equation. The application of the new energy–size relation has been shown to be valid across the size range covered by most modern grinding circuits, i.e. 0.1–100 mm.

Grindability

Ore grindability refers to the ease with which materials can be comminuted, and data from grindability tests are used to evaluate crushing and grinding efficiency.

Probably the most widely used parameter to measure ore grindability is the Bond work index W_i. If the breakage characteristics of a material remain constant over all size ranges, then the calculated work index would be expected to remain constant since it expresses the resistance of material to breakage. However, for most naturally occurring raw materials, differences exist in the breakage characteristics depending on particle size, which can result in variations in the work index. For instance, when a mineral breaks easily at the boundaries but individual grains are tough, then grindability increases with fineness of grind. Consequently work index values are generally obtained for some specified grind size which typifies the comminution operation being evaluated (Magdalinovic, 1989).

Grindability is based upon performance in a carefully defined piece of equipment according to a strict procedure. The Bond standard grindability test has been described in detail by Deister (1987), and Levin (1989) has proposed a method for determining the grindability of fine materials. Table 5.1 lists standard Bond work indices for a selection of materials.

Table 5.1 Selection of Bond work indices

Material	*Work index*	*Material*	*Work index*
Barite	4.73	Fluorspar	8.91
Bauxite	8.78	Granite	15.13
Coal	13.00	Graphite	43.56
Dolomite	11.27	Limestone	12.74
Emery	56.70	Quartzite	9.58
Ferro-silicon	10.01	Quartz	13.57

The standard Bond test is time-consuming, and a number of methods have been used to obtain the indices related to the Bond work index. Smith and Lee (1968) used batch-type grindability tests to arrive at the work index, and compared their results with work indices from the standard Bond tests, which require constant screening out of undersize material in order to simulate closed-circuit operation. The batch-type tests compared very favourably with the standard grindability test data, the advantage being that less time is required to determine the work index.

Berry and Bruce (1966) developed a comparative method of determining the grindability of an ore. The method requires the use of a reference ore of known grindability. The reference ore is ground for

a certain time and the power consumption recorded. An identical weight of the test ore is then ground for a length of time such that the power consumed is identical with that of the reference ore. If r is the reference ore and t the ore under test, then from Bond's Equation 5.2.

$$W_r = W_t = W_{ir}\left[\frac{10}{\sqrt{P_r}} - \frac{10}{\sqrt{F_r}}\right] = W_{it}\left[\frac{10}{\sqrt{P_t}} - \frac{10}{\sqrt{F_t}}\right]$$

Therefore

$$W_{it} = W_{ir}\left[\frac{10}{\sqrt{P_r}} - \frac{10}{\sqrt{F_r}}\right] \Big/ \left[\frac{10}{\sqrt{P_t}} - \frac{10}{\sqrt{F_t}}\right] \quad (5.3)$$

Reasonable values for the work indices are obtained by this method as long as the reference and test ores are ground to about the same product size distribution.

The low efficiency of grinding equipment in terms of the energy actually used to break the ore particles is a common feature of all types of mill, but there are substantial differences between various designs. Some machines are constructed in such a way that much energy is adsorbed in the component parts and is not available for breaking. Work indices have been obtained (Lowrison, 1974) from grindability tests on different sizes of several types of equipment, using identical feed materials. The values of work indices obtained are indications of the efficiencies of the machines. Thus, the equipment having the highest indices, and hence the largest energy consumers, are found to be jaw and gyratory crushers and tumbling mills; intermediate consumers are impact crushers and vibration mills, and roll crushers are the smallest consumers. The smallest consumers of energy are those machines which apply a steady, continuous, compressive stress on the material.

Values of *operating work indices*, W_{io}, obtained from specific units can be used to assess the effect of operating variables, such as mill speeds, size of grinding media, type of liner, etc. The higher the value of W_i, the lower is the grinding efficiency. The W_{io} can be obtained using Equation 5.2, by defining W as the specific energy being used (power draw/new feed rate), F and P as the actual feed and product 80% passing sizes, and W_i as the operating work index, W_{io}. Once corrected for the particular application and equipment-related factors, W_{io} can be compared on the same basis as grindability test results. This allows a direct comparison of grinding efficiency. Ideally W_i should be equal to W_{io} and grinding efficiency should be unity. It should be noted that the value of W is the power applied to the pinion shaft of the mill. Motor input power thus has to be converted to power at the mill pinion shaft unless the motor is coupled direct to the pinion shaft.

While Bond is the best-known grindability test for rod and ball mills, in recent years the SPI (SAG Power Index) test has become popular for SAG mills. The SPI test is a batch test, conducted in a 30.5 cm diameter by 10.2 cm long grinding mill charged with 5 kg of steel balls. Two kilograms of sample are crushed to 100% minus 1.9 cm and 80% minus 1.3 cm and placed in the mill. The test is run with several screening iterations until the sample is reduced to 80% minus 1.7 mm. The time required to reach a P80 of 1.7 mm is then converted to an SAG power index W_{sag} via the use of a proprietary transformation (Starkey and Dobby, 1996):

$$W_{sag} = Kf_{sag}\left(\frac{SPI}{T_{80}^{0.5}}\right)^n$$

The parameters K and n are empirical factors whilst f_{sag} incorporates a series of calculations (unpublished), which estimate the influence of factors such as pebble crusher recycle load, ball load, and feed size distribution. The test is essentially an indicator of an ore's breakage response to SAG abrasion events. As with other batch tests, the test is limited by the fact that a steady-state mill load is never reached.

Simulation of comminution processes and circuits

Simulation of comminution, particularly of grinding and classification, has received great attention in recent years, due to the fact that this is by far the most important unit operation both in terms of energy consumption and overall plant performance. Other aspects of mineral processing have not received the same intensive research accorded to grinding.

The Bond work index has little use in simulation, as it does not predict the complete product size distribution, only the 80% passing size, nor does it predict the effect of operating variables

on mill circulating load, nor classification performance. The complete size distribution is required in order to simulate the behaviour of the product in ancillary equipment such as screens and classifiers, and for this reason population balance models are finding increased usage in the design, optimisation and control of grinding circuits (Napier-Munn et al., 1996). One of the most successful applications of these models has been through the mineral processing simulator, JKSimMet. A range of case studies can be found in the literature, covering both design and optimization of grinding circuits. Recent examples include Richardson (1990), Lynch and Morrell (1992), McGhee et al. (2001), and Dunne et al. (2001). In the model formulation the particulate assembly that undergoes breakage in a mill is divided into several narrow size intervals (e.g. $\sqrt{2}$ sieve intervals). The size reduction process is defined by the matrix equation:

$$p = K \cdot f$$

where p represents the product and f the feed elements. The element p_{ij} in the product array is given by:

$$p_{ij} = K_{ij} \cdot f_j$$

where K_{ij} represents the mass fraction of the particles in the jth size range which fall in the ith size range in the product. The product array for n size ranges can thus be written as:

Product array

The product array is only useful if K is known. The behaviour of particles in each size interval is characterised by a size-discretised selection, or breakage rate function, S, which is the probability of particles in that size range being selected for breakage, the remainder passing through the process unbroken, and a set of size-discretised breakage functions, B, which give the distribution of breakage fragments produced by the occurrence of a primary breakage event in that size interval. $S \cdot f$ represents the portion of particles which are broken, $(1 - S) \cdot f$ thus representing the unbroken fraction. K in Equation 5.4 is thus replaced by B, and the equation for a primary breakage process becomes:

$$p = B \cdot S \cdot f + (1 - S) \cdot f$$

The model can be combined with information on the distribution of residence times in the mill to provide a description of open-circuit grinding, which can be coupled with information concerning the classifier to produce closed-circuit grinding conditions (Napier-Munn et al., 1996). These models can only realise their full potential, however, if accurate methods of estimating model parameters are available for a particular system. The complexity of the breakage environment in a tumbling mill precludes the calculation of these values from first principles, so that successful application depends on the development of efficient techniques for the estimation of model parameters from experimental data. The methods used for the determination of model parameters have been compared by Lynch et al. (1986). This comparison shows that, while all the modern ball mill models use a similar method for describing the breakage rate and the breakage distribution functions, each model has its own way of representing the material transport mechanisms.

Parameter estimation techniques can be classified into three broad categories:

(a) Graphical methods which are based mainly on the grinding of narrow size distributions.
(b) Tracer methods, involving the introduction of a tracer into one of the size intervals of the feed, followed by analysis of the product for the tracer.
(c) Non-linear regression methods, which allow all parameters to be computed from a minimum of experimental data.

Rajamani and Herbst (1984) report the development of an algorithm for simultaneous estimation of selection and breakage functions from experimental data with the use of non-linear regression, and present the results of estimation for batch and continuous operations. The estimated parameter values show good agreement with parameters determined by direct experimental methods, and a computer program based on the algorithm has been developed. The program is said to be capable of simulating tumbling mill grinding behaviour for a specified set of model parameters, and of estimating the model parameters from experimental data. Wiseman and Richardson (1991) give a detailed review of the JKSimMet software package for simulating mineral processing operations, particularly comminution and classification. It is based on

more than 25 years of modelling and simulation research and development at the Julius Kruttschnitt Mineral Research Centre (JKMRC). One of the main applications for the software package is the analysis and optimization of the performance of existing operations using experimental circuit data. Kojovic and Whiten (1994) outline a procedure for evaluating the quality of models typical of those used in mineral processing simulation.

Single particle breakage tests have been used by a number of researchers to investigate some salient features of the complex comminution process. A comparison of the results from single particle breakage tests with grindability and ball mill tests is given by Narayanan (1986). Application of the results from single particle breakage tests to modelling industrial comminution processes is described, and the necessity for further research into single particle breakage tests to develop a simple but comprehensive technique for estimating the breakage characteristics of ores is discussed. Napier-Munn et al. (1996) give a detailed description of the single particle breakage tests developed at the JKMRC, and their application to the determination of ore-specific parameters used in comminution models.

Although selection and breakage functions for homogeneous materials can be determined on a small scale and used to predict large-scale performance, it is more difficult to predict the behaviour of mixtures of two or more components. Furthermore, the relationship of material size reduction to subsequent processing is even more difficult to predict, due to the complexities of mineral release. However, recent work has focused on the development of grinding models which include mineral liberation in the size-reduction description (Choi et al., 1988; Herbst et al., 1988). In terms of liberation models for comminution, King (1994) and Gay (2004) have made the most significant progress. Gay's entropy-based multiphase approach models particles individually rather than using the standard approach of using composite classes. The development of such liberation models is essential if true simulation of integrated plants is ever to be developed.

The Discrete Element Method (DEM) approach is recognized as an effective tool for modelling (in both two and three dimensions) the flow of granular materials in a variety of mining industry applications, including the motion of grinding media in a mill. The technique combines detailed physical models to describe the motion of balls, rocks, and slurry and attendant breakage of particles as they are influenced by moving liner/lifters and grates.

The DEM has been used to model many industrial applications over the past decade. Of specific interest to comminution is the modelling of ball mills by Mishra and Rajamani (1992, 1994), Inoue and Okaya (1995), Cleary (1998), Datta et al. (1999) and SAG mills by Rajamani and Mishra (1996), Bwalya et al. (2001), Cleary (2001), Nordel et al. (2001), and Djordjevic (2004, 2005). One of the features of three-dimensional DEM simulation is the cutaway images of particle motion in the mill, an example of which is presented in Figure 5.4 for a 1.8 m diameter pilot SAG mill.

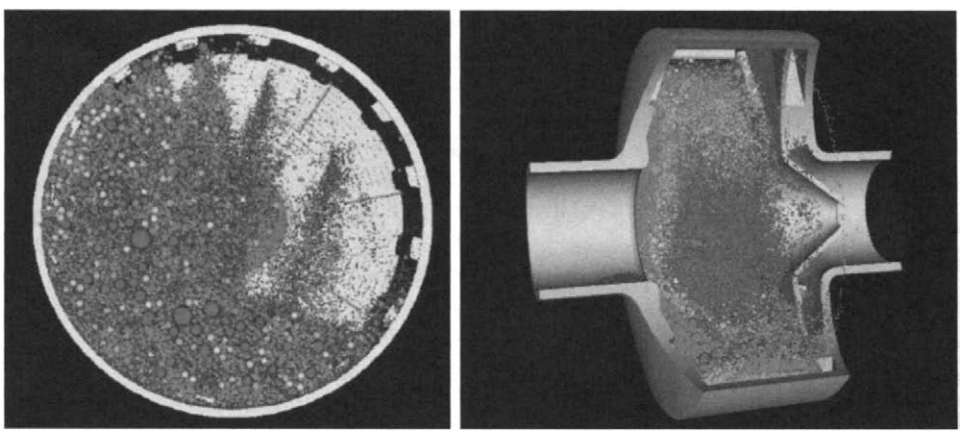


Figure 5.4 Example of ball and particle motion in a slice of a pilot SAG mill using three-dimensional DEM simulation (Courtesy CSIRO (Dr. Paul Cleary))

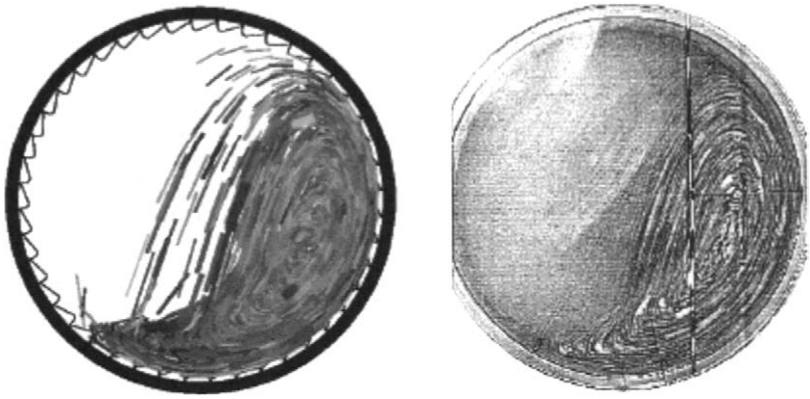


Figure 5.5 Comparison of three-dimensional DEM with experiment for 75% critical speed, scale model 0.6 m diameter SAG mill (Courtesy CSIRO (Dr. Paul Cleary))

Modelling of SAG mills by DEM is leading to improved understanding of charge dynamics, and offers the potential to improve mill design and control, and reduce wear. This could lead to reduced downtime, increased mill efficiency, increased throughput, lower costs, and lower energy consumption. DEM has not yet advanced to the stage of surpassing the predictive capability of the current milling models, but the improved understanding may in the short term lead to improved mechanistic models and design equations. Coupling of slurry to particles and adding direct prediction of particle breakage to the full scale DEM model are two of the major unresolved issues.

Validation of the predictions made by DEM is a critical part of understanding the effect of various modelling assumptions and for separating more accurate DEM variants from less accurate ones. Examples of such validations can be found in Cleary and Hoyer (2000) and Cleary et al. (2001). Govender et al. (2001) uses an automated three-dimensional tracking technique utilising biplanar X-ray filming for providing rigorous validation data on the motion of particles in an experimental small scale mill. Figure 5.5 shows a good agreement between DEM simulation and experiment in terms of the charge motion for a scale model SAG mill.

Though advances in computing power have enabled DEM simulations to tackle increasingly more complex processes, three-dimensional DEM simulation of large mills with many thousands of particles can be a time-consuming task. The speed of computation is determined principally by two parameters: number of particles involved and material properties. Large-scale simulations, with over 100,000 particles can take weeks for a single simulation. The computational time step is determined by the size of the smallest particle present in the model and material properties (elastic). These computational demands and lack of detailed experimental verification have limited the value of DEM techniques in the mining industry. Hence there is much effort around the world seeking to fill the vital gap linking computational results to rigorous experimental data. It is only with validated DEM that any confidence can be given to the predictive capability of such computational tools, especially when the predictive range lies beyond that for which the existing semi-empirical models were developed.

References

Berry, T.F. and Bruce, R.M. (1966). A simple method of determining the grindability of ores, *Can. Min. J.* (Jul.), 63.

Bond, F.C. (1952). The third theory of comminution, *Trans. AIMF*, **193**, 484.

Bwalya, B.W., Moys, M.H., and Hinde, A.L. (2001). The use of discrete element method and fracture mechanics to improve grinding rate predictions, *Minerals Engng.*, **14(6)**, 565–573.

Choi, W.Z., Adel, G.T., and Yoon, R.H. (1988). Estimation of model parameters for liberation and size reduction, *Min. Metall. Proc.*, **5** (Feb.), 33.

Cleary, P.W. (1998). Predicting charge motion power draw, segregation and wear in ball mill using discrete element methods, *Minerals Engng.*, **11(11)**, 1061–1080.

Cleary, P.W. (2001). Modelling comminution devices using DEM, *Int. J. Numer. Anal. Meth. Geomechan.*, **25**, 83–105.

Cleary, P.W. and Hoyer, D. (2000), Centrifugal mill charge motion and power draw: Comparison of DEM predictions with experiment, *Int. J. Min. Proc.*, **59(2)**, 131–148.

Cleary, P.W., Morrison, R.D., and Morrell, S. (2001). DEM validation for a full scale model SAG mill, *SAG2001 Conference*, Vancouver, Canada, IV, 191–206.

Datta, A., Mishra, B.K., and Rajamani, R.K. (1999). Analysis of power draw in ball mills by discrete element method, *Can. Metall. Q.*, **38**, 133–140.

Deister, R.J. (1987). How to determine the Bond work index using lab. ball mill grindability tests, *Engng. Min. J.*, **188**(Feb.), 42.

Djordjevic, N. (2005). Influence of charge size distribution on net-power draw of tumbling mill based on DEM modeling, *Minerals Engng.*, **18(3)**, 375–378.

Djordjevic, N., Shi, F.N., and Morrison, R.D. (2004). Determination of lifter design, speed and filling effects in AG mills by 3D DEM, *Minerals Engng.*, **17(11–12)**, 1135–1142.

Dunne, R., Morrell, S., Lane, G., Valery, W., and Hart, S. (2001). Design of the 40 foot diameter SAG mill installed at the Cadia gold copper mine, *SAG2001 Conference*, Vancouver, Canada, I, 43–58.

Esna-Ashari, M. and Kellerwessel, H. (1988). Interparticle crushing of gold ore improves leaching, *Randol Gold Forum 1988*, Scottsdale, USA, 141–146.

Flavel, M.D. (1978). Control of crushing circuits will reduce capital and operating costs, *Min. Mag.*, Mar., 207.

Gay, S. (2004). Application of multiphase liberation model for comminution, *Comminution '04 Conference*, Perth (Mar.).

Govender, I., Balden, V., Powell, M.S., and Nurick, G.N. (2001). Validating DEM – Potential major improvements to SAG modeling, *SAG2001 Conference*, Vancouver, Canada, IV, 101–114.

Griffith, A.A. (1921). *Phil. Trans. R. Soc.*, **221**, 163.

Hartley, J.N., Prisbrey, K.A., and Wick, O.J. (1978). Chemical additives for ore grinding: How effective are they?, *Engng. Min. J.* (Oct.), 105.

Herbst, 1.A., et al. (1988). Development of a multicomponent-multisize liberation model, *Minerals Engng.*, **1(2)**, 97.

Hukki, R.T. (1975). The principles of comminution: An analytical summary, *Engng. Min. J.*, **176**(May), 106.

Inglis, C.E. (1913). Stresses in a plate due to the presence of cracks and sharp comers. *Proc. Inst. Nav. Arch.*

Inoue, T. and Okaya, K. (1995). Analysis of grinding actions of ball mills by discrete element method, *Proc. XIX Int. Min. Proc. Cong.*, **1**, SME, 191–196.

Kick, F. (1885). *Des Gesetz der Proportionalem widerstand und Seine Anwendung*, Felix, Leipzig.

King, R.P. (1994). Linear stochastic models for mineral liberation, *Powder Tech.*, **81**, 217–234.

Knecht, J. (1994). High-pressure grinding rolls – a tool to optimize treatment of refractory and oxide gold ores. *Fifth Mill Operators Conf.*, AusIMM, Roxby Downs, Melbourne (Oct.), 51–59.

Kojovic, T. and Whiten, W.J. (1994). Evaluating the quality of simulation models, *IIMP Conf.*, Sudbury, 437–446.

Levin, J. (1989). Observations on the Bond standard grindability test, and a proposal for a standard grindability test for fine materials, *J.S. Afr. Inst. Min. Metall*, **89** (Jan.), 13.

Lowrison, G.C. (1974). *Crushing and Grinding*, Butterworths, London.

Lynch, A.J. and Narayanan, S.S. (1986). Simulation – the design tool for the future, in *Mineral Processing at a Crossroads – Problems and Prospects*, ed. B.A. Wills and R.W. Barley. Martinus Nijhoff Publishers, Dordrecht, 89.

Lynch, A.J. and Morrell, S. (1992). The understanding of comminution and classification and its practical application in plant design and optimisation, *Comminution: Theory and Practice*, ed. Kawatra, AIME, 405–426.

Lynch, A.J., et al. (1986). Ball mill models: Their evolution and present status, in *Advances in Minerals Processing.*, ed. P. Somasundaran, Chapter 3, 48, SME Inc., Littleton.

Magdalinovic, N.M. (1989). Calculation of energy required for grinding in a ball mill, *Int. J. Min. Proc.* **25** (Jan.), 41.

McGhee, S., Mosher, J., Richardson, M., David, D., and Morrison, R. (2001). SAG feed pre-crushing at ASARCO's ray concentrator: development, implementation and evaluation. *SAG2001 Conf.*, Vancouver, Canada, **1**, 234–247.

Mishra, B.K. and Rajamani, R.J. (1992). The discrete element method for the simulation of ball mills, *App. Math. Modelling*, **16**, 598–604.

Mishra, B.K. and Rajamani, R.K. (1994). Simulation of charge motion in ball mills. Part 1: Experimental verifications, *Int. J. Min. Proc.*, **40**, 171–186.

Morrell, S. (2004). An alternative energy-size relationship to that proposed by Bond for the design and optimisation of grinding circuits. *Int. J. Min. Proc.* (in press).

Napier-Munn, T.J., Morrell, S., Morrison, R.D., and Kojovic, T. (1996). JKMRC, University of Queensland, Brisbane, 413pp.

Narayanan, S.S. (1986). Single particle breakage tests: A review of principles and applications to comminution modelling, *Bull. Proc. Australas. Inst Min. Metall.*, **291**(June), 49.

Nordell, L., Potapov, A.V. and Herbst, J.A. (2001). Comminution simulation using discrete element method (DEM) approach – from single particle

breakage to full-scale SAG mill operation, *SAG2001 Conf.*, Vancouver, Canada, **4**, 235–236.

Partridge, A.C. (1978). Principles of comminution, *Mine and Quarry*, **7**(Jul./Aug.), 70.

Rajamani, K. and Herbst, J.A. (1984). Simultaneous estimation of selection and breakage functions from batch and continuous grinding data, *Trans. Inst. Min. Metall.*, **93** (June), C74.

Rajamani, R.K. and Mishra, B.K. (1996). Dynamics of ball and rock charge in SAG Mills, *SAG1996 Conf.*, Vancouver, Canada, 700–712.

Richardson, J.M. (1990). Computer simulation and optimisation of mineral processing plants, three case studies, *Control 90*, ed. Rajamani and Herbst, AIME, 233–244.

Schönert, K. (1988). A first survey of grinding with high-compression roller mills, *Int. J. Min. Proc.*, **22**, 401–412.

Smith, R.W. and Lee, K.H. (1968). A comparison of data from Bond type simulated closed-circuit and batch type grindability tests, *Trans. SME/AIME*, **241**, 91.

Starkey, J. and Dobby, G. (1996). Application of the minnovex SAG power index at five canadian SAG plants, *SAG1989 Conf.*, Vancouver, Canada, 345–360.

Stehr N. and Schwedes J. (1983). Investigation of the grinding behaviour of a stirred ball mill, *Ger. Chem. Engng.*, **6**, 337–343.

Stief, D.E., Lawruk, W.A., and Wilson, L.J. (1987). Tower mill and its application to fine grinding. *Min. Metall. Proc.*, **4(1)**, Feb., 45–50.

Von Rittinger, P.R. (1867). *Lehrbuch der Aufbereitungs Kunde*, Ernst and Korn, Berlin.

Wills, B.A. and Atkinson, K. (1993). Some observations on the fracture and liberation of mineral assemblies, *Minerals Engng.*, **6(7)**, 697.

Wiseman, D.M. and Richardson, J.M. (1991). JKSimMet – The mineral processing simulator, *Proceedings 2nd Can. Conf. on Comp. Applications in the Min. Ind.*, ed. Paulin, Pakalnis and, Mular, **2**, Univ. B.C. and CIM. 427–438.

6

Crushers

Introduction

Crushing is the first mechanical stage in the process of comminution in which the main objective is the liberation of the valuable minerals from the gangue.

It is generally a dry operation and is usually performed in two or three stages. Lumps of run-of-mine ore can be as large as 1.5 m across and these are reduced in the primary crushing stage to 10–20 cm in heavy-duty machines.

In most operations, the primary crushing schedule is the same as the mining schedule. When primary crushing is performed underground, this operation is normally a responsibility of the mining department; when primary crushing is on the surface, it is customary for the mining department to deliver the ore to the crusher and for the mineral processing department to crush and handle the ore from this point through the successive ore-processing unit operations. Primary crushers are commonly designed to operate 75% of the available time, mainly because of interruptions caused by insufficient crusher feed and by mechanical delays in the crusher (Lewis et al., 1976).

Secondary crushing includes all operations for reclaiming the primary crusher product from ore storage to the disposal of the final crusher product, which is usually between 0.5 and 2 cm in diameter. The primary crusher product from most metalliferous ores can be crushed and screened satisfactorily, and the secondary plant generally consists of one or two size-reduction stages with appropriate crushers and screens. If, however, the ore tends to be slippery and tough, the tertiary crushing stage may be substituted by coarse grinding in rod mills. On the other hand, more than two size-reduction stages may be used in secondary crushing if the ore is extra-hard, or in special cases where it is important to minimise the production of fines.

A basic flowsheet for a crushing plant is shown in Figure 6.1, incorporating two stages of secondary crushing. A washing stage is included, which is often necessary for sticky ores containing clay, which may lead to problems in crushing and screening (see Chapter 2).

Vibrating screens are sometimes placed ahead of the secondary crushers to remove undersize material, or *scalp* the feed, and thereby increase the capacity of the secondary crushing plant. Undersize material tends to pack the voids between the large particles in the crushing chamber, and can choke the crusher, causing damage, because the packed mass of rock is unable to swell in volume as it is broken.

Crushing may be in open or closed circuit depending on product size (Figure 6.2).

In open-circuit crushing, undersize material from the screen is combined with the crusher product and is then routed to the next operation. Open-circuit crushing is often used in intermediate crushing stages, or when the secondary crushing plant is producing a rod mill feed. If the crusher is producing ball-mill feed it is good practice to use closed-circuit crushing in which the undersize from the screen is the finished product. The crusher product is returned to the screen so that any over-size material will be recirculated. One of the main reasons for closing the circuit is the greater flexibility given to the crushing plant as a whole. The crusher can be operated at a wider setting if necessary, thus altering the size distribution of the product and by making a selective cut on the screen, the finished product can be adjusted to give the required specification. There is the added factor that if the material is wet or sticky (and climatic conditions can vary), then it is possible to open the setting of the crusher to prevent the possibility of packing, and by this means the throughput of the machine is increased, which will compensate for the additional circulating load. Closed-circuit operation also allows compensation for wear which

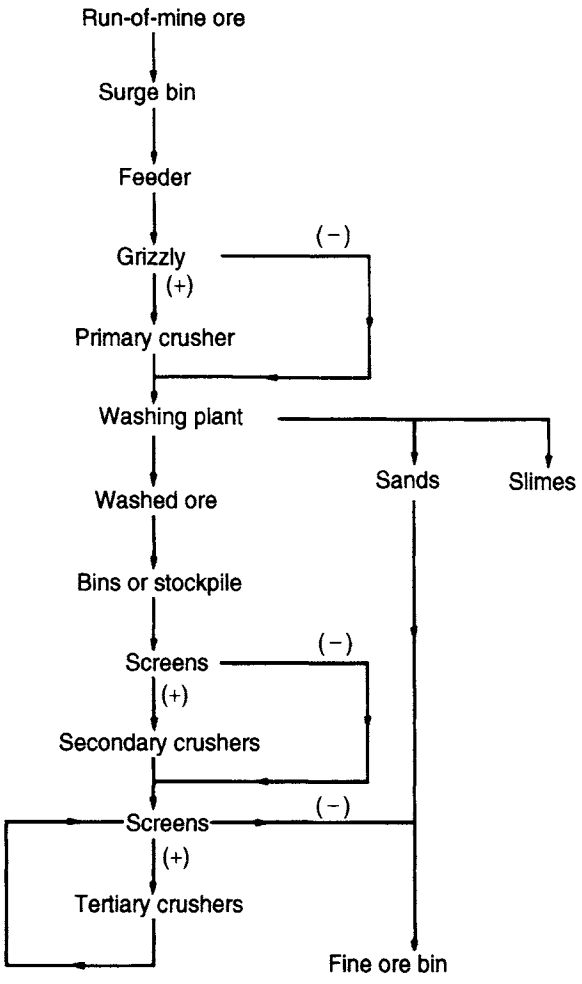


Figure 6.1 Basic crushing plant flowsheet

takes place on liners, and generally gives greater freedom to meet changes in requirements from the plant.

Surge bins precede the primary crusher to receive dumped loads from skips or lorries and should have enough storage capacity to maintain a steady feed to the crusher. In most mills the crushing plant does not run for 24 h a day, as hoisting and transport of ore is usually carried out on two shifts only, the other shift being used for drilling and blasting. The crushing section must therefore have a greater hourly capacity than the rest of the plant, which is run continuously. Ore is always stored after the crushers to ensure a continuous supply to the grinding section. The obvious question is, why not have similar storage capacity before the crushers and run this section continuously also? Apart from the fact that it is cheaper in terms of power consumption to crush at off-peak hours, large storage bins are expensive, so it is uneconomic to have bins at the crushing *and* grinding stage. It is not practicable to store large quantities of run-of-mine ore, as it is "long-ranged", i.e. it consists of a large range of particle sizes and the small ones move down in the pile and fill the voids. This packed mass is difficult to move after it has settled. Run-of-mine ore should therefore be kept moving as much as possible, and surge bins should have sufficient capacity only to even out the flow to the crusher.

Primary crushers

Primary crushers are heavy-duty machines, used to reduce the run-of-mine ore down to a size suitable for transport and for feeding the secondary crushers or AG/SAG mills. They are always operated in open circuit, with or without heavy-duty scalping screens (grizzlies). There are two main types of primary crusher in metalliferous operations – jaw and gyratory crushers – although the impact crusher has limited use as a primary crusher and will be considered separately.

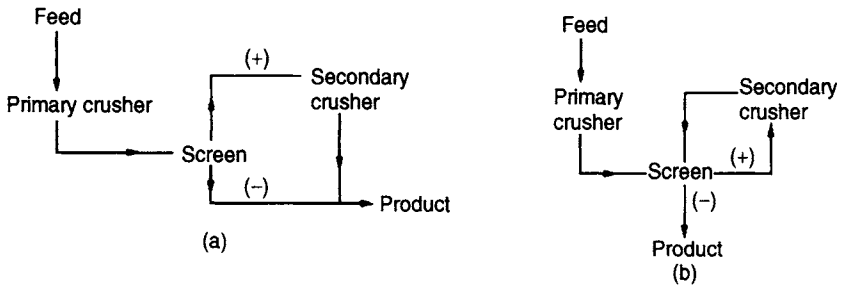


Figure 6.2 (a) Open-circuit crushing, (b) closed-circuit crushing

Jaw crushers

The distinctive feature of this class of crusher is the two plates which open and shut like animal jaws (Grieco and Grieco, 1985). The jaws are set at an acute angle to each other, and one jaw is pivoted so that it swings relative to the other fixed jaw. Material fed into the jaws is alternately *nipped* and released to fall further into the crushing chamber. Eventually it falls from the discharge aperture.

Jaw crushers are classified by the method of pivoting the swing jaw (Figure 6.3). In the *Blake crusher* the jaw is pivoted at the top and thus has a fixed receiving area and a variable discharge opening. In the *Dodge crusher* the jaw is pivoted at the bottom, giving it a variable feed area but fixed delivery area. The Dodge crusher is restricted to laboratory use, where close sizing is required, and is never used for heavy-duty crushing as it chokes very easily. The *Universal crusher* is pivoted in an intermediate position, and thus has a variable delivery and receiving area.

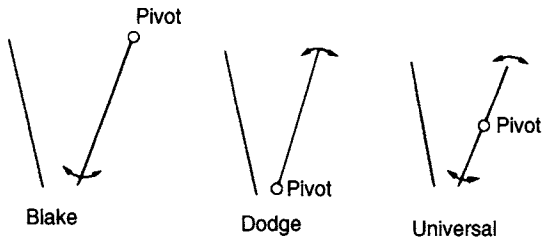


Figure 6.3 Jaw-crusher types

The Blake crusher was patented by W.E. Blake in 1858 and variations in detail on the basic form are found in most of the jaw crushers used today.

There are two forms of the Blake crusher – double toggle and single toggle.

Double-toggle Blake crushers In this model (Figure 6.4), the oscillating movement of the swinging jaw is effected by vertical movement of the pitman. This moves up and down under the influence of the eccentric. The back toggle plate causes the pitman to move sideways as it is pushed upward. This motion is transferred to the front toggle plate and this in turn causes the swing jaw to close on the fixed jaw. Similarly, downward movement of the pitman allows the swing jaw to open.

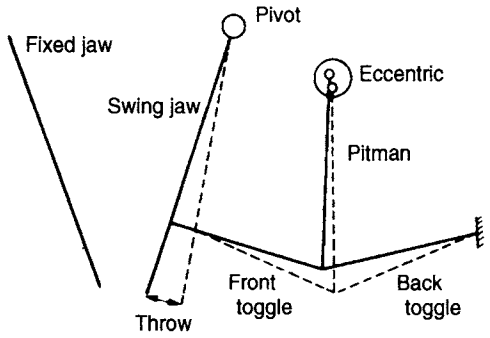


Figure 6.4 Blake jaw crusher (functional diagram)

The important features of the machine are:

(1) Since the jaw is pivoted from above, it moves a *minimum* distance at the entry point and a *maximum* distance at the delivery. This maximum distance is called the *throw* of the crusher.
(2) The horizontal displacement of the swing jaw is greatest at the bottom of the pitman cycle and diminishes steadily through the rising half of the cycle as the angle between the pitman and the back toggle plate becomes less acute.
(3) The crushing force is *least* at the start of the cycle, when the angle between the toggles is most acute, and is strongest at the top, when full power is delivered over a reduced travel of the jaw.

Figure 6.5 shows a cross-section through a double-toggle jaw crusher. All jaw crushers are rated according to their receiving areas, i.e. the *width* of the plates and the *gape*, which is the distance between the jaws at the feed opening. For example, an 1830 × 1220 mm crusher has a width of 1830 mm and a gape of 1220 mm.

Consider a large piece of rock falling into the mouth of the crusher. It is nipped by the jaws, which are moving relative to each other at a rate depending on the size of the machine and which usually varies inversely with the size. Basically, time must be given for the rock broken at each "bite" to fall to a new position before being nipped again. The ore falls until it is arrested. The swing jaw closes on it, quickly at first and then more slowly with increasing power towards the end of the stroke. The fragments now fall to a new arrest point

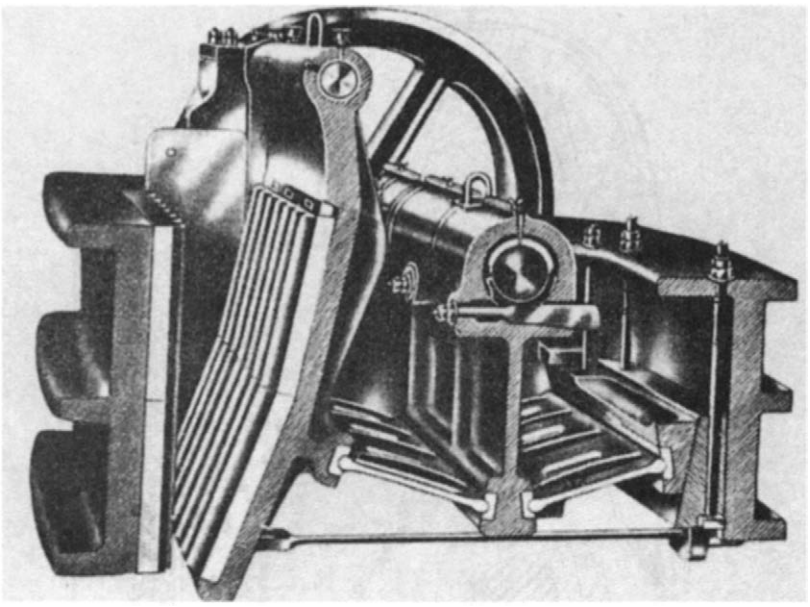


Figure 6.5 Cross-section through double-toggle crusher

as the jaws move apart and are then gripped and crushed again. During each "bite" of the jaws the rock swells in volume due to the creation of voids between the particles. Since the ore is also falling into a gradually reducing cross-sectional area of the crushing chamber, choking of the crusher would soon occur if it were not for the increasing amplitude of swing towards the discharge end of the crusher. This accelerates the material through the crusher, allowing it to discharge at a rate sufficient to leave space for material entering above. This is *arrested* or *free* crushing as opposed to *choked crushing*, which occurs when the volume of material arriving at a particular cross-section is greater than that leaving. In arrested crushing, crushing is by the jaws only, whereas in choked crushing, particles break each other. This *interparticle comminution* can lead to excessive production of fines, and if choking is severe can damage the crusher.

The discharge size of material from the crusher is controlled by the *set*, which is the *maximum* opening of the jaws at the discharge end. This can be adjusted by using toggle plates of the required length. Wear on the jaws can be taken up by adjusting the back pillow into which the back toggle plate bears. A number of manufacturers offer jaw setting by hydraulic jacking, and some fit electromechanical systems which allow remote control (Anon., 1981).

A feature of all jaw crushers is the heavy flywheel attached to the drive, which is necessary to store energy on the idling half of the stroke and deliver it on the crushing half. Since the jaw crusher works on half-cycle only, it is limited in capacity for its weight and size. Due to its alternate loading and release of stress, it must be very rugged and needs strong foundations to accommodate the vibrations.

Single-toggle jaw crushers In this type of crusher (Figure 6.6) the swing jaw is suspended on the eccentric shaft, which allows a lighter, more compact design than with the double-toggle machine. The motion of the swing jaw also differs from that of the double-toggle design. Not only does the swing jaw move towards the fixed jaw, under the action of the toggle plate, but it also moves vertically as the eccentric rotates. This elliptical jaw motion assists in pushing rock through the crushing chamber. The single-toggle machine therefore has a somewhat higher capacity than the double-toggle machine of the same gape. The eccentric movement, however, increases the rate of wear on the jaw plates. Direct attachment of the swing jaw to the eccentric imposes a high degree of strain on the drive shaft, and so maintenance

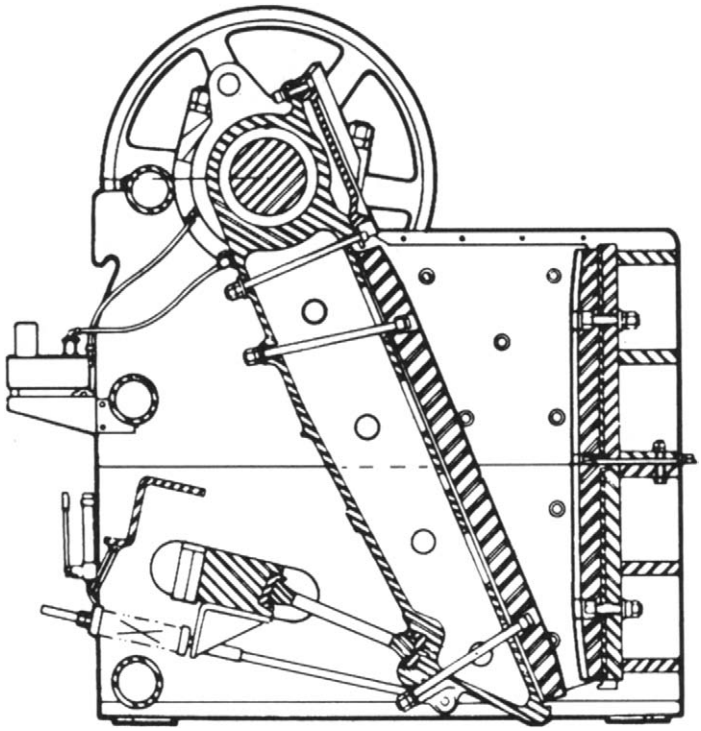


Figure 6.6 Cross-section of single-toggle jaw crusher

costs tend to be higher than with the double-toggle machine.

Double-toggle machines cost about 50% more than single-toggle machines of the same size, and are usually used on tough, hard, abrasive materials, although the single-toggle crusher is used in Europe, especially Sweden, for heavy-duty work on tough taconite ores, and it is often choke fed, since the jaw movement tends to make it self-feeding.

Jaw-crusher construction Jaw crushers are extremely heavy-duty machines and hence must be robustly constructed. The main frame is often made from cast iron or steel, connected with tie-bolts. It is often made in sections so that it can be transported underground for installation. Modern jaw crushers may have a main frame of mild steel plate welded together.

The jaws themselves are usually constructed from cast steel and are fitted with replaceable liners, made from manganese steel, or "Ni-hard", a Ni–Cr alloyed cast iron. Apart from reducing wear, hard liners are essential in that they minimise crushing energy consumption, reducing the deformation of the surface at each contact point. They are bolted in sections on to the jaws so that they can be removed easily and reversed periodically to equalise wear. Cheek plates are fitted to the sides of the crushing chamber to protect the main frame from wear. These are also made from hard alloy steel and have similar lives to the jaw plates. The jaw plates themselves may be smooth, but are often corrugated, the latter being preferred for hard, abrasive materials. Patterns on the working surface of the crushing members also influence capacity, especially at small settings. Laboratory tests have demonstrated that the capacity is reduced about 50 times when a corrugated profile is used rather than a smooth surface. The corrugated profile is claimed to perform compound crushing by compression, tension, and shearing. Conventional smooth crushing plates tend to perform crushing by compression only, though irregular particles under compression loading might still break in tension. Since rocks are around 10 times weaker in tension than compression, power consumption and wear costs should be lower with the corrugated profiles. Nevertheless, some type of pattern is desirable for

the jaw plate surface in a jaw crusher, partly to reduce the risk of undesired large flakes easily slipping through the straight opening, and partly to reduce the contact surface when crushing flaky blocks. In several installations, a slight wave shape has proved successful. The angle between the jaws is usually less than 26°, as the use of a larger angle than this causes slipping, which reduces capacity and increases wear.

In order to overcome problems of choking near the discharge of the crusher, which is possible if fines are present in the feed, curved plates are sometimes used. The lower end of the swing jaw is concave, whereas the opposite lower half of the fixed jaw is convex. This allows a more gradual reduction in size as the material nears the exit, hence minimising the chances of packing. Less wear is also reported on the jaw plates, since the material is distributed over a larger area.

The speed of jaw crushers varies inversely with the size, and usually lies in the range of 100–350 rev min^{-1}. The main criterion in determining the optimum speed is that particles must be given sufficient time to move down the crusher throat into a new position before being nipped again.

The maximum amplitude of swing of the jaw, or "throw", is determined by the type of material being crushed and is usually adjusted by changing the eccentric. It varies from 1 to 7 cm depending on the machine size, and is highest for tough, plastic material and lowest for hard, brittle ore. The greater the throw, the less danger is there of chokage, as material is removed more quickly. This is offset by the fact that a large throw tends to produce more fines, which inhibits arrested crushing. Large throws also impart higher working stresses to the machine.

In all crushers, provision must be made for avoiding the damage which could result from uncrushable material entering the chamber. Many jaw crushers are protected from such "tramp" material (usually metal objects) by a weak line of rivets on one of the toggle plates, although automatic trip-out devices are now becoming more common, and one manufacturer uses automatic overload protection based on hydraulic cylinders between the fixed jaw and the frame. In the event of excessive pressure caused by an overload, the jaw is allowed to open, normal gap conditions being reasserted after clearance of the blockage. This allows a full crusher to be started under load (Anon., 1981).

Jaw crushers range in size up to 1680 mm gape by 2130 mm width. This size machine will handle ore with a maximum size of 1.22 m at a crushing rate of approximately 725 t h^{-1} with a 203 mm set. However, at crushing rates above 545 t h^{-1} the economic advantage of the jaw crusher over the gyratory diminishes; and above 725 t h^{-1} jaw crushers cannot compete with gyratory crushers (Lewis et al., 1976).

Gyratory crushers

Gyratory crushers are principally used in surface-crushing plants, although a few currently operate underground. The gyratory crusher (Figure 6.7) consists essentially of a long spindle, carrying a hard steel conical grinding element, the head, seated in an eccentric sleeve. The spindle is suspended from a "spider" and, as it rotates, normally between 85 and 150 rev min^{-1}, it sweeps out a conical path within the fixed crushing chamber, or shell, due to the gyratory action of the eccentric. As in the jaw crusher, maximum movement of the head occurs near the discharge. This tends to relieve the choking due to swelling, the machine thus being a good arrested crusher. The spindle is free to turn on its axis in the eccentric sleeve, so that during crushing the lumps are compressed between the rotating head and the top shell segments, and abrasive action in a horizontal direction is negligible.

At any cross-section there are in effect two sets of jaws opening and shutting like jaw crushers. In fact, the gyratory crusher can be regarded as an infinitely large number of jaw crushers each of infinitely small width. Since the gyratory, unlike the jaw crusher, crushes on full cycle, it has a much higher capacity than a jaw crusher of the same gape, and is usually favoured in plants handling very large throughputs. In mines with crushing rates above 900 t h^{-1}, gyratory crushers are always selected.

Crushers range in size up to gapes of 1830 mm and can crush ores with top size of 1370 mm at a rate of up to 5000 t h^{-1} with a 200 mm set. Power consumption is as high as 750 kW on such crushers. Large gyratories often dispense with expensive feeding mechanisms and are often fed direct from trucks (Figure 6.8). They can be operated

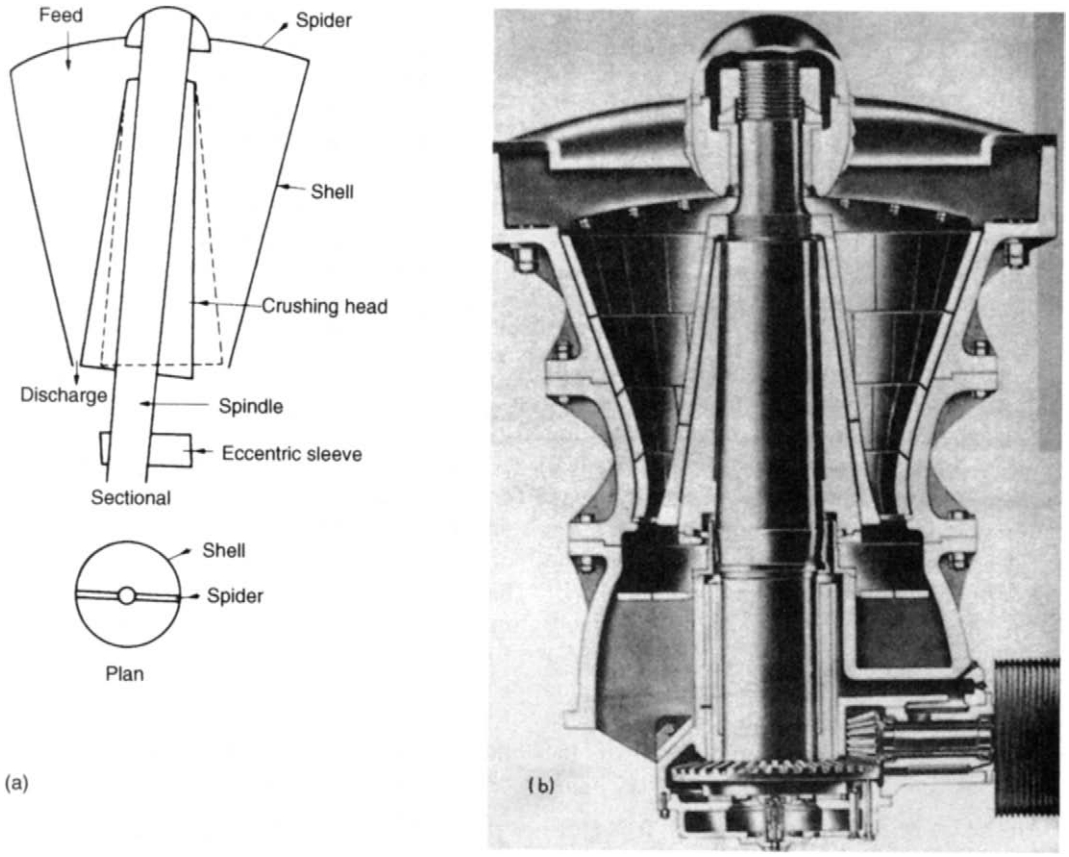


Figure 6.7 Gyratory crusher: (a) functional diagram, (b) cross-section

satisfactorily with the head buried in feed. Although excessive fines may have to be "scalped" from the feed, the modern trend in large-capacity plants is to dispense with grizzlies if the ore allows. This reduces capital cost of the installation and reduces the height from which the ore must fall into the crusher, thus minimising damage to the spider. Choked crushing is encouraged to some extent, but if this is not serious, the rock-to-rock crushing produced in the primaries reduces the rock-to-steel crushing required in the secondaries, thus reducing steel consumption (McQuiston and Shoemaker, 1978). Choke feeding of a gyratory crusher has been claimed to be also beneficial when the crusher is followed by SAG mills, whose throughput is sensitive to the mill feed size (Simkus and Dance, 1998). Operating crushers under choke feeding conditions gives more even mantle wear and longer life.

Gyratory-crusher construction The outer shell of the crusher is constructed from heavy steel casting or welded steel plate, with at least one constructional joint, the bottom part taking the drive shaft for the head, the top, and lower shells providing the crushing chamber. If the spindle is carried on a suspended bearing, as in the bulk of primary gyratories, then the spider carrying the bearing forms a joint across the reinforced alloyed white cast-iron (Ni-hard) liners or *concaves*. In small crushers the concave is one continuous ring bolted to the shell. Large machines use sectionalised concaves, called *staves*, which are wedge-shaped, and either rest on a ring fitted between the upper and the lower shell, or are bolted to the shell. The concaves are backed with some soft filler material, such as white metal, zinc, or plastic cement, which ensures even seating against the steel bowl.

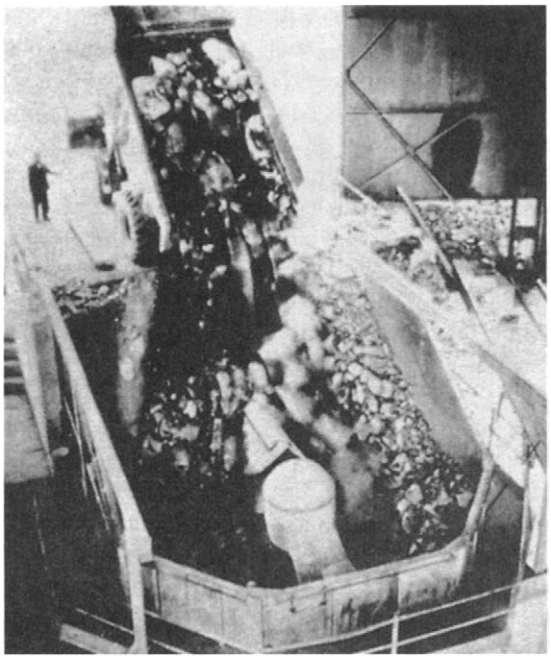


Figure 6.8 Gyratory crusher fed direct from truck

The head is one of the steel forgings which make up the spindle (Figure 6.9). The head is protected by a manganese steel *mantle*, which is fastened on to the head by means of nuts, on threads which are pitched so that they are self-tightening during operation. The mantle is backed with zinc, plastic cement, or, more recently, with an epoxy resin. The vertical profile is often bell-shaped to assist the crushing of material having a tendency to choke.

Some gyratory crushers have a hydraulic mounting and, when overloading occurs, a valve is tripped which releases the fluid, thus dropping the spindle and allowing the "tramp" material to pass out between the head and the bowl. This mounting is also used to adjust the set of the crusher at regular intervals so as to compensate for wear on the concaves and mantle. Many crushers use simple mechanical means to control the set, the most common method being by the use of a ring nut on the main shaft suspension.

In deciding whether a jaw or a gyratory crusher should be used in a particular plant, the main factor is the maximum size of ore which the crusher will be required to handle and the capacity required.

Gyratory crushers are, in general, used where high capacity is required. Since they crush on full cycle, they are more efficient than jaw crushers,

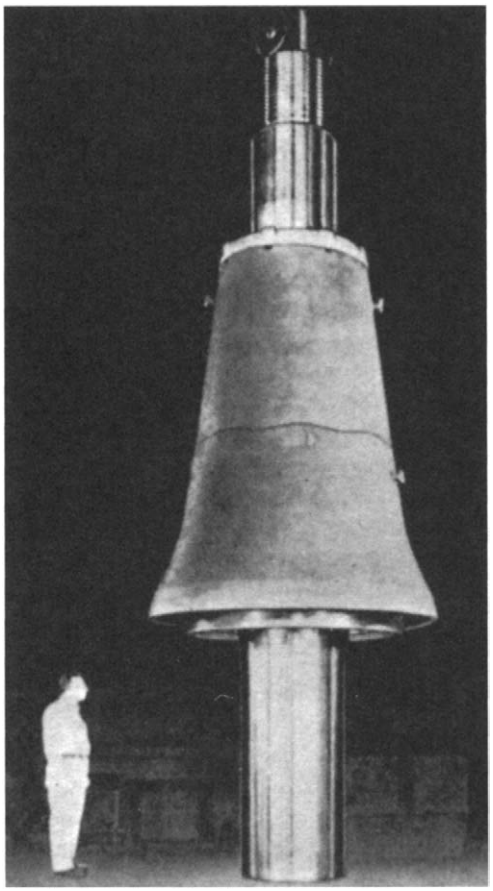


Figure 6.9 Crusher head

provided that the chamber can be kept full, which is normally easy, since the crusher can work with the head buried in ore.

Jaw crushers tend to be used where the crusher gape is more important than the capacity. For instance, if it is required to crush material of a certain maximum diameter, then a gyratory having the required gape would have a capacity about three times that of a jaw crusher of the same gape. If high capacity is required, then a gyratory is the answer. If, however, a large gape is needed but not capacity, then the jaw crusher will probably be more economical, as it is a smaller machine and the gyratory would be running idle most of the time. A useful relationship, which is often used in plant design, is that given by Taggart (1945):

If $t\,h^{-1} < 161.7\ (\text{gape in metres})^2$, use a jaw crusher.

Conversely, if the tonnage is greater than this value, use a gyratory crusher.

Because of the complex nature of jaw and gyratory crushers, exact formulae expressing their capacities have never been entirely satisfactory. Crushing capacity depends on many factors, such as the angle of nip (i.e. the angle between the crushing members), stroke, speed, and the liner material, as well as on the feed material, and its initial particle size. Capacity problems do not usually occur in the upper and middle sections of the crushing cavity, providing the angle of nip is not too great. It is normally the discharge zone, the narrowest section of the crushing chamber, which determines the crushing capacity.

Broman (1984) describes the development of simple models for optimising the performance of jaw and gyratory crushers. The volumetric capacity of a jaw crusher is expressed as:

$$Q = BSs \cdot \cot[a \cdot k \cdot 60n]\,\mathrm{m}^3/\mathrm{h}$$

where $B =$ inner width of crusher (m); $S =$ open side setting (m); $s =$ throw (m); $a =$ angle of nip; $n =$ speed of crusher (rpm); and k is a material constant, the size of which varies with the characteristics of the crushed material, the feeding method, liner type, etc., normally having values between 1.5 and 2.

For gyratory crushers, the corresponding formula is:

$$Q = (D - S)\pi Ss \cot(a \cdot k \cdot 60n)\,\mathrm{m}^3/\mathrm{h}$$

where $D =$ diameter of the outer head mantle at the discharge point (m), and k the material constant normally varying between 2 and 3.

The capital and maintenance costs of a jaw crusher are slightly less than those of the gyratory, but they may be offset by the installation costs, which are lower with the gyratory, since it occupies about two-thirds the volume and has about two-thirds the weight of a jaw crusher of the same capacity. This is because the circular crushing chamber allows a more compact design with a larger proportion of the total volume being accounted for by the crushing chamber than in the jaw crusher. Jaw-crusher foundations need to be much more rugged than those of the gyratory, due to the alternating working stresses.

The better self-feeding capability of the gyratory compared with the jaw results in a capital cost saving in some cases, with the elimination of expensive feeding devices, such as the heavy-duty chain feeder. This is, however, often false economy as the capital cost saving is considered of less importance in many cases than the improved performance and the pre-crusher scalping which is available with separate feeding devices.

In some cases, the jaw crusher has found favour, due to the ease with which it can be sectionalised. Thus, because of the need for transportation to remote locations and for underground use, it may be advantageous to install jaw crushers.

The type of material being crushed may also determine the crusher used. Jaw crushers perform better than gyratories on clayey, plastic material, due to their greater throw. Gyratories have been found to be particularly suitable for hard, abrasive material, and they tend to give a more cubic product than jaw crushers if the feed is laminated or "slabby".

Secondary crushers

Secondary crushers are much lighter than the heavy-duty, rugged primary machines. Since they take the primary crushed ore as feed, the maximum feed size will normally be less than 15 cm in diameter and, because most of the harmful constituents in the ore, such as tramp metal, wood, clays, and slimes have already been removed, it is much easier to handle. Similarly, the transportation and feeding arrangements serving the crushers do not need to be as rugged as in the primary stage. Secondary crushers also operate with dry feeds, and their purpose is to reduce the ore to a size suitable for grinding. In those cases where size reduction can be more efficiently carried out by crushing, there may be a tertiary stage before the material is passed to the grinding mills.

Tertiary crushers are, to all intents and purposes, of the same design as secondaries, except that they have a closer set.

The bulk of secondary crushing of metalliferous ores is performed by cone crushers, although crushing rolls and hammer mills are used for some applications.

The cone crusher

The cone crusher is a modified gyratory crusher. The essential difference is that the shorter spindle

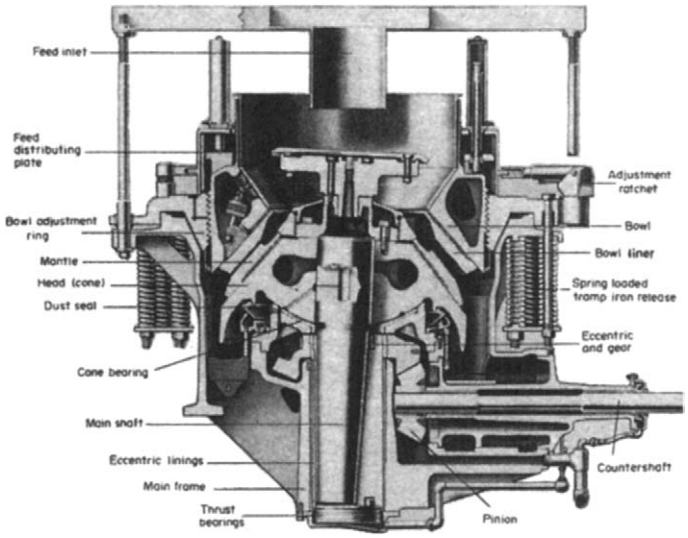


Figure 6.10 Cross-section of heavy-duty Symons cone crusher

of the cone crusher is not suspended, as in the gyratory, but is supported in a curved, universal bearing below the gyratory head or *cone* (Figure 6.10).

Power is transmitted from the source to the countershaft through a V-belt or direct drive. The countershaft has a bevel pinion pressed and keyed to it, and drives the gear on the eccentric assembly. The eccentric has a tapered, offset bore and provides the means whereby the head and main shaft follow an eccentric path during each cycle of rotation.

Since a large gape is not required, the crushing shell or "bowl" flares outwards which allows for the swell of broken ore by providing an increasing cross-sectional area towards the discharge end. The cone crusher is therefore an excellent arrested crusher. The flare of the bowl allows a much greater head angle than in the gyratory crusher, while retaining the same angle between the crushing members (Figure 6.11). This gives the cone crusher a high capacity, since the capacity of gyratory crushers is roughly proportional to the diameter of the head.

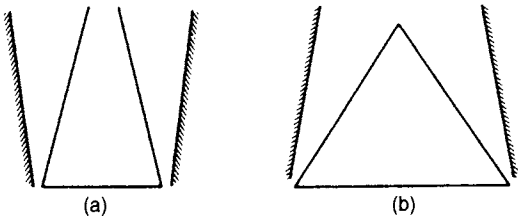


Figure 6.11 Head and shell shapes of (a) gyratory, and (b) cone crushers

The head is protected by a replaceable mantle, which is held in place by a large locking nut threaded onto a collar bolted on the top of the head. The mantle is backed with plastic cement, or zinc, or more recently with an epoxy resin.

Unlike a gyratory crusher, which is identified by the dimensions of the feed opening and the mantle diameter, a cone crusher is rated by the diameter of the cone lining. Cone crushers range in size from 559 mm to 3.1 m and have capacities up to $1100\,t\,h^{-1}$ with a discharge setting of 19 mm, although two 3.1 m Symons cone crushers, each with capacities of $3000\,t\,h^{-1}$, have been installed in a South African iron-ore plant (White, 1976).

The throw of cone crushers can be up to five times that of primary crushers, which must withstand heavier working stresses. They are also operated at much higher speeds. The material passing through the crusher is subjected to a series of hammer-like blows rather than being gradually compressed as by the slowly moving head of the gyratory.

The high-speed action allows particles to flow freely through the crusher, and the wide travel of the head creates a large opening between it and the bowl when in the fully open position. This permits

the crushed fines to be rapidly discharged, making room for additional feed.

The fast discharge and non-choking characteristics of the cone crusher allow a reduction ratio in the range 3–7:1, but this can be higher in some cases.

The Symons cone crusher is the most widely used type of cone crusher. It is produced in two forms: the Standard for normal secondary crushing and the Short-head for fine, or tertiary duty (Figures 6.12 and 6.13). They differ mainly in the shape of their crushing chambers. The Standard cone has "stepped" liners which allow a coarser feed than in the Short-head (Figure 6.14). They deliver a product varying from 0.5 to 6 cm. The Short-head has a steeper head angle than the Standard, which helps to prevent choking from the much finer material being handled. It also has a narrower feed opening and a longer parallel section at the discharge, and delivers a product of 0.3–2.0 cm.

The parallel section between the liners at the discharge is a feature of all cone crushers and is incorporated to maintain a close control on product size. Material passing through the parallel zone receives more than one impact from the crushing members. The set on the cone crusher is thus the minimum discharge opening.

The distributing plate on the top of the cone helps to centralise the feed, distributing it at a uniform rate to all of the crushing chamber.

An important feature of the crusher is that the bowl is held down either by an annular arrangement of springs or by a hydraulic mechanism. These allow the bowl to yield if "tramp" material enters the crushing chamber, so permitting the offending object to pass. If the springs are continually "on the work", as may happen with ores containing many tough particles, oversize material will be allowed to escape from the crusher. This is one of the reasons for using closed-circuit crushing in the final stages. It may be necessary to choose a screen for the circuit which has apertures slightly larger than the set of the crusher. This is to reduce the tendency for very tough particles, which are slightly oversize, to "spring" the crusher, causing an accumulation of such particles in the closed-circuit and a build-up of pressure in the crushing throat.

The set on the crusher can easily be changed, or adjusted for liner wear, by screwing the bowl up or down by means of a capstan and chain

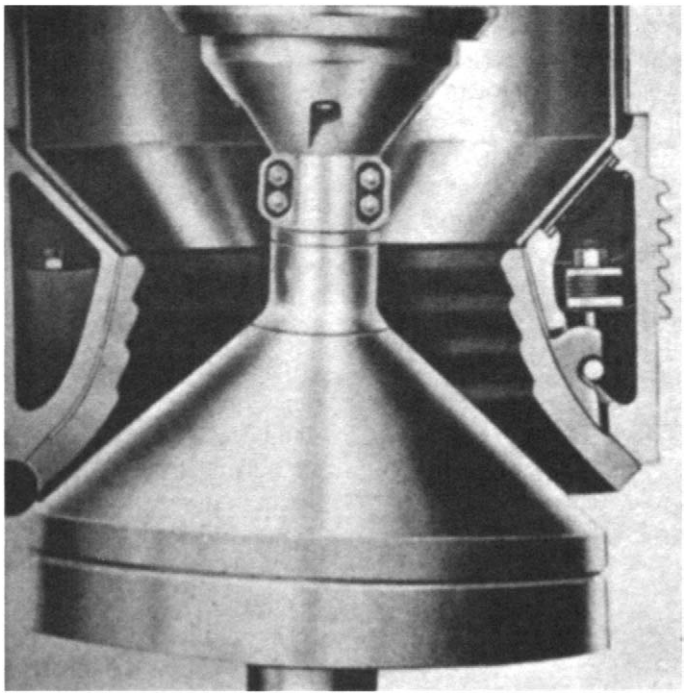


Figure 6.12 Standard cone crusher

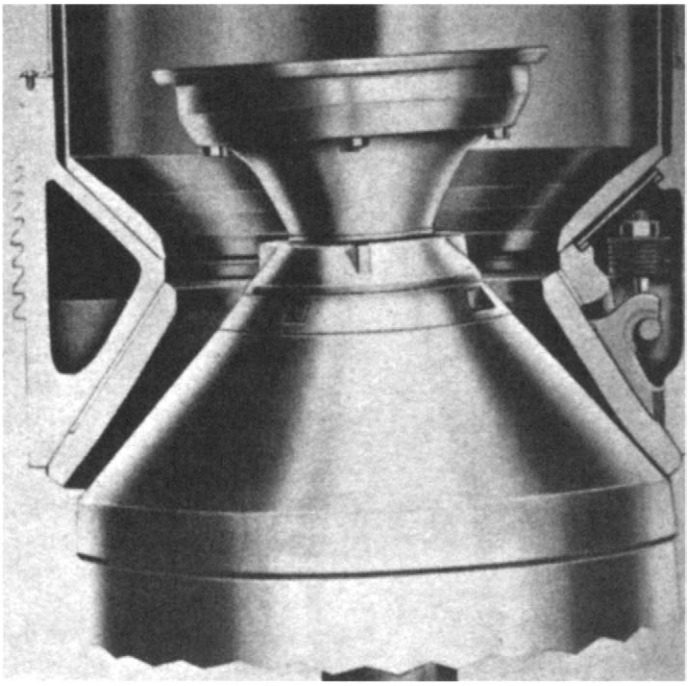


Figure 6.13 Short-head cone crusher

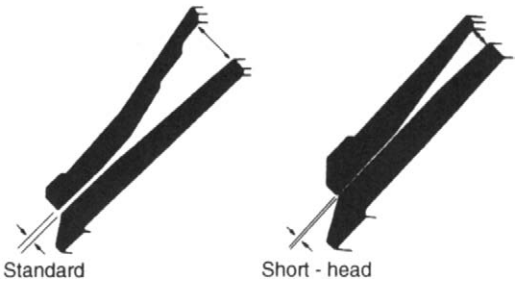


Figure 6.14 Liners of standard and short-head cone crushers

arrangement or by adjusting the hydraulic setting, as on the "425 Vari-Cone" crusher manufactured by Hewitt-Robins, which allows the operator to change settings even if the equipment is operating under maximum load (Anon., 1985). To close the setting, the operator opens a valve and presses a button starting a pump that adds hydraulic oil to the cylinder supporting the crusher head. To open the setting, another valve is opened allowing the oil to flow out of the cylinder. Efficiency is enhanced through automatic tramp iron clearing and reset. When tramp iron enters the crushing chamber, the crushing head will be forced down, causing hydraulic oil to flow into the accumulator. When the tramp iron has passed from the chamber, nitrogen pressure forces the hydraulic oil from the accumulator back into the supporting hydraulic cylinder, thus restoring the original setting.

Liner wear monitoring is possible using a Faro Arm (Figure 6.15), which is a portable coordinate measurement machine. A typical profile of a Symons concave liner is shown in Figure 6.16. More advanced systems use lasers to profile the mantle and concave in a vertical plane. This is accomplished by driving a laser/mirror arrangement into the crushing cavity along a track, guided by a computer-controlled motor/drive belt assembly. The laser calculates the relative distance from the mirror to the liner surface. Some of the benefits of the liner profiling systems include:

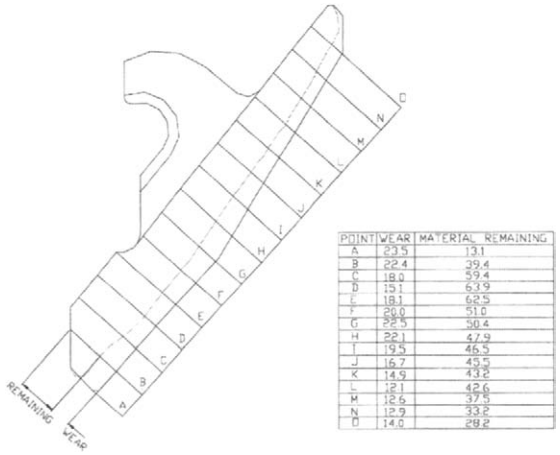
- Improved information for predicting mantle and concave liner replacement
- Identifying high wear areas
- Quantifying wear life with alternative liner alloys

In 1988 Nordberg Inc. introduced wet tertiary cone crushing at a Brazilian lead–zinc mine (Karra,



FARO, FAROARM and the Faro Blue color are registered trademarks and trademarks of FARO Technologies Inc. © 2006 FARO Technologies Inc. All Rights Reserved.

Figure 6.15 Faro Arm (Courtesy Faro Technologies)



POINT	WEAR	MATERIAL REMAINING
A	23.5	13.1
B	22.4	39.4
C	18.9	59.4
D	15.1	63.9
E	18.1	62.5
F	20.8	51.0
G	22.5	50.4
H	22.1	47.9
I	19.5	46.5
J	16.7	45.5
K	14.9	43.2
L	12.1	42.6
M	12.6	37.5
N	12.9	33.2
O	14.0	28.2

Figure 6.16 Example of a worn Symons concave liner profile, overlaid on the new liner profile (Courtesy Rio Tinto Technical Services)

1990). The so-called *Water Flush* technology uses a cone crusher incorporating special seals, internal components, and lubricants to handle the large flow of water, which is added to the crusher to produce a product slurry containing 30–50% solids, which can be fed directly to ball mills. Such technology has potential for the crushing of sticky ores, for improving productivity in existing circuits, and for developing more cost-effective conventional circuits.

However, the presence of water during crushing can increase the liner wear rates substantially, depending on the application. In pebble crushing applications found in AG/SAG circuits, Water Flush crushers have been problematic due to high wear and resulting maintenance demand.

The gyradisc crusher This is a specialised form of cone crusher, used for producing very fine material, and such crushers have found application in the quarrying industry for the production of large quantities of sand at economic cost (Anon., 1967).

The main modification to the conventional cone crusher is that the machine has very short liners and a very flat angle for the lower liner (Figure 6.17). Crushing is by *interparticle comminution* by the impact and attrition of a *multi*-layered mass of particles (Figure 6.18).

The angle of the lower liner is less than the angle of repose of the ore, so that when the liner is at rest the material does not slide. Transfer through the crushing zone is by movement of the head. Each time the lower liner moves away from the upper liner, material enters the attrition chamber from the surge load above. When reduction begins, material is picked up by the lower liner and is moved outward. Due to the slope of the liner it is carried to an advanced position and caught between the crushing members.

The length of stroke and the timing are such that after the initial stroke the lower liner is withdrawn faster than the previously crushed material falls by gravity. This permits the lower liner to recede and return to strike the previously crushed mass as it is falling, thus scattering it so that a new alignment of particles is obtained prior to another impact. At each withdrawal of the head, the void is filled by particles from the surge chamber.

At no time does single-layer crushing occur, as with conventional crushers. Crushing is by particle on particle, so that the setting of the crusher is not as directly related to the size of product as it is on the cone crusher.

Their main use is in quarries, for producing sand and gravel. When used in open circuit they will produce a product of chippings from about 1 cm downwards, of good cubic shape, with a satisfactory amount of sand, which obviates the use of blending and rehandling. In closed circuit they are

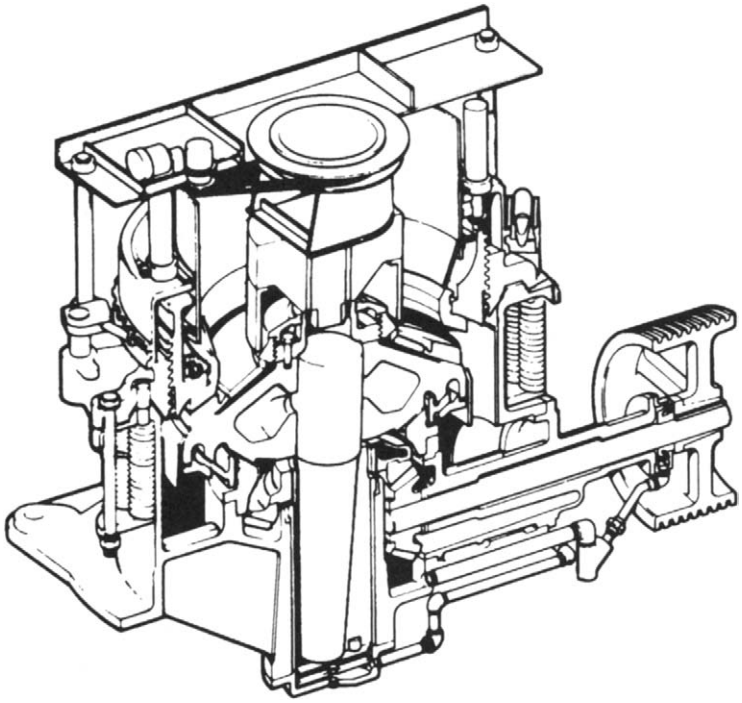


Figure 6.17 Gyradisc crusher

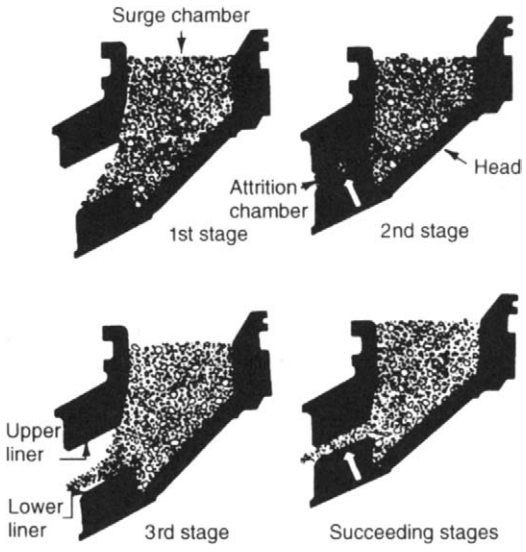


Figure 6.18 Action of gyradisc crusher

used to produce large quantities of sand. They may be used in open circuit on clean metalliferous ores with no primary slimes to produce an excellent ball-mill feed. Less than 19 mm material may be crushed to about 3 mm (Lewis et al., 1976).

The Rhodax crusher

This is a specialised form of a cone crusher, referred to as an inertial cone crusher. Developed by the FCB Research Centre in France, the Rhodax crusher is claimed to offer process advantages over conventional cone crushers and is based on inter-particle compression crushing. It consists of a frame supporting a cone and a mobile ring, and a set of rigid links forming a set of ties between the two parts (Figure 6.19).

The frame is supported on elastic suspensions isolating the environment from dynamic stresses created by the crushing action. It contains a central shaft fixed on a structure. A grinding cone is mounted on this shaft and is free to rotate. A sliding sleeve on this shaft is used to adjust the vertical position of the cone and therefore the gap, making it simple to compensate for wear. The ring structure is connected to the frame by a set of tie rods. The ring and the cone are made of wear resistant steel.

One set of synchronised unbalanced masses transmits a known and controlled crushing force to the ring when they rotate. This fragmentation force is proportional to $m\omega^2 r$, and stays constant even if

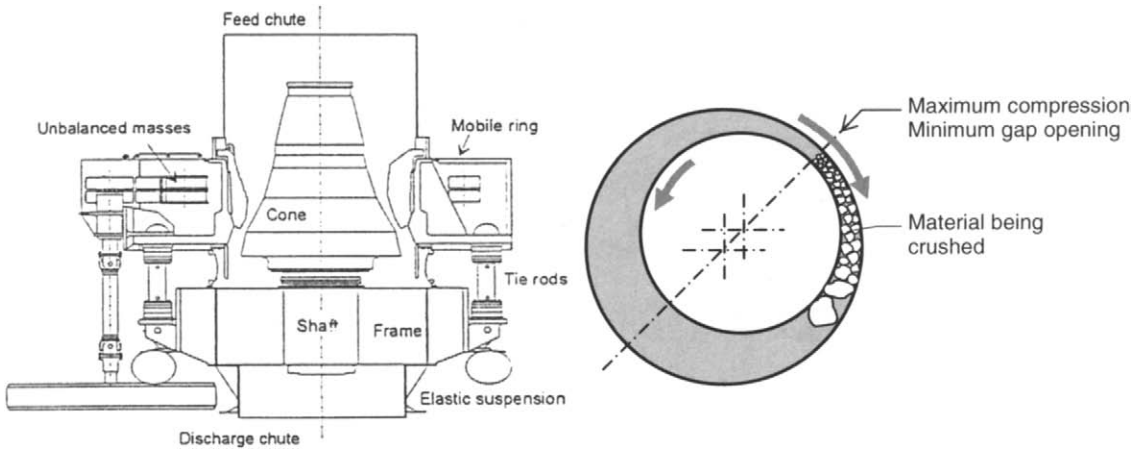


Figure 6.19 Schematic of the Rhodax crusher, and principle of operation (Courtesy JKMRC and JKTech Pty Ltd)

the feed varies, or an unbreakable object enters the crushing chamber. The Rhodax is claimed to achieve reduction ratios varying from 4 to more than 30 in open circuit. The relative positions of the unbalanced masses can be changed if required, so the value of the crushing force can thus be remotely controlled. As feed particles enter the fragmentation chamber, they slowly advance between the cone and the moving ring. These parts are subjected to horizontal circular translation movements and move towards and away from each other at a given point.

During the approach phase, materials are subjected to compression. The maximum pressure to which a material bed may be subjected is 10–50 MPa. During the separation phase, fragmented materials pass further down in the chamber until the next compression cycle. The number of cycles is typically 4–5. During these cycles the cone rolls on a bed of stressed material a few millimetres thick, with a rotation speed of a 10–20 rpm. This rotation is actually an epicyclical movement due to the lack of sliding friction between the cone and the feed material. The unbalanced masses rotate at 100–300 rpm. The following three parameters can be adjusted on the Rhodax crusher:

- the gap between the cone and the ring,
- the total static moment of unbalanced masses, and
- the rotation speed of these unbalanced masses.

The combination of the latter two settings enables the operator to fix the required fragmentation force very easily and quickly. Two series of machines have been developed on this basis, one for the production of aggregates (maximum pressure on the material bed between 10 and 25 MPa), and the other for coarse grinding or fine grinding (25–50 MPa maximum pressure on the material bed). Given the design of the machine (relative displacement of two non-imposed wear surfaces), the product size distribution is independent of the gap and wear. These are distinct advantages over conventional crushers which suffer problems with the variable product quality caused by wear. In conjunction with FCB in France, Multotec Process Equipment from South Africa is participating in the ongoing development of the Rhodax crusher in the mineral industry.

Roll crushers Roll crushers, or crushing rolls, are still used in some mills, although they have been replaced in most installations by cone crushers. They still have a useful application in handling friable, sticky, frozen, and less abrasive feeds, such as limestone, coal, chalk, gypsum, phosphate, and soft iron ores. Jaw and gyratory crushers have a tendency to choke near the discharge when crushing friable rock with a large proportion of maximum size pieces in the feed.

The mode of operation of roll crushers is extremely simple, the standard spring rolls (Figure 6.20) consisting of two horizontal cylinders which revolve towards each other. The set is determined by shims which cause the spring-loaded roll to be held back from the solidly mounted roll.

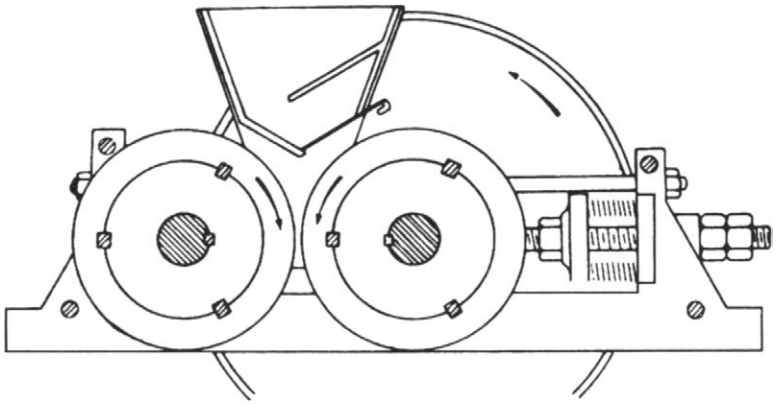


Figure 6.20 Crushing rolls

Unlike jaw and gyratory crushers, where reduction is progressive by repeated pressure as the material passes down to the discharge point, the crushing process in rolls is one of single pressure.

Roll crushers are also manufactured with only one rotating cylinder, which revolves towards a fixed plate. Other roll crushers use three, four, or six cylinders. In some crushers the diameters and speeds of the rolls may differ. The rolls may be gear driven, but this limits the distance adjustment between the rolls; and modern rolls are driven by V-belts from separate motors.

Multi-roll machines may use rolls in pairs or in sets of three. Machines with more than two rolls are, however, rare in modern mills. The great disadvantage of roll crushers is that, in order for reasonable reduction ratios to be achieved, very large rolls are required in relation to the size of the feed particles. They therefore have the highest capital cost of all crushers.

Consider a spherical particle, of radius r, being crushed by a pair of rolls of radius R, the gap between the rolls being $2a$ (Figure 6.21). If μ is the coefficient of friction between the rolls and the particle, θ is the angle formed by the tangents to the roll surfaces at their points of contact with the particle (the angle of nip), and C is the compressive force exerted by the rolls, acting from the roll centres through the particle centre, then for a particle to be *just* gripped by the rolls, equating vertically,

$$C \sin\left(\frac{\theta}{2}\right) = \mu C \cos\left(\frac{\theta}{2}\right) \qquad (6.1)$$

Therefore

$$\mu = \tan\left(\frac{\theta}{2}\right) \qquad (6.2)$$

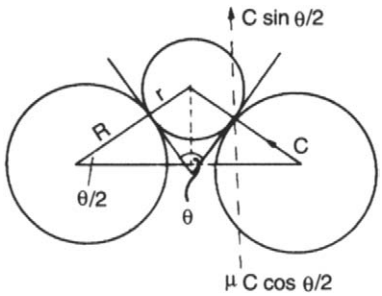


Figure 6.21 Forces on a particle in crushing rolls

The coefficient of friction between steel and most ore particles is in the range 0.2–0.3, so that the value of the angle of nip θ should never exceed about 30°, or the particle will slip. It should also be noted that the value of the coefficient of friction decreases with speed, so that the speed of the rolls depends on the angle of nip, and the type of material being crushed. The larger the angle of nip (i.e. the coarser the feed), the slower the peripheral speed needs to be to allow the particle to be nipped. For smaller angles of nip (finer feed), the roll speed can be increased, so increasing the capacity. Peripheral speeds vary between about $1\,\mathrm{m\,s^{-1}}$ for small rolls, up to about $15\,\mathrm{m\,s^{-1}}$ for the largest sizes of 1800 mm diameter upwards.

The value of the coefficient of friction between a particle and moving rolls can be calculated from the equation

$$\mu_k = \left[\frac{1+1.12v}{1+6v}\right]\mu \qquad (6.3)$$

where μ_k is the kinetic coefficient of friction and v is the peripheral velocity of the rolls ($m\,s^{-1}$). From Figure 6.21,

$$\cos\left(\frac{\theta}{2}\right) = \frac{R+a}{R+r} \qquad (6.4)$$

Equation 6.4 can be used to determine the maximum size of rock gripped in relation to roll diameter and the reduction ratio (r/a) required. Table 6.1 lists such values for rolls crushing material where the angle of nip should be less than 20° in order for the particles to be gripped (in most practical cases the angle of nip should not exceed about 25°).

It can be seen that unless very large diameter rolls are used, the angle of nip limits the reduction ratio of the crusher, and since reduction ratios greater than 4:1 are rarely used, a flow-line may require coarse crushing rolls to be followed by fine rolls.

Smooth-surfaced rolls are usually used for fine crushing, whereas coarse crushing is often performed in rolls having corrugated surfaces, or with stub teeth arranged to present a chequered surface pattern. "Sledging" or "slugger" rolls have a series of intermeshing teeth, or slugs, protruding from the roll surfaces (Figure 6.22). These dig into the rock so that the action is a combination of compression and ripping, and large pieces in relation to the roll diameter can be handled. Their main application is in the coarse crushing of soft or sticky iron ores, friable limestone, coal, etc., rolls of 1 m diameter being used to crush material of top size 400 mm.

Wear on the roll surfaces is very high and they often have a manganese steel tyre, which can be

Table 6.1 Maximum diameter of rock gripped in crushing rolls relative to roll diameter

Roll diameter (mm)	*Maximum size of rock gripped* (mm) *Reduction ratio*				
	2	*3*	*4*	*5*	*6*
200	6.2	4.6	4.1	3.8	3.7
400	12.4	9.2	8.2	7.6	7.3
600	18.6	13.8	12.2	11.5	11.0
800	24.8	18.4	16.3	15.3	14.7
1000	30.9	23.0	20.4	19.1	18.3
1200	37.1	27.6	24.5	22.9	22.0
1400	43.3	32.2	28.6	26.8	25.7

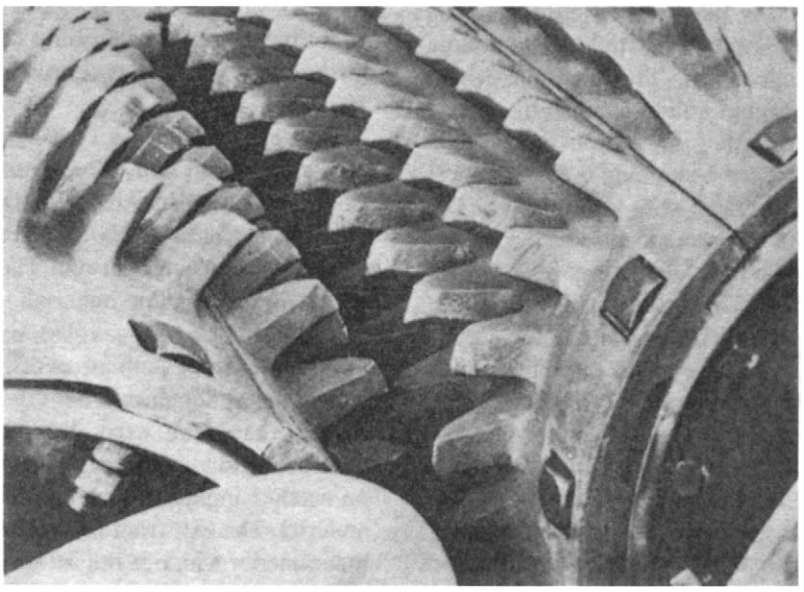


Figure 6.22 Toothed crushing mills

replaced when worn. The feed must be spread uniformly over the whole width of the rolls in order to give even wear. One simple method is to use a flat feed belt of the same width as the rolls.

Since there is no provision for the swelling of broken ore in the crushing chamber, roll crushers must be "starvation fed" if they are to be prevented from choking. Although the floating roll should only yield to an uncrushable body, choked crushing causes so much pressure that the springs are continually "on the work" during crushing, and some oversize escapes. Rolls should therefore be used in closed circuit with screens. Choked crushing also causes interparticle comminution, which leads to the production of material finer than the set of the crusher.

The capacity of the rolls can be calculated in terms of the ribbon of material that will pass the space between the rolls. Thus theoretical capacity is equal to

$$188.5\ NDW\ sd\ \mathrm{kg\,h^{-1}} \qquad (6.5)$$

where N is the speed of rolls ($\mathrm{rev\,min^{-1}}$), D is the roll diameter (m), W is the roll width (m), s is the specific gravity of feed material ($\mathrm{kg\,m^{-1}}$), and d is the distance between the rolls (m).

In practice, allowing for voids between the particles, loss of speed in gripping the feed, etc., the capacity is usually about 25% of the theoretical.

The pressure exerted on the feed particles in conventional roll crushers is in the range 10–30 MPa, but work in Germany led to the development in the mid-1980s of the *High-Compression Roller Mill*, which utilises forces in excess of 50 MPa, by the action of a hydraulic pressures system acting on a piston which presses the movable roller against the material bed (Figure 6.23) (density >70% solids by volume). Under such high forces, the product is a compacted cake containing a high proportion of fines and grains with microcracks. The compacted cake is subsequently deagglomerated, releasing the fines, and it has been shown (Brachthauser and Kellerwessel, 1988; Schwechten and Milburn, 1990) that the specific energy consumption for compression and ball mill-deagglomeration is considerably less than that of ball mill grinding alone. The typical comminution energy in an HPGR unit is 2.5–3.5 kW h/t, compared to 15–25 kW h/t in ball mill grinding. These mills are now being utilised in the cement, diamond, and limestone industries, and there is some evidence to show that mineral liberation can be improved by using these devices, so that they may be useful in the comminution of industrial and metalliferous ores (Esna-Ashari and Kellerwessel, 1988; Clark and Wills, 1989; Knecht, 1994; Watson and Brooks, 1994; Daniel, 2004). The mills were originally designed to be operated with smooth rolls, but studded rolls have become standard in the new designs, because of their improved wear-resistant characteristics (Figure 6.24).

Impact crushers

In this class of crusher, comminution is by impact rather than compression, by sharp blows applied at high speed to free-falling rock. The moving parts are beaters, which transfer some of their kinetic

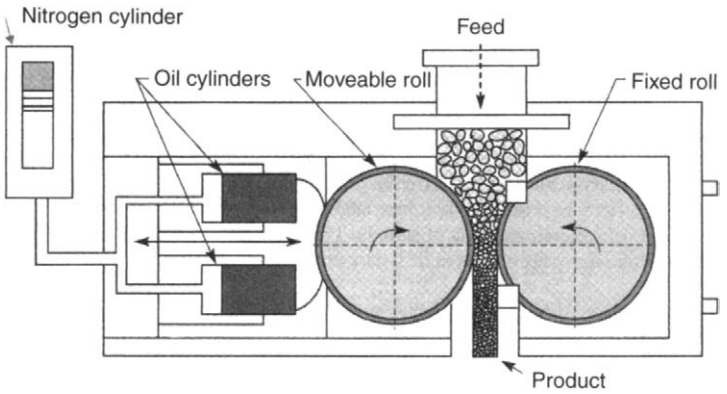


Figure 6.23 High pressure grinding rolls (from Napier-Munn et al., 1996; Courtesy JKMRC, The University of Queensland)

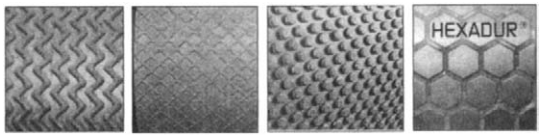


Figure 6.24 HPGR roll surface types: welded, chevron, studded and hexadur (Courtesy Humboldt Wedag Australia)

energy to the ore particles on contacting them. The internal stresses created in the particles are often large enough to cause them to shatter. These forces are increased by causing the particles to impact upon an anvil or breaker plate.

There is an important difference between the states of materials crushed by pressure and by impact. There are internal stresses in material broken by pressure which can later cause cracking. Impact causes immediate fracture with no residual stresses. This stress-free condition is particularly valuable in stone used for brick-making, building, and roadmaking, in which binding agents, such as bitumen, are subsequently added to the surface. Impact crushers, therefore, have a wider use in the quarrying industry than in the metal-mining industry. They may give trouble-free crushing on ores that tend to be plastic and pack when the crushing forces are applied slowly, as is the case in jaw and gyratory crushers. These types of ore tend to be brittle when the crushing force is applied instantaneously by impact crushers (Lewis et al., 1976).

Impact crushers are also favoured in the quarry industry because of the improved product shape. Cone crushers tend to produce more elongated particles because of their high reduction ratios and ability of such particles to pass through the chamber unbroken. In an impact crusher, all particles are subjected to impact and the elongated particles, having a lower strength due to their thinner cross section, would be broken (Ramos et al., 1994; Kojovic, 1995).

Figure 6.25 shows a cross-section through a typical *hammer mill*. The hammers are made from manganese steel or, more recently, nodular cast iron, containing chromium carbide, which is extremely abrasion resistant. The breaker plates are made of the same material.

The hammers are pivoted so that they can move out of the path of oversize material, or tramp metal,

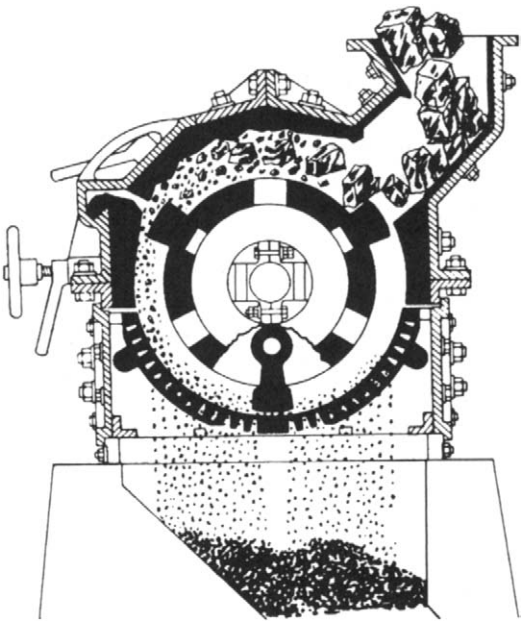


Figure 6.25 Hammer mill

entering the crushing chamber. Pivoted hammers exert less force than they would if rigidly attached, so they tend to be used on smaller impact crushers or for crushing soft material. The exit from the mill is perforated, so that material which is not broken to the required size is retained and swept up again by the rotor for further impacting.

This type of machine is designed to give the particles velocities of the order of that of the hammers. Fracture is either due to the severity of impact with the hammers or to the subsequent impact with the casing or grid. Since the particles are given very high velocities, much of the size reduction is by attrition, i.e. breaking of particle on particle, and this leads to little control on product size and a much higher proportion of fines than with compressive crushers.

The hammers can weigh over 100 kg and can work on feed up to 20 cm. The speed of the rotor varies between 500 and 3000 rev min^{-1}.

Due to the high rate of wear on these machines (wear can be taken up by moving the hammers on the pins) they are limited in use to relatively non-abrasive materials. They have extensive use in limestone quarrying and in the crushing of coal. A great advantage in quarrying is in the fact that they produce a very good cubic product.

Hammer mills have been used by Australian coking coal producers to prepare coke oven feeds (0.125–6 mm). To assist in the beneficiation of coke oven feeds, recent work has led to the development of a model of the swing hammer mill (Shi et al., 2003). The energy-based model comprises a mechanistic model for the mill power draw and a perfect mixing mill model with a dual-classification function to describe the operation of the hammers and underscreen. The model is able to accurately predict the product size distribution and power draw for given hammer mill configurations (breaker gap, under-screen orientation, screen aperture) and operating conditions (feed rate, feed size distribution, and coal breakage characteristics).

For much coarser crushing, the fixed hammer *impact mill* is often used (Figure 6.26). In these machines the material falls tangentially on to a rotor, running at 250–500 rev min^{-1}, receiving a glancing impulse, which sends it spinning towards the impact plates. The velocity imparted is deliberately restricted to a fraction of the velocity of the rotor to avoid enormous stress and probable failure of the rotor bearings.

The fractured pieces which can pass between the clearances of the rotor and breaker plate enter a second chamber created by another breaker plate, where the clearance is smaller, and then into a third smaller chamber. This is the *grinding path* which is designed to reduce flakiness and gives very good cubic particles.

The rotary impact mill gives a much better control of product size than does the hammer mill, since there is less attrition. The product shape is much more easily controlled and energy is saved by the removal of particles once they have reached the size required.

The blow bars are reversible to even out wear, and can easily be removed and replaced.

Large impact crushers will reduce 1.5 m top size run-of-mine ore to 20 cm, at capacities of around 1500 t h^{-1}, although crushers with capacities of 3000 t h^{-1} have been manufactured. Since they depend on high velocities for crushing, wear is greater than for jaw or gyratory crushers. Hence impact crushers should not be used on ores containing over 15% silica (Lewis et al., 1976). However, they are a good choice for primary crushing when high reduction ratios are required (the ratio can be as high as 40:1) and a high percentage of fines, and the ore is relatively non-abrasive.

The Tidco Barmac Crusher was developed in New Zealand in the late 1960s, and is finding increasing application (Rodriguez, 1990). The mill combines impact crushing, high-intensity grinding, and multi-particle pulverising, and as such, is best suited in the tertiary crushing or primary grinding stage, producing products in the 0.06–12 mm size range. A cross-section of the *Duopactor*, which can handle feeds of up to 650 t h^{-1}, at a top size of over 50 mm, is shown in Figure 6.27. The basic

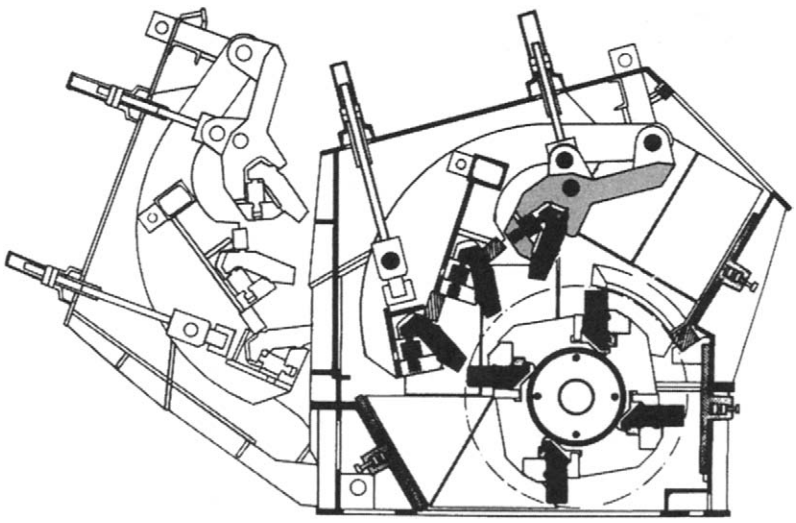


Figure 6.26 Impact mill

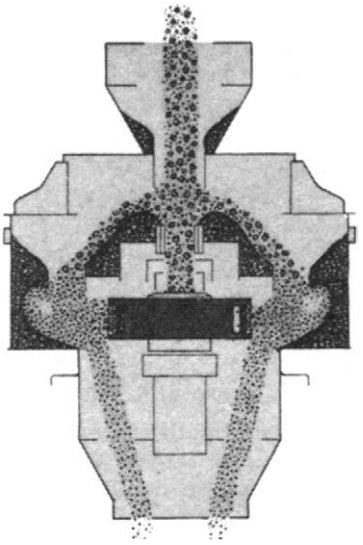


Figure 6.27 Cross-section of Tidco Barmac Duopactor Crusher

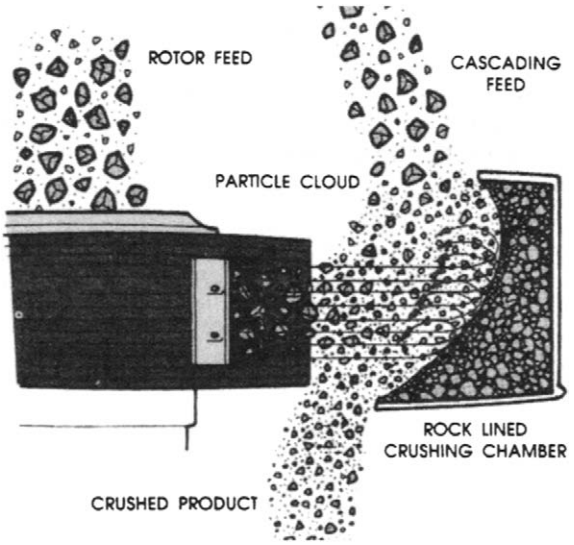


Figure 6.28 Action within Barmac crushing chamber

comminution principle employed involves acceleration of particles within a special ore-lined rotor revolving at high speed (Figure 6.28). Grinding commences when rock enters the rotor, and is thrown centrifugally, achieving exit velocities of up to 90 m/s. The rotor continuously discharges into a highly turbulent particle cloud contained within the crushing chamber, where reduction occurs primarily by rock-on-rock impact, attrition, and abrasion.

Other impact crushers include the *Canica Vetical Shaft Impact Crusher* developed by Jaques (Figure 6.29). These units typically operate with five iron impellors or hammers, with a ring of thin anvils. Rock is hit or accelerated to impact on the anvils, after which the broken fragments are free to fall into a discharge chute onto a product conveyor belt. This true impact size reduction process was successfully modelled by Kojovic (1996) and Djordjevic et al. (2003), using rotor dimensions and speed, and rock breakage characteristics measured in the laboratory. The model was also extended to the Barmac crushers (Napier-Munn et al., 1996).

Rotary coal breakers

Where large tonnages of coal are treated, the rotary coal breaker is often used (Figure 6.30).

This is very similar in operation to the cylindrical trommel screen (Chapter 8), consisting of a cylinder of 1.8–3.6 m in diameter and length of about $1\frac{1}{2}$ to $2\frac{1}{2}$ times the diameter, revolving at a speed of about 12–18 rev min^{-1}. The machine is massively constructed, with perforated walls, the size of the perforations being the size to which the coal is to be broken. The run-of-mine coal is fed into the rotating cylinder, at up to 1500 t h^{-1} in the larger machines. The machine utilises differential breakage, the coal being much more friable than the associated stones and shales, and rubbish such as wood, steel, etc., from the mine. The small particles of coal and shale quickly fall through the holes, while the larger lumps are retained, and are lifted by longitudinal lifters within the cylinder until they reach a point where they slide off the lifters and fall to the bottom of the cylinder, breaking by their own impact, and fall through the holes. The lifters are inclined to give the coal a forward motion through the breaker. Large pieces of shale and stone do not break as easily, and are usually discharged from the end of the breaker, which thus cleans the coal to a certain degree and, as the broken coal is quickly removed from the breaker, produces few fines. Although the rotary breaker is an expensive piece of equipment, maintenance costs are relatively low, and it produces positive control of top size product.

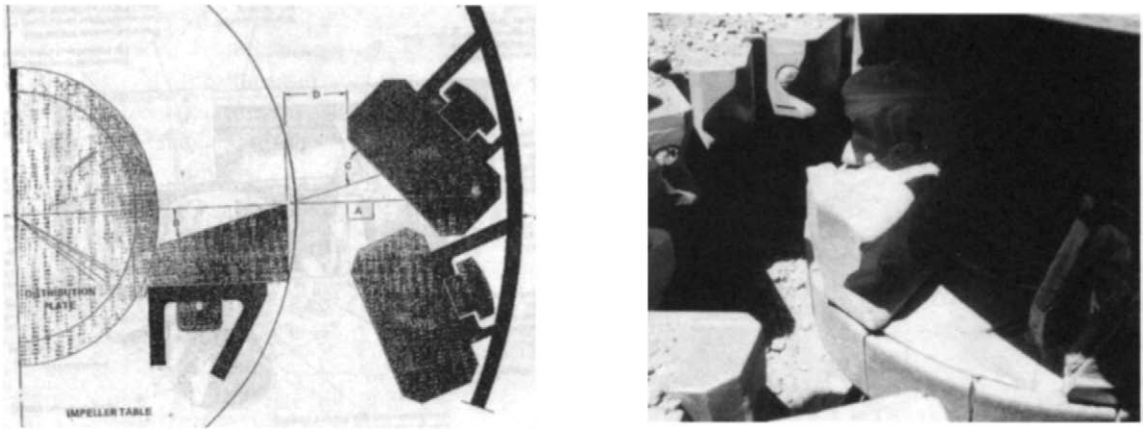


Figure 6.29 Canica VSI crusher impeller and anvil schematic; Model 100 wear profile (Courtesy JKMRC and JKTech Pty Ltd)

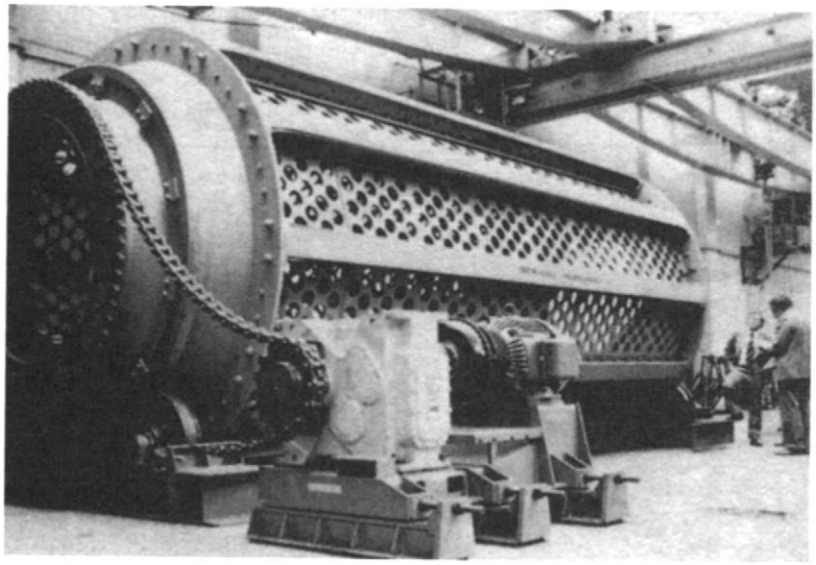


Figure 6.30 Rotary coal breaker

An overview of some of the recent work on modelling rotary breakers has been given by Esterle et al. (1996). The work was based at three open cut coal mines in Central Queensland, Australia, where 3 m diameter breakers were handling ROM coal.

Crushing circuits and control

In recent years, efforts have been made to improve crusher efficiency in order to reduce capital and operating costs. Automatic control of crushing circuits is increasingly used, larger crushers have been constructed, and mobile crushing units have been used, which allow relatively cheap ore transportation by conveyor belts rather than by trucks to a fixed crushing station (Kok, 1982; Woody, 1982; Gresshaber, 1983; Frizzel, 1985). A mobile crusher is a completely self-contained unit, mounted on a frame that is moved by means of a transport mechanism in the open pit as mining progresses. Mobile units typically use jaw, hammer, or roll crushers, fed directly or by apron feeders, at rates of up to 1000 t h^{-1}. Some

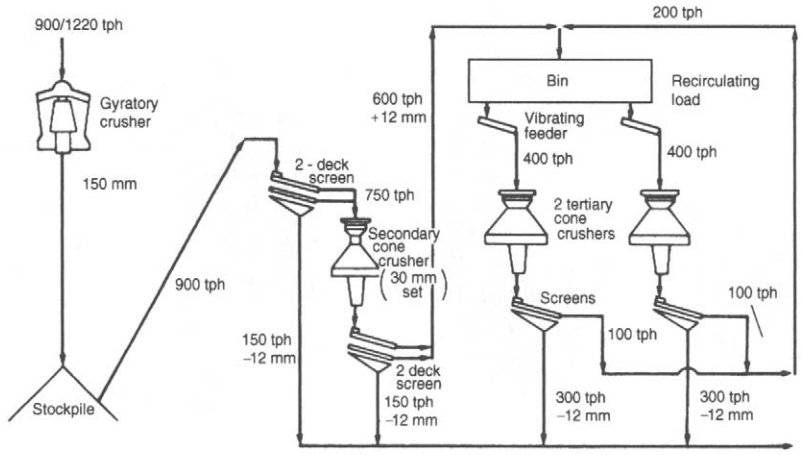


Figure 6.31 Three-stage crushing circuit for ball mill feed (after Motz, 1978)

units employ large gyratory crushers with capacities of up to 6000 t h^{-1} (Wyllie, 1989).

A typical flowsheet for a crushing plant producing ball mill feed is shown in Figure 6.31 (Motz, 1978). The circuit is typical of current practice in that the secondary product is screened and conveyed to a storage bin, rather than feeding the tertiary crushers directly. The intermediate bins allow good mixing of the secondary screen oversize with the circulating load, and regulation of the tertiary crusher feed, providing more efficient crushing. The circuit is also more readily adaptable to automatic feed control to maintain maximum power utilisation (Mollick, 1980).

In some cases, the crushing circuit is designed not only to produce mill feed, but also to provide media for autogenous grinding. Figure 6.32 shows the flowsheet for the crushing circuit at Pyhasalmi

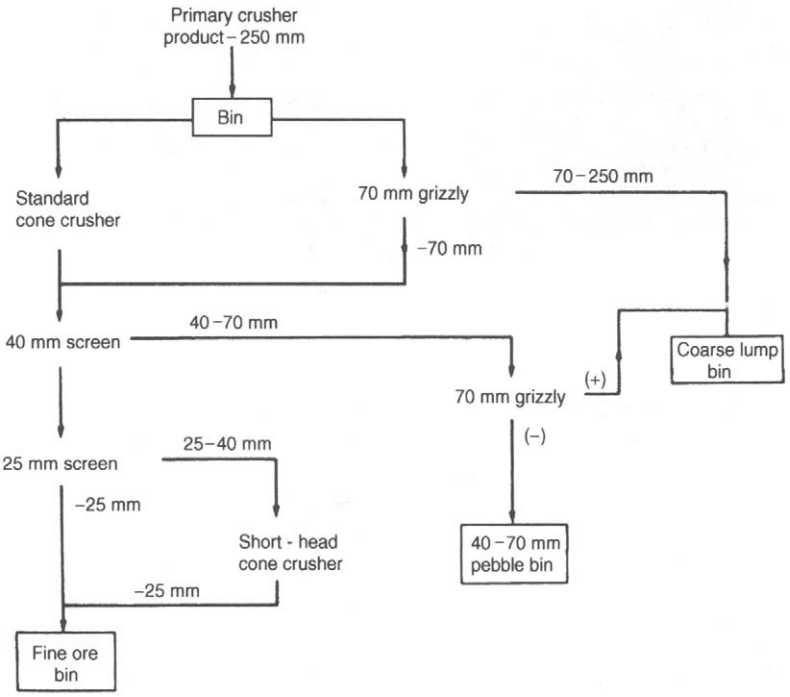


Figure 6.32 Pyhasalmi crushing circuit

in Finland, where grinding is performed in lump mills, followed by pebble mills (Wills, 1983). Primary crushing is carried out underground and the product is hoisted to the fine crushing plant on top of the fine ore bin. This plant consists of two parallel crushing lines, one including a standard Symons cone crusher as the first stage, and the other commencing with a vibrating grizzly of 70 mm set. The grizzly oversize of 70–250 mm is conveyed directly to a coarse lump bin, while the undersize joins the cone crusher product from the other line. This material is screened on two double deck vibrating screens, to produce a fine ore product of −25 mm, an intermediate product of 25–40 mm, which is crushed to −25 mm in an open circuit short-head Symons cone crusher, and a +40 mm fraction which is transferred to a 40–70 mm pebble bin via a 70 mm scalping grizzly.

Recent advances in instrumentation and process control hardware have made the implementation of computer control more common in crushing circuits. Instrumentation employed includes ore level detectors, oil flow sensors, power measurement devices, belt scales, variable speed belt drives and feeders, blocked chute detectors, and particle size measurement devices (Horst and Enochs, 1980). The importance of automatic control is exemplified by the crushing plant at Mount Isa in Australia, where the output increased by over 15% after controls were introduced (Manlapig and Watsford, 1983).

Supervisory control systems are not usually applied to primary crushers, the instrumentation basically being used to protect them. Thus lubrication flow indicators and bearing temperature detectors may be fitted, together with high and low level alarms in the chamber under the crusher.

The operating and process control objectives for secondary and tertiary crushing circuits differ from one plant to the next, but usually the main objective is to maximise crusher throughput at some specified product size. Numerous variables affect the performance of a crusher, but only three – ore feed rate, crusher opening and, in some cases, feed size – can be adjusted. Lynch (1977) has described case studies of automatic control systems for various applications. When the purpose of the crushing plant is to produce feed for the grinding circuit, the most important objective of the control system is to ensure a supply of crushed ore at the rate required by the grinding plant. The fineness of the crusher product is maintained by the selection of screens of the appropriate aperture in the final closed circuit loop. The most effective way of maximising throughput is to maintain the highest possible crusher power draw, and this has been used to control many plants. There is an optimum closed side setting for crushers operating in closed circuit which provides the highest tonnage of finished screen product for a particular power or circulating load limit, although the actual feed tonnage to the crusher increases at larger closed side settings. The power draw can be maintained by the use of a variable speed belt feeding the crusher. Changes in ore hardness and size distribution are compensated for by a change in belt speed. Operations under such choked conditions also require sensing of upper and lower levels of feed in the crusher by mechanical, nuclear, sonic, or proximity switches. Operation of the crusher at high power draw leads to increased fines production, such that if the increased throughput provided by the control system cannot be accommodated by the grinding plant, then the higher average power draw can be used to produce a finer product. This can be done by using screens with smaller apertures in the closed circuit, thus increasing the circulating load and hence the total crusher feed. In most cases, high screen loading decreases screening efficiency, particularly that of the particles close to the screen aperture size. This has the effect of reducing the effective "cut-size" of the screen, producing a finer product. Thus a possible control scheme during periods of excess closed circuit crushing capacity or reduced throughput requirement is to increase the circulating load by reducing the number of screens used, leading to a finer product. The implementation of this type of control loop requires accurate knowledge of the behaviour of the plant under various conditions.

In those circuits where the crushers produce a saleable product (e.g. road-stone quarries), the control objective is usually to maximise the production of certain size fractions from each tonne of feed. Since screen efficiency decreases as circulating load increases, producing a finer product size, circulating load can be used to control the product size. This can be affected by control of

the crusher setting, as on the Allis-Chalmers hydrocone crusher (Flavel, 1977, 1978; Anon., 1981), which has a hydraulic setting adjustment system which can be controlled automatically to optimise the crusher parameters. The required variation in crusher setting can be determined by the use of accurate mathematical models of crusher performance (Lynch, 1977; Napier-Munn et al., 1996), from empirical data, or by measuring product size on-line. Image processing based systems for the continuous measurement of fragment size for use in primary crushing and AG/SAG mill process control have been in use in the mining industry since the mid-1990s. Currently two systems are in use: Split-Online from Split Engineering and WipFrag from WipWare Inc. A description of the systems and how they work are given elsewhere (Maerz et al., 1996 for WipFrag; and Girdner et al., 2001 for Split). An example of the screen capture from a moving conveyor belt is shown in Figure 6.33 (see also Chapter 4).

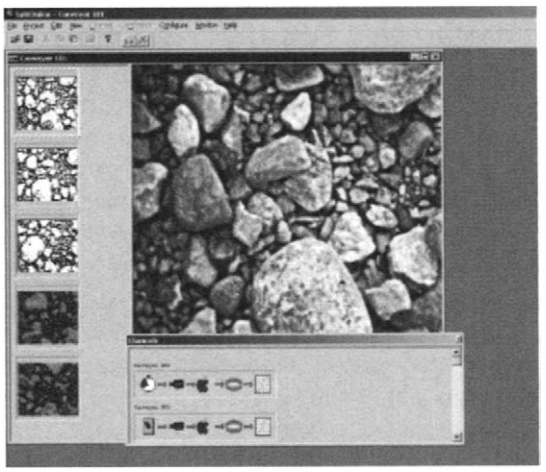


Figure 6.33 Screen capture of the Windows Version of Split-Online (Courtesy Split Engineering)

Additional loops are normally required in crushing circuits to control levels in surge bins between different stages. For instance, the crusher product surge bins can be monitored such that at high level, screen feed is increased to draw down the bins.

The importance of primary crusher control at Highland Valley Copper was well recognized, and through the use of image analysis, HVC was able to quantify the effect of feed size on crusher and mill performance, and thereby regulate crusher product size through a combination of feed rate and setting control (Dance, 2001). Figure 6.34 illustrates the effect of crusher feed size on the SAG mill throughput. As expected, as the amount of *medium* or critical size fed to the mill increased (−125 +50 mm), the tonnage of one of the semi-autogenous mills fell from 2000 to 1800 t/h. The effect of increasing the setting from 152 to 165 mm is shown in Figure 6.35. While the feed size % coarse (+125 mm) dropped from 15 to 8%, the larger setting allowed more to pass through uncrushed and the product % coarse values actually increased over time.

In most crushing plants there are long process delays, and standard PI controllers can be inadequate for the control loops. It is therefore desirable to provide a model of the process which incorporates the actual time delays, and use this model to adjust the controller inputs (McKee and Thornton, 1986). Such a dynamically compensated controller was developed for the Mount Isa crusher circuit (Manlapig and Watsford, 1983). The variation in operating conditions and significant circuit delays would seem to be well suited to control strategies based on modern model-based control techniques (see Chapter 3). In order to apply modern control theory to crushing, it is first necessary to develop dynamic models that are sufficiently detailed to reproduce the essential dynamic characteristics of crushing. For a cone crusher, this would involve accurately predicting the discharge size distribution, throughput, and power consumption as a function of time. Then optimal estimation using a Kalman filter has to be developed for the dynamic model. Finally, an optimal control algorithm is employed to determine the values of the manipulated variables which optimise the chosen control objectives. The optimal control algorithm will also supervise the set-points of the regulatory control loops. Herbst and Oblad (1986) have used a dynamic model of a cone crusher in conjunction with an extended Kalman filter to optimally estimate the size distributions of the material within the crusher as well as the measured output variables. In addition, estimation of the specific crushing rates has been implemented for the purpose of detecting ore hardness changes. The dynamic model and estimator are incorporated in a simulator as a first step in developing an optimal control scheme for

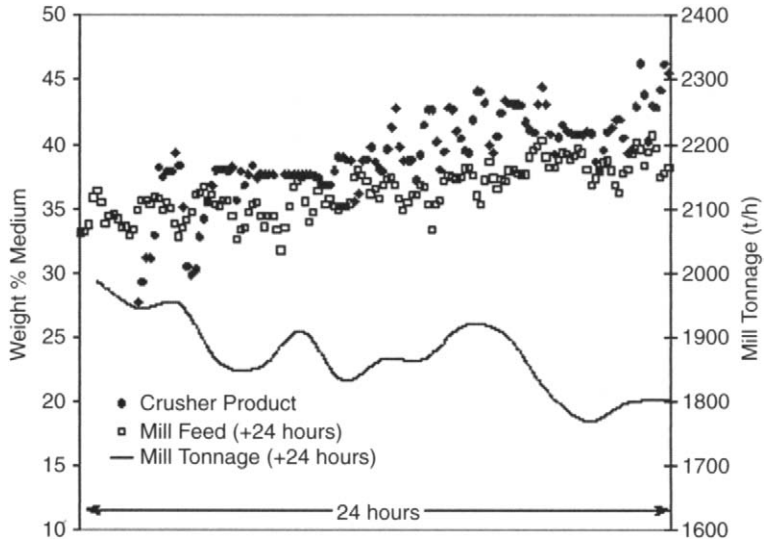


Figure 6.34 Crusher setting effect on mill product size (Courtesy Teck Cominco, Highland Valley Copper)

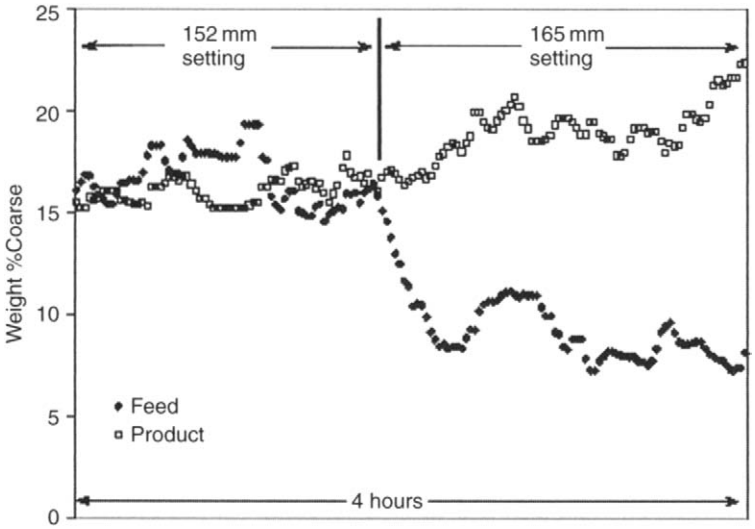


Figure 6.35 Effect of crusher setting on product size (Courtesy Teck Cominco, Highland Valley Copper)

crushing circuits. An overview of some of the recent work on crushing and screening models and a description of general policies for the control of crushing plants have been given by Whiten (1984) and Napier-Munn et al. (1996).

References

Anon. (1967). A new concept in the production of fine material, *Quarry Managers' J.*, (Jun.).

Anon. (1981). Crushers, *Min. Mag.* (Aug.), 94.

Anon. (1985). Rugged roller-bearing crusher, *Mining Mag.* (Sept.), 240.

Brachthauser, M. and Kellerwessel, H. (1988). High pressure comminution with roller presses in mineral processing, *Proc. XVIth Int. Min. Proc. Cong.* (ed. E. Forssberg), Elsevier, Amsterdam, 293.

Broman, J. (1984). Optimising capacity and economy in jaw and gyratory crushers, *Engng. Min. J.* (Jun.), 69.

Clarke, A.J. and Wills, B.A. (1989). Enhancement of cassiterite liberation by high pressure roller comminution, *Minerals Engng.*, **2(2)**, 259.

Cordonnier, A., Evrard, R., and Obry, C.H. (1995). New compression grinding technologies, *Int. Min. Proc. Cong.*, San Francisco, USA (Oct.).

Dance, A. (2001). The importance of primary crushing in mill feed size optimisation, *SAG2001 Conf.*, Vancouver, BC, Canada, **2**, 270–281.

Daniel, M.J. (2004). HPGR modeling and scale-up. *Comminution '04 Conference*, Perth (Mar.).

Djordjevic, N., Shi, F., and Morrison, R.D. (2003). Applying discrete element modelling to vertical and horizontal shaft impact crushers. *Minerals Engng.*, **16(10)**, 983–991.

Esna-Ashari, M. and Kellerwessel, H. (1988). Interparticle crushing of gold ore improves leaching, *Randol Gold Forum 1988*, Scottsdale, USA, 141–146.

Esterle, J.S., Kojovic, T., O'Brien, G., and Scott, A.C. (1996). Coal breakage modeling: A tool for managing fines generation. *Proceedings of the 1996 Mining Technology Conference*, ed. D. Howarth, H. Gurgenci, D. Sutherland, and B. Firth, Cooperative Research Centre for Mining Technology and Equipment (CMTE), Fremantle WA, 211–228.

Flavel, M.D. (1977). Scientific methods to design crushing and screening plants, *Min. Engng.*, **29**(Jul.), 65.

Flavel, M.D. (1978). Control of crushing circuits will reduce capital and operating costs, *Min. Mag.* (Mar.), 207.

Frizzel, E.M. (1985). Mobile in-pit crushing-product of evolutionary change, *Mining Engng.*, **37**(Jun.).

Girdner, K., Handy, J., and Kemeny, J. (2001). Improvements in fragmentation measurement software for SAG mill process control. *SAG2001 Conf.*, Vancouver, BC, Canada, **2**, 270–281.

Gresshaber, H.E. (1983), Crushing and grinding: Design considerations, *World Mining*, **36**(Oct.), 41.

Grieco, F.W. and Grieco, J.P. (1985). Manufacturing and refurbishing of jaw crushers, *CIM Bull.*, **78**(Oct.), 38.

Herbst, J.A. and Oblad, A.E. (1986). Modern control theory applied to crushing, Part 1: Development of a dynamic model for a cone crusher and optimal estimation of crusher operating variables, *Automation for Mineral Resource Development*, Pergamon, Oxford, 301.

Horst, W.E. and Enochs, R.C. (1980). Instrumentation and process control, *Engng. Min. J.*, **181**(Jun.), 70.

Karra, V. (1990). Developments in cone crushing. *Minerals Engng.*, **3(1/2)**, 75.

Knecht, J. (1994). High-pressure grinding rolls – a tool to optimize treatment of refractory and oxide gold ores, *Fifth Mill Operators Conf.*, AusIMM, Roxby Downs, Melbourne, (Oct.), 51–59.

Kojovic, T. (1996). Vertical shaft impactors: Predicting performance, *Quarry Aust J.*, **4(6)**, 35–39.

Kojovic, T. (1997). The development of a flakiness model for the prediction of crusher product shape, *Proc. of the 41st Annual Institute of Quarrying Conf.*, Brisbane, 135–148.

Kok, H.G. (1982). Use of mobile crushers in the minerals industry, *Min. Engng.*, **34**(Nov.), 1584.

Lewis, F.M., Coburn, J.L., and Bhappu, R.B. (1976). Comminution: A guide to size-reduction system design. *Min. Engng.*, **28**(Sept.), 29.

Lynch, A.J. (1977). *Mineral Crushing and Grinding Circuits*, Elsevier, Amsterdam.

Maerz, N.H., Palangio, T.C., and Franklin, J.A. (1996). WipFrag image based granulometry system. *Fragblast-5 Workshop on Measurement of Blast Fragmentation*, A A Balkema, Montreal, Canada, 91–99.

Manlapig, E.V. and Watsford, R.M.S. (1983). Computer control of the lead-zinc concentrator crushing plant operations of Mount Isa Mines Ltd, *Proc. 4th IFAC Symp. on Automation in Mining*, Helsinki, Aug.

McKee, D.J. and Thornton, A.J. (1986). Emerging automatic control approaches in mineral processing, in *Mineral Processing at a Crossroads – Problems and Prospects*, ed. B.A. Wills and R.W. Barley, Martinus Nijhoff, Dordrecht, Netherlands, 117.

McQuiston, F.W. and Shoemaker, R.S. (1978). *Primary Crushing Plant Design*, AIMME, New York.

Mollick, L. (1980). Crushing, *Engng. Min. J.*, **181**(Jun.), 96.

Motz, J.C. (1978). Crushing, in *Mineral Processing Plant Design*, ed. A.L. Mular and R.B. Bhappu, 203, AIMME, New York, 203.

Napier-Munn, T.J., Morrell, S., Morrison, R.D., and Kojovic, T. (1996). *Mineral Comminution circuits – Their Operation and Optimisation* (Appendix 3), JKMRC, The University of Queensland, Brisbane, 413.

Ramos, M., Smith, M.R., and Kojovic, T. (1994). Aggregate shape – Prediction and control during crushing, *Quarry Management* (Nov.), 23–30.

Rodriguez, D.E. (1990). The Tidco Barmac Autogenous Crushing Mill – A circuit design primer. *Minerals Engng.*, **3(1/2)**, 53.

Schwechten, D. and Milburn, G.H. (1990). Experiences in dry grinding with high compression roller mills for end product quality below 20 microns. *Minerals Engng.*, **3(1/2)**, 23.

Shi, F., Kojovic, T., Esterle, J.S., and David, D. (2003). An energy-based model for swing hammer mills, *Int. J. Min. Proc.*, **71(1–4)**, 147–166.

Simkus, R. and Dance, A. (1998). Tracking hardness and size: Measuring and monitoring ROM ore properties at Highland Valley copper. *Mine to Mill 1998 Conf.*, AusIMM, Oct., 113–119.

Taggart, A.F. (1945). *Handbook of Mineral Dressing*, Wiley, New York.

Watson, S. and Brooks, M. (1994). KCGM evaluation of high pressure grinding roll technology, *Fifth Mill Operators' Conf.*, Roxby Downs, AusIMM, 69–83.

White, L. (1976). Processing responding to new demands, *Engng. Min. J.* (Jun.), 219.

Whiten, W.J. (1984). Models and control techniques for crushing plants, in *Control'84 Minerals/Metallurgical Processing*, ed. J.A. Herbst, AIME, New York, 217.
Wills, B.A. (1983). Pyhasalmi and Vihanti concentrators, *Min. Mag.* (Sept.), 174.
Woody, R. (1982). Cutting crushing costs, *World Mining*, (Oct.), 76.
Wyllie, R.J.M. (1989). In-pit crushers. *Engng. Min. J.*, **190**(May), 22.

7

Grinding mills

Introduction

Grinding is the last stage in the process of comminution; in this stage the particles are reduced in size by a combination of impact and abrasion, either dry or in suspension in water. It is performed in rotating cylindrical steel vessels which contain a charge of loose crushing bodies – the grinding medium – which is free to move inside the mill, thus comminuting the ore particles. According to the ways by which motion is imparted to the charge, grinding mills are generally classified into two types: *tumbling mills* and *stirred mills*. In tumbling mills the mill shell is rotated and motion is imparted to the charge via the mill shell. The grinding medium may be steel rods, balls, or rock itself. Tumbling mills are typically employed in the mineral industry for coarse-grinding processes, in which particles between 5 and 250 mm are reduced in size to between 40 and 300 μm. In stirred mills the mill shell with either a horizontal or a vertical orientation is stationary and motion is imparted to the charge by the movement of an internal stirrer. Fine grinding media inside the mill are agitated or rotated by a stirrer, which typically comprises a central shaft to which are attached pins or discs of various designs. Stirred mills find application in fine (15–40 μm) and ultra-fine (<15 μm) grinding.

All ores have an economic optimum particle size (Chapter 1), which will depend on many factors, including the extent to which the values are dispersed in the gangue, and the subsequent separation process to be used. It is the purpose of the grinding section to exercise close control on this product size and, for this reason, correct grinding is often said to be the key to good mineral processing. Undergrinding of the ore will, of course, result in a product which is too coarse, with a degree of liberation too low for economic separation; poor recovery and enrichment ratio will be achieved in the concentration stage. Overgrinding needlessly reduces the particle size of the subsequently liberated major constituent (usually the gangue) and may reduce the particle size of the minor constituent (usually the mineral value) below the size required for most efficient separation. Much expensive energy is wasted in the process. It is important to realise that grinding is the most energy-intensive operation in mineral processing. It has been estimated that 50% of the energy consumed in US mills is used in comminution. On a survey of the energy consumed in a number of Canadian copper concentrators it was shown that the average energy consumption in $kWh\,t^{-1}$ was 2.2 for crushing, 11.6 for grinding, and 2.6 for flotation (Joe, 1979). Since grinding is the greatest single operating cost, the ore should not be ground any finer than is justified economically. Finer grinding should not be carried out beyond the point where the NSR for the increased recovery becomes less than the added operating cost (Steane, 1976). It can be shown, using Bond's Equation (5.2), that 19% extra energy must be consumed in grinding one screen size finer on a $\sqrt{2}$ screen series.

Although tumbling mills have been developed to a high degree of mechanical efficiency and reliability, they are extremely wasteful in terms of energy expended, since the ore is mostly broken as a result of repeated, random impacts, which break liberated as well as unliberated particles. At present there is no practical way that these impacts can be directed at the interfaces between the mineral grains, which would produce optimum liberation, although various ideas have been postulated (Wills and Atkinson, 1993).

Although the correct degree of liberation is the principal purpose of grinding in mineral processing, this treatment is sometimes used to increase the

surface area of the valuable minerals even though they may already be essentially liberated from the gangue. This is very important in processes where grinding is followed by hydrometallurgical methods of treatment. Thus in gold-ore treatment, leaching with cyanide solution follows the grinding process, and in some cases takes place during the grinding process. Leaching is much more efficient on particles which have large surface areas in relation to their mass and in such cases overgrinding may not be a disadvantage, as the increase in energy consumption may be offset by the increased gold recovery. This may not, however, be the case in the leaching of base metal ores, where a relatively coarse grind may be required in order to merely expose the valuable minerals to the lixivant, any further increase in metal extraction by finer grinding not being justified.

Grinding within a tumbling mill is influenced by the size, quantity, the type of motion, and the spaces between the individual pieces of the medium in the mill. As opposed to crushing, which takes place between relatively rigid surfaces, grinding is a more random process, and is subject to the laws of probability. The degree of grinding of an ore particle depends on the probability of the ore entering a zone between the medium shapes and the probability of some occurrence taking place after entry. Grinding can be done by several mechanisms, including impact or compression, due to forces applied almost normally to the particle surface; chipping due to oblique forces; and abrasion due to forces acting parallel to the surfaces (Figure 7.1). These mechanisms distort the particles and change their shape beyond certain limits determined by their degree of elasticity, which causes them to break.

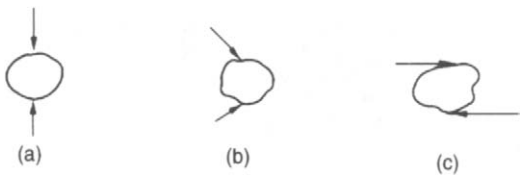


Figure 7.1 Mechanisms of breakage: (a) impact or compression, (b) chipping, (c) abrasion

Grinding is usually performed wet, although in certain applications dry grinding is used. When the mill is rotated, the mixture of medium, ore, and water, known as the *mill charge*, is intimately mixed, the medium comminuting the particles by any of the above methods depending on the speed of rotation of the mill and the shell liner structure. Most of the kinetic energy of the tumbling load is dissipated as heat, noise, and other losses, only a small fraction being expended in actually breaking the particles.

Apart from laboratory testing, grinding in mineral processing is a continuous process, material being fed at a controlled rate from storage bins into one end of the mill and overflowing at the other end after a suitable dwell time. Control of product size is exercised by the type of medium used, the speed of rotation of the mill, the nature of the ore feed, and the type of circuit used.

The motion of the charge in a tumbling mill

The distinctive feature of tumbling mills is the use of loose crushing bodies, which are large, hard, and heavy in relation to the ore particles, but small in relation to the volume of the mill, and which occupy slightly less than half the volume of the mill.

Due to the rotation and friction of the mill shell, the grinding medium is lifted along the rising side of the mill until a position of dynamic equilibrium is reached, when the bodies cascade and cataract down the free surface of the other bodies, about a dead zone where little movement occurs, down to the *toe* of the mill charge (Figure 7.2).

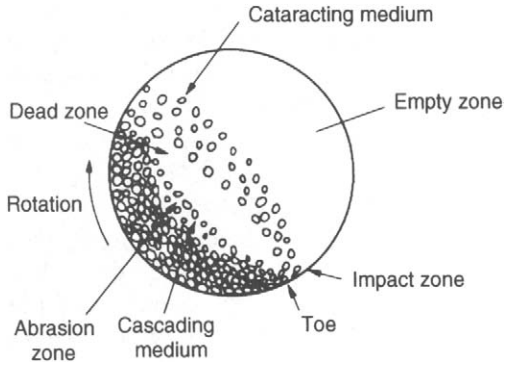


Figure 7.2 Motion of charge in a tumbling mill

The speed at which a mill is run is important, since it governs the nature of the product and the amount of wear on the shell liners. For instance,

a practical knowledge of the trajectories followed by the steel balls in a mill determines the speed at which it must be run in order that the descending balls shall fall on to the toe of the charge, and not on to the liner, which could lead to rapid liner wear.

The driving force of the mill is transmitted via the liner to the charge. At relatively low speeds, or with smooth liners, the medium tends to roll down to the toe of the mill and essentially abrasive comminution occurs. This *cascading* leads to finer grinding, with increased slimes production and increased liner wear. At higher speeds the medium is projected clear of the charge to describe a series of parabolas before landing on the toe of the charge. This *cataracting* leads to comminution by impact and a coarser end product with reduced liner wear. At the *critical speed* of the mill the theoretical trajectory of the medium is such that it would fall outside the shell. In practice, *centrifuging* occurs and the medium is carried around in an essentially fixed position against the shell.

In travelling around inside the mill the medium (and the large lumps of ore) follows a path which has two parts. The lifting section near to the shell liners is circular while the drop back to the toe of the mill charge is parabolic (Figure 7.3a).

Consider a ball, or rod, which is lifted up the shell of a mill of radius R metres, revolving at N rev min^{-1}. The rod abandons its circular path for a parabolic path at point P (Figure 7.3b), when the weight of the rod is just balanced by the centrifugal force, i.e. when

$$mV^2/R = mg\cos\alpha$$

where m is the mass of the rod or ball (kg), V is the linear velocity of the rod (m s^{-1}), and g is the acceleration due to gravity (m s^{-2}).

Since

$$V = \frac{2\pi RN}{60}$$

$$\cos\alpha = \frac{4\pi^2 N^2 R}{60^2 g}$$

$$= 0.0011 N^2 R$$

When the diameter of the rod, or ball, is taken into account, the radius of the outermost path is $(D-d)/2$, where D is the mill diameter and d the rod or ball diameter in metres.

Thus

$$\cos\alpha = \frac{0.0011 N^2 (D-d)}{2} \qquad (7.1)$$

The critical speed of the mill occurs when $\alpha = 0$, i.e. the medium abandons its circular path at the highest vertical point. At this point, $\cos\alpha = 1$.

Therefore

$$N_c = \frac{42.3}{\sqrt{D-d}} \text{ rev min}^{-1} \qquad (7.2)$$

where N_c is the critical speed of the mill.

Equation 7.2 assumes that there is no slip between the medium and the shell liner and, to allow for a margin of error, it has been common practice to increase the value of the calculated critical speed by as much as 20%. It is questionable, however, whether with modern liners maintained in reasonable condition this increase in the value is necessary or desirable.

Mills are driven, in practice, at speeds of 50–90% of critical speed, the choice being influenced by economic considerations. Increase in speed increases capacity, but there is little increase in

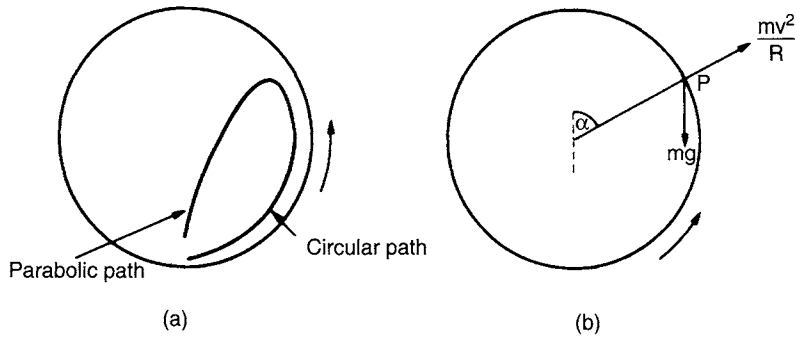


Figure 7.3 (a) Trajectory of grinding medium in tumbling mill, (b) forces acting on the medium

efficiency (i.e. $kW\,h\,t^{-1}$) above about 40–50% of the critical speed. Very low speeds are sometimes used when full mill capacity cannot be attained. High speeds are used for high-capacity coarse grinding. Cataracting at high speeds converts the potential energy of the medium into kinetic energy of impact on the toe of the charge and does not produce as much very fine material as the abrasive grinding produced by cascading at lower speeds. It is essential, however, that the cataracting medium should fall well inside the mill charge and not directly onto the liner, thus excessively increasing steel consumption. Most of the grinding in the mill takes place at the toe of the charge, where not only is there direct impact of the cataracting medium on to the charge, but also the ore packed between the cascading medium receives the shock transmitted.

At the extreme toe of the load the descending liner continuously underruns the churning mass, and moves some of it into the main mill charge. The medium and ore particles in contact with the liners are held with more firmness than the rest of the charge due to the extra weight bearing down on them. The larger the ore particle, rod, or ball, the less likely it is to be carried to the breakaway point by the liners. The cataracting effect should thus be applied in terms of the rod or ball of largest diameter.

Tumbling mills

Tumbling mills are of three basic types: rod, ball, and autogenous. Structurally, each type of mill consists of a horizontal cylindrical shell, provided with renewable wearing liners and a charge of grinding medium. The drum is supported so as to rotate on its axis on hollow *trunnions* attached to the end walls (Figure 7.4). The diameter of the mill determines the pressure that can be exerted by the medium on the ore particles and, in general, the larger the feed size the larger needs to be the mill diameter. The length of the mill, in conjunction with the diameter, determines the volume, and hence the capacity of the mill.

The feed material is usually fed to the mill continuously through one end trunnion, the ground product leaving via the other trunnion, although in certain applications the product may leave the mill through a number of ports spaced around the periphery of the shell. All types of mill can be used for wet or dry grinding by modification of feed and discharge equipment.

Construction of mills

Shell Mill shells are designed to sustain impact and heavy loading, and are constructed from rolled mild steel plates, buttwelded together. Holes are drilled to take the bolts for holding the liners.

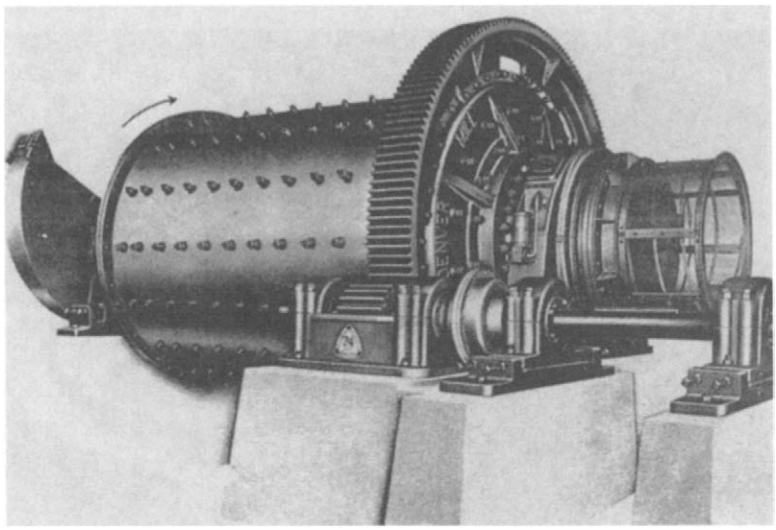


Figure 7.4 Tumbling mill

Normally one or two access manholes are provided. For attachment of the trunnion heads, heavy flanges of fabricated or cast steel are usually welded or bolted to the ends of the plate shells, planed with parallel faces which are grooved to receive a corresponding spigot on the head, and drilled for bolting to the head.

Mill ends The mill ends, or trunnion heads, may be of nodular or grey cast iron for diameters less than about 1 m. Larger heads are constructed from cast steel, which is relatively light, and can be welded. The heads are ribbed for reinforcement and may be flat, slightly conical, or dished. They are machined and drilled to fit shell flanges (Figure 7.5).

Trunnions and bearings (see also Anon., 1990) The trunnions are made from cast iron or steel and are spigoted and bolted to the end plates, although in small mills they may be integral with the end plates. They are highly polished to reduce bearing friction. Most trunnion bearings are rigid high-grade iron castings with 120–180° lining of white metal in the bearing area, surrounded by a fabricated mild steel housing, which is bolted into the concrete foundations (Figure 7.6).

The bearings in smaller mills may be grease lubricated, but oil lubrication is favoured in large mills, via motor-driven oil pumps. The effectiveness of normal lubrication protection is reduced when the mill is shut down for any length of time, and many mills are fitted with manually operated hydraulic starting lubricators, which force oil between the trunnion and trunnion bearing, preventing friction damage to the bearing surface, on starting, by re-establishing the protecting film of oil (Figure 7.7).

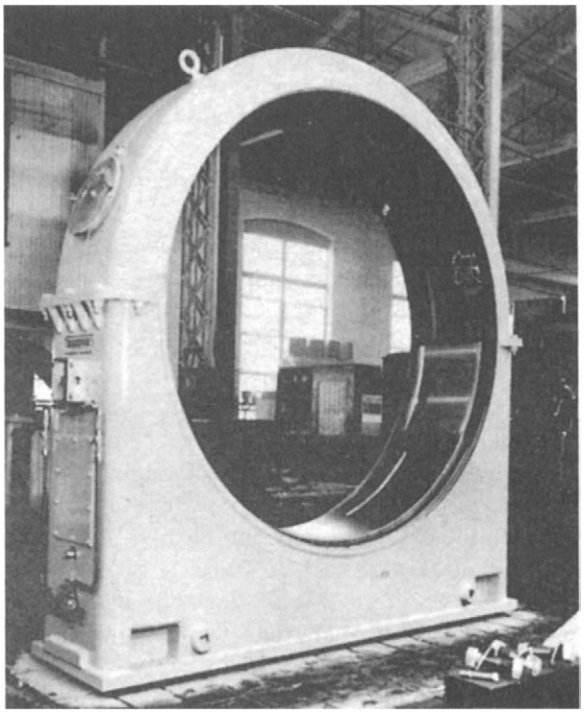


Figure 7.6 180° oil-lubricated trunnion bearing

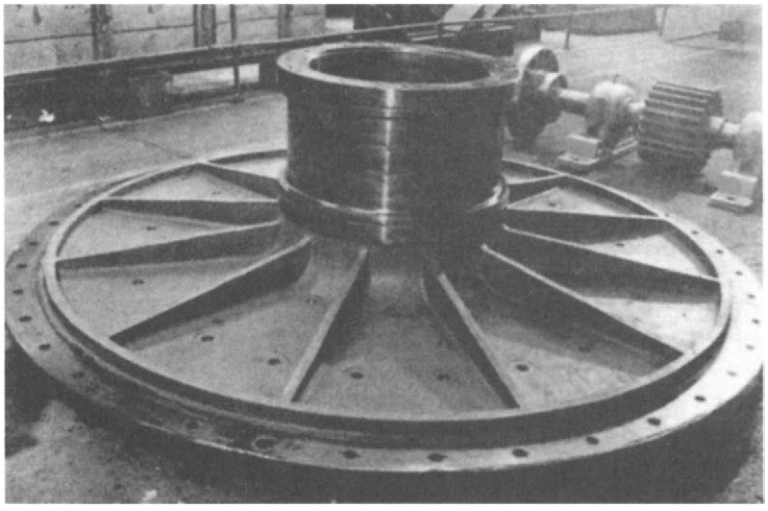


Figure 7.5 Tube mill end and trunnion

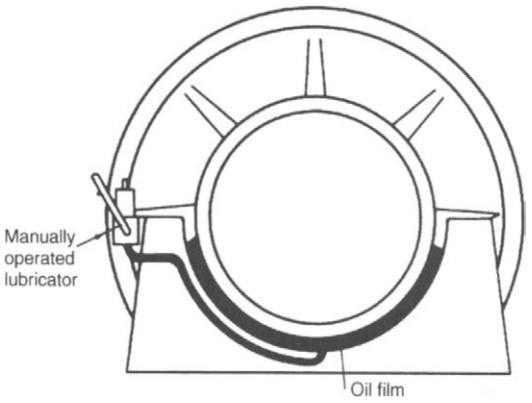


Figure 7.7 Hydraulic starting lubricator

Some manufacturers install large roller bearings, which can withstand higher forces than plain metal bearings (Figure 7.8).

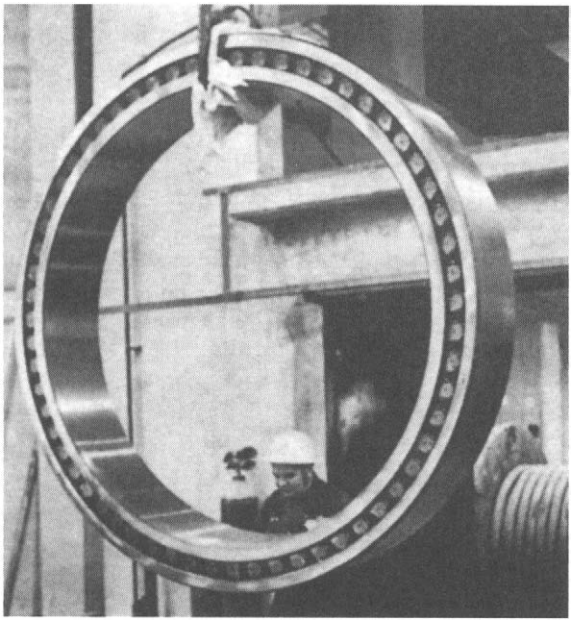


Figure 7.8 Trunnion with roller-type bearings

Drive (see also Knecht, 1990) Tumbling mills are most commonly rotated by a pinion meshing with a girth ring bolted to one end of the machine (Figure 7.9).

The pinion shaft is driven from the prime mover through vee-belts, in small mills of less than about 180 kW. For larger mills the shaft is coupled directly

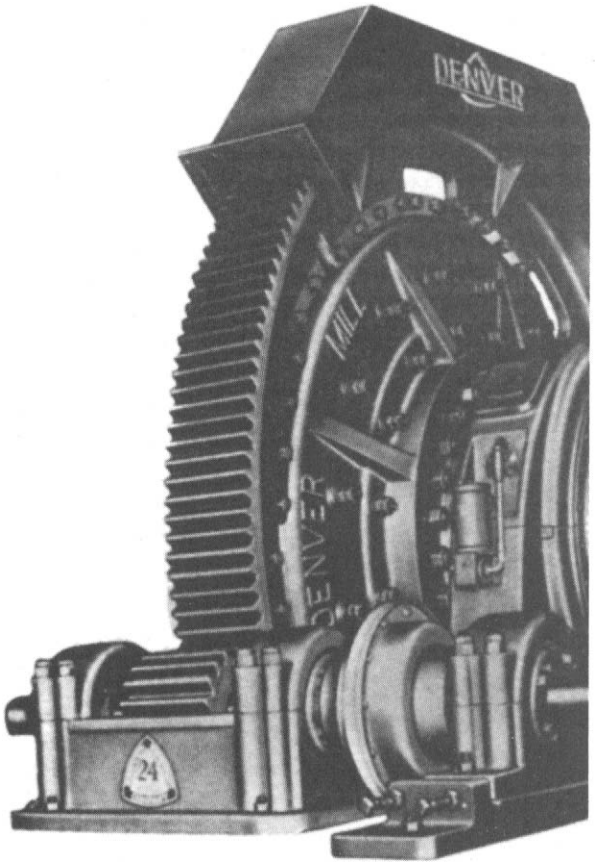


Figure 7.9 Gear/pinion assembly on ball mill

to the output shaft of a slow-speed synchronous motor, or to the output shaft of a motor-driven helical or double helical gear reducer. In some mills thyristors and DC motors are used to give variable speed control. Very large mills driven by girth gears require two to four pinions, and complex load sharing systems must be incorporated.

Large mills can be rotated by a central trunnion drive, which has the advantage of requiring no expensive ring gear, the drive being from one or two motors, with the inclusion of two- or three-speed gearing (Anon., 1982).

The larger the mill, the greater are the stresses between the shells and heads and the trunnions and heads. In the early 1970s, maintenance problems related to the application of gear and pinion and large speed reducer drives on dry grinding cement mills of long length drove operators to seek an alternative drive design. As a result, a number of gearless drive (ring motor) cement mills

were installed and the technology became relatively common in the European cement industry.

The gearless drive design features motor rotor elements bolted to a mill shell, a stationary stator assembly surrounding the rotor elements, and electronics converting the incoming current from 50/60 Hz to about 1 Hz. The mill shell actually becomes the rotating element of a large low speed synchronous motor. Mill speed is varied by changing the frequency of the current to the motor, allowing adjustments to the mill throughput as ore grindability changes.

The gearless drive design was not applied to the mills in the mineral industry until 1981 when the then-world's largest ball mill, 6.5 m diameter and 9.65 m long driven by a 8.1 MW motor, was installed at Sydvaranger in Norway (Meintrup and Kleiner, 1982). Currently the world's largest semi-autogenous grinding mill (SAG), 12 m diameter and 6.1 m length (belly inside liners) with a motor power of more than 20 MW, is in operation at Newcrest Mining's Cadia Hill gold and copper mine in Australia (Figure 7.10), with a throughput of over 2000 t/h (Dunne et al., 2001). A case study on a 13.4 m SAG mill with a drive power of 30 MW has been reported (Riezinger et al., 2001).

The major advantages of the gearless drive include variable speed capacity, removal of limits of design power, very high drive efficiency, low maintenance requirements, and less floor space for installation.

Liners The internal working faces of mills consist of renewable liners, which must withstand impact, be wear-resistant, and promote the most favourable motion of the charge. Rod mill ends have plain flat liners, slightly coned to encourage the self-centring and straight-line action of rods. They are made usually from manganese or chrome–molybdenum steels, having high impact strength. Ball-mill ends usually have ribs to lift the charge with the mill rotation. These prevent excessive slipping and increase liner life. They can be made from white cast iron, alloyed with nickel (Ni-hard), other wear-resistant materials, and rubber (Durman, 1988). Trunnion liners are designed for each application and can be conical, plain, with advancing or retarding spirals. They are manufactured from hard cast iron or cast alloy steel, a rubber lining often being bonded to the inner surface for increased life.

Shell liners have an endless variety of lifter shapes. Smooth linings result in much abrasion, and hence a fine grind, but with associated high metal wear. The liners are therefore generally shaped to provide lifting action and to add impact and crushing, the most common shapes being wave, Lorain, stepped, and shiplap (Figure 7.11). The liners are attached to the mill shell and ends by forged steel countersunk liner bolts.

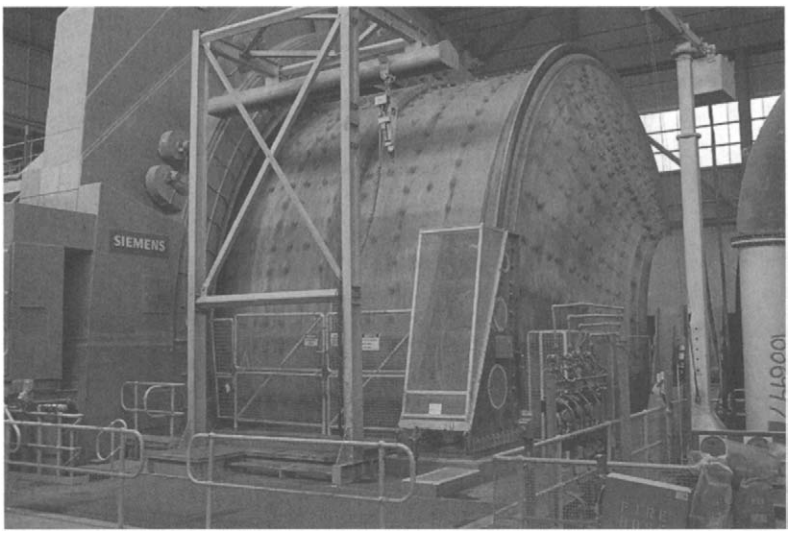


Figure 7.10 The 12 m diameter SAG mill operated at Cadia Hill Gold Mine (Photo by S. Hart; Courtesy Newcrest Mining)

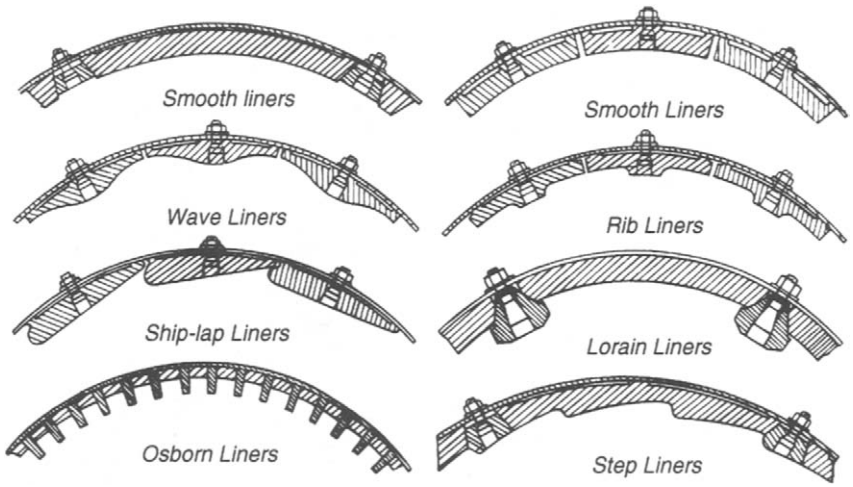


Figure 7.11 Mill shell liners

Rod mill liners are also generally of alloyed steel or cast iron, and of the wave type, although Ni-hard step liners may be used with rods up to 4 cm in diameter. Lorain liners are extensively used for coarse grinding in rod and ball mills, and consist of high carbon rolled steel plates held in place by manganese or hard alloy steel lifter bars. Ball mill liners may be made of hard cast iron when balls of up to 5 cm in diameter are used, but otherwise cast manganese steel, cast chromium steel, or Ni-hard are used.

Mill liners are a major cost in mill operation, and efforts to prolong liner life are constantly being made. There are at least ten wear-resistant alloys used for ball-mill linings, the more abrasion-resistant alloys containing large amounts of chromium, molybdenum, and nickel being the most expensive (De Richemond, 1982). However, with steadily increasing labour costs for replacing liners, the trend is towards selecting liners which have the best service life regardless of cost (Malghan, 1982).

Rubber liners and lifters have supplanted steel in some operations, and have been found to be longer lasting, easier and faster to install, and their use results in a significant reduction of noise level. However, increased medium consumption has been reported using rubber liners rather than Ni-hard liners. Rubber lining may also have drawbacks in processes requiring the addition of flotation reagents directly into the mill, or temperatures exceeding 80 °C. They are also thicker than their steel counterparts, which reduces mill capacity, a particularly important factor in small mills. There are also important differences in design aspects between steel and rubber linings (Moller and Brough, 1989).

The engineering advantage of rubber is that, at relatively low impact forces, it will yield, resuming its shape when the forces are removed. However, if the forces are too powerful, or the speed of the material hitting the rubber is too high, the wear rate is dramatic. In primary grinding applications, with severe grinding forces, the wear rate of rubber inhibits its use. Even though the wear cost per tonne of ore may be similar to that of the more expensive steel lining, the more frequent interruptions for maintenance often make it uneconomical. The advantage of steel is its great hardness, and steel-capped liners have been developed which combine the best qualities of rubber and steel. These consist of rubber lifter bars with steel inserts embedded in the face, the steel providing the wear resistance and the rubber backing cushioning the impacts (Moller, 1990).

A concept which has found some application for ball mills is the "angular spiral lining". The circular cross-section of a conventional mill is changed to a square cross-section with rounded corners by the addition of rubber-lined, flanged frames, which are offset to spiral in a direction opposite to the mill rotation. Double wave liner plates are fitted to these frames, and a sequential lifting of the charge down the length of the mill

results, which increases the grinding ball to pulp mixing through axial motion of the grinding charge, along with the normal cascading motion. Substantial increases in throughput, along with reductions in energy and grinding medium consumptions, have been reported (Korpi and Dopson, 1982).

To avoid the rapid wear of rubber liners, a new patented technology for a magnetic metal liner has been developed by China Metallurgical Mining Corp. The magnets keep the lining in contact with the steel shell and the end plates without using bolts, while the ball "scats" in the charge and magnetic minerals are attracted to the liner to form a 30–40 mm protective layer, which is continuously renewed as it wears. Over 10 years the magnetic metal liner has been used in more than 300 full-scale ball mills at over 100 mine sites in China (Zhou et al., 2003). For example, one set of the magnetic metal liner was installed in a 3.2 m (D) × 4.5 m (L) secondary ball mill (60 mm ball charge) at Waitoushan concentrator of Benxi Iron and Steel Corp. in 1992. Over nine years, 2.6 Mt of iron ore were ground at zero additional liner cost and zero maintenance of the liners (Zhou and Duan, 2004). The magnetic metal liner has also found applications in large ball mills, such as the 5.5 m (D) × 8.8 m (L) mills installed at Diaojuntai concentrator in Qidashan Iron Ore Mines.

Another advantage of the magnetic metal liner is that as the liners are thinner and lighter than conventional manganese steel, the effective mill volume is larger, and the mill weight is reduced. An 11.3% decrease in mill power draw at the same operational conditions has been realised in a 2.7 m (D) × 3.6 m (L) ball mill by using the magnetic metal liner.

Mill feeders The type of feeding arrangement used on the mill depends on whether the grinding is done in open or closed circuit and whether it is done wet or dry. The size and rate of feed are also important. Dry mills are usually fed by some sort of vibratory feeder. Three types of feeder are in use in wet-grinding mills. The simplest form is the *spout feeder* (Figure 7.12), consisting of a cylindrical or elliptical chute supported independently of the mill, and projecting directly into the trunnion liner. Material is fed by gravity through the spout to feed the mills. They are often used for feeding rod mills operating in open circuit or mills in closed circuit with hydrocyclone classifiers.

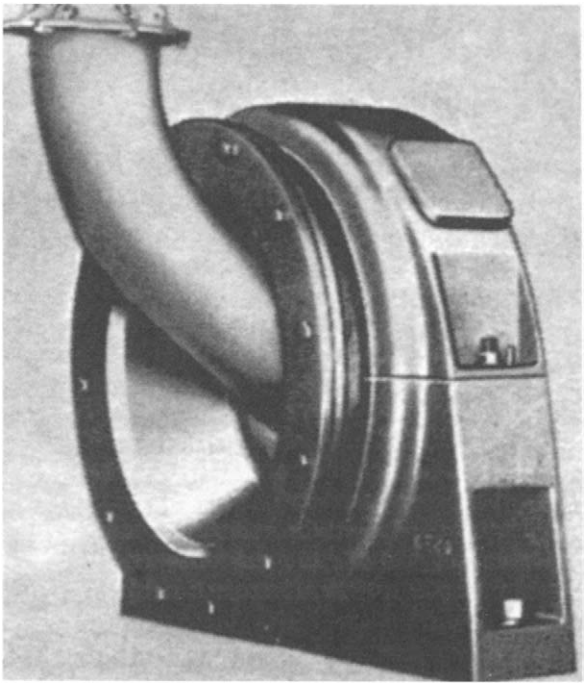


Figure 7.12 Spout feeder

Drum feeders Drum feeders (Figure 7.13) may be used as an alternative to a spout feeder when headroom is limited. The entire mill feed enters the drum via a chute or spout and an internal spiral carries it into the trunnion liner. The drum also provides a convenient method of adding grinding balls to a mill.

Combination drum-scoop feeders These (Figure 7.14) are generally used for wet grinding in closed circuit with a spiral or rake classifier. New material is fed directly into the drum, while the scoop picks up the classifier sands for regrinding. Either a single or a double scoop can be used, the latter providing an increased feed rate and more uniform flow of material into the mill; the counter-balancing effect of the double-scoop design serves to smooth out power fluctuation and it is normally incorporated in large-diameter mills. *Scoop feeders* are sometimes used in place of the drum-scoop combination when mill feed is in the fine-size range.

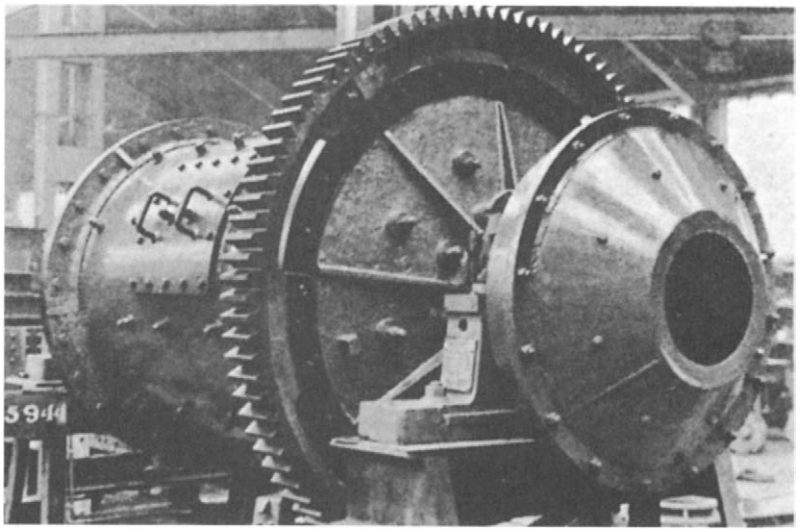


Figure 7.13 Drum feeder on ball mill

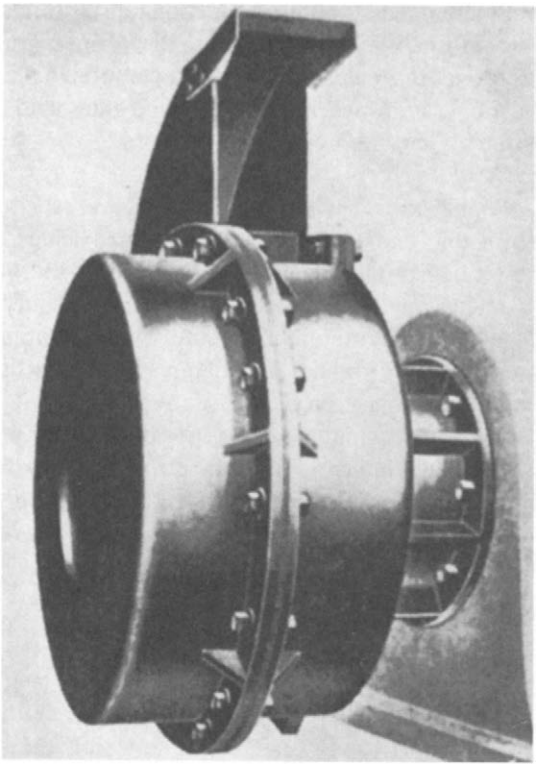


Figure 7.14 Drum-scoop feeder

Types of mill

Rod mills These may be considered as either fine crushers or coarse grinding machines. They are capable of taking feed as large as 50 mm and making a product as fine as 300 μm, reduction ratios normally being in the range 15–20:1. They are often preferred to fine crushing machines when the ore is "clayey" or damp, thus tending to choke crushers.

The distinctive feature of a rod mill is that the length of the cylindrical shell is between 1.5 and 2.5 times its diameter (Figure 7.15).

This ratio is important because the rods, which are only a few centimetres shorter than the length of the shell, must be prevented from turning so that they become wedged across the diameter of the cylinder. The ratio must not, however, be so large for the maximum diameter of the shell in use that the rods deform and break. Since rods longer than about 6 m will bend, this establishes the maximum length of the mill. Thus, with a mill 6.4 m long the diameter should not be over 4.57 m. Rod mills of up to 4.57 m in diameter by 6.4 m in length are in use, run by 1640 kW motors (Lewis et al., 1976). Rod and other grinding mills are rated by power rather than capacity, since the capacity is determined by many factors, such as the grindability, determined by laboratory testing (Chapter 5), and the reduction in size required. The power required for a certain required capacity may be estimated by the use of Bond's equation:

$$W = \frac{10W_i}{\sqrt{P}} - \frac{10W_i}{\sqrt{F}} \qquad (7.3)$$

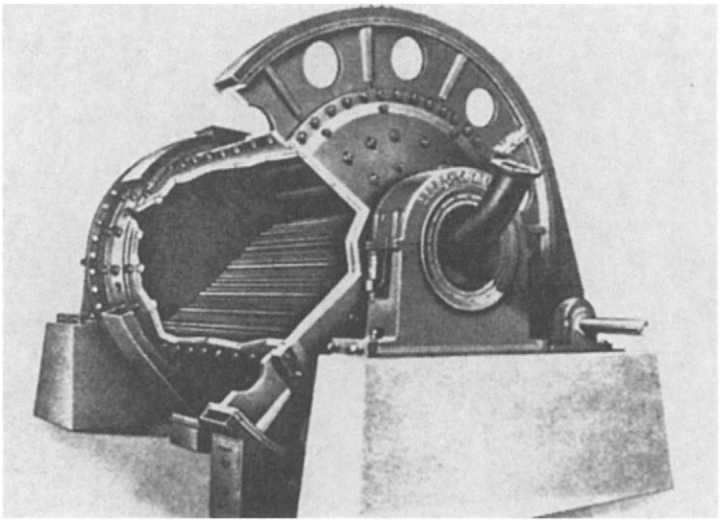


Figure 7.15 Rod mill

The calculated power requirement is adjusted by utilising efficiency factors dependent on the size of mill, size and type of media, type of grinding circuit, etc., to give the operating power requirement (Rowland and Kjos, 1978).

Rod mills are classed according to the nature of the discharge. A general statement can be made that the closer the discharge is to the periphery of the shell, the quicker the material will pass through and less overgrinding will take place.

Centre peripheral discharge mills (Figure 7.16) are fed at both ends through the trunnions and discharge the ground product through circumferential ports at the centre of the shell. The short path and steep gradient give a coarse grind with a minimum of fines, but the reduction ratio is limited. This mill can be used for wet or dry grinding and has found its greatest use in the preparation of specification sands, where high tonnage rates and an extremely coarse product are required.

End peripheral discharge mills (Figure 7.17) are fed at one end through the trunnion, discharging the ground product from the other end of the mill by means of several peripheral apertures into a close-fitting circumferential chute. This type of mill is used mainly for dry and damp grinding, where moderately coarse products are involved.

The most widely used type of rod mill in the mining industry is the *trunnion overflow* (Figure 7.18), in which the feed is introduced

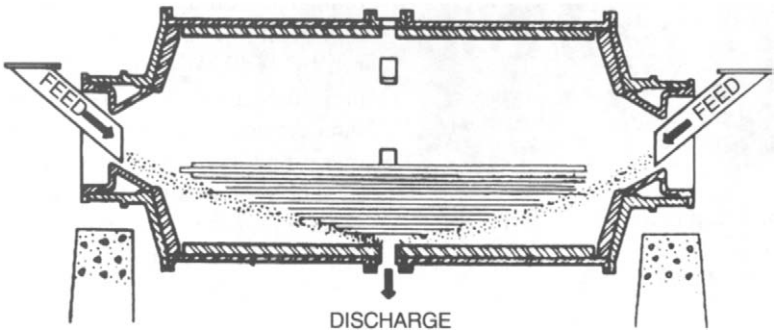


Figure 7.16 Central peripheral discharge mill

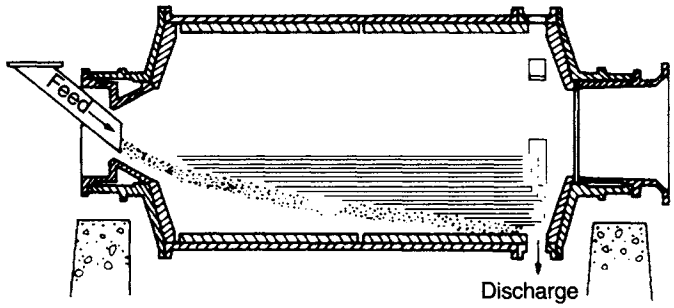


Figure 7.17 End peripheral discharge mill

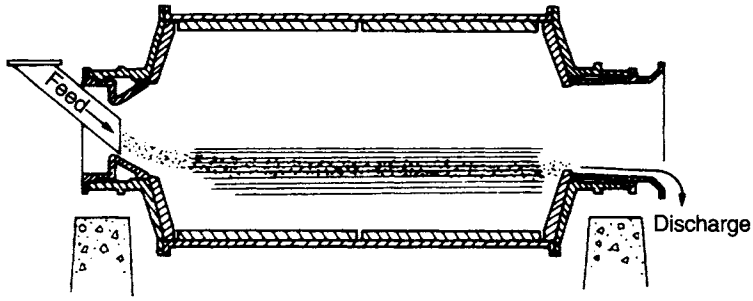


Figure 7.18 Overflow mill

through one trunnion and discharges through the other. This type of mill is used only for wet grinding and its principal function is to convert crushing-plant product into ball-mill feed. A flow gradient is provided by making the overflow trunnion diameter 10–20 cm larger than that of the feed opening. The discharge trunnion is often fitted with a spiral screen to remove tramp material.

Rod mills are charged initially with a selection of rods of assorted diameters, the proportion of each size being calculated to provide maximum grinding surface and to approximate to a seasoned or equilibrium charge. A seasoned charge will contain rods of varying diameters ranging from fresh replacements to those which have worn down to such a size as to warrant removal. Actual diameters in use range from 25 to 150 mm. The smaller the rods the larger is the total surface area and hence the greater is the grinding efficiency. The largest diameter should be no greater than that required to break the largest particle in the feed. A coarse feed or product normally requires larger rods. Generally, rods should be removed when they are worn down to about 25 mm in diameter or less, depending on the application, as small ones tend to bend or break. High carbon steel rods are used as they are hard, and break rather than warp when worn, so do not entangle with other rods. Optimum grinding rates are obtained with new rods when the volume is 35% of that of the shell. This reduces to 20–30% with wear and is maintained at this figure by substitution of new rods for worn ones. This proportion means that with normal voidage, about 45% of the mill volume is occupied. Overcharging results in inefficient grinding and increased liner and rod consumption. Rod consumption varies widely with the characteristics of the mill feed, mill speed, rod length, and product size; it is normally in the range 0.1–1.0 kg of steel per tonne of ore for wet grinding, being less for dry grinding.

Rod mills are normally run at between 50 and 65% of the critical speed, so that the rods cascade rather than cataract; many operating mills have been sped up to close to 80% of critical speed without any reports of excessive wear (McIvor and Finch, 1986). The feed pulp density is usually between 65 and 85% solids by weight, finer feeds requiring lower pulp densities. The grinding action results from line contact of the rods on the ore particles; the rods tumble in essentially a parallel alignment, and also spin, thus acting rather like a series of crushing rolls. The coarse feed tends to

spread the rods at the feed end, so producing a wedge- or cone-shaped array. This increases the tendency for grinding to take place preferentially on the larger particles, thereby producing a minimum amount of extremely fine material (Figure 7.19). This selective grinding gives a product of relatively narrow size range, with little oversize or slimes. Rod mills are therefore suitable for preparation of feed to gravity concentrators, certain flotation processes with slime problems, magnetic cobbing, and ball mills. They are nearly always run in open circuit because of this controlled size reduction.

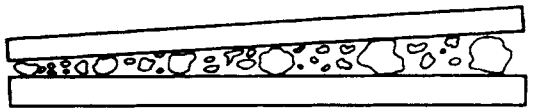


Figure 7.19 Grinding action of rods

Ball mills The final stages of comminution are performed in tumbling mills using steel balls as the grinding medium and so designated "ball mills."

Since balls have a greater surface area per unit weight than rods, they are better suited for fine finishing. The term ball mill is restricted to those having a length to diameter ratio of 1.5 to 1 and less. Ball mills in which the length to diameter ratio is between 3 and 5 are designated *tube mills*. These are sometimes divided into several longitudinal compartments, each having a different charge composition; the charges can be steel balls or rods, or pebbles, and they are often used dry to grind cement clinker, gypsum, and phosphate. Tube mills having only one compartment and a charge of hard, screened ore particles as the grinding medium are known as *pebble mills*. They are widely used in the South African gold mines. Since the weight of pebbles per unit volume is 35–55% of that of steel balls, and as the power input is directly proportional to the volume weight of the grinding medium, the power input and capacity of pebble mills are correspondingly lower. Thus in a given grinding circuit, for a certain feed rate, a pebble mill would be much larger than a ball mill, with correspondingly higher operating cost. However, it is claimed that the increment in capital cost can be justified economically by a reduction in operating cost attributed to the lower cost of the grinding medium. This may, however, be partially offset by higher energy cost per tonne of finished product (Lewis et al., 1976).

Ball mills are also classified by the nature of the discharge. They may be simple trunnion overflow mills, operated in open or closed circuit, or *grate discharge* (low-level discharge) mills. The latter type is fitted with discharge grates between the cylindrical mill body and the discharge trunnion. The pulp can flow freely through the openings in the grate and is then lifted up to the level of the discharge trunnion (Figure 7.20). These mills have a lower pulp level than overflow mills, thus reducing the dwell time of particles in the mill. Very little overgrinding takes place and the product contains a large fraction of coarse material, which is returned to the mill by some form of classifying device. Closed-circuit grinding (Figure 7.21), with high circulating loads, produces a closely sized end product and a high output per unit volume compared with open circuit grinding. Grate discharge mills usually take a coarser feed than overflow mills and are not required to grind so

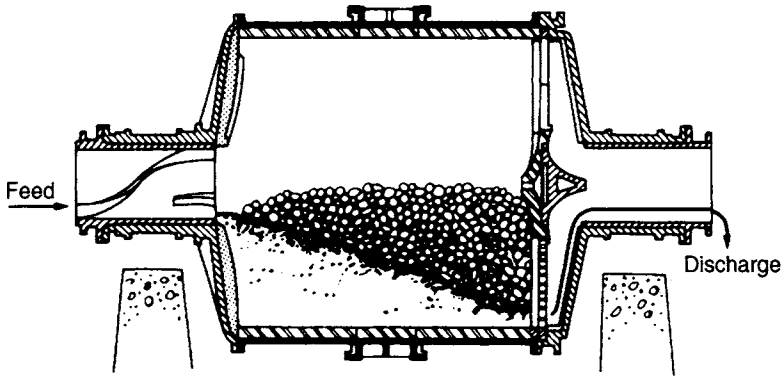


Figure 7.20 Grate discharge mill

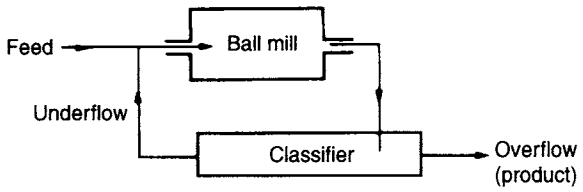


Figure 7.21 Simple closed-grinding circuit

finely, the main reason being that with many small balls forming the charge the grate open area plugs very quickly. The trunnion overflow mill is the simplest to operate and is used for most ball-mill applications, especially for fine grinding and regrinding. Energy consumption is said to be about 15% less than that of a grate discharge mill of the same size, although the grinding efficiencies of the two mills are the same (Lewis et al., 1976).

Ball mills are rated by power rather than capacity. Today the largest ball mill in operation is 7.3 m in diameter with a corresponding motor power of more than 11 MW (Figure 7.22).

The trend in recent years has been to use fewer comminution machines per grinding line with the result that units have increased considerably in capacity. For example, in the 1980s, the largest operating ball mill was 5.5 m in diameter by 7.3 m in length driven by a 4 MW motor. Today, ball mills of 5 m plus are commonplace, and 7 m ball mills are currently employed on at least two sites. However, there are several cases where large ball mills have not achieved design capabilities. One example was the 5.5 m diameter by 6.4 m ball mills at Bougainville Copper Ltd where the coarse material grinding was particularly inefficient (Tilyard, 1986). The "post-Bougainville Copper" literature has been reviewed recently (Morrell, 2001). Operational data from a wide range of large diameter ball mills were collected and analysed. The issues related to sizing of large diameter ball mills included power draw, residence time, feed size, and the applicability of Bond's equations. It was concluded that the power draw of large diameter mills follows the same relationships that hold for smaller diameter mills, as described in Morrell's power equation (Morrell, 1996).

Ball-mill scale-up studies have been conducted in Australia and the United States, the results emphasizing that there are limitations to conventional procedures for estimating large mill requirements from small-scale results (Arbiter and Harris, 1984; Rowland and Erickson, 1984; Whiten and Kavetsky, 1984; Rowland, 1986, 1988; Lo et al., 1988). Attempts have been made to use laboratory ball-mill test results to calibrate a suitable ball mill mathematical model, and a set of scale-up criteria have been developed for scaling the parameters of the model to predict full-scale ball-mill performance (Morrell and Man, 1997; Man, 2001).

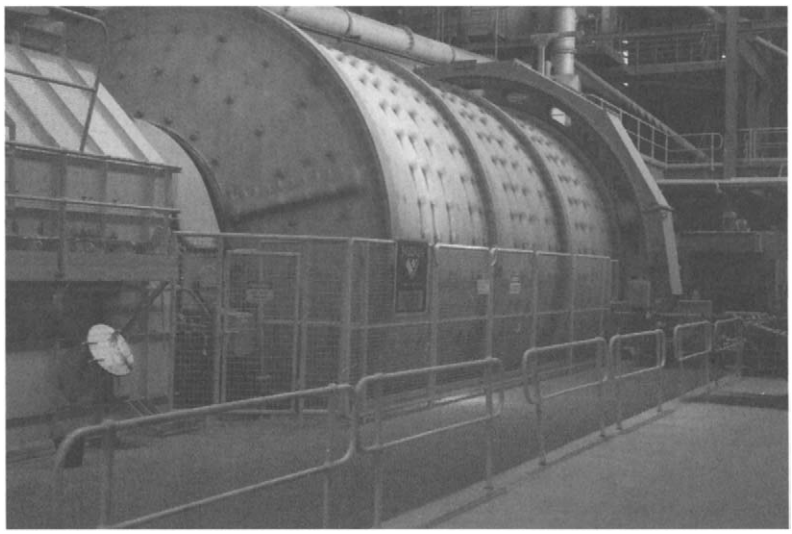


Figure 7.22 The 7.3 m diameter ball mill operated at Cadia Hill Gold Mine (Photo by S. Hart; Courtesy Newcrest Mining)

Further validation of these ball-mill scale-up procedures is under way (Shi, 2004). If proved, it offers a useful tool in greenfield design of ball milling circuit.

Grinding in a ball mill is effected by point contact of balls and ore particles and, given time, any degree of fineness can be achieved. The process is completely random – the probability of a fine particle being struck by a ball is the same as that of a coarse particle. The product from an open-circuit ball mill therefore exhibits a wide range of particle size, and overgrinding of at least some of the charge becomes a problem. Closed-circuit grinding in mills providing low residence time for the particles is almost always used in the last stages to overcome this.

Several factors influence the efficiency of ball-mill grinding. The pulp density of the feed should be as high as possible, consistent with ease of flow through the mill. It is essential that the balls are coated with a layer of ore; too dilute a pulp increases metal-to-metal contact, giving increased steel consumption and reduced efficiency. Ball mills should operate between 65 and 80% solids by weight, depending on the ore. The viscosity of the pulp increases with the fineness of the particles, therefore fine-grinding circuits may need lower pulp densities. The major factors affecting the pulp rheology and its effects on grinding circuits have been discussed by a number of researchers (Klimpel, 1982, 1983, 1984; Kawatra and Eisele, 1988; Moys, 1989; Shi, 1994; Shi and Napier-Munn, 2002). It was found that not only the viscosity of the pulp but also the rheological type (Newtonian or non-Newtonian) would affect ball milling performance.

The efficiency of grinding depends on the surface area of the grinding medium. Thus, balls should be as small as possible and the charge should be graded such that the largest balls are just heavy enough to grind the largest and hardest particles in the feed. A seasoned charge will consist of a wide range of ball sizes and new balls added to the mill are usually of the largest size required. Undersize balls leave the mill with the ore product and can be removed by passing the discharge over screens. Various formulae have been proposed for the required ratio of ball size to ore size, none of which is entirely satisfactory. The correct sizes are often determined by trial and error, primary grinding usually requiring a graded charge of 10–5 cm diameter balls, while secondary grinding requires 5–2 cm. Concha et al. (1988) have developed a method to calculate ball-mill charge by using a grinding circuit simulator with a model of ball wear in a tumbling mill.

Segregation of the ball charge within the mill is achieved in the *Hardinge mill* (Figure 7.23).

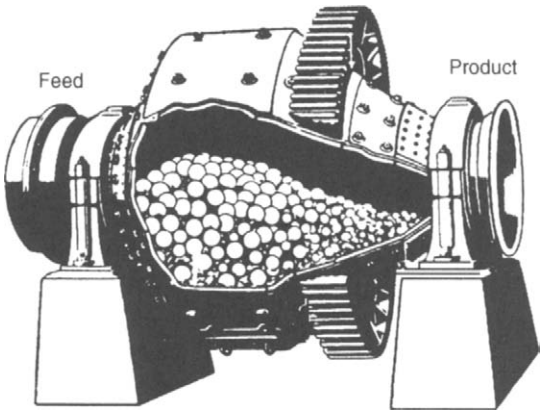


Figure 7.23 Hardinge mill

The conventional drum shape is modified by fitting a conical section, the angle of the cone being about 30°. Due to the centrifugal force generated, the balls are segregated so that the largest are at the feed end of the cone, i.e. the largest diameter and greatest centrifugal force, and the smallest are at the discharge. By this means, a regular gradation of ball size and of size reduction is produced.

In the current market, there are other shapes of grinding media such as Doering Cylpebs, Wheelabrator Allevard Enterprise (WAE) Millpebs, and Donhad Powerpeb. The Cylpebs are slightly tapered cylindrical grinding media with length equalling diameter, and all the edges being radiused (Figure 7.24). The largest Cylpebs available in the market are of the size 85 mm × 85 mm, and the

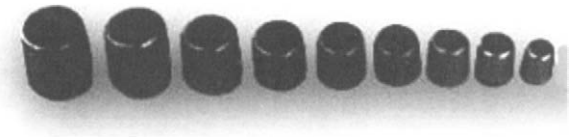


Figure 7.24 Doering Cylpebs used as grinding media (Courtesy JKMRC and Pty Ltd)

smallest ones are 8 mm × 8 mm. The shape of Powerpebs is slightly different from the Cylpebs with length being 1.5 times the diameter. Because of their geometry, these grinding media have greater surface area than balls of the same mass. For instance, Cylpebs with a diameter to height ratio of unity have 14.5% more surface area than the balls. It was thus supposed that these grinding media would produce more fines in a grinding mill. However, in a carefully designed laboratory test it was found that the Cylpebs produce a marginally coarser product than the balls at the identical specific energy (Shi, 2004). This is probably due to the breakage mechanism of line contact and area contact of the Cylpebs on the ore particles, similar to the grinding action of rods in a rod mill (see Figure 7.19).

Grinding balls are usually made of forged or rolled high-carbon or alloy steel, or cast alloy steel (Sailors, 1989), and consumption varies between 0.1 and as much as 1 kg/t of ore depending on hardness of ore, fineness of grind, and medium quality. Medium consumption can be a very high proportion, sometimes as much as 40% of the total milling cost, so is an area that often warrants special attention. Good quality grinding media may be more expensive, but may be economic due to lower wear rates. Very hard media, however, may lead to lower grinding efficiencies due to slippage, and this also should be taken into account. Finer grinding may lead to improved metallurgical efficiency, but at the expense of higher grinding energy and media consumption. Therefore, particularly with ore of low value, where milling costs are crucial, the economic limit of grinding has to be carefully assessed.

As the medium consumption contributes significantly to the total milling cost, great effort has been expended in the study of medium wear. Three wear mechanisms are generally recognised: abrasion, corrosion, and impact (Rajagopal and Iwasaki, 1992). Abrasion refers to the direct removal of metal from the grinding media surface. Corrosion means the less resistant corrosion product films being abraded away during wet grinding (Gangopadhyay and Moore, 1985; Meulendyke and Purdue, 1989). Impact wear refers to pitting, spalling, breaking, or flaking caused in the ore-metal-environment contact (Misra and Finnie, 1980; Gangopadhyay and Moore, 1987). Operational data show that abrasion is the major cause of metal loss in grinding, while corrosion represents less than 10% of the total loss (Dodd et al., 1985). In recent years, attempts have been extended to predict media wear by developing a total media wear model incorporating the abrasive, corrosive, and impact wear mechanisms (Radziszewski, 2002). The model parameters were determined from three ore-metal-environment-specific laboratory tests and validated with full-scale grinding operation data.

The charge volume is about 40–50% of the internal volume of the mill, about 40% of this being void space. The energy input to a mill increases with the ball charge, and reaches a maximum at a charge volume of approximately 50% (Figure 7.25), but for a number of reasons, 40–50% is rarely exceeded. The efficiency curve is in any case quite flat about the maximum. In overflow mills the charge volume is usually 40%, but there is a greater choice in the case of grate discharge mills. The optimum mill speed increases with charge volume, as the increased weight of charge reduces the amount of cataracting taking place.

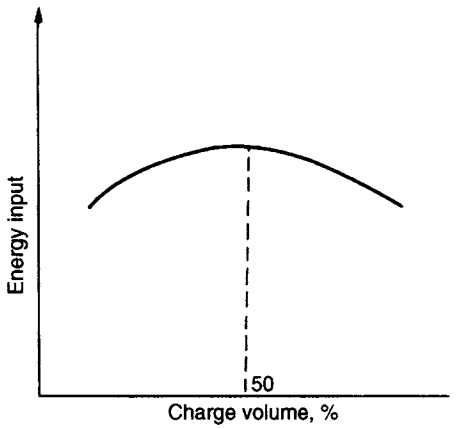


Figure 7.25 Energy input versus charge volume

Ball mills are often operated at higher speeds than rod mills, so that the larger balls cataract and impact on the ore particles. The work input to a mill increases in proportion to the speed, and ball mills are run at as high a speed as is possible without centrifuging. Normally this is 70–80% of the critical speed, the higher speeds often being used to increase the amount of cataracting taking place in order to break hard or coarse feeds.

Autogenous mills

One of the major developments in the mining industry during recent years is the use of

autogenous grinding (AG) and semi-autogenous grinding (SAG) mills. An AG mill is a tumbling mill that utilises the ore itself as grinding media. The ore must contain sufficient competent pieces to act as grinding media. An SAG mill is an autogenous mill that utilises steel balls in addition to the natural grinding media. Experience indicates that the ball charges used in SAG have generally been most effective in the range of 4–15% of the mill volume, including voids. In South African practice, however, semi-autogenous mills can have a ball charge as high as 35% of mill volume (Powell et al., 2001).

The first paper describing ore as grinding media was delivered to the American Institute of Mining and Metallurgical Engineers in 1908. In the early 1930s, Alvah Hadsel installed the Hadsel crushing and pulverizing machine, which was later improved by the Hardinge Company and was called the Hardinge Hadsel Mill. Early progression of AG mill size can be attributed primarily to a need in the iron ore industry to economically process large quantities of ore in the late 1950s. Since then the first 5.5 m (18 ft), 7.3 m (24 ft), 9.1 m (30 ft), 9.8 m (32 ft), and 11.0 m (36 ft) diameter AG/SAG mills were purchased by the iron ore producers. Non-ferrous operations (most copper and gold) utilised AG milling to a lesser extent before recognising that SAG milling was ideal for ore bodies with a variety of ore types. By December 2000, at least 1075 commercial AG/SAG mills had been sold worldwide with a total installed power exceeding 2.7 MkW. For a medium ore, those mills could process 7.2 Mt/d (Jones, 2001).

The main advantages of AG/SAG mills are their lower capital cost, the ability to treat a wide range of ore type including sticky and clayey feeds, relatively simple flowsheets, the large size of available equipment, lower manpower requirements, and reduced grinding media expense. The use of AG/SAG milling has grown to the point where many existing plants are retrofitting them, whilst new plants rarely choose a design that does not include them. This may not continue in the future, as new technologies such as fine crushing, the high pressure grinding rolls, and ultra-fine grinding offer alternative flowsheet options.

A schematic of various sections of the autogenous grinding mill is shown in Figure 7.26. AG or SAG mills are defined by the aspect ratio of the mill shell design and the product discharge mechanisms. The aspect ratio is defined as the ratio of diameter to length. Aspect ratios generally fall into three main groups: high aspect ratio mills where the diameter is 1.5–3 times of the length, "square mills" where the diameter is approximately equal to the length, and low aspect ratio mills where the length is 1.5–3 times that of the diameter. Although Scandinavian and South African practice favours low aspect ratio AG or SAG mills, in North America and Australia AG or SAG mills are distinguished by high aspects. The largest SAG mill in present use is 12 m in diameter by 6.1 m length (belly inside liners) driven by a motor power of more than 20 MW installed in an Australian gold-copper mine (Figure 7.10). Between 2000 and 2005, 92% of the newly installed AG/SAG mill power drove high aspect ratio mills (Jones, 2001). Many high aspect ratio mills, particularly the larger diameter units, have conical rather

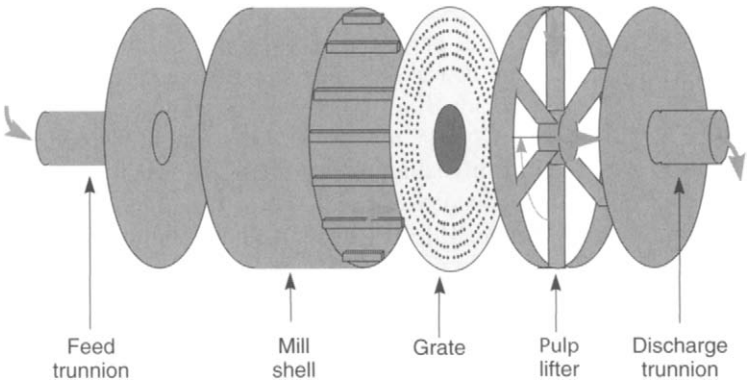


Figure 7.26 Schematic of various sections of an AG mill (Courtesy Latchireddi, 2002)

than flat ends. Attention should therefore be given to the mill length definition.

Inside the milling chamber the mill is lined with wearing plates held by lifter bars bolted to the shell. Lifter bars are essential to reduce slippage of the mill load, which causes rapid wear of the liners and also impairs the grinding action. The shape and geometry of the lifter bars, particularly the height and the face angle, have a significant influence on milling performance.

The grate as shown in Figure 7.26 is used to hold back the grinding media and allow fine particles and slurry to flow through its holes. Shapes of the grate apertures can be square, round, or slotted, with size varying from 10 to 40 mm. In some installations there are large holes varying from 40 to 100 mm in the grate, designated as pebble ports, which allow pebbles to be extracted. The total open area of the grate is approximately 2–12% of the mill cross-sectional area.

The mixture of particles smaller than the grate apertures and water in the form of a slurry discharges into the pulp lifter chambers. The pulp lifters, which are radially arranged as shown in Figure 7.26, rotate with the mill and lift the slurry into the discharge trunnion and out of the mill. Each pulp lifter chamber is emptied before its next cycle to create a gradient across the grate for slurry transportation from the milling chamber into the pulp lifter chambers.

There are two types of pulp lifter design – radial and curved (also known as spiral, refer to Figure 7.27). The radial or the straight type is most commonly used in the mineral processing industry.

While the major portion of the slurry passing through the grate is discharged from the mill via the discharge trunnion, a proportion of the slurry in the pulp lifter chamber flows back into the mill as the mill rotates. This flow-back process often leads to higher slurry hold-up inside an AG or SAG mill, and may sometimes contribute to the occurrence of "slurry pool", which has adverse effects on the grinding performance (Morrell and Kojovic, 1996). To improve the slurry transportation efficiency of the pulp lifters, particularly where slurry pooling limits capacity, a new concept of a Twin Chamber Pulp Lifter was developed by the JKMRC (Latchireddi and Morrell, 2003) and installed in a bauxite plant (Alcoa's 7.7 m diameter mill) in Western Australia (Morrell and Latchireddi, 2000). In this design, the slurry first enters the section exposed to the grate, the transition chamber, and then flows into the lower section, the collection chamber, which is not exposed to the grate. This mechanism prevents the pulp from flowing backwards into the mill, which can significantly increase the capacity of the mill.

Autogenous milling may be performed wet or dry. Dry mills have more environmental problems, do not handle materials containing clay well, and are more difficult to control than wet mills. However, in certain applications, involving grinding of minerals such as asbestos, talc, and mica, dry SAG mills are operated in closed circuit.

AG/SAG mills can handle feed ore as large as 200 mm, normally the product of the primary crusher or the run-of-mine ore, and achieve a product of 0.1 mm in one piece of equipment. The particle size distribution of the product depends on the characteristics and structure of the ore being ground. The main mechanism of comminution in AG/SAG mills is considered to be abrasion and impact. Fractures in rock composed of strong equidimensional mineral grains in a weaker matrix are principally at the grains or crystal boundaries, due to the relatively gentle comminution

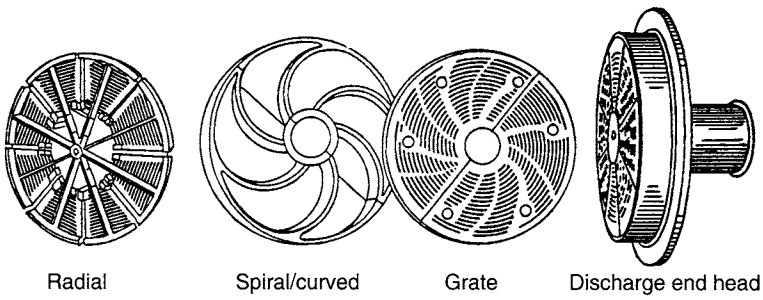


Figure 7.27 Conventional designs of pulp lifter (from Taggart, 1945; Courtesy John Wiley and Sons)

action. Thus the product sizing is predominantly around the region of grain or crystal size. This is generally desirable for mineral treatment as the wanted minerals are liberated with minimal overgrinding, and the grains keep their original prismatic shape more intact. A pilot plant study was made of the liberation characteristics of a nickel sulphide ore with full autogenous and semi-autogenous milling conditions. The mill products were sized and assayed, and then analysed by QEM*SEM. Assay evidence indicated that selective breakage was occurring in both cases leading to preferential liberation of sulphides (Wright et al., 1991). However, in their study it was not possible to establish any differences between the AG and SAG milling results, though it is frequently claimed that AG milling yields superior liberation.

Smoother particle surfaces are also obtained, which is desirable for flotation, particularly for the attachment of air bubbles. Investigations have shown that ores ground autogenously float faster and with better selectivity than if ground conventionally (Forssberg et al., 1988; Söderlund et al., 1989). Grinding in steel mills can also suppress the natural floatability of minerals, due to release of iron into the slurry, and galvanic interaction between sulphide minerals and medium can affect flotation efficiency (Rao and Natarajan, 1991).

In comparison with high aspect ratio mills, which are usually operated at 75–80% of critical speed, semi-autogenous mills in the gold mines of South Africa (locally known as "run-of-mine" mills, or RoM mills) have been limited in size to 4.88 m diameter and up to 12.2 m in length, and are normally operated at very high ball charge (up to 35%), very high total filling (up to 45%), and very high speeds (up to 90% critical). They are often operated in a single stage of grinding to produce final product of 75–80% passing 75 μm from a feed top size around 200 mm, but the mill throughput is relatively small. The initial cost of low aspect ratio AG/SAG mills is less than high aspect ratio mills, but they consume more power per tonne of product. The development of the different operating practice in South Africa occurred for historical rather than operational reasons. The RoM mills evolved from pebble tube mills used for fine secondary grinding that were converted to primary mills by directing the full run-of-mine feed to them (Mokken, 1978).

The influence of feed size and hardness on AG or SAG mill operation is much more significant than that on rod mill or ball-mill operation. In rod mills or ball mills, the mass of the rods or balls accounts for approximately 80% of the total mass of the charge and dominates both the power draw and the grinding performance of the mills. In SAG mills a significant proportion (or all of it, in AG mills) of the grinding media derives from the feed ore. Any change in the feed size distribution will therefore result in a change in the grinding media size distribution. It is equally true that any change in the feed ore hardness will affect breakage of the ore, and result in a change in the grinding media size distribution as well. The grinding media size distribution in turn will affect the breakage characteristics of the mill. Associated with the change of the breakage characteristics, the mill charge level will be changed, which affects the mill power draw. As a result, the measured AG/SAG mill power draw often varies widely with time. This is one of the significant differences in operation between the AG/SAG mill and the ball/rod mill, power draw of the latter being relatively stable. In response to the variation in feed size and hardness, the mill feed rate has to be changed significantly. At BHP-Billiton OK Tedi Mine located in Papua New Guinea, the ore hardness varied widely between 5 and 16 kW h/t, and the throughput to the 9.8 m by 4.3 m (7.5 MW) SAG mill could vary between 700 and 3000 t/h (Sloan et al., 2001). The effects of feed size and hardness on AG/SAG mill operation have been reported in the literature (Bouajila et al., 2001; Hart et al., 2001; Morrell and Valery, 2001).

The AG and SAG mills respond in a different manner to feed size changes. In an AG mill, the large rocks generate higher kinetic energy to break smaller rocks. Sufficient numbers of large rocks need to be provided to maintain a high enough frequency of breakage collisions. In general, AG mill performance is better with coarser feeds. In SAG mills, however, a relatively high ball charge dominates rock breakage, and the contribution of rock grinding media will decrease. The coarser feed rocks provide less of a role in providing grinding media and will instead provide a rock burden which requires to be ground. By reducing the feed size in these circumstances the grinding burden will be reduced (Napier-Munn et al., 1996).

Since the feed size and hardness exert a very important influence on AG/SAG mill performance, there are incentives to take account of the mine to mill operation as a whole optimisation campaign through controlling blasting practices, mining methods, run-of-mine stockpiling, partial or fully secondary crushing, and selective pre-screening of SAG mill feed. The mine-to-mill exercise has resulted in significant benefits to mining companies in terms of improving AG/SAG mill throughput, energy consumption, and grinding product size distribution (Scott and Morrell, 1998; Scott et al., 2002).

Unlike rod or ball mills, autogenous or semi-autogenous mills cannot usually be selected from bench scale grinding tests as they require more extensive testing. While grinding rods and balls can be obtained in the required sizes and quantities and their actions during milling can be reasonably predicted, in an autogenous mill the grinding medium is also the material to be ground and consequently is itself a variable. Thorough pilot scale testing of ore samples is therefore a necessity in assessing the feasibility of autogenous milling, predicting the energy requirement, flowsheet, and product size (Rowland, 1987; Mular and Agar, 1989; Mosher and Bigg, 2001).

However, the cost of a thorough pilot testing programme can be prohibitive, particularly for deposits with highly variable ore types. The use of mathematical modelling and simulation can help reduce the cost of the pilot tests by narrowing the choice of processing route at the pre-feasibility stage. This approach includes collection of representative ore samples that are typically drill cores or larger samples taken throughout the ore body. The rock breakage characterisation data are obtained through laboratory tests such as the drop-weight impact and tumbling tests (Napier-Munn et al., 1996), the SMC test using small diameter drill core samples (Morrell, 2004), the MacPherson autogenous mill work index test (MacPherson, 1989; Mosher and Bigg, 2001), and MinnovEx SPI (SAG Power Index) test (Starkey and Dobby, 1996). The breakage characteristics of the ore samples are compared with databases of extensive ore types and plant performance, which provides an indication of the ore relative strength and amenability to processing in various circuit configurations. Following pilot scale tests, computer simulation software such as JKSimMet (Napier-Munn et al., 1996) is used to scale-up to the full-size plant. There are some other computer software available for plant simulation, such as MODSIM developed by King and others at the university of the Witwatersrand in South Africa (Ford and King, 1984), USIM-PAC developed by BRGM in France (Evans et al., 1979), and CEET (Comminution Economic Evaluation Tool) (Dobby et al., 2001; Starkey et al., 2001). Even in the absence of pilot data, simulation can still provide reasonably accurate prediction of full-scale plant performance. This method is increasingly used as a standard in design and optimisation study of AG or SAG circuits worldwide.

Vibratory mills Vibratory mills are designed for continuous, or batch, grinding to give a very fine end product from a wide variety of materials, the operation being performed either wet or dry.

Two tubes functioning as vibrating grinding cylinders are located one above the other in a plane inclined at 30° to the perpendicular (Figure 7.28). Between them lies an eccentrically supported weight connected by a flexible universal joint to a 1000–1500 rev min^{-1} motor. Rotation of the eccentric vibrates the tubes to produce an oscillation circle of a few millimetres. The cylinders are filled to about 60–70% with grinding medium, usually steel balls of diameter 10–50 mm. The material being ground passes longitudinally through the cylinders like a fluid, in a complex spinning helix, thus allowing the grinding medium to reduce it by attrition. The material is fed and discharged through flexible bellow-type hoses.

The outstanding features of correctly designed vibratory ball mills are their small size and lower energy consumption relative to throughput when compared with other types of mill.

High-energy vibration mills can grind materials to surface areas of around 500 $m^2 g^{-1}$, a degree of fineness which is impossible in a conventional mill (Russell, 1989). Vibratory mills are made with capacities up to 15 $t h^{-1}$, although units of greater capacity than about 5 $t h^{-1}$ involve considerable engineering problems. The processed material size range is between approximately 30 mm feed and −10 μm end product, although the mill product size is very sensitive to feed-size variation, which limits its use for controlled grinding. Among their uses has been the regrinding of tin concentrates prior to

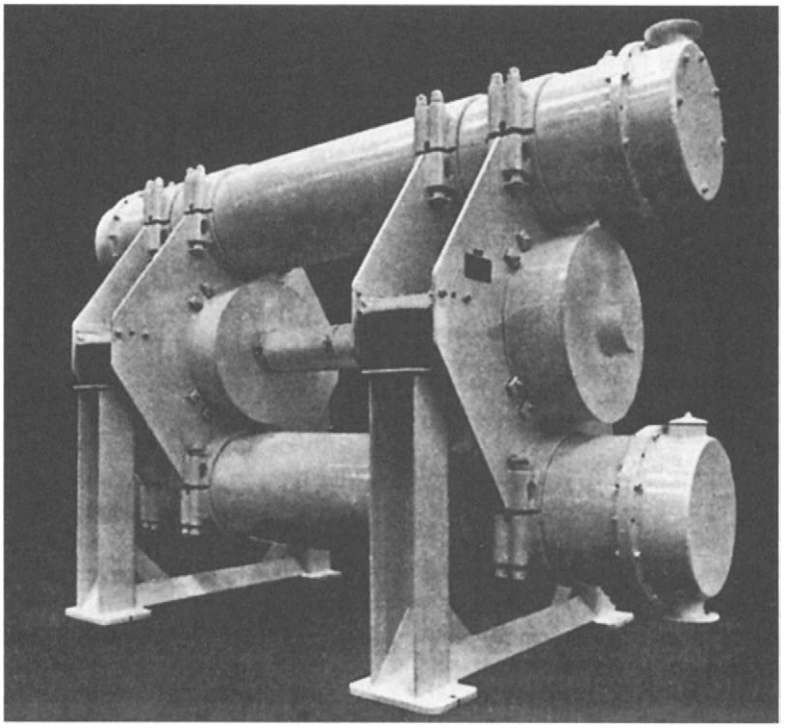


Figure 7.28 Vibratory mill

cleaning, their function being to remove the waste from the cassiterite crystals without destroying the crystals, which often happens in the conventional ball-mill environment.

Centrifugal mills The concept of centrifugal grinding is an old one, and although a patent of 1896 describes this process, it has so far not gained full-scale industrial application. Conventional mills have critical speeds above which centrifugal force prevents the mill charge mixing and tumbling to its best advantage. Throughput can therefore be increased only by increasing the size of the mill, particularly its diameter, and there are serious design and engineering problems associated with this.

In centrifugal milling, the forces on the charge inside the mill are increased by operating the mill in a centrifugal, rather than a gravitational, field. Comminution is more rapid, and the size of machine needed for a given grinding duty is thus reduced.

The Chamber of Mines of South Africa studied centrifugal milling concepts in detail, which led to a co-operative development programme with Lurgi of West Germany (Kitschen et al., 1982; Lloyd et al., 1982). Operation of a prototype 1 m diameter, 1 m long, 1 MW mill over an extended period at Western Deep Levels gold mine has proved it to be the equivalent of a conventional 4 m × 6 m ball mill in every respect.

Tower mills As tumbling mills such as ball and AG/SAG mills are not very effective in fine grinding due to their relatively low power intensity, alternatives for fine and ultra-fine grinding are tower mills and stirred mills. In contrast to tumbling mills where motion is imparted to the charge via the rotational mill shell, in tower and stirred mills motion is imparted to the charge by the movement of an internal stirrer while the shells are stationary. In a tower mill (Figure 7.29) such as that manufactured by Kubota in Japan and the Metso Vertimill, steel balls or pebbles are placed in a vertical grinding chamber in which an internal screw flight provides medium agitation. The feed enters at the top, with mill water, and is reduced in size by attribution and abrasion as it falls, the finely ground particles being carried upwards by pumped liquid and overflowing

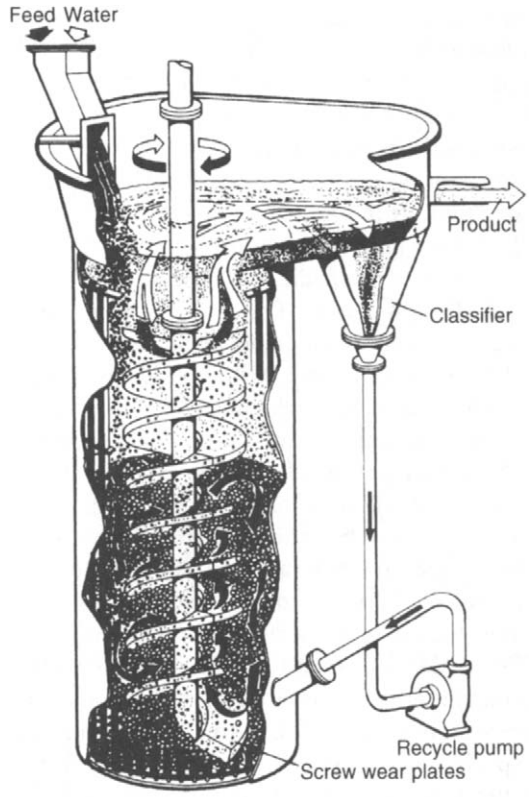


Figure 7.29 Tower mill

to a classifier. Oversize particles are returned to the bottom of the chamber, and final classification is by hydrocyclones, which return underflow to the mill sump for further grinding. According to the manufacturer's claims, advantages are a small installation area, low noise levels, efficient energy usage, minimal overgrinding, and low capital and operating costs. Product sizes may be 1–100 μm at capacities of up to 100 t/h or more. The Japanese have been the primary users of these mills, grinding a variety of materials including limestone, silica, rock salt, coal, and copper concentrates. The mill was introduced into the United States in 1979 for the purpose of grinding limestone, and has proved to provide a means of comminution in an area where the tumbling mill becomes inefficient (Stief et al., 1987).

Metso has carried out improvements to the original vertical stirred mill since the mid-1990s and the name Vertimill™ was created to describe the new design (Kalra, 1999). The principle of the Vertimill™ is similar to the tower mill. Grinding is by attrition/abrasion. Grinding efficiency is enhanced by the relatively high pressure between the media and particles to be ground. Product size has been claimed to range from 74 to 2 microns depending on the operating conditions. Currently, over 150 Vertimills™ have been placed into operation worldwide.

Stirred mills Despite the manufacturers claim that tower mills can achieve a product size of 1 μm, they are generally used at the coarse end of the fine grinding spectrum due to the use of coarse media (around 6 mm), and operation of their stirrer at a relatively slow velocity (less than 3 m/s tip speed). Finer grinding is normally achieved with stirred mills. These employ stirrers comprising a shaft with pins or disks. Stirred mills can be classified by their shell orientations: vertical such as the Sala Agitated Mill (SAM) or horizontal such as the IsaMill. They are distinguished by the designed power intensity. For tower mills, the power intensity is 20–40 kW/m^3; for a vertical pin stirrer mill it is 50–100 kW/m^3; and for horizontal stirred mills it is around 300–1000 kW/m^3 (Weller and Gao, 1999). The power intensity for horizontal stirred mills is thus an order of magnitude higher than that of vertical ones.

The IsaMill grinding chamber is a horizontally mounted shell, with a total volume of 10,000 litres in the currently largest IsaMill M10000. Inside the shell are rotating grinding discs mounted on a shaft which is coupled to a motor and gearbox (Figure 7.30). The grinding discs agitate the media

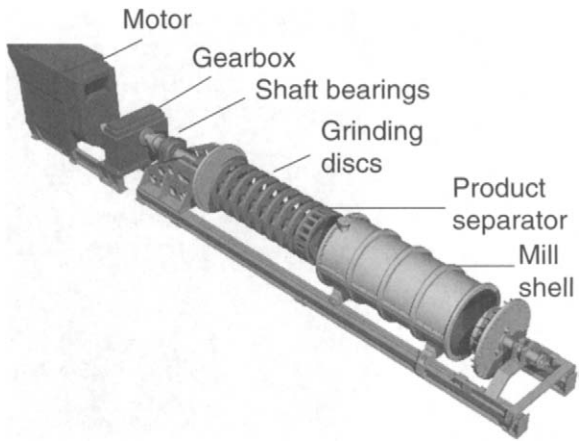


Figure 7.30 Schematic view of M10000 IsaMill with the mill shell removed (Courtesy Xstrata Technology)

and ore particles in a slurry that is continuously fed into the feed port. A patented product separator keeps the media inside the mill allowing only the product to exit. Rather than the use of screens as a classifier, the IsaMill uses the g-forces generated in the product separator to achieve a sharp cut in the product. This advantage is particularly beneficial to leaching operations, as excessive amounts of coarser particles would adversely affect the leaching recovery.

The IsaMill uses small grinding media and high stirrer velocity to impart energy to the media, which increases the breakage rate of fine particles caused by attrition/abrasion at relatively low power consumption. It is claimed that the IsaMill can efficiently grind minerals to below 10 microns. The grinding media that can be used include granulated slag, river sand, or a sized portion of the ore itself.

The world's then largest ultra-fine grinding mill, the 2.6 MW M10000 IsaMill, was commissioned in 2003 at Anglo Platinum's Western Limb Tailings Retreatment Plant (WLTRP) in South Africa (Figure 7.31).

Stirred media detritors The stirred sand media mill was first developed in the UK by English China Clays International, which later licensed the Stirred Media Detritor (SMD) technology to Metso Minerals. The SMD is a vertical mill (Figure 7.32). Unlike the stirred mill, which uses a shaft with discs or pins rotating at a very high speed, the SMD uses impellers rotating at a low speed. Normally, a natural silica or ceramic media is used as the grinding media (hence the SMD is also known as the "Sand Mill"). Grinding media is added through a pneumatic feed port or the manual feed chute located on top of the mill. Feed slurry enters through a port in the top of the unit.

The impellers thoroughly intermix the feed slurry and the media. The charge depth of the SMD is shallow. The axial flow within the charge constantly circulates particles across the media retention screens. Milled product discharges through these screens which are located around the top half of the unit. During the process, a proportion of the media will be abraded to below the screen aperture size and pass through the screens with the product. The number of exit screens depends on the grinding requirements and the required feed flow rate. The position of these screens automatically defines the operating level within the SMD.

The SMD has found its major applications in the metalliferous mining industry for fine or ultra-fine grinding duty. The normal operating range of specific energy is 5–100 kW h/t. Maximum size for the top screen SMD currently available is an installed power of 1100 kW. Feed size range is 30–100 microns and feed slurry solids concentration range is 20–60% by weight. The SMD normally operates in open circuit, although closed circuit is possible.

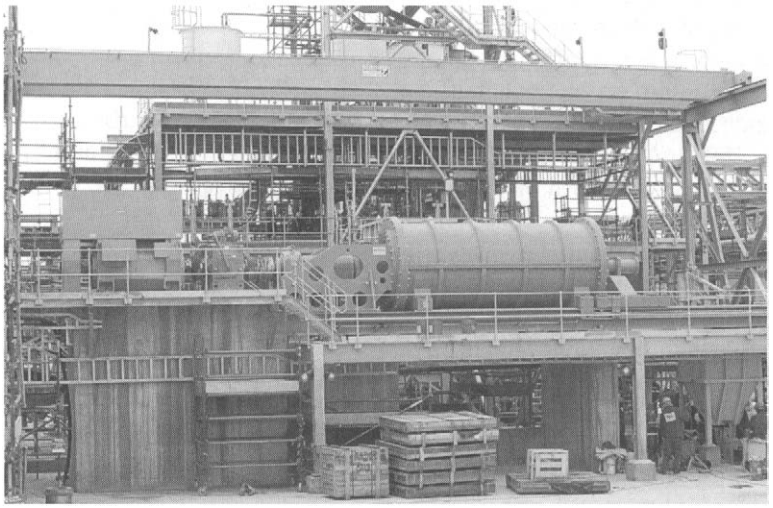


Figure 7.31 The large 10,000 litre, 2.6 MW IsaMill during the installation phase at Anglo Platinum's Western Limb Tailings Retreatment Plant in South Africa (Courtesy Xstrata Technology)



Figure 7.32 The stirred media detritor (Courtesy Mesto Minuals)

Roller mills These mills are often used for the dry grinding of medium soft materials of up to 4–5 mohs hardness (Hilton, 1984). Above this hardness, excessive wear offsets the advantage of lower energy consumption compared with conventional mills.

Table and roller mills are used to grind medium hard materials such as coal, limestone, phosphate rock, and gypsum. Two or three rollers, operating against coiled springs, grind material which is fed onto the centre of a rotating grinding table (Figure 7.33). Ground material spilling over the edge of the table is air-swept into a classifier mounted on the mill casing, coarse particles being returned for further grinding.

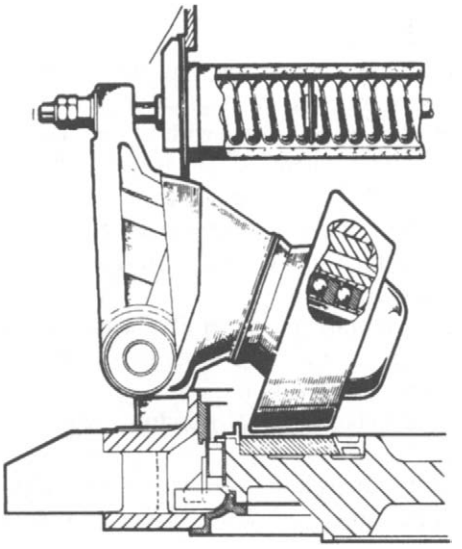


Figure 7.33 Section through table and roller mill

Pendulum roller mills are used for fine grinding non-metallic minerals such as barytes and limestone. Material is reduced by the centrifugal action of suspended rollers running against a stationary grinding ring (Figure 7.34). The rollers are pivoted on a spider support fitted to a gear-driven shaft. Feed material falls onto the mill floor, to be scooped up by ploughs into the "angle of nip" between the rolls and the grinding ring. Ground material is air-swept from the mill into a classifier, oversize material being returned.

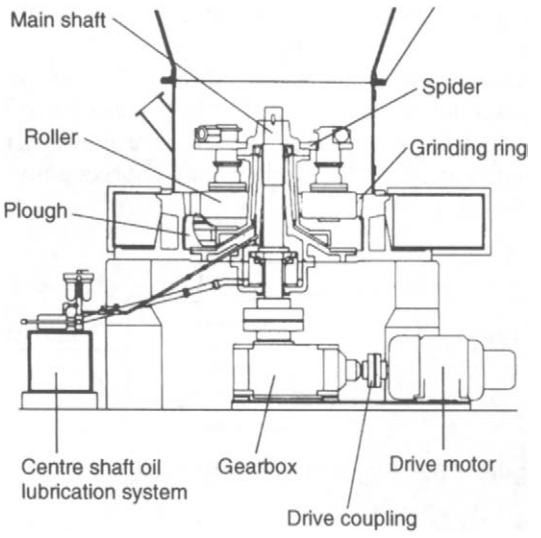


Figure 7.34 Section through pendulum roller mill

Grinding circuits

The feed can be wet or dry, depending on the subsequent process and the nature of the product. Dry grinding is necessary with some materials due to physical or chemical changes which occur if water is added. It causes less wear on the liners and grinding media and there is a higher proportion of fines in the product, which may be desirable in some cases.

Wet grinding is generally used in mineral processing operations because of the overall economies of operation.

The advantages of wet grinding are:

(1) It consumes lower power per tonne of product.
(2) It has higher capacity per unit mill volume.
(3) It makes possible the use of wet screening or classification for close product control.
(4) It eliminates the dust problem.
(5) It makes possible the use of simple handling and transport methods such as pumps, pipes, and launders.

The type of mill for a particular grind, and the circuit in which it is to be used, must be considered simultaneously. Circuits are divided into two broad classifications: *open* and *closed*. In open circuit the material is fed into the mill at a rate calculated to produce the correct product in one pass (Figure 7.35). This type of circuit is rarely used in mineral processing applications as there is no control on product size distribution. The feed rate must be low enough to ensure that every particle spends enough time in the mill to be broken down to product size. As a result, many particles in the product are overground, which consumes energy needlessly, and the product may subsequently be difficult to treat.

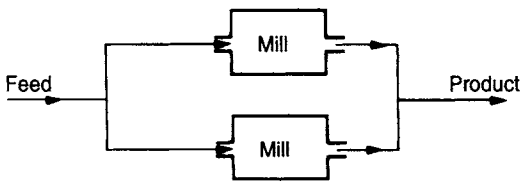


Figure 7.35 Single-stage open circuit

Grinding in the mining industry is almost always in closed circuit (Figure 7.21), in which material of the required size is removed by a classifier, which returns oversize to the mill. Although virtually every grinding circuit has some form of classification, individual mills in the circuit can be open or closed.

In closed-circuit operation, no effort is made to effect all the size reduction in a single pass. Instead, every effort is made to remove material from the circuit as soon as it reaches the required size. When grinding to a specified size, an increase in capacity of up to 35% can be obtained by closed-circuit operation.

The material returned to the mill by the classifier is known as the *circulating load*, and its weight is expressed as a percentage of the weight of new feed.

Closed-circuit grinding reduces the residence time of particles in each pass, and so the proportion of finished sizes in the mill, compared with open-circuit grinding. This decreases overgrinding and increases the energy available for useful grinding as long as there is an ample supply of unfinished material present. As the tonnage of new feed increases, so the tonnage of circulating load increases, since the classifier underflow becomes coarser, but the *composite* mill feed becomes finer due to this increase in circulating load. Due to the reduced residence time in the mill, the mill discharge correspondingly becomes coarser, so that the difference in mean size between the composite feed and the discharge decreases. The capacity of a mill increases with decreasing ball diameter due to the increase in grinding surface, to the point where the angle of nip between contacting balls and particles is exceeded. Consequently, the more near-finished material there is in the composite feed, the higher is the proportion of favourable nip angles, and the finer the composite feed the smaller need be the mean ball diameter. Within limits, therefore, the larger the circulating load the greater is the useful capacity of the mill. The increase is most rapid in the first 100% of circulating load, then continues up to a limit, depending on the circuit, just before chokage of the mill occurs. The optimum circulating load for a particular circuit depends on the classifier capacity and the cost of transporting the load to the mill. It is usually in the range of 100–350%, although it can be as high as 600%.

Rod mills are generally operated in open circuit because of their grinding action, especially when

preparing feed for ball mills. The parallel grinding surfaces simulate a slotted screen and tend to retard the larger particles until they are broken. Smaller particles slip through the spaces between the rods and are discharged without appreciable reduction. Ball mills, however, are virtually always operated in closed circuit with some form of classifier.

Various types of classifying device can be used to close the circuit, mechanical classifiers being used in many of the older mills. They are robust, easy to control, and smooth out, and tolerate surges well. They can handle very coarse sands products and are still used on many coarse-grinding circuits. They suffer from the severe disadvantage of classifying by gravitational force, which restricts their capacity when dealing with extremely fine material, hence reducing the circulating load possible.

Hydrocyclones (Chapter 9) classify by centrifugal action, which speeds up the classification of fine particles, giving much sharper separations and increasing the optimum circulating load. They occupy much less floor space than mechanical classifiers of the same capacity and have lower capital and installation costs. Due to their much quicker action, the grinding circuit can rapidly be brought into balance if changes are made and the reduced dwell time of particles in the return load gives less time for oxidation to occur, which is important with sulphide minerals which are to be subsequently floated. They have therefore become widely used in fine grinding circuits preceding flotation operations.

The action of all classifiers in grinding circuits is dependent on the differential settling rates of particles in a fluid, which means that particles are classified not only by size but also by specific gravity. A small dense particle may therefore behave in a similar way to a large, low-density particle. Thus, when an ore containing a heavy valuable mineral is ground, overgrinding of this material is likely to occur, due to it being returned in the circulating load, even though it is below the required product size.

Selective grinding of heavy sulphides in this manner prior to flotation can allow a coarser overall grind, the light gangue reporting to the classifier overflow, while the heavy particles containing valuable mineral are selectively reground. It can, however, pose problems with gravity and magnetic separation circuits, where particles should be as coarse and as closely sized as possible in order to achieve maximum separation efficiency. Such circuits are often closed by screens rather than classifiers. Fine screens have the disadvantage, however, of being relatively inefficient and delicate, and often a combination of classification and screening is used to reduce the load on the screens.

Such a circuit was used at Wheal Jane Ltd, UK, for the primary grinding of the complex copper-zinc-tin ore. The secondary crusher product was fed on to a wedge-wire screen, which routed the oversize into the primary ball mill; the mill discharge was pumped to a cyclone, and the underflow passed on to the screen to remove any fine heavy minerals before being returned to the ball mill (Figure 7.36).

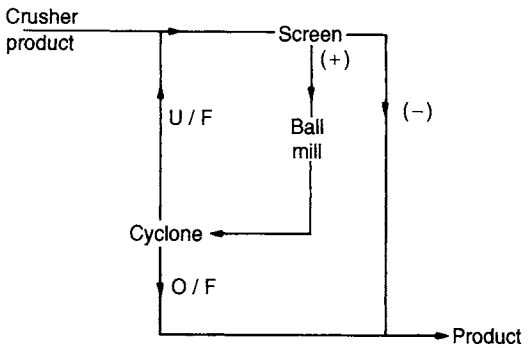


Figure 7.36 Cyclone and screen in the closed circuit

In order to solve the problem of overgrinding of small dense materials coming from the hydrocyclone underflow, a three-product cyclone has been developed by the JKMRC (Obeng and Morrell, 2003). This is a conventional hydrocyclone with a modified top cover plate and a second vortex finder inserted so as to generate three product streams (Chapter 9). By optimising the length and diameter of the second vortex finder, the amount of small dense mineral particles that normally report to the hydrocyclone underflow can be reduced. The middling stream can be classified with a microscreen to separate the valuables from the gangue (Figure 7.37). The three-product cyclone has been successfully tested in the platinum industry in South Africa for dealing with the dense chromite found in UG2 ores (Mainza and Powell, 2003; Mainza et al., 2004).

It is universal in gold recovery plants, where coarse-free gold is present, to incorporate some form of gravity concentrator into the grinding

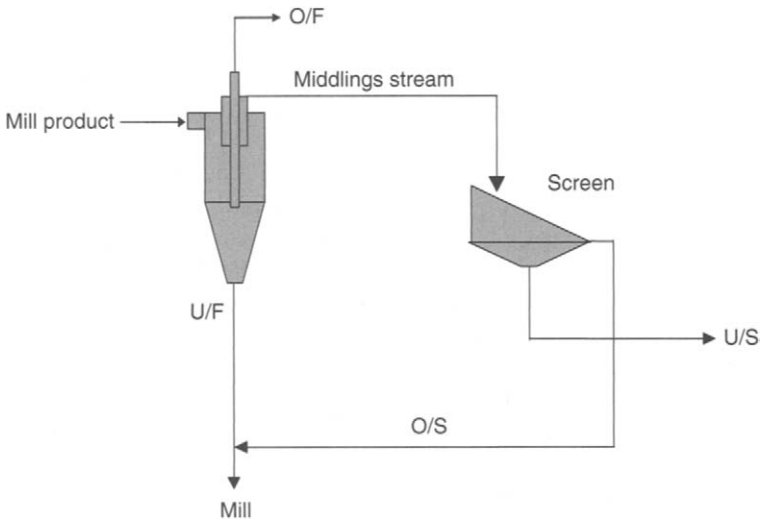


Figure 7.37 Removal of small dense mineral particles using the three-product cyclone

circuit. Native gold is extremely dense, and is invariably returned to the mill via the classifier. Being extremely malleable, once liberated it is merely deformed in the mill with no further breakage, so is continually recycled in the circuit.

At the Western Deep Levels Gold Mine in South Africa, the mill feed is first classified to remove fines, which are sent to the cyanidation plant in order to leach out the gold. The coarse fraction is fed to tube mills, the discharge being classified, and the fines returned to the primary cyclone. The classifier oversize, which contains any free gold present, is then treated by gravity concentrators, the tailings being returned to the primary cyclone, while the gravity concentrate is sent for further treatment by amalgamation (Figure 7.38). A similar system was used at the Afton copper concentrator in Canada, where jigs were used to remove coarse native copper from the primary grinding circuit (Anon., 1978).

Grinding circuits are fed at a uniform rate from bins holding the crusher plant product. There may be a number of ball mills in parallel, each circuit being closed by its own classifier, and taking a definite fraction of the feed (Figure 7.39).

Parallel mill circuits increase circuit flexibility, since individual units can be shut down or the feed rate can be changed, with little effect on the flowsheet. Fewer mills are, however, easier to control and capital and installation costs are lower, so the

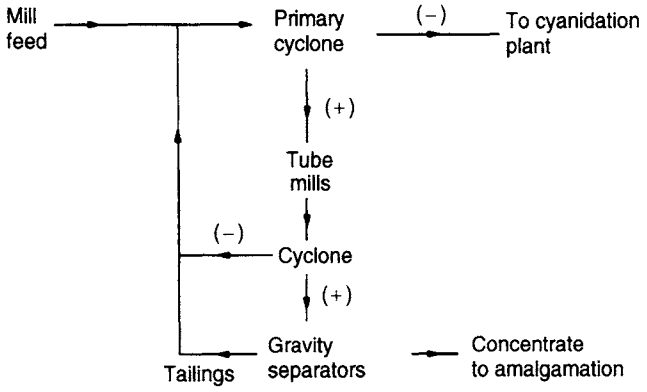


Figure 7.38 Typical gold recovery grinding circuit

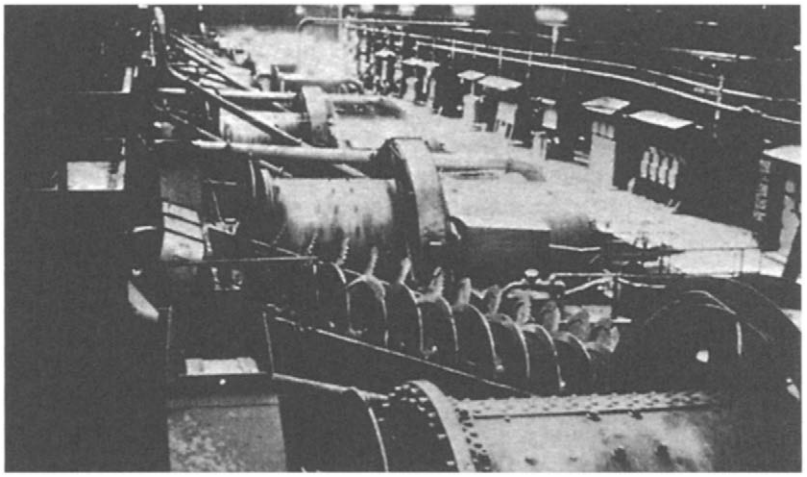


Figure 7.39 Closed-circuit ball mills

optimum number of mills must be decided at the design stage.

Multi-stage grinding in which mills are arranged in series can be used to produce successively finer products but the present trend is towards large single-stage primary ball mills, which greatly reduces capital and operating costs, and facilitates automatic control. The disadvantage of single-stage milling is that if too high a reduction ratio is produced, then relatively large balls are required for coarse feed, which may not efficiently grind the finer particles.

Two-stage grinding is used where rod milling is substituted for tertiary crushing (Figure 7.40).

The crusher product is fed to the rod mills, which operate in open circuit, producing ball-mill feed. This should, if capacity permits, be fed to the classifier rather than directly to the ball mill, as any finished material is immediately removed, and the rod mill product, which may need diluting prior to pumping, is thickened before being fed to the ball mill.

In recent years SAG milling has revolutionised the mining industry. Its high unit capacity has contributed towards substantial savings in capital and operating costs, which has in turn made many low-grade, high-tonnage operations such as copper and gold ores grinding economical feasible. SAG milling is a mature technology, and there is now a generation of metallurgists who believe that "conventional" grinding implies a SAG ball-mill circuit instead of three stages of crushing followed by rod and ball milling.

The AG/SAG mills can be operated in open or closed circuit. However, even in open circuit a coarse classifier such as a trommel attached to the mill, or a vibrating screen can be used. The oversize material is recycled either externally or internally. The external recycling can be achieved by conveyor belt in a continuous manner or in a batch mode where the material is stockpiled and periodically fed back into the mill by front-end loader. In the internal recycling the coarse material is conveyed

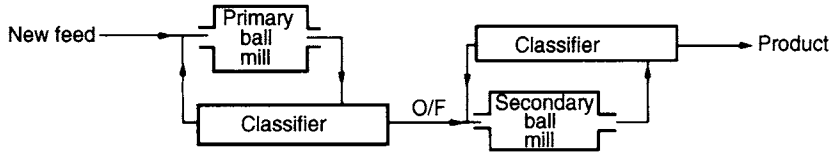


Figure 7.40 Two-stage grinding circuit

by a reverse spiral or water jet back down the centre of the trommel into the mill.

There are two closed circuit configurations that are common in AG/SAG operations. A single stage AG or SAG mill in closed circuit with hydrocyclone is favoured in the South African gold industry to process the run-of-mine ore and to produce a final grind. The mill discharge is pumped into a cluster of hydrocyclones, and the hydrocyclone underflow, together with the fresh ore, feeds the mill. The South African RoM mills are often designed with a low aspect ratio (defined as a ratio of shell diameter to length), and operated at a high filling level and a high mill rotational speed. As a general rule an AG/SAG mill in closed circuit with a fine classifier will produce a finer product, but will have a lower throughput capacity than an open circuit unit of the same size treating the same ore.

Another circuit configuration is the AG/SAG mill closed with a recycle or pebble crusher. In AG/SAG mill operation, the "critical size" of 25–50 mm is too small to act as grinding media to provide sufficient kinetic energy for other rock breakage, but is too large to be broken. If the critical size material is accumulated inside an AG/SAG mill, the mill energy efficiency will deteriorate, and the mill feed rate decreases. As a solution, additional large holes or pebble ports (40–100 mm) are cut into the mill grate allowing coarse material to exit the mill. The crusher in closed circuit is then used to reduce the size of the critical size material and return it to the mill. As the pebble ports also allow steel balls to exit the mill, a steel removal system (such as an electromagnet) must be installed to prevent them from entering the crusher. This circuit configuration has become increasingly popular in recent years as it usually produces a significant increase in throughput due to the removal of the critical size material. Compared with the open circuit, however, it gives a coarser product.

Some circuits have been trialled in which both a fine classifier and recycle crusher are used to close the mill. As the action of the recycle crusher is to remove rocks from the mill which are important as grinding media for fine particles, operating with a fine classifier as well can produce a build-up of sand-like material. This may lead to a drop in throughput and hence nullifies the advantage given by the recycle crusher (Napier-Munn et al., 1996).

In many recently designed plants the traditional three stages crushing followed by rod and ball milling circuit has been replaced by the popular SABC circuit, denoting a circuit comprising **SA**G mill followed by **B**all mill closed with **C**yclone. Figure 7.41 shows the comminution circuit at Newcrest Mining's Cadia Hill Gold Mine in New South Wales. The Cadia comminution circuit comprises a primary crusher, a single SAG mill, two pebble crushers and two parallel ball mills in closed circuit with cyclones (Dunn et al., 2001). Ore from the open cut mine is directly dump-trucked into a Fuller 1.5 m × 2.8 m (60 inch × 110 inch) gyratory crusher with a gap setting of 130–200 mm. Maximum design capacity of the primary crusher is 5800 t/h with a product size of 80% passing 200 mm. The primary crusher product is conveyed to a coarse ore stockpile with a live capacity of 41,000 t. A concrete tunnel under the stockpile houses three hydraulically driven belt feeders with variable speed drives. Each feeder draws ore from a mass flow hopper and has a capacity of 1800 t/h. A minimum of two feeders operating at 82% capacity is required to feed the SAG mill. The belt feeders discharge onto the main SAG mill feed conveyor. This conveyor has a capacity of 3700 t/h.

As the project economics study indicated a better performance with a maximum throughput through a single comminution line, the world's largest SAG mill and two of the world's largest ball mills were employed. The SAG mill is of Metso design and 12 m diameter by 6.1 m in length (belly inside liners) operating in semi-autogenous mode. It is fitted with a 20 MW Siemens gearless drive motor with bi-directional rotational capacity. The SAG mill was designed to treat 2065 t/h of monzonite ore at a ball charge of 8% volume, total filling of 25% volume, and an operating mill speed of 74% of critical. The mill is fitted with 80 mm grates with total grates open area of 7.66 m^2 (Hart et al., 2001). A 4.5 m diameter by 5.2 m long trommel screens the discharge product. Discharge material less than 12 mm falls directly into a cyclone feed sump hopper, where it is combined with discharge from the ball mills. Oversize pebbles from the trommel are conveyed to a surge bin of 735 t capacity, adjacent to the recycle crushers. Two Nordberg MP1000 cone crushers with a closed side setting gap of 12–16 mm are used to crush the pebbles with a designed product P80 being 12 mm and an

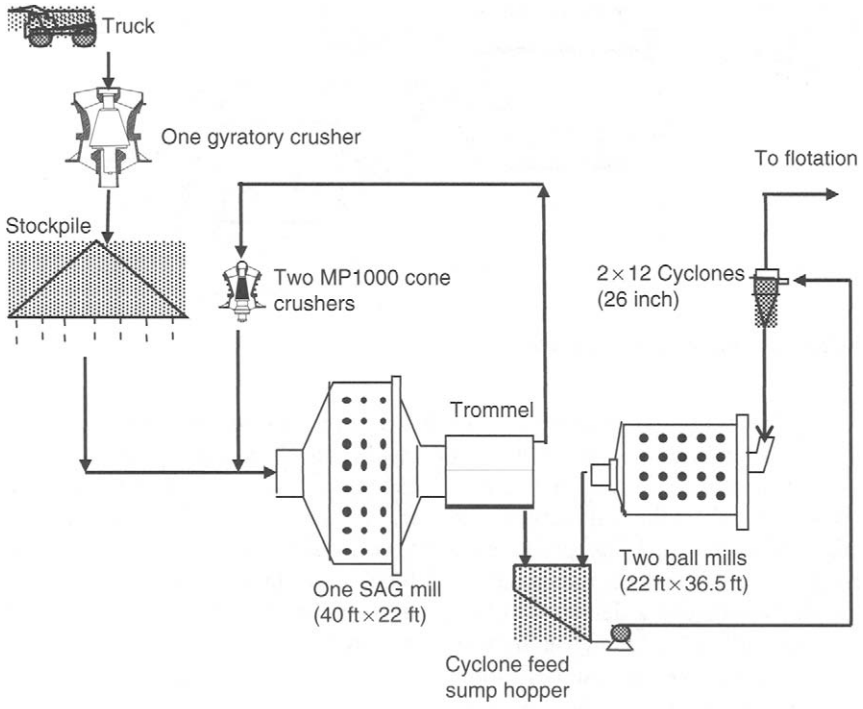


Figure 7.41 Diagram of the SABC circuit at Newcrest Mining's Cadia Mine employing the world's largest SAG mill and ball mills

expected total recycle pebble rate of 725 t/h. The crushed pebbles fall directly onto the SAG mill feed belt and return to the SAG mill.

SAG mill product feeds two parallel Metso ball mills of 6.6 m × 11.1 m (internal diameter × length), each with a 9.7 MW twin pinion drive. The ball mills are operated at a ball charge volume of 30–32% and 78.5% mill critical speed. The SAG mill trommel undersize combined with the ball mills discharge are pumped by two parallel cyclone feed pumps, each delivering to a pack of 12 Krebs 660 mm diameter cyclones. The cyclone underflow from each line reports to a ball mill while the cyclone overflow is directed to the flotation circuit. The designed ball milling circuit product is 80% passing 150 microns.

Control of the grinding circuit

The purpose of milling is to reduce the size of the ore particles to the point where economic liberation of the valuable minerals takes place. Thus, it is essential that not only should a mill accept a certain tonnage of ore per day, but should also yield a product that is of known and controllable particle size. The principal variables which can affect control are: changes in the new feed rate and the circulating load, size distribution and hardness of the ore, and the rate of water addition to the circuit. Also important are interruptions in the operation of the circuit, such as stoppages for such reasons as to feed new grinding medium or to clear a choked cyclone. For the purposes of stabilising control, feed rate, densities, and circulating loads can be maintained at values which experience has shown will produce the required product, but this method fails when disturbances cause deviations from normal operation. Fluctuation in feed size and hardness are probably the most significant factors disturbing the balance of a grinding circuit. Such fluctuations may arise from differences in composition, mineralisation, grain size, and crystallisation of the ore from different parts of the mine, from changes in the crusher settings, often due to wear, and from damage to screens in the crushing circuit. Minor fluctuations can be smoothed out by blending material excavated at different points in space and time. Ore storage tends to smooth out

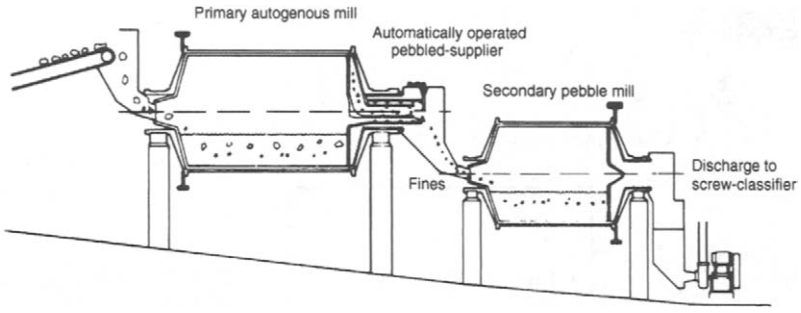


Figure 7.42 Boliden two-stage grinding system

variations providing that segregation does not take place in the bins, and the amount of storage capacity available depends on the nature of the ore (such as its tendency to oxidise) and on the mill economics.

Increase in feed size or hardness produces a coarser mill product unless the feed rate is correspondingly reduced. Conversely, a decrease in feed size or hardness may allow an increase in mill throughput. A coarser mill product results in there being a greater circulating load from the classifier, thus increasing the volumetric flow rate. Since the product size from a hydrocyclone is affected by flow rate (Chapter 9), the size distribution of the circuit product will change. Control of the circulating load is therefore important in control of particle size. A high circulating load at a fixed product size means lower energy consumption, but excessive circulating loads can result in mill, classifier, or pump overloading, hence there is an upper limit to mill feed rate.

Measurement of the circulating load can be made by sampling various slurry streams in the circuit. It may not be practicable to physically weigh the tonnage of circulating material, although the weight of new feed to each mill may be known from weightometers or other weighing methods used on the feeders.

In the simple ball-mill–classifier circuit shown in Figure 7.21, suppose the new feed rate is $F\,\mathrm{t\,h^{-1}}$ and the circulating load (i.e classifier underflow) is $C\,\mathrm{t\,h^{-1}}$, then:

$$\text{circulating load ratio} = \frac{C}{F}.$$

A mass balance on the mill classifier gives:

ball-mill discharge = circulating load + product

or

$$F + C = C + F$$

If samples of ball-mill discharge, circulating load, and classifier overflow (circuit product) are taken, and screen analyses are performed, then if a, b and c are the percentage weights in any specific size fraction in the mill product, circulating load, and classifier overflow respectively, then a mass balance on the classifier in terms of such sized material is:

$$(F + C)a = Fc + Cb$$

$$\text{or } \frac{C}{F} = \frac{a - c}{b - a} \tag{7.4}$$

Using all the size analysis data available, the "best-fit" value of the circulating load ratio can be determined by the method of least-squares (Chapter 3).

The variables a, b, and c may also represent the water/solid ratio of the products, since the relationship is then a mass balance of the weight of water in the circuit; since a, b, and c can be measured online by nuclear density gauges, the circuit circulating load can be continuously monitored.

Since grinding is extremely energy intensive, and the product from grinding affects subsequent processes, the need for close control is extremely important, and it is now generally accepted that some form of automatic control is required to maintain efficient performance. Automatic control of grinding circuits is the most advanced and most successful area of the application of process control in the minerals industry (Herbst et al., 1988; Mular, 1989).

In implementing instrumentation and process control for grinding circuits the control objective must first be defined, which may be:

(1) to maintain a constant product size at maximum throughput

(2) to maintain a constant feed rate within a limited range of product size
(3) to maximise production per unit time in conjunction with downstream circuit performance (e.g. flotation recovery).

The most important variables associated with a conventional grinding circuit are shown in Figure 7.43. Of the variables shown, only the ore feed rate and the water addition rates can be varied independently, as the other variables depend upon and respond to changes in these items. It is therefore ore feed rate and water addition to the mill and classifier which are the major variables used to control grinding circuits. In recent years, it has been reported that slurry viscosity, rather than or in addition to the density, should be used as a key operating variable for milling circuit control (Kawatra et al., 1988; Moys, 1989; Shi, 2002a). For a copper slurry, 1% increase from 55 to 56 vol% density results in a change in viscosity from 329 to 390 mPa s. The plant control system may not be able to distinguish the increment of 1% solids, but the viscometer can easily identify the associated change in viscosity (Shi, 2002a). In a closed grinding circuit, since hydrocyclone performance exerts a significant influence on solids concentration and particle size of grinding slurry, and the solids concentration and particle size affect the rheological characteristics of the slurry, the hydrocyclone classifier could be used as a rheological controller for the grinding mill (Shi, 2002b; Shi and Napier-Munn, 2002). The use of a variable speed pump feeding the classifiers introduces another independent variable, and has a significant effect on the stability of the circuit. Pump speed should, however, be viewed as a variable that provides the conditions under which particular control objectives can be achieved, rather than as a variable that actually achieves them.

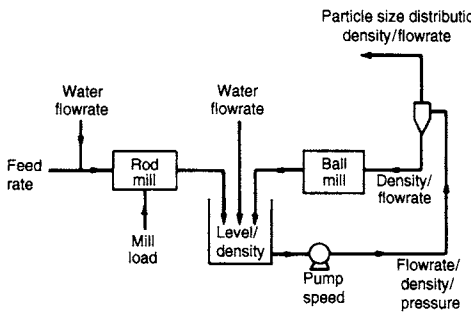


Figure 7.43 Grinding circuit control variables

Control of the feed rate is essential, and devices such as variable speed feeder belts in conjunction with weightometers are often used. Control of the grinding medium charge can be made by continuous monitoring of the mill power consumption. A fall in power consumption to a certain level necessitates charging of fresh grinding medium.

Continuous power monitoring finds its greatest use in autogenous grinding, the power drawn being used to control the mill feed rate. Control of power draft has been mainly made by load cells which measure directly the mass of material in the mill, but a dual microphone system has recently been tested and has been found to have considerable advantages over load cells (Jaspan et al., 1986; Timms, 1994; Perry and Anderson, 1996; Pax, 2001). Microphones have been used before, but mainly on air-swept mills, the sound intensity providing the set-point for feed control. The new system differs in that it uses two microphones, placed above and below the normal level of impact of the charge on the mill shell. As the mill load increases, the point of impact of the charge on the shell moves towards the upper microphone, and conversely down towards the lower microphone as it decreases. By comparing the output from the two microphones, it becomes possible to determine whether the charge level is rising or falling. This information is correlated with the power draw of the mill and used to calculate the rate of addition of the new feed. It was found in the full-scale operation that the sound level changed several minutes ahead of detectable changes in the mill bearing pressure, power, torque, motor current, and mill weight. Therefore the plant took the sound reading as an excellent indicator of changes in SAG load for the milling circuit control (Perry and Anderson, 1996). An unexpected benefit was that there proved to be a strong correlation between the sound intensity of the lower microphone and the pulp density in the mill. At the low pulp densities the fluidity of the charge permits stronger media-liner impacts and therefore more noise, while at high pulp density the viscosity tends to cushion the collisions, muffling the sound output. By using the output from the lower microphone to control water addition, a constant pulp density can be maintained.

The use of mill noise measurements as indicators of mill pulp density and viscosity has also been demonstrated on a laboratory ball mill (Watson and Morrison, 1986). The results suggest that as pulp density increases, the change in mill noise can be used to identify the pulp rheological regime and that knowledge of the rheology can be advantageous in optimising grinding.

Flow rates and densities are measured continuously mainly by the use of magnetic flowmeters and nuclear density gauges respectively, sump level is commonly indicated by bubble tube, capacitance-type detectors or other electronic devices, and product particle size can be either measured directly by the use of online monitors (Chapter 4) or inferred by the use of mathematical models (Chapter 9).

There is an important difference in the dynamic response of the circuit to changes in ore feed rate and to changes in water addition rate. Changes in ore feed rate initiate a slow progressive change in which the final equilibrium state represents the maximum product response, while changes in classifier water addition initiate an immediate maximum response, the equilibrium product response being relatively small. Increase in water addition rate also results in a simultaneous increase in circulating load and sump level, confirming the necessity of using a large capacity sump and variable speed pump to maintain effective control.

If the requirement of the control system is constant product size at constant feed rate, then the only manipulated variable is the classifier water, and the circuit must therefore tolerate variations in the cyclone overflow density and volumetric flow rate when ore characteristics change. Large variations in circulating load will also occur.

In many applications, the control objective is maximum throughput at constant particle size, which allows manipulation of both ore feed rate and classifier water addition. Allowing for the fact that the circuit has a limited capacity, this objective can be stated as a fixed product particle size set-point at a circulating load set-point corresponding to a value just below the maximum tonnage constraint. The circulating load is either calculated from measured values, measured directly, or inferred.

Since both ore feed rate and classifier water addition rate can be varied independently, two control strategies are available. In the first system product size is controlled by ore feed rate, and circulating load by classifier water addition rate, while in the second system product size is controlled by the ore feed rate. The choice of control strategy depends on which of the control loops, the particle size loop or the circulating load loop, is required to respond faster; this depends on many factors, such as the ability of the grinding and concentration circuits to handle variations in flow, the sensitivity of the concentration process to deviations from the optimum particle size, time lags within the grinding circuit, and the number of grinding stages. If the particle size response must be fast, then this loop is controlled by the classifier water, whereas if a fast mill throughput response is more important, then the product size is controlled by the ore feed rate.

At Vihanti in Finland (Wills, 1983), the latter strategy was employed, as the flotation circuit could tolerate short-term changes in particle size. The flowsheet and instrumentation for the No. 2 grinding circuit are shown in Figure 7.44. The control concentrates on keeping the particle size constant by regulating the crushed ore feed to the rod mill, and on stabilising the cyclone feed density by regulating the water addition to the cyclone pump sump.

The rod mill feed is measured by means of an electric belt weigher, and is kept constant by regulating the speed of the belt feeder. Water addition to the mill is controlled according to the feed rate set-point to maintain a constant slurry density. The rod mill discharge is fed to a sump where it joins the discharge from grinding circuit No. 1. The sump level is monitored by means of a pressure transducer and controlled by a variable speed pump, the slurry density being stabilised by water addition to the sump. The slurry is pumped to a 500 mm cyclone, the flow rate and density in the feed-line being monitored. The cyclone underflow is fed to a 1.6 m diameter Hukki cone classifier (Hukki, 1977), the overflow from this joining the cyclone overflow and providing feed to the flotation plant. Such two-stage classification is reported to increase the sharpness of separation (Heiskanen, 1979). The particle size was originally inferred from the cyclone feed data by means of an empirical mathematical model, but was later measured directly by an Autometrics PSM-200 system, the particle size being controlled

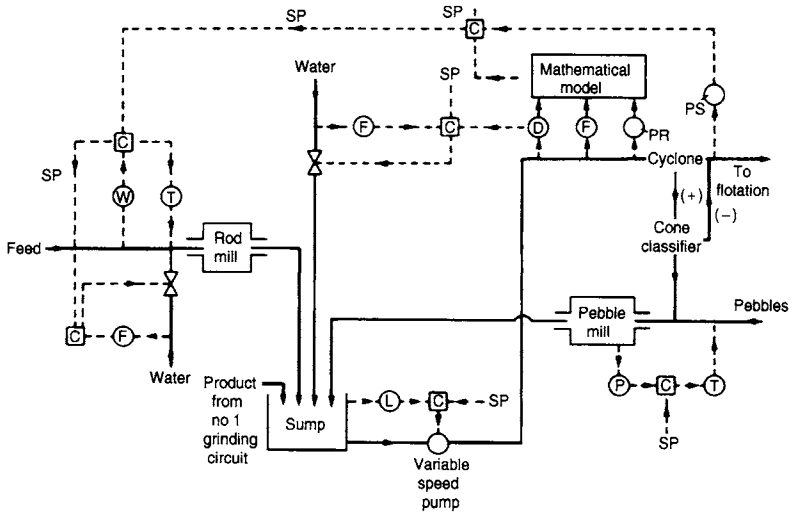


Figure 7.44 Vihanti No. 2 grinding circuit. F = Flow rate; W = Weight (belt scale); T = Thyristor control; D = Density; PR = Pressure; PS = Particle size; P = Power; L = Level; SP = Set-point; C = Controller

at 60% – 75 μm. The coarse product from the cone classifier was fed to a pebble mill, the pebble feed being controlled according to the power consumed.

The grinding circuit at Amax Lead Co's Buick concentrator, which controls product size by classifier water addition rate, is shown in Figure 7.45 (Perkins and Marnewecke, 1978).

The plant treats 1.6 m t a^{-1} of a complex copper–lead–zinc ore by flotation, the circuit being extremely sensitive to particle size. The control system uses a weightometer to measure the rod mill feed rate, orifice plate measurement of feed water and sump water flow rates, and sonic detection of sump level. An Autometrics PSM-100 particle size analyser measures the percentage passing

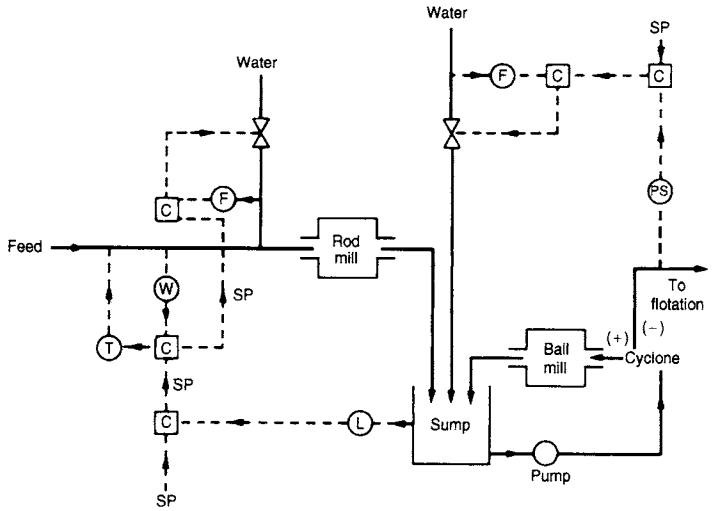


Figure 7.45 Amax Buick Concentrator – Zinc Circuit. F = Flow rate; W = Weight; T = Thyristor control; L = Level; PS = Particle size; SP = Set-point; C = Controller

75 μm and the percentage solids in the cyclone overflow.

The feed control loop matches the actual rod mill feed, indicated by the belt weightometer, with the feed set-point, which is cascaded from the cyclone sump level detector. The feed water control loop maintains a constant ratio between rod mill feed rate and rod mill water addition to provide a constant slurry density in the rod mill. The particle size monitor signal is compared with the particle size set-point, the controller adjusting the set-point of water addition to the sump accordingly, in order to maintain a product which is 59% – 75 μm in the cyclone overflow. Circulating load and sump level are controlled without the use of mass flow measurements or a variable speed pump, the sump level being a good indication of the circulating load, since the largest volume of flow into the sump comes from the ball-mill discharge. The mill throughput loop therefore maintains as high a sump level as possible by manipulating the ore feed rate to the rod mill.

The major limitation of the control strategies discussed above is that control of the numerous plant variables by independent controllers to their optimum values is made difficult by the interaction of these variables. For instance, in the example quoted above, particle size is controlled by water addition to the sump, but increase in sump water also increases the circulating load. Similarly, circulating load is controlled by the ore feed rate loop, but increase in ore feed rate also increases the particle size of the product. It is also apparent that if the circulating load (in this case the sump level) is above its set-point value *and* the product size is also above the set-point value, then the water addition loop will increase the sump water addition to reduce the particle size, this action increasing the circulating load faster than the slower acting feed loop can reduce it. In practice, one or more control loops are de-tuned to minimise such interactions, which results in a general slow down in control response.

Alternative approaches to grinding circuit control based on multivariable control systems have been investigated. Despite the apparent complexity of the multivariable controller (Hulbert, 1977), it has been successful in finding repeated and sustained applications in many industrial plants in the South African gold-mining industry (Metzner, 1993).

A common problem in the operation of a milling circuit, particularly when particle size control is attempted, is that the control actions are often constrained by physical or operational limitations. This problem is particularly relevant in the case of multivariable control, in which control of the process depends critically on the correct combination of several control actions. The saturation of one of these control actions may result in partial loss of control, or even instability of the process. In order to deal with this problem, a new method has been developed, in which the multivariable control scheme includes a robust "limit algorithm", thus retaining effective stabilising control of the milling process (Hulbert et al., 1990; Craig et al., 1992; Metzner, 1993; Galán et al., 2002).

Expert systems are becoming an accepted form of control for complex grinding circuits. Expert systems are computer programs that compile the process knowledge and rules employed by the control room operators. They allow continuous monitoring of the grinding circuit, apply logic in a consistent manner, and allow the circuit to be operated beyond a comfort zone. They require little additional investment and infrastructure and can operate from a desktop computer. Generally, there are three fundamental elements that comprise a plant expert system – the instrumentation, the software, and the integration. Several commercial systems are in use, such as MINTEK's Interpreting Expert System (Smith et al., 2001; Louw et al., 2003; van der Spuy et al., 2003), the MinnovEx expert system (Sloan et al., 2001), and the Outokumpu/Helsinki University's expert control system using the cluster model (Pulkkinen et al., 1993).

The sustainability of an expert system has been traced to the integration methodology, i.e. the human factors (Sloan et al., 2001). The major limitations of expert system control are that they are a knowledge-based methodology. Due to the complexity of the interrelationships among various grinding units, particularly those involving AG/SAG mills, the required control strategy is sometimes beyond existing knowledge.

Model-predictive control has its origins in work done in the 1970s (Lynch, 1977) but has received considerable attention in recent years with the

advent of more reliable models and more powerful computing platforms (Herbst et al., 1993; Evans, 2001; Galán et al., 2002; Lestage et al., 2002; Muller et al., 2003; Schroder et al., 2003). This approach involves development of mathematical models of a unit or a circuit based on existing knowledge, operating mechanisms, and experimental data. Such models often incorporate a number of model parameters that need to be calibrated by experimental data from a specific unit or circuit. Once the model parameters are determined and the ore breakage characteristics are known, the models can predict the performance of the unit or the circuit in response to changes in the feed condition or the operational conditions, either steady-state performance or the dynamic response. The model can also be used in conjunction with an expert system (Herbst et al., 1989).

JKDynaGrind developed by JKTech, Australia, is a typical dynamic model-based simulator that provides the information needed for online grinding control. Figure 7.46 illustrates the grinding circuit configuration and the models used to simulate the circuit performance (Schroder et al., 2003).

JKDynaGrind contains the JKMRC models for crushing, ball milling, and classification processes (Napier-Munn et al., 1996) and a dynamic AG/SAG mill model (Valery, 1997). It takes online data and updates once every 10 s as the inputs to provide continuous information about the mill operation such as charge volume, charge shape, degree of slurry pooling, product sizing, etc., which are difficult to acquire by conventional instrumentation. A Kalman filter is incorporated to provide dynamic fitting of model parameters. The information permits diagnosis of circuit behaviour, management of circuit operation, and automatic control.

Site trials indicated that model predictions closely matched the actual plant performance (Figure 7.47). During this trial, the JKDynaGrind system was used to augment the existing expert system, by providing information about the

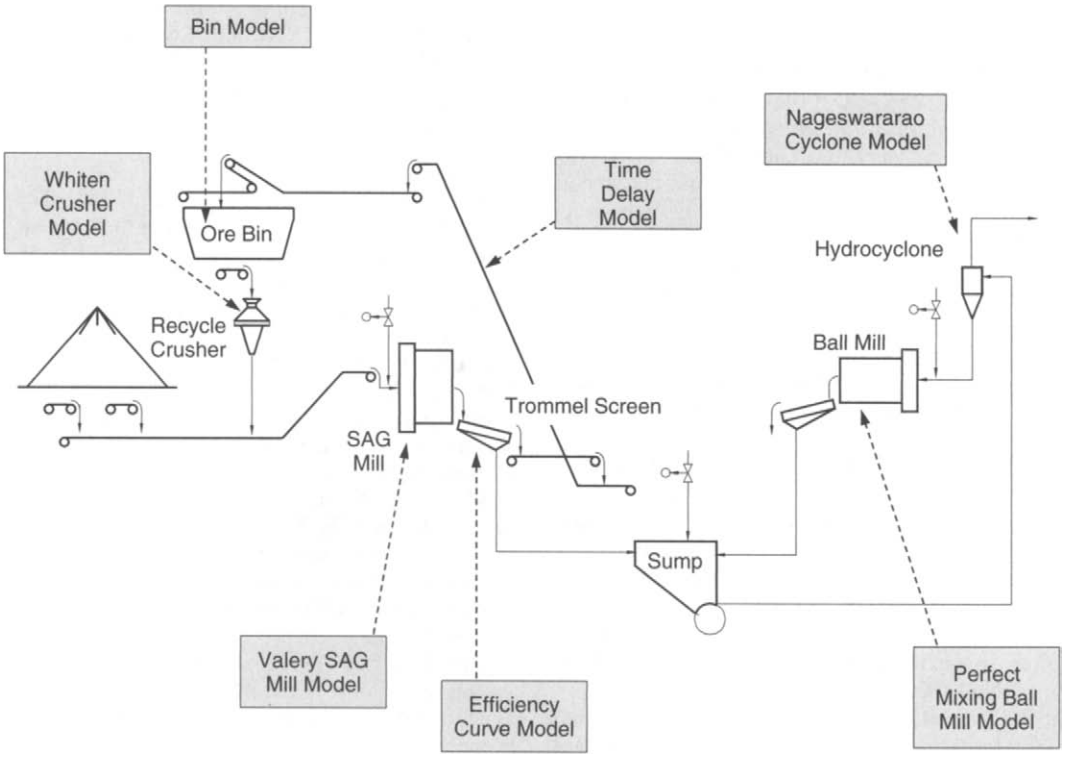


Figure 7.46 Construction of a grinding circuit model

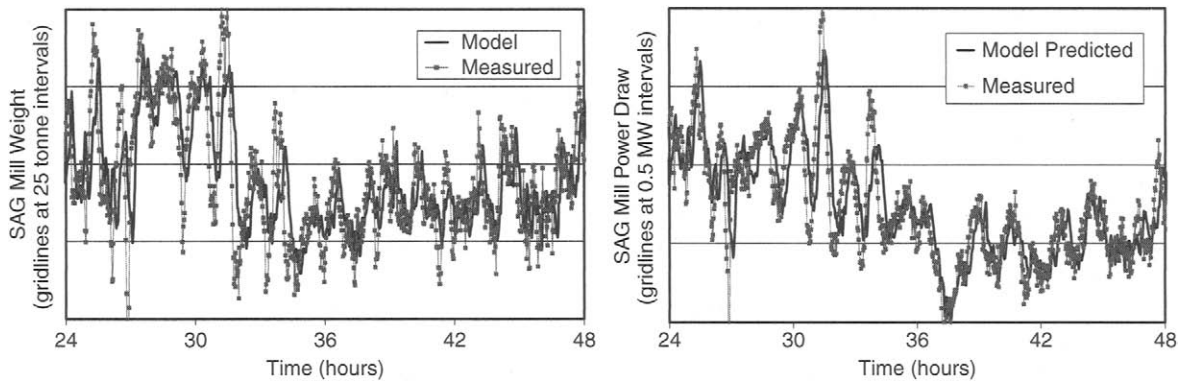


Figure 7.47 Measured SAG load and power compared with model predictions by JKDynaGrind (Courtesy JKMRC and JKTech Pty Ltd)

condition of the SAG mill load and ore hardness. This resulted in a 25% reduction in load variability (Schroder et al., 2003).

References

Anon. (1978). Afton – new Canadian copper mine, *World Mining*, **31**(Apr.), 42.

Anon. (1982). Grinding mills – rod, ball and autogenous, *Min. Mag.* (Sept.), 197.

Anon. (1990). Modern tube mill design for the mineral industry – Part I. *Mining Mag.*, **163**(Jul.), 20.

Arbiter, N. and Harris, C.C. (1984). Scale-up problems with large ball mills, *Min. Metall. Proc.*, **1**(May), 23.

Bouajila, A., Bartolacci, G., and Coté, C. (2001). The impact of feed size analysis on the autogenous grinding mill, *Proc. of SAG 2001 Conf.*, Vancouver, Canada, Vol. II, 317–330.

Concha, F., et al. (1988). Optimization of the ball charge in a tumbling mill, in *Proc. XVI Int. Min. Proc. Cong.* **A**, ed. K.S.E. Forssberg, Elsevier, Amsterdam, 147.

Craig, I.K., Hulbert, D.G., Metzner, G., and Moult, S.P. (1992). Optimised multivariable control of an industrial run-of-mine milling circuit, *J. S. Afr. I. Min. Metall.*, **6**, 169–176.

De Richemond, A.L. (1982). Choosing liner materials for ball mills, *Pit and Quarry*, (Sept.), 62.

Dobby, G., Bennett, C., and Kosick, G. (2001). Advances in SAG circuit design and simulation applied to the mine block model, *Proc. of SAG 2001 Conf.*, Vancouver, Canada, Vol. IV, 221–234.

Dodd, J., et al. (1985). Relative importance of abrasion and corrosion in metal loss in ball milling, *Min. Metall. Proc.*, **2**(Nov.), 212.

Dunne, R., Morrell, S., Lane, G., Valery, W., and Hart, S. (2001). Design of the 40 foot diameter SAG mill installed at the Cadia Gold Copper Mine, *Proc. of SAG 2001 Conf.*, Vancouver, Canada, Vol. I, 43–58.

Durman, R.W. (1988). Progress in abrasion-resistant materials for use in comminution processes. *Int. J. Min. Proc.* (Apr.), 381.

Evans, G. (2001). A new method for determining charge mass in AG/SAG mills, *Proc. of SAG 2001 Conf.*, Vancouver, Canada, Vol. II, 331–345.

Evans, L.B., et al. (1979). ASPEN – an advanced system for process engineering, *12th Symp. of Comp. Applications in Chem. Engng.*, Montreux.

Ford, M.A. and King, R.P. (1984). The simulation of ore-dressing plants, *Int. J. Min. Proc.*, **12**, 285–304.

Galán, O., Barton, G.W., and Romagnoli, J.A. (2002). Robust control of a SAG mill, *Powder Tech.*, **124**, 264–271.

Gangopadhyay, A.K. and Moore, J.J. (1985). Assessment of wear mechanisms in grinding media, *Min. Metall. Proc.*, **2**(Aug.), 145.

Gangopadhyay, A.K. and Moore, J.J. (1985). The role of abrasion and corrosion in grinding media wear, *Wear*, **104**, 49–64.

Gangopadhyay, A.K. and Moore, J.J. (1987). Effect of impact on the grinding media and mill liner in a large semi-autogenous mill, *Wear*, **114**, 249–260.

Hart, S., Valery, W., Clements, B., Reed, M., Song, M., and Dunne, R. (2001). Optimisation of the cadia Hill SAG mill circuit, *Proc. of SAG 2001 Conf.*, Vancouver, Canada, Vol. I, 11–30.

Heiskanen, K. (1979). Two-stage classification, *World Mining*, **32**(Jun.), 44.

Herbst, J., Pate, W.T., and Lo, Y.C. (1993). A model-based methodology for steady state and dynamic optimisation of autogenous and semiautogenous grinding mills, *Proc. XVIII Int. Min. Proc. Cong.*, Sydney, 519–527.

Herbst, J.A., et al. (1988). Optimal control of comminution operations. *Int. J. Min. Proc.* (Apr.), 275.

Herbst, J.A., et al. (1989). Experiences in the use of model based expert control systems in autogenous and semi autogenous grinding circuits, *Advances in Autogenous and Semiautogenous Grinding Technology*, ed.

A.L. Mular and G.E. Agar, Vol. 2, Dept. of Mining and Mineral Process Engineering, University of British Columbia, 669.

Hilton, W. (1984). Comminution and classification of barites, *Trans. Inst. Min. Metall.*, **93**, A145.

Hulbert, D.G. (1977). Multivariable control of a wet-grinding circuit, PhD Thesis, University of Natal, South Africa.

Hulbert, D.G., Craig, I.K., Coetzee, M.L., and Tudor, D. (1990). Multivariable control of a run-of-mine milling circuit, *J. S. Afr. I. Min. Metall.*, **90**, 173–181.

Hukki, R.T. (1977). A new way to grind and recover minerals, *Engng. Min. J.*, **178**(Apr.), 66.

Jaspan, R.K., et al. (1986). ROM mill power control using multiple microphones to determine mill load, *Proc. Gold 100 Conf.*, SAIMM, Jo'burg.

Joe, E.G. (1979). Energy consumption in Canadian mills, *CIM Bull.*, **72**(Jun.), 147.

Jones, S.M., and Holmberg, K.L. (1996). Modern grinding mill designs, in *Changing Scopes in Mineral Processing*, ed. M. Kemal et al., A.A. Balkema, Rotterdam.

Kalra, R. (1999). Overview on alternative methods for fine and ultra-fine grinding, *IIR Conference: Crushing and Grinding '99.*

Kawatra, S.K. and Eisele, T.C. (1988). Rheology effects in grinding circuits, in *Proc. XVI Int. Min. Proc. Cong.* A, ed. K.S.E. Forssberg, **195**, Elsevier, Amsterdam.

Kawatra, S.K., Eisele, T.C., Zhang, D., and Rusesky, M. (1988). Effects of temperature on hydrocyclone efficiency, *Int. J. Min. Proc.*, **23**, 205–211.

Kitschen, L.P., Lloyd, P.J.D. and Hartman, R. (1982). The centrifugal mill: Experience with a new grinding system and its applications, *Proc. XIV Int. Min. Proc. Cong.*, Paper no. 1–9, CIM, Toronto, Canada.

Klimpel, R.R. (1982). Slurry rheology influence on the performance of mineral/coal grinding circuit. Part 1, *Minerals Engng.*, **34(12)**, 1665–1668.

Klimpel, R.R. (1983). Slurry rheology influence on the performance of mineral/coal grinding circuit. Part 2, *Minerals Engng.*, **35(1)**, 21–26.

Klimpel, R.R. (1984). Influence of material breakage properties and associated slurry rheology on breakage rates in wet grinding of coal/ores in tumbling media mills, in *Reagents in the Mineral Industry*, ed. M.J. Jones and R. Oblatt, I.M.M., London, 265–270.

Knecht, J. (1990). Modern tube mill design for the mineral industry – Part II, *Mining Mag.*, **163**(Oct.), 264.

Korpi, P.A. and Dopson, G.W. (1982). Angular spiral lining systems in wet grinding grate discharge ball mills, *Min. Engng.*, **34**(Jan.), 57.

Latchireddi, S. (2002). Modelling the performance of grates and pulp lifters in autogenous and semi-autogenous mills, PhD Thesis, JKMRC, The University of Queensland.

Latchireddi, S. and Morrell, S. (2003). Slurry flow in mills: Grate-only discharge mechanism (Parts 1 and 2) *Minerals Engng.*, **16**, 625–642.

Lestage, R., Pomerleau, A., and Hodouin, D. (2002). Constrained real-time optimisation of a grinding circuit using steady-state linear programming supervisory control, *Powder Tech.*, **124**, 254–263.

Lewis, F.M., Coburn, J.L., and Bhappu, R.B. (1976). Comminution: A guide to size reduction system design, *Min. Engng.*, **28**(Sept.), 29.

Lloyd, P.J.D., et al. (1982). Centrifugal grinding on a commercial scale, *Engng. Min. J.* (Dec.), 49.

Lo, Y.C., et al. (1988). Design considerations for large diameter ball mills, *Int. J. Min. Proc.*, **22**(Apr.), 75.

Louw, J.J., Hulbert, D.G., Smith, V.C., Singh, A., and Smith, G.C. (2003). MINTEK's process control tools for milling and flotation control, *Proc. XXII Int. Min. Proc. Cong.*, Cape Town, **1**, 1581–1589.

Lynch, A.J. (1977). *Mineral Crushing and Grinding Circuits: Their simulation, optimisation and control*, Elsevier, 340pp.

MacPherson, A.R. (1989). Autogenous grinding, 1987-update, *CIM Bull.*, **82(921)**, 75–82.

Mainza, A. and Powell, M. (2003). Use of the three-product cyclone in dual-density ore classification, *Proc. XXII Int. Min. Proc. Cong.*, Cape Town, **1**, 317–326.

Mainza, A., Powell, M., and Knopjes, B. (2004). Differential classification of dense material in a three-product cyclone, *Minerals Engng.*, **17(5)**, 573–580.

Malghan, S.G. (1982). Methods to reduce steel wear in grinding mills, *Min. Engng.* (Jun.), 684.

Man, Y.T. (2001). Model-based procedure for scale-up of wet, overflow ball mills – Part 1: Outline of the methodology, *Minerals Engng.*, **14(10)**, 1237–1246.

McIvor, R.E. and Finch, J.A. (1986). The effects of design and operating variables on rod mill performance, *CIM Bull.*, **79**(Nov.), 39.

Meintrup, W. and Kleiner, F. (1982). World's largest ore grinder without gears, *Min. Engng.*, Sept., 1328.

Meulendyke, M.J. and Purdue, J.D. (1989). Wear of grinding media in the mineral processing industry: An overview, *Min. Metall. Proc.*, **6**, 167–171.

Metzner, G. (1993). Multivariable and optimising mill control – the South African experience, *Proc. XVIII Int. Min. Proc. Cong.*, Sydney, 293–299.

Misra A. and Finnie L. (1980). A classification of three-body abrasive wear and design of a new tester, *Wear*, **60**, 111–121.

Mokken, A.H. (1978). Progress in run-of-mine (autogenous) milling as originally introduced and subsequently developed in the gold mines of the Union Corporation Group, *Proc. 11 Commonwealth Mining and Metall. Cong.*, Hong Kong, 49.

Moller, T.K. and Brough, R. (1989). Optimizing the performance of a rubber – lined mill, *Mining Engng.*, **41**(Aug.), 849.

Moller, J. (1990). The best of two worlds – a new concept in primary grinding wear protection, *Minerals Engng.*, **3(1/2)**, 221.

Morrell, S. (1996). Power draw of wet tumbling mills and its relationship to charge dynamics, *Trans. Inst. Min. Metall.*, **105**, C43–C62.

Morrell, S. (2001). Large diameter SAG mills need large diameter ball mills – What are the issues?, *Proc. of SAG 2001 Con.*, Vancouver, Canada, Vol. III, 179.

Morrell, S. (2004). Predicting the specific energy of autogenous and semi-autogenous mills from small diameter drill core samples, *Minerals Engng.*, **17**, 447–451.

Morrell, S. and Latchireddi, S. (2000). The operation and interaction of grates and pulp lifter in autogenous and semi-autogenous mills, *Proc. of Seventh Mill Operators Conf.*, AusIMM, Kalgoorlie, Australia, 13–22.

Morrell, S. and Kojovic, T. (1996). The influence of slurry transport on the power draw of autogenous and semi-autogenous mills, *Proc. 2nd Int. Conf. on Autogenous and Semi-autogenous Grinding Technology*, Vancouver, Canada, 378.

Morrell, S. and Man, Y.T. (1997). Using modelling and simulation for the design of full scale ball mill circuits, *Minerals Engng.*, **10(12)**, 1311–1327.

Morrell, S. and Valery, W. (2001). Influence of feed size on AG/SAG mill performance, *Proc. of SAG 2001 Conf.*, Vancouver, Canada, Vol. I, 203–214.

Mosher, J. and Bigg, T. (2001). SAG mill test methodology for design and optimisation, *Proc. of SAG 2001 Conf.*, Vancouver, Canada, Vol. I, 348–361.

Moys, M.H. (1989). Slurry rheology – the key to a further advance in grinding mill control, *Proc. of SAG 1989 Conf.*, Vancouver, Canada, 713–727.

Mular, A.L. and Agar, G.E. (eds) (1989). *Advances in Autogenous and Semiautogenous Grinding Technology* (2 vols), Dept. of Mining and Mineral Process Engineering, University of British Columbia.

Mular, A.L. (1989). Automatic control of conventional and semi-autogenous grinding circuits, *CIM Bull.*, **82**(Feb.), 68.

Muller, B., Singh, A., van der Spuy, D., and Smith, V.C. (2003). Model predictive control in the minerals processing industry, *Proc. XXII Int. Min. Proc. Cong.*, Cape Town, 1692–1702.

Napier-Munn, T.J., Morrell, S., Morrison, R.D., and Kojovic, T. (1996). *Mineral Comminution Circuits: Their Operation and Optimisation*, ISBN 0 646 28861, JKMRC.

Obeng, D.P. and Morrell, S. (2003). The JK three-product cyclone – performance and potential applications, *Int. J. Min. Proc.*, **69**, 129–142.

Pax, R.A. (2001). Non-contact acoustic measurement if in-mill variables of SAG mills, *Proc. of SAG 2001 Conf.*, Vancouver, Canada, Vol. II, 386–393.

Perkins, T.E. and Marnewecke, L. (1978). Automatic grind control at Amax Lead Co., *Mining Engng.*, **30**(Feb.), 166.

Perry, R. and Anderson, L. (1996). Development of grinding circuit control at P.T. Freeport Indonesia's new SAG concentrator, *Proc. of SAG 1996 Conf.*, Vancouver, Canada, 671–699.

Powell, M.S., Morrell, S., and Latchireddi, S. (2001). Developments in the understanding of South African style SAG mills, *Minerals Engng.*, **14(10)**, 1143–1153.

Pulkkinen, K., Ylinen, R., Jamsa-Jounela, S.L., and Jarvensivu, M. (1993). Integrated expert system for grinding and flotation, *Proc. XVIII Int. Min. Proc. Cong.*, Sydney, 325–334.

Radziszewski, P. (2002). Exploring total media wear. *Minerals Engng.*, **15**, 1073–1087.

Rajagopal and Iwasaki (1992). The properties and performance of cast iron grinding media, *Min. Proc. Extra. Metall. Rev.*, **11**, 75–106.

Rao, M.K.Y. and Natarajan, K.A. (1991). Factors influencing ball wear and flotation with respect to ore grinding, *Min. Proc. Extra Metall. Rev.*, **7(3–4)**, 137.

Riezinger, F.M., Knecht, J., Patzelt, N., and Errath, R.A. (2001). How big is big – exploring today's limits of SAG and ball mill technology, *Proc. of SAG 2001 Conf.*, Vancouver, Canada, Vol. II, 25.

Rowland, C.A. (1986). Ball mill scale-up diameter factors, in *Advances in Mineral Processing.*, ed. P. Somasundaran, SME Inc., Littleton, 605.

Rowland, C.A. (1987). New developments in the selection of comminution circuits, *Engng. Min. J.* (Feb.), 34.

Rowland, C.A. (1988). Diameter factors affecting ball mill scale-up, *Int. J. Min. Proc.*, **22**(Apr.), 95.

Rowland, C.A. and Kjos, D.M. (1978). Rod and ball mills, *Mineral Processing Plant Design*, ed. A.L. Mular and R.B. Bhappu, AIMME, New York.

Rowland, C.A. and Erickson, M.T. (1984). Large ball mill scale-up factors to be studied relative to grinding efficiency, *Min. Metall. Proc.*, **1**(Aug.), 165.

Russell, A. (1989). Fine grinding – a review, *Industrial Minerals* (Apr.), 57.

Sailors, R.H. (1989). Cast high chromium media in wet grinding, *Min. and Metall. Proc.*, **6**(Nov.), 172.

Scott, A. and Morrell, S. (Co-Chairmen) (1998). Exploring the relationship between mining and mineral processing performance, *Proc. Mine to Mill Conf. 1998*, AusIMM, Brisbane.

Scott, A., Morrell, S., and Clark, D. (2002). Tracking and quantifying value from "mine to mill" improvement, *Proc. Value Tracking Symposium*, AusIMM, Brisbane, Australia, 77–84.

Schroder, A.J., Corder, G.D., and David, D.M. (2003). On-line dynamic simulation of milling operations, *Proc. Copper 2003*, Santiago, Chile, Vol III – Min. Proc., 27–44.

Shi, F. (1994). Slurry rheology and its effects on grinding, PhD Thesis, JKMRC, The University of Queensland.

Shi, F. (2002a). Investigation of the effects of chrome ball charge on slurry rheology and milling performance, *Minerals Engng.*, **15**, 297–299.

Shi, F. (2002b). The effects of hydrocyclone classification on slurry rheology and milling performance of industrial grinding circuits, *Proc. The 4th World Cong. of Particle Technology*, Paper No. 153.

Shi, F. (2004). A comparison of grinding media: Cylpebs versus balls, *Minerals Engng*. (in press).

Shi, F. and Napier-Munn, T.J. (2002). Effects of slurry rheology on industrial grinding performance, *Int. J. Min. Proc.*, **65**, 125–140.

Sloan, R., Parker, S., Craven, J., and Schaffer, M. (2001). Expert systems on SAG circuits: Three comparative case studies, *Proc. of SAG 2001 Conf.*, Vancouver, Canada, Vol. II, 346–357.

Smith, V.C., Hulbert, D.G., and Singh, A. (2001). AG/SAG control and optimization with PLANTSTAR 2000, *Proc. of SAG 2001 Conf.*, Vancouver, Canada, Vol. II, 282–293.

Starkey, J. and Dobby, G. (1996). Application of the MinnovEx SAG power index at five Canadian SAG plants, *Proc. of SAG 1996 Conf.*, Vancouver, Canada, 345–360.

Starkey, J., Robitaille, J., Cousin, P., Jordan, J., and Kosick, G. (2001). Design of the Agnico-Eagle Laronde Division SAG mill, *Proc. of SAG 2001 Conf.*, Vancouver, Canada, Vol. III, 165–178.

Steane, H.A. (1976). Coarser grind may mean lower metal recovery but higher profits, *Can. Min. J.*, **97**(May), 44.

Stief, D.E., et al. (1987). Tower mill and its application to fine grinding, *Min. Metall. Proc.*, **4**(Feb.), 45.

Taggart, A.F. (1945). *Handbook of Mineral Dressing*, Chapter 5, John Wiley & Sons Inc., New York.

Tilyard, P.A. (1986). Process developments at Bougainville Copper Ltd, *Bull. Proc. Australas. Inst. Min. Metall.*, **291**(Mar.), 33.

Timms, S.R. (1994). Investigation of semi-autogenous mill operating parameter estimation by means of TESPAR based on mill noise analysis at St. Ives Gold Mines, *Proc. Fifth Mill Operators Conference*, AusIMM, Roxby Downs, Australia, 297.

Valery, W. (1997). A model for dynamic and steady-state simulation of autogenous and semi-autogenous mills, PhD Thesis, JKMRC, The University of Queensland.

van der Spuy, D., Hulbert, D.G., Oosthuizen, D.J., and Muller, B. (2003). An online expert for minerals processing plants, *Proc. XXII Int. Min. Proc. Cong.*, Cape Town, 1594–1602.

Watson, J.L. and Morrison, S.D. (1986). Estimation of pulp viscosity and grinding mill performance by means of mill noise measurement, *Min. Metall. Proc.*, **3**(Nov.), 216.

Weller, K. and Gao, M. (1999). Ultra-fine grinding, *AJM Crushing and Grinding Conf.*, Kalgoolie, Australia.

Whiten, W.J. and Kavetsky, A. (1984). Studies on scale-up of ball mills, *Min. Metall. Proc.*, **1**(May), 23.

Wills, B.A. and Atkinson, K. (1993). Some observations on the fracture and liberation of mineral assemblies, *Minerals Engng.*, **6(7)**, 697.

Wright, P., Hayward, N., Wilkie G., and Sutherland, D. (1991). A liberation study of autogenous and SAG mills, *Proc. Fourth Mill Operators Conf.*, AusIMM, Burnie, Australia, 171–174.

Zhou, L. and Duan, Q. (2004). Application and prospect of Hanma-branded magnetic metal linings, *Comminution '04 Conf., Min. Engng.*, Perth.

Zhou, W., Zhou, L., and Duan, Q. (2003). Magnetic metal liners: 10 questions and answers, *Mining and Metall. Engng.*, **23(5)**, 93–94.

8

Industrial screening

Introduction

Industrial sizing is extensively used for size separations from 300 mm down to around 40 μm, although the efficiency decreases rapidly with fineness. Dry screening is generally limited to material above about 5 mm in size, while wet screening down to around 250 μm is common. Although there are screen types that are capable of efficient size separations down to 40 μm, sizing below 250 μm is also undertaken by classification (Chapter 9). Selection between screening and classification is influenced by the fact that finer separations demand large areas of screening surface and therefore can be expensive compared with classification for high-throughput applications.

The types of screening equipment are many and varied. Likewise, there are a wide range of screening objectives. The main purposes in the minerals industry are:

(a) *Sizing* or *Classifying*, to separate particles by size, usually to provide a downstream unit process with the particle size range suited to that unit operation;
(b) *Scalping*, to remove the coarsest size fractions in the feed material, usually so that they can be crushed or removed from the process;
(c) *Grading*, to prepare a number of products within specified size ranges. This is important in quarrying and iron ore, where the final product size is an important part of the specification;
(d) *Media recovery*, for washing magnetic media from ore in dense medium circuits;
(e) *Dewatering*, to drain free moisture from a wet sand slurry;
(f) *Desliming* or *de-dusting*, to remove fine material, generally below 0.5 mm from a wet or dry feed; and
(g) *Trash removal*, usually to remove wood fibres from a fine slurry stream.

Performance of screens

In its simplest form, the screen is a surface having many apertures, or holes, usually with uniform dimensions. Particles presented to that surface will either pass through or be retained, according to whether the particles are smaller or larger than the governing dimensions of the aperture. The efficiency of screening is determined by the degree of perfection of separation of the material into size fractions above or below the aperture size.

There has been no universally accepted method of defining screen performance and a number of methods are employed. The most common screen performance criteria are those which define an efficiency based on the recovery of material at a given size, or on the mass of misplaced material in each product. This immediately leads to a range of possibilities, such as undersize in the overscreen product, oversize in the through-screen product, or a combination of the two.

An efficiency equation can be calculated from a mass balance across a screen as follows:

Consider a screen (Figure 8.1) the feed to which is $F\,\mathrm{t\,h^{-1}}$. Two products are generated. A coarse product of $C\,\mathrm{t\,h^{-1}}$ overflows from the screen, and a fine product of $U\,\mathrm{t\,h^{-1}}$ passes through the screen.

Let f be the fraction of material above the cut point size in the feed; c be the fraction of material above the cut point size in the overflow; and u be the fraction of material above the cut point size in

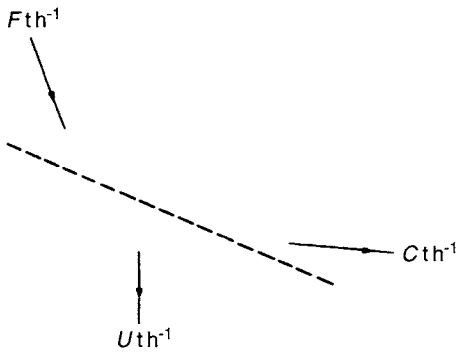


Figure 8.1 Mass balance on a screen

the underflow. f, c, and u can be determined by sieving a representative sample of each of the fractions on a laboratory screen of the same aperture size as the industrial screen and assuming this to be 100% efficient.

The mass balance on the screen is:

$$F = C + U$$

The mass balance of the oversize material is:

$$Ff = Cc + Uu$$

and the mass balance of the undersize material is:

$$F(1-f) = C(1-c) + U(1-u)$$

Hence

$$\frac{C}{F} = \frac{f-u}{c-u}$$

and

$$\frac{U}{F} = \frac{c-f}{c-u}$$

The recovery of oversize material into the screen overflow is:

$$= \frac{Cc}{Ff} = \frac{c(f-u)}{f(c-u)} \tag{8.1}$$

and the corresponding recovery of undersize material in the screen underflow is:

$$= \frac{U(1-u)}{F(1-f)} = \frac{(1-u)(c-f)}{(1-f)(c-u)} \tag{8.2}$$

These two relationships (8.1) and (8.2), measure the effectiveness of the screen in separating the coarse material from the underflow and the fine material from the overflow.

A combined effectiveness, or overall efficiency, E, is then obtained by multiplying the two equations together:

$$E = \frac{c(f-u)(1-u)(c-f)}{f(c-u)^2(1-f)} \tag{8.3}$$

For screens where the aperture and the cut point are similar (and if there are no broken or deformed apertures), the amount of coarse material in the underflow is usually very low. A simplification of Equation 8.3 can be obtained by assuming that it is, in fact, zero (i.e., $u = 0$), in which case the formula for fines recovery and that for the overall efficiency both reduce to:

$$E = \frac{c-f}{c(1-f)} \tag{8.4}$$

This formula is widely used and implies that recovery of the coarse material in the overflow is 100%.

Formulae such as the one derived are acceptable for assessing the efficiency of a screen under different conditions, operating on the *same feed.*

They do not, however, give an absolute value of the efficiency, as no allowance is made for the difficulty of the separation. A feed composed mainly of particles of a size near to that of the screen aperture – "near size" material – presents a more difficult separation than a feed composed mainly of very coarse and very fine particles with a screen aperture intermediate between them.

An *efficiency* or *partition curve* for a screen is drawn by plotting the partition coefficient, defined as the percentage of the feed reporting to the oversize product, against the geometric mean size on a logarithmic scale. (For particles in the range, say, 8.0 + 6.3 mm, the geometric mean size is $\sqrt{(8 \times 6.3)} = 7.1$ mm. Figure 8.2 shows ideal and real partition curves (see also Chapter 9).

The separation size, or *cut point*, is obtained at 50% probability, i.e. the size at which a particle has equal chance of reporting to the undersize or oversize product. The cut point is always less than the size of the largest apertures.

The efficiency of separation is assessed from the steepness of the curve (see Chapter 9). The efficiency curve effectively models the screen, and can be used for simulation and design purposes (Ferrara and Preti, 1975; Lynch and Narayanan, 1986; Napier-Munn et al., 1996).

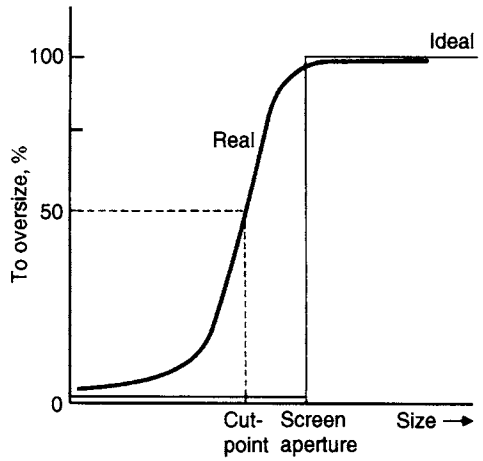


Figure 8.2 Partition curve

Factors affecting screen performance

Screen effectiveness must always be coupled with capacity as it is often possible by the use of a low feed rate and a very long screening time to effect an almost complete separation. At a given capacity, the effectiveness depends on the nature of the screening operation, i.e. on the overall chance of a particle passing through the screen once it has reached it.

The process of screening is frequently described as a series of probabilistic events, where particles are presented to a screening surface many times, and on each presentation there exists a given probability that a particle of a given size will pass. In its simplest form, the probability of passage for a single spherical particle size d passing a square aperture with a size x bordered by a wire diameter w in a single event is given by the Gaudin (1939) equation:

$$p = \left(\frac{x-d}{x+w}\right)^2 \tag{8.5}$$

or given that the fraction of open area f_o is defined as $x^2/(x+w)^2$:

$$p = f_o\left(1-\frac{d}{x}\right)^2 \tag{8.6}$$

The probability of passage for n presentations is calculated by:

$$p' = (1-p)^n \tag{8.7}$$

Screening performance is therefore affected by factors that influence the probability of particle passage, and factors that influence the number of opportunities the particles are given to pass through the screen mesh.

Particle size Taggart (1945) calculates some probabilities of passage related to the particle size using Equation 8.7, which are shown in Table 8.1. The figures relate the probable chance per thousand of unrestricted passage through a square aperture of a spherical particle and give the probable number of apertures in series in the path of the particle necessary to ensure its passage through the screen.

Table 8.1 Probability of passage

Ratio of particle to aperture size	*Chance of passage per 1000*	*Number of apertures required in path*
0.001	998	1
0.01	980	2
0.1	810	2
0.2	640	2
0.3	490	2
0.4	360	3
0.5	250	4
0.6	140	7
0.7	82	12
0.8	40	25
0.9	9.8	100
0.95	2.0	500
0.99	0.1	10^4
0.999	0.001	10^6

It can be seen from Table 8.1 that as the particle size approaches that of the aperture, the chance of passage falls off very rapidly. The overall screening efficiency is markedly reduced by the proportion of these *near-mesh* particles. The effect of near-mesh particles is compounded because these particles tend to "peg" or "plug" the apertures, reducing the available open area. This problem is often found on screens run in closed circuit with crushers, where a build-up of near-mesh material can occur and progressively reduce screening efficiency.

Feed rate The principle of sieve sizing analysis is to use a low feed rate and a very long screening time to effect an almost complete separation. In industrial screening practice, economics dictate that relatively high feed rates and short particle dwell

times on the screen should be used. At these high feed rates, a thick bed of material is presented to the screen, and fines must travel to the bottom of the particle bed before they have an opportunity to pass through the screen surface. The net effect is reduced efficiency. High capacity and high efficiency are often opposing requirements for any given separation, and a compromise is necessary to achieve the optimum result.

Screen angle The Gaudin Equation (8.6) assumes that the particle approaches the aperture perpendicular to the aperture. If a particle approaches the aperture at a shallow angle, it will "see" a narrower effective aperture dimension and near-mesh particles are less likely to pass. The slope of the screening surface affects the angle at which particles are presented to the screen apertures. Some screens utilise this effect to achieve separations significantly finer than the screen aperture. For example, sieve bends cut at approximately half the aperture size. Where screening efficiency is important, horizontal screens are selected.

The screen angle also affects the speed at which particles are conveyed along the screen, and therefore the dwell time on the screen and the number of opportunities particles have of passing the screen surface.

Particle shape Most granular materials processed on screens are non-spherical. While spherical particles pass with equal probability in any orientation, irregular-shaped near-mesh particles must orient themselves in an attitude that permits them to pass. Elongated and slabby particles will present a small cross-section for passage in some orientations and a large cross-section in others. The extreme particle shapes therefore have a low screening efficiency. Mica, for instance, screens poorly on square aperture screens, its flat, plate-like crystals tending to "ride" over the screen apertures.

Open area The chance of passing through the aperture is proportional to the percentage of *open area* in the screen material, which is defined as the ratio of the net area of the apertures to the whole area of the screening surface. The smaller the area occupied by the screen deck construction material, the greater the chance of a particle reaching an aperture.

Open area generally decreases with the fineness of the screen aperture. In order to increase the open area of a fine screen, very thin and fragile wires or deck construction must be used. This fragility and the low throughput capacity are the main reasons for classifiers replacing screens at fine aperture sizes.

Vibration Screens are vibrated in order to throw particles off the screening surface so that they can again be presented to the screen, and to convey the particles along the screen. The right type of vibration also induces stratification of the feed material (Figure 8.3), which allows the fines to work through the layer of particles to the screen surface while causing larger particles to rise to the top. Stratification tends to increase the rate of passage in the middle section of the screen (Soldinger, 1999).

The vibration must be sufficient to prevent pegging and blinding. However, excessive vibration intensity will cause particles to bounce from the screen deck and be thrown so far from the surface that there are very few effective presentations to the screen surface. Higher vibration rates can, in general, be used with higher feed rates, as the deeper bed of material has a "cushioning" effect which inhibits particle bounce.

Vibration can be characterised by the vibration frequency, f cycles per second, and amplitude, a metres. The term "stroke" is commonly used and refers to the peak-to-peak amplitude, or $2a$. Generally, screening at larger apertures is performed using larger amplitudes and lower frequencies; whereas for fine apertures, small amplitudes and high frequencies are preferred. The intensity of vibration is defined by the vibration g-force, Γ:

$$\Gamma = \frac{a(2\pi f)^2}{9.81} \tag{8.8}$$

Vibrating screens typically operate with a vibration force of between 3 and 7 times the gravitational acceleration, or 3G–7G. Vibrations are induced by mechanical exciters driven by electric motors or electrical solenoids in the case of high frequency screens. The power required is small compared to other unit operations within the concentrator, and is approximately proportional to the loaded mass of the screen.

Moisture The amount of surface moisture present in the feed has a marked effect on screening efficiency, as does the presence of clays and other

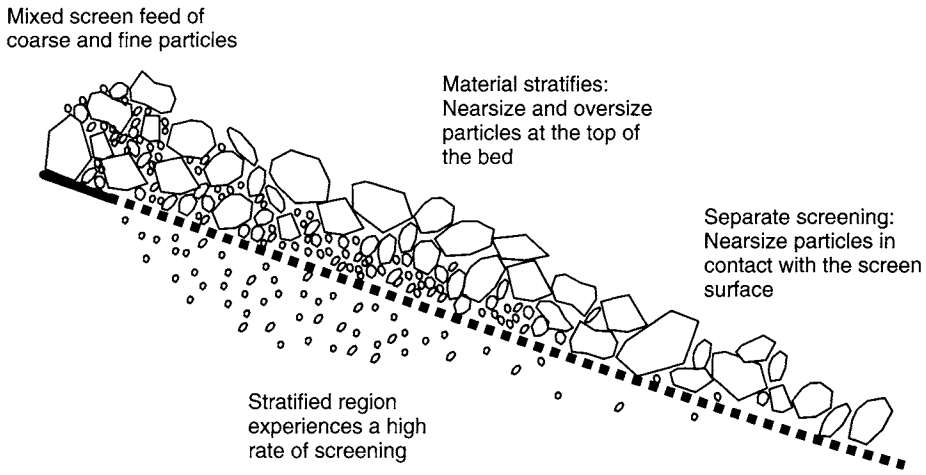


Figure 8.3 Stratification of particles on a screen (Courtesy JKMRC and JKTech Pty Ltd)

sticky materials. Damp feeds screen very poorly as they tend to agglomerate and "blind" the screen apertures. As a rule of thumb, screening at less than around 5 mm aperture size must be performed on perfectly dry or wet material, unless special measures are taken to prevent blinding. These measures may include using heated decks to break the surface tension of water between the screen wire and particles, ball-decks (a wire cage containing balls directly below the screening surface) to impart additional vibration to the underside of the screen cloth, or the use of non-blinding screen cloth weaves.

Wet screening allows finer sizes to be processed efficiently down to 250 μm and finer. Adherent fines are washed off large particles, and the screen is cleaned by the flow of pulp and additional water sprays.

Mathematical models of screens

Screen models aim to predict the size distribution and flow of the screen products. Models in the literature can be classified as:

(1) phenomenological models that incorporate a theory of the screening process;
(2) empirical models based on empirical data; and
(3) numerical models based on computer solutions of Newtonian mechanics.

Phenomenological models Phenomenological models are based on the theory of particle passage through a screening surface. The two dominant theories are *probabilistic*, treating the process as a series of probabilistic events, and *kinetic*, treating the process as one or more kinetic rate processes.

The model by Whiten (1972) extends the theory developed by Gaudin (Equation 8.6) to develop an efficiency curve model containing a single model parameter.

The model by Ferrara and Preti (1975) describes rate of passage through the screen as a function of the screen length. They proposed a zero-order rate of passage for the heavily loaded section of the screen, followed by a first-order rate governing the passage of particles in the lightly loaded section of the process.

Both of these models have been used extensively to model industrial screening data.

Empirical models *Empirical* or *capacity* models aim to predict the required area of screen and are frequently used by screen manufacturers. There are a number of different formulations of these models. Most aim to predict the quantity of undersize that can pass through the screen.

$$\text{Theoretical area required} = \frac{\text{Total t/h undersize in feed}}{C \times F_1 \times F_2 \times F_3 \times \cdots \times F_n}$$

where

C = Base-line screen capacity in t/h of undersize per unit area.

F_1 to F_n are correction factors.

Common correction factors include corrections for the quantity of oversize (material larger than the aperture), half-size (material less than half the aperture size), and near-size (material between 75 and 125% of the aperture size; the density of material being screened; whether the screen is a top deck or a lower deck on a multi-deck screen; the open area of the screen cloth; whether square or slotted apertures are used; whether wet-screening is employed; and the desired screening efficiency.

The values of the base-line capacity and for each of the factors are given in the form of tables or charts. Karra (1979) has converted these data into equation form so that they can be implemented in a spreadsheet.

While these capacity-based calculations are popular, they should be treated as a guide only (Olsen and Coombe, 2003). They have been developed for a specific type of screen: inclined circular stroke vibrating screens using standard wire-mesh screen cloth. Because there are many other variables and many other screen types and screening surfaces in use, accurate screen selection for a particular application is best done by seeking advice from reputable equipment suppliers together with pilot-scale testing.

Numerical models Numerical computer simulations are being increasingly used to model the behaviour of particles in various processing equipment including screens (Cleary, 2003); see Figure 8.4. It is expected that numerical simulation techniques such as the Discrete Element Method (DEM) will gain wider application in the modelling of industrial screens, and assist in the design and optimisation of new screening machines.

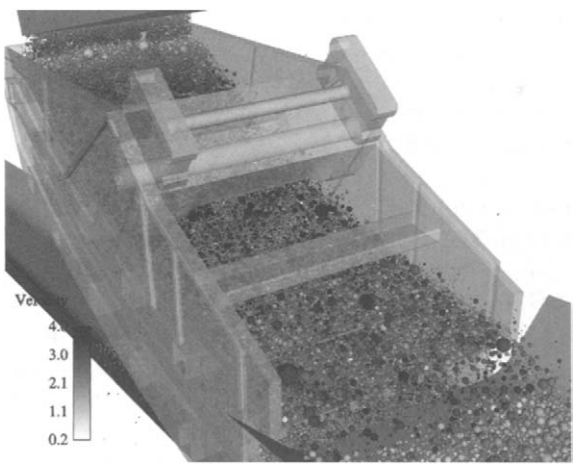


Figure 8.4 Screen simulated with DEM (Courtesy CSIRO (Dr. Paul Cleary))

Screen types

There are numerous different types of industrial screens available. The dominant screen type in industrial applications is the vibrating screen, of which there are many sub-types in use for coarse and fine-screening applications. There are also numerous other screen types in wide use for both coarse and fine screening applications.

Vibrating screens

Vibrating screens are the most important and versatile screening machines for mineral processing applications (Crissman, 1986). The success of the vibrating screen has made many older screen types obsolete in the minerals industry including shaking and reciprocating screens, details of which can be found in Taggart (1945). Vibrating screens have a rectangular screening surface with feed and oversize discharge at opposite ends. They perform size separations from 300 mm in size down to 45 μm and they are used in a variety of sizing, grading, scalping, dewatering, wet screening, and washing applications.

Vibrating screens of most types can be manufactured with more than one screening deck. On multiple-deck systems, the feed is introduced to the top coarse screen; the undersize falling through to the lower screen decks, thus producing a range of sized fractions from a single screen.

Inclined screens Inclined or circular motion screens (Figure 8.5) are widely used as sizing screens. A vertical circular or elliptical vibration is induced mechanically by the rotation of unbalanced weights or flywheels attached usually to a single drive shaft (see Box 8.1). The amplitude of throw can be adjusted by adding or removing weight elements bolted to the flywheels. The rotation direction can be contra-flow or in-flow. Contra-flow slows the material more and permits more efficient separation, whereas in-flow permits a greater throughput. Single-shaft screens must be installed on a slope, usually between 15° and 28°, to permit flow of material along the screen.

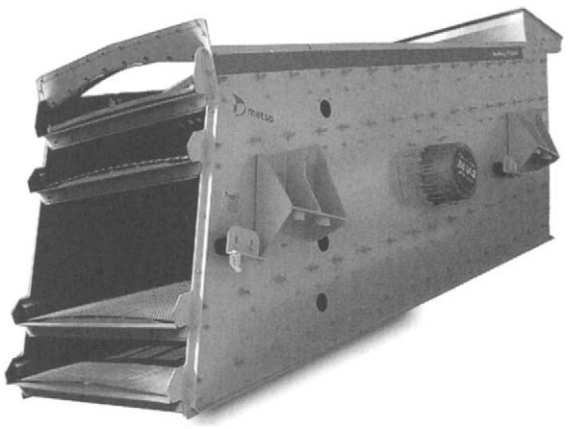


Figure 8.5 Inclined four-deck vibrating screen (Courtesy Metso Minerals)

Grizzly screens Very coarse material is usually screened on an inclined screen called a grizzly screen. Grizzlies are characterised by parallel steel bars or rails (Figure 8.7) set at a fixed distance apart and installed in line with the flow of ore. The gap between grizzly bars is usually greater than 50 mm and can be as large as 300 mm, with feed topsize as large as 1 m. Vibrating grizzlies are usually inclined at an angle of around 20° and have a circular-throw mechanism (see Box 8.1). The capacity of the largest machines exceeds 5000 $t\,h^{-1}$.

The most common use of grizzlies in mineral processing is for sizing the feed to primary and secondary crushers. If a crusher has a 100 mm setting, then feed can be passed over a grizzly with a 100 mm gap in order to reduce the load on the crusher.

The bars are typically made from wear-resistant manganese steel, and are usually tapered to create gaps that become wider towards the discharge end of the screen to prevent rocks from wedging between the bars. Domed or peaked profiles on the tops of the bars give added wear protection and prevent undersized rocks from "riding" along the bars and being misplaced.

Horizontal screens Horizontal, low-head or *linear vibrating screens* (Figure 8.8) have a horizontal or near-horizontal screening surface, and therefore need less headroom than inclined screens. Horizontal screens must be vibrated with a linear or an elliptical vibration produced by a double or triple-shaft vibrator (see Box 8.1). The accuracy of particle sizing on horizontal screens is superior to that on inclined screens; however because gravity does not assist the transport of material along the screen they have lower capacity than inclined screens (Krause, 2005). Horizontal screens are used in sizing applications where screening efficiency is critical, and in drain-and-rinse screens in heavy medium circuits.

Resonance screens are a type of horizontal screen consisting of a screen frame connected by rubber buffers to a dynamically balanced frame having a natural resonance frequency which is the same as that of the vibrating screen body. The vibration energy imparted to the screen frame is stored up in the balancing frame, and re-imparted to the screen frame on the return stroke. The energy losses are reduced to a minimum, and the sharp return motion produced by the resonant action imparts a lively action to the deck and promotes good screening.

Dewatering screens are a type of vibrating screen that are fed a thick slurry and produce a drained sand product. Dewatering screens are often installed with a slight up-hill incline to ensure that water does not flow over with the product. A thick bed of particles forms, trapping particles finer than the screen aperture.

Banana screens Banana or *Multi-slope* screens have become widely used in high-tonnage sizing applications where both efficiency and capacity are important. Banana screens (Figure 8.9) typically have a variable slope of around 40–30° at the feed end of the screen, reducing to around 0–15° in increments of 3.5–5° (Beerkircher, 1997). Banana screens are usually designed with a linear-stroke vibrator (see Box 8.1).

The steep sections of the screen cause the feed material to flow rapidly at the feed end of the screen. The resulting thin bed of particles stratifies more quickly and therefore has a faster screening rate for the very fine material than would be possible on a slower moving thick bed. Towards the discharge end of the screen, the slope decreases to slow down the remaining material, enabling more efficient screening of the near-size material. The capacity of banana screens is significantly greater and is reported to be up to three or four times that of conventional vibrating screens (Meinel, 1998).

Box 8.1: Screen vibration

Circular motion (Single-shaft) screens. When the shaft of an inclined screen is located precisely at the screen's centre of gravity, the entire screen body vibrates with a circular vibration pattern (Figure 8.6a). Occasionally, the shaft is installed above or below the centre of gravity as in the system shown in Figure 8.6b. This placement results in an elliptical motion, slanting forward at the feed end; a circular motion at the centre; and an elliptical motion, slanting backwards at the discharge end. Forward motion at the feed end serves to move oversize material rapidly out of the feed zone to keep the bed as thin as possible. This action facilitates passage of fines which should be completely removed in the first one-third of the screen length. As the oversize bed thins down, near the centre of the screen, the motion gradually changes to the circular pattern to slow down the rate of travel of the solids. At the discharge end, the oversize and remaining near-size materials are subjected to the increasingly retarding effect of the backward elliptical motion. This allows the near-size material more time to find openings in the screen cloth.

Linear-vibration (Double-shaft) screens. A linear vibration is induced by using mechanical exciters containing matched unbalanced weights rotating in opposite directions on two shafts as shown in Figure 8.6c. Linear stroke screens can be installed on a slope, horizontally or even on a small up-hill incline. The angle of stroke is typically between 30 and 60° to the screen deck. Linear-vibration exciters are used on horizontal screens and banana screens.

Oval motion (Triple-shaft) screens. A three-shaft exciter design can be used to generate an elliptical vibratory motion as shown in Figure 8.6d, which can also be used on horizontal and banana screens. The three shafts are connected by gears and one of the shafts is driven. The elliptical motion is claimed to offer the efficiency benefit of a linear vibrating screen with the tumbling action of a circular motion screen. Higher capacities and increased efficiencies are claimed over either linear or circular motion machines.

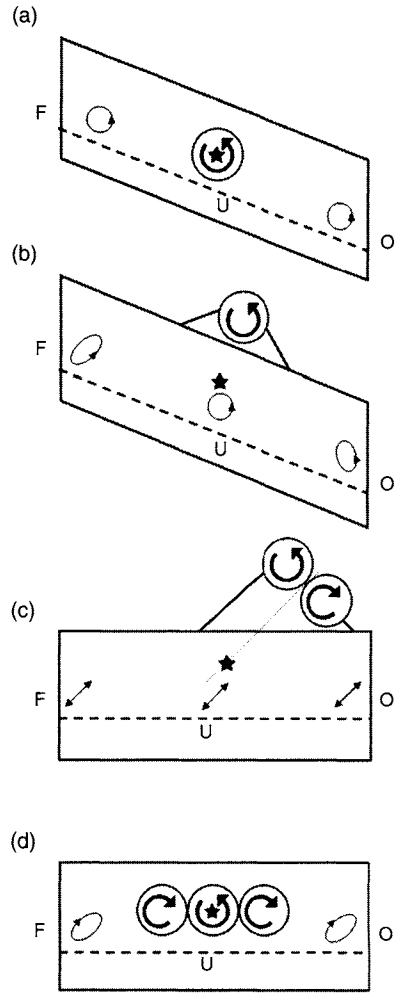


Figure 8.6 Vibration patterns generated by various exciter designs. The star represents the location of the screen's centre of gravity (Courtesy JKMRC and JKTech Pty Ltd)

Modular screens such as the *OmniScreen* (Figure 8.10), consist of two or more independent screen modules arranged in series, effectively making a large screen from a number of smaller units. A key advantage of this arrangement is that each screen module can be separately configured with a unique screen slope, screen surface type, vibration stroke, and frequency. This allows screening performance to be optimised separately on different sections of the screen. The individual

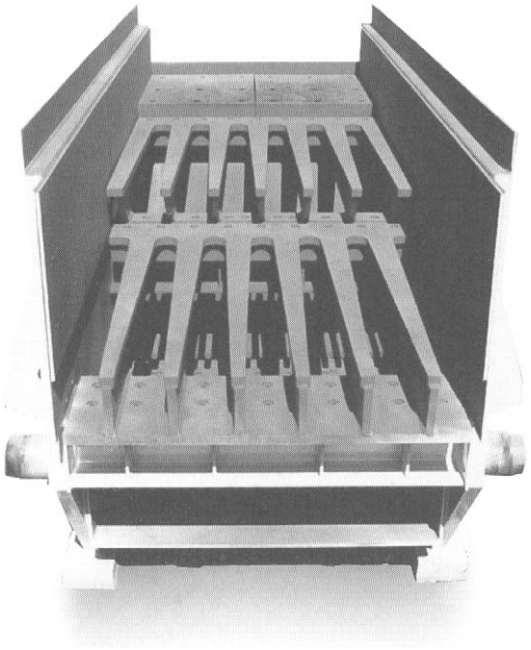


Figure 8.7 Vibrating grizzly screen (Courtesy Metso Minerals)

screen sections being smaller and lighter are mechanically more robust compared with a single screen with an equivalent total size. Modular screens are frequently installed in a multi-slope configuration.

Mogensen sizers The *Mogensen Sizer* is a vibrating screen that uses the principle that particles smaller than the aperture statistically require a certain number of presentations to the screen in order to pass (refer to Table 8.1). The Mogensen Sizer (Figure 8.11) consists of a system of oscillating and sloping screens of decreasing aperture size, the smallest of which has a mesh size up to twice the size of the desired separation size (Hansen, 2000). This arrangement allows particles very much finer than the screens to pass through quickly, but causing larger particles to be rejected by one of the screen surfaces.

A thin layer of particles on each screen surface is maintained, enabling high capacity such that a particular screening duty can be met with a machine occupying less floor space than a conventional screen, and blinding and wear are reduced.

The *Mogensen 2000 Sizer* is a similar device designed for fine separations, incorporating direct rapping of the screen mesh rather than vibration of the entire unit.

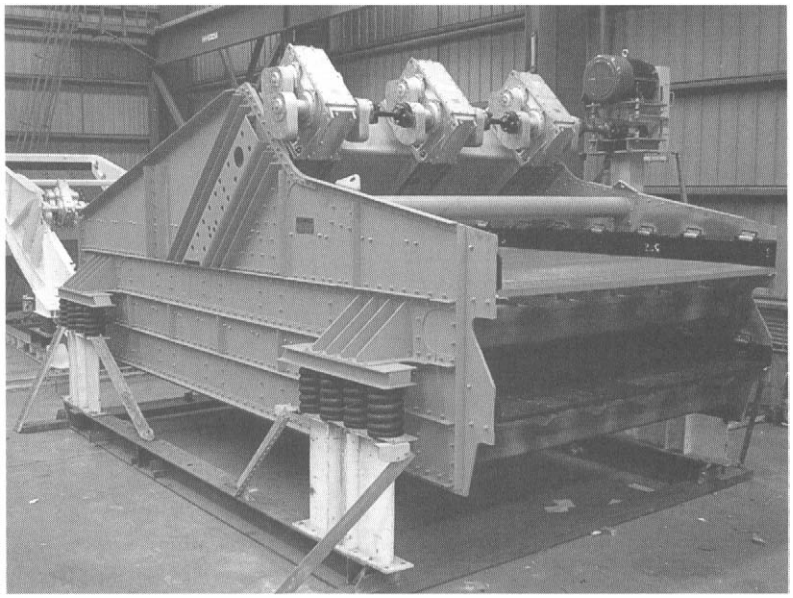


Figure 8.8 Horizontal screen (Courtesy Schenk Australia)

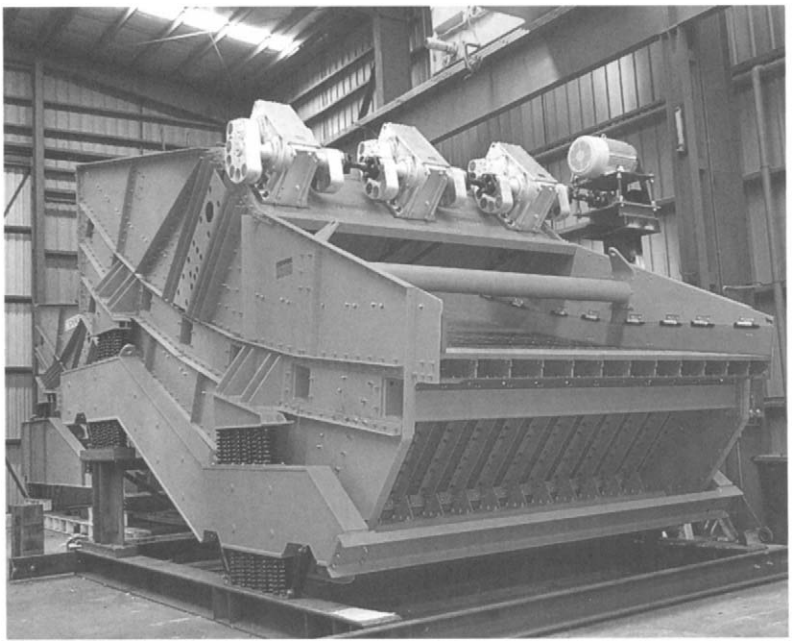


Figure 8.9 Banana screen (Courtesy Schenk Australia)



Figure 8.10 Omni screen (Courtesy Omni Crushing and Screening)

High frequency screens Efficient screening of fine particles requires a vibration with small amplitude and high frequency. Frequencies up to 3600 rpm are used to separate down to 100 microns compared with vibrating screens for coarser applications that are vibrated at around 700–1200 rpm. The vibration of the screening surface can be created by electric motors or with electrical solenoids. In the case of the *Tyler H-series* (or *Hum-mer*) screen, the vibrators are mounted above

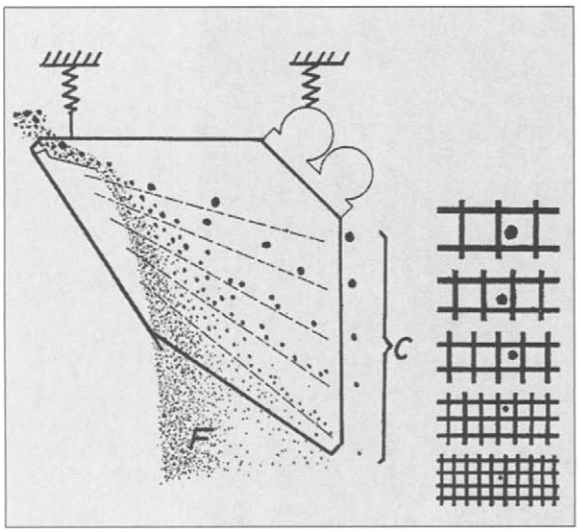


Figure 8.11 Mogensen sizer separting into coarse C and fines F (from Hansen, 2000)

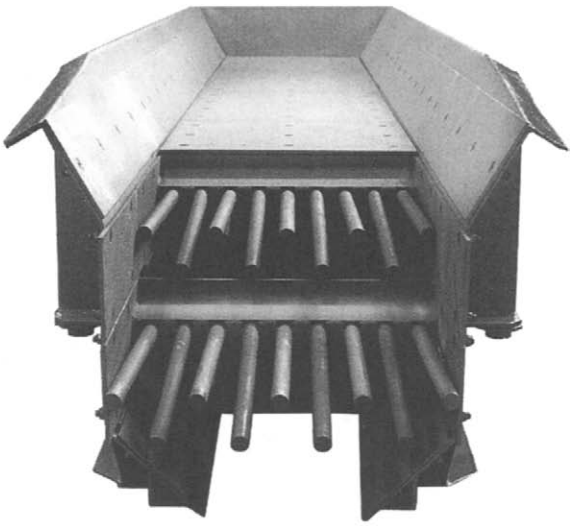


Figure 8.12 Self-cleaning grizzly attached to a feeder (Courtesy Metso Minerals)

and connected by rods directly to the screening surface so that energy is not wasted in vibrating the entire screen body.

High-frequency wet screens such as the *Derrick repulp screen* permit screening down to 45 microns. Screening efficiency decreases rapidly once the free water has passed through the screen, therefore these screens incorporate water-sprays to periodically re-pulp the screen oversize to ensure good washing.

Other screen types

Static screens *Static grizzlies* with no vibration mechanism are used in scalping applications. They are installed at a slope of 35–50° to assist material flow (Taggart, 1945). Static grizzlies are less efficient than their vibrating counterparts and are usually used in scalping applications when the proportion of oversize material in the feed is small.

Mogensen divergators and self-cleaning grizzly screens (Figure 8.12) use round bars in two rows – alternate bars at different angles, and fixed at one end to prevent the possibility of blinding. Divergators are used for coarse separations between 25 and 400 mm. Divergators are used in grizzly scalping duties and in chutes to direct the fine material onto the conveyor first to cushion the impact from coarser lumps.

Trommels One of the oldest screening devices is the trommel or revolving screen, which is a cylindrical screen (Figure 8.13) typically rotating at between 35 and 45% critical speed. Trommels are installed on a small angle to the horizontal or use a series of internal baffles to transport material along the cylinder. Trommels can be made to deliver several sized products by using trommel screens in series from finest to coarsest such as the one shown; or using concentric trommels with the coarsest mesh being innermost. Trommels can handle material from 55 mm down to 6 mm, and even smaller sizes can be handled under wet screening conditions. Although trommels are cheaper, vibration-free, and mechanically robust; they typically have lower capacities than vibrating screens since only part of the screen surface is in use at any one time, and they can be more prone to blinding.

Trommels remain widely used in some screening duties including aggregate screening plants and the screening of mill discharge streams. AG, SAG, and ball mill discharge streams usually pass through a trommel screen attached to the mill outlet to prevent ball scats from reaching subsequent processing equipment and to prevent a build-up of pebbles in the mill. Trommels are also used for wet-scrubbing ores such as bauxite.

The *Rotaspiral*, introduced in 2001 by Particle Separation Systems, is a trommel-like device designed for ultra-fine screening between 1000 and

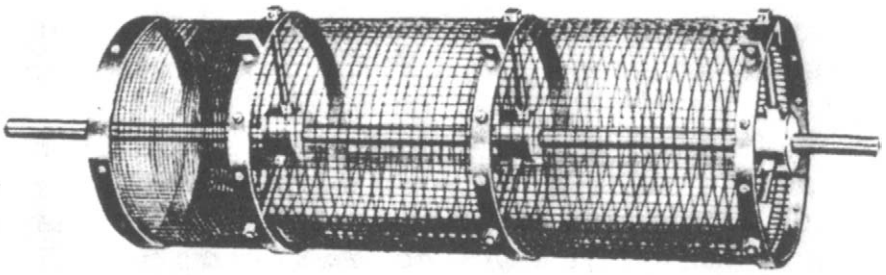


Figure 8.13 Trommel screen

75 microns. The drum contains an internal spiral to move the material through the screen. Water sprays are used to fluidise the screen bed and wash the screen surface. The Rotaspiral can also be used in a dewatering duty.

The *Bradford Breaker* (Figure 8.14) is a variation of the trommel screen used in the coal industry. It serves a dual function of breaking coal, usually to between −75 and −100 mm, and separating the harder shale, rock tramp metal, and wood contaminants into the oversize. Bradford breakers are operated at between 60 and −70% critical speed.

Roller screen Roller screens can be used for screening applications from 3 to 300 mm (Clifford, 1999). Roller screens (Figure 8.15) use a series of parallel driven rolls (circular, elliptical, or profiled) or discs to transport oversize across the series of rolls while allowing fines to fall through the gaps between rolls or discs. Roller screens offer advantages of high capacity, low noise levels, require little head-room, subject the material to less impact, and permit screening of very sticky materials.

Flip-flow screen The concept used in the Liwell "Flip-flow" screens and also Binder "Bivi-TEC", IFE "Trisomat" and Jöst "Trampolin", is a system of flexible screen panels that are alternately stretched and relaxed to impart motion to the screen bed instead of relying only on mechanical vibration of the screen body. The throwing action can generate forces of up to 50 G on the screen surface, preventing material from blinding in the apertures. The screen body may be static or subjected to accelerations in the range 2–4 G (Kingsford, 1991).

Flip-flow screens can be used for separations ranging from 0.5 up to 50 mm and for feed rates up to 800 $t\,h^{-1}$. Flip-flow screens are particularly suited for fine separations of damp material that cannot be screened efficiently on conventional vibrating screens (Meinel, 1998).

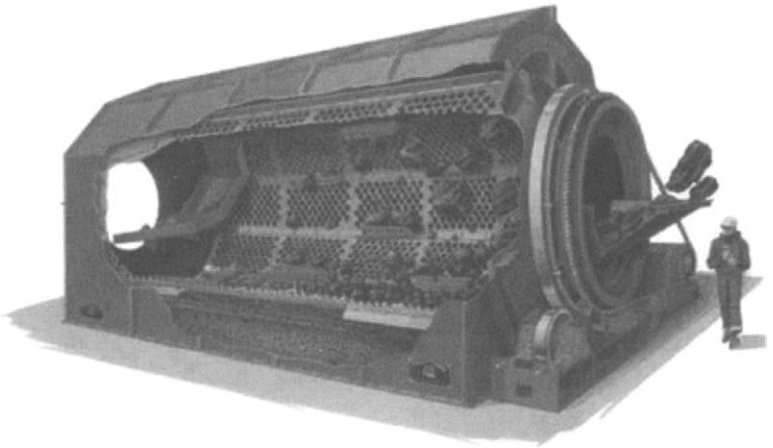


Figure 8.14 Bradford breaker (Courtesy Pennsylvania Crusher)

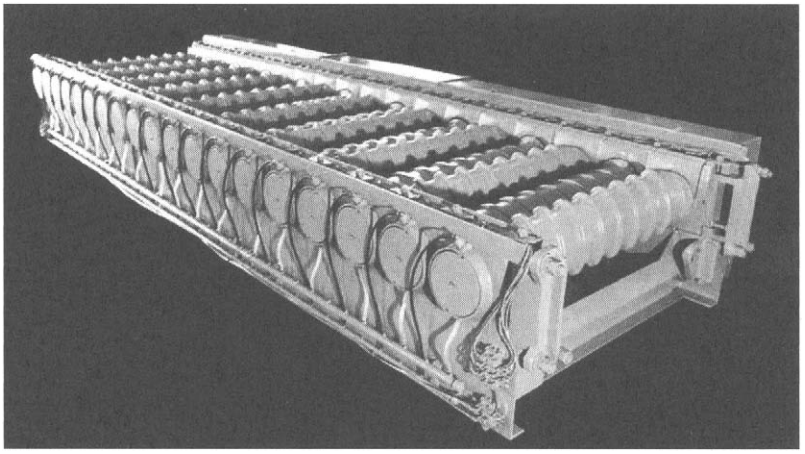


Figure 8.15 Roller screen (Courtesy Metso Minerals)

Circular screens Circular, Gyratory, or *Tumbler* screens (Figure 8.16) impart a combined gyratory and vertical motion. They are widely used for fine-screening applications, wet or dry, down to 40 μm. The basic components consist of a nest of sieves up to around 2.7 m in diameter supported on a table which is mounted on springs on a base, suspended from beneath the table is a motor with double-shaft extensions, which drives eccentric weights and in doing so effects horizontal gyratory motion. Vertical motion is imparted by the bottom weights, which swing the mobile mass about its centre of gravity, producing a circular tipping motion to the screen, the top weights producing the horizontal gyratory motion. Ball trays and ultrasonic devices may be fitted below the screen surfaces to reduce blinding. Circular screens are often configured to produce multiple size fractions.

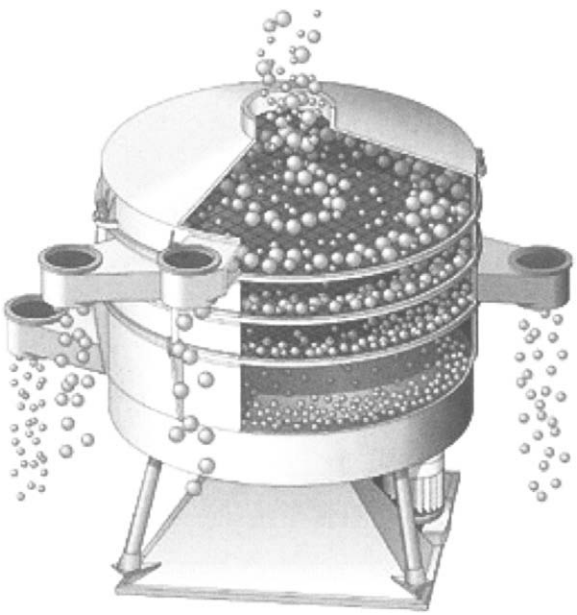


Figure 8.16 Gyratory screen

Sieve bend screens Wedge or profile wire or slotted polyurethane panels are used in *sieve bends* and *inclined flat screens* for dewatering and very fine screening applications. The sieve bend has a curved screen composed of horizontal wedge bars, whereas flat screens are installed on a slope of between 45 and 60°. Feed slurry enters the upper surface of the screen tangentially and flows down the surface in a direction perpendicular to the openings between the wedge bars. As the stream of slurry passes each opening a thin layer is peeled off and directed to the underside of the screen. According to Fontein (1954), particles roughly twice the thickness of this layer are dragged along with the undersize fraction; particles larger than this size pass across the openings as their greatest part projects into the liquid flowing over the slot. In general, therefore, a separation is produced at a size roughly equivalent to half the bar spacing and so very little plugging of the apertures should take place. Separation can be undertaken down to 50 μm and screen capacities are up to $180\,m^3\,h^{-1}$.

One of the most important applications for sieve bends is in draining water from the feed to drain and

rinse screens in dense medium separation circuits. When treating abrasive materials sieve bends will require regular reversal of the screen surface as the leading edge of the apertures will lose their sharpness over time.

Sieve bends and inclined wedge-wire screens are sometimes installed with mechanical devices to periodically vibrate or rap the screen surface in order to removed blinded particles.

Linear screen The linear screen developed by Delkor is predominantly used for removing wood chips and fibre from the ore stream feeding carbon-in-pulp systems, and for the recovery of loaded carbon in gold CIP circuits (Anon., 1986). The machine (Figure 8.17) comprises a synthetic monofilament screen cloth supported on rollers and driven by a head pulley coupled to a variable speed drive unit. Mesh sizes in use are typically around 500 microns. Dilute slurry enters through a distributor on to the moving cloth. The undersize drains through the cloth by gravity and is collected in the underpan. The oversize material retained on the screen is discharged at the drive pulley, and any adhering material is washed from the screen cloth using water sprays.

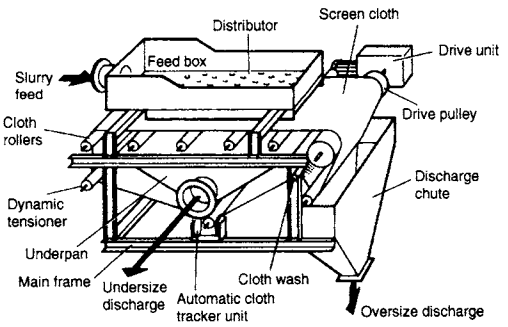


Figure 8.17 Linear screen (Courtesy Delkor)

As the screen is not vibrated, linear screens are quiet and the energy consumption is much less than that required for vibrating screens.

Pansep screen The Pansep screen (Figure 8.18) has a similar principle to the linear screen but rather than a continuous screen surface, the deck is divided into a series of pans that move in a manner similar to a conveyor. The base of each pan consists of a tensioned wire screen mesh permitting finer cut points than on linear screens. Cut points in the range 45–600 μm are possible.

Screening occurs both on the top of the "conveyor" motion and on the bottom giving high screening capacity for the occupied area as well as providing a cleaning action of the screen deck by continually reversing the screening direction (Buisman, 2000). Panels are washed twice each rotation.

Pansep screens are able to create a significantly sharper size separation than hydrocyclones (Mohanty, 2003). As screens do not have density effects as do hydraulic classifiers, Pansep screens can be used to separate coarse material from hydrocyclone overflow in grinding circuits to increase recovery, or to recover low-ash coal from desliming cyclones.

Screening surfaces

There are many types of screening surface available for industrial vibrating screens. The selection of screening surface for a particular duty will depend on the aperture required and the nature of the work. The selection of the size and shape of the apertures, the proportion of open area, the material properties of the screening surface, and flexibility of the screen surface can be critical to the performance of a screening machine.

Screening surfaces are usually manufactured from steel, rubber, or polyurethane, and can be classified according to how they are fixed to the screen. Bolt-in, tensioned, and modular fixing systems are used on industrial screens.

Bolt-in screening surfaces Screening surfaces for screening duties with particles larger than around 50 mm frequently consist of large sheets of punched, laser-cut, or plasma-cut steel plate, often sandwiched with a polyurethane or rubber wear surface to maximise wear life. These sheets are rigid and are bolted to the screen (Figure 8.19). Curved sections of screens of this type are also commonly used on trommels.

These screening surfaces are available with custom-designed aperture shapes and sizes. Apertures usually have a tapered profile, becoming wider with depth, thereby reducing the propensity of particles pegging in the aperture.

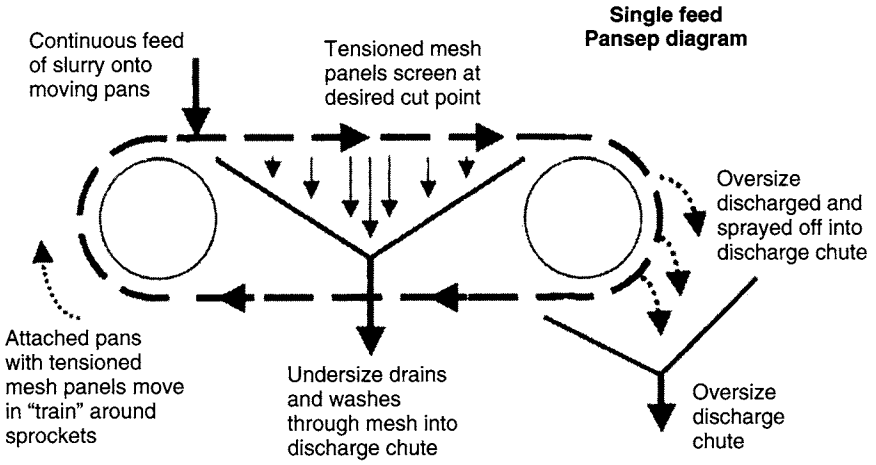


Figure 8.18 Principle of the Pansep screen (from Buismann, 2000)

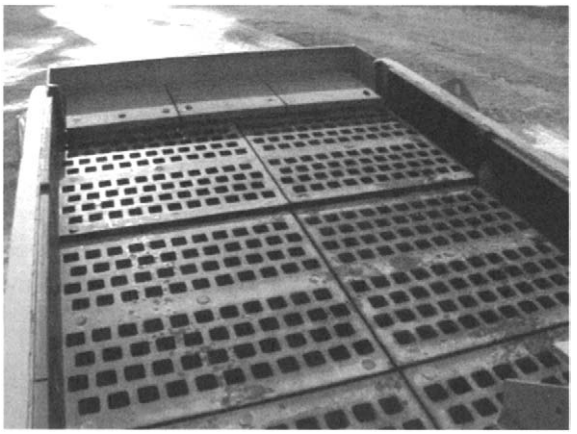


Figure 8.19 Bolt-in screening surface

Tensioned screening surfaces Tensioned screen surfaces consist of cloths that are stretched taut, either between the sides of the screen (cross tensioned) or along the length of the screen (end tensioned). Maintaining the correct tension in the screen cloth is essential to ensure screening efficiency and to prevent premature failure of the screening surface. Tensioned screens are available in various wire weaves as well as polyurethane and rubber mats.

Traditional *woven-wire cloth*, usually constructed from steel or stainless steel, remains popular. Wire cloths are the cheapest screening surfaces, have a high open area, and are comparatively light. The high open area generally allows a screen to be smaller than a screen with modular panels for the same capacity duty. In relatively light screening duties, therefore, wire-tensioned screens are often preferred. Increasing the wire thickness increases their strength, but decreases open area and hence capacity.

Various types of square and rectangular weaves are available. Rectangular screen apertures have a greater open area than square-mesh screens of the same wire diameter. The wire diameter chosen depends on the nature of the work and the capacity required. Fine screens can have the same or greater open areas than coarse screens, but the wires used must be thinner and hence more fragile.

"Self-cleaning" wire Traditionally, blinding problems have been countered by using wire with long-slotted apertures or no cross-wires at all (piano-wire) but at the cost of lower screening efficiency. Self-cleaning wire (Figure 8.20) is a variation on this, having wires that are crimped to form "apertures" but individual wires are free to vibrate and therefore have a high resistance to blinding and pegging. Screening accuracy can be close to that of conventional woven wire mesh; and they have a longer wear life, justifying their higher initial cost. There are three main types of self-cleaning weave: diamond, triangle, and wave or zig-zag shaped apertures. The triangle and diamond weaves give a more efficient separation.

Tensioned rubber and polyurethane mats that can be interchanged with tensioned wire cloths

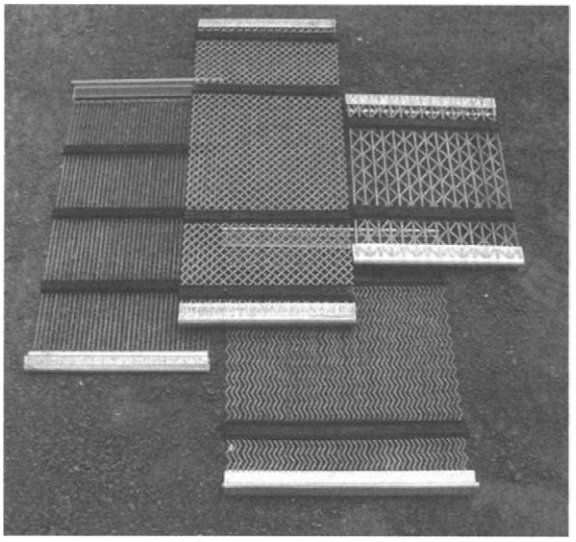


Figure 8.20 Various types of self-cleaning wire mesh

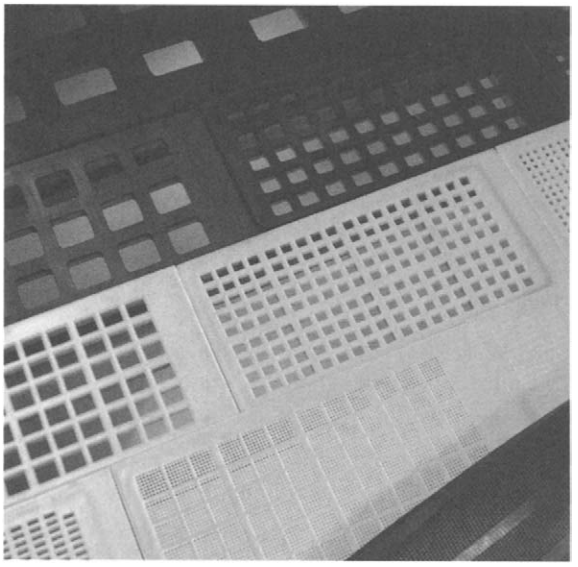


Figure 8.21 Modular screen panels (Courtesy Metso Minerals)

are also available. These mats are usually reinforced with internal steel cables or synthetic cords. Rubber and polyurethane can have significantly longer wear life than steel, although the open area is generally lower than wire. Aggregate producers prefer tensioned media because they must be able to make frequent deck changes to produce different specifications, and tensioned media are quicker to replace than modular screening systems.

Modular screening surfaces The most popular screening surfaces in harsh screening duties are polyurethane and rubber screen decks (Figure 8.21), usually assembled in modules or panels that are fixed onto a sub-frame. Both materials offer exceptional resistance to abrasion. Rubber also has excellent impact resistance; therefore rubber is often used in applications where top size can be greater than around 2″ (50 mm). Polyurethane is generally preferred in wet screening applications.

Modular polyurethane and rubber screen panels are typically 1″ × 1″ (305 × 305 mm), 2″ × 1″ (610 × 305 mm) or similar in size. The edges of the panel typically contain a rigid steel internal frame to give the panel strength. Panel systems allow for rapid replacement of the deck. Different panel types and aperture sizes can be installed at different positions along the screen to address high wear areas and to optimise any given screening task.

The major advantage of modular polyurethane panels is the exceptional wear resistance in most applications; often 10 times the wear life is reported over traditional wire cloth. Modular screens do not require tensioning and re-tensioning and damaged sections of the screen can be replaced *in situ*. Polyurethane and rubber screens are also quieter and the more flexible apertures reduce blinding compared with steel wire cloths.

Square, rectangular, and slot apertures are the most commonly used aperture shapes. Rectangular and slot apertures can be in-flow (usual for sizing applications), cross-flow orientations (usual for dewatering applications), or diagonal. Rectangular and slot apertures provide greater open area, throughput, resistance to pegging and efficiency with slabby particles compared with square apertures. Other aperture shapes include circles, hexagons, octagons, rhomboids, and tear-drops. Combinations of shapes and configurations are also possible. Circular apertures are considered to give the most accurate cut, but are more prone to pegging. Slotted, tear-drop, and more complex aperture shapes are used where blinding or pegging can be a problem. Apertures are tapered, being wider at the bottom than the top, to ensure that a particle that has passed through the aperture at the deck surface can fall freely to undersize.

Modular wire and *wedge wire panels* are also available. These have much greater open area compared with modular polyurethane screens. These wire panels consist of a polyurethane or rubber fixing system moulded around a woven-wire or wedge-wire screening surface.

References

Anon. (1986). New linear screen offers wide applications, *Engng. Min. J.*, **187**(Sept.), 79.

Beerkircher, G., (1997). Banana screen technology, *Comminution Practices*, ed. S.K. Kawatra, SME, 37–40.

Buisman, R. (2000). *Fine Coal Screening Using the New Pansep Screen.*

Chalk, P.H. (1974). Screening on inclined decks, *Processing*, Oct., 6.

Cleary, P.W. (2003). DEM as a tool for design and optimisation of mineral processing equipment, *Proc. XXII IMPC*, 1648–1657.

Clifford, D. (1999). Screening for profit, *Mining Mag.*, **180(5)**, May, 236–248.

Crissman, H.(1986). Vibrating screen selection, *Pit and Quarry*, **78**(June), 39 and **79**(Nov.), 46.

Ferrara, G. and Preti, U. (1975). A contribution to screening kinetics, *Proc. 11th Int. Min. Proc. Cong.*, Cagliari.

Fontein, F.J. (1954). The D.S.M. sievebend, new tool for wetscreening on fine sizes, application in coal washeries, *Second Int. Coal Prep. Cong.*, Essen.

Gaudin, A.M. (1939). *Principles of Mineral Dressing*, McGraw-Hill.

Hansen, H. (2000). Fundamentals and further development of sizer technology, *Aufbereitungs Technik*, **41(7)**.

Karra, V.K. (1979). Development of a model for predicting the screening performance of a vibrating screen, *CIM Bull.*, **72**, 167–171.

Kingsford, G.R. (1991). The evaluation of a non-blinding screen for screening iron ore fines, *Proc. 4th Mill Operators Conf.*, 25–29.

Krause, M. (2005). Horizontal versus inclined screens, *Quarry*, Mar., 26–27.

Lynch, A.J. and Narayanan, S.S. (1986). Simulation – the design tool for the future, in *Mineral Processing at a Crossroads*, ed. B.A. Wills and R.W. Barley, Martinus Nijoff Publishers, Dordrecht, 89.

Meinel, A. (1998). Classification of fine, medium-sized and coarse particles on shaking screens, *Aufbereitungs-Technik*, **39(7)**.

Mogensen, F.A. (1965). A new method of screening granular materials, *Quarry Managers J.*, Oct., 409.

Mohanty, M. K. (2003). Fine coal screening performance enhancement using the Pansep screen, *Int. J. Min. Proc.*, **69**, 205–220.

Napier-Munn, T.J., Morrell, S., Morrison, R.D., and Kojovic, T. (1996). *Mineral comminution Circuits – Their Operation and Optimisation*, Chapter 12, JKMRC, The University of Queensland, Brisbane, 413.

Olsen, P. and Coombe A. (2003). Is screening a science or art?, *Quarry*, **11(8)**, Aug., 20–25.

Soldinger, M. (1999). Interrelation of the stratification and passage in the screening process, *Minerals Engng.*, **12(5)**, 497–519.

Taggart, A.F. (1945). *Handbook of Mineral Dressing*, Wiley, New York.

Whiten, W.J. (1972). The simulation of crushing plants with models developed using multiple spline regression, *10th Int. Symp. on the Application of Computer Methods in the Min. Ind*, Johannesburg, 317–323.

9

Classification

Introduction

Classification is a method of separating mixtures of minerals into two or more products on the basis of the velocity with which the grains fall through a fluid medium (Heiskanen, 1993). In mineral processing, this is usually water, and wet classification is generally applied to mineral particles which are considered too fine to be sorted efficiently by screening. Since the velocity of particles in a fluid medium is dependent not only on the size, but also on the specific gravity and shape of the particles, the principles of classification are important in mineral separations utilising gravity concentrators. Classifiers also strongly influence the performance of grinding circuits.

Principles of classification

When a solid particle falls freely in a vacuum, it is subject to constant acceleration and its velocity increases indefinitely, being independent of size and density. Thus a lump of lead and a feather fall at exactly the same rate.

In a viscous medium, such as air or water, there is resistance to this movement and the value increases with velocity. When equilibrium is attained between the gravitational and fluid resistances forces, the body reaches its *terminal velocity* and thereafter falls at a uniform rate.

The nature of the resistance depends on the velocity of the descent. At low velocities motion is smooth because the layer of fluid in contact with the body moves with it, while the fluid a short distance away is motionless. Between these two positions is a zone of intense shear in the fluid all around the descending particle. Effectively all resistance to motion is due to the shear forces or viscosity of the fluid and is hence called *viscous resistance*. At high velocities the main resistance is due to the displacement of fluid by the body, and viscous resistance is relatively small; this is known as *turbulent resistance*.

Whether viscous or turbulent resistance predominates, the acceleration of particles in a fluid rapidly decreases and the terminal velocity is quickly reached.

Classifiers consist essentially of a *sorting column* in which a fluid is rising at a uniform rate (Figure 9.1). Particles introduced into the sorting column either sink or rise according to whether their terminal velocities are greater or lesser than the upward velocity of the fluid. The sorting column therefore separates the feed into two products – an *overflow* consisting of particles with terminal velocities lesser than the velocity of the fluid and an *underflow* or *spigot product* of particles with terminal velocities greater than the rising velocity.

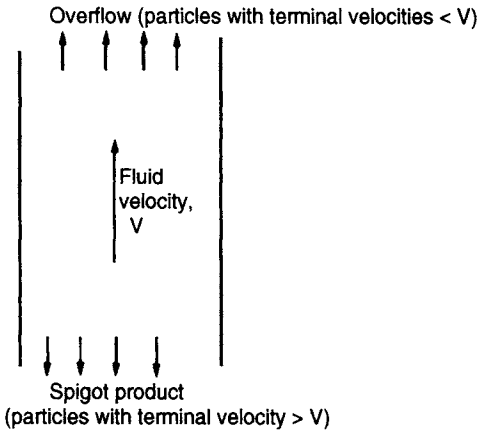


Figure 9.1 Classifier sorting column

Free settling

Free settling refers to the sinking of particles in a volume of fluid which is large with respect to the total volume of particles, hence particle crowding

is negligible. For well-dispersed ore pulps, free settling predominates when the percentage of solids by weight is less than about 15 (Taggart, 1945).

Consider a spherical particle of diameter d and density D_s falling under gravity in a viscous fluid of density D_f under free-settling conditions, i.e. ideally in a fluid of infinite extent. The particle is acted upon by three forces: a gravitational force acting downwards, an upward buoyant force due to the displaced fluid, and a drag force D acting upwards. The equation of motion of the particle is

$$mg - m'g - D = \frac{m\,dx}{dt} \tag{9.1}$$

where m is the mass of the particle, m' is the mass of the displaced fluid, x is the particle velocity, and g is the acceleration due to gravity.

When the terminal velocity is reached, $dx/dt = 0$, and hence $D = (m - m')g$.

Therefore

$$D = \left(\frac{\pi}{6}\right) g d^3 (D_s - D_f) \tag{9.2}$$

Stokes (1891) assumed the drag force on a spherical particle to be entirely due to viscous resistance and deduced the expression

$$D = 3\pi d\eta v \tag{9.3}$$

where η is the fluid viscosity and v is the terminal velocity.

Hence, substituting in Equation 9.2,

$$3\pi d\eta v = \left(\frac{\pi}{6}\right) g d^3 (D_s - D_f)$$

and

$$v = \frac{g d^2 (D_s - D_f)}{18\eta} \tag{9.4}$$

This expression is known as *Stokes' law*.

Newton assumed that the drag force was entirely due to turbulent resistance, and deduced:

$$D = 0.055\pi d^2 v^2 D_f \tag{9.5}$$

Substituting in Equation 9.2 gives

$$v = \left[\frac{3gd(D_s - D_f)}{D_f}\right]^{1/2} \tag{9.6}$$

This is *Newton's law* for turbulent resistance.

Stokes' law is valid for particles below about 50 μm in diameter. The upper size limit is determined by the dimensionless Reynolds number (Chapter 4). Newton's law holds for particles larger than about 0.5 cm in diameter. There is, therefore, an intermediate range of particle size, which corresponds to the range in which most wet classification is performed, in which neither law fits experimental data.

Stokes' law (9.4) for a particular fluid can be simplified to

$$v = k_1 d^2 (D_s - D_f) \tag{9.7}$$

and Newton's law (9.6) can be simplified to

$$v = k_2 [d(D_s - D_f)]^{1/2} \tag{9.8}$$

where k_1 and k_2 are constants, and $(D_s - D_f)$ is known as the *effective density* of a particle of density D_s in a fluid of density D_f.

Both laws show that the terminal velocity of a particle in a particular fluid is a function only of the particle size and density. It can be seen that:

(1) If two particles have the same density, then the particle with the larger diameter has the higher terminal velocity.
(2) If two particles have the same diameter, then the heavier particle has the higher terminal velocity.

Consider two mineral particles of densities D_a and D_b and diameters d_a and d_b respectively, falling in a fluid of density D_f at exactly the same settling rate. Their terminal velocities must be the same, and hence from Stokes' law (9.7):

$$d_a^2 (D_a - D_f) = d_b^2 (D_b - D_f)$$

or

$$\frac{d_a}{d_b} = \left(\frac{D_b - D_f}{D_a - D_f}\right)^{1/2} \tag{9.9}$$

This expression is known as the *free-settling ratio* of the two minerals, i.e. the ratio of particle size required for the two minerals to fall at equal rates.

Similarly from Newton's law (9.8), the free settling ratio of large particles is

$$\frac{d_a}{d_b} = \frac{D_b - D_f}{D_a - D_f} \tag{9.10}$$

Consider a mixture of galena (density 7.5) and quartz (density 2.65) particles classifying in water.

For small particles, obeying Stokes' law, the free settling ratio (Equation 9.9) is

$$\left(\frac{7.5-1}{2.65-1}\right)^{1/2}=1.99$$

i.e. a small particle of galena will settle at the same rate as a small particle of quartz which has a diameter 1.99 times as large.

For particles obeying Newton's law, the free settling ratio (Equation 9.10) is

$$\frac{7.5-1}{2.65-1}=3.94$$

The free-settling ratio is therefore larger for coarse particles obeying Newton's law than for fine particles obeying Stokes' law. This means that *the density difference between the particles has a more pronounced effect on classification at coarser size ranges*. This is important where gravity concentration is being utilised. Over-grinding of the ore must be avoided, such that particles are fed to the separator in as coarse a state as possible, so that a rapid separation can be made, exploiting the enhanced effect of specific gravity difference. The enhanced gravity effect does, however, mean that fine heavy minerals are more likely to be overground in conventional ball mill-classifier circuits, so it is preferable where possible to use rod mills for the primary coarse grind.

The general expression for free-settling ratio can be deduced from Equations 9.9 and 9.10 as

$$\frac{d_a}{d_b}=\left(\frac{D_b-D_f}{D_a-D_f}\right)^n \qquad (9.11)$$

where $n=0.5$ for small particles obeying Stokes' law and $n=1$ for large particles obeying Newton's law.

The value of n lies in the range 0.5–1 for particles in the intermediate size range of 50 μm–0.5 cm.

Hindered settling

As the proportion of solids in the pulp increases, the effect of particle crowding becomes more apparent and the falling rate of the particles begins to decrease. The system begins to behave as a heavy liquid whose density is that of the pulp rather than that of the carrier liquid; *hindered-settling* conditions now prevail. Because of the high density and viscosity of the slurry through which a particle must fall in a separation by hindered settling, the resistance to fall is mainly due to the turbulence created (Swanson, 1989), and a modified form of Newton's law (9.8) can be used to determine the approximate falling rate of the particles

$$v=k[d(D_s-D_p)]^{1/2} \qquad (9.12)$$

where D_p is the *pulp density*.

The lower the density of the particle, the more marked is the effect of reduction of the effective density, D_s-D_p, and the greater is the reduction in falling velocity. Similarly, the larger the particle, the greater is the reduction in falling rate as the pulp density increases.

This is important in classifier design; in effect, *hindered-settling reduces the effect of size, while increasing the effect of density on classification.*

This is illustrated by considering a mixture of quartz and galena particles settling in a pulp of density 1.5. The *hindered-settling ratio* can be derived from Equation 9.12 as

$$\frac{d_a}{d_b}=\frac{D_b-D_p}{D_a-D_p} \qquad (9.13)$$

Therefore, in this system,

$$\frac{d_a}{d_b}=\frac{7.5-1.5}{2.65-1.5}=5.22$$

A particle of galena will thus fall in the pulp at the same rate as a particle of quartz which has a diameter 5.22 times as large. This compares with the free-settling ratio, calculated as 3.94 for turbulent resistance.

The *hindered-settling ratio is always greater than the free-settling ratio*, and the denser the pulp, the greater is the ratio of the diameter of equal settling particles. For quartz and galena, the greatest hindered-settling ratio that we can attain practically is about 7.5. Hindered-settling classifiers are used to increase the effect of density on the separation, whereas free-settling classifiers use relatively dilute suspensions to increase the effect of size on the separation (Figure 9.2). Relatively dense slurries are fed to certain gravity concentrators, particularly those treating heavy alluvial sands. This allows high tonnages to be treated, and enhances the effect of specific gravity difference on the separation. The efficiency of separation, however, may be reduced since the viscosity of a slurry increases with density. For separations involving feeds with

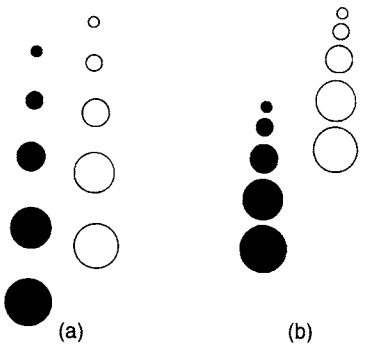


Figure 9.2 Classification by (a) free settling, (b) hindered settling

a high proportion of particles close to the required density of separation, lower slurry densities may be necessary, even though the density difference effect is reduced.

As the pulp density increases, a point is reached where each mineral particle is covered only with a thin film of water. This condition is known as a *quicksand*, and because of surface tension, the mixture is a perfect suspension and does not tend to separate. The solids are in a condition of *full teeter*, which means that each grain is free to move, but is unable to do so without colliding with other grains and as a result stays in place. The mass acts as a viscous liquid and can be penetrated by solids with a higher specific gravity than that of the mass, which will then move at a velocity impeded by the viscosity of the mass.

A condition of teeter can be produced in a classifier sorting column by putting a constriction in the column, either by tapering the column or by inserting a grid into the base (Figure 9.3).

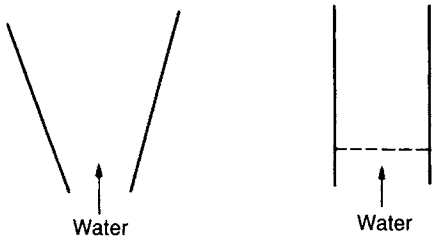


Figure 9.3 Teeter chambers

Such hindered-settling sorting columns are known as *teeter chambers*. Due to the constriction, the velocity of the introduced water current is greatest at the bottom of the column. A particle falls until it reaches a point where its falling velocity equals that of the rising current. The particle can now fall no further. Many particles reach this condition, and as a result, a mass of particles becomes trapped above the constriction and pressure builds up in the mass. Particles move upward along the path of least resistance, which is usually the centre of the column, until they reach a region of lower pressure at or near the top of the settled mass; here, under conditions in which they previously fell, they fall again. As particles from the bottom rise at the centre, those from the sides fall into the resulting void. A general circulation is built up, the particles being said to *teeter*. The constant jostling of teetering particles has a scouring effect which removes any entrained or adhering slimes particles, which then leave the teeter chamber and pass out through the classifier overflow. Cleaner separations can therefore be made in such classifiers.

Types of classifier

Many different types of classifier have been designed and built. They may be grouped, however, into two broad classes depending on the direction of flow of the carrying current. Horizontal current classifiers such as mechanical classifiers are essentially of the free-settling type and accentuate the sizing function; vertical current or hydraulic classifiers are usually hindered-settling types and so increase the effect of density on the separation.

A useful guide to some of the major types of classification equipment used in mineral processing can be found elsewhere (Anon., 1984; Heiskanen, 1993).

Hydraulic classifiers

These are characterised by the use of water additional to that of the feed pulp, introduced so that its direction of flow opposes that of the settling particles. They normally consist of a series of sorting columns through each of which a vertical current of water is rising and particles are settling out (Figure 9.4).

The rising currents are graded from a relatively high velocity in the first sorting column, to a relatively low velocity in the last, so that a series of spigot products can be obtained, with the coarser,

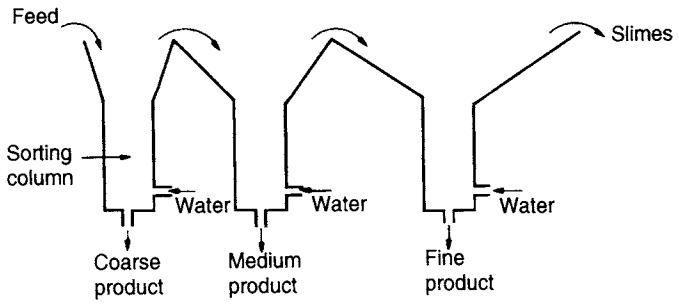


Figure 9.4 Principle of hydraulic classifier

denser particles in the first spigot and the fines in the latter spigots. Very fine slimes overflow the final sorting column of the classifier. The size of each successive vessel is increased, partly because the amount of liquid to be handled includes all the water used for classifying in the previous vessels and partly because it is desired to reduce, in stages, the surface velocity of the fluid flowing from one vessel to the next.

Hydraulic classifiers may be free- or hindered-settling types. The former are rarely used; they are simple and have high capacities, but are inefficient in sizing and sorting. They are characterised by the fact that each sorting column is of the same cross-sectional area throughout its length.

The greatest use for hydraulic classifiers in the mineral industry is for sorting the feed to certain gravity concentration processes so that the size effect can be suppressed and the density effect enhanced (Chapter 10). Such classifiers are of the hindered-settling type. These differ from the free-settling classifiers in that the sorting column is constricted at the bottom in order to produce a teeter chamber (Figure 9.3). The hindered-settling classifier uses much less water than the free-settling type, and is more selective in its action, due to the scouring action in the teeter chamber, and the buoyancy effect of the pulp, as a whole, on those particles which are to be rejected. Since the ratio of sizes of equally falling particles is high, the classifier is capable of performing a concentrating effect, and the first spigot product is normally of higher grade than the other products (Figure 9.5).

This is known as the *added increment* of the classifier and the first spigot product may in some cases be rich enough to be classed as a concentrate.

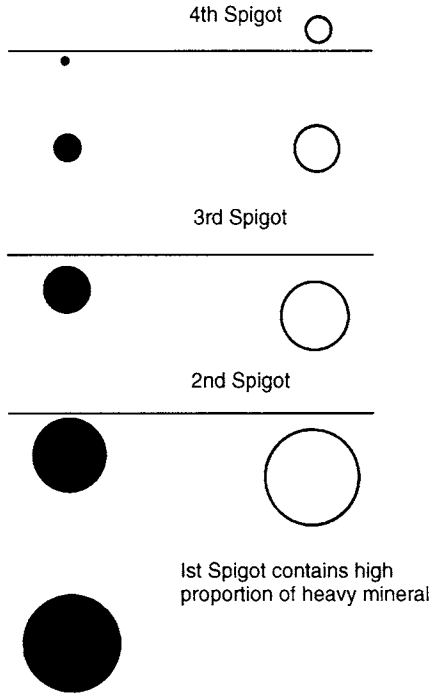


Figure 9.5 Added increment of hindered-settling classifier

During classification the teeter bed tends to grow, as it is easier for particles to become entangled in the bed rather than leave it. This tends to alter the character of the spigot discharge, as the density builds up. In modern multi-spigot *hydrosizers* the teeter bed composition is automatically controlled. The Stokes hydrosizer (Figure 9.6) is commonly used to sort the feed to gravity concentrators (Mackie et al., 1987).

Each teeter chamber is provided at its bottom with a supply of water under constant head which is used for maintaining a teetering condition in the

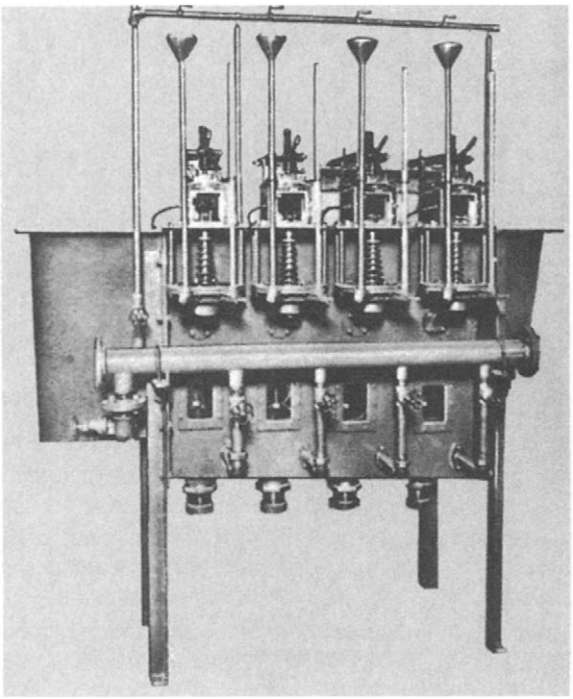


Figure 9.6 Stokes multi-spigot hydrosizer

solids that find their way down against the interstitial rising flow of water. Each teeter chamber is fitted with a discharge spigot which is, in turn, connected to a pressure-sensitive valve so that the classifying conditions set by the operator can be accurately controlled (Figure 9.7).

The valve may be hydraulically or electrically operated; in operation it is adjusted to balance the pressure set up by the teetering material. The concentration of solids in a particular compartment can be held extremely steady in spite of the normal variations in feed rate taking place from time to time. The rate of discharge from each spigot will, of course, change in sympathy with these variations, but since these changing tendencies are always being balanced by the valve, the discharge will take place at a nearly constant density. For a quartz sand this is usually about 65% solids by weight, but is higher for heavier minerals.

Horizontal current classifiers

Settling cones These are the simplest form of classifier, in which there is little attempt to do more than separate the solids from the liquid, i.e. they are sometimes used as dewatering units in small-scale operations. They are often used in the aggregate industry to de-slime coarse sands products. The principle of the settling cone is shown in Figure 9.8. The pulp is fed into the tank as a distributed stream at F, with the spigot discharge S initially closed. When the tank is full, overflow of water and slimes commences, and a bed of settled sand builds up until it reaches the level shown. If the spigot valve is now opened and sand discharge maintained at a rate equal to that of the input, classification by horizontal current action takes place radially across zone D from the feed cylinder B to the overflow lip. The main difficulty in operation of such a device is the balancing of the sand discharge and deposition; it is virtually impossible to maintain a regular discharge of sand through an open pipe under the influence of gravity. Many different designs of cone have been introduced to overcome this problem (Taggart, 1945).

In the "Floatex" separator, which consists essentially of a hindered-settling classifier over a dewatering cone, automatic control of the coarse lower discharge is governed by the specific gravity of the teeter column. The use of the machine as a desliming unit and in upgrading coal and mica, as well as its possible application in closed-circuit classification of metalliferous ores, is discussed by Littler (1986).

Mechanical classifiers Several forms of classifier exist in which the material of lower settling velocity is carried away in a liquid overflow, and the material of higher settling velocity is deposited on the bottom of the equipment and is dragged upwards against the flow of liquid by some mechanical means.

Mechanical classifiers have widespread use in closed-circuit grinding operations and in the classification of products from ore-washing plants (Chapter 2). In washing plants they act more or less as sizing devices, as the particles are essentially unliberated, so are of similar density. In closed-circuit grinding they have a tendency to return small dense particles to the mill, causing overgrinding (Chapter 7). They have also been used to densify dense media (Chapter 11).

The principle of the mechanical classifier is shown in Figure 9.9.

The pulp feed is introduced into the inclined trough and forms a settling pool in which particles

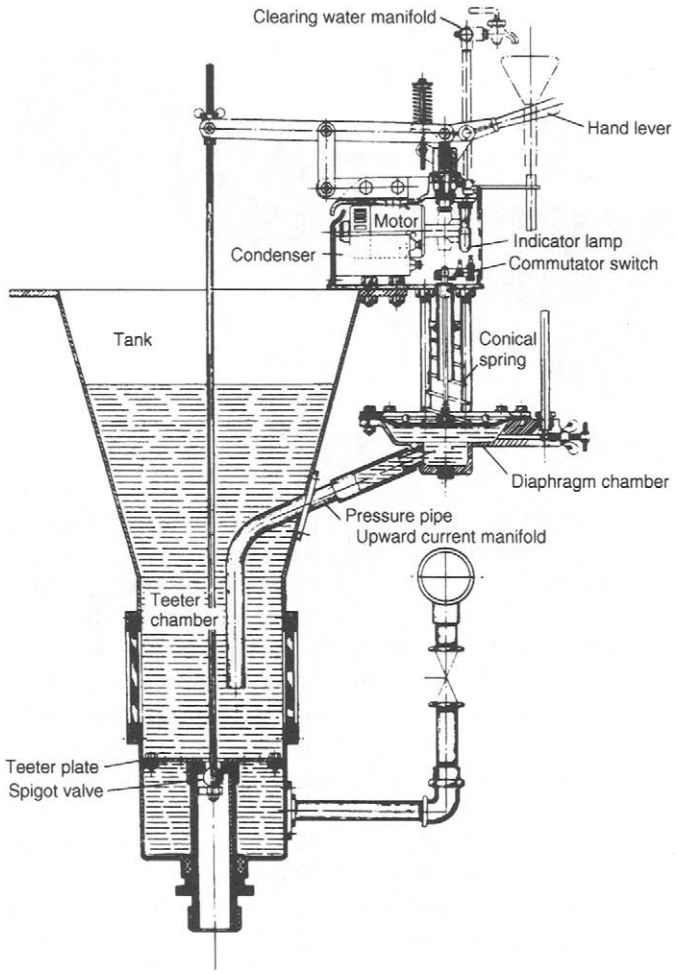


Figure 9.7 Section through sorting column of hydrosizer

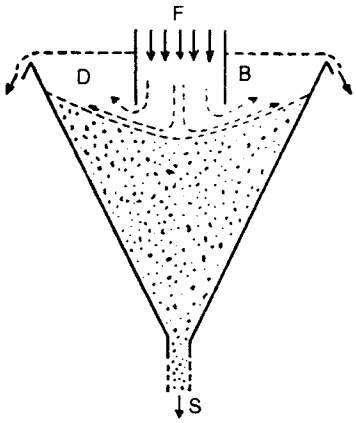


Figure 9.8 Settling cone operation

of high falling velocity quickly fall to the bottom of the trough. Above this coarse sand is a quicksand zone where essentially hindered settling takes place. The depth and shape of this zone depends on the classifier action and on the feed pulp density. Above the quicksand is a zone of essentially free settling material, comprising a stream of pulp flowing horizontally across the top of the quicksand zone from the feed inlet to the overflow weir, where the fines are removed.

The settled sands are conveyed up the inclined trough by mechanical rakes or by a helical screw. The conveying mechanism also serves to keep fine particles in suspension in the pool by gentle agitation and when the sands leave the pool they are slowly turned over by the raking action, thus releasing entrained slimes and water, increasing the

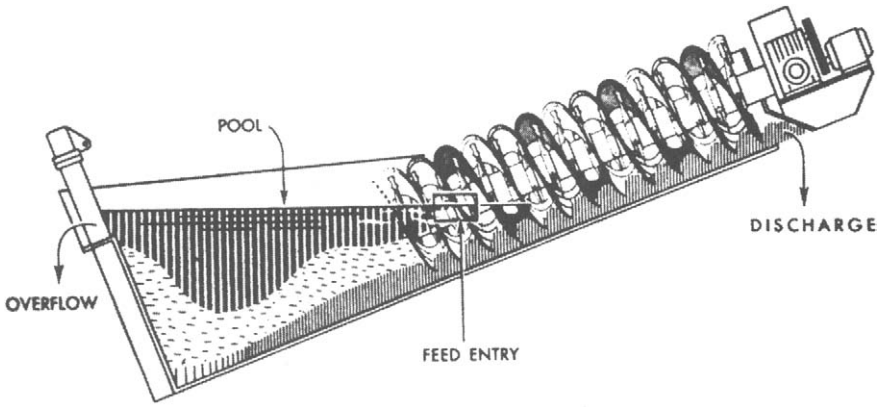


Figure 9.9 Principle of mechanical classifier

efficiency of the separation. Washing sprays are often directed on the emergent sands to wash the released slimes back into the pool.

The rake classifier (Figure 9.10) utilises rakes actuated by an eccentric motion, which causes them to dip into the settled material and to move it up the incline for a short distance. The rakes are then withdrawn, and return to the starting-point, where the cycle is repeated; the settled material is thus slowly moved up the incline to the discharge.

In the *duplex* type shown, one set of rakes is moving up, while the other set returns; Simplex and quadruplex machines are also made in which there are one or four raking assemblies.

Spiral classifiers (Figure 9.11) use a continuously revolving spiral to move the sands up the slope. They can be operated at steeper slopes than the rake classifier, in which the sands tend to slip back when the rakes are removed. Steeper slopes aid the drainage of sands, giving a cleaner, drier product. Agitation in the pool is less than in the rake classifier which is important in separations of very fine material.

The size at which the separation is made and the quality of the separation depend on a number of factors.

Increasing the feed rate increases the horizontal carrying velocity and thus increases the size of particle leaving in the overflow. The feed should

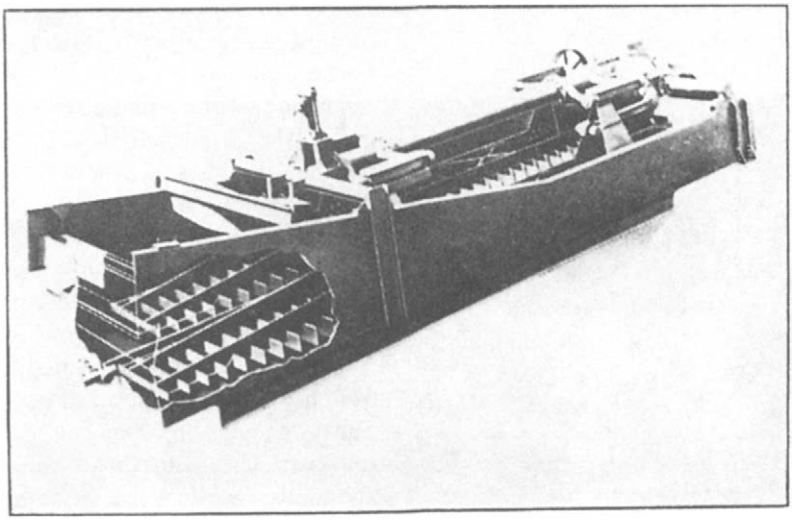


Figure 9.10 Rake classifier

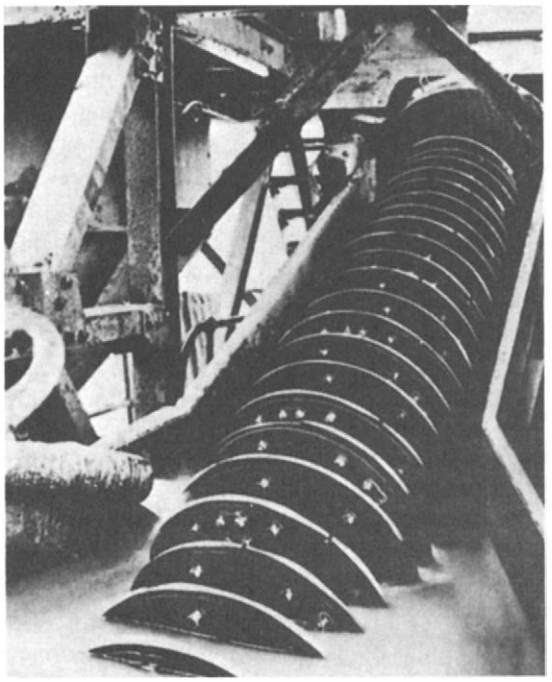


Figure 9.11 Spiral classifier

not be introduced directly into the pool, as this causes agitation and releases coarse material from the hindered-settling zone, which may report to the overflow. The feed stream should be slowed down by spreading it on an apron, partially submerged in the pool, and sloped towards the sand discharge end, so that most of the kinetic energy is absorbed in the part of the pool furthest from the overflow.

The speed of the rakes or spiral determines the degree of agitation of the pulp and the tonnage rate of sand removal. For coarse separations, a high degree of agitation may be necessary to keep the coarse particles in suspension in the pool, whereas for finer separations, less agitation and thus lower raking speeds are required. It is essential, however, that the speed is high enough to transport the sands up the slope.

The height of the overflow weir is an operating variable in some mechanical classifiers. Increasing the weir height increases the pool volume, and hence allows more settling time and decreases the surface agitation, thus reducing the pulp density at overflow level, where the final separation is made. High weirs are thus used for fine separations.

Dilution of the pulp is the most important variable in the operation of mechanical classifiers. In closed-circuit grinding operations, ball mills rarely discharge at less than 65% solids by weight, whereas mechanical classifiers never operate at more than about 50% solids. Water to control dilution is added in the feed launder, or onto the sand near the vee of the pool. Water addition determines the rate of settling of the particles; increased dilution reduces the density of the weir overflow, and increases free settling, allowing finer particles to settle out of the influence of the horizontal current. Finer separations are thus produced, providing that the overflow pulp density is above a value known as the *critical dilution*, which is normally about 10% solids. Below this density, the effect of increasing rising velocity with dilution becomes more important than the increase in particle settling rates produced by decrease of pulp density. The overflow therefore becomes coarser with increasing dilution (Figure 9.12). In mineral processing applications, however, very rarely is the overflow density less than the critical dilution.

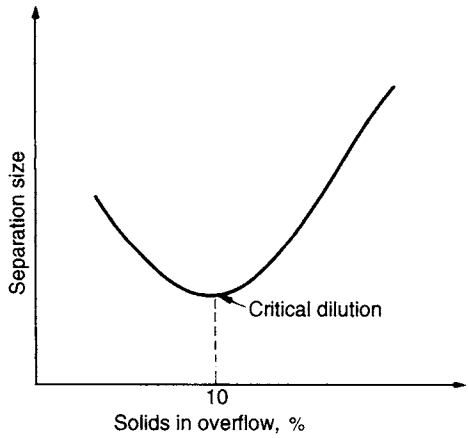


Figure 9.12 Effect of dilution of overflow on classifier separation

One of the major disadvantages of the mechanical classifier is its inability to produce overflows of very fine particle size at reasonable pulp densities. To produce such separations, the pulp may have to be diluted to such an extent to increase particle settling rates that it becomes too thin for subsequent operations. It may therefore require thickening before concentration can take place. This is undesirable as, apart from the capital cost and floor

space of the thickener, oxidation of liberated particles may occur in the thickener, which may affect subsequent processes, especially froth flotation.

The hydrocyclone

This is a continuously operating classifying device that utilises centrifugal force to accelerate the settling rate of particles. It is one of the most important devices in the minerals industry, its main use in mineral processing being as a classifier, which has proved extremely efficient at fine separation sizes. It is widely used in closed-circuit grinding operations (Napier-Munn et al., 1996) but has found many other uses, such as de-sliming, de-gritting, and thickening.

It has replaced mechanical classifiers in many applications, its advantages being simplicity and high capacity relative to its size. A variant, the "water-only-cyclone", has been used for the cleaning of fine coal (Osborne, 1985) and other minerals.

A typical hydrocyclone (Figure 9.13) consists of a conically shaped vessel, open at its apex, or underflow, joined to a cylindrical section, which has a tangential feed inlet. The top of the cylindrical section is closed with a plate through which passes an axially mounted overflow pipe. The pipe is extended into the body of the cyclone by a short, removable section known as the *vortex finder*, which prevents short-circuiting of feed directly into the overflow.

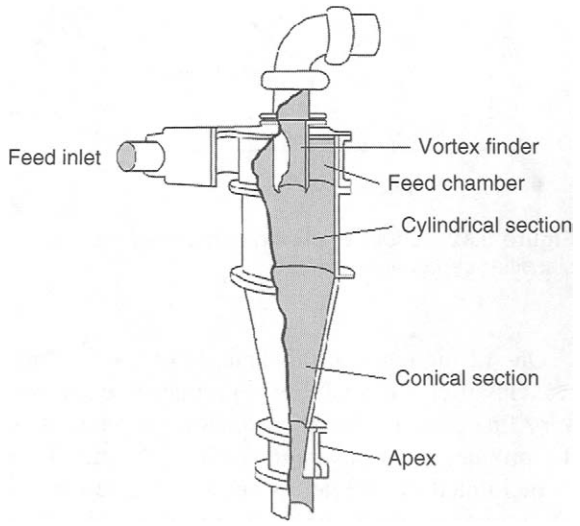


Figure 9.13 Hydrocyclone (from Napier-Munn et al., 1996; Courtesy JKMRC, The University of Queensland)

The feed is introduced under pressure through the tangential entry which imparts a swirling motion to the pulp. This generates a vortex in the cyclone, with a low-pressure zone along the vertical axis. An air core develops along the axis, normally connected to the atmosphere through the apex opening, but in part created by dissolved air coming out of solution in the zone of low pressure.

The classical theory of hydrocyclone action is that particles within the flow pattern are subjected to two opposing forces – an outward centrifugal force and an inwardly acting drag (Figure 9.14). The centrifugal force developed accelerates the settling rate of the particles thereby separating particles according to size, shape, and specific gravity. Faster settling particles move to the wall of the cyclone, where the velocity is lowest, and migrate to the apex opening. Due to the action of the drag force, the slower-settling particles move towards the zone of low pressure along the axis and are carried upward through the vortex-finder to the overflow.

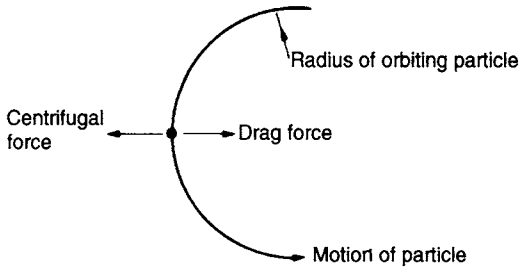


Figure 9.14 Forces acting on an orbiting particle in the hydrocyclone

The existence of an outer region of downward flow and an inner region of upward flow implies a position at which there is no vertical velocity. This applies throughout the greater part of the cyclone body, and an envelope of zero vertical velocity should exist throughout the body of the cyclone (Figure 9.15). Particles thrown outside the envelope of zero vertical velocity by the greater centrifugal force exit via the underflow, while particles swept to the centre by the greater drag force leave in the overflow. Particles lying on the envelope of zero velocity are acted upon by equal centrifugal and drag forces and have an equal chance of reporting either to the underflow or overflow.

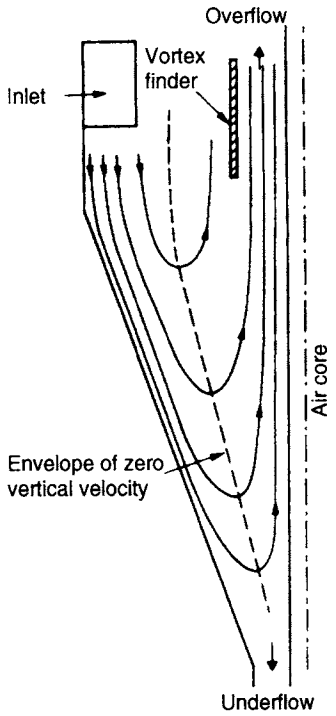


Figure 9.15 Distribution of the vertical and radial components of velocity in a hydrocyclone

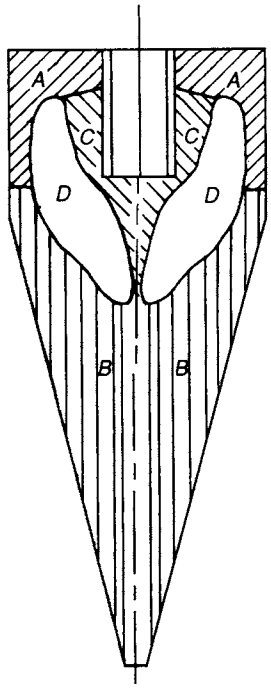


Figure 9.16 Regions of similar size distribution within cyclone

Experimental work reported by Renner and Cohen (1978) has shown that classification does not take-place throughout the whole body of the cyclone as the classical model postulates. Using a high-speed probe, samples were taken from several selected positions within a 150-mm diameter cyclone, and were subjected to size analysis. The results showed that the interior of the cyclone may be divided into four regions that contain distinctively different size distributions (Figure 9.16).

Essentially unclassified feed exists in a narrow region A adjacent to the cylinder wall and roof of the cyclone. Region B occupies a very large part of the cone of the cyclone and contains fully classified coarse material, i.e. the size distribution is practically uniform and resembles that of the coarse underflow product. Similarly, fully classified fine material is contained in region C, a narrow region surrounding the vortex finder and extending below the latter along the cyclone axis. Only in the toroid-shaped region D does classification appear to be taking place. Across this region, size fractions are radially distributed, so that decreasing sizes show maxima at decreasing radial distances from the axis. The cyclone was run at low pressure, so the region D may be larger in production units.

Hydrocyclones are almost universally used in grinding circuits (Figure 9.17) because of their high capacity and relative efficiency. They can also classify over a very wide range of sizes (typically 5–500 μm), smaller diameter units being used for finer classification.

Cyclone efficiency

The commonest method of representing cyclone efficiency is by a *performance* or *partition* curve (Figure 9.18), which relates the weight fraction, or percentage, of each particle size in the feed which reports to the apex, or underflow, to the particle size. It is analogous to the partition curve for density separation (Chapter 11). The *cut point*, or separation size, of the cyclone is defined as the size for which 50% of the particles in the feed report to the underflow, i.e. particles of this size have an equal chance of going either with the overflow or underflow (Svarovsky, 1984). This point

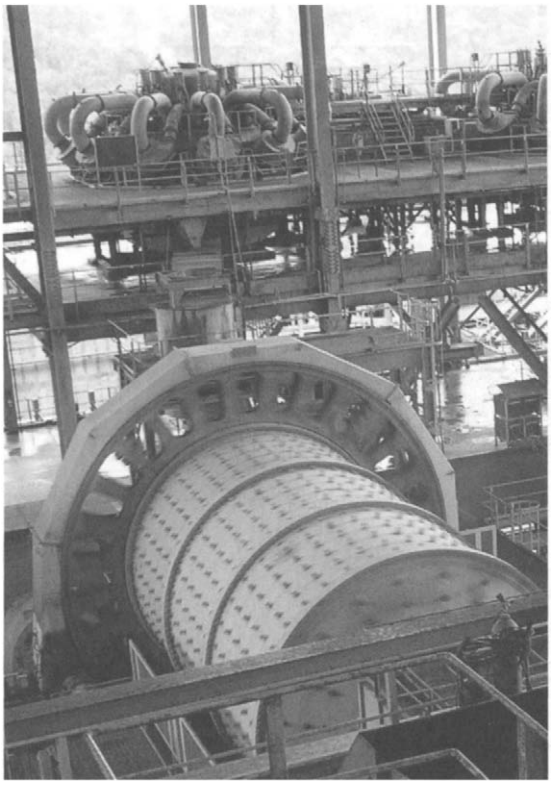


Figure 9.17 Ball mill in closed circuit with hydrocyclones, Batu Hijau mine, Indonesia (Courtesy JKMRC and JKTech Pty Ltd)

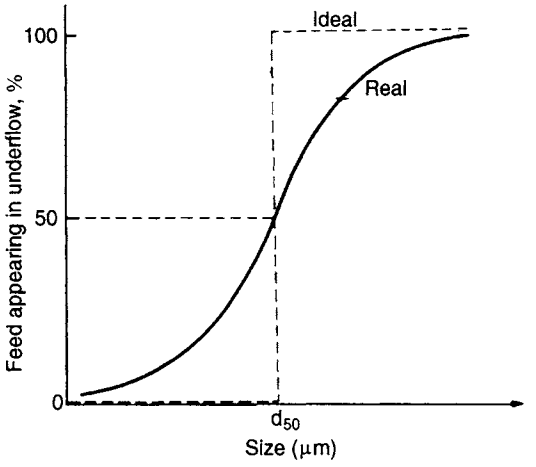


Figure 9.18 Partition curve for hydrocyclone

is usually referred to as the d_{50} size. The sharpness of the cut depends on the slope of the central section of the partition curve; the closer to vertical is the slope, the higher is the efficiency. The slope of the curve can be expressed by taking the points at which 75 and 25% of the feed particles report to the underflow. These are the d_{75} and d_{25} sizes, respectively. The efficiency of separation, or the so-called *imperfection I*, is then given by

$$I = \frac{d_{75} - d_{25}}{2d_{50}} \tag{9.14}$$

Many mathematical models of hydrocyclones include the term "corrected d_{50}" taken from the "corrected" classification curve. Kelsall (1953) suggested that solids of all sizes are entrained in the coarse product liquid by short-circuiting in direct proportion to the fraction of feed water reporting to the underflow.

For example, if the feed contains $16\,t\,h^{-1}$ of material of a certain size, and $12\,t\,h^{-1}$ reports to the underflow, then the percentage of this size reporting to the underflow, and plotted on the normal partition curve, is 75%.

However, if, say, 25% of the feed water reports to the underflow, then 25% of the feed material will short-circuit with it; therefore, $4\,t\,h^{-1}$ of the size fraction will short-circuit to the underflow, and only $8\,t\,h^{-1}$ leave in the underflow due to classification. The corrected recovery of the size fraction is thus

$$100 \times \frac{(12-4)}{(16-4)} = 67\%$$

The uncorrected partition curve can therefore be corrected by utilising the equation

$$y' = \frac{y - R}{1 - R} \tag{9.15}$$

where y' is the corrected mass fraction of a particular size reporting to underflow, y is the actual mass fraction of a particular size reporting to the underflow, and R is the fraction of the feed liquid which is recovered in the coarse product stream. The corrected curve thus describes particles recovered to the underflow by true classification. It should be noted that Kelsall's assumption has been questioned, and Flintoff et al. (1987) reviewed some of the arguments. However, the Kelsall correction has the advantages of simplicity, utility, and familiarity through long use. Figure 9.19 shows uncorrected and corrected classification curves.

The method of construction of the partition curve can be illustrated by means of an example. It is easily performed in a spreadsheet. Suppose

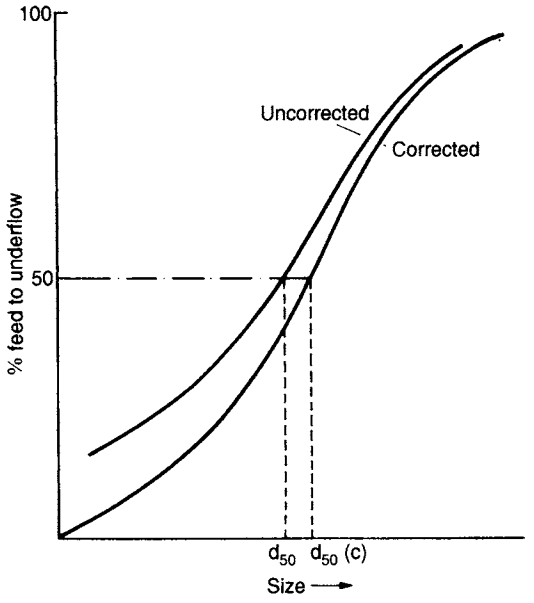


Figure 9.19 Uncorrected and corrected classification curves

a cyclone is being fed with quartz (density $2700\,kg\,m^{-3}$) in the form of a slurry of pulp density $1670\,kg\,m^{-3}$. The cyclone underflow density is $1890\,kg\,m^{-3}$, and the overflow $1460\,kg\,m^{-3}$.

Using Equation 3.6, the percentage solids by weight in the cyclone feed is 63.7%. Therefore, the dilution ratio (water–solids ratio) of feed is

$$\frac{36.3}{63.7} = 0.57$$

Similarly, the underflow and overflow dilution ratios can be calculated to be 0.34 and 1.00 respectively.

If the cyclone is fed at the rate of $F\,t\,h^{-1}$ of dry solids and the underflow and overflow mass flowrates are U and $V\,t\,h^{-1}$ respectively, then, since the total amount of water entering the cyclone must equal the amount leaving in unit time:

$$0.57F = 0.34U + V$$

or

$$0.57F = 0.34U + (F - U)$$

Therefore

$$\frac{U}{F} = 0.652$$

The underflow is thus 65.2% of the total feed weight and the overflow is 34.8% of the feed.

The performance curve for the cyclone can now be prepared by tabulating the data as in Table 9.1.

Columns 1, 2, and 3 represent the screen analyses of the overflow and underflow, and columns 4 and 5 relate these results in relation to the feed material. Column 4, e.g., is prepared by multiplying the results of column 2 by 0.652. Adding column 4 to column 5 produces column 6, the reconstituted size analysis of the feed material. Column 8 is determined by dividing each weight in column 4 by the corresponding weight in column 6. Plotting column 8 against column 7, the arithmetic mean of the sieve size ranges, produces the partition curve, from which the d_{50} (177.5 μm) can be determined. The partition curve can be corrected by utilising Equation 9.15. The value of R in this example is

$$\frac{65.2 \times 0.34}{100 \times 0.57} = 0.39$$

Lynch and Rao (reported in Lynch [1977]) describe the application of the "reduced efficiency curve", which is obtained by plotting corrected weight percentage of particles reporting to the underflow against the actual size divided by the corrected d_{50} (Figure 9.20), and suggests that it can be used to derive the actual performance curve after any changes in operating conditions, the curve being independent of hydrocyclone diameter, outlet dimensions, or operating conditions. A number of mathematical functions have been suggested to describe the reduced efficiency curve. The commonest are reviewed by Napier-Munn et al. (1996).

Although partition curves are extremely useful in assessing classifier performance, the minerals engineer is usually more interested in knowing fineness of grind (i.e. cyclone overflow size analysis) than the cyclone d_{50}. A simple fundamental relationship between fineness of grind and the efficiency curve of a hydrocyclone has been developed by Kawatra and Seitz (1985).

Mathematical models of hydrocyclones

Many attempts have been made to capture the key relationships between hydrocyclone operating and geometrical variables in models for use in design and optimisation, with some success. Progress is being made in using computational fluid dynamics

Table 9.1

(1) Size (μm)	(2) Wt %	(3)	(4) Wt % of feed	(5)	(6) Reconstituted feed	(7) Nominal size (arithmetic mean)	(8) % of feed to U/F
	U/F	O/F	U/F	O/F			
+1168	14.7	–	9.6	–	9.6	–	100.0
589–1168	21.8	–	14.2	–	14.2	878.5	100.0
295–589	25.0	5.9	16.3	2.1	18.4	442.0	88.6
208–295	7.4	9.0	4.8	3.1	7.9	251.5	60.8
147–208	6.3	11.7	4.1	4.1	8.2	177.5	50.0
104–147	4.8	11.2	3.1	3.9	7.0	125.5	44.3
74–104	2.9	7.9	1.9	2.7	4.6	89.0	41.3
−74	17.1	54.3	11.2	18.9	30.1	–	37.2
Total	100.0	100.0	65.2	34.8	100.0		

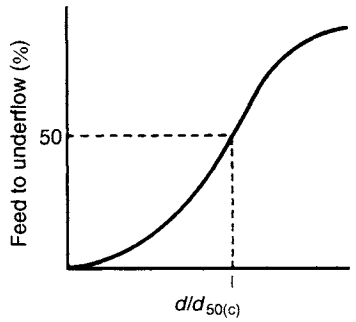


Figure 9.20 Reduced efficiency curve

to model hydrocyclones from first principles (e.g. Brennan et al., 2003; Nowakowski et al., 2004) though this approach is very computationally-intensive and not yet mature. All the models commonly used in practice are still essentially empirical in nature.

Bradley's seminal book (1965) listed eight equations for the cut-size, and these have increased significantly since then. Bradley's own equation based on the equilibrium orbit hypothesis (Figures 9.14 and 9.15) was:

$$d_{50} = k\left[\frac{D_c^3 \eta}{Q_f(\rho_s - \rho_l)}\right]^n \qquad (9.16)$$

where D_c = cyclone diameter, ρ = fluid viscosity, Q_f = feed flow rate, ρ_s = solids density, ρ_l = fluid density, n = hydrodynamic constant (0.5 for particle laminar flow), k = constant incorporating other factors, particularly cyclone geometry. This demonstrates some of the process trends well, but cannot be used directly in practical design or operational situations.

The most widely used of the published empirical models are probably those of Plitt (1976) and Nageswararao (1995, though first published in 1978). Plitt published a slightly modified form of his model in 1980 (Flintoff et al., 1987). These models, based on a phenomenological description of the process with numerical constants determined from large databases, are described in Napier-Munn et al. (1996) and were reviewed and compared more recently by Nageswararao et al. (2004).

Plitt's modified model for the corrected cut size $d_{50(c)}$ in microns is:

$$d_{50c} = \frac{F_1\ 39.7\ D_c^{0.46}\ D_i^{0.6}\ D_o^{1.21}\ \eta^{0.5}\ \exp(0.063 C_v)}{D_u^{0.71}\ h^{0.38}\ Q_f^{0.45}\left(\frac{\rho_s - 1}{1.6}\right)^k} \qquad (9.17)$$

where D_c, D_i, D_o, and D_u are the inside diameters of the cyclone, inlet, vortex finder, and apex respectively (cm), η is the liquid viscosity (cP), C_v is the feed solids volume concentration (%), h is the distance between apex and end of vortex finder (cm), k is a hydrodynamic exponent to be estimated from data (default value for laminar flow 0.5), Q_f is the feed flow rate (l/min), and ρ_s is the solids density (g/cm^3). Note that for non-circular inlets, $D_i = \sqrt{4A/\pi}$ where A (cm^2) is the cross-sectional area of the inlet.

The equation for the volumetric flow rate of slurry to the cyclone, Q_f, is:

$$Q_f = \frac{F_2 P^{0.56} D_c^{0.21} D_i^{0.53} h^{0.16} (D_u^2 + D_o^2)^{0.49}}{\exp(0.0031 C_v)} \quad (9.18)$$

where P is the pressure drop across the cyclone in kPa (1 psi = 6.896 kPa). F_1 and F_2 in Equations 9.17 and 9.18 are material-specific constants that must be determined from tests with the feed material concerned.

Plitt also reports equations for the flow split between underflow and overflow, and for the efficiency parameter in the reduced efficiency curve.

Nageswararao's model includes correlations for corrected cut size, pressure-flow rate, and flow split, though not efficiency. It also requires the estimate of feed-specific constants from data, though first approximations can be obtained from libraries of previous case studies. This requirement for feed-specific calibration emphasises the important effect which feed conditions have on hydrocyclone performance.

Asomah and Napier-Munn (1997) reported an empirical model which incorporates the angle of inclination of the cyclone, as well as explicitly the slurry viscosity, but this has not yet been validated in the large-scale use which has been enjoyed by the Plitt and Nageswararao models.

A useful general approximation for the flow rate in a hydrocyclone is

$$Q \approx 9.5 \times 10^{-3} \sqrt{P}\, D^2 \quad (9.19)$$

Flow rate and pressure drop together define the useful work done in the cyclone:

$$\text{Power} = \frac{PQ}{3600} \text{ kW} \quad (9.20)$$

where Q = flow rate (m^3/h), P = pressure drop (kPa), and D = cyclone diameter (cm). The power can be used as a first approximation to size the pump motor, making allowances for head losses and pump efficiency.

These models are easy to incorporate in spreadsheets, but are particularly useful in process design and optimisation using dedicated computer simulators such as JKSimMet (Napier-Munn et al., 1996) and MODSIM (King, 2001), or the flowsheet simulator Limn (Hand and Wiseman, 2002). They can also be used as a virtual instrument or "soft sensor" (Morrison and Freeman, 1990; Smith and Swartz, 1999), inferring cyclone product size from geometry and operating variables as an alternative to using an on-line sizer (Chapter 4).

Scale-up and design of hydrocyclones

A preliminary scale-up from a known situation (e.g. a laboratory or pilot plant test) to the unknown (e.g. a full production installation) can be done via the basic relationships between cut-size, cyclone diameter, flow rate, and pressure drop. These are:

$$\frac{d_{50c_2}}{d_{50c_1}} = \left(\frac{D_2}{D_1}\right)^{n_1} \left(\frac{Q_1}{Q_2}\right)^{n_2} = \left(\frac{D_2}{D_1}\right)^{n_3} \left(\frac{P_1}{P_2}\right)^{n_4} \quad (9.21)$$

and

$$\frac{P_1}{P_2} \simeq \left(\frac{Q_1}{Q_2}\right)^{n_5} \left(\frac{D_2}{D_1}\right)^{n_6} \quad (9.22)$$

where P is pressure drop, Q flow rate, D cyclone diameter, the subscripts 1 and 2 indicate the known and scale-up applications respectively, and n_{1-6} are constants which are a function of the flow conditions. The theoretical values (for dilute slurries and particle laminar flow in small cyclones) are: $n_1 = 1.5$, $n_2 = 0.5$, $n_3 = 0.5$, $n_4 = 0.25$, $n_5 = 2.0$, and $n_6 = 4.0$. The constants to be used in practice will depend on conditions and which particular model is favoured. In particular, high feed solids concentrations will substantially influence both cut size (increase) and pressure drop at a given flow rate (reduce). There is no general consensus, but in most applications the following values will give more realistic predictions: $n_1 = 1.54$, $n_2 = 0.43$, $n_3 = 0.72$, $n_4 = 0.22$, $n_5 = 2.0$, and $n_6 = 3.76$.

These relationships tell us that the diameter, flow rate, and pressure must be considered together. For example, cut-size cannot be scaled purely on cyclone diameter, as a new diameter will bring either a new flow rate or pressure or both. For example, if it is desired to scale to a larger cyclone at the same cut size, then $d_{50c_1} = d_{50c_2}$ and $D_2 = D_1 (P_2/P_1)^{n_4/n_3}$.

Classification efficiency can sometimes be improved by arranging several cyclones in series to re-treat overflow, underflow or both. Svarovsky (1984) has pointed out that if N cyclones with identical classification curves are arranged in series, each treating the overflow of the previous one, then

the overall recovery of size d to the combined coarse product, $R_{d(T)}$, is given by

$$R_{d(T)} = 1 - (1 - R_d)^N \qquad (9.23)$$

where R_d = recovery of size d in one cyclone.

The appropriate way of specifying a cyclone installation is by process simulation using a simulation package such as those mentioned above. These packages incorporate empirical cyclone models such as those by Plitt and Nageswararao, and can be used for optimising processing circuits incorporating hydrocyclones (e.g. Morrison and Morrell, 1998).

An alternative is to use the simple empirical methods of sizing cyclones for a particular duty developed by the manufacturers. Arterburn (1982) published a method based on the performance of a "typical" Krebs cyclone with graphical corrections for other conditions; from this the required cut-point can be calculated, and thus the cyclone size, capacity, and number of units determined. A version of this paper is available on the Krebs Engineers website, and a more recent approach was given by Olson and Turner (2002).

Mular and Jull (1978) developed empirical formulae from the graphical information for "typical" cyclones, relating d_{50} to the operating variables for cyclones of varying diameter.

A "typical" cyclone has an inlet area of about 7% of the cross-sectional area of the feed chamber, a vortex finder of diameter 35–40% of the cyclone diameter, and an apex diameter normally not less than 25% of the vortex-finder diameter.

The equation for the cyclone cut-point is:

$$d_{50(c)} = \frac{0.77 D_c^{1.875}}{Q^{0.6}(S-1)^{0.5}} \times \frac{\exp(-0.301 + 0.0945V - 0.00356V^2 + 0.0000684V^3)}{Q^{0.6}(S-1)^{0.5}} \qquad (9.24)$$

Equations such as these have been used in computer-controlled grinding circuits to infer cut-points from measured data, but their use in this respect is declining with the increased application of on-line particle size monitors (Chapter 4). Their great value, however, is in the design and optimisation of circuits employing cyclones by the use of computer simulation. For instance, Krebs Engineers applied mathematical models to a grinding-classification circuit and predicted that two-stage cycloning, as opposed to the more common single stage, would allow a 6% increase in grinding circuit throughput. Without the aid of cyclone modelling, such work would be costly and time-consuming.

The equations can also be very valuable in the selection of cyclones for a particular duty, the final control of cut-point and capacity made by adjusting the size of inlet, vortex-finder, and apex.

For example, consider a primary grinding mill, fed with ore (sp. gr. 3.7 g cm^{-3}) at the rate of 201.5 t h^{-1}. The mill is to be in closed circuit with cyclones, to produce a circulating load of 300% and a cut-point of 74 μm.

The total cyclone feed is therefore 806 t h^{-1}. Assuming 50% solids in the cyclone feed, then the slurry density (Equation 3.6) is 1.574 kg l^{-1}, and the volumetric flow rate to the cyclones (Equation 3.7) is 1024 m^3 h^{-1}.

The volumetric % solids in the feed is 1.574 × 50/3.7 = 21.3%. Combining Equations 9.19 and 9.24:

$$d_{50(c)} = \frac{12.67 D_c^{0.675}}{P^{0.3}(S-1)^{0.5}} \times \frac{\exp(-0.301 + 0.0945V - 0.00356V^2 + 0.0000684V^3)}{P^{0.3}(S-1)^{0.5}} \qquad (9.25)$$

For a cyclone cutting at 74 μm ($d_{50(c)}$) operating at a pressure of, say, 12 psi (82.74 kPa), D_c = 66 cm. Therefore, 660 mm cyclones, or their nearest manufactured equivalent, would probably be chosen; final adjustments to the cut-size being made by changing the vortex-finder, spigot openings, pressure, etc.

The maximum volume handled by 660 mm cyclones at 12 psi is 372.5 m^3 (Equation 9.20), so three cyclones would be required to handle the total flow rate.

Factors affecting cyclone performance

The empirical models and scale-up correlations, tempered by experience, are helpful in summarising the effects of operating and design variables on cyclone performance. The following process trends generally hold true:

Cut-size (inversely related to solids recovery)
- Increases with cyclone diameter
- Increases with feed solids concentration and/or viscosity

Decreases with flow rate
Increases with small apex or large vortex finder
Increases with cyclone inclination to vertical

Classification efficiency
Increases with correct cyclone size selection
Decreases with feed solids concentration and/or viscosity
Increased by limiting water to underflow
Increased by certain geometries

Flow split of water to under flow
Increases with larger apex or smaller vortex finder
Decreases with flow-rate
Decreases with inclined cyclones (especially low pressure)
Increases with feed solids concentration and/or viscosity

Flow rate
Increases with pressure
Increases with cyclone diameter
Decreases (at a given pressure) with feed solids concentration and/or viscosity

Since the operating variables have an important effect on the cyclone performance, it is necessary to avoid fluctuations in flow rate, etc., during operation. Pump surging should be eliminated either by automatic control of level in the sump, or by a self-regulating sump, and adequate surge capacity should be installed to eliminate flow rate fluctuations.

The feed flow rate and the pressure drop across the cyclone are closely related (Equation 9.19). The value of the pressure drop is required to permit design of the pumping system for a given capacity or to determine the capacity for a given installation. Usually the pressure drop is determined from a feed-pressure gauge located on the inlet line some distance upstream from the cyclone. Within limits, an increase in feed flow rate will improve fine particle efficiency by increasing the centrifugal force on the particles. All other variables being constant, this can only be achieved by an increase in pressure and a corresponding increase in power, since this is directly related to the product of pressure drop and capacity. Since increase in feed rate, or pressure drop, increases the centrifugal force effect, finer particles are carried to the underflow, and d_{50} is decreased, but the change has to be large to have a significant effect. Figure 9.21 shows the effect of pressure on the capacity and cut-point of cyclones.

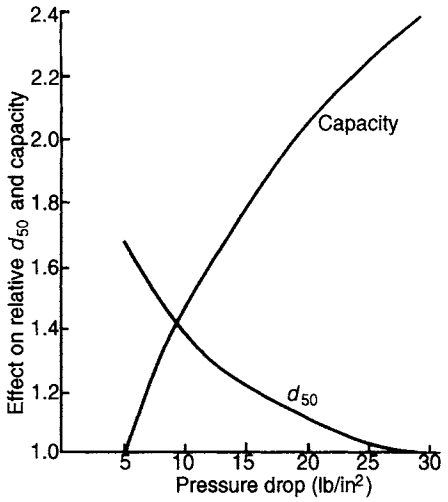


Figure 9.21 Effect of pressure on capacity and cut-point of hydrocyclones

The effect of increase in feed pulp density is complex, as the effective pulp viscosity and degree of hindered settling is increased within the cyclone. The sharpness of the separation decreases with increasing pulp density and the cut-point rises due to the greater resistance to the swirling motion within the cyclone, which reduces the effective pressure drop. Separation at finer sizes can only be achieved with feeds of low solids content and large pressure drop. Normally, the feed concentration is no greater than about 30% solids by weight, but for closed-circuit grinding operations, where relatively coarse separations are often required, high feed concentrations of up to 60% solids by weight are often used, combined with low-pressure drops, often less than 10 psi (68.9 kPa). Figure 9.22 shows that feed concentration has an important effect on the cut-size at high pulp densities.

The shape of the particles in the feed is also an important factor in separation, very flat particles such as mica often reporting to the overflow, even though they are relatively coarse.

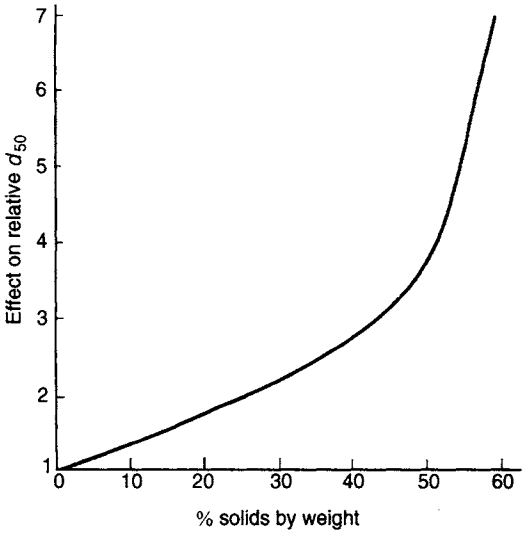


Figure 9.22 Effect of solids concentration on cut-point of hydrocyclones

In practice, the cut-point is mainly controlled by the cyclone design variables, such as inlet, vortex-finder, and apex openings, and most cyclones are designed such that these are easily changed.

The area of the inlet determines the entrance velocity and an increase in area increases the flow rate. Also important is the geometry of the feed inlet. In most cyclones the shape of the entry is developed from circular cross-section to rectangular cross-section at the entrance to the cylindrical section of the cyclone. This helps to "spread" the flow along the wall of the chamber. The inlet is normally tangential, but involuted feed entries are also common (Figure 9.23). Involuted entries are said to minimise turbulence and reduce wear.

Such design differences are reflected in proprietary cyclone developments such as Weir Warman's CAVEX® and Krebs' gMAX® units.

The diameter of the vortex finder is a very important variable. At a given pressure drop across the cyclone, an increase in the diameter of the vortex finder will result in a coarser cut-point and an increase in capacity.

The size of the apex, or spigot opening, determines the underflow density, and must be large enough to discharge the coarse solids that are being separated by the cyclone. The orifice must also permit the entry of air along the axis of the cyclone in order to establish the air vortex. Cyclones should be operated at the highest possible underflow density, since unclassified material leaves the underflow in proportion to the fraction of feed water leaving via the underflow. Under correct operating conditions, the discharge should form a hollow cone spray with a 20–30° included angle (Figure 9.24). Air can then enter the cyclone, the classified coarse particles will discharge freely, and solids concentrations greater than 50% by weight can be achieved. Too small an apex opening can lead to the condition known as "roping", where an extremely thick pulp stream of the same diameter as the apex is formed, and the air vortex may be lost, the separation efficiency will fall, and oversize material will discharge through the vortex finder. (This condition is sometimes encouraged where a very high underflow solids concentration is required, but is otherwise deleterious). Too large an apex orifice results in the larger hollow cone pattern seen in Figure 9.24. The underflow will be excessively dilute and the additional water will carry unclassified fine solids that would otherwise report to the overflow.

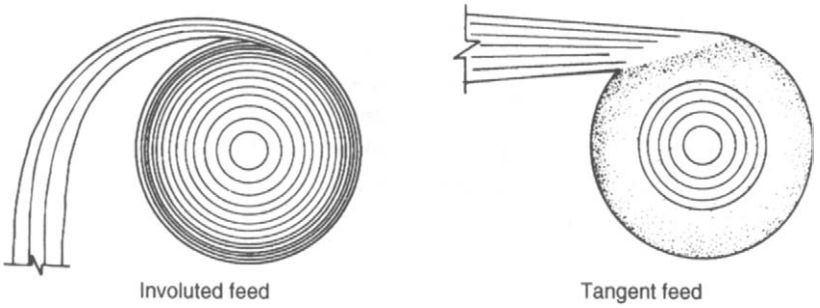


Figure 9.23 Involuted and tangential feed entries

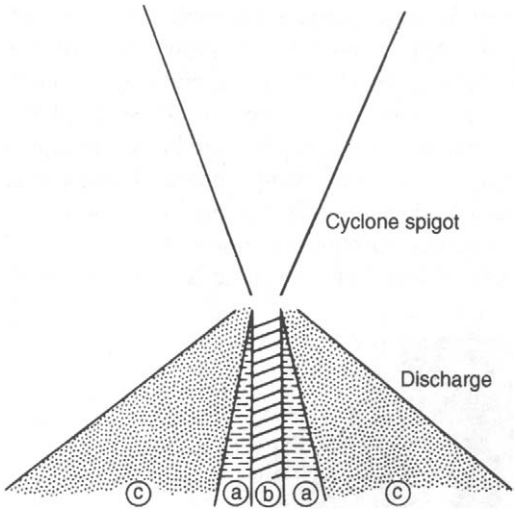


Figure 9.24 Effect of spigot size on cyclone underflow: zone (a), correct operation; zone (b), "roping" – spigot too small; zone (c), excessively dilute – spigot too large

Some investigators have concluded that the cyclone diameter has no effect on the cut-point and that for geometrically similar cyclones the efficiency curve is a function only of the feed material characteristics; the inlet and outlet diameters are the critical design variables, the cyclone diameter merely being the size of the housing required to accommodate these apertures (Lynch et al., 1974; 1975; Rao et al., 1976). This is true where the inlet and outlet diameters are essentially proxies for cyclone diameter for geometrically similar cyclones. However, from theoretical considerations, it is the cyclone diameter which controls the radius of orbit and thus the centrifugal force acting on the particles. As there is a strong interdependence between the aperture sizes and cyclone diameter, it is difficult to distinguish the true effect, and Plitt (1976) concludes that the cyclone diameter has an independent effect on separation size.

For geometrically similar cyclones at constant flow rate, $d_{50} \propto \text{diameter}^x$, but the value of x is open to much debate. The value of x using the Krebs-Mular-Jull model is 1.875, for Plitt's model it is 1.18, and Bradley (1965) concluded that x varies from 1.36 to 1.52. The discussion of Equation 9.21 above suggests $x = 1.54$.

In practice, the cut-point is determined to a large extent by the cyclone size. The size required for a particular application can be estimated from the empirical models developed, but these tend to become unreliable with extremely large cyclones due to the increased turbulence within the cyclone, and it is therefore more common to choose the required model by referring to manufacturers' charts, which show capacity and separation size range in terms of cyclone size. A typical performance chart is shown in Figure 9.25. This is for Krebs cyclones, operating at less than 30% feed solids by weight, and with solids density in the range 2.5–3.2 kg^{-1}.

Since fine separations require small cyclones, which have only small capacity, several have

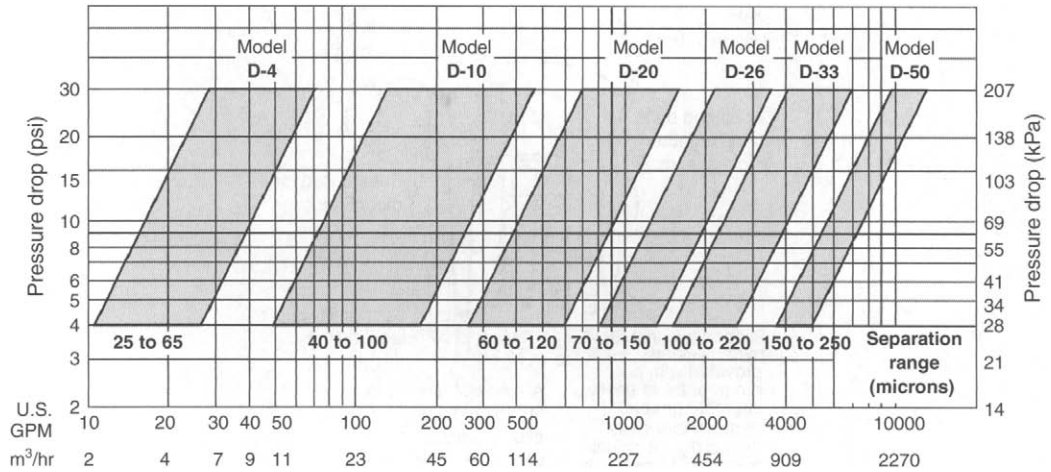


Figure 9.25 Hydrocyclone performance chart (Krebs) (from Napier-Munn et al., 1996; Courtesy JKMRC, The University of Queensland)

to be connected in parallel if high capacity is required (Figure 9.26). Cyclones used for desliming duties are usually of very small diameter, and a large number may be required if substantial flow rates must be handled. The desliming plant at the Mr. Keith Nickel concentrator in Western Australia has 4000 such cyclones. The practical problems of distributing the feed evenly and minimising blockages have been largely overcome by the use of Mozley cyclone assemblies (Anon., 1983). A 16 × 44 mm assembly is shown in Figure 9.27. The feed is introduced into a housing via a central inlet at pressures of up to 50 psi (344.8 kPa). The housing contains an assembly of 16 × 44 mm cyclones, the feed being forced through a trash screen and into each cyclone without the need for separate distributing ports (Figure 9.28). The overflow from each cyclone leaves via the inner

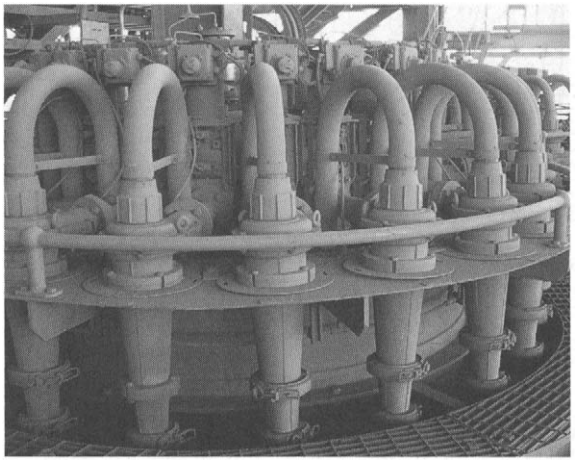


Figure 9.26 A nest of 150 mm cyclones at the Century Zinc mine, Australia (Courtesy JKMRC and JKTech Pty Ltd)

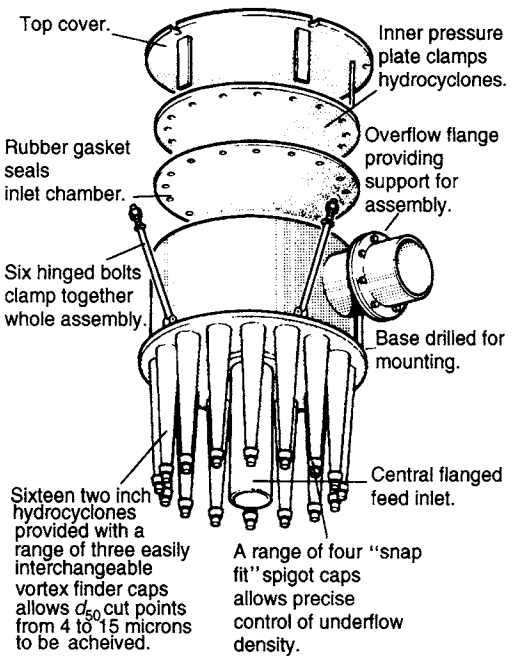


Figure 9.27 Mozley 16 mm × 44 mm cyclone assembly

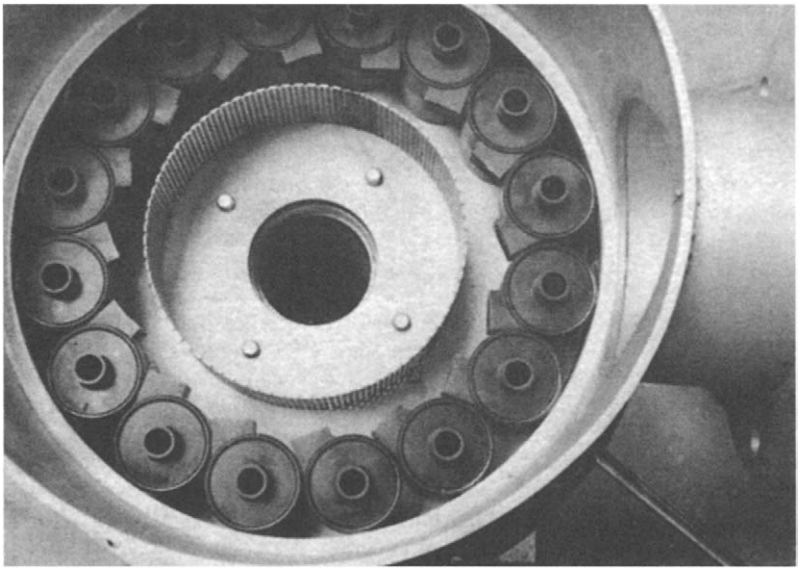


Figure 9.28 Interior of Mozley cyclone assembly

pressure plate, and leaves the housing through the single overflow pipe on the side. The assembly design reduces maintenance to a minimum, the removal of the top cover allowing easy access so that individual cyclones can be removed without disconnecting feed or overflow pipework.

Since separation at large particle size requires large diameter cyclones with consequent high capacities, in many cases, where coarse separations are required, cyclones cannot be utilised, as the plant throughput is not high enough. This is often a problem in pilot plants where simulation of the full-size plant cannot be achieved, as scaling down the size of cyclones to allow for smaller capacity also reduces the cut-point produced.

References

Anon. (1977). *The Sizing of Hydrocyclones*, Krebs Engineers, California.

Anon. (1983). Small diameter hydrocyclones Richard Mozley prominent in UK development, *Ind. Min.* (Jan.), 33.

Anon. (1984). Classifiers Part 2: Some of the major manufacturers of classification equipment used in mineral processing, *Mining Mag.* (Jul.), 40.

Arterburn, R.A. (1982). The sizing and selection of hydrocyclones, in *Design and Installation of Comminution Circuits*, ed. A.L. Mular, and G.V. Jergensen, Vol. 1, Chapter 32, 597–607, AIME.

Asomah, I.K. and Napier-Munn, T.J. (1997). An empirical model of hydrocyclones, incorporating angle of cyclone inclination, *Minerals Eng.*, **10(3)**, 339–347.

Austin, L.G. and Klimpel, R.R. (1981). An improved method for analysing classifier data, *Powder Tech.*, **29**(Jul./Aug.), 227.

Bradley, D. (1965). *The Hydrocyclone*, Pergamon Press, Oxford.

Brennan, M., Subramanian, V., Rong, R.X., Lyman, G.J., Holtham, P.N., and Napier-Munn, T.J. (2003). Towards a new understanding of the cyclone separator, *XXII Int. Min. Proc. Cong.*, Cape Town, Oct.

Flintoff, B.C., Plitt, L.R., and Turak, A.A. (1987). Cyclone modelling: A review of present technology, *CIM Bull.*, **80(905)**, Sept. 39–50.

Hand, P. and Wiseman, D. (2002). Optimisation of moisture adjusted products using spreadsheets, *XIV International Coal Preparation Congress and Exhibition (XIV ICPC)*, SAIMM, Johannesburg, Mar.

Heiskanen, K. (1993). *Particle Classification*, Chapman and Hall, London, 321.

Kawatra, S.K. and Seitz, R.A. (1985). Calculating the particle size distribution in a hydrocyclone product for simulation purposes, *Min. Metall. Proc.*, **2**(Aug.), 152.

Kelsall, D.F. (1953). A further study of the hydraulic cyclone. *Chem. Engng. Sci.*, **2**, 254–272.

King, R.P. (2001). *Modelling and Simulation of Mineral Processing Systems*, Butterworth-Heinemann, Oxford.

Littler, A. (1986). Automatic hindered-settling classifier for hydraulic sizing and mineral beneficiation, *Trans. Inst. Min. Metall.*, **95**(Sept.), C133.

Lynch, A.J., Rao, T.C., and Bailey, C.W. (1975). The influence of design and operating variables on the

capacities of hydrocyclone classifiers, *Int. J. Min. Proc.*, **2**(Mar.), 29.

Lynch, A.J., Rao, T.C., and Prisbrey, K.A. (1974). The influence of hydrocyclone diameter on reduced efficiency curves, *Int. J. Min. Proc.*, **1**(May), 173.

Lynch, A.J. (1977). *Mineral Crushing and Grinding Circuits*, Elsevier, Amsterdam.

Mackie, R.I., et al. (1987). Mathematical model of the Stokes hydrosizer, *Trans. Inst. Min. Metall.*, **96**(Sept.), C130.

Morrison, R.D. and Freeman, N. (1990). Grinding control development at ZC Mines. *Proc. AusIMM*, **295(2)**, Dec., 45–49.

Morrison, R.D. and Morrell, S. (1998). Comparison of comminution circuit energy efficiency using simulation, *SME Annual Meeting*, SME, Orlando (Mar.), Reprint 98–36.

Mular, A.L. and Jull, N.A. (1978). The selection of cyclone classifiers, pumps and pump boxes for grinding circuits, *Mineral Processing Plant Design*, AIMME, New York.

Nageswararao, K. (1995). A generalised model for hydrocyclone classifiers, *AusIMM Proc.*, **2(21)**.

Nageswararao, K, Wiseman, D.M., and Napier-Munn, T.J. (2004). Two empirical hydrocyclone models revisited, *Minerals Engng.*, **17(5)**, May, 671–687.

Napier-Munn, T.J., Morrell, S., Morrison, R.D., and Kojovic, T. (1996). *Mineral Comminution Circuits – Their Operation and Optimisation*, Chapter 12, JKMRC, The University of Queensland, Brisbane, 413 pp.

Nowakowski, A.F., Cullivan, J.C., Williams, R.A., and Dyakowski, T. (2004). Application of CFD to modelling of the flow in hydrocyclones. Is this a realisable option or still a research challenge? *Minerals Engng.*, **17(5)**, 661–669.

Olson, T.J. and Turner, P.A. (2002). Hydrocyclone selection for plant design, *Proc. Min. Proc. Plant Design, Practice and Control*, Vancouver, ed. Mular, Halbe, and Barratt, SME (Oct.), 880–893.

Osborne, D.G. (1985). Fine coal cleaning by gravity methods: a review of current practice. *Coal Prep.*, **2**, 207–242.

Plitt, L.R. (1976). A mathematical model of the hydrocyclone classifier, *CIM Bull.*, **69**(Dec.), 114.

Rao, T.C., Nageswararao, K., and Lynch, A.J. (1976). Influence of feed inlet diameter on the hydrocyclone behaviour, *Int. J. Min. Proc.*, **3**(Dec.), 357.

Renner, V.G. and Cohen, H.E. (1978). Measurement and interpretation of size distribution of particles within a hydrocyclone, *Trans. IMM*, Sec. C, **87**(June), 139.

Smith, V.C. and Swartz, C.L.E. (1999). Development of a hydrocyclone product size soft-sensor. *Control and Optimisation in Minerals, Metals and Materials Processing*, Proc. Int. Symp. at 38th Ann. Conf. Mets. of CIM, Quebec, Aug. ed. D. Hodouin et al., Can. Inst. Min. Metall. Pet., 59–70.

Stokes, G.G. (1891). *Mathematical and Physical Paper III*, Cambridge University Press.

Svarovsky, L. (1984). *Hydrocyclones*, Holt, Rinehart & Winston Ltd, Eastbourne.

Swanson, V.F. (1989). Free and hindered settling, *Min. Metall. Proc.*, **6**(Nov.), 190.

Taggart, A.F. (1945). *Handbook of Mineral Dressing*, Wiley, New York.

10

Gravity concentration

Introduction

Gravity methods of separation are used to treat a great variety of materials, ranging from heavy metal sulphides such as galena (sp. gr. 7.5) to coal (sp. gr. 1.3), at particle sizes in some cases below 50 μm.

These methods declined in importance in the first half of the twentieth century due to the development of the froth-flotation process, which allows the selective treatment of low-grade complex ores. They remained, however, the main concentrating methods for iron and tungsten ores and are used extensively for treating tin ores, coal and many industrial minerals.

In recent years, many companies have re-evaluated gravity systems due to increasing costs of flotation reagents, the relative simplicity of gravity processes, and the fact that they produce comparatively little environmental pollution. Modern gravity techniques have proved efficient for concentration of minerals having particle sizes in the 50 μm range and, when coupled with improved pumping technology and instrumentation, have been incorporated in high-capacity plants (Holland-Batt, 1998). In many cases a high proportion of the mineral in an orebody can at least be pre-concentrated effectively by cheap and ecologically acceptable gravity systems; the amount of reagents and fuel used can be cut significantly when the more expensive methods are restricted to the processing of gravity concentrate. Gravity separation of minerals at coarser sizes as soon as liberation is achieved can also have significant advantages for later treatment stages due to decreased surface area, more efficient dewatering, and the absence of adhering chemicals which could interfere with further processing.

Gravity techniques to recover residual valuable heavy minerals in flotation tailings are being increasingly used. Apart from current production, there are many large tailings dumps which could be excavated cheaply and processed to give high value concentrates using recently developed technology.

Principles of gravity concentration

Gravity concentration methods separate minerals of different specific gravity by their relative movement in response to gravity and one or more other forces, the latter often being the resistance to motion offered by a viscous fluid, such as water or air.

It is essential for effective separation that a marked density difference exists between the mineral and the gangue. Some idea of the type of separation possible can be gained from the *concentration criterion*

$$\frac{D_h - D_f}{D_l - D_f} \qquad (10.1)$$

where D_h is the specific gravity of the heavy mineral, D_l is the specific gravity of the light mineral, and D_f is the specific gravity of the fluid medium.

In very general terms, when the quotient is greater than 2.5, whether positive or negative, then gravity separation is relatively easy, the efficiency of separation decreasing as the value of the quotient decreases.

The motion of a particle in a fluid is dependent not only on its specific gravity, but also on its size (Chapter 9); large particles will be affected more than smaller ones. The efficiency of gravity processes therefore increases with particle size, and

the particles should be sufficiently coarse to move in accordance with Newton's law (Equation 9.6). Particles which are so small that their movement is dominated mainly by surface friction respond relatively poorly to commercial high-capacity gravity methods. In practice, close size control of feeds to gravity processes is required in order to reduce the size effect and make the relative motion of the particles specific gravity-dependent.

Gravity separators

Many different machines have been designed and built in the past to effect separation of minerals by gravity, and they are comprehensively reviewed by Burt (1985). Many gravity devices have become obsolete, and only equipment that is used in modern mills will be described in this chapter. Contact details for manufacturers of gravity concentrators can be found in the annual Buyer's Guide of products and services published by Mining Magazine in December each year.

A classification of the more commonly used gravity separators on the basis of feed size range is shown in Figure 1.8.

The dense medium separation (DMS) process is widely used to preconcentrate crushed material prior to grinding and will be considered separately in the next chapter.

It is essential for the efficient operation of all gravity separators that the feed is carefully prepared. Grinding is particularly important in adequate liberation; successive regrinding of middlings is required in most operations. Primary grinding should be performed where possible in open-circuit rod mills, but if fine grinding is required, closed-circuit ball milling should be used, preferably with screens closing the circuits rather than hydrocyclones in order to reduce selective overgrinding of heavy friable valuable minerals.

Gravity separators are extremely sensitive to the presence of *slimes* (ultra-fine particles), which increase the viscosity of the slurry and hence reduce the sharpness of separation, and obscure visual cut-points. It is common practice in most gravity concentrators to remove particles less than about 10 μm from the feed, and divert this fraction to the tailings, and this can account for considerable loss of values. De-sliming is often achieved by the use of hydrocyclones, although if hydraulic classifiers are used to prepare the feed it may be preferable to de-slime at this stage, since the high shear forces produced in hydrocyclones tend to cause degradation of friable minerals.

The feed to jigs, cones, and spirals should, if possible, be screened before separation takes place, each fraction being treated separately. In most cases, however, removal of the oversize by screening, in conjunction with de-sliming, is adequate. Processes which utilise flowing-film separation, such as shaking tables and tilting frames, should always be preceded by good hydraulic classification in multi-spigot hydrosizers.

Although most slurry transportation is achieved by centrifugal pumps and pipelines, as much as possible should be made of natural gravity flow; many old gravity concentrators were built on hillsides to achieve this. Reduction of slurry pumping to a minimum not only reduces energy consumption, but also reduces slimes production in the circuit. To minimise degradation of friable minerals, slurry pumping velocities should be as low as possible, consistent with maintaining the solids in suspension.

One of the most important aspects of gravity circuit operations is correct water balance within the plant. Almost all gravity concentrators have an optimum feed pulp-density, and relatively little deviation from this density causes a rapid decline in efficiency. Accurate pulp-density control is therefore essential, and this is most important on the raw feed. Automatic density control should be used where possible, and the best way of achieving this is by the use of nucleonic density gauges (Chapter 3) controlling the water addition to the new feed. Although such instrumentation is expensive, it is usually economic in the long term. Control of pulp density within the circuit can be made by the use of settling cones preceding the gravity device. These thicken the pulp, but the overflow often contains solids, and should be directed to a central large sump or thickener. For substantial increase in pulp density, hydrocyclones or thickeners may be used. The latter are the more expensive, but produce less particle degradation and also provide substantial surge capacity. It is usually necessary to recycle water in most plants, so adequate thickener or cyclone capacity should be provided, and slimes build-up in the recycled water must be minimised.

If the ore contains an appreciable amount of sulphide minerals then, if the primary grind is finer than about 300 μm, these should be removed by froth flotation prior to gravity concentration, as they reduce the performance of spirals, tables, etc. If the primary grind is too coarse for effective sulphide flotation, then the gravity concentrate must be reground prior to removal of the sulphides. The sulphide flotation tailing is then usually cleaned by further gravity concentration.

The final gravity concentrate often needs cleaning by magnetic separation, leaching, or some other method, in order to remove other mineral contaminants. For instance, at the South Crofty tin mine in Cornwall, the gravity concentrate was subjected to cleaning by magnetic separators, which removed wolframite from the cassiterite product.

The design and optimisation of gravity circuits is discussed by Wells (1991).

Jigs

Jigging is one of the oldest methods of gravity concentration, yet the basic principles are only now beginning to be understood. A mathematical model developed by Jonkers et al. (1998) shows considerable promise in predicting jig performance on a size by density basis.

The jig is normally used to concentrate relatively coarse material and, if the feed is fairly closed sized (e.g. 3–10 mm), it is not difficult to achieve good separation of a fairly narrow specific gravity range in minerals in the feed (e.g. fluorite, sp. gr. 3.2, from quartz, sp. gr. 2.7). When the specific gravity difference is large, good concentration is possible with a wider size range. Many large jig circuits are still operated in the coal, cassiterite, tungsten, gold, barytes, and iron-ore industries. They have a relatively high unit capacity on classified feed and can achieve good recovery of values down to 150 μm and acceptable recoveries often down to 75 μm. High proportions of fine sand and slime interfere with performance and the fines content should be controlled to provide optimum bed conditions.

In the jig the separation of minerals of different specific gravity is accomplished in a bed which is rendered fluid by a pulsating current of water so as to produce stratification. The aim is to dilate the bed of material being treated and to control the dilation so that the heavier, smaller particles penetrate the interstices of the bed and the larger high specific gravity particles fall under a condition probably similar to hindered settling (Lyman, 1992).

On the pulsion stroke the bed is normally lifted as a mass, then as the velocity decreases it tends to dilate, the bottom particles falling first until the whole bed is loosened. On the suction stroke it then closes slowly again and this is repeated at every stroke, the frequency usually varying between 55 and 330 c min^{-1}. Fine particles tend to pass through the interstices after the large ones have become immobile. The motion can be obtained either by using a fixed sieve jig, and pulsating the water, or by employing a moving sieve, as in the simple hand-jig (Figure 10.1).

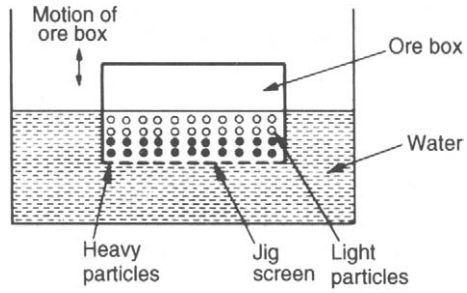


Figure 10.1 Hand jig

The jigging action

It was shown in Chapter 9 that the equation of motion of a particle settling in a viscous fluid is

$$m\,dx/dt = mg - m'g - D \qquad (9.1)$$

where m is the mass of the mineral grain, dx/dt is the acceleration, g is the acceleration due to gravity, m' is the mass of displaced fluid, and D is the fluid resistance due to the particle movement.

At the beginning of the particle movement, since the velocity x is very small, D can be ignored as it is a function of velocity.

Therefore

$$dx/dt = \left(\frac{m - m'}{m}\right) g \qquad (10.2)$$

and since the particle and the displaced fluid are of equal volume,

$$dx/dt = \left(\frac{D_s - D_f}{D_s}\right) g$$
$$= \left(\frac{1 - D_f}{D_s}\right) g \qquad (10.3)$$

where D_s and D_f are the respective specific gravities of the solid and the fluid.

The initial acceleration of the mineral grains is thus independent of size and dependent only on the densities of the solid and the fluid. Theoretically, if the duration of fall is short enough and the repetition of fall frequent enough, the total distance travelled by the particles will be affected more by the differential initial acceleration, and therefore by density, than by their terminal velocities and therefore by size. In other words, to separate small heavy mineral particles from large light particles a short jigging cycle is necessary. Although relatively short fast strokes are used to separate fine minerals, more control and better stratification can be achieved by using longer, slower strokes, especially with the coarser particle sizes. It is therefore good practice to screen the feed to jigs into different size ranges and treat these separately. The effect of differential initial acceleration is shown in Figure 10.2.

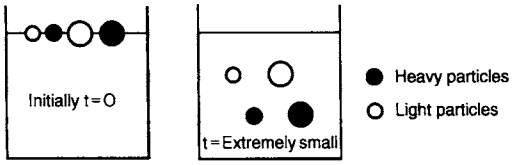


Figure 10.2 Differential initial acceleration

If the mineral particles are examined after a longer time they will have attained their terminal velocities and will be moving at a rate dependent on their specific gravity and size. Since the bed is really a loosely packed mass with interstitial water providing a very thick suspension of high density, hindered-settling conditions prevail, and the settling ratio of heavy to light minerals is higher than that for free settling (Chapter 9). Figure 10.3 shows the effect of hindered settling on the separation.

The upward flow can be adjusted so that it overcomes the downward velocity of the fine light

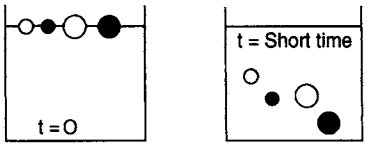


Figure 10.3 Hindered settling

particles and carries them away, thus achieving separation. It can be increased further so that only large heavy particles settle, but it is apparent that it will not be possible to separate the small heavy and large light particles of similar terminal velocity.

Hindered settling has a marked effect on the separation of coarse minerals, for which longer, slower strokes should be used, although in practice, with coarser feeds, it is improbable that the larger particles have time to reach their terminal velocities.

At the end of a pulsion stroke, as the bed begins to compact, the larger particles interlock, allowing the smaller grains to move downwards through the interstices under the influence of gravity. The fine grains may not settle as rapidly during this *consolidation trickling* phase (Figure 10.4) as during the initial acceleration or suspension, but if consolidation trickling can be made to last long enough, the effect, especially in the recovery of the fine heavy minerals, can be considerable.

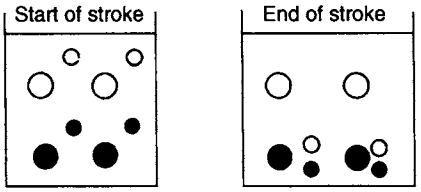


Figure 10.4 Consolidation trickling

Figure 10.5 shows an idealised jigging process by the described phenomena.

In the jig the pulsating water currents are caused by a piston having a movement which is a harmonic waveform (Figure 10.6).

The vertical speed of flow through the bed is proportional to the speed of the piston. When this speed is greatest, the speed of flow through the bed is also greatest (Figure 10.7).

The upward speed of flow increases after point A, the beginning of the cycle. As the speed

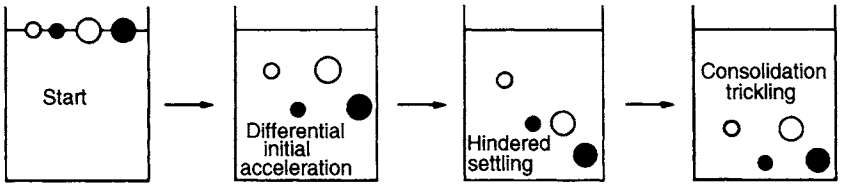


Figure 10.5 Ideal jigging process

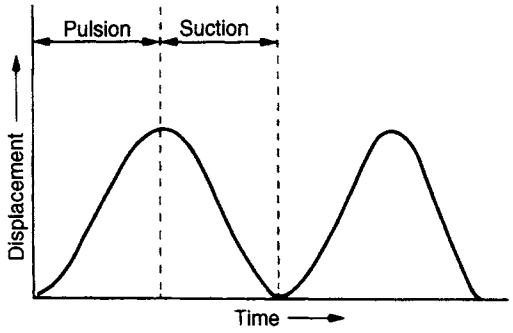


Figure 10.6 Movement of the piston in a jig

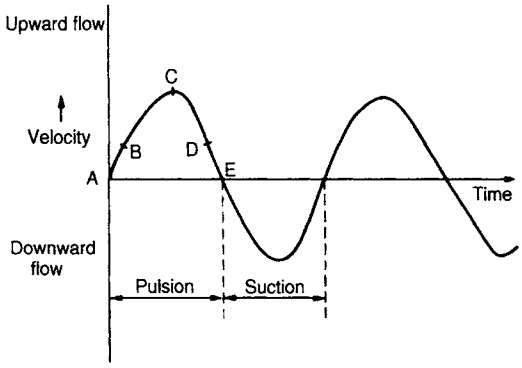


Figure 10.7 Speed of flow through bed during jig cycle

increases, the grains will be loosened and the bed will be forced open, or dilated. At, say, point B, the grains are in the phase of hindered settling in an upward flow, and since the speed of flow from B to C still increases, the fine grains are pushed upwards by the flow. The chance of them being carried along with the top flow into the tailings is then at its greatest. In the vicinity of D, first the coarser grains and later on the remaining fine grains will fall back. Due to the combination of initial acceleration and hindered settling, it is mainly the coarser grains that will lie at the bottom of the bed.

At the point of transition between the pulsion and the suction stroke, at point E, the bed will be compacted. Consolidation trickling can now occur to a limited extent. In a closely sized ore the heavy grains can now penetrate only with difficulty through the bed and may be lost to the tailings. Severe compaction of the bed can be reduced by the addition of *hutch water*, a constant volume of water, which creates a constant upward flow through the bed. This flow, coupled with the varying flow caused by the piston, is shown in Figure 10.8. Thus suction is reduced by hutch-water addition, and is reduced in duration; by adding a large quantity of water, the suction may be entirely eliminated. The coarse ore then penetrates the bed more easily and the horizontal transport of the feed over the jig is also improved. However, fines losses will increase, partly because of the longer duration of the pulsion stroke, and partly because the added water increases the speed of the top flow.

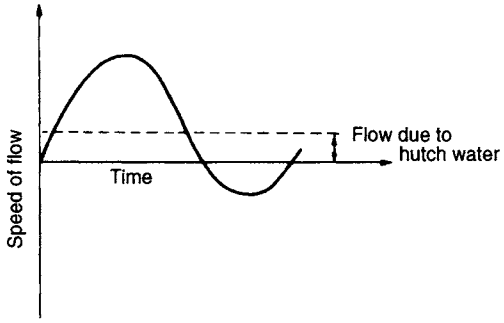


Figure 10.8 Effect of hutch water on flow through bed

Types of jig

Essentially the jig is an open tank filled with water, with a horizontal jig screen at the top, and provided with a spigot in the bottom, or *hutch* compartment, for concentrate removal (Figure 10.9). Current

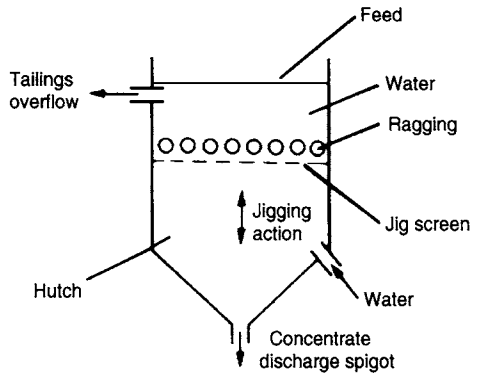


Figure 10.9 Basic jig construction

types of jig are reviewed by Cope (2000). The jig bed consists of a layer of coarse, heavy particles, or *ragging*, placed on the jig screen on to which the slurry is fed. The feed flows across the ragging and the separation takes place in the jig bed so that grains with a high specific gravity penetrate through the ragging and screen to be drawn off as a concentrate, while the light grains are carried away by the cross-flow to be discarded as tailings. The harmonic motion produced by the eccentric drive is supplemented by a large amount of continuously supplied hutch water, which enhances the upward and diminishes the downward velocity of the water (Figure 10.8).

One of the oldest types of jig is the *Harz* (Figure 10.10) in which the plunger moves up and down vertically in a separate compartment. Up to four successive compartments are placed in series in the hutch. A high-grade concentrate is produced in the first compartment, successively lower grades being produced in the other compartments, tailings overflowing the final compartment. If the feed particles are larger than the apertures of the screen, jigging "over the screen" is used, and the concentrate grade is partly governed by the thickness of the bottom layer, determined by the rate of withdrawal through the concentrate discharge port.

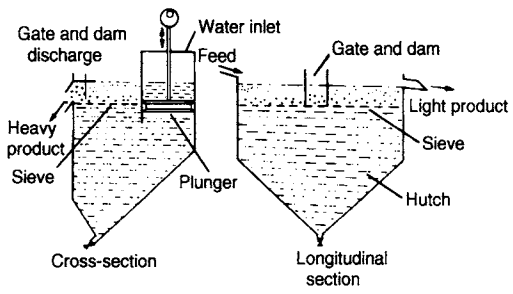


Figure 10.10 Harz jig

The *Denver mineral jig* (Figure 10.11) is widely used, especially for removing heavy minerals from closed grinding circuits, thus preventing overgrinding. The rotary water valve can be adjusted so as to open at any desired part of the jig cycle, synchronisation between the valve and the plungers being achieved by a rubber timing belt. By suitable adjustment of the valve, any desired variation can be achieved, from complete neutralisation of the suction stroke with hydraulic water to a full balance between suction and pulsion.

Conventional mineral jigs consist of square or rectangular tanks, sometimes combined to form two, three, or four cells in series. In order to compensate for the increase in cross-flow velocity over the jig bed, caused by the addition of hutch water, trapezoidal-shaped jigs were developed. By arranging these as sectors of a circle, the modular *circular*, or *radial*, jig was introduced, in which the feed enters in the centre and flows radially over the jig bed towards the tailings discharge at the circumference (Figure 10.12).

The main advantage of the circular jig is its very large capacity, and *IHC Radial Jigs* (Figure 10.13) have been installed on most newly built tin dredges in Malaysia and Thailand since their development in 1970. They are also in use for the treatment of gold, diamonds, iron ore, etc., the largest, of 7.5 m in diameter, being capable of treating up to $300\,m^3\,h^{-1}$ of feed with a maximum particle size of 25 mm. In the IHC jig, the harmonic motion of the conventional eccentric-driven jig is replaced by an asymmetrical "saw-tooth" movement of the diaphragm, with a rapid upward, followed by a slow downward, stroke (Figure 10.14). This produces a much larger and more constant suction stroke, giving the finer particles more time to settle in the bed, thus reducing their loss to tailings, the jig being capable of accepting particles as fine as 60 microns.

The *InLine Pressure Jig (IPJ)* is a recent Australian development in jig technology which is finding wide application for the recovery of free gold, sulphides, native copper, tin/tantalum, diamonds and other minerals (Figure 10.15). The IPJ is unique in that it is fully encapsulated and pressurised, allowing it to be completely filled with

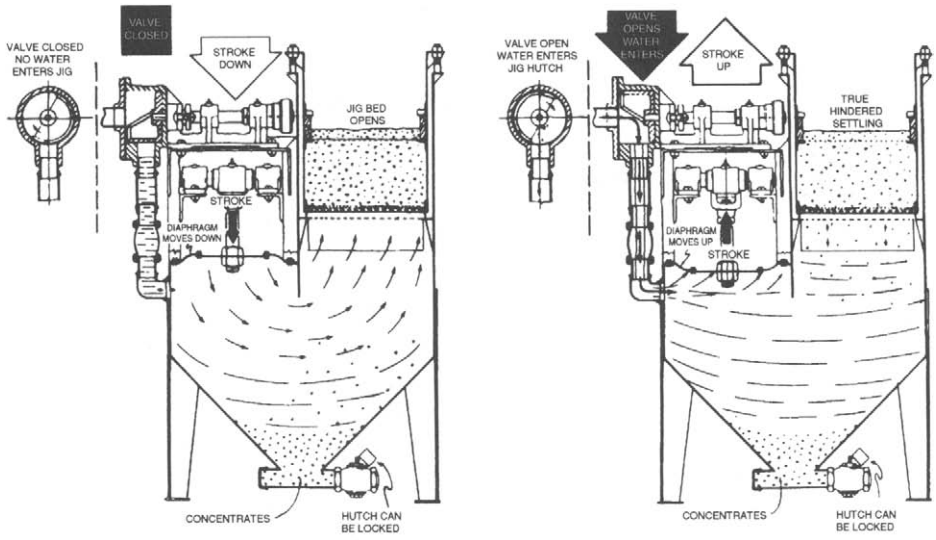


Figure 10.11 Denver mineral jig

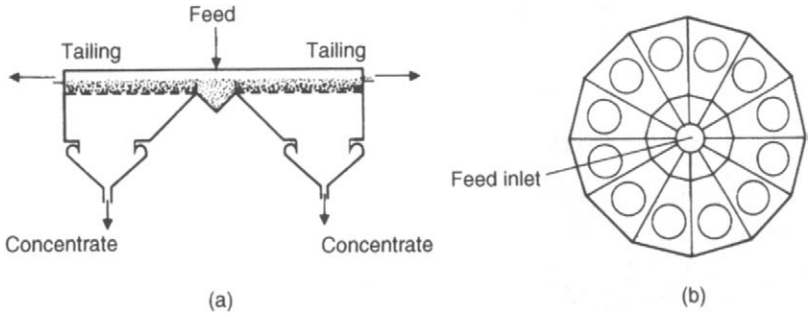


Figure 10.12 (a) Outline of circular jig; (b) radial jig up to twelve modules

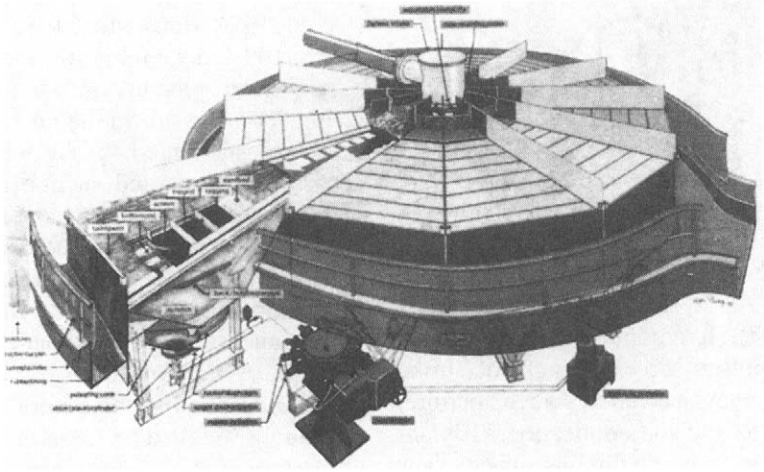


Figure 10.13 IHC modular radial jig

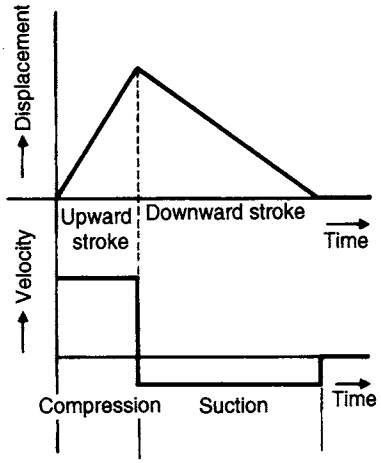


Figure 10.14 IHC jig drive characteristics

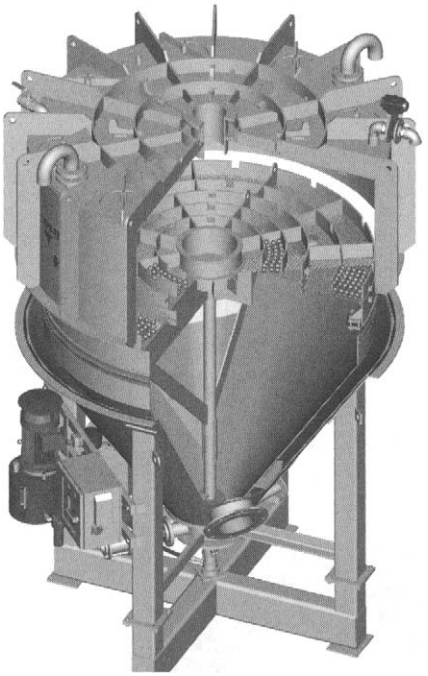


Figure 10.15 The Gekko Systems Inline Pressure Jig (Courtesy Gekko Systems)

slurry (Gray, 1997). It combines a circular bed with a vertically pulsed screen. Length of stroke and pulsation frequency, as well as screen aperture, can all be altered to suit the application. IPJs are typically installed in grinding circuits, where their low water requirements allow operators to treat the full circulating load, maximising recovery of liberated values. Both concentrates and tailings are discharged under pressure.

In an attempt to recover fine particles using gravity concentration methods, jigs have been developed to make use of centrifugal force. Such jigs have all the elements of a standard jig except that the bed of mineral is rotated at high speed while being pulsed. The *Kelsey Centrifugal Jig* (KCJ) takes a conventional jig and spins it in a centrifuge. The ability to change the apparent gravitational field is a major departure in the recovery of fine minerals. The main operating variables which are adjusted to control processing of different types of material are centrifugal force, ragging material, and size distribution. The 16 hutch J1800 KCJ can treat over 100 t/h, depending on the application. The use of a J650 KCJ in tin recovery is described by Beniuk et al. (1994).

Coal jigs

Jigs are widely used coal-cleaning devices, and are preferred to the more expensive dense medium process when the coal has relatively little middlings, or "near-gravity" material, as is often the case with British coals. No feed preparation is required, as is necessary with DMS, and for coals which are easily washed, i.e. those consisting predominantly of liberated coal and denser rock particles, the lack of close density control is not a disadvantage.

Two types of air-pulsated jig – *Baum* and *Batac* – are used in the coal industry. The standard Baum jig (Figure 10.16), with some design modifications (Green, 1984; Harrington, 1986), has been used for nearly 100 years, and is still the dominant device.

Air under pressure is forced into a large air chamber on one side of the jig vessel causing pulsations and suction to the jig water, which in turn causes pulsations and suction through the screen plates upon which the raw coal is fed, thus causing stratification. Various methods are used to continuously separate the refuse from the lighter coal product, and all the modern Baum jigs are fitted with some form of automatic refuse extraction (Adams, 1983). One form of control incorporates a float immersed in the bed of material. The float is suitably weighed to settle on the dense layer of refuse moving across the screen plates. An increase in the depth of refuse raises the float, which automatically controls the refuse discharge, either by

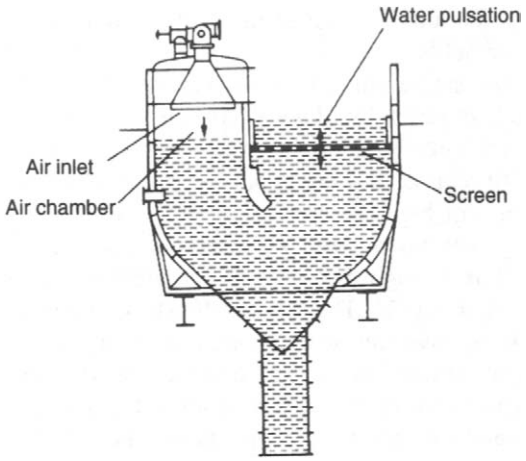


Figure 10.16 Baum jig

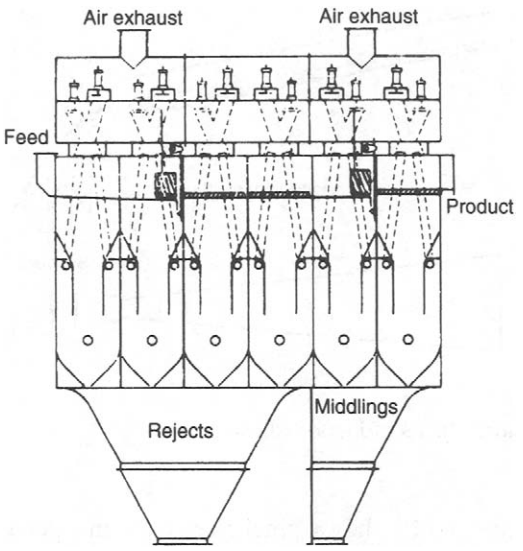


Figure 10.17 Batac jig

adjusting the height of a moving gate, or by controlling the pulsating water which lifts the rejects over a fixed weir plate (Wallace, 1979). This system is reported to respond quickly and accurately.

In Britain it is now commonplace for the automatic control system to determine the variations in refuse bed thickness by measuring the differences in water pressure under the screen plates arising from the resistance offered to pulsation. The JigScan control system developed at the Julius Kruttschnitt Mineral Research Centre measures bed conditions and pulse velocity many times within the pulse using pressure sensing and nucleonic technology (Loveday and Jonkers, 2002). Evidence of a change in the pulse is an indicator of a fundamental problem with the jig, allowing the operator to take corrective action. Increased yields of greater than 2 per cent have been reported for JigScan-controlled jigs.

In many situations the Baum jig still performs satisfactorily, with its ability to handle large tonnages (up to $1000\,t\,h^{-1}$) of coal of a wide size range. However, the distribution of the stratification force, being on one side of the jig, tends to cause unequal force along the width of jig screen and therefore uneven stratification and some loss in the efficiency of separation of the coal from its heavier impurities. This tendency is not so important in relatively narrow jigs, and in the United States multiple float and gate mechanisms have been used to counteract the effects. The *Batac jig* (Zimmerman, 1975) is also pneumatically operated (Figure 10.17), but has no side air chamber like the Baum jig. Instead, it is designed with a series of multiple air chambers, usually two to a cell, extending under the jig for its full width, thus giving uniform air distribution. The jig uses electronically controlled air valves which provide a sharp cut-off of the air input and exhaust. Both inlet and outlet valves are infinitely variable with regard to speed and length of stroke, allowing for the desired variation in pulsation and suction by which proper stratification of the bed may be achieved for differing raw coal characteristics. As a result, the Batac jig can wash both coarse and fine sizes well (Chen, 1980). The jig has also been successfully utilised to produce high-grade lump ore and sinter-feed concentrates from such iron ore deposits which cannot be upgraded by heavy-medium techniques (Hasse and Wasmuth, 1988; Miller, 1991).

Pinched sluices and cones

Pinched sluices of various forms have been used for heavy mineral separations for centuries. In its simplest form (Figure 10.18), it is an inclined launder about 1 m long, narrowing from about 200 mm in width at the feed end to about 25 mm at the discharge. Pulp of between 50 and 65% solids enters gently and stratifies as it descends; at the discharge end these strata are separated by various means, such as by splitters, or by some type of tray (Sivamohan and Forssberg, 1985b).

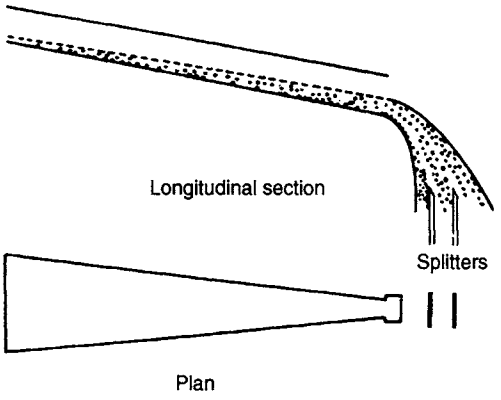


Figure 10.18 Pinched sluice

Figure 10.19 shows pinched sluices in operation on an Australian heavy mineral sand concentrator. The fundamental basis for gravity concentration in sluices is described by Schubert (1995).

The *Reichert cone* is a wet gravity concentrating device designed for high-capacity applications. Its principle of operation is similar to that of a pinched sluice, but the pulp flow is not restricted or influenced by side-wall effect, which is somewhat detrimental to pinched-sluice operation.

The Reichert cone concentrator was developed in Australia in the early 1960s primarily to treat titanium-bearing beach sands, and the success of cone circuits has led to their application in many other fields.

The single unit comprises several cone sections stacked vertically (Figure 10.20), so as to permit several stages of upgrading. The cones are made of fibreglass and are mounted in circular frames over 6 m high. Each cone is 2 m in diameter and there are no moving parts in the unit. A cross-section through a Reichert cone system is shown in Figure 10.21. The system shown is one of many possible systems using double and single cones, together with trays, which direct heavy mineral fractions from the centre draw-off areas of the cones to external collection boxes and also serve to further upgrade the fraction, acting as a sort of pinched sluice.

The feed pulp is distributed evenly around the periphery of the cone. As it flows towards the centre of the cone the heavy particles separate to the bottom of the film. This concentrate is removed by an annular slot in the bottom of the concentrating cone; the part of the film flowing over the slot is the tailings. The efficiency of this separation process is relatively low and is repeated a number of times within a single machine to achieve effective performance. A typical machine system for rougher concentration duties will consist of four double single-cone stages in series, each retreating the tailings of the preceding stage. This machine

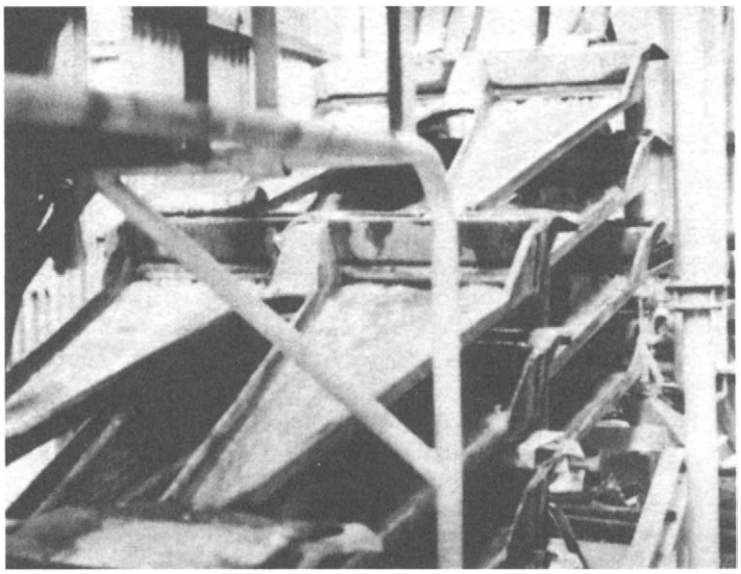


Figure 10.19 Pinched sluices in operation

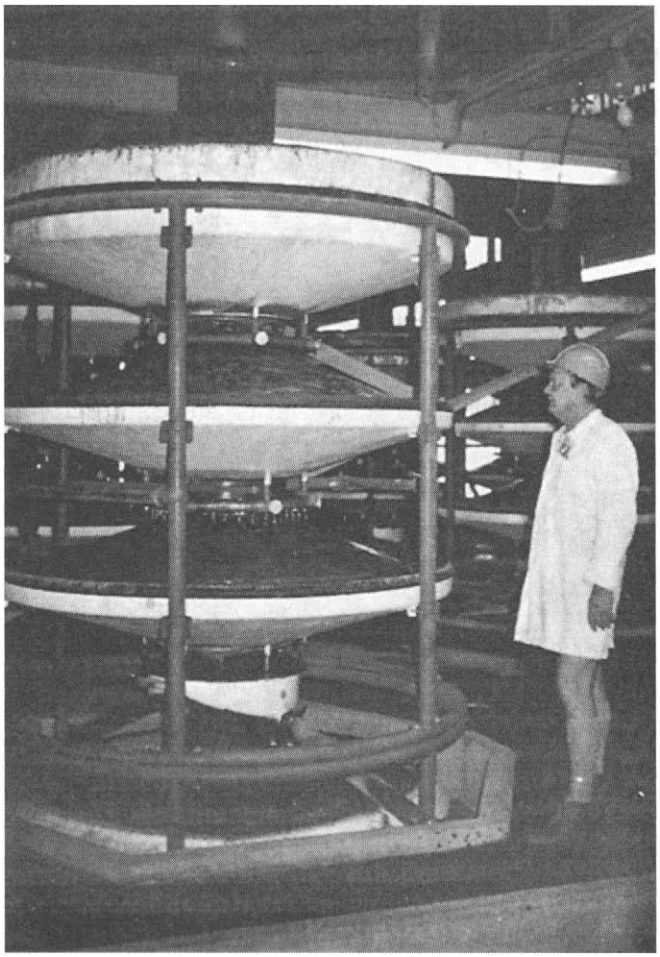


Figure 10.20 Reichert cones

will produce a concentrate from the upper three stages and the product from the fourth stage as middlings (Anon., 1977). A cone concentration system can be set to produce a marked reverse classification effect, in that the slots tend to reject coarser, lighter particles to tailings, while retaining finer, heavier particles in the concentrate flows.

Reichert cones have a high capacity, operating normally in the range 65–90 $t\,h^{-1}$, but in exceptional cases this can be from 40 to 100 $t\,h^{-1}$, with a feed density of between 55 and 70% solids by weight. They accept feeds of up to 3 mm in size and can treat material as fine as 30 μm, although they are most efficient in the 100–600 μm size range (Forssberg and Sandström, 1979). In recent years the capacity of cones has been increased by increasing the cone diameter to 3.5 m. The longer deck not only provides improved throughput but also greater upgrading per cone. The equivalent overall metallurgical performance can be achieved using fewer stages in a 3.5 m diameter cone (Richards and Palmer, 1997).

The success of cone circuits in the Australian mineral sand industry has led to their application in other fields. Preconcentration of tin and gold, the recovery of tungsten, and the concentration of magnetite are all successful applications. In many of these applications, cones, due to their high capacities and low operating costs, have replaced spirals and shaking tables.

One of the largest single installations is operated at Palabora Mining Co. in South Africa. Sixty-eight Reichert cones treat 34,000 $t\,d^{-1}$ of flotation tailings, after preliminary de-sliming and low intensity

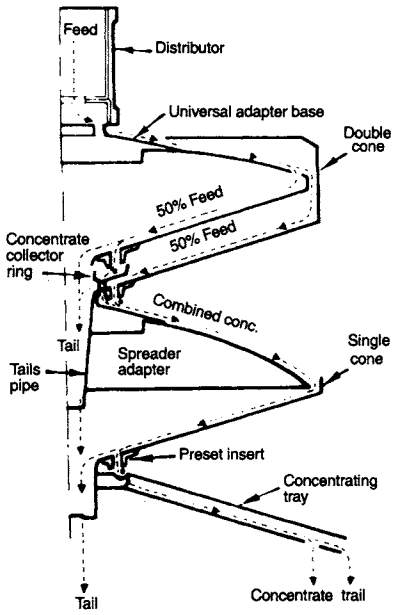


Figure 10.21 Cross-section through Reichert cone concentrator system

magnetic separation for removal of magnetite. A complex circuit consists of 48 rougher-scavenger units, each with a six-cone configuration, and 20 cleaner recleaners with eight-cone configurations

The cone section of the plant produces an upgrading of about 200:1, with a recovery of 85% of +45 μm material. The concentrate is further upgraded on shaking tables to produce final concentrates of uranothorite and baddeleyite.

Cone circuits have been successfully used as preconcentrators ahead of flotation to recover gold and silver values from base metal sulphides in a number of operations in Scandinavia, Papua New Guinea, and Australia.

King (2000) describes the use of the MODSIM flowsheet simulator to evaluate different cone configurations in rougher, scavenger, and cleaner applications.

Spirals

Spiral concentrators have, over numerous years, found many varied applications in mineral processing, but perhaps their most extensive usage has been in the treatment of heavy mineral sand deposits, such as those carrying ilmenite, rutile, zircon, and monazite (see Chapter 13), and in recent years in the recovery of fine coal.

The Humphreys spiral (Figure 10.22) was introduced in 1943, its first commercial application being on chrome-bearing sands (Hubbard et al., 1953). It is composed of a helical conduit of modified semicircular cross-section. Feed pulp of between 15 and 45% solids by weight and in the size range 3 mm to 75 μm is introduced at the top of the spiral and, as it flows spirally downwards, the particles stratify due to the combined effect of centrifugal force, the differential settling rates of the particles, and the effect of interstitial trickling through the flowing particle bed. These mechanisms are complex, being much influenced by the slurry density and particle size. Some workers (Mills, 1978) have reported that the main separation effect is due to hindered settling, with the largest, densest particles reporting preferentially to the concentrate, which forms in a band along the inner edge of the stream (Figure 10.23). Bonsu (1983), however, reported that the net effect is reverse classification, the smaller, denser particles preferentially entering the concentrate band.

Ports for the removal of the higher specific-gravity particles are located at the lowest points in the cross-section. Wash-water, added at the inner edge of the stream, flows outwardly across the concentrate band. The width of concentrate band removed at the ports is controlled by adjustable splitters. The grade of concentrate taken from descending ports progressively decreases, tailings being discharged from the lower end of the spiral conduit.

Until relatively recently, all spirals were very similar, based upon the original Humphreys design, which is now obsolete. However, in recent years, there have been considerable developments in spiral technology, and a wide range of devices are now available. The main areas of development have been in the introduction of spirals with only one concentrate take-off, at the bottom of the spiral, and the use of spirals without added wash water. Wash waterless spirals reportedly offer lower cost, easy operation, and simple maintenance, and have been installed at several gold and tin processing plants. Holland-Batt (1995) discusses the design considerations affecting the pitch of the trough and the trough shape, while the modern high capacity spirals which result from careful design are described by Richards and Palmer (1997).

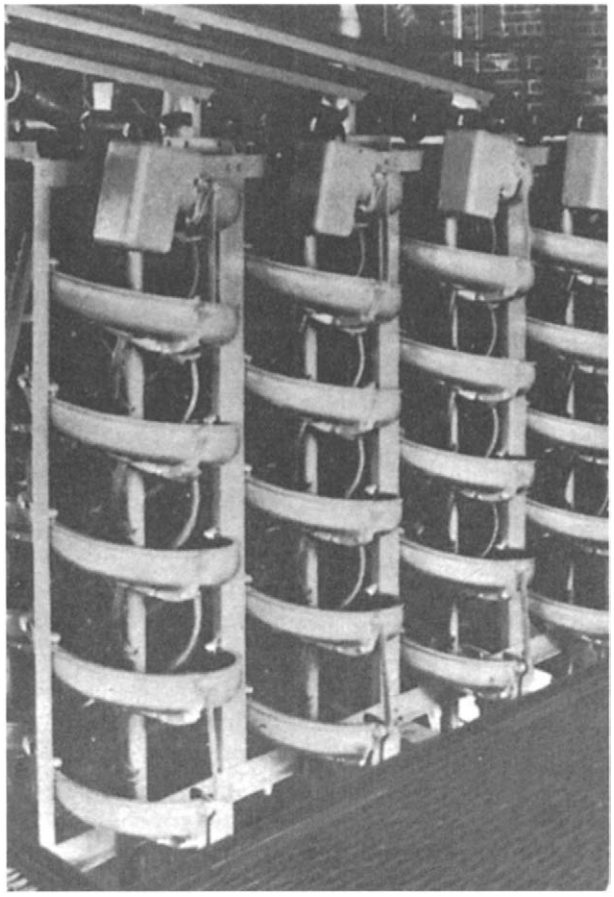


Figure 10.22 Humphreys spiral concentrators

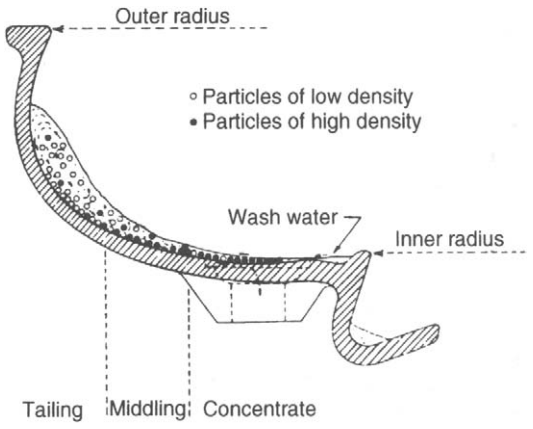


Figure 10.23 Cross-section of spiral stream

A comprehensive semi-empirical mathematical model of the spiral has been developed by Holland-Batt (1989), while a detailed CFD model of the fluid flow has been developed and validated by Matthews et al. (1998).

Improved spiral concentrator design has offered an efficient and economic alternative to the Reichert cone concentrator (Ferree, 1993). Davies et al. (1991) have reviewed the development of new spiral models and describe the mechanism of separation and the effects of operating parameters. Some of the traditional areas of spiral application are described, together with examples of new applications such as treatment of fine alluvials and tailings, and fine coal recovery. One of the most important developments in fine coal washing was the introduction in the 1980s of spiral separators specifically designed for coal. It is common practice to separate down to 0.5 mm coal using dense medium cyclones (Chapter 11), and below this by froth flotation. Spiral circuits have been installed to process the size range which is least effectively

treated by these two methods, typically 0.1–2 mm (Weale and Swanson, 1991).

Double-spiral concentrators, with two starts integrated into the one space around a common column, have been used in Australia for many years and have also been accepted elsewhere. At Mount Wright in Canada 4300 double-start spirals are upgrading specular hematite ore at $6900\,t\,h^{-1}$ at 86% recovery (Hyma and Meech, 1989).

Spirals are made with slopes of varying steepness, the angle affecting the specific gravity of separation, but having little effect on the concentrate grade and recovery. Shallow angles are used, for example, to separate coal from shale, while steeper angles are used for normal heavy mineral-silica separations. The steepest angles are used to separate heavy minerals from heavy waste minerals, for example zircon (sp. gr. 4.7) from kyanite and staurolite (sp. gr. 3.6). Capacity ranges from 1 to $3\,t\,h^{-1}$ on low slope spirals to about double this for the steeper units. Spiral length is usually five or more turns for roughing duty and three turns in some cleaning units. Because treatment by spiral separators involves a multiplicity of units, the separation efficiency is very sensitive to the pulp distribution system employed. Lack of uniformity in feeding results in substantial falls in operating efficiency and can lead to severe losses in recovery, this is especially true with coal spirals (Holland-Batt, 1993).

Shaking tables

When a flowing film of water flows over a flat, inclined surface the water closest to the surface is retarded by the friction of the water absorbed on the surface; the velocity increases towards the water surface. If mineral particles are introduced into the film, small particles will not move as rapidly as large particles, since they will be submerged in the slower-moving portion of the film. Particles of high specific gravity will move more slowly than lighter particles, and so a lateral displacement of the material will be produced (Figure 10.24).

The flowing film effectively separates coarse light particles from small dense particles, and this mechanism is utilised to some extent in the shaking-table concentrator (Figure 10.25), which is perhaps the most metallurgically efficient form of gravity concentrator, being used to treat the smaller, more difficult flow-streams, and to produce finished concentrates from the products of other forms of gravity system.

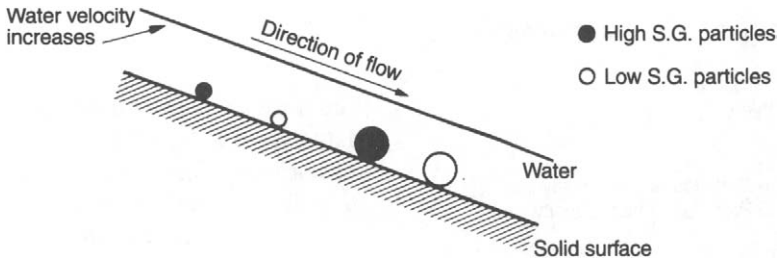


Figure 10.24 Action in a flowing film

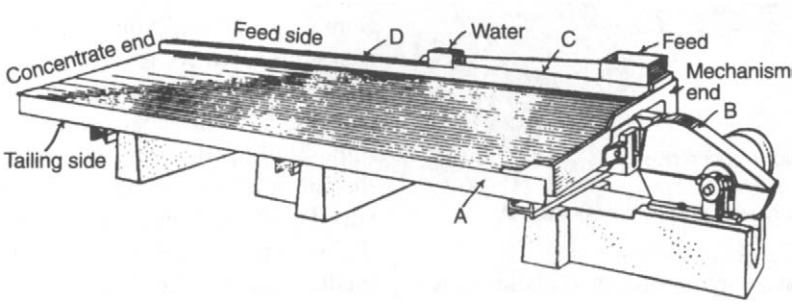


Figure 10.25 Shaking table

It consists of a slightly inclined deck, A, on to which feed, at about 25% solids by weight, is introduced at the feed box and is distributed along C; wash water is distributed along the balance of the feed side from launder D. The table is vibrated longitudinally, by the mechanism B, using a slow forward stroke and a rapid return, which causes the mineral particles to "crawl" along the deck parallel to the direction of motion. The minerals are thus subjected to two forces, that due to the table motion and that, at right angles to it, due to the flowing film of water. The net effect is that the particles move diagonally across the deck from the feed end and, since the effect of the flowing film depends on the size and density of the particles, they will fan out on the table, the smaller, denser particles riding highest towards the concentrate launder at the far end, while the larger lighter particles are washed into the tailings launder, which runs along the length of the table. Figure 10.26 shows an idealised diagram of the distribution of table products. An adjustable splitter at the concentrate end is often used to separate this product into two fractions – a high-grade concentrate and a middlings fraction.

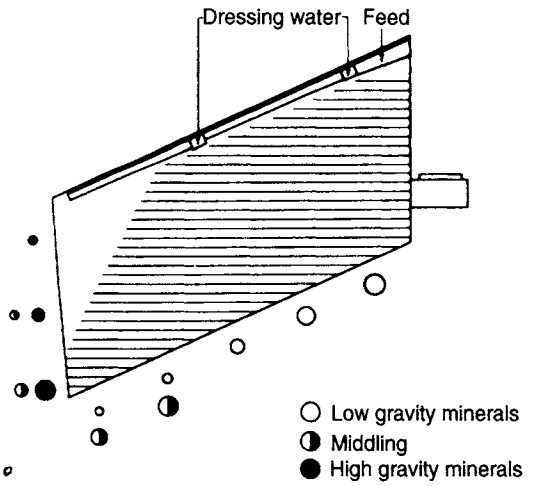


Figure 10.26 Distribution of table products

Although true flowing film concentration requires a single layer of feed, in practice a multi-layered feed is introduced on to the table, enabling much larger tonnages to be dealt with. Vertical stratification due to shaking action takes place behind the *riffles*, which generally run parallel with the long axis of the table and are tapered from a maximum height on the feed side, till they die out near the opposite side, part of which is left smooth (Figure 10.26). In the protected pockets behind the riffles the particles stratify so that the finest and heaviest particles are at the bottom and the coarsest and lightest particles are at the top (Figure 10.27). Layers of particles are moved across the riffles by the crowding action of new feed and by the flowing film of wash water. Due to the taper of the riffles, progressively finer sized and higher density particles are continuously being brought into contact with the flowing film of water that tops the riffles. Final concentration takes place at the unriffled area at the end of the deck, where the layer of material is at this stage usually only one or two particles deep.

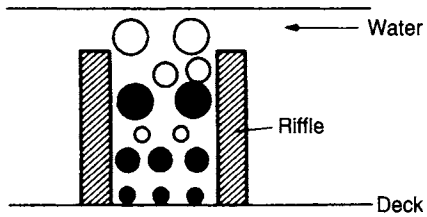


Figure 10.27 Vertical stratification between riffles

The significance of the many design and operating variables and their interactions have been reviewed by Sivamohan and Forssberg (1985a), and the development of a mathematical model of a shaking table is described by Manser et al. (1991). The separation on a shaking table is controlled by a number of operating variables, such as wash water, feed pulp density, deck slope, amplitude, and feed rate, and the importance of these variables in the model development is discussed.

Many other factors, including particle shape and the type of deck, play an important part in table separations. Flat particles, such as mica, although light, do not roll easily across the deck in the water film; such particles cling to the deck and are carried down to the concentrate discharge. Likewise, spherical dense particles may move easily in the film towards the tailings launder.

The table decks are usually constructed of wood, lined with materials with a high coefficient of friction, such as linoleum, rubber, and plastics. Decks made from fibreglass are also used which, although more expensive, are extremely hard wearing. The riffles on such decks are incorporated as part of the mould.

Particle size plays a very important role in table separations; as the range of sizes in a table feed increases, the efficiency of separation decreases. If a table feed is made up of a wide range of particle sizes, some of these sizes will be cleaned inefficiently. As can be seen from Figure 10.26, in an idealised separation, the middlings produced are not "true middlings", i.e. particles of associated mineral and gangue, but relatively coarse dense particles and fine light particles. If these particles are returned to the grinding circuit, together with the true middlings, then they will be needlessly reground.

Since the shaking table effectively separates coarse light from fine dense particles, it is common practice to classify the feed, since classifiers put such particles into the same product, on the basis of their equal settling rates. In order to feed as narrow a size range as possible on to the table, classification is usually performed in multi-spigot hydrosizers (Chapter 9), each spigot product, comprising a narrow range of equally settling particles, being fed to a separate set of shaking tables. A typical gravity concentrator employing shaking tables (Figure 10.28) may have an initial grind in rod mills in order to liberate as much mineral at as coarse a size as possible to aid separation. The hydrosizer products feed separate sets of tables, the middlings being reground before returning to the hydrosizer. Riffled tables, or *sand tables*, normally operate on feed sizes in the range 3 mm to 100 μm, and the hydrosizer overflow, consisting primarily of particles finer than this, is usually thickened and then distributed to tables whose decks have a series of planes rather than riffles and are designated *slime tables*.

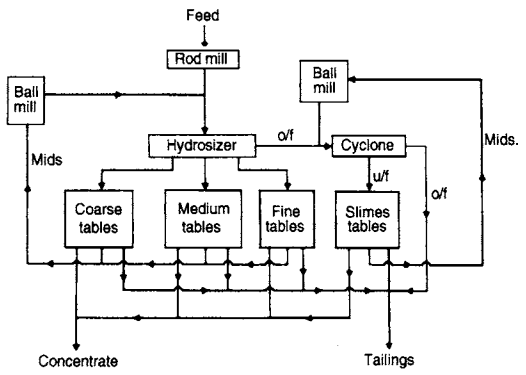


Figure 10.28 Typical shaking-table concentrator flowsheet

Dewatering of the hydrosizer overflow is often performed by hydrocyclones, which also remove particles in the overflow smaller than about 10 μm, which will not separate efficiently by gravity methods due to their extremely slow settling rates.

Successive stages of regrinding are a feature of many gravity concentrators. The mineral is separated at all stages in as coarse a state as possible in order to achieve reasonably fast separation and hence high throughputs.

The capacity of a table varies according to size of feed particles and the concentration criteria. Tables can handle up to $2\,t\,h^{-1}$ of 1.5 mm sand and perhaps $1\,t\,h^{-1}$ of fine sand. On 100–150 μm feed materials, table capacities may be as low as $0.5\,t\,h^{-1}$. On coal feeds, however, which are often tabled at sizes of up to 15 mm, much higher capacities are common. A normal 5 mm raw coal feed can be tabled with high efficiency at $12.5\,t\,h^{-1}$ per deck, whilst tonnages as high as $15.0\,t\,h^{-1}$ per deck are not uncommon when the top size in the feed is 15 mm (Terry, 1974).

The introduction of double and triple-deck units (Figure 10.29) has improved the area/capacity ratio at the expense of some flexibility and control.

Separation can be influenced by the length of stroke, which can be altered by means of a handwheel on the vibrator, or head motion, and by the reciprocating speed (Figure 10.30). The length of stroke usually varies within the range of 10–25 mm or more, the speed being in the range 240–325 strokes per minute. Generally, a fine feed requires a higher speed and shorter stroke which increases in speed as it goes forward until it is jerked to a halt before being sharply reversed, allowing the particles to slide forward during most of the backward stroke due to their built-up momentum.

The quantity of water used in the feed pulp varies, but for ore tables normal feed dilution is 20–25% solids by weight, while for coal tables pulps of 33–40% solids are used. In addition to the water in the feed pulp, clear water flows over the table for final concentrate cleaning. This varies from a few litres to almost $100\,l\,min^{-1}$ according to the nature of the feed material.

Tables slope from the feed to the tailings discharge end and the correct angle of incline is obtained by means of a handwheel. In most cases the line of separation is clearly visible on the table so this adjustment is easily made.

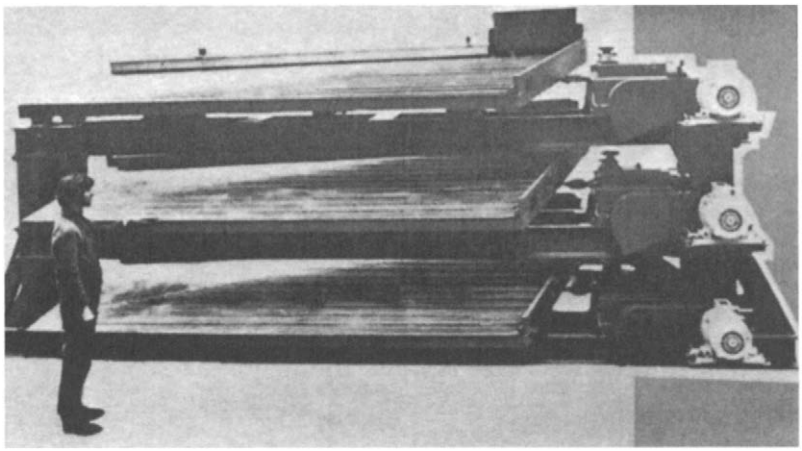


Figure 10.29 Trible-deck table

The table is slightly elevated along the line of motion from the feed end to the concentrate end. The moderate slope, which the high-density particles climb more readily than the low-density minerals, greatly improves the separation, allowing much sharper cuts to be made between concentrate, middlings, and tailings. The correct amount of end elevation varies with feed size and is greatest for the coarsest and highest gravity feeds. The end elevation should never be less than the taper of the riffles, otherwise there is a tendency for water to flow out towards the riffle tips rather than across the riffles. Normal end elevations in ore tabling range from a maximum of 90 mm for a very heavy, coarse sand to as little as 6 mm for an extremely fine feed.

Ore-concentrating tables are used primarily for the concentration of minerals of tin, iron, tungsten, tantalum, mica, barium, titanium, zirconium, and, to a lesser extent, gold, silver, thorium, uranium, and others. Tables are now being used in the recycling of electronic scrap to recover precious metals.

Pneumatic tables

Originally developed for seed separation, pneumatic or air tables have an important use in the treatment of heavy mineral sand deposits, and in the upgrading of asbestos, and in applications where water is at a premium. Pneumatic tables use a throwing motion to move the feed along a flat riffled deck, and blow air continuously up through a porous bed. The stratification produced is somewhat different from that of wet tables. Whereas in wet tabling the particle size increases and the density decreases from the top of the concentrate band to the tailings, on an air table both particle size and density decrease from the top down, the coarsest particles in the middlings band having the lowest density. Pneumatic tabling is therefore similar in effect to hydraulic classification. They are commonly used in combination with wet tables to clean zircon concentrates, one of the products obtained from heavy mineral sand deposits. Such concentrates are often contaminated with small amounts of fine silica, which can effectively be separated from the coarse zircon particles by air tabling. Some fine zircon may be lost in the tailings, and can be recovered by treatment on wet shaking tables.

Duplex concentrator

This machine was originally developed for the recovery of tin from low grade feeds, but has a wider application in the recovery of tungsten, tantalum, gold, chromite and platinum from fine feeds (Pearl et al., 1991). Two decks are used alternately to provide continuous feeding, the feed slurry being fed onto one of the decks, the lower density minerals running off into the discharge launder, while the heavy minerals remain on the deck. The deck is washed with water after a preset time, in order to remove the gangue minerals, after which the deck is tilted and the concentrate

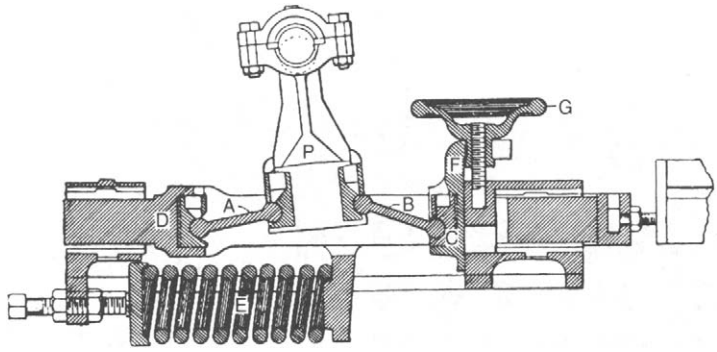


Figure 10.30 Head motion of Wilfley table

is washed off. One table is always concentrating, while the other is being washed or is discharging concentrates. The concentrator has a capacity of up to $5\,t\,h^{-1}$ of $-100\,\mu m$ feed producing enrichment ratios of between 20 and 500, and is available with various sizes and numbers of decks.

Mozley Laboratory Separator

This flowing film device, which uses orbital shear, is now used in many mineral processing laboratories, and is designed to treat small samples (100 g) of ore, allowing a relatively unskilled operator to obtain information for a recovery grade curve within a very short time (Anon., 1980).

Cordingley et al. (1994) used a Mozley Laboratory Mineral Separator to obtain data for the optimisation of both gravity circuit performance and comminution requirements with respect to liberation size at the Wheal Jane tin concentrator.

Centrifugal concentrators

The Kelsey centrifugal jig was described above. Other non-jig centrifugal separators have also been developed over the last 20 years.

The *Knelson* concentrator is a compact batch centrifugal separator with an active fluidised bed to capture heavy minerals (Knelson, 1992; Knelson and Jones, 1994). Unit capacities range from laboratory scale to 150 tonnes of solids per hour. A centrifugal force up to 200 times the force of gravity acts on the particles, trapping denser particles in a series of rings located in the machine, while the gangue particles are flushed out. The Knelson concentrator can treat particles ranging in size from 10 microns to a maximum of 6 mm. It is generally used for feeds in which the dense component to be recovered is a very small fraction of the total material, less than 500 g/t (0.05% by weight).

Feed slurry is then introduced through the stationary feed tube and into the concentrate cone. When the slurry reaches the bottom of the cone it is forced outward and up the cone wall under the influence of centrifugal force. Fluidisation water is introduced into the concentrate cone through a series of fluidisation holes. The slurry fills each ring to capacity to create a concentrating bed. Compaction of the bed is prevented by the fluidisation water. The flow of water that is injected into the rings is controlled to achieve optimum bed fluidisation. High specific gravity particles are captured and retained in the concentrating cone. When the concentrate cycle is complete, concentrates are flushed from the cone into the concentrate launder. Under normal operating conditions, this automated procedure is achieved in under 2 min in a secure environment.

The batch Knelson Concentrator has been widely applied in the recovery of gold, platinum, silver, mercury, and native copper.

The *Falcon* SB concentrator is another spinning fluidised bed batch concentrator (Figure 10.31). It is designed principally for the recovery of free gold in grinding circuit classifier underflows where a very small (<1%) mass pull to concentrate is required. The feed first flows up the sides of a cone-shaped bowl, where it stratifies according to particle density before passing over a concentrate bed fluidised from behind by back pressure water. The bed retains dense particles such as gold, and lighter gangue particles are washed over the top.

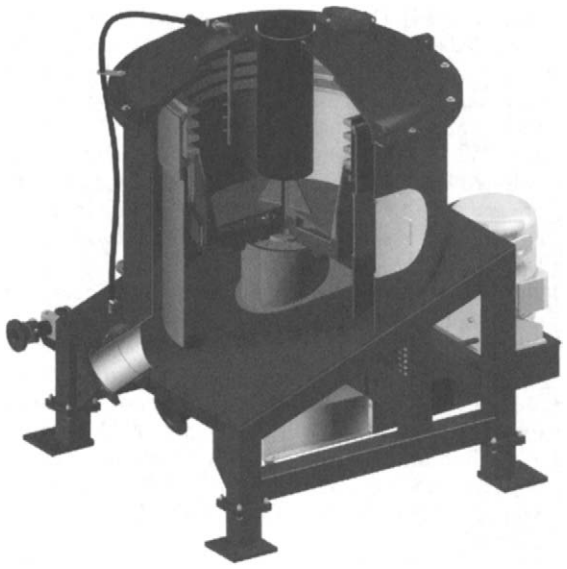


Figure 10.31 The Falcon SB5200B Centrifugal Separator (Courtesy Falcon Concentrators)

Periodically the feed is stopped and the concentrate rinsed out. Rinsing frequency, which is under automatic control, is determined from grade and recovery requirements. Accelerations of up to 300 times the force of gravity are used in the SB machine (McAlister and Armstrong, 1998). The SB5200 can treat nearly $400\,t\,h^{-1}$ of feed solids, depending on the specific application.

The principle of the Mozley *Multi-Gravity Separator* (MGS) can be visualised as rolling the horizontal surface of a conventional shaking table into a drum, then rotating it so that many times the normal gravitational pull can be exerted on the mineral particles as they flow in the water layer across the surface. Figure 10.32 shows a cross-section of the pilot scale MGS. The Mine Scale MGS consists of two slightly tapered open-ended drums, mounted "back to back", rotating at speeds variable between 90 and 150 rpm, enabling forces of between 5 and 15 g to be generated at the drum surfaces. A sinusoidal shake with an amplitude variable between 4 and 6 cps is superimposed on the motion of the drum, the shake imparted to one drum being balanced by the shake imparted to the other, thus balancing the whole machine. A scraper assembly is mounted within each drum on a separate concentric shaft, driven slightly faster than the drum but in the same direction. This scrapes the settled solids up the slope of the drum, during which

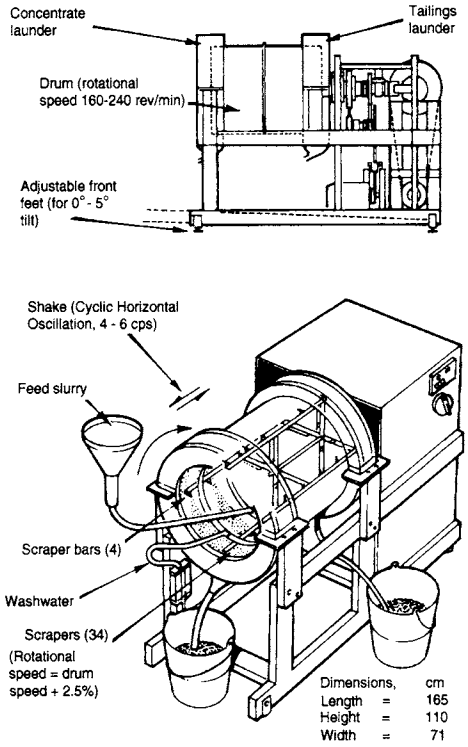


Figure 10.32 Pilot Scale MGS

time they are subjected to counter-current washing before being discharged as concentrate at the open, outer, narrow end of the drum. The lower density minerals, along with the majority of the wash water, flow downstream to discharge as tailings via slots at the inner end of each drum. The MGS has been used to effect improvements in final tin concentrate grade by replacing column flotation as the final stage of cleaning (Turner and Hallewell, 1993).

Gold ore concentrators

Although most of the gold from gold mines worldwide is recovered by dissolution in cyanide solution, a proportion of the coarse (+75 μm) gold is recovered by gravity separators. It has been argued that separate treatment of the coarse gold in this way constitutes a security risk and increases costs. Gravity concentration can remain an attractive option only if it can be implemented with very low capital and operating costs. A test designed to characterise the gravity recoverable gold (GRG) in the main circulating load of a grinding circuit has been described by Laplante et al. (1995).

The coarse gold must be concentrated in the grinding circuit to prevent it from being flattened into thin platelets (see Chapter 7). The rise of new gravity concentration devices such as the Knelson, Falcon, and IPJ have made this possible. In certain cases where sulphide minerals are the gravity gold carrier, flash flotation combined with modern gravity concentration technology provides the most effective gold recovery (Laplante and Dunne, 2002).

The deposits of the Yukon use sluice boxes to treat large tonnages of low grade gravels. Kelly et al. (1995) show that the simple sluice box can be a relatively efficient gravity concentrator provided they are correctly operated.

References

Adams, R.J. (1983). Control system increases jig performance, *Min. Equip. Int.* (Aug.), 37.

Anon. (1977). How Reichert cone concentration recovers minerals by gravity, *World Mining*, **30**(Jul.), 48.

Anon. (1980). Laboratory separator modification improves recovery of coarse-grained heavy minerals, *Min. Mag.* (Aug.), 158.

Beniuk, V.G., Vadeikis, C.A., and Enraght-Moony, J.N. (1994). Centrifugal jigging of gravity concentrate and tailing at Renison Limited, *Minerals Engng*, **7(5/6)**, 577.

Bonsu, A.K. (1983). Influence of pulp density and particle size on spiral concentration efficiency, *M.Phil. Thesis*, Camborne School of Mines.

Burt, R.O. (1985). *Gravity Concentration Technology*, Elsevier, Amsterdam.

Chen, W.L. (1980). Batac jig in five U.S. plants, *Mining Engng.*, **32**(Sept.), 1346.

Cope, L.W. (2000). Jigs: The forgotten machine, *Engng. and Mining. J.* (Aug.), 30.

Cordingley, M.G., Hallewell M.P., and Turner, J.W.G. (1994) Release analysis and its use in the optimization of the comminution and gravity circuits at the Wheal Jane tin concentrator, *Minerals Engng.*, **7(12)**, 1517.

Davies, P.O.J., et al. (1991). Recent developments in spiral design, construction and application, *Minerals Engng.*, **4(3/4)**, 437.

Ferree, T.J. (1993). Application of MDL Reichert cone and spiral concentrators for the separation of heavy minerals *CIM Bull.*, **86**, 35.

Forssberg, K.S. and Sandström, E. (1979). Operational characteristics of the Reichert cone in ore processing, *13th IMPC, Warsaw*, **2**, 259.

Gray, A.H. (1997). InLine pressure jig – an exciting, low cost technology with significant operational benefits in gravity separation of minerals, *AusIMM Annual Conf.*, Ballarat, Victoria (AusIMM).

Green, P. (1984). Designers improve jig efficiency, *Coal Age*, **89**(Jan.), 50.

Harrington, G. (1986). Practical design and operation of Baum jig installations, *Mine and Quarry Special Chines Supplement* (Jul., Aug.), 16.

Hasse, W. and Wasmuth, H.D. (1988). Use of air-pulsated Batac jigs for production of high-grade lump ore and sinterfeed from intergrown hematite iron ores, ed. K.S.E. Forssberg, *Proc. XVI Int. Min. Proc. Cong.*, Stockholm, **A**, 1053, Elsevier, Amsterdam.

Holland-Batt, A.B. (1989). Spiral separation: Theory and simulation. *Trans IMM C*, **98**, C46.

Holland-Batt, A.B. (1993). The effect of feed rate on the performance of coal spirals, *Coal Preparation*, 199.

Holland-Batt, A.B. (1995). Some design considerations for spiral separators, *Minerals Engng.*, **8(11)**, 1381.

Holland-Batt, A.B. (1998). Gravity separation: A revitalized technology, *SME Preprint 98–45*, Society for Mining, Metallurgy and Exploration, Inc., Littelton, Colorado.

Hubbard, J.S., Humphreys, I.B. and Brown, E.W. (1953). How Humphreys spiral concentrator is used in modern dressing practice, *Mining World* (May).

Hyma, D.B. and Meech, J.A. (1989). Preliminary tests to improve the iron ore recovery from the −212 micron fraction of new spiral feed at Quebec Cartier Mining Company, *Minerals Engng.*, **2(4)**, 481.

Jonkers, A., Lyman G.J., and Loveday, G.K. (2002). Advances in modelling of stratification in jigs. *Roc-XIII Int. Coal. Prepn. Cong.*, Jonannesburg (Mar.), Vol. 1, 266–276.

Karantzavelos, G.E. and Frangiscos, A.Z. (1984). Contribution to the modelling of the jigging process, in *Control '84 Min./Metall. Proc.*, ed. J.A. Herbst, AIME, New York, 97.

King, R.P. (2000). Flowsheet optimization using simulation: A gravity concentrator using Reichert cones, in *Proc. XXI Int. Min. Proc. Cong.*, Rome, B9–1.

Knelson, B. (1992). The Knelson Concentrator. Metamorphosis from crude beginning to sophisticated world wide acceptance, *Minerals Engng.*, **5(10–12)**.

Knelson, B. and Jones, R. (1994). A new generation of Knelson Concentrators – a totally secure system goes on line, *Minerals Engng.*, **7(2/3)**, 201.

Laplante, A., Woodcock, F., and Noaparast, M. (1995). Predicting gravity separation gold recovery, *Min. and Metall. Proc.* (May), 74.

Laplante, A. and Dunne, R.C. (2002). The gravity recoverable gold test and flash flotation, *Proc. 34th Annual Meeting of the Canadian Min. Proc.*, Ottawa.

Loveday, B.K. and Forbes, J.E. (1982). Some considerations in the use of gravity concentration for the recovery of gold, *J.S.Afr.I.M.M.* (May), 121.

Loveday, G., and Jonkers, A. (2002). The Apic jig and the JigScan controller take the guesswork out of jigging, *XIV Int. Coal Prep. Cong., S.Afr.I.M.M*, 247.

Lyman, G.J. (1992). Review of jigging principles and control, *Coal Preparation*, **11(3–4)**, 145.

Manser, R.J., et al. (1991). The shaking table concentrator – the influence of operating conditions and table parameters on mineral separation – the development of a mathematical model for normal operating conditions, *Minerals Engng.*, **4(3/4)**, 369.

Matthews, B.W., Holtham, P.N., Fletcher, C.A.J., Golab, K., and Partridge, A.C. (1998). Fluid and particulate flow on spiral concentrators: Computational simulation and validation, *Proc. XIII Int. Coal Prep. Cong.*, Brisbane, Australia, 833.

McAlister, S. and Armstrong, K.C. (1998). Development of the Falcon concentrators, *SME Preprint*, 98–172.

Miller, D.J. (1991). Design and operating experience with the Goldsworthy Mining Limited Batac jig and spiral separator iron ore beneficiation plant, *Minerals Engng.*, **4(3/4)**, 411.

Mills, C. (1978). Process design, scale-up and plant design for gravity concentration, in *Mineral Processing Plant Design*, ed. A.L. Mular and R.B. Bhappu, AIMME, New York.

Pearl, M., et al. (1991). A mathematical model of the Duplex concentrator, *Minerals Engng.*, **4(3/4)**, 347.

Richards, R.G. and Palmer, M.K. (1997). High capacity gravity separators – a review of current status, *Minerals Engng.*, **10(9)**, 973.

Schubert, H. (1995). On the fundamentals of gravity concentration in sluices and spirals, *Aufbereitungs-Technik*, **36(11)**, 497.

Sivamohan, R. and Forssberg, E. (1985a). Principles of tabling, *Int. J. Min. Proc.*, **15**(Nov.), 281.

Sivamohan, R. and Forssberg, E. (1985b). Principles of sluicing, *Int. J. Min. Proc.*, **15**(Oct.), 157.

Terry, R.L. (1974). Minerals concentration by wet tabling, *Min. Proc.*, **15**(Jul./Aug.), 14.

Tiernon, C.H. (1980). Concentrating tables for fine coal-cleaning, *Mining Engng.*, **32**(Aug.), 1228.

Turner, J.W.G. and Hallewell, M.P. (1993). Process improvements for fine cassiterite recovery at Wheal Jane, *Minerals Engng.*, **6(8–10)**, 817.

Wallace, W. (1981). Practical aspects of Baum jig coal washing, *Mine and Quarry*, **10**(Sept.), 40.

Wallace, W.M. (1979). Electronically controlled Baum jig washing, *Mine and Quarry*, **8** (Jul./Aug.), 43.

Weale, W.G. and Swanson, A.R. (1991). Some aspects of spiral plant design and operation, in *Proc. 5th Australian Coal Prep. Conf.*, Aust. Coal Prep. Soc., **99**.

Wells, A. (1991). Some experiences in the design and optimisation of fine gravity concentration circuits, *Minerals Engng.*, **4(3/4)**, 383.

Zimmerman, R.E. (1975). Performance of the Batac jig for cleaning fine and coarse coal sizes, *Trans. Soc. Min. Engng.*, AIME, **258**(Sept.), 199.

11

Dense medium separation (DMS)

Introduction

Dense medium separation (or heavy medium separation (HMS), or the sink-and-float process) is applied to the pre-concentration of minerals, i.e. the rejection of gangue prior to grinding for final liberation. It is also used in coal preparation to produce a commercially graded end-product, clean coal being separated from the heavier shale or high-ash coal.

In principle, it is the simplest of all gravity processes and has long been a standard laboratory method for separating minerals of different specific gravity. Heavy liquids of suitable density are used, so that those minerals lighter than the liquid float, while those denser than it sink (Figure 11.1).

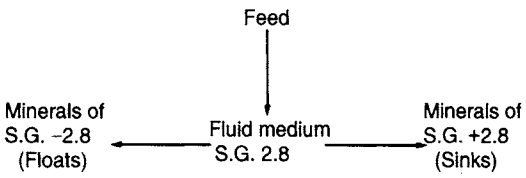


Figure 11.1 Principle of dense medium separation

Since most of the liquids used in the laboratory are expensive or toxic, the dense medium used in industrial separations is a thick suspension, or pulp, of some heavy solid in water, which behaves as a heavy liquid.

The process offers some advantages over other gravity processes. It has the ability to make sharp separations at any required density, with a high degree of efficiency even in the presence of high percentages of near-density material. The density of separation can be closely controlled, within a relative density of $\pm 0.005\,kg\,l^{-1}$ and can be maintained, under normal conditions, for indefinite periods. The separating density can, however, be changed at will and fairly quickly, to meet varying requirements. The process is, however, rather expensive, mainly due to the ancillary equipment needed to clean the medium and the cost of the medium itself.

Dense medium separation is applicable to any ore in which, after a suitable degree of liberation by crushing, there is enough difference in specific gravity between the particles to separate those which will repay the cost of further treatment from those which will not. The process is most widely applied when the density difference occurs at a coarse particle size, as separation efficiency decreases with size due to the slower rate of settling of the particles. Particles should preferably be larger than about 4 mm in diameter, in which case separation can be effective on a difference in specific gravity of 0.1 or less.

Separation down to 500 μm, and less, in size can, however, be made by the use of centrifugal separators. Providing a density difference exists, there is no upper size limit except that determined by the ability of the plant to handle the material.

Dense medium separation is possible with ores in which the minerals are coarsely aggregated. If the values are finely disseminated throughout the host rock, then a suitable density difference between the crushed particles cannot be developed by coarse crushing.

Preconcentration is most often performed on metalliferous ores which are associated with relatively light country rock. Thus finely disseminated galena and sphalerite often occur with pyrite as replacement deposits in rocks such as limestone or dolomite. Similarly in some of the Cornish tin ores the cassiterite is found in lodes with some degree of banded structure in which it is associated with other high specific-gravity minerals such as the sulphides of iron, arsenic, and copper, as well as iron oxides. The lode fragments containing these minerals therefore have a greater density than the siliceous waste and will, therefore, allow early separation. Wall rock adjacent to the lode may likewise be disposed of and will in many cases form the majority of the waste generated, since the working of narrow lodes often involves the removal of waste rock from the walls to facilitate access. Problems may arise if the wall rock is mineralised with low-value, high-density minerals such as iron oxides and sulphides, a situation which is often encountered. A good example is a wolfram mine in France where the schist wall rock was found to contain pyrrhotite which raised its density to such an extent that dense medium separation to preconcentrate the wolfram lode material was impossible. As a result, the whole of the run-of-mine ore had to be comminuted in order to obtain the wolfram.

The dense medium

Liquids

Heavy liquids have wide use in the laboratory for the appraisal of gravity-separation techniques on ores. Heavy liquid testing may be performed to determine the feasibility of dense medium separation on a particular ore, and to determine the economic separating density, or it may be used to assess the efficiency of an existing dense medium circuit by carrying out tests on the sink and float products. The aim is to separate the ore samples into a series of fractions according to density, establishing the relationship between the high and the low specific gravity minerals.

Tetrabromoethane (TBE), having a specific gravity of 2.96, is commonly used and may be diluted with white spirit or carbon tetrachloride (sp. gr. 1.58) to give a range of densities below 2.96.

Bromoform (sp. gr. 2.89) may be mixed with carbon tetrachloride to give densities in the range 1.58–2.89. For densities of up to 3.3, diiodomethane is useful, diluted as required with triethyl orthophosphate. Aqueous solutions of sodium polytungstate have certain advantages over organic liquids, such as being virtually non-volatile, non-toxic and of lower viscosity, and densities of up to 3.1 can easily be achieved (Anon., 1984).

Clerici solution (thallium formate-thallium malonate solution) allows separation at densities up to 4.2 at 20 °C, or 5.0 at 90 °C. Separations of up to 18 kg l^{-1} can be achieved by the use of *magneto-hydrostatics*, i.e. the utilisation of the supplementary weighting force produced in a solution of a paramagnetic salt or ferrofluid when situated in a magnetic field gradient. This type of separation is applicable primarily to non-magnetic minerals with a lower limiting particle size of about 50 μm (Parsonage 1977; Domenico et al., 1994).

Many heavy liquids give off toxic fumes and must be used with adequate ventilation: the Clerici liquids are extremely poisonous and must be handled with extreme care. The use of pure liquids on a commercial scale has therefore not been found practicable, and industrial processes employ finely ground solids suspended in water.

Suspensions

Below a concentration of about 15% by volume, finely ground suspensions in water behave essentially as simple Newtonian fluids. Above this concentration, however, the suspension becomes non-Newtonian and a certain minimum stress, or yield stress, has to be applied before shear will occur and the movement of a particle can commence. Thus small particles, or those close to the medium density, are unable to overcome the rigidity offered by the medium before movement can be achieved. This can be overcome to some extent either by increasing the shearing forces on the particles, or by decreasing the apparent viscosity of the suspension. The shearing force may be increased by substituting centrifugal force for gravity. The viscous effect may be decreased by agitating the medium, which causes elements of liquid to be sheared relative to each other. In practice the medium is never static, as motion is imparted to it by paddles, air, etc., and also by the sinking material itself. All these factors, by reducing the yield stress, tend to bring the parting

or separating density as close as possible to the density of the medium in the bath.

In order to produce a stable suspension of sufficiently high density, with a reasonably low viscosity, it is necessary to use fine, high specific-gravity solid particles, agitation being necessary to maintain the suspension and to lower the apparent viscosity. The solids comprising the medium must be hard, with no tendency to slime, as degradation increases the apparent viscosity by increasing the surface area of the medium. The medium must be easily removed from the mineral surfaces by washing, and must be easily recoverable from the fine-ore particles washed from the surfaces. It must not be affected by the constituents of the ore and must resist chemical attack, such as corrosion.

Galena was initially used as the medium and, when pure, it can give a bath density of about 4.0. Above this level, ore separation is slowed down by the viscous resistance. Froth flotation, which is an expensive process, was used to clean the contaminated medium, but the main disadvantage is that galena is fairly soft and tends to slime easily, and it also has a tendency to oxidise, which impairs the flotation efficiency.

The most widely used medium for metalliferous ores is now ferrosilicon, whilst magnetite is used in coal preparation. Recovery of medium in both cases is by magnetic separation.

Magnetite (sp. gr. 5.1) is relatively cheap, and is used to maintain bath densities of up to 2.5 kg l^{-1}.

Ferrosilicon (sp. gr. 6.7–6.9) is an alloy of iron and silicon which should contain not less than 82% Fe and 15–16% Si (Collins et al., 1974). If the silicon content is less than 15%, the alloy will tend to corrode, while if it is more than 16% the magnetic susceptibility and density will be greatly reduced. Losses of ferrosilicon from a dense medium circuit vary widely, from as little as 0.1 to more than 2.5 kg/t of ore treated, the losses, apart from spillages, mainly occurring in magnetic separation and by the adhesion of medium to ore particles. Corrosion usually accounts for relatively small losses, and can be effectively prevented by maintaining the ferrosilicon in its passive state. This is normally achieved by atmospheric oxygen diffusing into the medium, or by the addition of small quantities of sodium nitrite (Stewart and Guerney, 1998).

Milled ferrosilicon is produced in a range of size distributions, from 30 to 95% – 45 μm, the finer grades being used for finer ores and centrifugal separators. The coarser, lower viscosity grades can achieve medium densities up to about 3.3. Atomised ferrosilicon consists of rounded particles which produce media of lower viscosity and can be used to achieve densities as high as 4 (Myburgh, 2002; Dunglison et al., 1999).

Separating vessels

Several types of separating vessel are in use, and these may be classified into gravitational ("static-baths") and centrifugal (dynamic) vessels. There is an extensive literature on the performance of these processes, and effective mathematical models are now being developed, which can be used for simulation purposes (Napier-Munn, 1991).

Gravitational vessels

Gravitational units comprise some form of vessel into which the feed and medium are introduced and the floats are removed by paddles, or merely by overflow. Removal of the sinks is the most difficult part of separator design. The aim is to discharge the sinks particles without removing sufficient of the medium to cause disturbing downward currents in the vessel.

The *Wemco cone separator* (Figure 11.2) is widely used for ore treatment, since it has a relatively high sinks capacity. The cone, which has a diameter of up to 6 m, accommodates feed particles of up to 10 cm in diameter, with capacities of up to 500 t h^{-1}.

The feed is introduced on to the surface of the medium by free-fall, which allows it to plunge several centimetres into the medium. Gentle agitation by rakes mounted on the central shaft helps keep the medium in suspension. The float fraction simply overflows a weir, whilst the sinks are removed by pump or by external or internal air lift.

Drum separators (Figure 11.3) are built in several sizes, up to 4.3 m diameter by 6 m long, with maximum capacities of 450 t h^{-1}, and can treat feeds of up to 30 cm in diameter. Separation is accomplished by the continuous removal of the sink product through the action of lifters fixed to the inside of the rotating drum. The lifters empty into the sink launder when they pass the horizontal position. The float product overflows a weir at

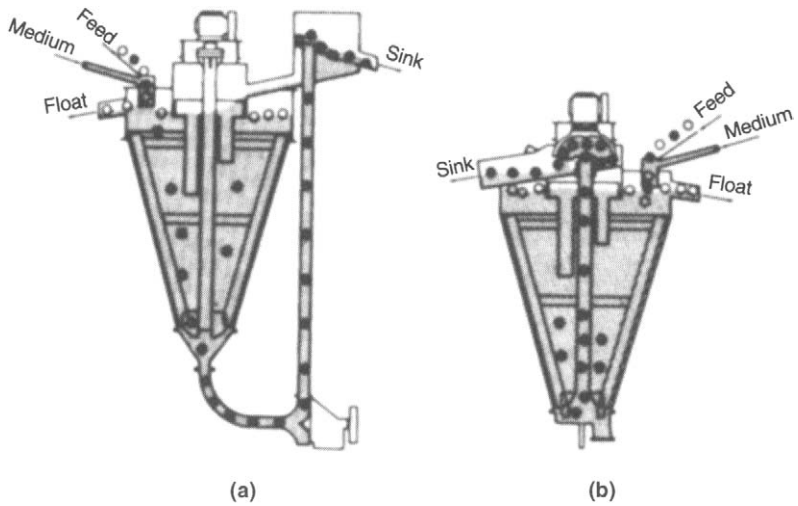


Figure 11.2 Wemco cone separator. (a) Single-gravity, two-product system with torque-flow-pump sink removal; (b) Single-gravity, two-product system with compressed-air sink removal

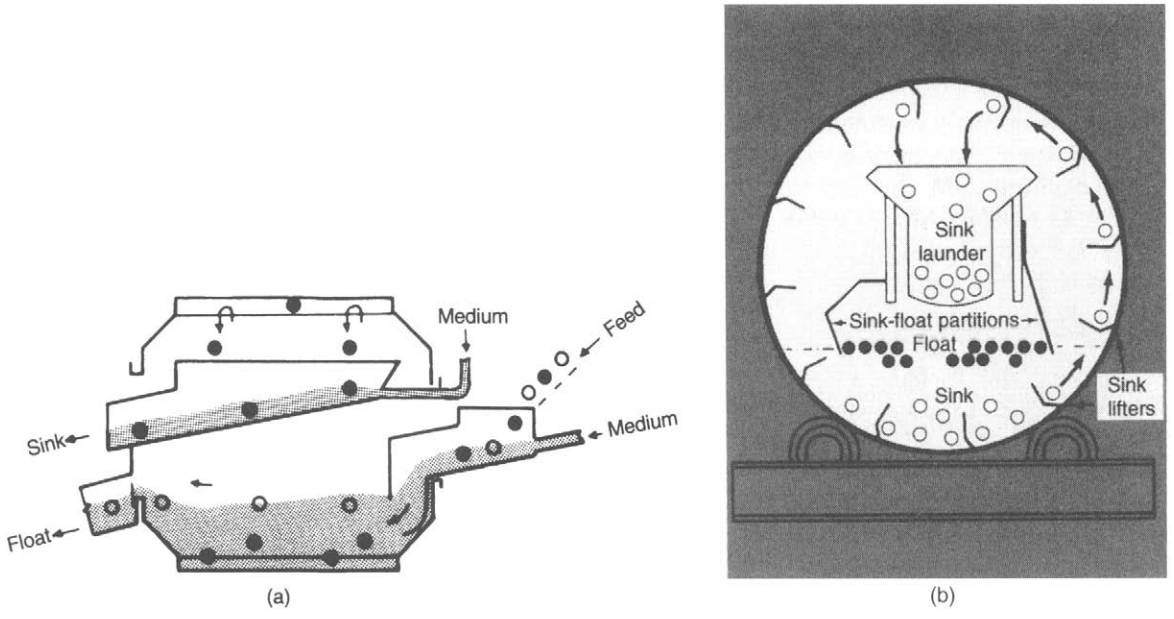


Figure 11.3 Drum separator: (a) side view, (b) end view

the opposite end of the drum from the feed chute. Longitudinal partitions separate the float surface from the sink-discharge action of the revolving lifters.

The comparatively shallow pool depth in the drum compared with the cone separator minimises settling out of the medium particles giving a uniform gravity throughout the drum.

Where single-stage dense-medium treatment is unable to produce the desired recovery, two-stage separation can be achieved in the *two-compartment drum separator* (Figure 11.4), which is, in effect, two drum separators mounted integrally and rotating together, one feeding the other. The lighter medium in the first compartment separates a pure float product. The sink product is lifted and

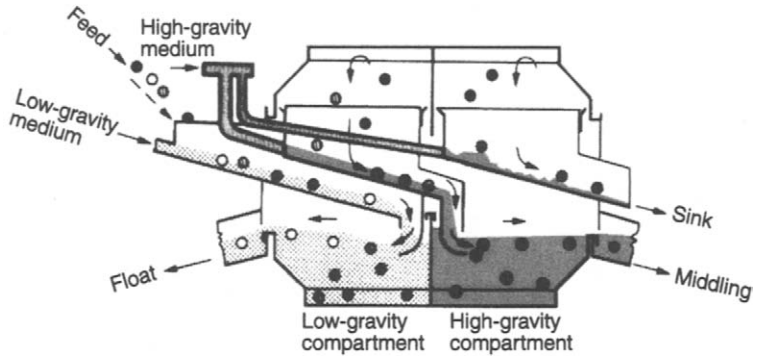


Figure 11.4 Two-compartment drum separator

conveyed into the second compartment where the middlings and the true sinks are separated.

Although drum separators have very large sinks capacities, and are inherently more suited to the treatment of metallic ores, where the sinks product is normally 60–80% of the feed, rather than to coal, where the sinks product is only 5–20% of the feed, they are very commonly used in the coal industry because of their simplicity, reliability, and relatively small maintenance needs. A mathematical model of the DM drum has been developed by Baguley and Napier-Munn (1996).

The *Drewboy bath* is widely used in the UK coal industry because of its high floats capacity (Figure 11.5).

The raw coal is fed into the separator at one end, and the floats are discharged from the opposite end by a star-wheel with suspended rubber, or chain straps, while the sinks are lifted out from the bottom of the bath by a radial-vaned wheel mounted on an inclined shaft. The medium is fed into the bath at two points – at the bottom of the vessel and with the raw coal – the proportion being controlled by valves.

The *Norwalt washer* was developed in South Africa, and most installations are to be found in that country. Raw coal is introduced into the centre of the annular separating vessel, which is provided with stirring arms (Figure 11.6).

The floats are carried round by the stirrers, and are discharged over a weir on the other side of the vessel, being carried out of the vessel by the medium flow. The discard sinks to the bottom of the vessel and is dragged along by scrapers attached to the bottom of the stirring arms, and is discharged via a hole in the bottom of the bath into

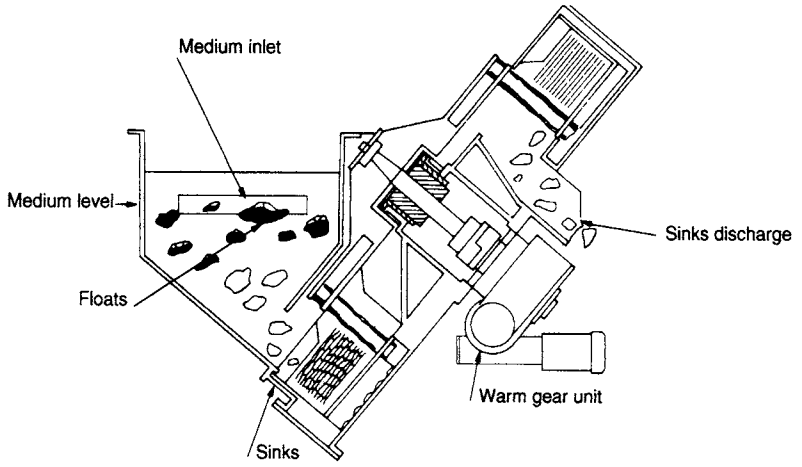


Figure 11.5 Drewboy bath

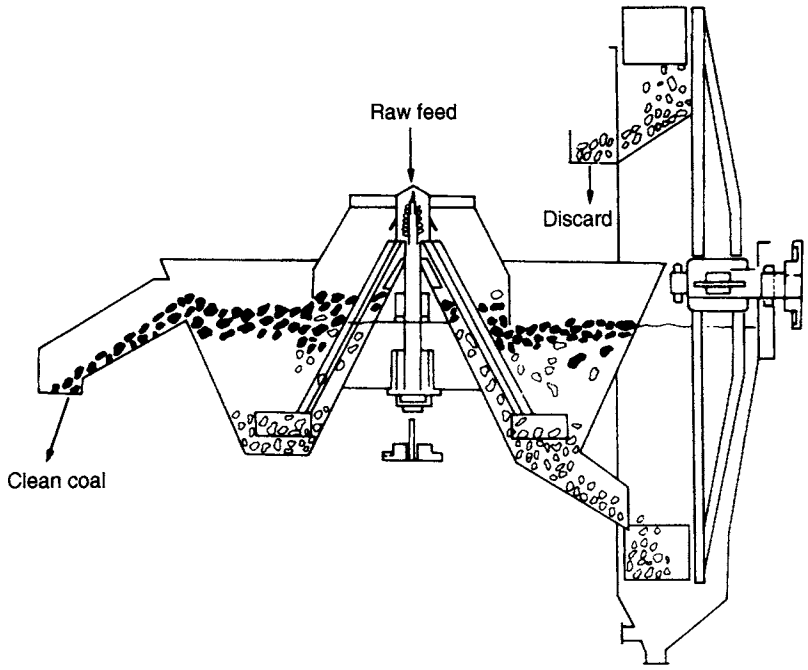


Figure 11.6 Norwalt bath

a sealed elevator, either of the wheel or bucket type, which continuously removes the sinks product.

The *Teska Bath*, developed in Germany, uses a rotating bucket wheel to remove coal reject.

Centrifugal separators

Cyclone dense medium separators have now become widely used in the treatment of ores and coal. They provide a high centrifugal force and a low viscosity in the medium, enabling much finer separations to be achieved than in gravitational separators. Feed to these devices is typically de-slimed at about 0.5 mm, to avoid contamination of the medium with slimes, and to minimise medium consumption. A finer medium is required than with gravitational vessels, to avoid medium instability. In recent years work has been carried out in many parts of the world to extend the range of particle size treated by centrifugal separators, particularly those operating in coal preparation plants, where advantages to be gained are elimination of de-sliming screens and reduced froth flotation of the screen undersize, as well as more accurate separation of fine coal. Froth flotation has little effect on sulphur reduction, whereas pyrite can be removed, and oxidised coal treated by DMS. The work has shown that good separations can be achieved for coal particles as fine as 0.1 mm, but below this size separation efficiency is very low. Since a typical British coal can contain 10% material less than 0.1 mm, froth flotation must be retained to clean these finer fractions, although DMS with no de-sliming has been performed in the United States (Anon., 1985). Tests on a lead–zinc ore have shown that good separations can be achieved down to 0.16 mm using a centrifugal separator (Ruff, 1984). These and similar results elsewhere, together with the progress made in automatic control of medium consistency, add to the growing evidence that DMS can be considered for finer material than had been thought economical or practical until recently. As the energy requirement for grinding, flotation, and dewatering is often up to ten times that required for DMS, a steady increase of fines pre-concentration plants is likely.

By far the most widely used centrifugal DM separator is the cyclone (Figure 11.7) whose principle of operation is similar to that of the conventional hydrocyclone (Chapter 9). The commonest form of DM cyclone is that developed by the Dutch State Mines in the 1940s, which has an included

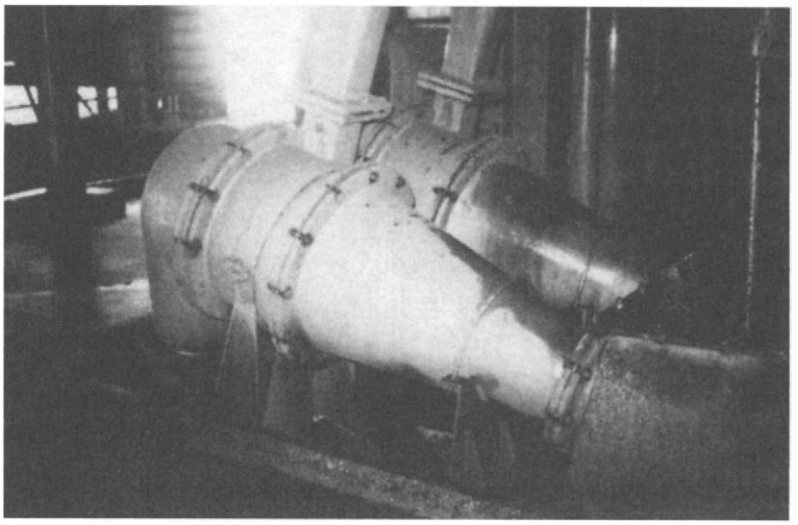


Figure 11.7 DSM cyclones

cone angle of 20°. Cyclones typically treat ores and coal in the range 0.5–40 mm. The largest cyclones now exceed 1 m in diameter and are capable of throughputs in coal preparation of over 250 t/h (Lee et al., 1995).

The ore or coal is suspended in the medium and introduced tangentially to the cyclone either via a pump or it is gravity-fed. Gravity feeding requires a taller and therefore more expensive building but achieves a more consistent flow and less pump wear and ore degradation. The dense material (reject in the case of coal, product in the case of iron ore) is centrifuged to the cyclone wall and exits at the apex. The light product "floats" to the flow around the axis and exits via the vortex finder.

Mathematical models of the DM cyclone for coal have been developed by King and Juckes (1988) and Wood et al. (1987) and for minerals by Scott and Napier-Munn (1992). A more general model has been reported by Dunglison and Napier-Munn (1997).

The *Vorsyl separator* (Figure 11.8) is used in many coal-preparation plants for the treatment of small coal sizes up to about 50 mm at feed rates of up to $120\,t\,h^{-1}$ (Shaw, 1984). The feed to the separator, consisting of de-slimed raw coal, together with the separating medium of magnetite, is introduced tangentially, or more recently by an involute entry, at the top of the separating chamber, under pressure. Material of specific gravity less than that of the medium passes into the clean coal outlet via the vortex finder, while the near gravity material and the heavier shale particles move to the wall of the vessel due to the centrifugal acceleration induced. The particles move in a spiral path down the chamber towards the base of the vessel where the drag caused by the proximity of the orifice plate reduces the tangential velocity and creates a strong inward flow towards the throat. This carries the shale, and near gravity material, through zones of high centrifugal force, where a final precise separation is achieved. The shale, and a proportion of the medium, discharge through the throat into the shallow shale chamber, which is provided with a tangential outlet, and is connected by a short duct to a second shallow chamber known as the vortextractor. This is also a cylindrical vessel with a tangential inlet for the medium and reject and an axial outlet. An inward spiral flow to the outlet is induced, which dissipates the inlet pressure energy and permits the use of a large outlet nozzle without the passing of an excessive quantity of medium.

The *LARCODEMS* (Large Coal Dense Medium Separator) was developed to treat a wide size range of coal (−100 mm) at high capacity in one vessel (Shah, 1987). It has also been used in concentrating iron ore. The unit (Figure 11.9) consists of a cylindrical chamber which is inclined at approximately 30° to the horizontal. Feed medium at the required relative density is introduced under pressure, either by pump or static head, into the involute tangential

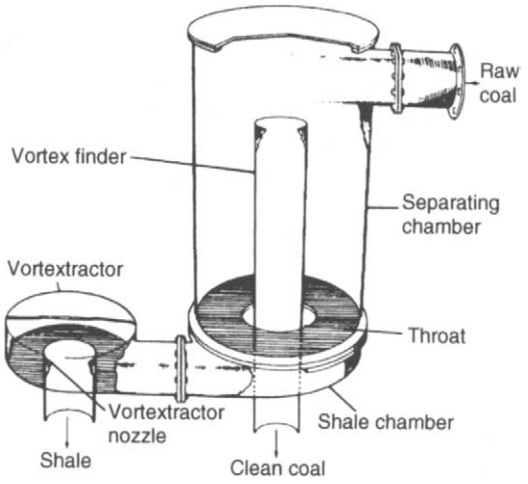


Figure 11.8 Vorsyl separator

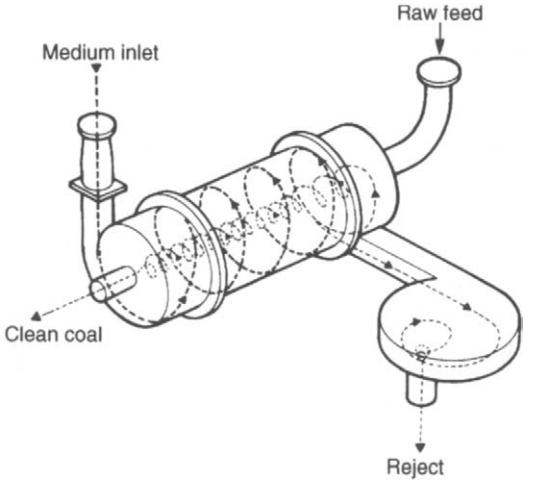


Figure 11.9 LARCODEMS separator

inlet at the lower end. At the top end of the vessel is another involute tangential outlet connected to the vortextractor. Raw coal of 0.5–100 mm is fed into the separator by a chute connected to the top end, the clean coal after separation being removed through the bottom outlet. High relative density particles pass rapidly to the separator wall and are removed through the top involute outlet and the vortextractor.

The first installation of the device was as the main processor in the 250 $t\,h^{-1}$ coal preparation plant at Point of Ayr Colliery in the United Kingdom (Lane, 1987). As the 250 $t\,h^{-1}$ LARCODEMS is only 1.2 m diameter by 3 m long, it could have a dramatic effect on the design and construction of future coal preparation plants.

The *Dyna Whirlpool* separator is similar to the LARCODEMS, and is used for treating fine coal, particularly in the Southern Hemisphere, as well as diamonds, fluorspar, tin, and lead–zinc ores, in the size range 0.5–30 mm (Wills and Lewis, 1980).

It consists of a cylinder of predetermined length (Figure 11.10), having identical tangential inlet and outlet sections at either end. The unit is operated in an inclined position and medium of the required density is pumped under pressure into the lower outlet. The rotating medium creates a vortex throughout the length of the unit and leaves via the upper tangential discharge and the lower vortex outlet tube. Raw feed entering the upper vortex tube is sluiced into the unit by a small quantity of medium and a rotational motion is quickly imparted by the open vortex. Float material passes down the vortex and does not contact the outer walls of the unit, thus greatly reducing wear. The floats are discharged from the lower vortex outlet tube. The heavy sink particles of the feed penetrate the rising medium towards the outer wall of the unit and are discharged with medium through the sink discharge pipe. Since the sinks discharge is close to the feed inlet, the sinks are removed from the unit almost immediately, again reducing wear

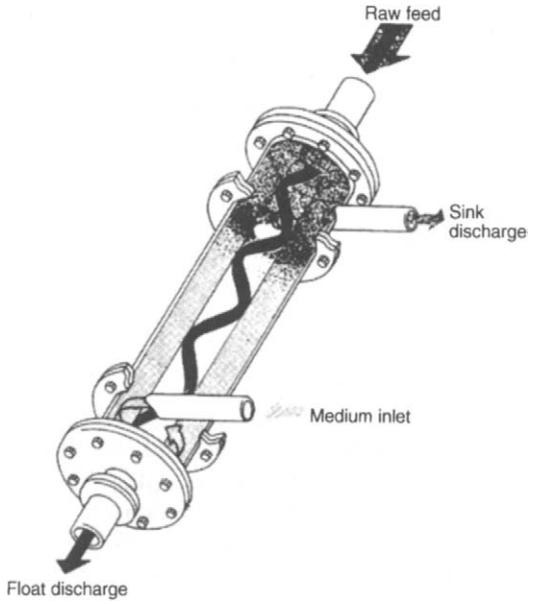


Figure 11.10 Dyna Whirlpool separator

considerably. Only near-gravity particles which are separated further along the unit actually come into contact with the main cylindrical body. The tangential sink discharge outlet is connected to a flexible sink hose and the height of this hose may be used to adjust back pressure to finely control the cut-point. The capacity of the separator can be as high as $100\,t\,h^{-1}$, and it has several advantages over the DSM cyclone. Apart from the reduced wear, which not only decreases maintenance costs but also maintains performance of the unit, operating costs are lower, since only the medium is pumped. The unit has a much higher sinks capacity and can accept large fluctuations in sink/float ratios (Hacioglu and Turner, 1985).

The *Tri-Flo* separator (Figure 11.11) can be regarded as two Dyna Whirlpool separators joined in series, and has been installed in a number of coal, metalliferous, and non-metallic ore treatment plants (Burton et al., 1991; Kitsikopoulos et al., 1991; Ferrara et al., 1994). Involute medium inlets and sink outlets are used, which produce less turbulence than tangential inlets.

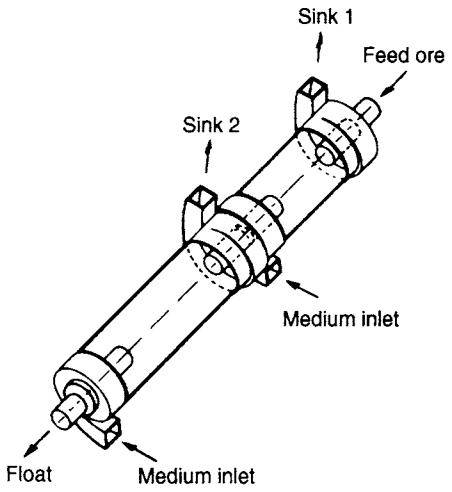


Figure 11.11 Tri-Flo separator

The device can be operated with two media of differing densities in order to produce sink products of individual controllable densities. Two-stage treatment using a single medium density produces a float and two sinks products with only slightly different separation densities. With metalliferous ores, the second sink product can be regarded as a scavenging stage for the dense minerals, thus increasing their recovery. This second product may be recrushed, and, after de-sliming, returned for retreatment. Where the separator is used for washing coal, the second stage cleans the float to produce a higher grade product. Two stages of separation also increase the sharpness of separation.

DMS circuits

Although the separating vessel is the most important element of a DMS process, it is only one part of a relatively complex circuit. Other equipment is required to prepare the feed, and to recover, clean, and re-circulate the medium (Symonds and Malbon, 2002).

The feed to a dense medium circuit must be screened to remove fine ore, and slimes should be removed by washing, thus alleviating any tendency which such slime content may have for creating sharp increases in medium viscosity.

The greatest expense in any dense medium circuit is the provision for reclaiming and cleaning the medium which leaves the separator with the sink and float products. A typical circuit is shown in Figure 11.12.

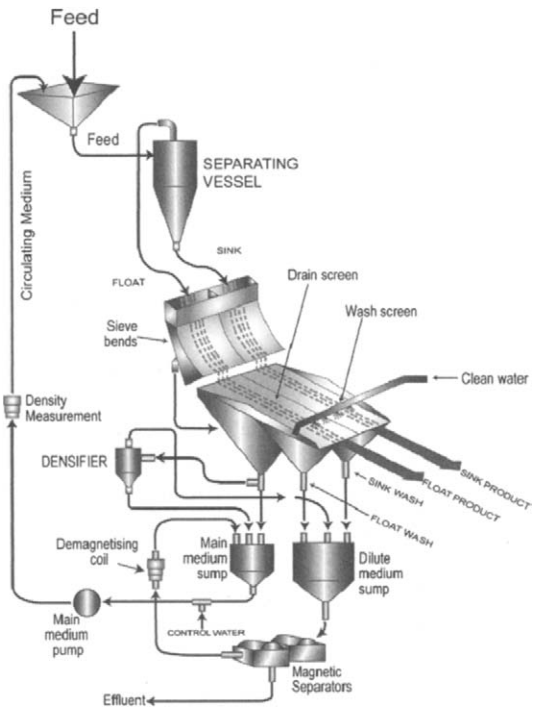


Figure 11.12 Typical DMS circuit

The sink and float fractions pass on to separate vibrating drainage screens where more than 90% of the medium in the separator products is recovered and pumped back via a sump into the separating vessel. The products then pass under washing sprays where substantially complete removal of medium and adhering fines is accomplished. The finished float and sink products are discharged from the screens for disposal or further treatment.

The undersize products from the washing screens, consisting of medium, wash water, and fines, are too dilute and contaminated to be returned directly as medium to the separating vessel. They are treated individually as shown, or together, by magnetic separation, to recover the magnetic ferrosilicon or magnetite from the non-magnetic fines. Reclaimed, cleaned medium is thickened to the required density by a centrifugal or spiral densifier, which continuously returns it to the DMS circuit. The densified medium discharge passes through a demagnetising coil to ensure a non-flocculated, uniform suspension in the separating vessel.

Most large DMS plants include automatic control of the feed medium density. This is done by densifying sufficient medium to cause the medium density to rise, measuring the feed density with a gamma attenuation gauge, and using the signal to adjust the amount of water added to the medium to return it to the correct density.

The major costs in DMS are power (for pumping) and medium consumption. Medium losses can account for 10–35% of total costs. They are principally due to adhesion to products and losses from the magnetic separators, though the proportions will depend on the size and porosity of the ore, the characteristics of the medium solids, and the plant design (Napier-Munn et al., 1995). Losses increase for fine or porous ore, fine media, and high operating densities.

Correct sizing and selection of equipment, together with correct choice of design parameters such as rinsing water volumes, are essential. As effluent water always contains some entrained medium, the more of this that can be recycled back to the plant the better (Dardis, 1987). Careful attention should also be paid to the quality of the medium used, Williams and Kelsall (1992) having shown that certain ferrosilicon powders are more prone to mechanical degradation and corrosion than others.

Medium rheology is critical to efficient operation of dense medium systems (Napier-Munn, 1990), although the effects of viscosity are difficult to quantify (Reeves, 1990; Dunglison et al., 1999). Management of viscosity includes selecting the correct medium specifications, minimising operating density, and minimising the content of clays and other fine contamination (Napier-Munn and Scott, 1990). If the amount of fines in the circuit reaches a high proportion due, say, to inefficient screening of the feed, it may be necessary to divert an increased amount of medium into the cleaning circuit. Many circuits have such a provision, allowing medium from the draining screen to be diverted into the washing screen undersize sump.

Typical dense medium separations

The most important use of DMS is in coal preparation where a relatively simple separation removes the low-ash coal from the heavier high-ash discard and associated shales and sand-stones.

DMS is preferred to the cheaper Baum jig method of separation when washing coals with a relatively large proportion of middlings, or near-density material, since the separating density can be controlled to much closer limits.

British coals, in general, are relatively easy to wash, and jigs are used in many cases. Where DMS is preferred, Drum and Drewboys separators are most widely used for the coarser fractions, with DSM cyclones and Vorsyl separators being preferred for the fines. DMS is essential with most Southern Hemisphere coals, where a high middlings fraction is present. This is especially so with the large, low-grade coal deposits found in the former South African Transvaal province. Drums and Norwalt baths are the most common separators utilised to wash such coals, with DSM cyclones and Dyna Whirlpools being used to treat the finer fractions.

At Amcoal's Landau Colliery in the Transvaal, a two-density operation is carried out in order to produce two saleable products. After preliminary screening of the run-of-mine coal, the coarse (+7 mm) fraction is washed in Norwalt bath separators, utilising magnetite as the medium to give a separating density of 1.6. The sinks product from

this operation, consisting predominantly of sand and shales, is discarded, and the floats product is routed to Norwalt baths operating at a lower density of 1.4. This separation stage produces a low-ash floats product, containing about 7.5% ash, which is used for metallurgical coke production, and a sinks product, which is the process middlings, containing about 15% ash, which is used as power-station fuel. The fine (0.5–7 mm) fraction is treated in a similar two-stage manner utilising Dyna Whirlpool separators.

In metalliferous mining, DMS is used in the preconcentration of lead–zinc ores, in which the disseminated sulphide minerals often associate together as replacement bandings in the light country rock, such that marked specific gravity differences between particles crushed to fairly coarse sizes can be exploited.

A dense medium plant was incorporated into the lead–zinc circuit at Mount Isa Mines Ltd., Australia, in 1982 in order to increase the plant throughput by 50%. The ore, containing roughly 6.5% lead, 6.5% zinc, and 200 ppm silver, consists of galena, sphalerite, pyrite, and other sulphides finely disseminated in distinct bands in quartz and dolomite (Figure 11.13). Liberation of the ore into particles which are either sulphide-rich or predominantly gangue begins at around −50 mm, and becomes substantial below 18 mm.

The plant treats about $800\,t\,h^{-1}$ of material, in the size range 1.7–13 mm by DSM cyclones, at a separating density of $3.05\,kg\,l^{-1}$, to reject 30–35% of the run-of-mine ore as tailings, with 96–97% recoveries of lead, zinc, and silver to the pre-concentrate. The pre-concentrate has a 25% lower Bond Work Index, and is less abrasive because the lower specific gravity siliceous material mostly reports to the rejects. The rejects are used as a cheap source of fill for underground operations. The plant is extensively instrumented, the process control strategy being described elsewhere (Munro et al., 1982).

DMS is also used to pre-concentrate tin and tungsten ores, and non-metallic ores such as fluorite, barite, etc. It has a very important use in the pre-concentration of diamond ores, prior to recovery of the diamonds by electronic sorting (Chapter 14) or grease-tabling (Chaston and Napier-Munn, 1974; Rylatt and Popplewell, 1999). Diamonds are the lowest grade of all ores mined, and concentration ratios of several million to one must be achieved. DMS produces an initial enrichment of the ore in the order of 100–1000 to 1 by making use of the fact that diamonds have a fairly high specific gravity (3.5), and are relatively easily liberated from the ore, since they are loosely held in the parent rock. Gravity and centrifugal separators are utilised, with ferrosilicon as the medium, and separating densities of between 2.6 and 3.0 are used. Clays in the ore sometimes present a problem by increasing the medium viscosity, thus reducing separating efficiency and the recovery of diamonds to the sinks.

DMS is also used for upgrading low grade iron ores for blast furnace feed. Both gravity and

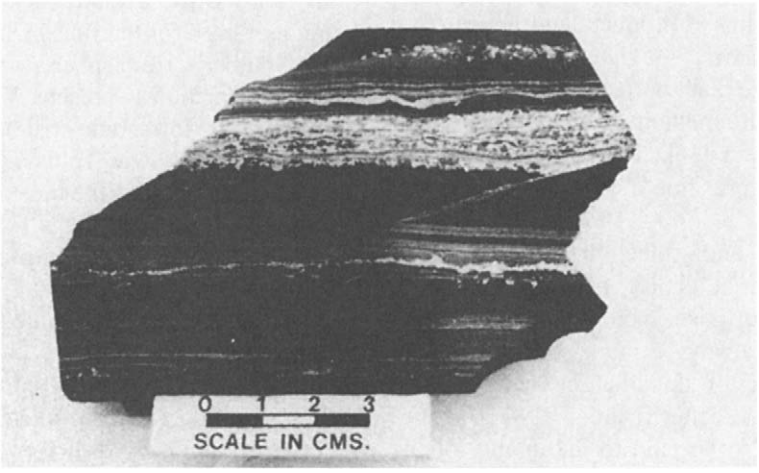


Figure 11.13 Mount Isa ore. Bands of sulphide minerals in carbonaceous host rock

centrifugal separators are used, and in some cases the medium density can exceed 4 (Myburgh, 2002).

Laboratory heavy liquid tests

Laboratory testing may be performed on ores in order to assess the suitability of dense medium separation and other gravity methods, and to determine the economic separating density.

Liquids covering a range of densities in incremental steps are prepared, and the representative sample of crushed ore is introduced into the liquid of highest density. The floats product is removed and washed and placed in the liquid of next lower density, whose float product is then transferred to the next lower density and so on. The sinks product is finally drained, washed, and dried, and then weighed, together with the final floats product, to give the density distribution of the sample by weight (Figure 11.14).

Care should be taken when evaluating ores of fine particle size that sufficient time is given for the particles to settle into the appropriate fraction. Centrifuging is often carried out on fine materials to reduce the settling time, but this should be done with care, as there is a tendency for the floats to become entrained in the sinks fraction. Unsatisfactory results are often obtained with porous materials, such as magnesite ores, due to the entrainment of liquid in the pores, which changes the apparent density of the particles.

After assaying the fractions for metal content, the distribution of material and metal in the density fractions of the sample can be tabulated. Table 11.1 shows such a distribution from tests performed on a tin ore. The computations are easily accomplished in a spreadsheet. It can be seen from columns 3 and 6 of the table that if a separation density of 2.75 was chosen, then 68.48% of the material, being lighter than 2.75, would be discarded as a float product, and only 3.81% of the tin would be lost in this fraction. Similarly, 96.19% of the tin would be recovered into the sink product, which accounts for 31.52% of the original total feed weight.

The choice of *optimum* separating density must be made on economic grounds. In the example shown in Table 11.1, the economic impact of rejecting 68.48% of the feed to HMS on downstream performance must be assessed. The smaller throughput will lower grinding and concentration operating costs, the impact on grinding energy and steel costs often being particularly high. Against these savings, the cost of operating the DMS plant and the effect of losing 3.81% of the run-of-mine tin to floats must be considered. The amount of *recoverable* tin in this fraction has to be estimated, together with its subsequent loss in smelter revenue. If this loss is lower than the saving in overall milling costs, then DMS is economic. The optimum density is that which maximises the difference between overall reduction in milling costs per tonne of run-of-mine ore and loss in smelter revenue. Schena et al. (1990) have analysed the economic choice of separating density and have developed computer software for the evaluation.

Heavy liquid tests are important in coal preparation in order to determine the required density of separation and the expected yield of coal of the required ash content. The "ash" content refers to the amount of incombustible material in the coal. Since coal is lighter than the contained minerals, the higher the density of separation the higher is the *yield*:

$$\text{yield} = \frac{\text{weight of coal floats product} \times 100\%}{\text{total feed weight}}$$

but the higher is the ash content. The ash content of each density fraction from heavy liquid testing is determined by taking about 1 g of the fraction, placing it in a cold well-ventilated furnace, and

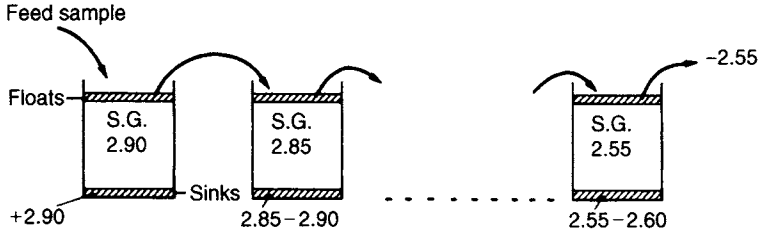


Figure 11.14 Heavy liquid testing

Table 11.1 Heavy liquid test results

(1) *Specific gravity fraction*	(2) *% Weight*	(3) *Cumulative % Weight*	(4) *Assay (% Sn)*	(5) *Distribution (% Sn)*	(6) *Cumulative distribution (% Sn)*
−2.55	1.57	1.57	0.003	0.004	0.004
2.55–2.60	9.22	10.79	0.04	0.33	0.37
2.60–2.65	26.11	36.90	0.04	0.93	1.30
2.65–2.70	19.67	56.57	0.04	0.70	2.00
2.70–2.75	11.91	68.48	0.17	1.81	3.81
2.75–2.80	10.92	79.40	0.34	3.32	7.13
2.80–2.85	7.87	87.27	0.37	2.60	9.73
2.85–2.90	2.55	89.82	1.30	2.96	12.69
+2.90	10.18	100.00	9.60	87.34	100.00

slowly raising the temperature to 815° C, maintaining the sample at this temperature until constant weight is obtained. The residue is cooled and then weighed. The ash content is the mass of ash expressed as a percentage of the initial sample weight taken.

Table 11.2 shows the results of heavy liquid tests performed on a coal sample. The coal was separated into the density fractions shown in column 1, and the weight fractions and ash contents are tabulated in columns 2 and 3 respectively. The weight per cent of each product is multiplied by the ash content to give the ash product (column 4).

The total floats and sinks products at the various separating densities shown in column 5 are tabulated in columns 6–11. To obtain the cumulative per cent for each gravity fraction, columns 2 and 4 are cumulated from top to bottom to give columns 6 and 7 respectively. Column 7 is then divided by column 6 to obtain the cumulative per cent ash (column 8). Cumulative sink ash is obtained in essentially the same manner, except that columns

Table 11.2

(1) *Sp. gr. fraction*	(2) *Wt %*	(3) *Ash %*	(4) *Ash product*	(5) *Separating density*	(6) *Cumulative float (Clean coal)*		(8)	(9) *Cumulative sink (Discard)*		(10)
					Wt %	*Ash product*	*Ash %*	*Wt %*	*Ash product*	*Ash %*
−1.30	0.77	4.4	3.39	1.30	0.77	3.39	4.4	99.23	2213.76	22.3
1.30–1.32	0.73	5.6	4.09	1.32	1.50	7.48	5.0	98.50	2209.67	22.4
1.32–1.34	1.26	6.5	8.19	1.34	2.76	15.67	5.7	97.24	2201.48	22.6
1.34–1.36	4.01	7.2	28.87	1.36	6.77	44.54	6.6	93.23	2172.61	23.3
1.36–1.38	8.92	9.2	82.06	1.38	15.69	126.60	8.1	84.31	2090.55	24.8
1.38–1.40	10.33	11.0	113.63	1.40	26.02	240.23	9.2	73.98	1976.92	26.7
1.40–1.42	9.28	12.1	112.29	1.42	35.30	352.52	10.0	64.70	1864.63	28.8
1.42–1.44	9.00	14.1	126.90	1.44	44.30	479.42	10.8	55.70	1737.73	31.2
1.44–1.46	8.58	16.0	137.28	1.46	52.88	616.70	11.7	47.12	1600.45	34.0
1.46–1.48	7.79	17.9	139.44	1.48	60.67	756.14	12.5	39.33	1461.01	37.1
1.48–1.50	6.42	21.5	138.03	1.50	67.09	894.17	13.3	32.91	1322.98	40.2
+1.50	32.91	40.2	1322.98	–	100.00	2217.15	22.2	0.00	0.00	0.0
Total	100.0	22.2	2217.15							

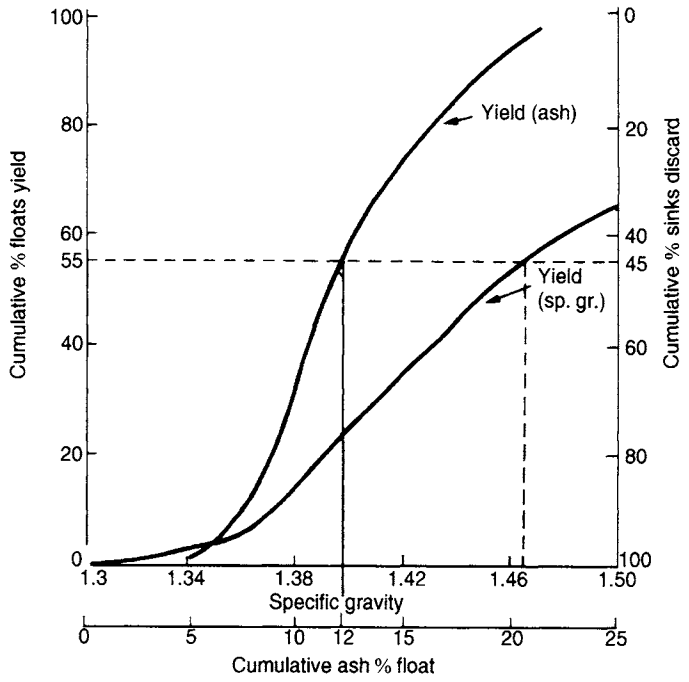


Figure 11.15 Typical coal washability curves

2 and 4 are cumulated from bottom to top to give columns 9 and 10 respectively.

The results of Table 11.2 are plotted in Figure 11.15 as typical *washability curves*.

Suppose an ash content of 12% is required in the coal product. It can be seen from the washability curves that such a coal would be produced at a yield of 55% (cumulative per cent floats), and the required density of separation is 1.465.

The difficulty of the separation in terms of operational control is dependent mainly on the amount of material present in the feed which is close to the required density of separation. For instance, if the feed were composed entirely of pure coal at a sp. gr. of 1.3 and shale at a density of 2.7, then the separation would be easily carried out over a wide range of operating densities. If, however, the feed consists of appreciable middlings, and much material is present very close to the chosen separating density, then only a small variation in this density will seriously affect the yield and ash content of the product.

The amount of near-gravity material present is sometimes regarded as being the weight of material in the range ± 0.1 or $\pm 0.05\,\mathrm{kg\,l^{-1}}$ of the separating density, and separations involving feeds with less than about 7% of ± 0.1 near-gravity material are regarded by coal preparation engineers as being fairly easy to control. Such separations are often performed in Baum jigs, as these are cheaper than dense medium plants, which require expensive media-cleaning facilities, and no feed preparation, i.e. removal of the fine particles by screening, is required. However, the density of separation in jigs is not as easy to control to fine limits, as it is in dense medium baths, and for near-gravity material much above 7%, dense medium separation is preferred.

Heavy liquid tests can be used to evaluate any gravity separation process on any ore, and Table 11.3 can be used to indicate the type of separator which could effect the separation in practice (Mills, 1978).

Table 11.3 takes no account of the particle size of the material and experience is therefore required in its application to heavy liquid results, although some idea of the effective particle size range of gravity separators can be gained from Figure 11.8. The throughput of the plant must also be taken into account with respect to the type of separator chosen. For instance, if a throughput of only a few tonnes per hour is envisaged, there would be little point in

Table 11.3

Wt % within ±0.1 gravity of separation	*Gravity process recommended*	*Type*
0–7	Almost any process	Jigs, tables, spirals
7–10	Efficient process	Sluices, cones, DMS
10–15	Efficient process with good operation	
15–25	Very efficient process with expert operation	DMS
Above 25	Limited to a few exceptionally efficient processes with expert operation	DMS with close control

installing Reichert cones, which are high-capacity units, operating most effectively at about $70\,t\,h^{-1}$.

Efficiency of dense medium separation

Laboratory testing assumes perfect separation and, in such batch tests, conditions are indeed close to the ideal, as sufficient time can be taken to allow complete separation to take place.

In a continuous production process, however, conditions are usually far from ideal and particles can be misplaced to the wrong product for a variety of reasons. The dominant effect is that of the density distribution of the feed. Very dense or very light particles will settle through the medium and report to the appropriate product quickly, but particles of density close to that of the medium will move more slowly and may not reach the right product in the time available for the separation. In the limit, particles of density the same as, or very close to, that of the medium will follow the medium and divide in much the same proportion.

Other factors also play a role in determining the efficiency of separation. Fine particles generally separate less efficiently than coarse, again because of their slower settling rates. The properties of the medium, the design and condition of the separating vessel, and the feed conditions, particularly feed rate, will all influence the separation.

The efficiency of separation can be represented by the slope of a *Partition* or *Tromp* curve, first introduced by K.F. Tromp (1937). It describes the separating efficiency for the separator whatever the quality of the feed and can be used for estimation of performance and comparison between separators.

The partition curve relates the *partition coefficient* or *partition number*, i.e. the percentage of the feed material of a particular specific gravity which reports to either the sinks product (generally used for minerals) or the floats product (generally used for coal), to specific gravity (Figure 11.16). It is exactly analogous to the classification efficiency curve, in which the partition coefficient is plotted against size rather than specific gravity.

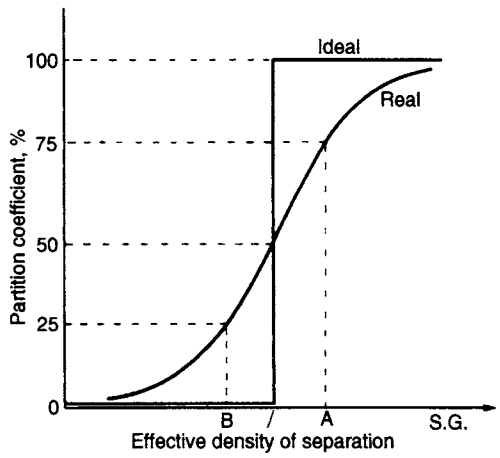


Figure 11.16 Partition or Tromp curve

The ideal partition curve reflects a perfect separation in which all particles having a density higher than the separating density report to sinks, and those lighter report to floats. There is no misplaced material.

The partition curve for a real separation shows that efficiency is highest for particles of density far from the operating density and decreases for particles approaching the operating density.

The area between the two curves is called the "error area" and is a measure of the degree of misplacement of particles to the wrong product.

Many partition curves give a reasonable straight-line relationship between the distribution of 25 and 75%, and the slope of the line between these distributions is used to show the efficiency of the process.

The *probable error of separation* or the *Ecart probable (Ep)* is defined as half the difference between the density where 75% is recovered to sinks and that at which 25% is recovered to sinks, i.e. from Figure 11.16,

$$Ep = (A - B)/2$$

The density at which 50% of the particles report to sinks is shown as the *effective density of separation*, which may not be exactly the same as the medium density, particularly for centrifugal separators, in which the separating density is generally higher than the medium density.

The lower the Ep, the nearer to vertical is the line between 25 and 75% and the more efficient is the separation. An ideal separation has a vertical line with an $Ep = 0$ whereas in practice the Ep usually lies in the range 0.01–0.10.

The Ep is not commonly used as a method of assessing the efficiency of separation in units such as tables, spirals, cones, etc., due to the many operating variables (wash water, table slope, speed, etc.) which can affect the separation efficiency. It is, however, ideally suited to the relatively simple and reproducible DMS process. However care should be taken in its application, as it does not reflect performance at the tails of the curve, which can be important.

Construction of partition curves

The partition curve for an operating dense medium vessel can be determined by sampling the sink and float products and performing heavy liquid tests to determine the amount of material in each density fraction. The range of liquid densities applied must envelope the working density of the dense medium unit. The results of heavy liquid tests on samples of floats and sinks from a vessel separating coal (floats) from shale (sinks) are shown in Table 11.4. The calculations are easily performed in a spreadsheet.

Columns 1 and 2 are the results of laboratory tests on the float and sink products and columns 3 and 4 relate these results to the total distribution of the feed material to floats and sinks which must be determined by weighing the products over a period of time. The weight fraction in columns 3 and 4 can be added together to produce the reconstituted feed weight distribution in each density fraction (column 5). Column 6 gives the nominal specific gravity of each density range, i.e. material in the density range 1.30–1.40 is assumed to have a specific gravity lying midway between these densities −1.35.

The partition coefficient (column 7) is the percentage of feed material of a certain nominal specific gravity which reports to sinks, i.e.

$$\frac{\text{column 4}}{\text{column 5}} \times 100\%.$$

It can also be determined by applying the two-product formula (Chapter 3) to the density distributions of feed, sinks, and floats, if all three are available and accurate.

The partition curve can then be constructed by plotting the partition coefficient against the nominal specific gravity, from which the probable error of separation of the vessel can be determined.

An alternative, rapid, method of determining the partition curve of a separator is to utilise density tracers. Specially developed colour-coded plastic tracers can be fed to the process, the partitioned products being collected and hand sorted by density (colour). It is then a simple matter to construct the partition curve directly by noting the proportion of each density of tracer reporting to either the sink or float product. Application of tracer methods has shown that considerable uncertainties can exist in experimentally determined Tromp curves unless an adequate number of tracers is used, and Napier-Munn (1985) presents graphs that facilitate the selection of sample size and the calculation of confidence limits. A system in operation in a US coal preparation plant uses sensitive metal detectors that automatically spot and count the number of different types of tracers passing through a stream. The tracers, of various size and density, are selectively fed into the feed stream of a Baum jig by a computer-controlled dispensing system, allowing the jig's real-time performance to be assessed (Chironis, 1987).

Table 11.4 Coal–shale separation evaluation

Specific gravity fraction	*(1) Floats analysis (wt %)*	*(2) Sinks analysis (wt %)*	*(3) Floats % of feed*	*(4) Sinks % of feed*	*(5) Reconstituted feed (%)*	*(6) Nominal sp. gr.*	*(7) Partition coefficient*
−1.30	83.34	18.15	68.83	3.15	71.98	–	4.39
1.30–1.40	10.50	10.82	8.67	1.89	10.56	1.35	17.80
1.40–1.50	3.35	9.64	2.77	1.68	4.45	1.45	37.75
1.50–1.60	1.79	13.33	1.48	2.32	3.80	1.55	61.05
1.60–1.70	0.30	8.37	0.25	1.46	1.71	1.65	85.38
1.70–1.80	0.16	5.85	0.13	1.02	1.15	1.75	88.70
1.80–1.90	0.07	5.05	0.06	0.88	0.94	1.85	93.62
1.90–2.00	0.07	4.34	0.06	0.75	0.81	1.95	92.68
+2.00	0.42	24.45	0.35	4.25	4.60	–	92.39
Totals	100.00	100.00	82.60	17.40	100.00		

Partition curves can be used to predict the products that would be obtained if the feed or separation gravity were changed. The curves are *specific to the vessel for which they were established* and are not affected by the type of material fed to it, provided:

(a) The feed size range is the same – efficiency generally decreases with decrease in size; Figure 11.17 shows typical efficiencies of bath (drum, cone, etc.) and centrifugal (cyclone, DWP, etc.) separators versus particle size. It can clearly be seen that, in general, below about 10 mm, centrifugal separators are better than baths;

(b) the separating gravity is in approximately the same range – the higher the effective separating density the greater the probable error, due to the increased medium viscosity. It has in fact been shown that the *Ep* is directly proportional to the separating density, all other factors being the same (Gottfried, 1978);

(c) the feed rate is the same.

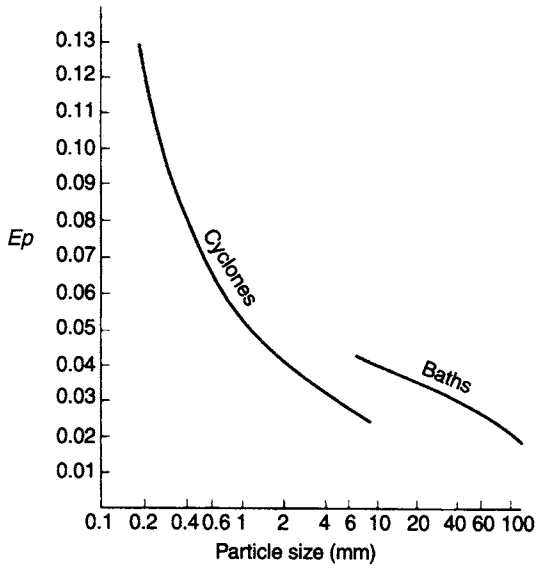


Figure 11.17 Effect of particle size on efficiency of dense media separators

The partition curve for a vessel can be used to determine the amount of misplaced material which will report to the products for any particular feed material. For example, the distribution of the products from the tin ore, which was evaluated by heavy liquid tests (Table 11.1) can be determined for treatment in an operating separator. Figure 11.18 shows a partition curve for a separator having an *Ep* of 0.07.

The curve can be shifted slightly along the abscissa until the effective density of separation corresponds to the laboratory evaluated separating density of 2.75. The distribution of material to sinks and floats can now be evaluated, e.g. at a nominal specific gravity of 2.725, 44.0% of the material reports to the sinks and 56.0% to the floats.

The performance is evaluated in Table 11.5. Columns 1, 2, and 3 show the results of the heavy liquid tests, which were tabulated in Table 11.1. Columns 4 and 5 are the distributions to sinks

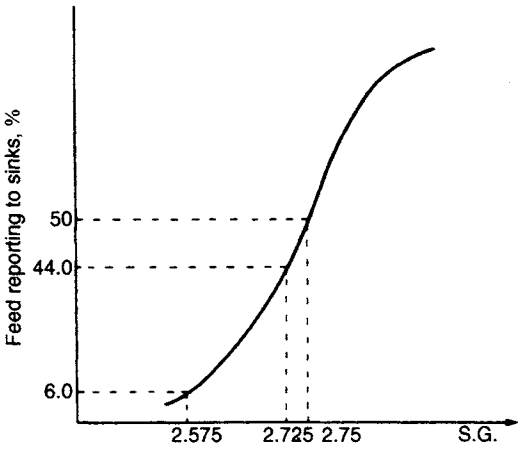


Figure 11.18 Partition curve for $Ep = 0.07$

and floats respectively, obtained from the partition curve. Column 6 = column 1 × column 4, and column 9 = column 1 × column 5. The assay of each fraction is assumed to be the same whether or not the material reports to sinks or floats (columns 2, 7, and 10). Columns 8 and 11 are then calculated as the amount of tin reporting to sinks and floats in each fraction (columns 6 × 7 and 9 × 10) as a percentage of the total tin in the feed (sum of columns 1 × 2).

The total distribution of the feed to sinks is the sum of all the fractions in column 6, i.e. 40.26%, while the recovery of tin into the sinks is the sum of the fractions in column 8, i.e. 95.29%. This compares with a distribution of 31.52% and a recovery of 96.19% of tin in the ideal separation.

This method of evaluating the performance of a separator on a particular feed is tedious and is ideal for a spreadsheet, providing that the partition numbers for each density fraction are known. These can be represented by a suitable mathematical function. There is a large literature on the selection and application of such functions. Some are arbitrary, and others have some theoretical or heuristic justification. The key feature of the partition curve is its S-shaped character. In this it bears a passing resemblance to a number of probability distribution functions and indeed the curve can be thought of as a statistical description of the DMS process, describing the probability with which a particle of given density (and other characteristics) reports to the sink product. Tromp himself recognised this in suggesting that the amount of misplaced material relative to a suitably transformed density scale was normally distributed, and Jowett (1986) showed that a partition curve for a process controlled by simple probability factors should have a normal distribution form.

However, many real partition curves do not behave ideally as does the one illustrated in Figure 11.16. In particular they are not asymptotic to 0 and 100% but exhibit evidence of short-circuit flow to one or both products. Stratford

Table 11.5 Tin ore evaluation

Specific gravity fraction	*Nominal sp. gr.*	*Feed*			*Distribution to (%)*		*Sinks*			*Floats*		
		(1) Wt %	*(2) % Sn*	*(3) % Dist.*	*(4) Sinks*	*(5) Floats*	*(6) Wt %*	*(7) % Sn*	*(8) % (feed) distribution*	*(9) Wt %*	*(10) % Sn*	*(11) % (feed) distribution*
−2.55	–	1.57	0.003	0.004	0.00	100.00	0.00	0.003	0.00	1.57	0.003	0.04
2.55–2.60	2.575	9.22	0.04	0.33	6.0	94.00	0.55	0.04	0.02	8.67	0.04	0.31
2.60–2.65	2.625	26.11	0.04	0.93	13.5	86.5	3.52	0.04	0.13	22.59	0.04	0.80
2.65–2.70	2.675	19.67	0.04	0.70	27.0	73.0	5.31	0.04	0.19	14.35	0.04	0.51
2.70–2.75	2.725	11.91	0.17	1.81	44.0	56.0	5.24	0.17	0.80	6.67	0.17	1.01
2.75–2.80	2.775	10.92	0.34	3.32	63.0	37.0	6.88	0.34	2.09	4.04	0.34	1.23
2.80–2.85	2.825	7.87	0.37	2.60	79.5	20.5	6.26	0.37	2.07	1.61	0.37	0.53
2.85–2.90	2.875	2.55	1.30	2.96	90.5	9.5	2.32	1.30	2.68	0.24	1.30	0.28
+2.90	–	10.18	9.60	87.34	100.00	0.00	10.18	9.60	87.31	0.00	9.60	0.00
Totals		100.00	1.12	100.00			40.26	2.65	95.29	59.74	0.09	4.71

and Napier-Munn (1986) identified four attributes required of a suitable function to represent the partition curve:

(1) It should have natural asymptotes, preferably described by separate parameters.
(2) It should be capable of exhibiting asymmetry about the separating density; ie the differentiated form of the function should be capable of describing skewed distributions.
(3) It should be mathematically continuous.
(4) Its parameters should be capable of estimation by accessible methods.

A two-parameter function asymptotic to 0 and 100% is the Rosin-Rammler function, originally developed to describe size distributions (Tarjan, 1974):

$$P_i = 100 - 100\exp\left[-\left(\frac{\rho_i}{a}\right)^m\right] \qquad (11.1)$$

In this form, P_i is the partition number (feed reporting to sinks, %), ρ_i is the mean density of density fraction i, and a and m are the parameters of the function; m describes the width of the curve (high values of m indicating more efficient separations). Partition curve functions are normally expressed in terms of the *normalised* density, ρ/ρ_{50}, where ρ_{50} is the separating density. The normalised curve is generally independent of cut-point and medium density, but dependent on particle size. Inserting this into Equation 11.1, and noting that $P = 50$ for $\rho = \rho_{50}$ $(\rho/\rho_{50} = 1)$, gives:

$$P_i = 100 - 100\exp\left[-\ln 2\left(\frac{\rho_i}{\rho_{50}}\right)^m\right] \qquad (11.2)$$

One of the advantages of Equation 11.2 is that it can be linearised so that simple linear regression can be used to estimate m and ρ_{50} from experimental data:

$$\ln\left[\frac{\ln\left(\frac{100}{100 - P_i}\right)}{\ln 2}\right] = m\ln\rho_i - m\ln\rho_{50} \qquad (11.3)$$

Gottfried (1978) proposed a related function, the Weibull function, with additional parameters to account for the fact that the curves do not always reach the 0 and 100% asymptotes due to short-circuit flow:

$$P_i = 100 - 100\left[f_0 + c\exp\left(-\frac{(\rho_i/\rho_{50} - x_0)^a}{b}\right)\right] \qquad (11.4)$$

The six parameters of the function (c, f_0, ρ_{50}, x_0, a, and b) are not independent, so by the argument of Equation 11.2 x_0 can be expressed as:

$$x_0 = 1 - \left[b\ln\left(\frac{c}{0.5 - f_0}\right)\right]^{1/a} \qquad (11.5)$$

In this version of the function, representing percent of feed to sinks, f_0 is the proportion of high density material misplaced to floats, and $1 - (c + f_0)$ is the proportion of low density material misplaced to sinks, so that $c + f_0 \leq 1$. The curve therefore varies from a minimum of $100[1 - (c + f_0)]$ to a maximum of $100(1 - f_0)$.

The parameters of Equation 11.4 have to be determined by non-linear estimation. Non-linear optimisation routines are available in spreadsheets. First approximations of c, f_0 and ρ_{50} can be obtained from the curve itself.

King and Juckes (1988) utilised Whiten's classification function with two additional parameters to describe the short-circuit flows or by-pass:

$$P_i = \beta + (1 - \alpha - \beta)\left[\frac{e^{b\rho_i/\rho_{50}} - 1}{e^{b\rho_i/\rho_{50}} + e^b - 2}\right] \qquad (11.6)$$

Here, for $P =$ proportion to underflow, α is the fraction of feed which short-circuits to overflow and β is the fraction of feed which short-circuits to underflow; b is an efficiency parameter, with high values of b indicating high efficiency. Again the function is non-linear in the parameters.

The Ep (Figure 11.16) can be predicted from these functions by substitution for ρ_{75} and ρ_{25}. Scott and Napier-Munn (1992) showed that for efficient separations (low Eps) without short-circuiting, the partition curve could be approximated by:

$$P_i = \frac{1}{1 + \exp\left[\frac{\ln 3(\rho_{50} - \rho_i)}{Ep}\right]} \qquad (11.7)$$

Organic efficiency

The term *organic efficiency* is often used to express the efficiency of coal preparation plants. It is defined as the ratio (normally expressed as a percentage) between the actual yield of a desired product and the theoretical possible yield at the same ash content.

For instance, if the coal, whose washability data is plotted in Figure 11.15, produced an operating

yield of 51% at an ash content of 12%, then, since the theoretical yield at this ash content is 55%, the organic efficiency is equal to 51/55, or 92.7%.

Organic efficiency cannot be used to compare the efficiencies of different plants, as it is a dependent criterion, and is much influenced by the washability of the coal. It is possible, for example, to obtain a high organic efficiency on a coal containing little near-gravity material, even when the separating efficiency, as measured by partition data, is quite poor.

References

Anon. (1984). Sodium metatungstate, a new medium for binary and ternary density gradient centrifugation, *Makromol. Chem.*, **185**, 1429.

Anon. (1985). Feeding to zero: Island Creek's experience in Kentucky, *Coal Age*, **90**(Jan.), 66.

Baguley, P.J., Napier-Munn, T.J. (1996). Mathematical model of the dense medium drum, *Trans. Inst. Min. Met.*, **105**, C1–C8.

Burton, M.W.A., et al. (1991). The economic impact of modern dense medium systems, *Minerals Engng.*, **4(3/4)**, 225.

Chaston, I.R.M. and Napier-Munn, T.J. (1974). Design and operation of dense-medium cyclone plants for the recovery of diamonds in Africa, *J. S. Afr. Inst. Min. Metall.*, **75(5)** (Dec.), 120–133.

Chironis, N.P. (1987). On-line coal-tracing system improves cleaning efficiencies. *Coal Age*, **92**(Mar.), 44.

Collins, B., Napier-Munn, T.J., and Sciarone, M. (1974). The production, properties and selection of ferrosilicon powders for heavy medium separation, *J. S. Afr. Inst. Min. Met.*, **75(5)** (Dec.), 103–119.

Dardis, K.A. (1987). The design and operation of heavy medium recovery circuits for improved medium recovery, *Dense Medium Operator's Conference*, Aust. Inst. Min. Metall., Victoria, 157.

Domenico, J.A., Stouffer, N.J., and Faye, C. (1994). Magstream as a heavy liquid separation alternative for mineral sands exploration, *SME Annual Meeting*, SME, Albuquerque (Feb.), Preprint 94–262.

Dunglison, M.E. and Napier-Munn, T.J. (1997). Development of a general model for the dense medium cyclone, *6th Samancor Symp. on DMS*, Broome, May (Samancor).

Dunglison, M.E., Napier-Munn, T.J., and Shi, F. (1999). The rheology of ferrosilicon dense medium suspensions, *Min. Proc. Ext. Review*, **20**, 183–196.

Fallon, N.E. and Gottfried, B.S. (1985). Statistical representation of generalized distribution data for float-sink coal-cleaning devices: Baum jigs, Batac jigs, Dynawhirlpools, *Int. J. Min. Proc.*, **15**(Oct.), 231.

Ferrara, G. and Schena, G.D. (1986). Influence of contamination and type of ferrosilicon on viscosity and stability of dense media, *Trans. Inst. Min. Metall.*, **95**(Dec.), C211.

Ferrara, G., Machiavelli, G., Bevilacqua, P., and Meloy, T.P. (1994). Tri-Flo: Multistage high-sharpness DMS process with new applications, *Minerals and Metallurgical Processing*, **11**(May), 63.

Gottfried, B.S. (1978). A generalisation of distribution data for characterizing the performance of float-sink coal cleaning devices, *Int. J. Min. Proc.*, **5**, 1.

Hacioglu, E. and Turner, J.F. (1985). A study of the Dynawhirlpool, *Proc. XVth Int. Min. Proc. Cong.*, **1**, 244, Cannes.

Hunt, M.S., et al. (1986). The influence of ferrosilicon properties on dense medium separation plant consumption, *Bull. Proc. Australas. Inst. Min. Metall.*, **291**(Oct.), 73.

Jowett, A. (1986). An appraisal of partition curves for coal-cleaning processes, *Int. J. Min. Proc.*, **16**(Jan.), 75.

King, R.P. and Juckes, A.H. (1988). Performance of a dense medium cyclone when beneficiating fine coal, *Coal Preparation*, **5**, 185–210.

Kitsikopoulos, H., et al. (1991). Industrial operation of the first two-density three-stage dense medium separator processing chromite ores, *Proc. XVII Int. Min. Proc. Cong.* Dresden, Vol. 3, Bergakademie Freiberg, 55.

Lane, D.E. (1987). Point of Ayr Colliery, *Mining Mag.* **157**(Sept.), 226.

Lee, D., Holtham, P.N., Wood, C.J. and Hammond R. (1995). Operating experience and performance evaluation of the 1150 mm primary dense medium cyclone at Warkworth Mining, *Proc. 7th Aus. Coal. Prep. Conf.*, Mudgee, Aus. Coal. Prep. Soc., Paper B1 (Sept.), 71–85.

Mills, C. (1978). Process design, scale-up and plant design for gravity concentration, in *Mineral Processing Plant Design*, ed. A.L. Mular and R.B. Bhappu, AIMME, New York.

Munro, P.D., et al. (1982). The design, construction and commissioning of a heavy medium plant of silver-lead-zinc ore treatment-Mount Isa Mines Ltd., *Proc. XIVth Int. Min. Proc. Cong.*, Paper VI-6, Toronto.

Myburgh, H.A. (2002). The influence of the quality of ferrosilicon on the rheology of dense medium and the ability to reach higher densities, *Proc. Iron Ore 2002*, Aus. IMM, Perth (Sept.), 313–317.

Napier-Munn, T.J. (1985). Use of density tracers for determination of the Tromp curve for gravity separation processes, *Trans. Inst. Min. Metall.*, **94**(Mar.), C45.

Napier-Munn, T.J. (1990). The effect of dense medium viscosity on separation efficiency, *Coal Preparation*, **8(3–4)**, 145.

Napier-Munn T.J. (1991). Modelling and simulating dense medium separation processes – a progress report, *Minerals Engng.*, **4(3/4)**, 329.

Napier-Munn, T.J. and Scott, I.A. (1990). The effect of demagnetisation and ore contamination on the viscosity of the medium in a dense medium cyclone plant, *Minerals Engng.*, **3(6)**, 607–613.

Napier-Munn T.J. et al. (1995). Some causes of medium loss in dense medium plants, *Minerals Engng.*, **8(6)**, 659.

Parsonage, P. (1980). Factors that influence performance of pilot-plant paramagnetic liquid separator for dense particle fractionation, *Trans. IMM*, Sec. C, **89**(Dec.), 166.

Reeves, T.J. (1990). On-line viscosity measurement under industrial conditions, *Coal Preparation*, **8(3–4)**, 135.

Ruff, H.J. (1984). New developments in dynamic dense-medium systems, *Mine and Quarry*, **13**(Dec.), 24.

Rylatt, M.G. and Popplewell, G.M. (1999). Diamond processing at Ekati in Canada, *Mining Engng.*, SME, (Feb.), 19–25.

Schena, G.D., Gochin, R.J., and Ferrara, G. (1990). Pre-concentration by dense-medium separation – an economic evaluation. *Trans. Inst. Min. Metall.*, sect. C (Jan.–Apr.), C21.

Scott, I.A. and Napier-Munn, T.J. (1992). Dense medium cyclone model based on the pivot phenomenon, *Trans. Inst. Min. Metall.*, **101**, C61–C76.

Shah, C.L. (1987). A new centrifugal dense medium separator for treating 250 t/h of coal sized up to 100 mm, *3rd Int. Conf. on Hydrocyclones*, Oxford, BHRA (Sept./Oct.), 91–100.

Shaw, S.R. (1984). The Vorsyl dense-medium separator: some recent developments, *Mine and Quarry*, **13**(Apr.), 28.

Stewart, K.J. and Guerney, P.J. (1998). Detection and prevention of ferrosilicon corrosion in dense medium plants, *6th Mill Ops. Conf.*, Aus. IMM, Madang (Oct.), 177–183.

Stratford, K.J. and Napier-Munn, T.J. (1986). Functions for the mathematical representation of the partition curve for dense medium cyclones, *Proc. 19th APCOM*, SME, Penn. State Univ. (Apr.), 719–728.

Symonds, D.F. and Malbon, S. (2002). Sizing and selection of heavy media equipment: Design and layout, *Proc. Min. Proc. Plant Design, Practice and Control*, ed. Mular, Halbe and Barratt, SME, 1011–1032.

Tarjan, G. (1974). Application of distribution functions to partition curves, *Int. J. Min. Proc.*, **1**, 261–265.

Tromp, K.F. (1937). New methods of computing the washability of coals, *Coll. Guard.*, 154, 955–959, 1009; May 21.

Williams, R.A. and Kelsall, G.H. (1992). Degradation of ferrosilicon media in dense medium separation circuits, *Minerals Engng.*, **5(1)**, 57.

Wills. B.A. and Lewis, P.A. (1980). Applications of the Dyna Whirlpool in the minerals industry, *Mining Mag.* (Sept.), 255.

Wood, C.J., Davis, J.J., and Lyman, G.J. (1987). Towards a medium behaviour based performance model for coal-washing DM cyclones, *Dense Medium Operators Conference*, Aus. IMM, Brisbane (Jul.), 247–256.

12

Froth flotation

Introduction

Flotation is undoubtedly the most important and versatile mineral processing technique, and both its use and application are continually being expanded to treat greater tonnages and to cover new areas.

Originally patented in 1906, flotation has permitted the mining of low-grade and complex ore bodies which would have otherwise been regarded as uneconomic. In earlier practice the tailings of many gravity plants were of a higher grade than the ore treated in many modern flotation plants.

Flotation is a selective process and can be used to achieve specific separations from complex ores such as lead–zinc, copper–zinc, etc. Initially developed to treat the sulphides of copper, lead, and zinc, the field of flotation has now expanded to include platinum, nickel, and gold-hosting sulphides, and oxides, such as hematite and cassiterite, oxidised minerals, such as malachite and cerussite, and non-metallic ores, such as fluorite, phosphates, and fine coal.

Principles of flotation

Flotation is a physico-chemical separation process that utilises the difference in surface properties of the valuable minerals and the unwanted gangue minerals. The theory of froth flotation is complex, involving three phases (solids, water, and froth) with many subprocesses and interactions, and is not completely understood. The subject has been reviewed comprehensively by a number of authors (Sutherland and Wark, 1955; Glembotskii et al., 1972; King, 1982; Leja, 1982; Ives, 1984; Jones and Woodcock, 1984; Schulze, 1984; Fuerstenau et al., 1985; Crozier, 1992; Laskowski and Poling, 1995; Harris et al., 2002; Johnson and Munro, 2002; Rao, 2004), and will only be dealt with briefly here.

The process of material being recovered by flotation from the pulp comprises three mechanisms:

(1) Selective attachment to air bubbles (or "true flotation").
(2) Entrainment in the water which passes through the froth.
(3) Physical entrapment between particles in the froth attached to air bubbles (often referred to as "aggregation").

The attachment of valuable minerals to air bubbles is the most important mechanism and represents the majority of particles that are recovered to the concentrate. Although true flotation is the dominant mechanism for the recovery of valuable mineral, the separation efficiency between the valuable mineral and gangue is also dependent on the degree of entrainment and physical entrapment. Unlike true flotation, which is chemically selective to the mineral surface properties, both gangue and valuable minerals alike can be recovered by entrainment and entrapment. Drainage of these minerals occurs in the froth phase and controlling the stability of this phase is important to achieve an adequate separation. In industrial flotation plant practice, entrainment of unwanted gangue can be common and hence a single flotation stage is uncommon. Often several stages of flotation (called "circuits") are required to reach an economically acceptable quality of valuable mineral in the final product.

True flotation utilises the differences in physico-chemical surface properties of particles of various minerals. After treatment with reagents, such differences in surface properties between the minerals within the flotation pulp become apparent and, for flotation to take place, an air bubble must be able to attach itself to a particle, and lift it to the water surface. Figure 12.1 illustrates the principles of flotation in a mechanical flotation cell. The agitator provides enough turbulence in the pulp phase to promote collision of particles and bubbles which

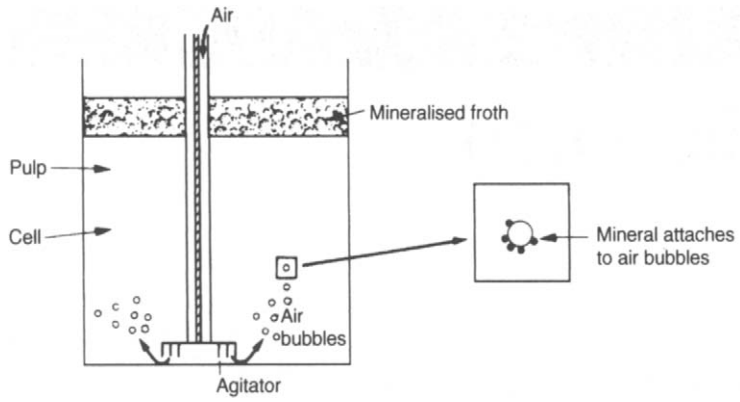


Figure 12.1 Principle of froth flotation

results in the attachment of valuable particles to bubbles and their transport into the froth phase for recovery.

The process can only be applied to relatively fine particles, because if they are too large the adhesion between the particle and the bubble will be less than the particle weight and the bubble will therefore drop its load. There is an optimum size range for successful flotation (Trahar and Warren, 1976; Crawford and Ralston, 1988; Finch and Dobby, 1990).

In flotation concentration, the mineral is usually transferred to the froth, or float fraction, leaving the gangue in the pulp or tailing. This is *direct flotation* and the opposite is *reverse flotation*, in which the gangue is separated into the float fraction.

The function of the froth phase is to enhance the overall selectivity of the flotation process. The froth achieves this by reducing the recovery of entrained material to the concentrate stream, while preferentially retaining the attached material. This increases the concentrate grade whilst limiting as far as possible the reduction in recovery of valuables. The relationship between recovery and grade is a trade-off that needs to be managed according to operational constraints and is incorporated in the management of an optimum froth stability. As the final separation phase in a flotation cell, the froth phase is a crucial determinant of the grade and recovery of the flotation process.

The mineral particles can only attach to the air bubbles if they are to some extent water-repellent, or *hydrophobic*. Having reached the surface, the air bubbles can only continue to support the mineral particles if they can form a stable froth, otherwise they will burst and drop the mineral particles. To achieve these conditions it is necessary to use the numerous chemical compounds known as *flotation reagents*, (Ranney, 1980; Crozier, 1984; Suttill, 1991; Nagaraj, 1994; Fuerstenau and Somasundaran, 2003).

The activity of a mineral surface in relation to flotation reagents in water depends on the forces which operate on that surface. The forces tending to separate a particle and a bubble are shown in Figure 12.2. The tensile forces lead to the development of an angle between the mineral surface and the bubble surface. At equilibrium,

$$\gamma_{s/a} = \gamma_{s/w} + \gamma_{w/a} \cos \theta \qquad (12.1)$$

where $\gamma_{s/a}$, $\gamma_{s/w}$ and $\gamma_{w/a}$ are the surface energies between solid and air, solid and water and water and air, respectively, and θ is the contact angle between the mineral surface and the bubble.

The force required to break the particle–bubble interface is called the *work of adhesion*, $W_{s/a}$, and

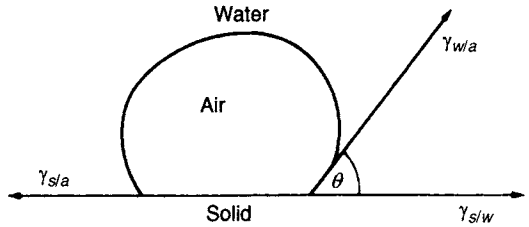


Figure 12.2 Contact angle between bubble and particle in an aqueous medium

is equal to the work required to separate the solid–air interface and produce separate air–water and solid–water interfaces, i.e.

$$W_{s/a} = \gamma_{w/a} + \gamma_{s/w} - \gamma_{s/a} \qquad (12.2)$$

Combining with Equation 12.1 gives

$$W_{s/a} = \gamma_{w/a}(1 - \cos\theta) \qquad (12.3)$$

It can be seen that the greater the contact angle the greater is the work of adhesion between particle and bubble and the more resilient the system is to disruptive forces. The hydrophobicity of a mineral therefore increases with the contact angle; minerals with a high contact angle are said to be *aerophilic*, i.e. they have a higher affinity for air than for water. The terms *hydrophobicity* and *floatability* are often used interchangeably. Hydrophobicity, however, refers to a thermodynamic characteristic, whereas floatability is a kinetic characteristic and incorporates other particle properties affecting amenability to flotation (Leja, 1982; Laskowski, 1986; Woods, 1994).

Most minerals are not water-repellent in their natural state and flotation reagents must be added to the pulp. The most important reagents are the *collectors*, which adsorb on mineral surfaces, rendering them hydrophobic (or aerophilic) and facilitating bubble attachment. The *frothers* help maintain a reasonably stable froth. *Regulators* are used to control the flotation process; these either activate or depress mineral attachment to air bubbles and are also used to control the pH of the system. Useful reviews of flotation reagents and their behaviour include those of Crozier (1984); Somasundaran and Sivakumar (1988), Ahmed and Jameson (1989), Adkins and Pearse (1992), Nagaraj (1994), Buckley and Woods (1997), and Ralston et al. (2001).

Classification of minerals

All minerals are classified into *polar* or *non-polar types* according to their surface characteristics. The surfaces of non-polar minerals are characterised by relatively weak molecular bonds. The minerals are composed of covalent molecules held together by van der Waals forces, and the non-polar surfaces do not readily attach to the water dipoles, and in consequence are hydrophobic. Minerals of this type, such as graphite, sulphur, molybdenite, diamond, coal, and talc, thus have high natural floatabilities with contact angles between 60 and 90°. Although it is possible to float these minerals without the aid of chemical agents, it is universal to increase their hydrophobicity by the addition of hydrocarbon oils or frothing agents. Creosote, for example, is widely used to increase the floatability of coal. Use is made of the natural hydrophobicity of diamond in *grease tabling*, a classical method of diamond recovery which is still used in some plants. The pre-concentrated diamond ore slurry is passed over inclined vibrating tables, which are covered in a thick layer of petroleum grease. The diamonds become embedded in the grease because of their water-repellency, while the water-wetted gangue particles are washed off the table. The grease is skimmed off the table either periodically or continuously, and placed in perforated pots (Figure 12.3), which are immersed in boiling water. The grease melts, and runs out through the perforations, and is collected and re-used, while the pot containing

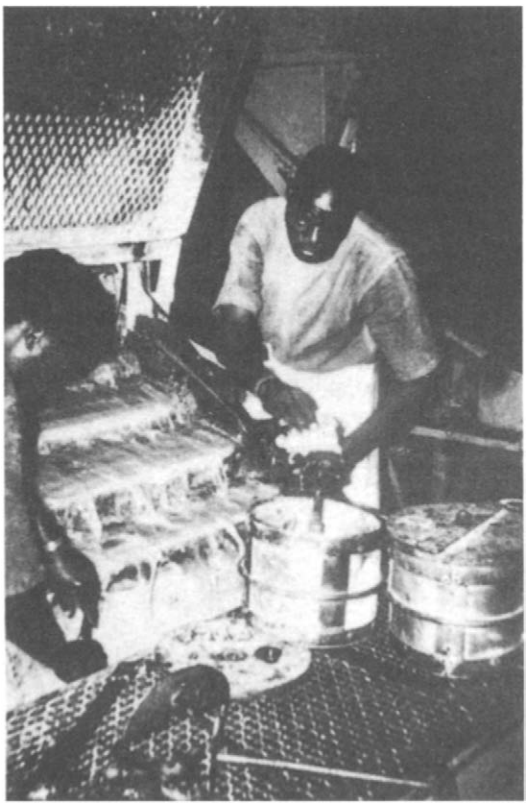


Figure 12.3 Diamond recovery grease table

Table 12.1 Classification of polar minerals

Group 1	*Group 2*	*Group 3(a)*	*Group 4*	*Group 5*
Galena	Barite	Cerrusite	Hematite	Zircon
Covellite	Anhydrite	Malachite	Magnetite	Willemite
Bornite	Gypsum	Azurite	Gothite	Hemimorphite
Chalcocite	Anglesite	Wulfenite	Chromite	Beryl
Chalcopyrite			Ilmenite	Feldspar
Stibnite		*Group 3(b)*	Corundum	Sillimanite
Argentite		Fluorite	Pyrolusite	Garnet
Bismuthinite		Calcite	Limonite	Quartz
Millerite		Witherite	Borax	
Cobaltite		Magnesite	Wolframite	
Arsenopyrite		Dolomite	Columbite	
Pyrite		Apatite	Tantalite	
Sphalerite		Scheelite	Rutile	
Orpiment		Smithsonite	Cassiterite	
Pentlandite		Rhodochrosite		
Realgar		Siderite		
Native Au, Pt, Ag, Cu		Monazite		

the diamonds is transported to the diamond-sorting section.

Minerals with strong covalent or ionic surface bonding are known as polar types, and exhibit high free energy values at the polar surface. The polar surfaces react strongly with water molecules, and these minerals are naturally hydrophilic.

The polar group of minerals have been subdivided into various classes depending on the magnitude of polarity (Wrobel, 1970), which increases from groups 1 to 5 (Table 12.1). Minerals in group 3(a) can be rendered hydrophobic by sulphidisation of the mineral surface in an alkaline aqueous medium. Apart from the native metals, the minerals in group 1 are all sulphides, which are only weakly polar due to their covalent bonding, which is relatively weak compared to the ionic bonding of the carbonate and sulphate minerals. In general, therefore, the degree of polarity increases from sulphide minerals, through sulphates, to carbonates, halites, phosphates, etc., then oxides-hydroxides, and, finally, silicates and quartz.

Collectors

Hydrophobicity has to be imparted to most minerals in order to float them. In order to achieve this, surfactants known as *collectors* are added to the pulp and time is allowed for adsorption during agitation in what is known as the *conditioning period.* Collectors are organic compounds which render selected minerals water-repellent by adsorption of molecules or ions on to the mineral surface, reducing the stability of the hydrated layer separating the mineral surface from the air bubble to such a level that attachment of the particle to the bubble can be made on contact.

Collector molecules may be ionising compounds, which dissociate into ions in water, or non-ionising compounds, which are practically insoluble, and render the mineral water-repellent by covering its surface with a thin film.

Ionising collectors have found very wide application in flotation. They have complex molecules which are asymmetric in structure and are *heteropolar*, i.e. the molecule contains a non-polar hydrocarbon group and a polar group which may be one of a number of types. The non-polar hydrocarbon radical has pronounced water-repellent properties, whereas the polar group reacts with water.

Ionising collectors are classed in accordance with the type of ion, anion or cation that produces the water-repellent effect in water. This classification is given in Figure 12.4.

The structure of sodium oleate, an anionic collector in which the hydrocarbon radical, which

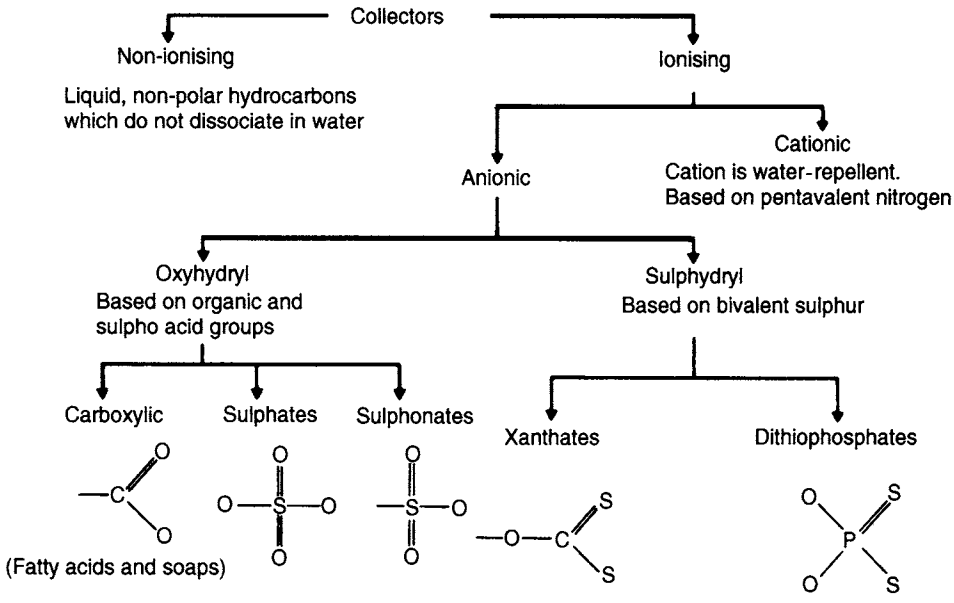


Figure 12.4 Classification of collectors (after Glembotskii et al., 1972)

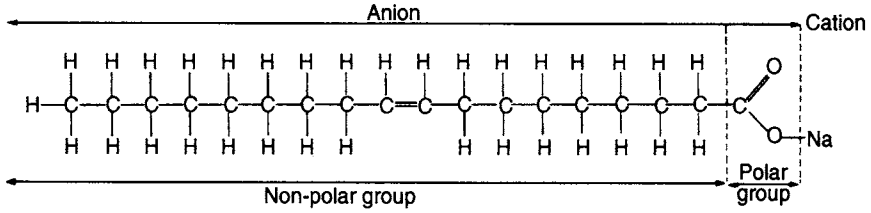


Figure 12.5 Structure of sodium oleate

does not react with water, constitutes the non-polar part of the molecule, is shown in Figure 12.5.

Amphoteric collectors possess a cationic and an anionic function, depending on the working pH, and have been used to treat sedimentary phosphate deposits (Houot et al., 1985) and to improve the selectivity of cassiterite flotation (Broekaert et al., 1984).

Because of chemical, electrical, or physical attraction between the polar portions and surface sites, collectors adsorb on the particles with their non-polar ends orientated towards the bulk solution, thereby imparting hydrophobicity to the particles (Figure 12.6). They are usually used in small amounts, substantially those necessary to form a monomolecular layer on particle surfaces (starvation level), as increased concentration, apart from the cost, tends to float other minerals, reducing selectivity. It is always harder to eliminate a collector already adsorbed than to prevent its adsorption.

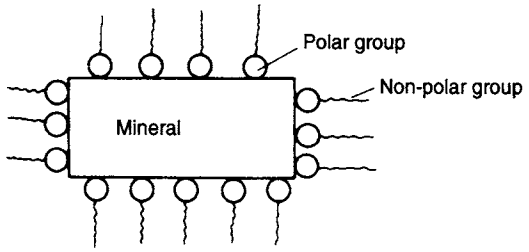


Figure 12.6 Collector adsorption on mineral surface

An excessive concentration of a collector can also have an adverse effect on the recovery of the valuable minerals, possibly due to the development of collector multi-layers on the particles, reducing the proportion of hydrocarbon radicals orientated into the bulk solution. The hydrophobicity of the

particles is thus reduced, and hence their floatability. The flotation limit may be extended without loss of selectivity by using a collector with a longer hydrocarbon chain, thus producing greater water-repulsion, rather than by increasing the concentration of a shorter chain collector. However, chain length is usually limited to two to five carbon atoms, since the solubility of the collector in water rapidly diminishes with increasing chain length and, although there is a corresponding decrease in solubility of the collector products, which therefore adsorb very readily on the mineral surfaces, it is, of course, necessary for the collector to ionise in water for chemisorption to take place on the mineral surfaces. Not only the chain length but also the chain structure, affects solubility and adsorption (Smith, 1989); branched chains have higher solubility than straight chains.

It is common to add more than one collector to a flotation system. A selective collector may be used at the head of the circuit, to float the highly hydrophobic minerals, after which a more powerful, but less selective one, is added to promote recovery of the slower floating minerals.

Anionic collectors

These are the most widely used collectors in mineral flotation and may be classified into two types according to the structure of the polar group (Figure 12.4). *Oxyhydryl* collectors have organic and sulpho-acid anions as their polar groups and, as with all anionic collectors, the cation takes no significant part in the reagent–mineral reaction.

Typically, oxyhydryl collectors are organic acids or soaps. The carboxylates are known as fatty acids, and occur naturally in vegetable oils and animal fats from which they are extracted by distillation and crystallisation. The salts of oleic acid, such as sodium oleate (Figure 12.5) and linoleic acid, are commonly used. As with all ionic collectors, the longer the hydrocarbon chain length, the more powerful is the water-repulsion produced, but solubility decreases. Soaps (the salts of fatty acids), however, are soluble even if the chain length is long. The carboxylates are strong collectors, but have relatively low selectivity. They are used for the flotation of minerals of calcium, barium, strontium, and magnesium, the carbonates of non-ferrous metals, and the soluble salts of alkali metals and alkaline earth metals (Finch and Riggs, 1986).

The sulphates and sulphonates are used more rarely. They possess similar properties to fatty acids, but have lower collecting power. However, they have greater selectivity and are used for floating barite, celestite, fluorite, apatite, chromite, kyanite, mica, cassiterite, and scheelite (Holme, 1986).

The oxyhydryl collectors have been used to float cassiterite, but have now been largely replaced by other reagents such as arsonic and phosphonic acids and sulphosuccinamates (Broekaert et al., 1984; Collins et al., 1984; Baldauf et al., 1985).

The most widely used collectors are of the *sulphydryl* type where the polar group contains bivalent sulphur (*thio* compounds). They are very powerful and selective in the flotation of sulphide minerals (Avotins et al., 1994). The *mercaptans* (thiols) are the simplest of thio compounds, having the general formula $RS^{-}Na$ (or $K)^{+}$, where R is the hydrocarbon group. They have been used as selective collectors for some of the more refractory sulphide minerals (Shaw, 1981). The most widely used thiol collectors are the *xanthogenates* (technically known as the *xanthates*) and the *dithiophosphates* (Aerofloat collectors). The xanthates are the most important for sulphide mineral flotation. They are prepared by reacting an alkali hydroxide, an alcohol and carbon disulphide:

$$ROH + CS_2 + KOH = RO \cdot CS \cdot SK + H_2O \quad (12.4)$$

where R is the hydrocarbon group and contains normally one to six carbon atoms, the most widely used xanthates being ethyl, isopropyl, isobutyl, amyl, and hexyl. Sodium ethyl xanthate is typical and has the structure shown in Figure 12.7. The anion consists of a hydrocarbon non-polar radical and a connected polar group. Although the cation (sodium or potassium) plays no part in the reactions leading to mineral hydrophobicity, it has been shown (Ackerman et al., 1986) that the sodium

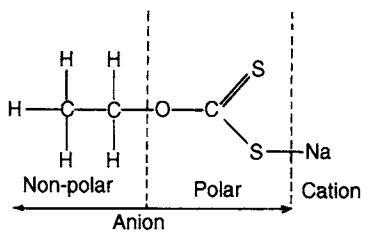


Figure 12.7 Structure of sodium ethyl xanthate

form of the alkyl xanthates decreases in efficacy with age, probably due to water absorption from the atmosphere, whereas the potassium salts are not affected by this problem.

The dithiophosphates have pentavalent phosphorus in the polar group, rather than tetravalent carbon (Figure 12.8).

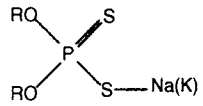


Figure 12.8 Dithiophosphates

The reaction between sulphide minerals and sulphydryl collectors is complex and various mechanisms have been proposed (Yoon and Basilio, 1993). Xanthates are assumed to adsorb on sulphide mineral surfaces due to chemical forces between the polar group and the surface, resulting in insoluble metal xanthates, which are strongly hydrophobic. Mechanisms involving the formation and adsorption of dixanthogen, xanthic acid, etc., have also been proposed. It has been established that the sulphide is not joined to the collector anions without the previous action of oxygen. The solubilities of sulphide minerals in water are very low, suggesting that sulphides should be relatively inert in aqueous solution. However, they are thermodynamically unstable in the presence of oxygen, and surface oxidation to S^{2-}, $S_2O_3^{2-}$, and SO_4^{2-} can occur, depending on the E_h-pH conditions. Figure 12.9 shows the E_h-pH (Pourbaix) diagram for galena. At cathodic potential, the surface of galena is converted to lead, and sulphide ions pass into solution. Under anodic conditions (i.e. when cathodic reduction of oxygen occurs, e.g. $\frac{1}{2}O_2 + H_2O + 2e \rightarrow 2OH^-$), lead will dissolve or form oxidised metal species on the surface, depending on the pH. The initial oxidation of sulphide leads to the formation of elemental sulphur, e.g. in acid solution:

$$MS \rightarrow M^{2+} + S^0 + 2e \qquad (12.5)$$

with its equivalent in neutral or alkaline solution:

$$MS + 2H_2O \rightarrow M(OH)_2 + S^0 + 2H^+ + 2e \qquad (12.6)$$

The presence of elemental sulphur in the mineral surface can lead to hydrophobicity, and the mineral

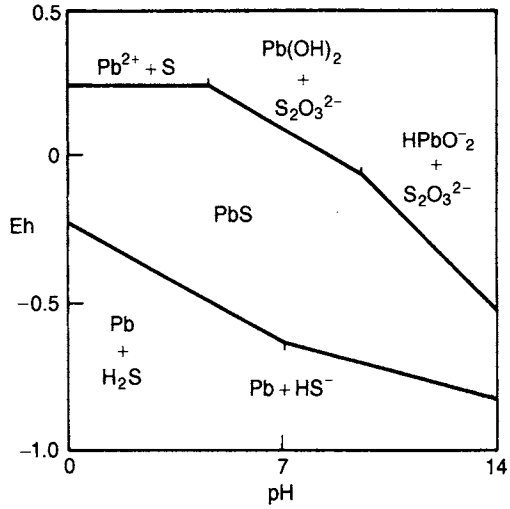


Figure 12.9 E_h-pH diagram for galena (equilibrium lines correspond to dissolved species at 10^{-4} M) (after Woods, 1976)

may be floated in the absence of collectors, although control of these redox conditions is difficult in practice. Usually the cathodic reduction of oxygen is strong enough to provide a sufficient electron sink for oxidation of the sulphide mineral surface to oxy-sulphur species, which are not hydrophobic, and so collectors are required to promote flotation. The oxidation products are more soluble than the sulphides, and the reaction of xanthates and other thiol collectors with these products by an ion-exchange process is the major adsorption mechanism for the flotation of sulphides (Shergold, 1984). For instance, if the sulphide surface oxidises to thiosulphate, the following reactions can occur:

$$2MS + 2O_2 + H_2O \rightarrow MS_2O_3 + M(OH)_2$$

and

$$MS_2O_3 + 2ROCS_2^- \rightarrow M(ROCS_2)_2 + S_2O_3^{2-}$$

or

$$2MS + 4ROCS_2^- + 3H_2O \rightarrow 2M(ROCS_2)_2 + S_2O_3^{2-} + 6H^+ + 8e \text{ (anodic reaction)} \qquad (12.7)$$

The insoluble metal xanthate so formed renders the mineral surface hydrophobic. However, strong

oxidising conditions can lead to the formation of sulphates, e.g.:

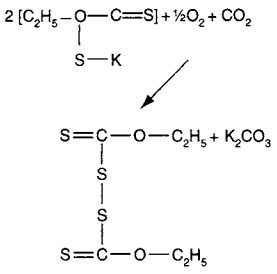
$$MS + 2ROCS_2^- + 4H_2O \rightarrow M(ROCS_2)_2 + SO_4^{2-} + 8H^+ + 8e \quad (12.8)$$

Although sulphates react strongly with xanthates, they are relatively soluble in aqueous solution, and so do not form stable hydrophobic surface products, the metal xanthates formed tending to scale off the mineral.

The solubilities of the hydrophobic xanthates of copper, lead, silver, and mercury are very low, but the xanthates of zinc and iron are much more soluble. Typically, ethyl xanthates are only weak collectors of pure sphalerite, but replacement of the crystal lattice zinc atoms by copper improves the flotation properties of the mineral. The alkali earth metal xanthates (calcium, barium, magnesium) are very soluble and xanthates have no collector action on the minerals of such metals, nor on oxides, silicates, or aluminosilicates, which permits extremely selective flotation of sulphides from gangue minerals.

Xanthates are used as collectors for oxidised minerals such as malachite, cerussite, and anglesite, and for native minerals such as gold, silver, and copper. Comparatively high concentrations are necessary with the oxidised minerals, and often higher xanthates such as amyl are preferred.

Xanthates and similar compounds tend to oxidise fairly easily, which can lead to complications in flotation. After a few months of storage, they develop a strong odour and a deeper colour due to the formation of "dixanthogen", e.g. with potassium ethyl xanthate:



Dixanthogens and similar products of oxidation are themselves collectors (Jones and Woodcock, 1983), and their formation can lead to loss of selectivity and control in complex flotation circuits.

Xanthates also form insoluble metal salts with ions of copper, lead, and other heavy metals which may be present in the slurry, which reduces the effectiveness of the collector. By using alkaline conditions, preferably as early as the grinding circuit, these heavy metal ions can be precipitated as relatively insoluble hydroxides. Alkaline conditions also inhibit xanthate breakdown, which proceeds more rapidly as the pH is lowered:

$$H^+ + ROCS^{2-} \leftrightarrow HX \rightarrow ROH + CS_2 \quad (12.10)$$

With xanthic acid (HX) and xanthate ions in equilibrium, the unstable xanthic acid decomposes to alcohol and carbon disulphide.

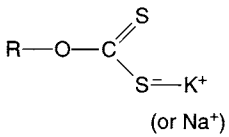
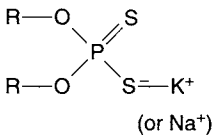
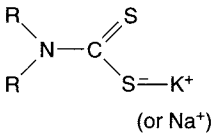
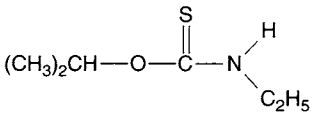
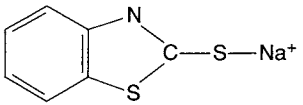
Dithiophosphates are not as widely used as the xanthates, but are still important reagents in practice. They are comparatively weak collectors, but give good results in combination with xanthates. They are often used in the separation of copper from lead sulphides, as they are effective selective collectors for copper sulphide minerals.

It appears that the water repulsion imparted to the mineral surface is due to the formation of an oxidation product of the dithiophosphate collector which adsorbs on to the mineral surface. Thus, as with xanthates, the presence of oxygen, or another oxidising agent, is essential for flotation. Strong oxidising conditions destroy the hydrophobic substances and are thus undesirable, while oxidisation of the mineral surface itself may impede collector adsorption.

Hartati et al. (1997) described the properties of monothiphosphate (MTP) and showed how this collector dramatically altered the collecting property of dithiophosphate (DTP) when one of the S atoms was replaced by an O atom particularly in the flotation of gold in porphyry copper ores. They showed that MTP achieved selectivity in the flotation of gold against pyrite at an alkaline environment.

Various reviews of the interaction between xanthates, dithiophosphates, other thiol collectors, and mixtures thereof with sulphide mineral surfaces have been made (Klimpel, 1986; Woods and Richardson, 1986; Aplan and Chander, 1987; Crozier, 1991; Adkins and Pearse, 1992; Bradshaw, 1997) and a list of the common thio collectors is given in Table 12.2, including references which provide more detail on these extremely important reagents.

Table 12.2 Common thiol collectors and their uses

Reagent	*Formula*	pH *range*	*Main uses*	*References*
O-alkyl dithiocarbonates (Xanthates)		8–13	Flotation of sulphides, oxidised minerals such as malachite, cerussite, and elemental metals	Leja (1982); Rao (1971)
Dialkyl dithiophosphates (Aerofloats)		4–12	Selective flotation of copper and zinc sulphides from galena	Mingione (1984)
Dialkyl dithiocarbamate		5–12	Similar properties to xanthates, but more expensive	Jiwu et al. (1984)
Isopropyl thionocarbamate (Minerec 1661/Z-200)		4–9	Selective flotation of copper sulphides from pyrite	Ackerman et al. (1984)
Mercaptobenzothiazole (R404/425)		4–9	Flotation of tarnished or oxidised lead and copper minerals. Floats pyrite at pH 4–5	Fuerstenau and Raghavan (1986)

Chelating reagents have potential as flotation collectors, in view of their ability to form stable, selective compounds with the cations present on mineral surfaces (Somasundaran et al., 1993; Marabini, 1994). They are highly specific complexing reagents consisting of large organic molecules capable of bonding to the metal ion via two or more functional groups. However, despite several successful attempts at laboratory scale to demonstrate their effectiveness, the number of commercial plants using these reagents is relatively insignificant, mainly due to their prohibitive cost.

Cationic collectors

The characteristic property of this group of collectors is that the water-repulsion is produced by the cation where the polar group is based on pentavalent nitrogen, the amines (Figure 12.10) being the most common (Gefvert, 1986; Zachwieja, 1994). The anions of such collectors are usually halides, or more rarely hydroxides, which take no active part in the reaction with minerals.

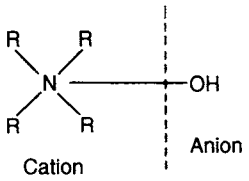


Figure 12.10 Cationic amine collector

Unlike the xanthates, the amines are considered to adsorb on mineral surfaces primarily due to electrostatic attraction between the polar head of the collector and the charged electrical double layer on the mineral surface. Such forces are not as strong or irreversible as the chemical forces characteristic of anionic collectors, so these collectors tend to be relatively weak in collecting power.

Cationic collectors are very sensitive to the pH of the medium, being most active in slightly acid solutions and inactive in strongly alkaline and acid media. They are used for floating oxides, carbonates, silicates, and alkali earth metals such as barite, carnallite, and sylvite. The primary amines (i.e. those where only one hydrocarbon group is present with two hydrogen atoms) are strong collectors of apatite and they can selectively float sedimentary phosphates from calcareous ores. The collector requirement can be reduced by adding a non-polar reagent such as kerosene, which is co-adsorbed on the mineral surface. Since the zeta potentials of both apatite and dolomite are negative in the relevant pH range, the selective flotation of the phosphate may not be interpreted solely by the electrostatic model of adsorption, and experimental evidence for chemical interaction has been presented (Soto and Iwasaki, 1985).

Frothers

Frothers are added to stabilise bubble formation in the pulp phase, to create a reasonably stable froth to allow selective drainage from the froth of entrained gangue, and to increase flotation kinetics. The importance of the froth phase to flotation performance is being increasingly recognised and the factors affecting froth stability are being extensively researched (Harris 1982; Melo and Laskowski 2003, 2005; Hatfield et al., 2004; Barbian et al., 2005).

Plant practice involving frothers has been reviewed by Crozier and Klimpel (1989).

Frothers are in many respects chemically similar to ionic collectors, and, indeed, many of the collectors, such as oleates, are powerful frothers, being in fact too powerful to be used as efficient frothers, since the froths which they produce can be too stable to allow efficient transport to further processing. Froth build-up on the surfaces of thickeners and excessive frothing of flotation cells are problems occurring in many mineral processing plants. A good frother should have negligible collecting power, and also produce a froth which is just stable enough to facilitate transfer of floated mineral from the cell surface to the collecting launder.

Frothers are generally heteropolar surface-active organic reagents, capable of being adsorbed on the air–water interface. When surface-active molecules react with water, the water dipoles combine readily with the polar groups and hydrate them, but there is practically no reaction with the non-polar hydrocarbon group, the tendency being to force the latter into the air phase. Thus the heteropolar structure of the frother molecule leads to its adsorption, i.e. the molecules concentrate in the surface layer with the non-polar groups oriented towards the air and the polar groups towards the water (Figure 12.11).

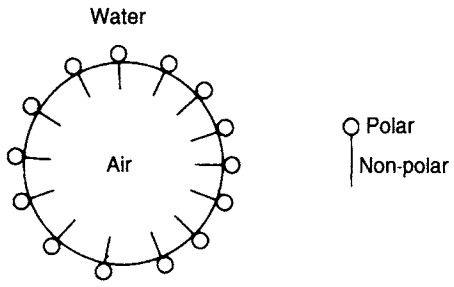


Figure 12.11 Action of the frother

Frothing action is thus due to the ability of the frother to adsorb on the air–water interface because of its surface activity and to reduce the surface tension, thus stabilising the air bubble.

Frothers must be to some extent soluble in water, otherwise they would be distributed very unevenly in an aqueous solution and their surface-active properties would not be fully effective. The most effective frothers include in their composition one of the following groups:

Hydroxyl	—OH
Carboxyl	
Carbonyl	=C=O
Amino group	— NH_2
Sulpho group	—OSO_2OH, —SO_2OH

The acids, amines, and alcohols are the most soluble of the frothers. The alcohols (—OH) are the most widely used, since they have practically no collector properties, and in this respect are preferable to other frothers, such as the carboxyls, which are also powerful collectors; the presence of collecting and frothing properties in the same reagent may make selective flotation difficult. Frothers with an amino group and certain sulpho group frothers also have weak collector properties.

Pine oil, which contains aromatic alcohols, the most active frothing component being terpineol, $C_{10}H_{17}OH$, has been widely used as a frother. Cresol (cresylic acid), $CH_3C_6H_4OH$, has also had wide use.

A wide range of synthetic frothers, based mainly on high molecular-weight alcohols, are now in use in many plants. They have the important advantage over industrial products such as pine oil and cresol in that their compositions are much more stable, which makes it easier to control the flotation process and improves performance. A widely used synthetic alcohol frother is methyl isobutyl carbinol (MIBC). Another range of synthetic frothers are based on polyglycol ethers, and have been found to be very effective. They are marketed under various names, such as Cytec Oreprep 549 and Cytec Aerofroth 65. Frothers based on polyglycols are also used, and it is not uncommon to blend all three chemical groups – alcohols, polyglycol ethers, and polyglycols – together to provide a specific frother for a particular flotation circuit (Riggs, 1986).

The alcohol groups provide a selective, often brittle, froth, which allows good control and materials transfer through the launders and pumps. The glycol ether group is stronger, with more persistence than the alcohol groups, while the polyglycols are the strongest surface active frothers utilised. They are very effective in maximising load support with coarse grinds and high grade feeds, at all pH ranges.

Although frothers are generally surface-active reagents, it has been shown that surface-inactive reagents, such as diacetone alcohol and ethyl acetal, behave as frothers in solid–liquid–air systems, although not in two-phase liquid–air systems (Lekki and Laskowski, 1975). Molecules of these reagents have two polar groups and are readily soluble in water. They adsorb on solid surfaces but do not appreciably change their hydrophobicity. When the mineral surface, on which the surface inactive frother is adsorbed, is approached by an air bubble, the molecules reorientate and produce a sufficiently stable three-phase froth. Being surface inactive, these reagents do not reduce surface tension, and apart from the slight reduction due to collectors, the forces available for flotation are maintained at their maximum.

Regulators

Regulators, or modifiers, are used extensively in flotation to modify the action of the collector, either by intensifying or by reducing its water-repellent effect on the mineral surface. They thus make collector action more selective towards certain minerals. Regulators can be classed as activators, depressants, or pH modifiers.

Activators

These reagents alter the chemical nature of mineral surfaces so that they become hydrophobic due to the action of the collector. Activators are generally soluble salts which ionise in solution, the ions then reacting with the mineral surface.

A classical example is the activation of sphalerite by copper in solution. Sphalerite is not floated satisfactorily by a xanthate collector, since the collector products formed, such as zinc xanthate, are relatively soluble in water, and so do not provide a hydrophobic film around the mineral. Floatability can be improved by the use of large quantities of long-chain xanthates, but a more satisfactory method is to use copper sulphate as an activator, which is readily soluble and dissociates into copper ions in solution. Activation is due to the formation of molecules of copper sulphide at the mineral surface, due to the fact that copper is more electronegative than zinc and therefore ionises less readily:

$$ZnS + Cu^{2+} \leftrightarrow CuS + Zn^{2+} \qquad (12.11)$$

The copper sulphide deposited on the sphalerite surface reacts readily with xanthate to form insoluble copper xanthate, which renders the sphalerite surface hydrophobic. Recent work, however, suggests that this simple ion-exchange mechanism may be oversimplified, and Wang et al. (1989a,b) propose a model based on surface oxidation of the mineral and reduction of the activator, surface precipitation of the activator hydroxide and a mixed potential mechanism.

The main use of copper sulphate as an activator is in the differential flotation of lead–zinc ores, where after lead flotation the sphalerite is activated and floated. To some extent, copper ions can also activate galena, calcite, and pyrite. When sphalerite is associated with pyrite or pyrrhotite, selectivity is usually ensured by the high alkalinity (pH 10.5–12) of the pulp, lime being added in conjunction with the copper sulphate activator.

Oxidised minerals of lead, zinc, and copper, such as cerussite, smithsonite, azurite, and malachite, float very inefficiently with sulphydryl collectors and require an extremely large amount, as heavy metal ions dissolved from the mineral lattice must be precipitated as metal xanthate before the collector interacts with the mineral. Adsorption at the mineral surface is also poor, the collector coating being readily removed by particle abrasion. Such minerals are activated by the use of sodium sulphide or sodium hydrosulphide (Fuerstenau et al., 1985; Malghan, 1986). Large quantities of up to $10\,kg\,t^{-1}$ of such "sulphidisers" may be required, due to the relatively high solubilities of the oxidised minerals.

In solution, sodium sulphide hydrolyses and then dissociates:

$$Na_2S + 2H_2O \leftrightarrow 2NaOH + H_2S \qquad (12.12)$$

$$NaOH \leftrightarrow Na^+ + OH^- \qquad (12.13)$$

$$H_2S \leftrightarrow H^+ + HS^- \qquad (12.14)$$

$$HS^- \leftrightarrow H^+ + S^{2-} \qquad (12.15)$$

Since the dissociation constants of Equations 12.14 and 12.15 are extremely low and that of Equation 12.13 is high, the concentration of OH^- ions increases at a faster rate than that of H^+ ions and the pulp becomes alkaline. Hydrolysis and dissociation of sodium sulphide release OH^-, S^{2-}, and HS^- ions into solution and these can react with and modify the mineral surfaces. Sulphidation causes sulphur ions to pass into the crystal lattice of the oxidised minerals, giving them a relatively insoluble pseudo-sulphide surface coating and allowing them to be floated by sulphydryl collectors. For example, in the sulphidisation of cerussite, the following reactions take place:

$$Na_2S + H_2O \leftrightarrow NaHS + NaOH \qquad (12.16)$$

$$PbCO_3 + 3NaOH = H_2O + Na_2CO_3 + NaHPbO_3 \qquad (12.17)$$

$$NaHS + NaHPbO_2 = 2NaOH + PbS \qquad (12.18)$$

or

$$Na_2S + PbCO_3 = Na_2CO_3 + PbS \qquad (12.19)$$

The amount of sodium sulphide added to the pulp must be very strictly controlled, as it is a very powerful depressant for sulphide minerals and will, if in excess, depress the activated oxide minerals, preventing collector adsorption. The amount required is dependent on the pulp alkalinity, as an increase in pH causes Equations 12.14 and 12.15 to proceed further to the right, producing more HS^- and S^{2-} ions. For

this reason sodium hydrosulphide is sometimes preferred to sodium sulphide, as the former does not hydrolyse and hence increase the pH. The amount of sulphidiser added should be sufficient only to produce a coherent film of sulphide on the mineral surface, such that xanthate can be adsorbed. With an increase in sulphidiser beyond that required for activation, concentrations of sulphide and hydrosulphide ions increase. The HS^- ions readily adsorb on the mineral surfaces, giving them a high negative charge, and preventing adsorption of the collector anions. Excess sodium sulphide also removes oxygen from the pulp:

$$Na_2S + 2O_2 = Na_2SO_4 \qquad (12.20)$$

Since oxygen is required in the pulp for the adsorption of sulphydryl collectors on sulphide surfaces, flotation efficiency is reduced.

In the flotation of mixed sulphide-oxidised ores, the sulphide minerals are usually floated first, before sulphidisation of the oxidised surfaces. This prevents the depression of sulphides by sodium sulphide and the sulphidiser is subsequently added to the pulp in stages, in starvation levels. It has recently been suggested (Zhang and Poling, 1991) that the detrimental effects of residual hydrosulphide can be eliminated by the addition of ammonium sulphate with the hydrosulphide. Use of the relatively inexpensive ammonium sulphate appears to reduce the consumption of the much more expensive sulphidising agent and enhances the activating effect of the hydrosulphide ions. Zhou and Chander (1991) have further suggested that sodium tetrasulphide may be superior to sodium sulphide in terms of flotation response, and propose mechanisms for the reactions.

Depressants

Depression is used to increase the selectivity of flotation by rendering certain minerals hydrophilic (water-avid), thus preventing their flotation. They are key to the economic flotation of certain ores such as platinum and nickel sulphides.

There are many types of depressants and their actions are complex and varied, and in most cases not fully understood, making depression more difficult to control than the application of other types of reagent, particularly when the froth phase is also affected by their action (Bradshaw et al., 2005).

Slime coating is an example of a naturally occurring form of depression. Slimes in a crushed and ground ore make flotation difficult, as they coat the mineral particles, retarding collector adsorption (Parsonage, 1985). The particle size at which these effects become significant depends on the flotation system, but in general particles below 20 microns are potentially deleterious, and some form of desliming is usually carried out prior to flotation, resulting in an inevitable loss of slime values. Sometimes slime can be removed from the mineral surfaces by vigorous agitation, or a slime dispersant may be used. Sodium silicate in solution increases the double-layer charge on particles, so that the slime layers which have formed readily disperse. The clean mineral surface can then interact with the collector. In this respect, therefore, sodium silicate is used as an activator, preventing depression by the slimes. Sodium silicate is also used as a depressant in some systems, being one of the most widely used regulating agents in the flotation of non-sulphide minerals, such as scheelite, calcite, and fluorite. Sodium oleate is the major collector in the flotation of these minerals, but the selectivity in the separation of scheelite from calcite and fluorite is often inadequate. Sodium silicate has therefore been used to improve selectivity. Shin and Choi (1985) have examined the mechanism of adsorption of sodium silicate and its interaction with these minerals.

Inorganic depressants

Cyanides are widely used in the selective flotation of lead–copper–zinc and copper–zinc ores as depressants for sphalerite, pyrite, and certain copper sulphides. Sphalerite rejection from copper concentrates is often of major concern, as zinc is a penalty element in copper smelting.

It is fairly well established that pure clean sphalerite does not adsorb short-chain xanthates until its surface is activated by copper ions (Equation 12.11). However, copper ions resulting from very slight dissolution of copper minerals present in the ore may cause unintentional activation and prevent selective separation. Cyanide is added to the pulp to desorb the surface copper and to react with copper in solution forming soluble cyanide complexes. Sodium cyanide is most commonly used, which hydrolyses in aqueous solution to

form free alkali and relatively insoluble hydrogen cyanide:

$$NaCN + H_2O \leftrightarrow HCN + NaOH \qquad (12.21)$$

The hydrogen cyanide then dissociates:

$$HCN \leftrightarrow H^+ + CN^- \qquad (12.22)$$

The dissociation constant of Equation 12.22 is extremely low compared with that of Equation 12.21, so that an increase in pulp alkalinity reduces the amount of free HCN, but increases the concentration of CN^- ions. An alkaline pulp is essential, as free hydrogen cyanide is extremely dangerous. The major function of the alkali, however, is to control the concentration of cyanide ions available for dissolution of the copper to cupro-cyanide:

$$3CN^- + Cu^{2+} \leftrightarrow [Cu(CN)_2]^- + \frac{1}{2}C_2N_2 \qquad (12.23)$$

Apart from the reactions of cyanide with metal ions in solution, it can react with metal xanthates to form soluble complexes, preventing xanthate adsorption on the mineral surface, although this cannot occur until the metal ions in solution have been complexed, according to Equation 12.23. Hence if Cu^{2+} ions are in solution, the prevention of xanthate adsorption cannot occur unless the ratio of CN^- ions to Cu^{2+} ions is greater than 3:1. The greater the solubility of the metal xanthate in cyanide, the less stable is the attachment of the collector to the mineral. It has been shown that lead xanthates have very low solubilities in cyanide, copper xanthates are fairly soluble, while the xanthates of zinc, nickel, gold, and iron are highly soluble. Iron and zinc can, therefore, be very easily separated from lead in complex ores. In the separation of chalcopyrite from sphalerite and pyrite, very close control of cyanide ion concentration is needed. Cyanide should be added sufficiently only to complex the heavy metal ions in solution, and to solubilise the zinc and iron xanthates. Excess cyanide forms soluble complexes with the slightly less soluble copper xanthate, depressing the chalcopyrite.

The depressive effect of cyanide depends on its concentration and on the concentration of the collector and the length of the hydrocarbon chain. The longer the chain, the greater is the stability of the metal xanthate in cyanide solutions and the higher the concentration of cyanide required to depress the mineral. Relatively low concentrations of xanthates with short hydrocarbon chains are therefore used for selective flotation where cyanides are used as depressants.

Cyanides are, of course, extremely toxic and must be handled with great care. They also have the disadvantage of being expensive and they depress and dissolve gold and silver, reducing the extraction of these metals into the froth product. Despite these disadvantages, they are widely used due to their high degree of selectivity in flotation. They also have the advantage of leaving the mineral surface relatively unaffected, so that subsequent activation is relatively simple, although residual cyanide ions in solution may interfere with the activator.

While many plants function efficiently with cyanide alone, in others an additional reagent, generally zinc sulphate, is added to ensure satisfactory depression of sphalerite. If copper ions are present, the introduction of zinc ions can prevent the copper depositing on the sphalerite surface by shifting Equation 12.11 to the left.

However, other, more complex, reactions occur to assist depression and it is considered that cyanide reacts with zinc sulphate to form zinc cyanide, which is relatively insoluble, and precipitates on the sphalerite surface, rendering it hydrophilic and preventing collector adsorption:

$$ZnSO_4 + 2NaCN = Zn(CN)_2 + Na_2SO_4 \qquad (12.24)$$

In an alkaline pulp, zinc hydroxide, which adsorbs copper ions, is also formed and it is precipitated on to the sphalerite surface, preventing collector adsorption.

The use of zinc sulphate thus reduces cyanide consumption and cases have been known where depression of sphalerite has been achieved by the use of zinc sulphate alone.

Although cyanides and zinc sulphate are widely used, they do have many disadvantages, for example many concentrators being loath to use cyanides due to environmental problems. Zinc sulphate is effective only at high pH values, at which zinc hydroxide precipitates from solution. There is a need, therefore, for alternative selective depressants. Research on Pb–Zn ores in Yugoslavia has shown that sphalerite depression by zinc sulphate and sodium cyanide can be successfully replaced by a combination of

ferrosulphate and sodium cyanide (Pavlica et al., 1986). This has the advantage of reducing sodium cyanide consumption, with consequent economic and ecological advantages. Zinc bisulphite used with cyanide in alkaline conditions is being used to treat bulk copper–zinc–iron concentrates at the Cerro Colorado mill in Spain (Ser and Nieto, 1985). This reagent combination was found to give results which were more favourable than those obtained using standard depression techniques, such as cyanide–zinc sulphate, which was found to be very sensitive to variations in the chalcocite content of the ore.

Sphalerite activation can be prevented by eliminating copper ions from the flotation pulp, and in some plants precipitation with hydrogen sulphide or sodium sulphide is carried out.

Sulphur dioxide has developed into a most versatile and almost indispensable conditioning reagent for polysulphide ores. Although widely used as a galena depressant in copper–lead separations, it also deactivates zinc sulphides and enhances the flotation differential between zinc and other base metal sulphides. In copper cleaner and copper–lead separation circuits, very effective zinc rejection is attained through acidification of pulps by injection of SO_2. However, SO_2 cannot be employed when treating ores which contain the secondary copper minerals covellite or chalcocite, since they become soluble in the presence of sulphur dioxide and the dissolved copper ions activate zinc sulphides (Konigsman, 1985). Sulphur dioxide does not appreciably depress chalcopyrite and other copper-bearing minerals. In fact, adsorption of xanthate on chalcopyrite is enhanced in the presence of SO_2, and the addition of SO_2 before xanthate results in effective sphalerite depression while increasing the floatability of chalcopyrite. The use of SO_2 in various Swedish concentrators is discussed by Broman et al. (1985), who point out that SO_2 has the advantage over cyanide in sphalerite depression in that there is little copper depression, and no dissolution of precious metals. However, it is indicated that the use of SO_2 demands adaptation of the other reagent additions, and in some cases a change of collector type is required.

Potassium dichromate ($K_2Cr_2O_7$) is also used to depress galena in copper–lead separations. The depressive action is due to the chemical reactions between the galena surface and CrO_4^- anions, which produces insoluble lead dichromate that increases wettability and prevents flotation.

More than 40% of the Western world's molybdenum is produced as a by-product from porphyry copper ores. The small amount of molybdenite is collected along with copper in a bulk Cu–Mo concentrate. The two minerals are then separated, almost always by depressing the copper minerals and floating the molybdenite. Sodium hydrosulphide (or sodium sulphide) is used most extensively, though several other inorganic compounds, such as cyanides, and Noke's reagent (a product of the reaction of sodium hydroxide and phosphorous pentasulphide), are also used (Nagaraj et al., 1986). Almost all the currently used depressants are inorganic. Numerous organic depressants have been developed over the years, but apart from sodium thioglycolate, none have been successfully commercialised (Agar, 1984).

Polymeric depressants

The use of polymeric depressants has the advantage of being less hazardous than the more widely used inorganic depressants, and interest in their use has been growing (Liu and Laskowski, 1989). Organic reagents such as starch, tannin, quebracho, and dextrin do not ionise in solution, but prevent flotation in a manner similar to a slime coating. They have been used for many years as gangue-mineral depressants, and are used in small amounts to depress talc, graphite, and calcite (Pugh, 1989). Starch and dextrin can also be used as supplementary lead depressants in copper–lead separations. Other applications include the selective depression of polymetallic sulphide ores in the processing of iron ore (Nyamekye and Laskowski, 1993), as blinders in potash flotation (Arsentiev et al., 1988) and the depression of talcaeous gangue minerals in platinum and base metal flotation (Steenberg and Harris, 1984; Liu and Laskowski 1999; Shortridge et al., 2000; Bradshaw et al., 2005; Smeink et al., 2005; Wang et al., 2005).

In the South African platinum group mineral (PGM) industry, polymeric depressants such as carboxymethyl cellulose (CMC) and guar are widely used to depress talcaeous gangue minerals. One of the major differences between these two polysaccharides is that CMC is negatively charged in solution, whereas guar is typically only slightly charged, if at all (Mackenzie, 1986).

The importance of pH

It is evident from the foregoing that pulp alkalinity plays a very important, though very complex, role in flotation, and, in practice, selectivity in complex separations is dependent on a delicate balance between reagent concentrations and pH.

Flotation where possible is carried out in an alkaline medium, as most collectors, including xanthates, are stable under these conditions, and corrosion of cells, pipework etc., is minimised. Alkalinity is controlled by the addition of lime, sodium carbonate (soda ash), and to a lesser extent sodium hydroxide or ammonia. Sulphuric or sulphurous acids are used where a decrease in pH is required.

These chemicals are often used in very significant amounts in almost all flotation operations. Although they are cheaper than collectors and frothers, the overall cost is generally higher with pH regulators per tonne of ore treated than with any other processing chemical. For example, the cost of lime in sulphide mineral flotation is roughly double that of the collector used, so significant operational cost savings can be achieved by the proper choice and use of pH regulators (Fee and Klimpel, 1986).

Lime, being cheap, is very widely used to regulate pulp alkalinity, and is used in the form of milk of lime, a suspension of calcium hydroxide particles in a saturated aqueous solution. Lime or soda ash is often added to the slurry prior to flotation to precipitate heavy metal ions from solution. In this sense, the alkali is acting as a "deactivator", as these heavy metal ions can activate sphalerite and pyrite and prevent their selective flotation from lead or copper minerals. Since the heavy metal salts precipitated by the alkali can dissociate to a limited extent and thus allow ions into solution, cyanide is often used with the alkali to complex them. Hydroxyl and hydrogen ions modify the electrical double layer and zeta potential (see Chapter 15) surrounding the mineral particles, and hence the hydration of the surfaces and their floatability is affected. With xanthates as collectors, sufficient alkali will depress almost any sulphide mineral, and for any concentration of xanthate there is a pH value below which any given mineral will float, and above which it will not float. This *critical pH* value depends on the nature of the mineral, the particular collector and its concentration, and the temperature (Sutherland and Wark, 1955). Figure 12.12 shows how the critical pH value for pyrite, galena, and chalcopyrite depends on the concentration of sodium aerofloat collector.

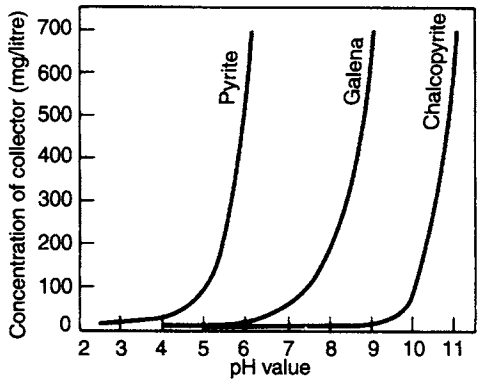


Figure 12.12 Relationship between concentration of sodium diethyl dithiophosphate and critical pH value (after Sutherland and Wark, 1955)

It is evident from the curves that using $50\,mg\,l^{-1}$ of sodium aerofloat, and a pH value of 8, chalcopyrite can be floated from galena and pyrite. On reducing the pH to 6, the galena can be floated from the pyrite.

Lime can also act as a strong depressant for pyrite and arsenopyrite when using xanthate collectors. Both the hydroxyl and calcium ions participate in the depressive effect on pyrite by the formation of mixed films of Fe(OH), FeO(OH), $CaSO_4$, and $CaCO_3$ on the surface, so reducing the adsorption of xanthate. Lime has no such effect with copper minerals, but does depress galena to some extent. In the flotation of galena, therefore, pH control is often affected by the use of soda ash, pyrite and sphalerite being depressed by cyanide.

As was shown earlier, the effectiveness of sodium cyanide and sodium sulphide is governed to such a large extent by the value of pH that these reagents are of scarcely any value in the absence of alkalis. Since, where cyanide is used as a depressant, the function of the alkali is to control the cyanide ion concentration (Equations 12.22 and 12.23), there is for each mineral and given concentration of collector a "critical cyanide ion concentration" above which flotation is impossible. Curves for several minerals are given in Figure 12.13, and it can be seen that chalcopyrite can be floated from pyrite at pH 7.5 and $30\,mg\,l^{-1}$ sodium cyanide.

Since, of the copper minerals, chalcopyrite lies closest to pyrite relative to the influence of alkali and cyanide, all the copper minerals will float with the chalcopyrite. Thus, by careful choice of pH value and cyanide concentration, excellent separations are theoretically possible, although in practice other variables serve to make the separation more difficult. Adsorption of xanthate by galena is uninfluenced by cyanide, the alkali alone acting as a depressant.

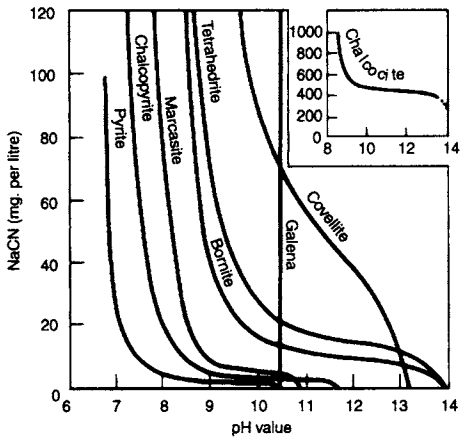


Figure 12.13 Contact curves for several minerals (ethyl xanthate = 25 mg/l) (after Sutherland and Wark, 1955)

The importance of pulp potential

Work conducted in Australia and the United States has shown that most sulphide minerals can, under certain conditions, be floated in the absence of collectors (Chander, 1988a; Woods, 1988; Ralston, 1991). All these studies imply that, if not oxygen itself, then at least an oxidising potential is required for collectorless flotation. It has been established that sulphide minerals oxidise through a continuum of metal-deficient sulphides of decreasing metal content through to elemental sulphur (Equations 12.5 and 12.6) by reactions of the type:

$$MS \rightarrow M_{1-x}S + xM^{2+} + 2xe \text{ (acid)} \qquad (12.25)$$

and

$$MS + xH_2O \rightarrow M_{1-x}S + xMO + 2xH^{+} + 2xe \text{ (alkali)} \qquad (12.26)$$

These sulphur-rich, metal-deficient zones can render the mineral hydrophobic, provided that the local conditions are such that the metal oxides/hydroxides formed by the reaction are solubilised. Excessive oxidation can produce thiosalts (Equation 12.7), and, ultimately, sulphate (Equation 12.8), together with metal ions which may re-adsorb, as hydrolysis products, on to the mineral, producing hydrophilic surfaces.

Buckley et al. (1985) studied the surface oxidation of galena, bornite, chalcopyrite, and pyrrhotite, and found that for each mineral the initial oxidation reaction is the removal of a metal component from the surface region to leave a sulphide with similar structure to the original mineral but with lower metal content. Metal-deficient sulphide layers containing high sulphur–metal ratios are probably stabilised by the underlying mineral because they have the same sulphur lattices. The authors showed that flotation of the minerals could be accomplished without the aid of collectors when a metal-deficient sulphide, rather than elemental sulphur, is formed. Naturally hydrophobic sulphide minerals, such as molybdenite, have such layer structures, the behaviour of these minerals being explained in terms of the work of adhesion of water to the surface being largely determined by dispersion forces, with hydrogen bonding and ionic interactions being small. It is possible that a similar situation exists at the surface of other sulphides where a metal-deficient layer is formed. Although the metal is dissolved at low pH (Equation 12.25), in neutral or alkaline conditions a hydroxy-oxide is formed (Equation 12.26), which could be expected to be hydrophilic. However, collectorless flotation occurs under these conditions, and the authors conclude that the metal oxides are dissolved due to the turbulence in the flotation cells, or are abraded from the mineral surfaces.

The collectorless flotation process has also been tested on six different chalcopyrite ores while monitoring the potentials of the pulp (Luttrell and Yoon, 1984). The results confirmed that collectorless flotation is effective only under oxidising conditions. In addition, the flotation requires that the chalcopyrite surface be relatively free of hydrophilic oxidation products, which can be accomplished by treating the ore pulp with sodium sulphide. The role of sodium sulphide in collectorless flotation was initially thought

to be one of sulphidising agent. However, the excess HS^-/S^{2-} ions that have not been consumed in sulphidisation may be oxidised to become elemental sulphur or polysulphides, depending on pH, which may deposit on the mineral surface. Thus, the collectorless flotation process using sodium sulphide may provide an external source for these hydrophobic species that could enhance flotation. Collectorless flotation was also found to be pH dependent, becoming more favourable with decreasing pH.

However, as explained by Guy and Trahar (1985), the application of such findings to realistic separations is not straightforward, as the areas of floatability determined from experiments with single sulphides do not necessarily coincide with those determined from experiments with sulphide mixtures. Cations produced by sulphide oxidation may react in different ways in a given system. Apart from modifying the surfaces of some minerals by surface interactions, they may be precipitated as hydroxides which have a profound effect on sulphide floatability.

For instance, pyrite and pyrrhotite occur together in many important ores, and the galvanic interaction between these two minerals and its effect on their floatabilities have been investigated (Nakazawa and Iwasaki, 1985). The galvanic contact decreased the formation of hydroxide or oxide and sulphate species of iron on pyrrhotite, whereas such formations were increased on pyrite. The effect was to improve the floatability of pyrrhotite, while reducing that of pyrite.

The control of redox conditions is complicated not only by the galvanic interactions between the different minerals in the ore but also by the interactions between the minerals and the steel grinding medium (Martin et al., 1991). The reducing conditions at a sulphide mineral surface created by the oxidation of steel in a galvanic interaction can hinder the adsorption of the collector.

Learmont and Iwasaki (1984) have studied the interaction between galena and steel media. They show that iron oxide, hydroxide, or sulphate species form on the galena surface on contact with mild steel, decreasing the galena floatability. The time of contact and aeration conditions affect the severity of the flotation depression. Adam and Iwasaki (1984) showed that the flotation response of pyrrhotite was similarly adversely affected. The formation of hydroxide or oxide and sulphate species of iron through the oxygen reduction reaction at the cathodically polarised surface of pyrrhotite was shown to be the mechanism responsible for the reduced floatability of pyrrhotite, the following reactions being proposed:

$$\frac{1}{2}O_2 + H_2O + 2e^- = 2OH^- \text{ (cathode)}$$

$$2H^+ + 2e^- = H_2 \text{ (cathode)}$$

$$FeS = Fe^{2+} + S^{2-} \text{ (dissociation)} \rightarrow Fe_2O(OH)_3$$

or

$$FeOOH \rightarrow Fe(OH)SO_4$$

The formation of an iron hydroxide coating covering the mineral surface reduces mineral floatability.

Due to these many complex interactions, measurement of the pulp oxidation–reduction potential is difficult in a plant environment (Johnson and Munro, 1988; Labonte and Finch, 1988). Electrodes which have different activities for the oxygen reduction reaction, such as platinum and gold, can give rise to different E_h values, and different sulphides can give rise to different E_h values in the same solution. Because of these complexities, on-line measurement of E_h to control redox conditions is still a control strategy of the future, although some concentrators do use such actions based on operating experience, and Outokumpu Oy is developing methods to control the electrochemical potentials of minerals directly in the ore pulps in order to attain the optimum combination of E_h and pH, as well as the optimum collector addition (Heimala et al., 1988).

Pre-flotation aeration of sulphide pulps has been practised in the Noranda Group (Canada) and other organisations for many years to help depress pyrite and pyrrhotite and promote chalcopyrite and galena (Konigsman, 1985).

The introduction of talc pre-flotation at Woodlawn in Australia had a detrimental effect on copper circuit performance, due to the aeration provided by the talc cells (Williams and Phelan, 1985). The aeration promoted the flotation of the other sulphides, especially galena, relative to that of chalcopyrite. Copper circuit performance was subsequently improved by the addition of a strong reducing agent, sodium sulphide, to the talc flotation tailing.

Nitrogen is used as the carrier gas in a few molybdenum flotation circuits, a reducing potential being used to minimise the consumption of the sulphide depressant which inhibits flotation of copper minerals. Nitrogen has great potential as a carrier gas in other flotation circuits (Martin et al., 1989), apart from chalcopyrite–molybdenite separation, because of its ready availability at smelter sites and its chemical inertness. The latter means that it is unlikely to be consumed by side reactions.

Only recently has there been a revival of interest in studying the mechanism of depression of sulphides. The influence of the strongly reducing nature of sodium hydrosulphide on depressant action has been monitored by means of solution redox-potential measurements, and it would appear that the depressant activity is to some extent electrochemical, the HS^- ions, by virtue of their large negative E_h, destabilising the coating of thiol collector (Nagaraj et al., 1986). The oxidation–reduction effects in sulphide mineral depression have been reviewed by Chander (1985).

The role of bubble generation and froth performance

In the science of flotation, one of the most critical components within the process is the role of the bubbles. Gorain et al. (1997, 1998) showed that the first order rate constant (k) achieved in a variety of industrial flotation cells of different types and sizes operated at a range of different air rates, impeller speeds and froth depths depended on the feed ore floatability (P), the bubble surface area flux (S_b) generated in the cell and the recovery across the froth phase (R_f), in a simple numerical relationship:

$$K = P \cdot S_b \cdot R_f \qquad (12.27)$$

where k = rate constant (s^{-1}); P = floatability (dimensionless); S_b = bubble surface area flux (s^{-1}); R_f = froth recovery (fraction).

Based on these findings, the performance of a flotation unit can be considered to arise from the interaction of a stream property – the particle floatability (P) – with parameters that characterise the operating conditions of the pulp and froth zones of the unit (S_b and R_f). In other words, the particle floatability is governed by the degree of hydrophobicity (as described earlier), the bubble surface area flux is a key driver within the pulp zone of a given cell, and the froth recovery describes the performance across the froth zone.

The bubble surface area flux, which is the rate at which bubble surface area moves through the cell per unit of cell cross-sectional area, can be measured directly within a cell from the measurements of superficial gas velocity (J_g) and the bubble size (d_b):

$$S_b = \frac{6J_g}{d_b} \qquad (12.28)$$

where J_g = the superficial gas velocity (m/s); d_b = the Sauter mean bubble diameter (m)

Both J_g and d_b are measurable using a suitable bubble size analyzer (e.g. Tucker et al., 1994; Hernandez et al., 2002) and a superficial gas velocity probe (Gorain et al., 1996). S_b can also be predicted using a correlation developed by Gorain et al. (1999) using a large number of data sets collected from different base metal flotation plants:

$$S_b = 123\, J_g^{0.75} N_s^{0.44} A_s^{-0.10} P_{80}^{-0.42} \qquad (12.29)$$

where N_s = impeller tip speed (rpm); A_s = impeller aspect ratio (impeller width/impeller height) (dimensionless); P_{80} = cell feed 80% passing size (μm).

Gorain et al. (1997) and Alexander et al. (2000) showed that the bubble surface area flux was linearly related to the first order rate constant at shallow froth depths. In addition, this relationship was shown to be independent of cell size and operating parameters. This is illustrated in Figure 12.14 which shows that the relationship measured in a pilot scale 60 litre cell was essentially identical to that measured in a parallel Outokumpu 100 m^3 tank cell.

At present, there are several techniques available to quantify the froth recovery factor, R_f. However, most of these methods are either intrusive in the froth zone or subject to assumptions that cannot be adopted in conventional cell modelling (e.g. no entrainment effects). A method initially developed for batch flotation cells by Feteris et al. (1987) was later modified by Vera et al. (1999) to determine R_f directly from industrial scale flotation froths. In this approach, froth recovery (R_f) is estimated by determining the cell recovery at a measured froth depth (and hence the first order rate constant, k) to the cell recovery at no froth depth (and hence the collection zone rate constant, k_c). The cell recovery at

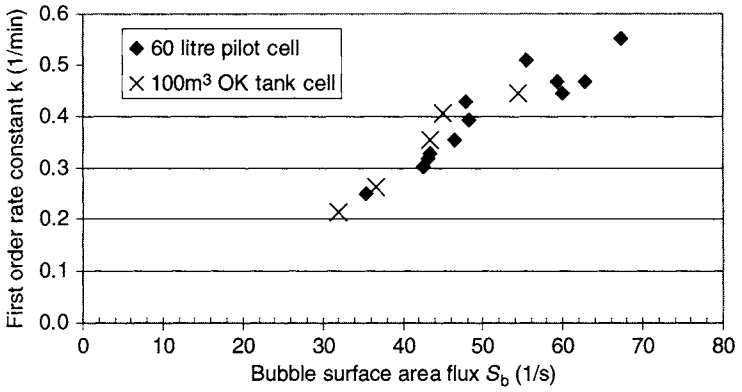


Figure 12.14 First order rate constant and bubble surface area flux relationship in a 60 l pilot cell and a 100 m^3 OK rougher cell (after Alexander et al. (2000))

no-froth depth cannot be measured directly, but can be estimated by extrapolation of results obtained at four or more froth depths.

An alternative technique for determining R_f in industrial flotation cells was developed by Savassi et al. (1998). A direct measurement of R_f is achieved by solving a set of mass balance equations with data obtained from a sample of the concentrate and samples taken below the pulp–froth interface. This direct measuring technique is a better approach than the first method, as no variation in the operating conditions of the flotation cell is needed. However, as noted by the authors, the technique is limited to use in roughers as it requires high bubble loads and a significant difference between the grade of the attached and suspended particles. Alexander et al. (2000) proposed a new direct method for measuring froth recovery which is applicable in other sections of the flotation circuit. This was based on the Savassi method of solving the mass balance equations across the froth but extended the technique using improved sampling methods. This is the current technique being used by many metallurgists to measure froth recovery in large industrial flotation cells.

Entrainment

The true flotation response has dominated the flotation literature since the separation process was first commercially used in 1905. Jowett (1966) first noted the recovery of fine particles by entrainment in water. Since then measuring techniques and mathematical models to measure and represent the entrainment mechanism have been developed by a number of authors. However, little work has been carried out in industrial scale cells. An exception was research conducted by Johnson (1972) which included industrial cell data to supplement laboratory data. This work showed that the recovery by entrainment is proportional to the feed water recovery to the concentrate. From this finding, the degree of entrainment was defined as the ratio of the recovery of entrained solids to that of water.

Johnson (1972) also showed that the degree of entrainment was a strong function of particle size: entrainment has been shown to be significant below particle sizes of 50 μm (Smith and Warren, 1989). Recently, Savassi et al. (1998) developed an empirical model to describe the relationship between the degree of entrainment and particle size. This model is represented in the equations below:

$$\mathrm{ENT}_i = \frac{2}{\exp(2.292(d_i/\xi)^{\mathrm{adj}}) + \exp(-2.292 d_i/\xi)} \tag{12.30}$$

and

$$\mathrm{adj} = 1 + \frac{\ln(\delta)}{\exp(d_i/\xi)} \tag{12.31}$$

where ENT_i = mass transfer of entrained particles to the concentrate ÷ mass transfer of water to the concentrate; d_i = particle size (μm); ξ = entrainment parameter, or the particle size for which the degree of entrainment is 20% (μm); δ = drainage parameter, related to the preferential drainage of coarse particles (dimensionless).

The engineering of flotation

The industrial application of the flotation process has been practised for 100 years. Although the process is effective, industrial flotation practice often requires several stages to produce the product quality desired by the market. These stages are combined in various methods and are referred to as "flotation circuits". In this section, the stages required in developing a flotation circuit including laboratory and pilot plant flotation testing, the types of circuits currently in practice and the types of flotation cells used are described. Lane et al. (2005) present a useful review of the logical approach to the design of a flotation flowsheet.

Laboratory flotation testing

In order to develop a flotation circuit for a specific ore, preliminary laboratory testwork must be undertaken in order to determine the choice of reagents and the size of plant for a given throughput as well as the flowsheet and peripheral data. Flotation testing is also carried out on ores in existing plants to improve procedures and for development of new reagents.

It is essential that testwork is carried out on ore which is representative of that treated in the commercial plant. Samples for testwork must be representative, not only in chemical composition but also relative to mineralogical composition and degree of dissemination. A mineralogical examination of drill cores or other individual samples should therefore be made before a representative sample is selected. Composite drill core samples are ideal for testing if drilling in the deposit has been extensive; the cores generally contain ore from points widely distributed over the area and in depth. It must be realised that ore bodies are variable and that a representative sample will not apply equally well to all parts of the ore body; it is used therefore for development of the *general* flotation procedure. Additional tests must be made on samples from various areas and depths to establish optimum conditions in each case and to give design data over the whole range of ore variation.

Characterisation of the flotation response of ore deposits must therefore recognise that the ore deposit could represent a variety of rock types, with different ore mineralogy, textures (fine or coarse grain) and faulting. It is therefore preferable that drill core samples be selected to represent the variations within the ore body. Each sample should be tested separately and the overall value of the deposit is then assessed by compositing the metallurgical responses of each sample mathematically.

Having selected representative samples of the ore, it is necessary to prepare them for flotation testing, which involves comminution of the ore to its optimum particle size. Crushing must be carried out with care in order to avoid accidental contamination of the sample by grease or oil, or with other materials which have been previously crushed. Even in a commercial plant, a small amount of grease or oil can temporarily upset the flotation circuit. Samples are usually crushed with small jaw crushers or cone crushers to about 0.5 cm and then to about 1 mm with crushing rolls in closed circuit with a screen.

Storage of the crushed sample is important, since oxidation of the surfaces is to be avoided, especially with sulphide ores. Not only does oxidation inhibit collector adsorption, but it also facilitates the dissolution of heavy metal ions, which may interfere with the flotation process. Sulphides should be tested as soon as possible after obtaining the sample and ore samples must be shipped in sealed drums in as coarse a state as possible. Samples should be crushed as needed during the testwork, although a better solution is to crush all the samples and to store them in an inert atmosphere.

Wet grinding of the samples should always be undertaken immediately prior to flotation testing to avoid oxidation of the liberated mineral surfaces. Batch laboratory grinding, using ball mills, produces a flotation feed with a wider size distribution than that obtained in continuous closed-circuit grinding; to minimise this, batch rod mills are used which give products having a size distribution which approximates closely to that obtained in closed-circuit ball mills. True simulation is never really achieved, however, as overgrinding of high specific gravity minerals, which is a feature of closed-circuit grinding, is avoided in a batch rod mill. It is also important to understand the effect of grinding media on flotation especially where scale-up is sought (Greet et al., 2005).

A soft dense mineral, such as galena, will be ground finer in closed circuit than predicted by

the batch tests, and its losses due to production of ultra-fine particles may be substantial. Some sulphide minerals, such as sphalerite and pyrite, can be depressed more easily at the coarser sizes produced in batch grinding, but may be more difficult to depress at the finer sizes resulting from closed-circuit grinding. Predictions from laboratory tests can be improved if the mineral recovery from the batch tests is expressed as a function of *mineral* size rather than overall product size. The optimum mineral size can be determined and the overall size estimated to give the optimum grind size (Finch et al., 1979). This method assumes that the same fineness of the valuable mineral will give the same flotation results both from closed-circuit and batch grinding, irrespective of the differences in size distributions of the other minerals.

It must be appreciated that the optimum grinding size of the particles depends not only on their grain size but also on their floatability. Initial examination of the ore should be made to determine the degree of liberation in terms of particle size in order to estimate the required fineness of grind.

The potential for liberation of the minerals contained in the ore can be determined by characterising the grain sizes of the minerals present. This can be achieved by breaking the drill core samples at a relatively coarse size (typically about 600 microns). This preserves the *in situ* texture of the samples, including grain size, association, and shape. The texture can be characterised by using a scanning electron microscope configured as a mineral liberation analyser, such as the MLA (Figure 12.15) or the QEMSCAN, as discussed in Chapter 1. Such an analyser can measure the grain sizes and composition of the component minerals of the ore. An example of an MLA image is shown in Figure 12.16.

Testwork should then be carried out over a range of grinding sizes in conjunction with flotation tests in order to determine the optimum flotation feed size distribution. In certain cases, it may be necessary to overgrind the ore in order that the particles are small enough to be lifted by the air bubbles. If the mineral is readily floatable a coarse grind may be utilised, the subsequent concentrate requiring regrinding to further free the mineral from the gangue, before further flotation is performed to produce a high-grade concentrate.

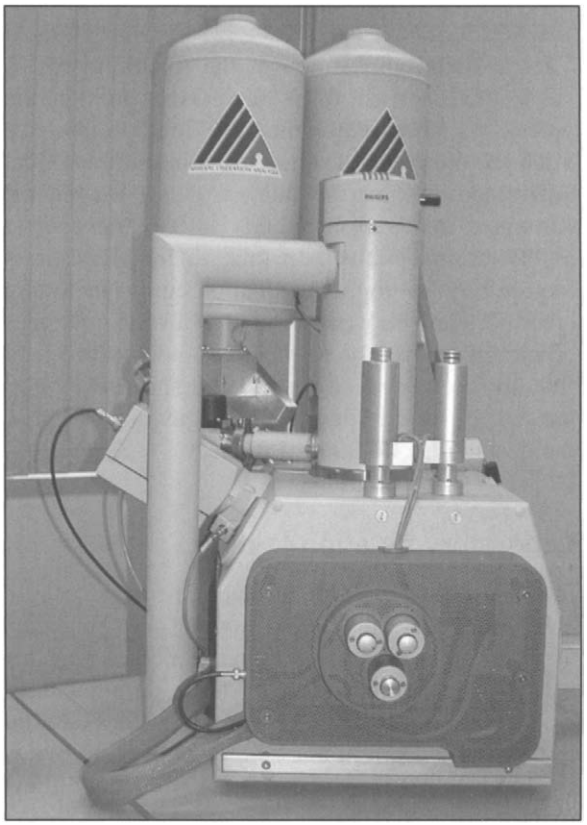


Figure 12.15 An example of an automated mineral liberation analyser – the FEI–JKMRC MLA (Courtesy JKMRC and JKTech Pty Ltd)

Mineral surface analysis

A useful laboratory method is that of *contact angle measurement* (Laskowski, 1986; Ralston and Newcombe, 1992; Woods, 1994), where, in its simplest form, a clean smooth surface of mineral is placed in distilled water, and a bubble of air from the end of a capillary tube is pressed down upon it. If, after a short time, no adhesion is visible on withdrawal of the bubble, the mineral surface is assumed to be clean, and the collector is then added. If the mineral surface now becomes hydrophobic, adherence of the introduced bubble to the surface results. The contact angle produced across the water phase (Figure 12.2) is a measure of the floatability of the mineral. The method suffers from many disadvantages; it is extremely difficult to obtain a truly representative surface of the mineral of the required size (at least 0.5 cm^2). The mineral may not be representative of the naturally liberated surface after the intense polishing required to produce

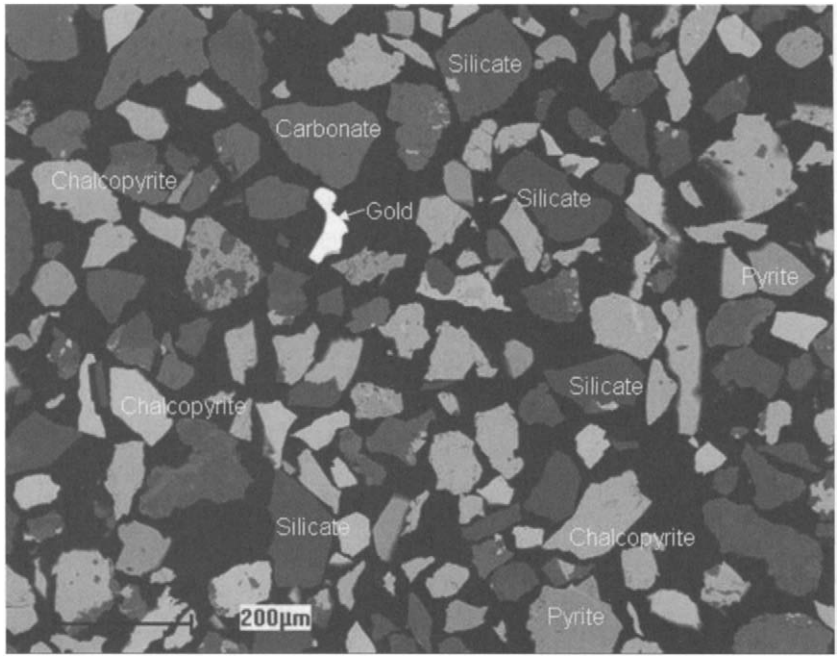


Figure 12.16 An image from an MLA showing the mineral grains in a copper–gold ore. The particles are 100–200 µm in size. These images are usually presented in false colour with each colour denoting a mineral or mineral class (Courtesy JKMRC and JKTech Pty Ltd)

a completely clean, flat surface. The method is static, whereas true flotation is dynamic, particles adhering after impact with bubbles rising in the pulp. Contact angle measurements should, therefore, be regarded only as indicators of flotation response.

Several sophisticated analytical techniques are now available for measuring the condition of the mineral surface and the products formed when adding collectors. These can be used both for a fundamental understanding of the processes of surface modification by reagents and for diagnosing particular separation problems or opportunities. They include Time of Flight Mass Spectroscopy (TOF-SIMS) either as a separate technique or in combination with X-Ray photoelectron spectroscopy (XPS) (Piantadosi et al., 2000; Hart et al., 2005, Hope et al., 2005), Infrared External Reflection Spectroscopy (Mielczarski and Mielczarski, 2005), Spectroelectrochemical Raman studies (Goh et al., 2005), and molecular modelling and verification (Rao et al., 2005).

Microflotation tests

Initial floatability tests are often made on the liberated mineral particles, as a means of assessing a range of suitable collectors and regulators, and to determine the effective pH for flotation. In the *Hallimond tube* technique (Figure 12.17), dynamic conditions prevail. The mineral particles are held on a support of sintered glass inside the tube containing the distilled water and the collector under test. Air bubbles are introduced through the sinter and any hydrophobic mineral particles are

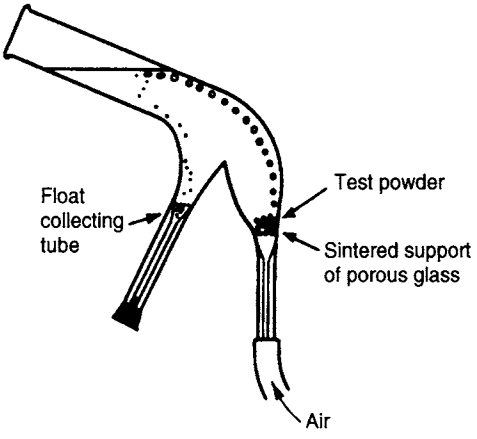


Figure 12.17 Hallimond tube

lifted by the bubbles, which burst at the water surface, allowing the particles to fall into the collecting tube. By treating a small weighed sample of pure mineral, or a mixture of pure minerals (e.g. galena and quartz), the weight collected in the tube can be related to the floatability. The Hallimond tube has the advantage of eliminating costly assaying. However, as frothers are not used in the test, it is doubtful whether the method truly simulates industrial flotation.

Other microflotation systems used to evaluate floatability on a microscale include those described by Partridge and Smith (1971), and the UCT microflotation cell (Bradshaw and O'Connor, 1996).

Batch flotation tests

The bulk of laboratory testwork is carried out in batch flotation cells (Figure 12.18), usually with 500 g, 1 kg, or 2 kg samples of ore. The cells are mechanically agitated, the speed of rotation of the impellers being variable, and simulate the large-scale models commercially available. Introduction of air to the cell is normally via a hollow standpipe surrounding the impeller shaft. The action of the impeller draws air down the standpipe, the volume being controlled by a valve and by the speed of the impeller. The air stream is sheared into fine bubbles by the impeller, these bubbles then rising through the pulp to the surface, where any particles picked up are removed as a mineralised froth.

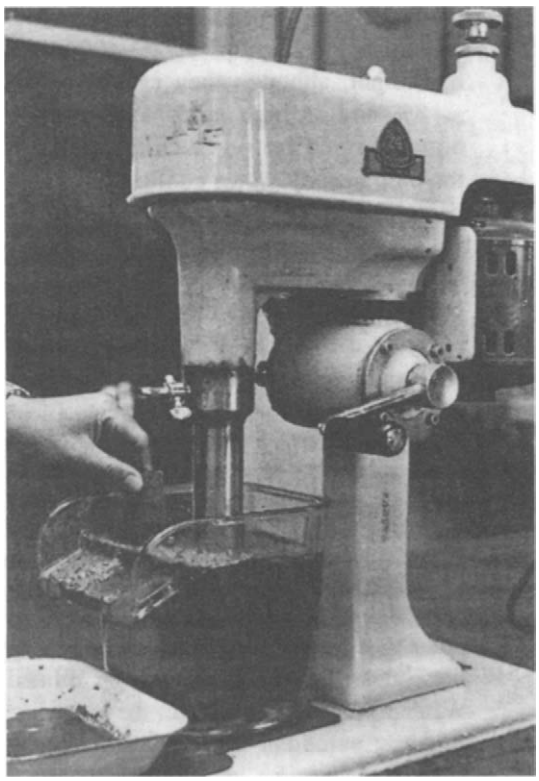


Figure 12.18 Laboratory flotation cell

Batch tests are fairly straightforward in practice, but a few experimental points are worth noting:

(1) Agitation of the pulp must be vigorous enough to keep all the solids in suspension, without breaking up the mineralised froth column.

(2) Conditioning of the pulp with the reagents is often required. This is a period of agitation, varying from a few seconds to 30 min, before the air is turned on, which allows the surface of the mineral particles to react with the reagents.

(3) Very small quantities of frother can have marked effects, and *stage additions* of frother are often needed to control the volume of froth. The froth depth should be between 2 and 5 cm, as very shallow froths entail the risk of losing pulp into the concentrate container. Reduction of the amount of air is sometimes used to limit the amount of froth produced. This should be standardised for comparative tests in order to prevent the introduction of another variable.

(4) As a matter of economics, flotation separations are carried out in as dense a pulp as possible consistent with good selectivity and operating conditions. The denser the pulp, the less cell volume is required in the commercial plant, and also less reagent is required, since the effectiveness of most reagents is a function of their concentrations in solution. The optimum pulp density is of great importance, as in general the more dilute the pulp, the cleaner the separation. Most commercial floats are in pulps of 25–40% solids by weight, although they can be as low as 8% and as high as 55%. It must be borne in mind that in batch flotation tests the pulp density varies continuously, from beginning to end, as solids are removed with the froth and water

is added to maintain the cell pulp level. This continuous variation changes the concentration of reagents as well as the character of the froth.

(5) As water contains dissolved chemicals which may affect flotation, water from the supply which will be used commercially should be used, rather than distilled water.

(6) Normally only very small quantities of reagent are required for batch tests. In order to give accurate control of their addition rates, they may have to be diluted. Water-soluble reagents can be added as aqueous solutions by pipette, insoluble liquid reagents by graduated dropper or hypodermic needle. Solids may either be emulsified or dissolved in organic solvents, providing the latter do not affect flotation.

(7) Recovery of froth is sensitive to operator technique.

(8) Most commercial flotation operations include at least one cleaning stage, in which froth is refloated to increase its grade, the cleaner tailings often being recycled. Since cleaner tails are not recycled in batch tests, they do not always closely simulate commercial plants. If cleaning is critical, cycle tests may have to be undertaken. These are multiple-step flotation tests designed to measure the effect of circulating materials. The main objectives of cycle tests are to determine:

- The increase in recovery obtained by recirculating cleaner tailings.
- The variation in reagent requirements to compensate for the circulating load of reagents.
- The effect of build-up of slimes or other undesirables which may interfere with flotation.
- The froth handling problems.

Normally at least six cycles are required before the circuit reaches equilibrium and a complete material balance should be made on each cycle. Since the reagents are in solution, it is essential that liquids as well as solids recirculate, so any liquid used to adjust pulp density must be circuit liquid obtained from decantation or filtration steps. Cycle tests are very laborious to carry out, and often the test fails to reach steady state. A method has been developed (Agar and Kipkie, 1978) whereby cycle test behaviour can be predicted from data developed from individual batch tests, and a computer program has been developed to arrive at a steady-state balance for a variety of simulated circuits.

Pilot plant testwork

Laboratory flotation tests provide the basis of design of the commercial plant. Prior to development of the plant, pilot scale testing is often carried out in order to:

(1) Provide continuous operating data for design. Laboratory tests do not closely simulate commercial plants, as they are batch processes.

(2) Prepare large samples of concentrate for survey by smelters, etc., in order to assess the possibility of penalties or bonuses for trace impurities.

(3) Compare costs with alternative process methods.

(4) Compare equipment performance.

(5) Demonstrate the feasibility of the process to non-technical investors.

Laboratory and pilot scale data should provide the optimum conditions for concentrating the ore and the effect of change of process variables. The most important data provided by testwork includes:

(a) The optimum grind size of the ore. This is the particle size at which the most economic recovery can be obtained. This depends not only on the grindability of the ore but also on its floatability. Some readily floatable minerals can be floated at well above the liberating size of the mineral particles, the only upper limit to size being that which the bubbles can no longer physically lift the particles to the surface. The upper size limit is normally around 300 μm. The lower size limit for flotation, at which problems of oxidation and other surface effects occur, is around 5 μm.

(b) Quantity of reagents required and location of addition points.

(c) Pulp density; important in determining size and number of flotation cells.

(d) Flotation time; experimental data gives the time necessary to make the separation into concentrate and tailings. This depends on the particle size and the reagents used and is needed to determine the plant capacity.
(e) Pulp temperature, which affects the reaction rates. Water at room temperature is, however, used for most separations.
(f) The extent of uniformity of the ore; variations in hardness, grindability, mineral content, and floatability should be investigated so that variations can be accommodated in the design.
(g) Corrosion and erosion qualities of the pulp; this is important in determining the materials used to construct the plant.
(h) Type of circuit; many different types of circuit can be used, and laboratory tests should provide data for the design of the best-suited circuit. This should be as basic as possible at this stage. Many flow schemes used in operating plants have evolved over a long period, and attempted duplication in the laboratory is often difficult and misleading. The laboratory procedures should be kept as simple as possible so that the results can be interpreted into plant operation.

A key issue in pilot plant testing is flexibility and consistency of operation. A standardised pilot plant has recently been developed called the floatability characterisation test rig (FCTR). The unit described by Rahal et al. (2000) is a fully automated pilot plant which is designed to move from plant to plant and characterise the floatability of each plant's ore according to standard procedures. It can be used both for testing modified circuits in existing plants and developing flowsheets for new ores. The FCTR is shown in operation in Figure 12.19.

Basic flotation circuits

Commercial flotation is a continuous process. Cells are arranged in series forming a *bank* (Figure 12.20). Pulp enters the first cell of the bank and gives up some of its valuable minerals as froth; the overflow from this cell passes to the second cell, where more mineralised froth is removed, and so on down the bank, until barren tailings overflow the last cell in the bank. In the case of flotation cells that use weir-type level control, the height of the froth column for each cell is determined by adjusting the height of the tailings overflow weir, the difference in height between this and the cell overflow lip determining the froth depth. In modern tank cells, pulp level is often maintained by adjusting the cell's tailings discharge with a rubber sleeve pinch valve.

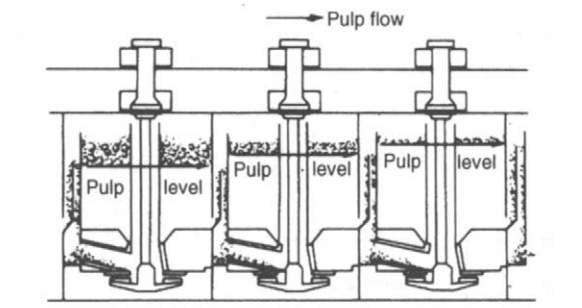
New feed enters the first cell of the bank, the froth column in the first few cells being kept high, since there are plenty of hydrophobic mineral particles to sustain it. The pulp level is raised from cell to cell, as the pulp becomes depleted in floatable minerals, by progressively raising the cell tailings weir height. The last few cells in the bank contain relatively low-grade froths, comprising weakly aerophilic particles. These are the *scavengers*, usually containing middlings particles, which are often recirculated to the head of the system.

In earlier cell designs, the scavenger cells, having little mineral to sustain a deep froth, have their tailings weirs raised so that pulp is almost overflowing the cell lip. This policy, which is used to remove all weakly floating material ("pulling the cells hard"), ensures maximum recovery from the bank of cells. Excessive circulating loads should be avoided, however, as the rougher feed may be diluted, and the flotation time reduced. In more recent cell designs, as the amount of minerals in the froth decreases (as in the scavenger cells described above) the froth is crowded using "froth crowders". This design allows the cell to be operated with a slightly deeper froth.

The flowsheet for this basic system is shown in Figure 12.21. This flowsheet can be successfully operated only when the gangue is relatively unfloatable, and it requires extremely careful control to produce an even grade of concentrate if there are any fluctuations in the head grade. A preferable system is to dilute the concentrate from the first few cells of the bank, known as *rougher* concentrates, and refloat them in *cleaner* cells, where the level of the pulp is kept low to maintain a deep froth and produce a high-grade concentrate. In this rougher–scavenger–cleaner system (Figure 12.22), the cleaning cells receive a comparatively high-grade feed, whilst the scavenging section can be run with an excess of air so as to obtain maximum recovery. Tailings from the cleaner cells, usually containing aerophilic mineral particles, can be



Figure 12.19 The Floatability Characterisation Test Rig (FCTR) (Courtesy JKMRC and JKTech Pty Ltd)



(a)



(b)

Figure 12.20 (a) Bank of flotation cells; (b) banks of cells in a concentrator

recirculated to the rougher cells, along with the scavengers. This type of circuit, besides being useful for ores that need the maximum amount of aeration at the end of the bank to produce profitable recovery, is often employed when the gangue has a tendency to float and is difficult to separate from the mineral. In such cases, it may be necessary to utilise one or more recleaning banks of cells (Figure 12.23).

It is worth noting that the diluting water used to lower the pulp density of the cleaning bank passes to the roughing cells and dilutes the primary feed, which should therefore contain a correspondingly smaller portion of water as it leaves the grinding section in order that the dilution of the cleaner tailing may bring it to the correct pulp ratio in the roughing cells.

Flowsheet design

In designing a suitable flowsheet for a flotation plant, the primary grind size is of major consideration. This is mainly due to the fact that the flotation response depends on the level of liberation of the minerals in the ore. The target grind size can be estimated based on past experience and from mineralogical evaluation, but laboratory

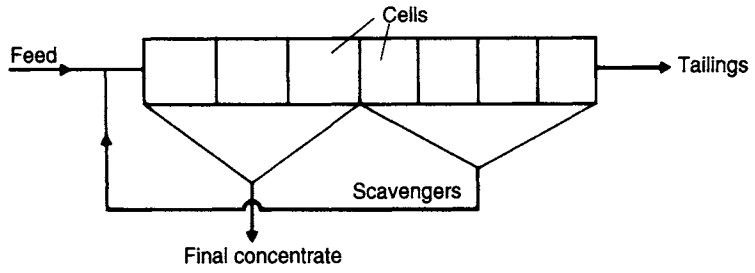


Figure 12.21 Simple flotation circuit

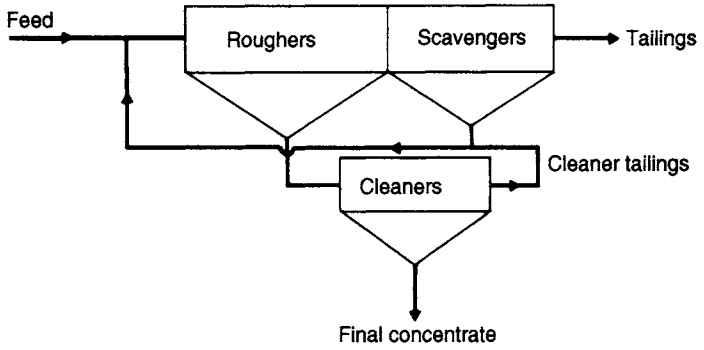


Figure 12.22 Rougher–scavenger–cleaner system

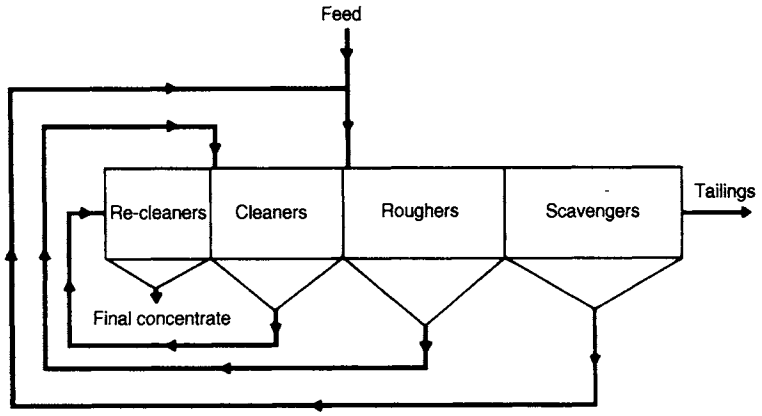


Figure 12.23 Circuit employing recleaning

grind-flotation tests must be conducted to determine optimum conditions. Grind size can be estimated knowing the size of the grains in the ore, and grain size can be estimated using mineral liberation analysers.

The purpose of the primary grind is to promote *economic recovery* of the valuable ore minerals. Batch tests are performed, utilising various reagent combinations, on samples of ore ground to various degrees. Incremental concentrate samples are weighed and assayed, and the results plotted as recovery–time and recovery–grade curves (Figure 12.24).

Initially, a grind size should be chosen which gives a reasonable rougher grade and recovery within an acceptable flotation time. If grinding is too coarse, some of the valuable mineral, locked in middlings grains, will not be floated. However, excessive flotation times may eventually allow some of these particles to report to the concentrate,

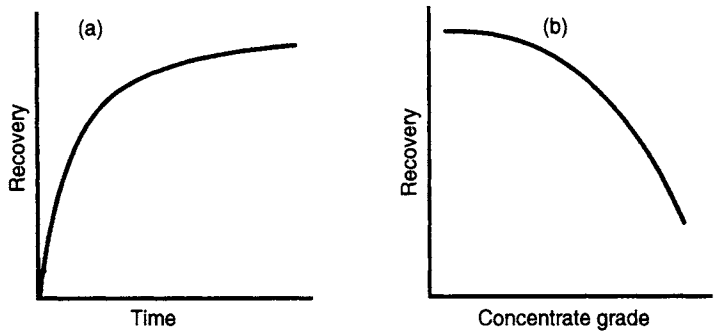


Figure 12.24 (a) Recovery of metal to concentrate versus time; (b) recovery versus concentrate grade curve

reducing its grade. It is here that the flotation engineers must use their experience in deciding what is, at this stage, a reasonable concentrate grade and flotation time.

As grinding is invariably the greatest single operating cost, it should not be carried out any finer than is justified economically. Later testwork, having improved on the basic flotation scheme, will modify the primary grind size, taking into account the amount of secondary grinding required to reach the specified concentrate grade, and the number of cleaning stages required. Finer grinding should not be performed beyond the point where the NSR for the increment saved becomes less than the operating cost (Steane, 1976).

After determining a suitable primary grind size (which may be modified in later testwork), further tests are performed to optimise reagent additions, pH, pulp densities, etc. Having optimised flotation recovery, testwork is then aimed at producing the required concentrate *grade*, and determining the flowsheet which must be utilised to achieve this.

As Figure 12.24(a) indicates, most of the valuable mineral floats within a few minutes, whereas it takes much longer for the residual small quantity to float. The rate equation for flotation can be expressed in a general way as follows:

$$v = -\mathrm{d}W/\mathrm{d}t = K_n W^n \qquad (12.32)$$

where v (weight/unit time) is the flotation rate, W is the weight of floatable mineral remaining in the pulp at time t, K_n is the rate constant, and n is the order of the reaction. The kinetics of flotation have been studied by many workers, the majority classifying flotation as a first order reaction ($n = 1$), others reporting second order kinetics (Mori et al., 1985). Dowling et al. (1985) applied thirteen rate models to batch copper flotation data and evaluated the results using statistical techniques. The flotation of the copper ore was shown to be essentially a first order process, and all the models tested were found to give a reasonably good fit to the experimental data, though some models were clearly better than others.

The first order rate equation is usually expressed as (Lynch et al., 1981):

$$R = 1 - \exp(-kt) \qquad (12.34)$$

where R is the cumulative recovery after time t; k is the first order rate constant (time^{-1}); t is the cumulative flotation time.

Plots of $\ln(1 - R)$ versus time should produce straight lines, but such plots are often concave upwards, which has led a number of workers to postulate the presence of fast and slow floating components. Agar (1985) argues that such postulates are false, the non-linear plots resulting from the assumption that the maximum possible recovery is 100%, whereas in practice some floatable material is usually totally irrecoverable, as it may be encased in gangue. A modified first order rate equation of the form:

$$R = RI[1 - \exp(-kt)] \qquad (12.35)$$

is proposed, where RI is the maximum theoretical flotation recovery.

The flotation rate constant is dependent on the particle size and the degree of liberation of the mineral, the curve shown in Figure 12.24(a) being a summation of the flotation rates of all the particles within the ore. Figure 12.25 shows the variation of flotation rate constant of an ore as a function of the particle size. Extensive studies of

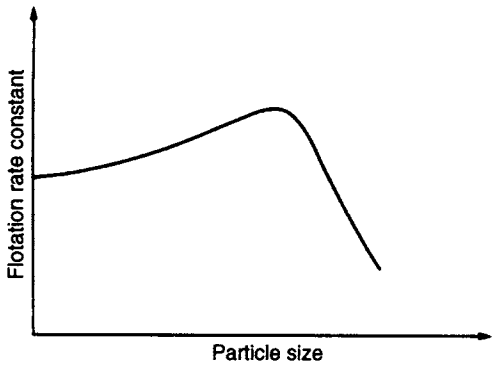


Figure 12.25 Flotation rate constant as a function of particle size

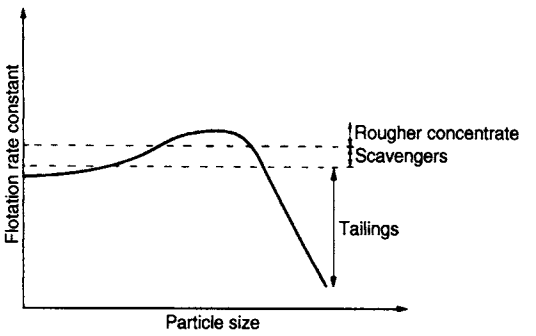


Figure 12.26
Rougher–scavenger system determined by flotation rate constant

the influence of particle size on flotation have been made (Trahar and Warren, 1976; Hemmings, 1980; Trahar, 1981).

It is clear that the flotation activity of an ore falls off slowly towards the range of fine particle size, mainly due to the increase in number of particles per unit weight and to the deteriorating conditions for bubble–particle contact and effects such as increased surface oxidation of the particles. Flotation activity falls off very rapidly above the optimum particle size, due to the lesser degree of liberation of the minerals and to the decreasing ability of the bubbles to lift the coarse particles. It can be seen that the floated material is composed of a fast floating fraction in the medium-size range and a more reluctant fraction comprising unliberated coarse material and fines. In a commercial flotation circuit the fast floating material will be recovered in the roughing section, while the more reluctant fraction is recovered by scavenging, certain losses into the tailings having to be accepted. Figure 12.26 relates the distribution in terms of the flotation rate constant.

The essential difference between the concentrates from the roughers and scavengers is that the latter comprise both coarse and fine particles while the rougher concentrate consists essentially of an intermediate-size fraction.

The grade of the final cleaner concentrate is dependent on the grade of the rougher concentrate (Figure 12.24(b)) and, in order to reach the specified optimum cleaning grade, it is necessary to keep the rougher grade at a predetermined value. The decision as to where the rougher–scavenger split should be can be made on the basis of batch tests where cumulative concentrate grade is plotted against time (Figure 12.27), the time limit for rougher flotation then being fixed as that required to give a rougher concentrate with a high enough grade to produce the specified final concentrate grade with the chosen number of cleaning stages. The remaining flotation time (Figure 12.24(a)) is for scavenging, this time sometimes being reduced by increasing the severity of the flotation conditions (i.e. increased aeration, addition of more powerful collector) after the removal of the rougher concentrate.

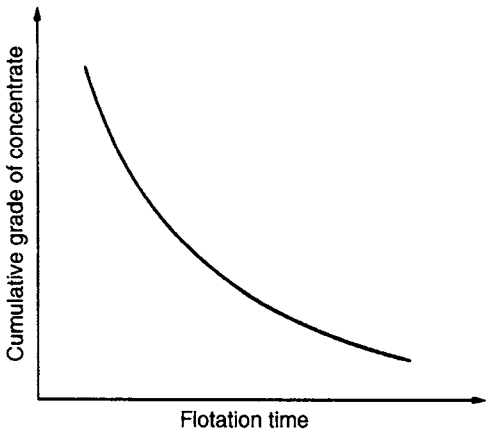


Figure 12.27 Cumulative grade in rougher flotation versus time

Agar et al. (1980) have argued that the rougher–scavenger split should be made at the flotation time where separation efficiency (Equation 1.1) is maximised. Separation efficiency (SE) reaches a

maximum value when dSE/dt is zero, so that from Equation 1.3:

$$\frac{\mathrm{dSE}}{\mathrm{d}t} = \frac{100m}{f(m-f)}\left[(c-f)\frac{\mathrm{d}C}{\mathrm{d}t} + C\frac{\mathrm{d}c}{\mathrm{d}t}\right] \quad (12.36)$$

$$= 0 \quad \text{at maximum separation efficiency.}$$

$$\int_0^t G\mathrm{d}C = Cc \quad (12.37)$$

Therefore, on differentiating Equation 12.37 with respect to t:

$$G\frac{\mathrm{d}C}{\mathrm{d}t} = C\frac{\mathrm{d}C}{\mathrm{d}t} + c\frac{\mathrm{d}C}{\mathrm{d}t} \quad (12.38)$$

and substituting Equation 12.38 in Equation 12.36:

$$\frac{\mathrm{dSE}}{\mathrm{d}t} = \frac{100\,m}{f(m-f)}\left[c\frac{\mathrm{d}C}{\mathrm{d}t} - f\frac{\mathrm{d}C}{\mathrm{d}t} + G\frac{\mathrm{d}C}{\mathrm{d}t} - c\frac{\mathrm{d}C}{\mathrm{d}t}\right] \quad (12.39)$$

Therefore, at maximum separation efficiency, where $\mathrm{dSE}/\mathrm{d}t = 0$, $G = f$.

This means that at maximum separation efficiency, the grade of concentrate produced is equal to the flotation feed, and after this time the flotation system is no longer concentrating the valuable mineral.

Since separation efficiency = recovery of mineral–recovery of gangue (Equation 1.1), separation efficiency is also maximised when:

$$\frac{\mathrm{d}(Rm - Rg)}{\mathrm{d}t} = 0, \quad \text{i.e. when} \quad \frac{\mathrm{d}Rm}{\mathrm{d}t} = \frac{\mathrm{d}Rg}{\mathrm{d}t}$$

Therefore, at maximum separation efficiency, the rate of flotation of valuable mineral is equal to that of the gangue, and above the optimum flotation time the gangue begins to float faster than the mineral. This optimum flotation time can be calculated from the first order rate Equation (12.35). However, as shown by Agar (1985), this equation has to be modified for batch flotation tests to incorporate a correction factor for time. In batch flotation some hydrophobic solids will have air attached to them during the conditioning period, which causes them to float more rapidly than they would naturally. This causes a positive correction to time zero, as flotation actually started before the air flow was introduced. On the other hand, when air flow commences, several seconds elapse before a full depth of loaded froth is present in the cell, and this gives a negative correction to time zero. Agar's modified rate equation for batch flotation tests is:

$$R = RI\{1 - \exp[-k(t+b)]\} \quad (12.40)$$

where b is correction for time zero.

A plot of $\ln[(RI-R)/RI]$ versus $(t+b)$ should produce a line of slope $-k$. However, RI and b are both unknown. Using experimental data, at the qth value of R and t:

$$\ln\left(\frac{RI - R_q}{RI}\right) + k(t_q + b) = r_q$$

where r_q is the residual due to errors in the experimental data.

Hence

$$r_q^2 = \left[\ln\left(\frac{RI - R_q}{RI}\right)\right]^2 + k^2(t_q+b)^2 + 2k(t_q+b)\cdot\ln\left(\frac{RI-R_q}{RI}\right).$$

Therefore, for n experimental data:

$$\sum_{q=1}^{n} r_q^2 = \sum_{q=1}^{n}\left[\ln\left(\frac{RI-R_q}{RI}\right)\right]^2 + k^2\sum_{q=1}^{n} t_q{}^2 + nk^2b^2 + 2k^2b\sum_{q=1}^{n} t_q + 2k\sum_{q=1}^{n}\left[t_q\cdot\ln\left(\frac{RI-R_q}{RI}\right)\right] + 2kb\sum_{q=1}^{n}\ln\left(\frac{RI-R_q}{RI}\right) \quad (12.41)$$

$\sum_{q=1}^{n} r^2$ is a minimum when $\frac{\partial}{\partial k}\left(\sum_{q=1}^{n} r^2\right)$ and $\frac{\partial}{\partial b}\left(\sum_{q=1}^{n} r^2\right)$ are zero,

i.e. when

$$\frac{\partial}{\partial k}\left(\sum_{q=1}^{n} r^2\right) = 2k\sum_{q=1}^{n} t^2 + 2nkb^2 + 4kb\sum_{q=1}^{n} t + 2\sum_{q=1}^{n}\left[t\cdot\ln\left(\frac{RI-R}{RI}\right)\right] + 2b\sum_{q=1}^{n}\ln\left(\frac{RI-R}{RI}\right) = 0 \quad (12.42)$$

and

$$\frac{\partial}{\partial b}\left(\sum_{q=1}^{n} r^2\right) = 2nk^2b + 2k^2\sum_{q=1}^{n} t + 2k\sum_{q=1}^{n}\ln\left(\frac{RI-R}{RI}\right) = 0 \quad (12.43)$$

Equations 12.42 and 12.43 can be solved to give:

$$\hat{k} = -\frac{\left\{n\sum_{q=1}^{n} t\cdot\ln\left[(RI-R)/RI\right]\right\}}{n\sum_{q=1}^{n} t^2 - \left(\sum_{q=1}^{n} t\right)^2} - \frac{\left\{\sum_{q=1}^{n}\ln\left[(RI-R)/RI\right]\cdot\sum_{q=1}^{n} t\right\}}{n\sum_{q=1}^{n} t^2 - \left(\sum_{q=1}^{n} t\right)^2} \quad (12.44)$$

and

$$\hat{b} = -\frac{\left\{\hat{k}\sum_{q=1}^{n} t + \sum_{q=1}^{n}\ln\left[(RI-R)/RI\right]\right\}}{n\hat{k}} \quad (12.45)$$

RI can initially be assigned a value of 100, and $\hat{k}$ and $\hat{b}$ are calculated from Equations 12.44 and 12.45. Using these values $\sum_{q=1}^{n} r^2$ is then calculated from Equation 12.41.

RI is then decremented and the procedure repeated until values of $\hat{k}$, $\hat{b}$, and $\hat{RI}$ are found which minimise $\sum_{q=1}^{n} r^2$.

From Equation 12.40:

$$dR/dt = RI\cdot k\exp\left[-k\left(t+b\right)\right]$$

so that if the computations are performed for mineral (m) and gangue (g), then at optimum flotation time:

$$RI_m k_m\cdot\exp\left[-k_m\left(t+b_m\right)\right] = RI_g k_g\cdot\exp\left[-k_g\left(t+b_g\right)\right]$$

from which optimum flotation time

$$= \left[\ln\frac{RI_m k_m}{RI_g k_g} - k_m b_m + k_g b_g\right] \Big/ \left(k_m - k_g\right) \quad (12.46)$$

In a complex flotation circuit, the rougher flotation may be divided into stages, each delivering its concentrate into the cleaning circuit at a different location according to its grade.

Thus, the basic flowsheet consisting of cleaners and recleaners may be supplemented by a low-grade cleaning circuit (Figure 12.28).

To ensure the recovery of the weakly aerophilic particles which are passed to the particular section of the cleaning plant, it is essential that the retention time in the cleaning stage is at least that of the corresponding roughing section.

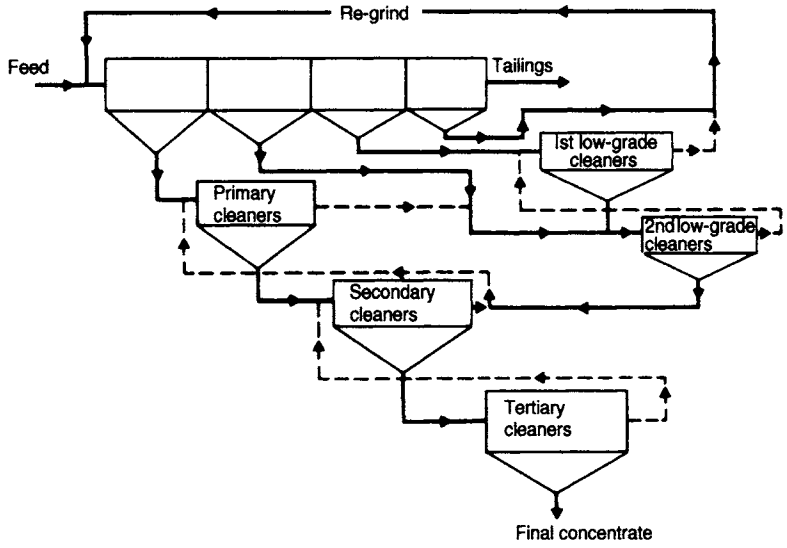


Figure 12.28 Complex flotation circuit

Since the object of the scavenging section is to promote maximum recovery by minimising the losses to tailings, it is advisable to dimension the scavengers generously, to allow not only for the slow-floating character of the particles but also for fluctuations in the circuit. However, it is important to avoid excessive overloading of the system with large volumes of low-grade material, so a compromise must be made in designing the scavenger circuit (Lindgren and Broman, 1976). It may be preferable to have a lower rougher concentrate grade (longer flotation time), and more cleaning stages, thus reducing the volume of scavenger concentrate produced.

This is particularly important in non-metallic flotation, where, due to the generally low ratio of concentration, large circulating loads are often produced. For instance, in the flotation of a low-grade metallic ore, the ratio of concentration may be as high as 50, so that only about 2% of the ore is removed as concentrate, and the circulating loads in the system are of this order of magnitude. Non-metallic ores, however, are often of high grade, and the ratio of concentration can be as low as 2, so that 50% of the ore is removed as concentrate, and very high circulating loads are produced. Control of such circuits can often be facilitated by the addition of a thickener, or agitator, which can act as surge capacity for large changes in circulating load which may arise when changes in ore grade occur.

If cleaning does not give the required concentrate grade, regrinding of the rougher concentrate may be needed, usually being necessary to at least regrind the scavenger concentrate, and sometimes the primary cleaner tailings, before recirculation to the rougher circuit. The purpose of primary grinding is to promote maximum recovery, by rendering most of the valuable mineral floatable so that the bulk of the gangue can be discarded, thus reducing the amount of material that must be further processed. In secondary grinding, or regrinding, the major consideration is the grade of the concentrate.

Regrinding of the middlings products is common practice in flotation plants. Both the scavenger product and the cleaner tailings contain essentially a slow floating, fairly metal-rich fine fraction and a coarse product consisting mainly of unliberated mineral. These products are generally classified if the amount of fines is appreciable, after which the coarse product is reground and returned to the system with the new feed. The fine classified product is either recycled to the rougher circuit, or cleaned in a separate circuit to a grade high enough to be fed to the final concentrate or the main cleaner system.

Regrinding practice depends to a large extent on the ore mineralogy. In certain circumstances, particularly when the mineral is of high floatability and is associated with an unfloatable gangue, it may be economical to grind at a relatively coarse size and regrind the rougher concentrate (Figure 12.29). This is common practice with such minerals as molybdenite, which is readily floatable, when associated with hard, abrasive gangues. Removing the gangue as a tailings at a coarse particle size considerably reduces the energy consumption in the grinding stage.

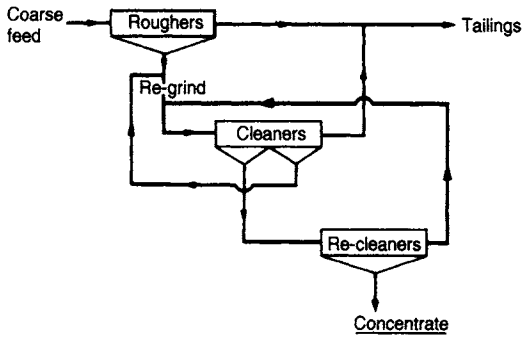


Figure 12.29 Regrinding of rougher concentrates

Figure 12.30 shows a circuit used at the Phoenix Copper Div. of Granby Mining Corp., Canada (Hardwicke et al., 1978). The main copper mineral is chalcopyrite, some of which is finely disseminated in the gangue, but it also occurs as complex grains with pyrite. The circuit removes the fairly coarse chalcopyrite early by one-stage rougher-scavenger-cleaning. The middlings from this stage, consisting essentially of the finely disseminated copper minerals, are reground and floated in a completely separate circuit utilising two cleaning stages, thus isolating the flotation of the coarse material (80%–188 μm) from the flotation of the very fine particles (80%–40 μm).

Selective flotation circuits, which concentrate two or more minerals, must incorporate substantial facilities for control. Where, for example, heavy sulphide ores are being treated, it is common for a bulk float to be initially removed. This

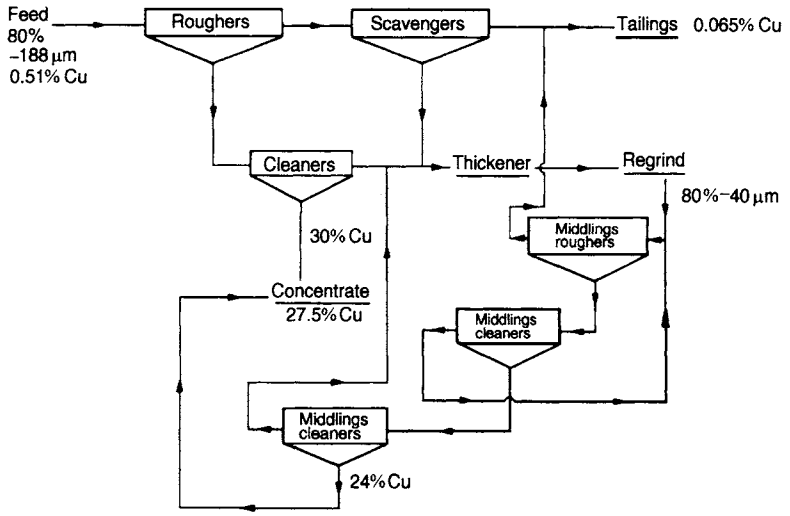


Figure 12.30 Phoenix Copper Div. flotation circuit

isolates the sulphides from the non-sulphides, thus simplifying the subsequent selective separation of each sulphide component, providing that this is not inhibited by the presence of reagents from the bulk float which are adsorbed on the mineral surfaces. If this is serious, direct selective flotation must be used, which is essentially two or more one-product circuits in series, although some plants treating difficult ores use a combination of bulk and selective flotation in the rougher operations. Mineral composition and the degree of intergrowth of the valuable minerals are also important factors. Extremely fine intergrowth inhibits selective flotation separation, and there are some complex ores, containing sulphides of copper, lead, and zinc, which cause extreme difficulties in selective flotation. Figure 12.31 gives an outline of three flowsheets in use for such ores, from an "easy" coarse-grained ore (a) to a "difficult" fine grained ore (c).

Some flotation plants are in operation where more than five concentrates are effectively recovered from a single feed, such operations demanding considerable modification in the chemical nature of the feed pulp for each stage in the total treatment. The pH of the pulp may have to span a range from as low as 2.5 to as high as 10.5 to recover sulphide minerals alone, and further complications can arise if non-sulphide minerals, such as cassiterite, fluorite, barytes, etc., are to be recovered with sulphides.

Figure 12.32 shows a circuit which has been used to treat a complex ore containing copper, zinc, and iron sulphides, and cassiterite disseminated in a siliceous gangue.

A relatively coarse primary grind is used in order to recover as much cassiterite at as coarse a size as possible in the subsequent gravity process. After conditioning with copper sulphate to activate the sphalerite, the relatively large amount of sulphide minerals, which would interfere with the recovery of the cassiterite, is removed by bulk flotation at neutral pH. The bulk rougher concentrate is reground to release finely disseminated cassiterite, after which cleaning is undertaken, the cleaner tailings being recirculated to the head of the system. The bulk cleaner concentrate is conditioned with lime to about pH 11, which depresses the pyrite, and the copper and zinc sulphides are floated and cleaned, leaving the pyrite in the rougher tailings.

A significant problem in connection with flotation circuit design is that of transposing times from batch tests to flotation times in the continuous working circuit. The fundamental difference between a batch test and a continuous process is that every part of the flotation pulp in a batch test remains in the cell for the same length of time, whereas in a cell with continuous flow there is a spread, often quite considerable, in the retention times of different unit volumes. Some of the pulp takes a short cut and passes out of the cell relatively quickly, with the result that flotation is incomplete.

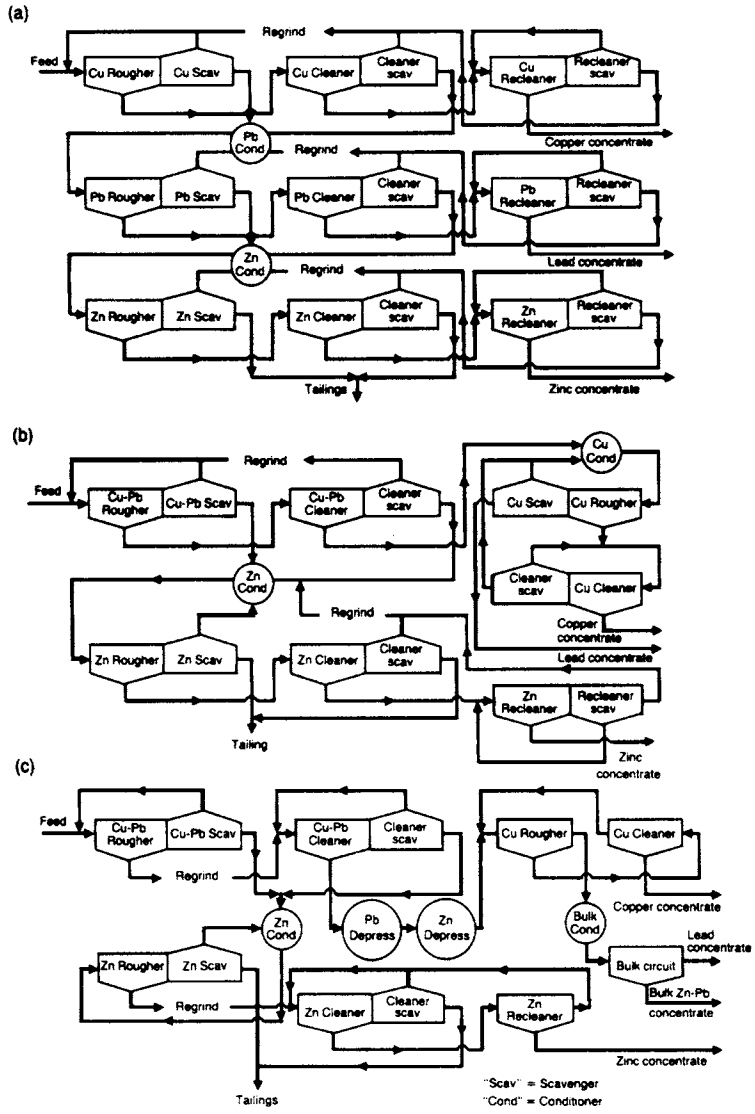


Figure 12.31 Typical flotation flowsheet used for complex sulphide processing – production of three concentrates (after Barbery, 1986)

To reduce this problem the desired total flotation volume is divided into smaller portions.

The total cell volume required to give the specified nominal flotation time must, of course, be computed with allowance for the fact that only a part of the actual cell volume is available for the pulp. From the gross volume must be subtracted the volumes of the rotor machinery and stator, the froth layer and the air present in the pulp during the flotation process. Calculations indicate that the net volume in some cases can be as small as 50% of the gross cell volume. It must be remembered, however, that this factor only gives an adequate nominal retention time, without providing a safety margin for partial short-circuits in the flow as mentioned above or for the fluctuations that are liable to occur in the system. A safety factor of two to three is usually applied to laboratory flotation times in order to determine the required cell volume of the full-scale plant.

It should be noted that although increased aeration results in faster flotation, it also results in shorter retention times, as a larger portion of the total volume is occupied by air. There is, therefore,

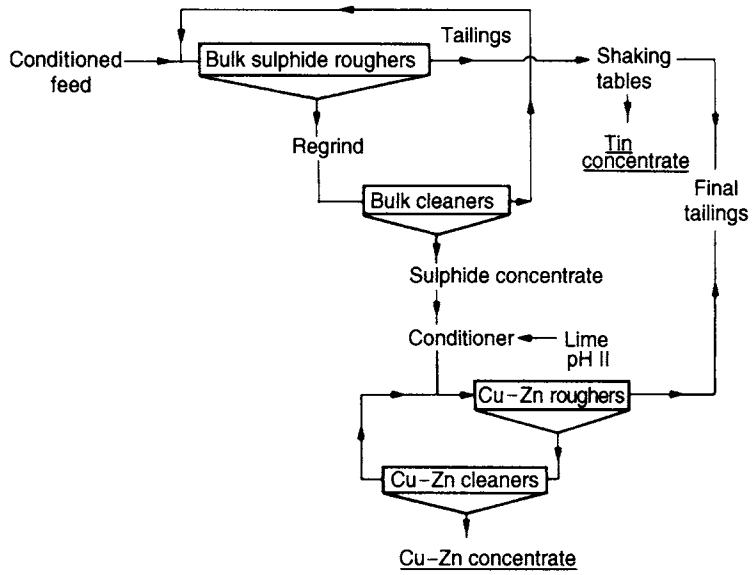


Figure 12.32 Copper–zinc–tin separation circuit

an optimum rate of air supply to the cells, above which recovery may be reduced. This is not evident from the results of batch tests.

Flotation circuits can now be designed and optimised using computer modelling and simulation software, e.g. JKSimFloat (Harris et al., 2002). This simulator has the capabilities of predicting the flotation performance of a circuit under conditions of changing:

- Feed throughput (assuming that flotation floatability remains constant and residence time varies);
- Bank residence time;
- Cell operating parameter, e.g. air flow rate, froth depth, etc.;
- Circuit stream destination.

Numerous scenarios can be simulated quickly, providing the flotation design engineer with a tool for assessing the optimum circuit flowsheet.

Circuit flexibility

The decision having been reached to design a flotation circuit according to a certain scheme, it is necessary to provide for fluctuations in the flow rate of ore to the plant, both large and small, and for minor fluctuations in grade of incoming ore.

The simplest way of smoothing out grade fluctuations and of providing a smooth flow to the plant is by interposing a large storage agitator between the grinding section and the flotation plant:

$$\text{Grind} \rightarrow \text{Storage Agitator} \rightarrow \text{Flotation Plant}$$

Any minor variations in grade and tonnage are smoothed out by the agitator, from which material is pumped at a controlled rate to the flotation plant. The agitator can also be used as a conditioning tank, reagents being fed directly into it. It is essential to precondition the pulp sufficiently with the reagents before feeding to the flotation banks, otherwise the first few cells in the bank act as an extension of the conditioning system, and poor recoveries result.

Control systems can be installed to maintain the flow rate of the slurry as constant as possible. The control system starts in the grinding circuit where the feed rate of ore to the grinding mills is maintained constant using variable speed feeders. The level of slurry in pump boxes is also maintained constant by automatically adjusting pump speed using variable speed drives. Levels of slurry in flotation cells are maintained constant by using automatic cell level control systems.

Provision must be made to accommodate any major changes in flow rate which may occur; for example, a number of mills may have to be shut

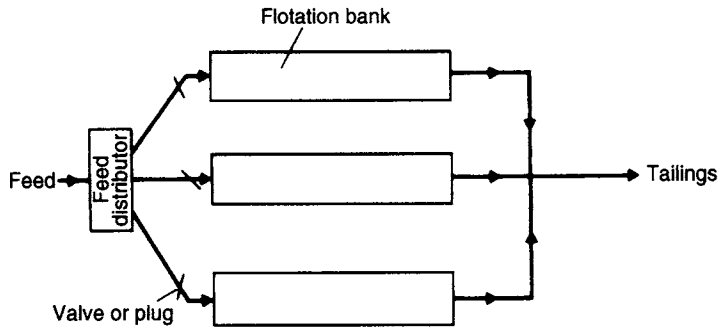


Figure 12.33 Parallel flotation banks

down for maintenance. This is achieved by splitting the feed into parallel banks of cells (Figures 12.33 and 12.20(b)), each bank requiring an optimum flow rate for maximum recovery. Major reductions in flow rate below the designed maximum can then be accommodated by shutting off the feed to the required number of banks. The optimum number of banks required will depend on the ease of control of the particular circuit. More flexibility is built into the circuit by increasing the number of banks, but the problems of controlling large numbers of banks must be taken into account, and in plants that have installed very large unit processes, such as grinding mills, flotation machines, etc., in order to reduce costs and facilitate automatic control, the need for many parallel banks has been reduced.

In designing each flotation bank, the number of cells required must be assessed: should a few large cells be incorporated or many small cells giving the same total capacity?

This is determined by many factors. If a small cell in a bank containing many such cells has to be shut down, then its effect on production and efficiency is not as large as that of shutting down a large cell in a bank consisting of only a few such cells. Maintenance costs, however, tend to be lower with large cells, since there are relatively fewer parts to change in a particular bank.

The desired residence time for maximum economic recovery, which is calculated from laboratory tests, assumes that every particle is given the chance to float in that time. This does not necessarily happen in a continuous process, as it is possible for particles to short-circuit immediately from one cell to the next. This becomes increasingly serious when there are the fewer cells in the bank. Designing a bank with many small cells gives particles which have short-circuited in one or more cells the chance to float in succeeding cells. The designer, therefore, must decide between small cells for greater flexibility and metallurgical performance, and large cells, which have a smaller total capital cost, less floor area per unit volume, and lower operating costs. In eastern Europe, it has been common to install 30 or more machines in a single bank, while in the West the trend is to install very large cells, especially in the roughing stage.

Flotation plants built in the 1970s and 1980s used between eight and fourteen cells in the rougher banks to produce an optimum design, depending on the most economic layout of the plant. This had the effect of limiting the use of $28\,m^3$ ($1000\,ft^3$) cells to mills with tonnage throughputs of $15{,}000\,t\,d^{-1}$ or higher, although some machine manufacturers, particularly Outokumpu, recommend using the largest cells possible, which reduces the number of mechanisms, in some cases to only two in a bank. There are reports that recovery is unimpaired, or even enhanced, at the same total retention time. As Young (1982) observed, a clear difference of opinion has emerged, which requires further research.

In the 1990s and 2000s the flotation cell suppliers that produced Outokumpu and Wemco cells developed the tank cell designs. These cells can be as big as $150\,m^3$ or more in volume and can treat more that 100,000 tonnes per day of ore, particularly in large copper operations in South America and Asia (Figure 12.20(b)). Tank cells of even greater volumes are under development from flotation cell suppliers (Weber et al., 2005). These cells are able to minimise short-circuiting of slurry by using big tanks with a single tailings discharge that is controlled by rubber sleeved pinch valves. A

bank is typically designed with about eight to ten cells in the rougher section.

Flexibility must be provided relative to the number of cells in a bank producing rougher and scavenger concentrates, in order to allow for changes in the grade of incoming ore. For instance, if the ore grade decreases, it may be necessary to reduce the number of cells producing rougher concentrate, in order to feed the cleaners with the required grade of material. A simple method of adjusting the "cell split" on a bank is shown in Figure 12.34. If the bank shown has, say, twenty cells, each successive four cells feeding a common launder, then by plugging outlet B, twelve cells produce rougher concentrate. Similarly, by plugging outlet A, only eight produce rougher concentrates, and by leaving both outlets free, a ten–ten cell split is produced.

At North Broken Hill in Australia, the lead recleaner concentrate grade was automatically controlled by stabilising the mass flow rate of recleaner feed. An increase in flow rate increased the cleaner concentrate grade, due to the decreased residence time within the cells. Automatically controlled froth diverter trays (Figure 12.35) increased the number of cells producing concentrate to compensate for the increase in feed rate, and the number of cells producing middlings was correspondingly reduced (Figure 12.36).

Flotation machines

Although many different machines are currently being manufactured and many more have been developed and discarded in the past, it is fair to state that two distinct groups have arisen: pneumatic and mechanical machines. The type of machine is of

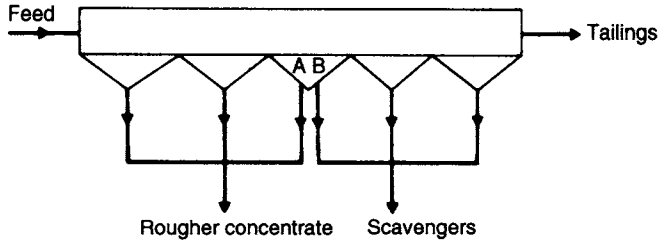


Figure 12.34 Control of cell split



Figure 12.35 Automatic froth diverter trays

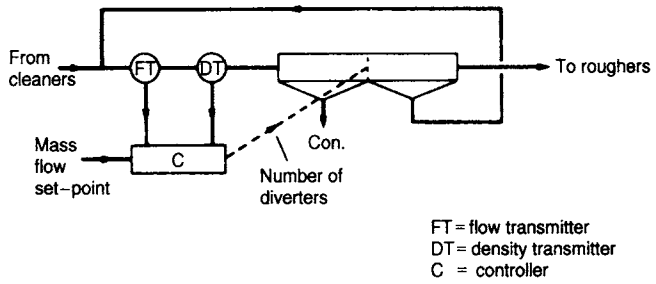


Figure 12.36 Lead recleaning circuit. North Broken Hill, Australia

great importance in designing a flotation plant and is frequently the characteristic causing most debate (Araujo et al., 2005; Lelinski et al., 2005).

Pneumatic machines either use air entrained by turbulent pulp addition (cascade cells), or more commonly air either blown in or induced, in which case the air must be dispersed either by baffles or by some form of permeable base within the cell. Generally pneumatic machines give a low-grade concentrate and little operating trouble. Since air is used not only to produce the froth and create aeration but also to maintain the suspension and to circulate it, an excessive amount is usually introduced and for this and other reasons they have been little used.

One of the early developments in the pneumatic field was the Davcra cell (Figure 12.37), which has been claimed to yield equivalent or better performance than a bank of mechanical machines.

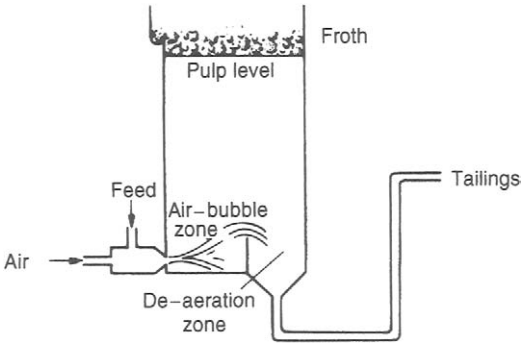


Figure 12.37 Davcra cell

The cell consists of a tank segmented by a vertical baffle. Air and feed slurry are injected into the tank through a cyclone-type dispersion nozzle, the energy of the jet of pulp being dissipated against the vertical baffle. Dispersion of air and collection of particles by bubbles allegedly occurs in the highly agitated region of tank confined by the baffle. The pulp flows over the baffle into a quiescent region designed for bubble–pulp disengagement. The cell can be used for roughing or cleaning applications on a variety of minerals. Although not widely used, Davcra cells replaced some mechanical cleaner machines at Chambishi copper mine in Zambia, with reported lower operating costs, reduced floor area, and improved metallurgical performance.

A significant development in recent years has been the increasing industrial use of flotation columns. The main advantages of columns include improved separation performance, particularly on fine materials, low capital and operational cost, less plant space demand, and adaptability to automatic control.

A typical configuration of a column is shown in Figure 12.38. It consists of two distinct sections. In the section below the feed point (the recovery section), particles suspended in the descending water phase contact a rising swarm of air bubbles produced by a sparger (Murdock and Wyslouzil, 1991) in the column base. Floatable particles collide with and adhere to the bubbles and are transported to the washing section above the feed point. Non-floatable material is removed from the base of the column as tailing. Gangue particles that are loosely attached to bubbles or are entrained in bubble slipstreams are washed back into the recovery section, hence reducing contamination of the concentrate. The wash water also serves to suppress the flow of feed slurry up the column towards the concentrate outlet. There is a downward liquid flow in all parts of the column

preventing bulk flow of feed material into the concentrate.

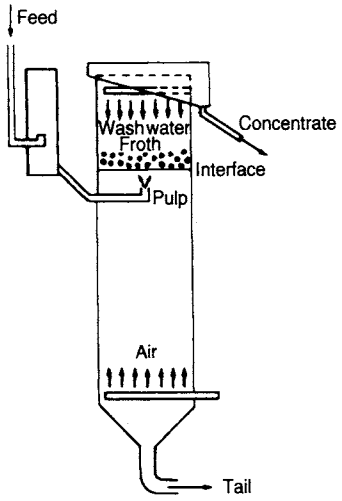


Figure 12.38 The flotation column

Columns were originally developed in Canada, and were used initially for cleaning molybdenum concentrates. Two-column flotation units were installed in the molybdenum circuit at Mines Gaspe, Canada, in 1980, and excellent results were reported (Cienski and Coffin, 1981). The units replaced mechanical machines in the cleaner banks. Since then many of the copper–molybdenum producers in North America have installed columns for molybdenum cleaning, and their use has been expanded into the roughing, scavenging, and cleaning of a variety of ore types, in many parts of the world. An indication of the interest in columns is that within a period of three years, they have been the subject of two international conferences (Sastry, 1988; Agar et al., 1991), a textbook (Finch and Dobby, 1990), and many other papers (Araujo et al., 2005).

The US Bureau of Mines compared column flotation with conventional flotation on a Montana chromite ore, the results showing that column flotation appears to be a physical improvement in the flotation separation process (McKay et al., 1986). Because of the excellent results achieved, further studies of column flotation were underway on ores containing fluorite, manganese, platinum, palladium, titanium, and other minerals. The United Coal Co. in the United States has also pioneered the use of columns for the flotation of fine coal (Chironis, 1986). It is possible that, due to their froth washing capability, columns may find an increasing use in the future for treating ores that need extensive fine grinding, followed by desliming and multi-stage cleaning.

Instrumentation and some degree of automatic control is a necessity for column operation. The methods currently used for the control of columns have been summarised by Moys and Finch (1988).

Flotation columns are usually about 12 m high, with diameters of up to about 3.5 m (round or square, the former being more popular), the importance of height/diameter ratio having been discussed by Yianatos et al. (1988). Several attempts have been made to develop column-type devices with much smaller height/diameter ratios, the Jameson cell (Kennedy, 1990; Cowburn et al., 2005) being a successful example (Figure 12.39 – Harbort et al., 2002). Contact between the feed and the air stream is made in a mixing device at the top of a vertical downcomer. The air–liquid mixture flows downwards to discharge into a shallow pool of pulp in the bottom of a short cylindrical column. The bubbles disengage and rise to the top of the column to overflow into a concentrate launder, while the tails are discharged from the bottom of the vessel. The main advantages of the device are that the overall height of the column is reduced to about 1 m, and the flotation column can be self-inducing with respect to the air supply,

The Jameson cell was developed jointly by Mount Isa Mines Ltd and the University of Newcastle, Australia. The cell was first installed for cleaning duties in base metal operations (Clayton et al., 1991; Harbort et al., 1994) but it has also found uses in other duties including roughing and preconcentrating. The major advantage of the cell is its ability to produce clean concentrates in one stage of operation. It also has a novel application in solvent extraction – electrowinning, where it is being used to recover entrained organic from copper-rich electrolyte (Miller and Readett, 1992) in many of the copper-leaching operations in Arizona and New Mexico in the United States as well as in Mexico.

The Jameson cell has also become widely used in the coal industry in Australia in the 1990s and 2000s. Typical cell layout is shown in Figure 12.40, which shows the fine coal slurry feeding a central distributor, splitting the stream and being treated

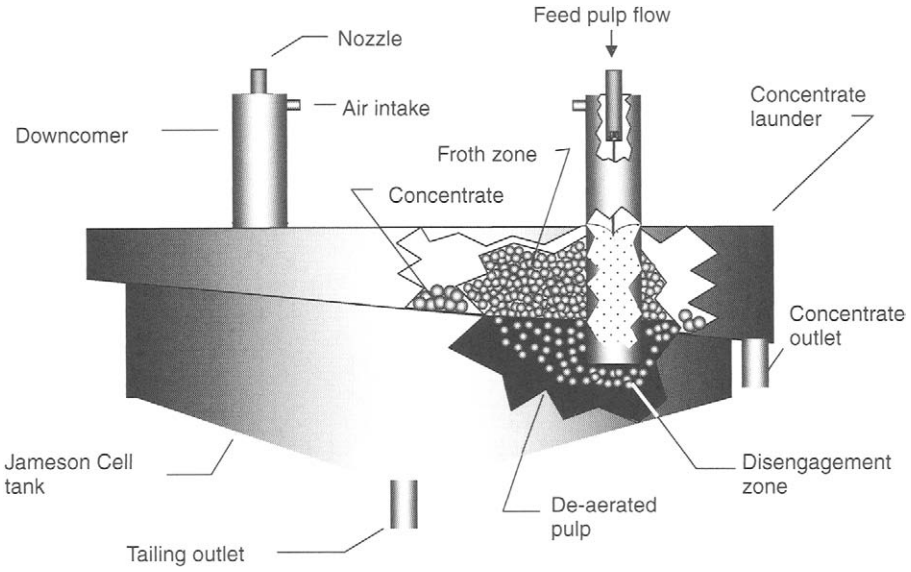


Figure 12.39 Principles of operation of the Jameson cell (Courtesy Xstrata Technology)

inside the downcomer. The clean coal then overflows as a concentrate from the separation chamber.

Froth separators were developed in the USSR in 1961 and had treated 9 M tonnes of various ores by 1972 (Malinovskii et al., 1973). The principle of the froth separator (Figure 12.41) is that conditioned feed is discharged onto the top of a froth bed, the hydrophobic particles being retained while the hydrophilic species pass through and are thereby separated. This method is particularly suited to the separation of coarse particles. The slurry is introduced at the top of the machine and descends over sloping baffles before entering an aeration trough, where it is strongly aerated before floating horizontally onto the top of the froth bed. Water and solids which penetrate the froth bed pass between aerator pipes into the pyramidal tank. The aerators are rubber pipes with 40–60 fine holes per cubic centimetre, into which air is blown at 115 kPa. The machine, which has two froth discharge lips, each 1.6 m long, is capable of treating $50\,t\,h^{-1}$ of solids at slurry densites of between 50 and 70% solids. Although used little in the western world, they have great potential for treating coarse feeds at up to ten times the rate of mechanical machines. The upper size limit for flotation is increased to about 3 mm, but they are not suited to fines treatment, a typical feed size range being about 75 pm to 2 mm. The role of flotation time is reversed, increasing flotation times reducing the recovery but increasing the concentrate grade.

Mechanical flotation machines are the most widely used, being characterised by a mechanically driven impeller which agitates the slurry and disperses the incoming air into small bubbles. The machines may be self-aerating, the depression created by the impeller inducing the air, or "supercharged" where air is introduced via an external blower. In a typical flotation bank, there are a number of such machines in series, "cell-to-cell" machines being separated by weirs between each impeller, whereas "open-flow" or "free-flow" machines allow virtually unrestricted flow of the slurry down the bank.

The most pronounced trend in recent years, particularly in the flotation of base metal ores, has been the move towards larger capacity flotation cells, with corresponding reduction in capital and operating costs, particularly where automatic control is incorporated. In the mid-1960s, flotation cells were commonly $5.7\,m^3$ ($200\,ft^3$) in volume, or less (Figure 12.42) and in the 1970s and 1980s $8.5\,m^3$ to $14.2\,m^3$ cells were widely used (Figure 12.43), with $28.3\,m^3$ cells, and larger, being increasingly adopted. Manufacturers in the forefront of this industry included Denver Equipment ($36.1\,m^3$), Galigher ($42.5\,m^3$), Wemco ($85\,m^3$), Outokumpu Oy ($38\,m^3$), and Sala ($44\,m^3$). Many

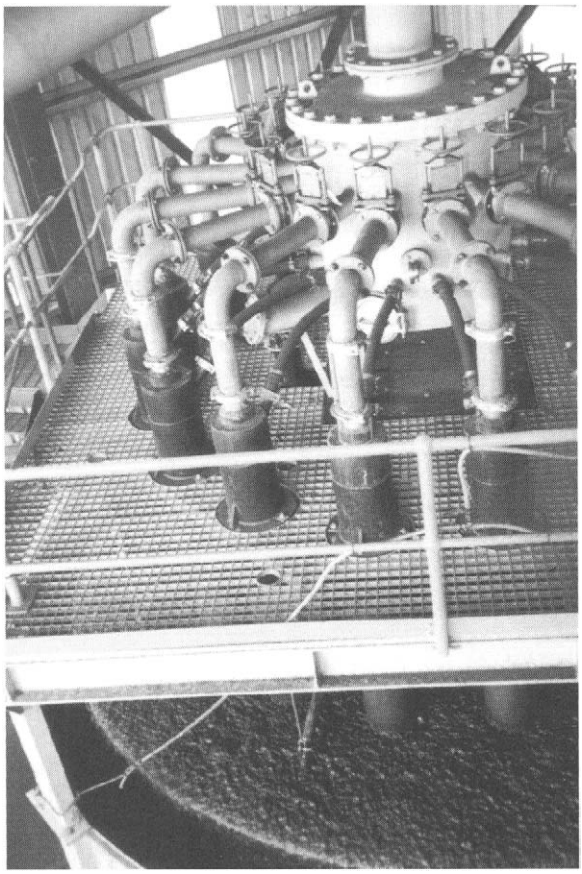


Figure 12.40 A Jameson cell in coal flotation, showing the downcomers and the clean coal concentrate being produced (Courtesy JKMRC and JKTech Pty Ltd)

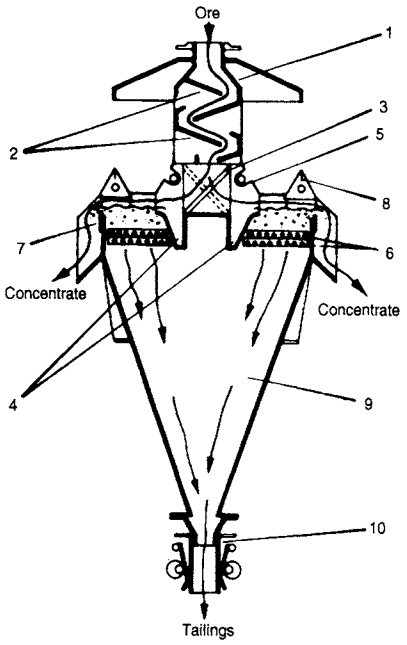


Figure 12.41 Froth separator

other machines were manufactured, however, and were comprehensively reviewed by Harris (1976) and Young (1982).

As described above, in the 1990s and 2000s flotation cell suppliers developed the tank cell designs (Figures 12.20(b), 12.44). These cells are currently 150 m^3 in volume but bigger cells are on the drawing boards (Weber et al., 2005). The cells are circular in shape, fitted with froth crowders, multiple froth launders and discharge and designed with effective level control systems.

In the 1970s most of the flotation machines were of the "open flow" type, as they were much better suited to high throughputs and are easier to maintain than cell-to-cell types. The Denver "Sub-A" was perhaps the most well-known cell-to-cell machine, having been used widely in the past in small plants, and in multi-stage cleaning circuits, where the pumping action of the impellers permitted the transfer of intermediate flowed without external pumps. They were manufactured with cell sizes of up to 14.2 m^3, and were used mostly as coal-cleaning devices, where the users reported a significant improvement in selectivity over open-flow designs.

The flotation mechanism is suspended in an individual square cell separated from the adjoining cell by an adjustable weir (Figure 12.45). A feed pipe conducts the flow of pulp from the weir of the preceding cell to the mechanism of the next cell, the flow being aided by the suction action of the impeller. The positive suction created by the impeller draws air down the hollow stand-pipe surrounding the shaft. This air stream is sheared into fine bubbles by the impeller action and is intimately mixed with the pulp which is drawn into the cell onto the rotating impeller. Directly above the impeller is a stationary hood, which prevented "sanding-up" of the impeller if the machine is shut down. Attached to this hood are four baffle vanes, which extend almost to the corners of the cell. These prevented agitation and swirling of the pulp above the impeller, thus producing a quiescent zone where bubbles can ascend with their mineral load without being subjected to scouring



Figure 12.42 Mechanical flotation cells

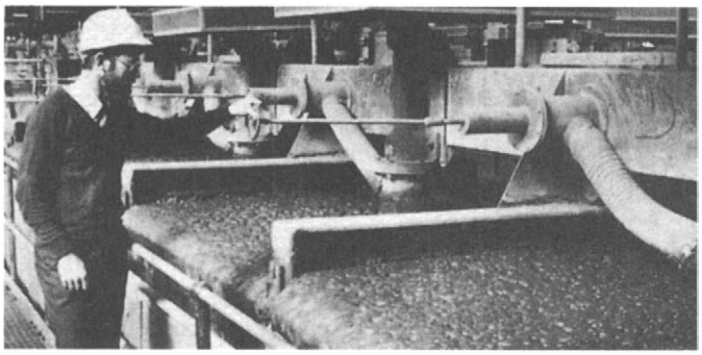


Figure 12.43 14.2 m^3 Denver D–R flotation cells

which may cause them to drop it. The mineral-laden bubbles separate from the gangue in this zone and pass upward to form a froth. As the bubbles move to the pulp level, they are carried forward to the overflow lip by the crowding action of succeeding bubbles, and quick removal of froth is accomplished by froth paddles which aid the overflow.

Pulp from the cell flowed over the adjustable tailings weir, and was drawn on to the impeller of the next cell where it was again subjected to intense agitation and aeration. Particles which are too heavy to flow over the tailings weir are by-passed through sand relief ports, which prevented the build-up of coarse material in the cell.

The amount of air introduced into the pulp depends upon the impeller speed, which is normally in the range of 7–10 ms^{-1} peripheral. More air may be obtained by increasing the impeller speed, but this may in certain circumstances overagitate the pulp as well as increase impeller wear and energy consumption. In such cases, supercharging may be applied by introducing additional air down the stand-pipe by means of an external blower.

Supercharging is required with the Denver D–R machine (Figures 12.43 and 12.46), which ranges in



Figure 12.44 160 m^3 Outokumpu tank cell (Courtesy JKMRC and JKTech Pty Ltd)

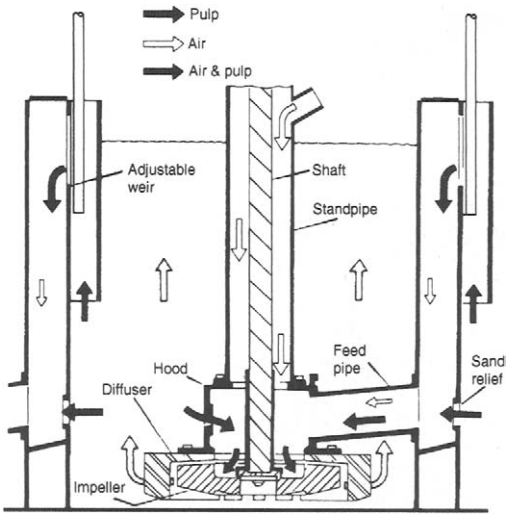


Figure 12.45 Denver sub-aeration cell

size from 2.8 m^3 to 36.1 m^3, and which was developed as a result of the need for a machine to handle larger tonnages in bulk-flotation circuits. These units are characterised by the absence of intermediate partitions and weirs between cells. Individual cell feed pipes have been eliminated, and pulp is free to flow through the machine without interference. The pulp level is controlled by a single tailings weir at the end of the trough. Flotation efficiency is high, operation is simple, and the need for operator attention is minimised. Most high-tonnage plants use a free-flow type of flotation machine and many are equipped with automatic control of pulp level and other variable factors.

A widely used flotation machine is the Wemco Fagergren (Figures 12.47 and 12.48) manufactured in sizes up to 85 m^3. The modern 1 + 1 design consists of a rotor-disperser assembly, rather than an impeller, and the unit usually comprises a long rectangular trough, divided into sections, each containing a rotor-disperser assembly. The feed enters below the first partition, and tails go over partitions from one section to the next, the pulp level being adjusted at the end tailings weir.

Pulp passing through each cell, or compartment, is drawn upwards into the rotor by the suction created by the rotation. The rotor also draws air down the standpipe, no external blower being needed. The air is thoroughly mixed with the pulp before being broken into small, firm bubbles by the disperser, a stationary, ribbed, perforated band encompassing the rotor, by abruptly diverting the whirling motion of the pulp.

Perhaps the most well known of the supercharged machines is the Galigher Agitair (Sorensen, 1982) (Figure 12.49). This system, again, offers a straight-line flow of pulp through a suitably proportioned row of cells, flow being produced by a gravity head. The Agitair machine is often used in large-capacity plants. In each compartment, which may be up to 42.5 m^3 in volume, is a separate impeller rotating in a stationary baffle system. Air is blown into the pulp through the hollow standpipe surrounding the impeller shaft, and is sheared into fine bubbles, the volume of air being controlled separately for each compartment. Pulp depth is controlled by means of weir bars or dart valves at the discharge end of the bank, while the depth of froth in each cell can be controlled by varying the number and size of froth weir bars provided for each cell. Agitair machines produce copious froths and have found favour in mills handling ores of poor floatability, which require large froth columns to help weakly aerophilic particles to overflow.

The Wemco cell has also experienced significant design change in the late 1990s and 2000s. The cell still uses the same rotor design as the Wemco Fagergren cell but the rotor is now inside a new Smart Cell tank design (Figures 12.50 and 12.51).

Outokumpu Oy has operated several base metal mines and concentrators in Finland and elsewhere, and is well known for its mineral processing equipment including its range of OK flotation cells.

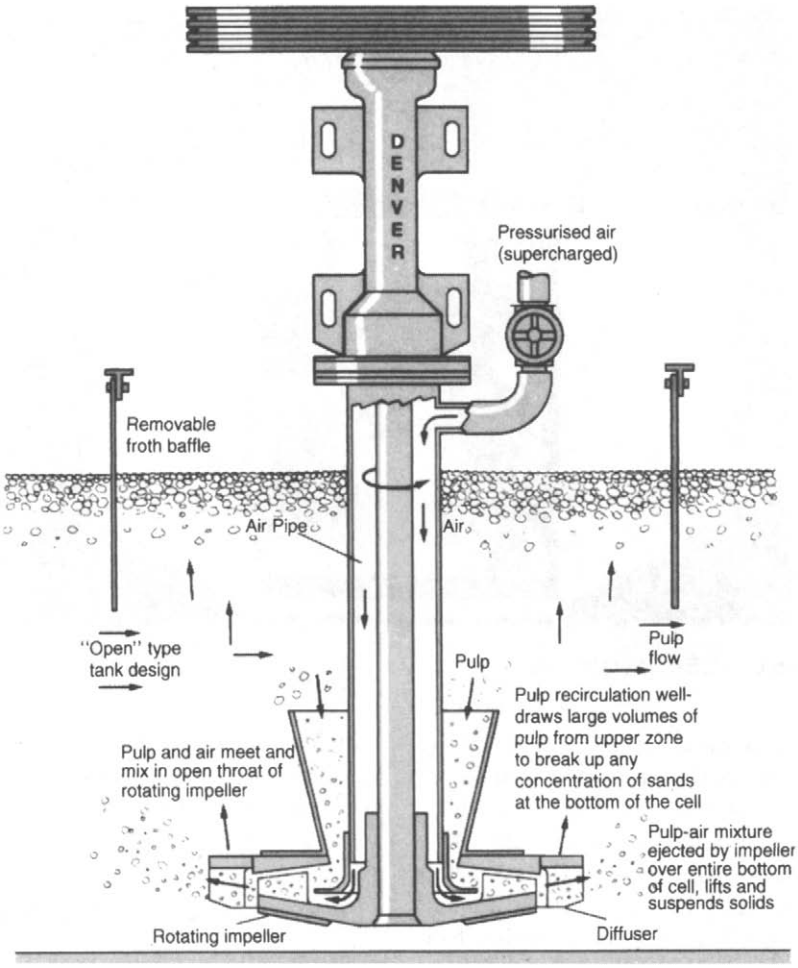


Figure 12.46 Denver D–R flotation machine

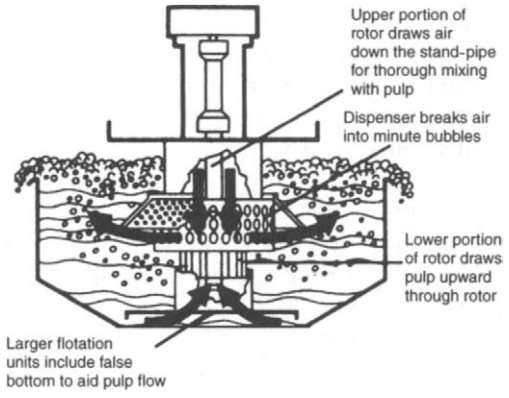


Figure 12.47 Wemco Fagergren cell

The OK impeller differs markedly from that of most other machines. It consists of a number of vertical slots which taper downwards, the top of the impeller being closed by a horizontal disc (Figure 12.52). As it rotates, slurry is accelerated in the slots and expelled near the point of maximum diameter. Air is blown down the shaft and the slurry and air flows are brought into contact with each other in the rotor-stator clearance, the aerated slurry then leaving the mechanism to the surrounding cell volume. The slurry flow is replaced by fresh slurry which enters the slots near their base where the diameter and peripheral speed are less. Thus the impeller acts as a pump, drawing in slurry at the base of the cell, and expelling it outwards. The tank cell design and the rotor design minimise short-circuiting, as pulp flow is towards the bottom of the

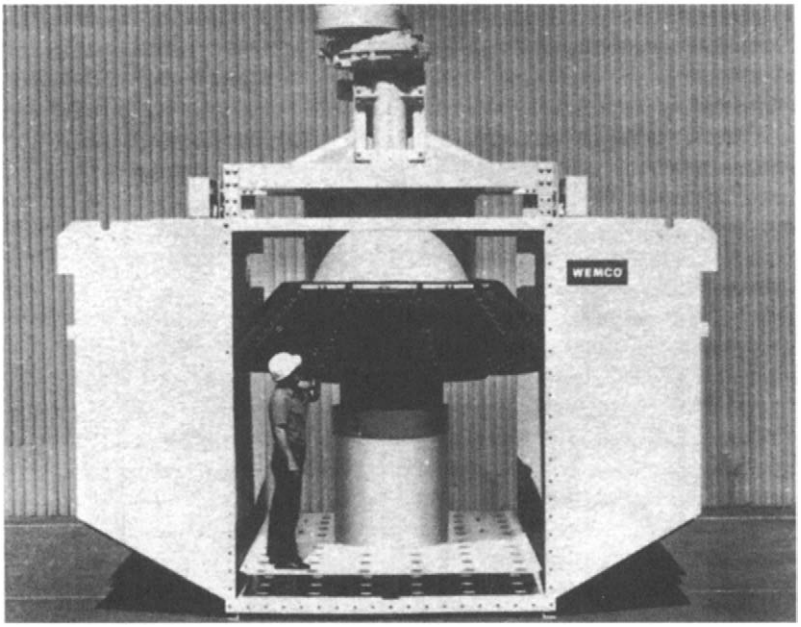


Figure 12.48 Wemco 42.5 m^3 flotation cell

cell and the new feed entering is directed towards the mechanism due to the suction action of the rotor. It is because of this that banks containing only two large cells are now in use in many of the world's concentrators (Niitti and Tarvainen, 1982).

The Sala AS series of flotation cells, ranging in size from 1.2 to 44 m^3, differs in design from the machines previously described. Most machines are designed to promote ideal mixing conditions, the vertical flows achieved maintaining solids in suspension. The Sala design (Figure 12.53) minimises vertical circulation, the manufacturers claiming that the natural stratification in the slurry is beneficial to the process. The impeller is positioned under a stationary hood which extends out to, and supports, the stationary diffuser. The impeller is a flat disc with vertical radial blades on both surfaces, the upper blades expelling air which is blown down the standpipe, and the lower blades expelling slurry from the central base area of the tank, all slurry flowing into the impeller being from below. The aerated slurry is then expelled through the conventional circular stator. Although the impeller has an unusually large diameter in relation to the rather shallow cell size, this preventing sanding in the corners, it is claimed that the air is dispersed into very closely sized fine bubbles, which are particularly suited to fines flotation. The machines are used to treat a variety of materials, including base metals, iron ore, coal, and non-metallic minerals.

Comparison of flotation machines

Selection of a particular type of flotation machine for a given circuit is usually the subject of great debate and controversy (Araujo et al., 2005; Lelinski et al., 2005).

The main criteria in assessing cell performance are:

(1) metallurgical performance, i.e. product recovery and grade
(2) capacity in tonnes treated per unit volume
(3) economics, e.g. initial costs, operating and maintenance costs.

In addition to the above factors, less tangible factors, such as the ease of operation and previous experience of personnel with the equipment, may contribute.

Direct comparison of cells is by no means a simple matter. Although comparison of different cell types, such as mechanical against pneumatic, should be based on metallurgical performance

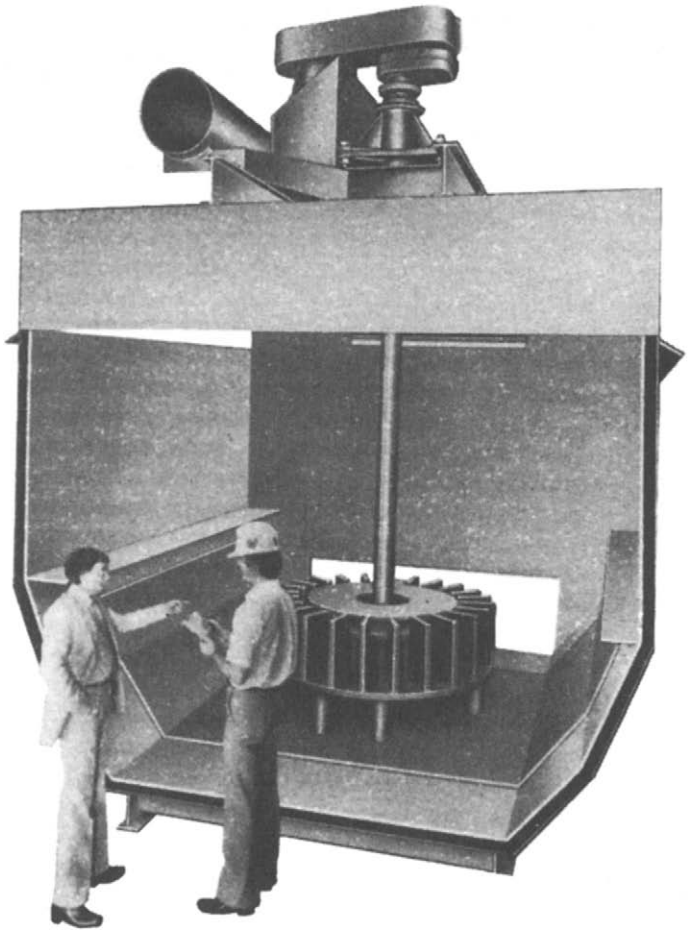


Figure 12.49 42.5 m^3 Agitair flotation machine

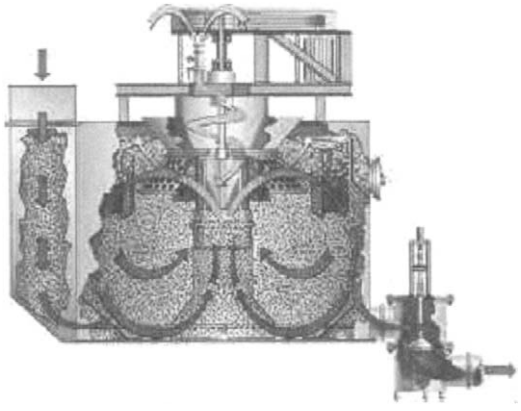


Figure 12.50 Wemco Smart Cell features

when testing the same pulp in parallel streams, even here results are suspect; much depends on the operator's skill and prejudices, as an operator trained on one type of cell will prefer it to others.

In general, the differences between mechanical machines are small and selection depends a lot on personal preference. One of the basic problems that hampers comparison of flotation cells is that a cell is required to perform more than a selective collection operation; it is required to deliver the collected solids to a concentrate product with minimal entrainment of pulp. The observed rate of recovery from a cell can be dependent on the froth-removal rate, which in turn can be affected by such process variables as reagent additions, impeller speed, position of the pulp-froth interface and aeration. Research has shown that bubble size

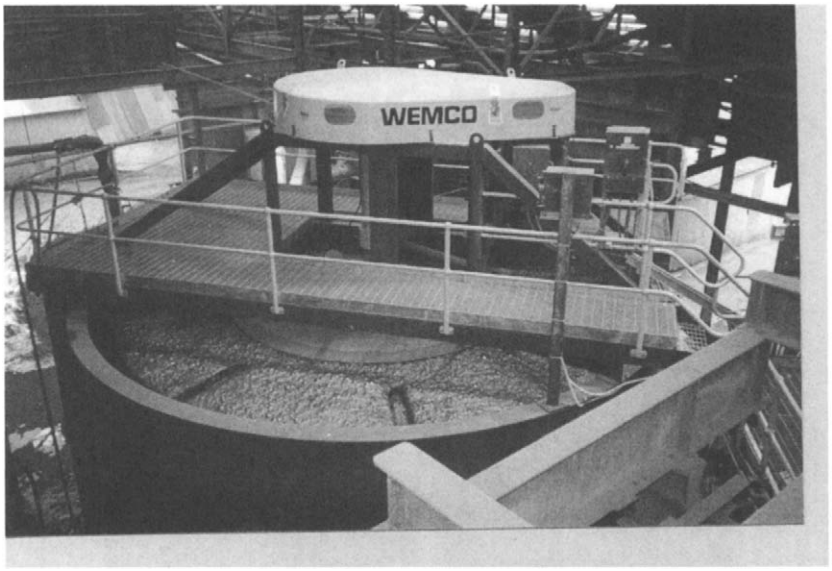


Figure 12.51 Wemco Smart Cell showing radial launders (Courtesy Outokumou Technology Minerals Oy)

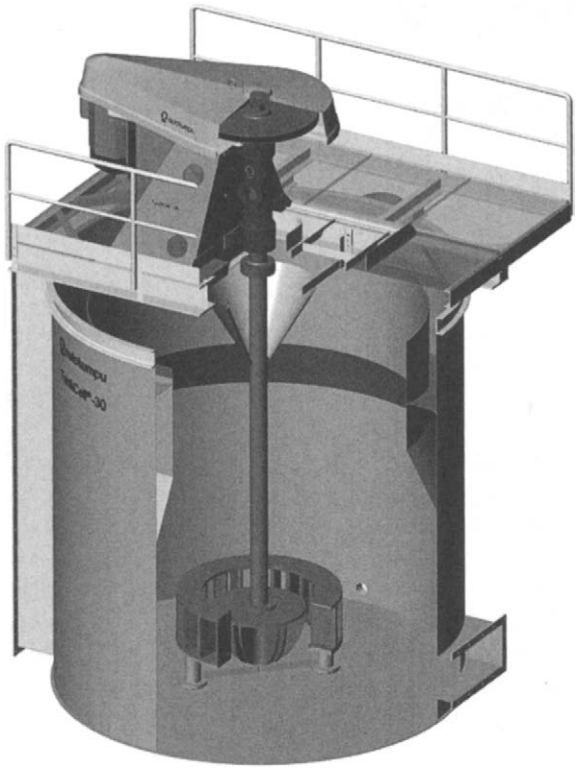


Figure 12.52 Outokumpu flotation cell showing the rotor assembly (Courtesy Outokumou Technology Minerals Oy)

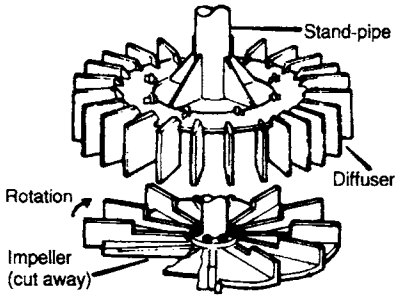


Figure 12.53 Sala flotation mechanism

in mechanical machines of all designs is between 0.1 and 1 mm, the size being controlled mainly by the frother. The machine stator does not change the bubble size, but only the flow pattern in the cell (Harris, 1976). Machine suppliers recommend impeller speeds that allow the machine to maintain the particles in suspension and disperse the bubbles throughout the cell.

Mechanical and conventional pneumatic machines have been used for many decades, whereas froth separators and columns are fairly recent developments. Mechanical machines have been the dominant type, pneumatic machines, apart from the Davcra, now rarely being seen, except in a few old concentrators. Columns now have a role in flotation but froth separators have, as yet, to gain wide acceptance.

Although there is very little information on pneumatic machines, Arbiter and Harris (1962) reported comparative tests on a number of mechanical and pneumatic cells showing the former to be generally superior. Gaudin (1957) suggested that mechanical machines are better suited to difficult separations, particularly where fines are present. The impellers tend to have a scouring effect which removes slimes from particle surfaces. An American survey of flotation columns was reported by Clingan and McGregor (1987). All the production columns surveyed were in use as cleaners or scavengers. All operators indicated that improved metallurgical performance was part of their justification for using flotation columns and most indicated operating-cost savings and ease of operation.

An analysis of the effectiveness of the various types of flotation machine has been made by Young (1982), who discusses machine performance with regard to the basic objectives of flotation, which are the recovery of the hydrophobic species into the froth product, and, at the same time, achieving a high selectivity by retaining as much of the hydrophilic species as possible in the slurry. Achievement of recovery is dependent on the mechanism of particle–bubble attachment, which may be by "coursing bubble" contact between an ascending bubble and a falling particle, by precipitation of dissolved gas onto a particle surface, or by contact between a particle and an unstable "nascent" bubble in a pressure gradient. Coursing bubble attachment requires non-turbulent conditions, which is not found in mechanical or Davcra cells. A mechanical impeller can be compared to a turbine operating in a cavitating mode, air bubbles forming on the trailing, low pressure side of the impeller blades, while slurry flows are concentrated mainly upon the leading, high pressure side. The air and slurry flows are therefore separated to some extent, and the possibility of air precipitation on particles and for contact between particles and nascent bubbles is low. Mechanical impellers, therefore, do not appear to be the ideal device for particle–bubble contact, and the nozzle in the Davcra cell would appear to be much more efficient, which may explain why the Davcra cell can give the same recovery as a short bank of mechanical cells.

The particle–bubble contact in column machines is by coursing bubble only, and these are ideal displacement machines, whereas the mechanical cells are ideal mixers. The more favourable conditions for particle–bubble attachment, together with a lower tendency to break established bonds, may account for the high recoveries reported from flotation columns.

As selectivity is reduced by slurry turbulence, it is clear that the column machines, which also improve selectivity by froth washing, have an advantage over the mechanical machines. The froth separators, however, are not well suited to achieving selectivity from fine feeds, as the fine hydrophilic particles must descend through the total froth bed to report to the tailings, and this is difficult to achieve.

As Young concludes, mechanical flotation machines dominate the Western industry, but the reasons for this may be more due to commercial realities than to design excellence. The major Western manufacturers make only this type, and many flotation engineers are familiar with no other. However, in the future, the mechanical machines will no doubt encounter the increasing challenge of other types, and there is no reason why a number of different units could not be installed in concentrators for specific duties.

Electroflotation

Industrial flotation is rarely applied to particles below 10 μm in size due to lack of control of air bubble size. With ultra-fine particles, extremely fine bubbles must be generated to improve attachment. Such bubbles can be generated by in situ electrolysis in a modified flotation cell. Electroflotation has been used for some time in waste-treatment applications to float solids from suspensions. Direct current is passed through the pulp within the cell by two electrodes, generating a stream of hydrogen and oxygen bubbles. Considerable work has been done on factors affecting the bubble size on detachment from the electrodes, such as electrode potential, pH, surface tension and contact angle of the bubble on the electrode. On detachment, the majority of bubbles are in the 10–60 μm range, and bubble density can be controlled by current density to yield optimum distribution of ultra-fine bubbles as well as adequate froth control. Conventional flotation processes produce bubbles ranging from 0.6 to 1 mm in diameter and there is considerable variation in bubble size.

Some other factors have also been noted in addition to the fine bubbles. For example, the flotation of cassiterite is improved when electrolytic hydrogen is used for flotation. This may be due to nascent hydrogen reducing the surface of the cassiterite to tin, allowing the bubbles to attach themselves.

Although the main applications of electroflotation are in sewage treatment, this technique is capable of selectively floating solids and has been used in the food industry. It may have a future role in the treatment of fine mineral particles (Venkatachalam, 1992).

Agglomeration-skin flotation

In agglomeration flotation, the hydrophobic mineral particles are loosely bonded with relatively smaller air bubbles to form agglomerates, which are denser than water but less dense than the particles wetted by the water. Separation of the agglomerated particles is achieved by flowing film gravity concentration. When the agglomerates reach a free water surface, they are replaced by skin-floating individual particles. In skin-flotation, surface tension forces result in the flotation of the hydrophobic particles, while the hydrophilic particles sink, effecting a separation.

In *table flotation*, the reagentised particles are fed onto a wet shaking table. The pulp is diluted to 30–35% solids and is aerated by air jets from a series of drilled pipes arranged above the deck, at right-angles to the riffles, in such a way that the holes are immediately above the material carried by the riffles. The hydrophobic particles form aggregates with the air bubbles and float to the water surface, from where they skin-float to the normal "tailings" side of the table. The wetted particles become caught in the riffles and discharge at the end of the table where the concentrate normally reports in most shaking table gravity-separation processes.

With table flotation, and other agglomeration processes, it is desirable to film and float the most abundant mineral, if possible, as the capacity of the table is limited to the amount of material that can be carried along the riffles. This is the reverse of the ideal conditions for froth flotation, where it is desirable to film and float the mineral that is least abundant, so as to reduce entrainment of unwanted material to the minimum. This difference renders table flotation most suitable for removing sulphide minerals from pyritic tin ore concentrate, or for the concentration of non-metallic minerals, such as fluorite, barite, and phosphate rock. Such minerals are often liberated at sizes too coarse for conventional flotation. Agglomeration separations are possible over a wide range of sizes, usually from a maximum of about 1.5 mm in diameter to 150 μm. Minerals with low specific gravities, such as fluorite, have been separated at sizes of up to 3 mm.

Table flotation was used until relatively recently in the treatment of coarse phosphate rock, but has been replaced by similar methods utilising pinched sluices and spirals as the flowing film devices (Moudgil and Barnett, 1979).

Flotation plant practice

The ore and pulp preparation

It is inevitable that there will be changes in the character of the ore being fed to a flotation circuit. There should therefore be means available for both observing and adjusting for such changes. Variation in the crystal structure and intergrowth may have an important effect on liberation and optimum grind size. Change in the proportion of associated minerals is a very common occurrence and one which may be largely overcome by blending the ore both before and after crushing has been completed. When the feed is high grade it is relatively easy to produce a highly mineralised froth and high-grade concentrate; when it is low grade it is harder to maintain a stable froth and it may be necessary to switch one of the final cleaning cells to a lower-grade section if cells and launders have suitable flexibility.

Fluctuation in the nature and proportion of minerals in the run-of-mine ore inevitably occurs when ores are drawn from more than one location, and the variation observed may be further accentuated by partial oxidation of the ore. This may occur from geological changes or from delayed transportation of broken ore from the stope in the mine to the processing plant. Oxidation also commonly occurs as a result of overlong storage in stockpiles or ore-bins and therefore it is necessary to determine how prone a particular ore is to oxidation and to ensure that the holding time is kept well below a

critical level. Oxidised ores are softened by lattice decomposition and become more inert to collector reagents and more prone to overgrinding.

Wet grinding is the most important factor contributing to the performance of the flotation circuit. It is therefore of vital importance that the grinding circuit shall provide a reliable means of control as a guarantee that the milled product will allow maximum liberation of the values. In the comminution section of the plant, poor operation in the crushing stage can be offset in grinding. There is, however, no way of offsetting poor grinding practice and it is wise to use experienced operators on this section.

The degree of grinding required is determined by testwork and removal of free mineral at the coarsest possible size is always desirable. Modern flotation takes this into account, as is evidenced by the general trend towards floating the mineral in stages: first coarse, then fine. The advantages of floating a mineral as coarse as possible include:

- lower grinding costs;
- increased recovery due to decreased slime losses;
- fewer overground particles;
- increased metallurgical efficiency;
- less flotation equipment;
- increased efficiency in thickening and filtration stages.

Laboratory control of grinding must be carried out on a routine basis, by screening and assaying the tailings in order to determine the losses in each size fraction and the reason for their occurrence. It is often found that the largest losses occur in the coarsest particles, due to inadequate liberation, and if grinding all the ore to a finer size improves recovery economically then it should be done. Often the losses occur in the very fine "sub-sieve" fractions, due to overgrinding of heavy mineral values. In this case it may be necessary to "scalp" the grinding circuit and remove heavy minerals, which are returned to the mill by the classifier at sizes below optimum grind. This can be done by adding flotation reagents to the mill discharge and removing fine liberated minerals by a unit flotation cell between this and the classifier (Figure 12.54). Apart from the advantages of reducing overgrinding, the density of the mill discharge can be controlled so as to give optimum flotation efficiency. In conventional circuits the mill discharge density is controlled according to the cyclone requirements, the cyclone overflows often requiring dewatering before feeding flotation.

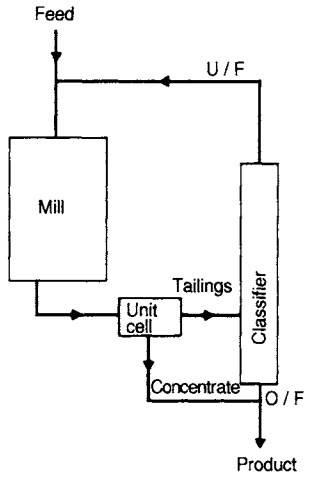


Figure 12.54 Removal of fine heavy minerals from the grinding circuit by unit flotation cell

Flotation within the grinding circuit, particularly of heavy, coarse lead minerals, is performed at several concentrators and the aim of Outokumpu's *flash flotation* method is to recover such coarse valuable minerals which would normally be recycled to the grinding circuit via classification (Warder and McQuie, 2005). The concentrate produced is final concentrate, needing no further cleaning, and is produced in a specially designed flotation machine, *Skim-air*, which removes the coarse floatable particles while allowing the others to return to the mill for further grinding, thus reducing the amount of valuable mineral lost to fines and increasing the average particle size of the final concentrate. A number of these cells have been installed in Finnish concentrators, with considerable benefits (Anon., 1986b).

As was shown earlier, if the mineral is readily floatable, and is associated with a relatively non-floatable gangue, it may be more economical to produce a coarse final tailings and regrind the resulting low-grade rougher concentrate, which may then be considered almost as a middlings product (Figure 12.29). The secondary, or regrind operation, treating only a small percentage of the original fine ore feed, can therefore be carried out

to a size fine enough to liberate. Subsequent flotation then produces the maximum recovery/grade results in the greatest economic return per tonne of ore milled. There is, of course, an upper limit on size at which flotation may be practised effectively, due to the physical limitations of the bubble in lifting coarse particles. Whilst it may be argued that factors such as shape, density, and aerophilic properties may be influential, the practical upper limit rarely exceeds 0.5 mm and is usually below 0.3 mm. For a wide variety of minerals, reagents, and flotation machines, recovery is greatest for particles in the size range 100–10 μm (Trahar and Warren, 1976; Trahar, 1981). Below about 10 μm recovery falls steadily. There is no evidence of a critical size below which particles become unfloatable. The reason for the difficulties experienced in selective flotation of fine particles is not fully understood and varies from ore to ore. Very fine particles have relatively high surface area in relation to mass and tend to oxidise readily, or be coated with slimes before reaching the conditioning section, which makes collector adsorption difficult. Particles of low mass tend to be repelled by the slip-stream which surrounds a fast-moving air bubble, and should therefore be offered small, slow-moving bubbles. On the other hand, if small particles are in suspension near the froth column, they tend to overflow with the froth column regardless of their composition, as the downward pull of gravity is offset by the upward force due to the drift of the bubbles. Fine hydrophilic particles can also be mechanically entrained in the interstices between bubbles or be entrained in the water overflowing with the froth (Kirjavainen and Laapas, 1988). Such entrainment can be reduced by froth washing (Kaya and Laplante, 1991), as is performed in flotation columns.

When the ore value is low, the *slimes* (the ultrafine fraction which may be detrimental to flotation) are often removed from the granular fraction by passing the feed through de-sliming cyclones, and discarding the overflow. Alternatively, de-sliming can be carried out between flotation stages; for instance, rougher flotation may be followed by a de-sliming operation, which improves recovery in the scavenging stage. If the slimes contain substantial values, they are sometimes treated separately, thus increasing overall recovery.

Figure 12.55 shows the flowsheet used by the White Pine Copper Co. of Michigan, USA, to treat an ore consisting of chalcocite and native copper finely disseminated in a shale gangue (Tveter and McQuiston, 1962). Rapid flotation of the fine chalcocite and native copper is followed by de-sliming of the primary flotation tailings. Elimination of these gangue slimes accelerates recovery of the middlings in the scavenging stage.

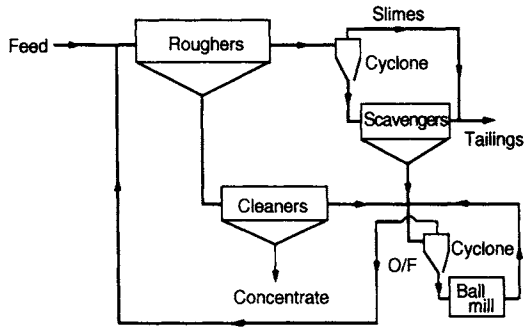


Figure 12.55 White Pine Copper Co. flotation circuit

Kaolin clay has been beneficiated for many years by *carrier flotation*, in which −60 μm particles of calcite are added to the system with oleic acid as collector. During conditioning, the fine anatase particles in the raw clay coat the coarse calcite particles and are separated from the clay when the calcite is recovered by flotation (Sivamohan, 1990). Fuerstenau et al. (1991) have demonstrated that carrier flotation can be carried out autogenously i.e. using the same mineral, and a hematite ore has been classified into a coarse and a fine fraction, the coarse hematite particles being used as carrier particles for the fine hematite. This phenomenon is an important type of shear flocculation (see Chapter 1), and has been used successfully in a number of mines in China, for the flotation of hematite, copper oxides, lead–zinc slimes, and tin slimes. In all cases concentrate is returned to the slimes feed, the coarser particles acting not only as carriers, but also promoting aggregation of the fines (Wang et al., 1988). Fuerstenau (1988) has argued that the consideration of such *multi-feed* circuits is expected to become an integral part of circuit selection for the separation of refractory ores.

The operating density of the pulp is determined by testwork, and is influenced by the mean size of particles within the feed. Coarse particles will

settle in a flotation cell at a relatively rapid rate, which may be substantially reduced by increasing the volume of particles in the pulp. As a general rule higher density pulps are applied to coarser sizes. In treating heavy sulphide ores, low-grade rougher concentrates are obtained from pulps of between 30 and 50% solids, whilst reground cleaner concentrates are obtained from pulps of between 10 and 30% solids.

Reagents and conditioning

Each ore is a unique problem and reagent requirements must be carefully determined by testwork, although it may be possible to obtain guidelines for reagent selection from examples of similar operations. An enormous amount of experience and information is freely available from reagent manufacturers. One vital requirement of a collector or frother is that it becomes totally emulsified prior to usage. Suitable emulsifiers must be used if this condition is not apparent.

Selection of reagents must be followed by careful consideration of the points of addition in the circuit. It is essential that reagents are fed smoothly and uniformly to the pulp, which requires close control of reagent feeding and on the pulp flow rate. Frothers are always added last when possible; since they do not react chemically they only require dispersion in the pulp, and long conditioning times are unnecessary. Adding frothers early tends to produce a mineralised froth floating on the surface of the pulp during the conditioning stage. This is due to entrained air, which can cause uneven distribution of the collector.

In flotation, the amount of agitation and consequent dispersion are closely associated with the time required for physical and chemical reactions to take place. Conditioning prior to flotation is now considered standard practice and is an important factor in decreasing flotation time. This is perhaps the most economical way of increasing the capacity of a flotation circuit. The minerals are converted to a readily floatable form as a result of ideal conditioning, and therefore a greater volume can be treated. Although it is possible to condition in a flotation machine, it is generally not economical to do so, although it is currently common practice for stage addition to include booster dosage of collector into cell banks, particularly at the transition from rougher to scavenger collection. Machines in the flow-line are often used as conditioners. Agitators are often interposed between the grinding mills and the flotation circuit to smooth out surges in grade and flow rate from the mills. Reagents are often added to these storage reservoirs for conditioning. Alternatively, reagents may be added to the grinding circuit in order to ensure optimum dispersion. The ball mill is a good conditioner and is often used when the collectors are oily and need emulsifying and long conditioning times. The advantage of conditioning in the mill is that the collector is present at the time that new surface is being formed, before oxidation can take place. The disadvantage is that reagent rate control is difficult, as the feed to the mill may have continual minor grade fluctuations, and the mill may have a high circulating load, which can become overconditioned. Where very close control of conditioning time is essential such as in the selective flotation of complex ores, special conditioning tanks are incorporated into the flow-line (Figure 12.56). The pulp and reagent are fed down the open stand-pipe and fall on to the propeller, which forces the mixture downwards and outwards. The outlet at the side of the tank can be adjusted to give a height sufficient to give the pulp its desired residence time within the tank.

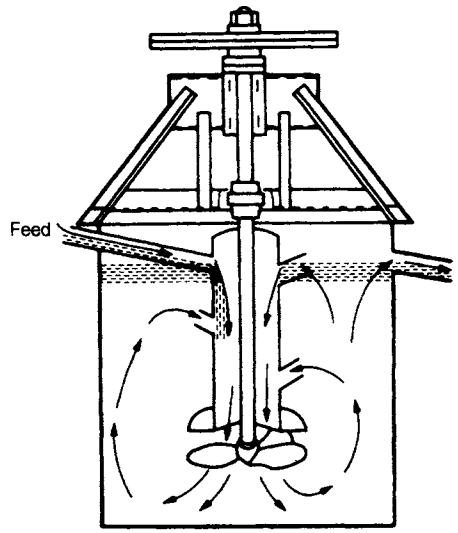


Figure 12.56 Denver conditioning tank

Stage addition of reagents often yields higher recoveries at substantially lower cost than if all reagents are added at the same point in the circuit

prior to flotation. The first 75% of the values is normally readily floatable, providing optimum grind size is achieved. The remaining values may well be largely composite in nature and will therefore require more careful reagent conditioning, but perhaps 15% are sufficiently large or sufficiently rich in value to be recovered relatively easily. The remaining 10% can potentially affect the whole economic balance of the process, being both fine in size and low in values. Because this fraction is such a critical one it must be examined extremely carefully and regularly, and reagent addition must be carefully and quickly controlled.

When feasible to do so, it is usually more desirable to float in an alkaline or neutral circuit. Acid circuits usually require specially constructed equipment to withstand corrosion. It is a common finding that the effectiveness of a separation may occur within very narrow pH limits, in which case the key to success for the whole process lies in the pH control system. In selective flotation where more than one mineral is concentrated, the separation pH may well vary from one stage to the next. This, of course, makes it vitally important to regulate reagents to bring about these conditions and control them accurately.

The first stage of pH control is often undertaken by adding dry lime to the fine ore-bins, which tend to reduce oxidation of sulphide mineral surfaces. Final close pH control may be carried out on the classifier overflow, by the addition of lime as a slurry. The slurry is usually taken from a ring main, as lime settles out quickly if not kept moving, and forms a hard cement within the pipelines.

Solid flotation reagents can be fed by rotating disc, vibro, and belt feeders, but more commonly reagents are added in liquid form. Insoluble liquids such as pine oil are often fed at full strength, whereas water-soluble reagents are made up to fixed solution strengths, normally about 10%, before addition. Reagent mixing is performed on day shifts in most mills, under close supervision, to produce a 24 h supply. The aqueous reagents are usually pumped through ring mains, from where they are drawn off to feeders as required.

Modern flotation plants typically add reagents via either positive displacement metering pumps or automatically controlled valves, where reagents are added in frequent short busts from a ring main or manifold. With the increased complexity of measurement and control these methods allow online reagent addition rates to be relayed to either remote monitors or computers within control rooms. For small quantities, peristaltic pumps can be used, where rollers squeeze a carrier tube seated in a curved track, thus displacing the reagent along the tube. In a number of older flotation plants reagents are still added via Clarkson feeders, which use small cups on a rotating wheel, and through flow rotameters.

Small amounts of frother can be injected directly into the pipeline carrying the flotation feed, by positive-displacement piston metering pumps.

Control of flotation plants

Automatic control is increasingly being used, the control strategies being almost as numerous as the number of plants involved. The key to effective control is online chemical analysis (Chapter 3), which produces real-time analysis of the metal composition of process streams. Control strategies are implemented in distributed control systems (DCS) or programmable logic controllers (PLC) and there are many vendor-supplied solutions.

However, although there are many reports of successful applications, in reality few if any plants can claim to be *fully* automatic in the sense of operating unattended overextended periods, despite the availability of robust instrumentation, a wide range of control algorithms, and powerful computing assets. McKee (1991) has reviewed some of the reasons. The main problems have been in first successfully stabilizing a complex process, and then developing process models which will define set-points and limits to accommodate changes in ore type, mineralogy, texture, chemical composition of the mine water, and contamination of the feed. Control systems have also been unsuccessful in some cases due to inadequate maintenance of instrumentation. It is essential, for instance, that pH probes are kept clean, and that all online instrumentation is regularly serviced and calibrated. Implementation of control strategies at the plant design stage have rarely been successful as the most significant control variables are often not identified until experience of the plant has been gained. Only then can control strategies based on these variables, and with specific objectives, be successfully attempted. Another limitation is the training of plant operating and metallurgical staff in the principles and

application of control, and the shortage of control engineers needed to keep control systems running. The most successful systems have been those which allow the control room operator to interact with the plant control system when necessary to adjust set-points and limits. In this respect it is doubtful whether automatic control can achieve better metallurgical efficiency than experienced, conscientious operators in the short term. Its great advantage, however, is that the DCS is constantly vigilant, not being affected by shift changeovers, tea breaks, and other interruptions which affect the human operator.

A flotation control system consists of various subsystems, some of which may be manually controlled, while others may have computer-controlled loops, but all contributing to the overall control objective (Paakkinen and Cooper, 1979; Lynch et al., 1981). The aim should be to improve the metallurgical efficiency, i.e. to produce the best possible grade–recovery curve, and to stabilise the process at the concentrate grade which will produce the most economic return from the throughput (Figure 12.57), despite disturbances entering the circuit. This has not, as yet, been achieved by automatic control alone.

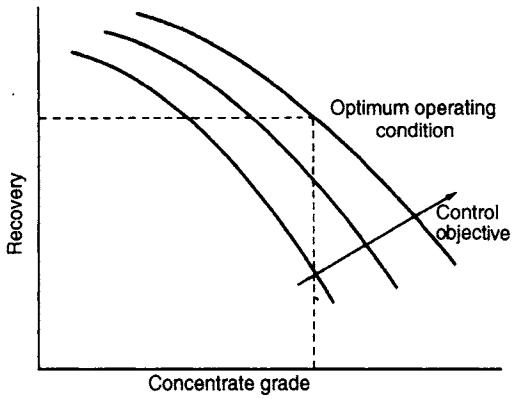


Figure 12.57 Flotation control objective

Disturbances caused by variations in feed rate, pulp density, and particle size distribution should be minimal if grinding circuit control is effective, such that the prime function of flotation control is to compensate for variations in mineralogy and floatability. The variables which are manipulated, either manually or automatically, to effect this are mass flows, reagent and air addition rates, pulp and froth levels, pH, and circulating loads by the control of cell-splits on selected banks.

Best practice involves getting the basic control objectives established first, such as stabilizing control of pulp and sump levels, air flow, and reagent flows. More advanced stabilizing control can then be attempted, such as pH, reagent ratio control (based on plant input flows and assays), pulp flow, circulating load, concentrate grade, and recovery. Finally, true optimising control can be developed, such as maximum recovery at a target grade. Higher level optimising control is generally not possible until stable operation has been achieved (McKee, 1991).

The key variable to control is pulp level in the cell, because a constant pulp level is very important to ensure stable and efficient flotation performance. The pulp level can be measured by a number of different means. Ultrasonic devices measure the time sound waves take to reach the pulp level, or a "float" resting at the froth/pulp interface. Floats can also be connected to sensing devices which measure how far the float moves as the pulp level changes, either through a vertical motion sensor or a horizontal lever. Conductivity probes register the difference in electrical conductivity between the froth and pulp to determine the pulp level. Differential pressure cells are submerged in the flotation tank and measure the pressure exerted on them by the liquid above. Bubble tubes also determine the pulp level based on pressure of the pulp compressing air within the bubble tube though these are not much used today.

Control of pulp level is effected by dart valves or pinch valves. In older flotation plants movable weirs are also used. In general each bank of cells will have a level detection transducer (usually a float-based device) and the level is then controlled by a simple feed back PI loop which adjusts the valve on the bank tailings outlet based on a set-point either entered by the operator or determined by a higher-level control strategy responding to changes in grade, recovery, froth condition, or other criteria. Feed forward in combination with feed back control is often required to avoid damaging interactions between different flotation banks. Feed forward control is based on feed flow measurement or inference (e.g. from a variable speed pump or preceding level controllers).

Level control can either be simple, as outlined above, or involve more complex interactions (Kampjarvi and Jamsa-Jounela, 2002). "FloatStar™", developed by Mintek in South Africa, is an integrated package providing level control throughout a flotation circuit, plus additional capabilities such as an algorithm to calculate optimum level set-points and/or aeration rates that aim to optimize the residence times, mass pulls, and circulating loads within a flotation circuit (Singh et al., 2003).

Control of slurry pH is a very important requirement in many selective flotation circuits, the control loop often being independent of the others, although in some cases the set-point is varied according to changes in flotation characteristics. For automatic control of lime or acid it is important that time delays in the control loop are minimised, which requires reagent addition as close as possible to the point of pH measurement. Lime is often added to the grinding mills in order to minimise corrosion and to precipitate heavy metal ions from solution. In the circuit shown in Figure 12.58, lime addition is controlled by the ratio of the mass flow to the mill, and the ratio set-point is adjusted by a pH controller which measures pH early in the flotation process with an operator-determined pH set-point. Lags are sufficient to allow sufficient mixing in the mill.

Control of collector addition rate is sometimes performed by feed-forward ratio control based on a linear response to assays or tonnage of valuable metal in the flotation feed. Typically, increase in collector dosage increases mineral recovery until a plateau is reached, beyond which further addition may either have no practical effect, or a slight reduction in recovery may occur. The gangue recovery also increases with collector addition, such that beyond the plateau region selectivity is reduced (Figure 12.59). The operator can intervene to change the ratio set-point or bias to respond to the changing feed conditions.

The most common aim of collector control is to maintain the addition rate at the edge of the plateau, the main difficulty being in identifying the optimum point, especially when the response changes due to changes in ore type, or the interaction with other reagents. For this reason, automatic control using feed-forward loops has rarely been successful in the long term. There are many cases of successful semi-automatic control, however, where the operator adjusts the set-point to accommodate changes in ore type, and the computer controls the reagent addition over fairly narrow limits of feed grade. For example, feed-forward control of copper sulphate activator and xanthate to the zinc roughers has been used in the control strategy at Mattagami Lake Mines, Canada (Konigsman et al., 1976). The reagents are varied in proportion to changes in feed grade according to a simple ratio/bias algorithm, which is a standard algorithm supplied with all DCSs or PLCs:

$$\text{Reagent flow rate} = A + (B \times \%\text{Zn in feed})$$

Where A and B vary for different reagents. The operator may change the base amount A as different

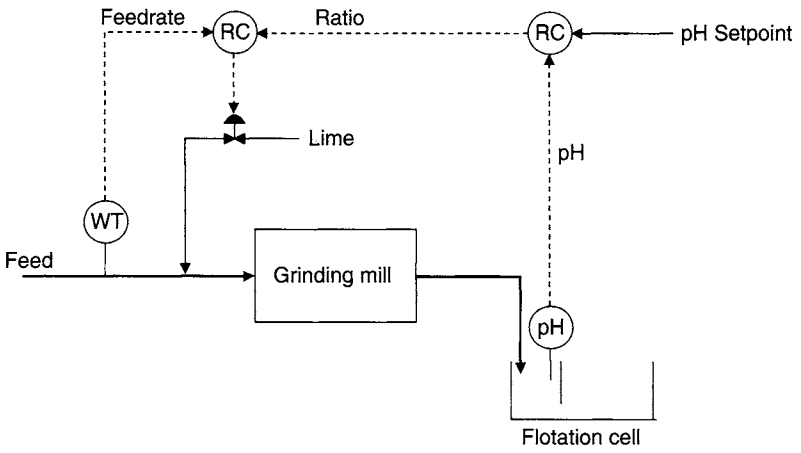


Figure 12.58 Control of pH in a flotation circuit

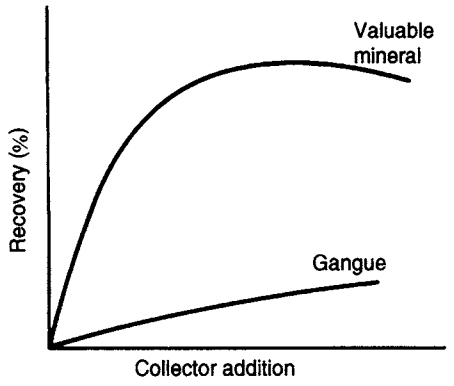


Figure 12.59 Effect of collector addition

ore types are encountered. The logic of the control system is shown in Figure 12.60.

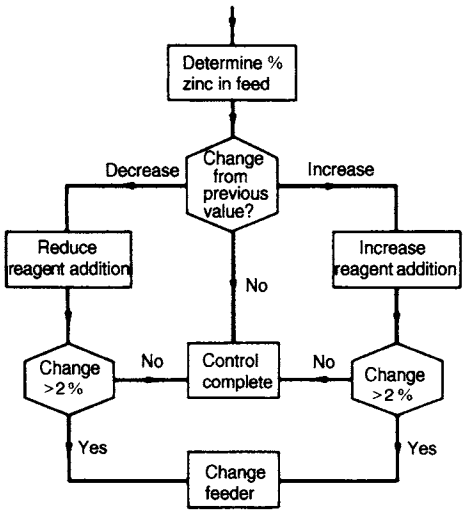


Figure 12.60 Feed-forward control strategy at Mattagami Lake

Although feed-forward ratio control can provide a degree of stability, stabilisation may be more effective using feed-back data. The distance–velocity lag experienced with feed-back loops utilising tailings assays can be overcome to some extent by making use of the fact that the circuit begins to respond to changes in flotation characteristics immediately the ore enters the banks, and this can be detected by measurements in the first few cells. For instance, control of rougher concentrate grade is a useful strategy, as this strongly influences the final cleaner concentrate grade.

At Mount Isa in Australia, feed-forward control of xanthate addition to the copper roughers was unsatisfactory, as the optimum addition rate was not simply related to the mass of copper in the flotation feed (Fewings et al., 1979). The assay of concentrate produced in the first four cells of the bank was combined with the four-cell tailings and feed assays to compute the four-cell recovery. It was found that there was a linear response between this recovery and the collector dosage required to maintain the overall recovery at the edge of the plateau. The control strategy, although fairly successful in the short-term, eventually failed when changes in ore type occurred. Computation of unit process recovery in this way is also subject to error due to inherent inaccuracies of on-stream analysis data (see Example 3.13).

The amount of frother added to the flotation system is an important variable, but automatic control has been unsuccessful in many cases, as the nature of the froth is dependent on only very minor changes in frother addition and is much affected by intangible factors such as contamination of the feed, mine water chemistry, etc. At low addition rates, the froth is unstable and recovery of minerals is low, whereas increasing frother addition rate has a marked effect on the flotation rate, increasing the weight, and reducing the grade of concentrate produced. The usual approach is to manually adjust the frother set-point, or less commonly to ratio the frother to the feed rate of solids and water.

Flow rate of concentrate has been controlled in some systems by regulating the frother addition. The grade is not as sensitive to changes in frother addition, but there may be a good relationship between grade and flow rate. Cascade control can be used, where the concentrate grade controls the concentrate flow rate set-point, which in turn controls the frother addition set-point (Figure 12.61). Stabilising control of conventional column cells, which generally operate with deep froths, is relatively simple (Finch and Dobby, 1989).

Air input to the flotation process and froth depth are parameters which, like frother addition, affect the recovery of minerals into the concentrate, and can be used to control concentrate grade, tailings grade, or mass flow rate of concentrate. Aeration and froth depth do not, however, affect subsequent cleaning operations, as will residual frother

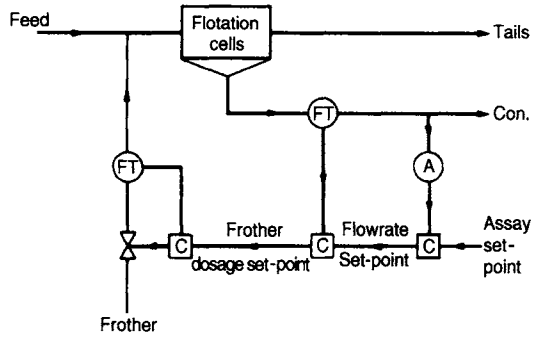


Figure 12.61 Cascade control of frother addition

carried over from the roughers, and they are often used as primary control variables. Flotation generally responds faster to changes in aeration than to changes in froth depth, and because of this aeration is often a more effective control variable, especially where circulating loads have to be controlled. There is obviously interaction between frother addition, aeration and froth depth, and where computer-controlled loops are used it is necessary to control these variables such that only minor changes are made. This can be done by manipulating only one of these variables, maintaining the others constant at predetermined optimum levels unless the conditions deviate outside acceptable limits, which may vary with ore type. At Vihanti in Finland (Figure 12.71), the copper grade of the bulk copper–lead rougher concentrate has been used to control the rate of aeration and frother addition to the roughers and scavengers. Aeration has priority, being the cheaper "reagent" and leaving no residual concentration if used in excess. However, if the addition rate reaches a certain upper limit, then the frother rate is increased (Wills, 1983).

The importance of froth depth is mainly due to the effect that it has on the gangue content of the concentrate. Free gangue can be carried into the concentrate mainly by mechanical entrainment, and the deeper the froth layer the more the drainage of gangue into the cell occurs. Froth depth is very commonly used to control the concentrate grade, an increase in froth depth increasing the grade, but often at the expense of a slight reduction in recovery. Froth depth is often regarded as the difference between the pulp level and the level of the flotation cell overflow lip, and as such is controlled by changing the pulp level by the control and measurement methods mentioned earlier.

Froth level set-points can be cascaded to aeration or frother set-point controllers in order to maintain the required depth. Specification of the actual froth depth requires a knowledge of the level of the froth column surface, which may not coincide with the height of the cell overflow lip. Figure 12.62 shows a device developed at Mattagami Lakes for sensing the level of the froth column, this level controlling the frother dosage set-point (Kitzinger et al., 1979). The sensor consists of a set of stainless steel electrodes connected to an electronic circuit which senses the number in contact with the froth. The seven electrodes, one of which is always immersed in the pulp, are of gradually decreasing length, so that the number in contact with the froth is directly proportional to the depth of the froth column.

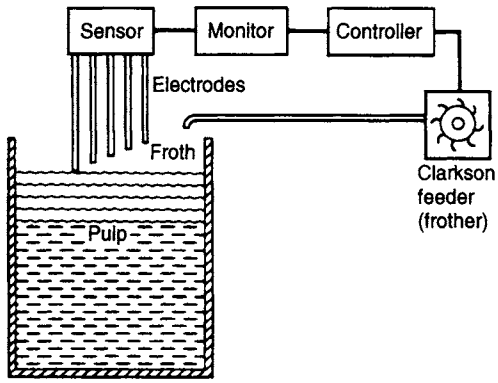


Figure 12.62 Froth measuring device

The most common, recent, froth measuremement device utilises ultrasonics. A ball float lies at the froth–pulp interface and is connected to a vertical shaft. A target plate is mounted on the upper end of the vertical shaft, above the top of the froth. An ultrasonic transmitter directs soundwaves to the target plate and the froth depth is calculated from the time taken for the sound waves to return to the source.

Froth level devices are used at Pyhasalmi in Finland (Figure 12.70). The addition of copper sulphate activator to the zinc circuit is controlled mainly by the on-stream analysis data but an excess tends to depress the froth level. The circuit contains several froth level measuring devices which indicate the improper addition of copper sulphate early enough to adjust the frother and sulphate addition to prevent a disturbance.

The ultimate aim of control is to increase the economic efficiency of the process by seeking to optimise performance, and there are several strategies which can be adopted to achieve this. Evolutionary optimisation (EVOP) methods (Chapter 3) (Oberg and Deming, 2000) have potential for flotation optimisation but have not been widely used. The control method involves periodically adjusting the set-points of the controlled variables according to a defined experimental design strategy such as a factorial or simplex search, the effect on economic efficiency being calculated and fed back to the operating system. The set-points are then shifted slightly to move in the direction of the optimum, and the process repeated until an optimum is encountered. Such methods cannot, however, be fully effective unless satisfactory stabilisation of plant performance can be achieved over long periods.

Herbst et al. (1986) discussed the use of advanced model-based control strategies in flotation, highlighting the advantages of these modern methods over classical control schemes. McKee (1991) also reviewed the progress in this area.

The Black Mountain concentrator in South Africa developed adaptive optimisation to control lead flotation (Twidle et al., 1985). Optimising control calculated the combination of metal recovery and concentrate grade which would achieve the highest economic return per unit of ore treated under the prevailing conditions. The criterion used to evaluate plant performance was the concept of economic efficiency (Chapter 1), in this case defined as the ratio between the revenue derived per tonne of ore at the achieved concentrate grade and recovery, and that derived at the target grade and recovery. Target concentrate grade and recovery were calculated from the operating recovery–grade curve, which was continuously updated based on a 24 h data bank, to allow for changes in the nature of the ore, quality of grinding, etc. Many factors influence the optimum combination of recovery and grade, such as commodity prices, reagent and treatment costs, transport costs, etc. The fundamental principle of adaptive optimisation is that concentrate grade and recovery can be predicted by online multivariable linear regression models, the coefficients of the models being continuously updated from the 24 h data bank. Independent variables that determine grade and recovery can be reagent additions, grades of rougher concentrate, final concentrate and cleaner tailing, feed grade and throughputs. Some independent variables are controllable whilst others are not.

The Pyhasalmi concentrator developed optimisation control based on a multi-linear response model, to optimise copper and zinc recoveries, and the balance of these metal values in each concentrate, to provide the highest economic efficiency (smelter value of metal in concentrate/value of metal in feed) (Miettunen, 1983). This took into account factors such as the penalties caused by the presence of zinc in the copper concentrate and the increasing costs of transportation due to a low copper content in the concentrate. Cyanide addition was the most influential variable in the copper circuit, while copper sulphate dosage to the zinc rougher bank was adjusted to maximise the economic recovery of the total zinc flotation circuit. The effect of copper sulphate on the rougher concentrate assays and the scavenger tailing assay was determined, and the approach used was to apply multiple linear regression to a 3 hour history of data stored in the process control computer. With this procedure, the effect of copper sulphate changes on economic recovery could be determined, and therefore the requirement to either increase or decrease copper sulphate to improve the economic recovery was known. Copper sulphate changes, determined by the optimising control system, were usually made every 6–30 min.

In recent years adaptive control (Thornton, 1991), expert systems (Kittel et al., 2001) and neural networks (Cubillos and Lima, 1997) have all been applied to the flotation problem with varying degrees of success. The texture, velocity, and colour of flotation froths are diagnostic of the flotation condition and are used by skilled operators to adjust set-points, particularly air addition rates. This function has now been implemented in machine vision systems which measure these properties online (van Olst et al., 2000; Holtham and Nguyen, 2002), allowing control systems to make use of froth characteristics in optimising performance (Kittel et al., 2001).

A comprehensive control system for a flotation plant requires extensive instrumentation and involves a considerable capital outlay. Figure 12.63 shows the instrumentation requirement for a simple

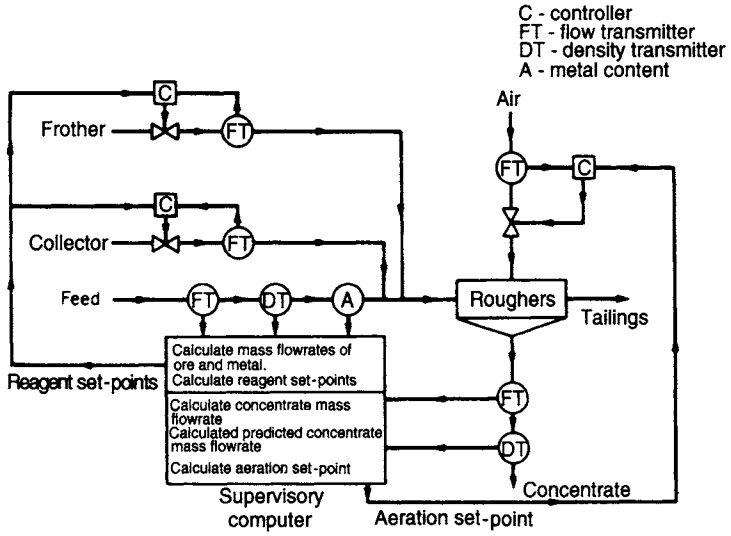


Figure 12.63 Instrumentation for rougher circuit control

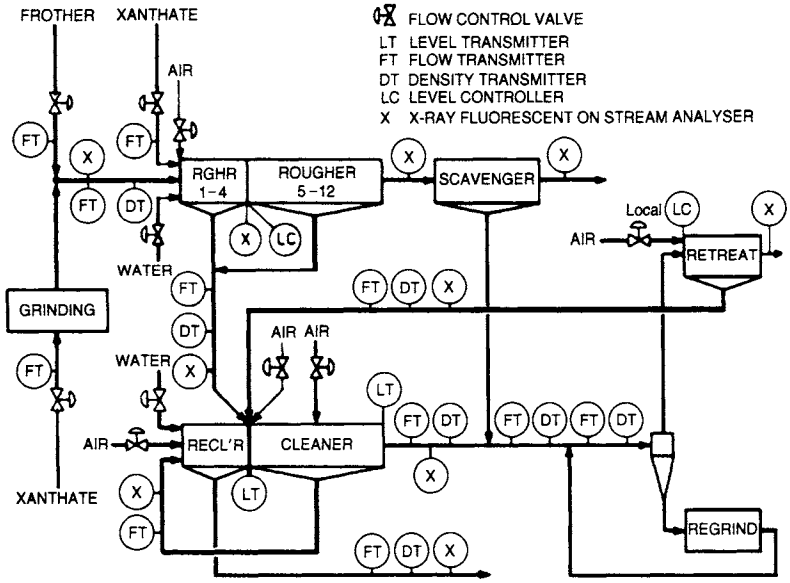


Figure 12.64 Instrumentation in Mount Isa copper flotation circuit

feed-forward system which could assist in control of a sulphide rougher bank, and Figure 12.64 shows the instrumentation used in the control of the Mount Isa copper flotation circuit in Queensland, Australia (Fewings et al., 1979). Although various cascade control loops have been attempted in this circuit, they have been unsuccessful in the long term due to changes in feed conditions, and set-points within the loops are mainly controlled by the operators.

Lynch et al. (1981) analysed the cost of such installations, which provide potentially significant economic and metallurgical benefits. The majority of plants which have installed instrumentation for manual or automatic control purposes have reported improved metal recoveries varying from 0.5 to 3.0%, sometimes with increased concentrate grades. Reduction in reagent consumptions of between 10 and 20% have also been reported.

Typical flotation separations

The expansion of flotation as a method of mineral concentration can be observed from the following data. According to surveys carried out by the US Bureau of Mines, the ore treated by flotation in the United States expressed as million tonnes was 180 in 1960, 368 in 1970, 440 in 1980, and 384 in 1985. Worldwide, froth flotation is used to treat 2000 Mt of material annually. In 1980, just before the recession in the American mineral industries, 55% of the total US tonnage was base metal sulphides, 27% phosphates, 9% iron ores, 6% industrial minerals, and 3% coal (Fuerstenau, 1988).

Although flotation is increasingly used for the non-metallic and oxidised minerals, the bulk of the world's tonnage currently processed is sulphide from the ores of copper, lead, and zinc, often associated in complex ore deposits. The treatment of such ores serves as an introduction to the flowsheets encountered in plant practice. Comprehensive reviews of the complete range of sulphide, oxide, and non-metallic flotation separations can be found elsewhere (Jordan et al., 1986; Malhotra et al., 1986; Redeker and Bentzen, 1986; Crozier, 1990) and good reviews of the flotation of specific materials such as coal (Osborne, 1988; Firth, 1999; Meenan, 1999), phosphates (Lawver et al., 1984; Hsieh and Lehr, 1985; Anon., 1986a; Moudgil, 1986; Wiegel, 1999), iron ore (Houot, 1983; Iwasaki, 1983, 1999; Nummela and Iwasaki, 1986), cassiterite (Lepetic, 1986; Senior and Poling, 1986; Andrews, 1990), scheelite (Beyzavi, 1985), chromium and manganese minerals (Fuerstenau et al., 1986), and gold (O'Connor and Dunne, 1994) are also available.

Flotation of copper ores

Over 15 Mt of copper are produced annually in the world, and in 2003 about 35% was from Chile (Yianatos, 2003). Significant tonnages were also produced in Canada (11%), Zambia (7.4%), Zaire (4.9%), and Australia (4.5%) (Thompson, 1991). During the 1990s, low copper prices resulted in a considerable quantity of mine capacity being unused, particularly in the United States, where many mines were forced to shut down or cut back on production. Ore grades in US mines average only 0.6% Cu, compared with 2.2% Cu in Africa and 1.2% Cu in South America, and to convert such low-grade ores to saleable concentrates, especially with current low metal prices and high production costs, requires a high level of technology and control, and a careful balance between concentrate grades, recovery and milling costs. Substantial increases in copper prices since 2003 (Chapter 1) have resulted in the reopening of many mines and significant increases in copper flotation capacity.

Copper is characterised by having a number of economic ore minerals (Appendix 1), many of which may occur in the same deposit, and in various proportions according to depth. Copper sulphides in the upper part of an ore body often oxidise and dissolve in water percolating down the outcrops of the deposit. A typical reaction with chalcopyrite is:

$$2CuFeS_2 + 17O + 6H_2O + CO_2 \rightarrow 2Fe(OH)_3 + 2CuSO_4 + 2H_2SO_4 + H_2CO_3$$

The residual ferric hydroxide left in this leached zone is called *gossan* and its presence has often been used to identify a copper ore body. As the water percolates through the zone of oxidation it may precipitate secondary minerals such as malachite and azurite to form an oxidised cap on the deeper primary ore.

The bulk of the dissolved copper, however, usually stays in solution until it passes below the water table into reducing conditions, where the dissolved metals may be precipitated from solution as secondary sulphides, e.g.:

$$CuFeS_2 + CuSO_4 \rightarrow FeSO_4 + 2CuS(\text{covellite})$$

$$5FeS_2 + 14CuSO_4 + 12H_2O \rightarrow 5FeSO_4 + 12H_2SO_4 + 7Cu_2S(\text{chalcocite})$$

As these secondary sulphide minerals contain relatively high amounts of copper, the grade of the ore in this *zone of supergene enrichment* is increased above that of the underlying primary mineralisation, and where supergene enrichment has been extensive, spectacularly rich copper "bonanzas" are formed.

The earliest copper miners worked the relatively small amount of metallic copper contained in the oxidised zone of the ore bodies. The discovery of smelting allowed high-grade oxidised copper minerals to be worked and processed. With improved developments in copper metallurgy, such as matte smelting and conversion, the

secondary sulphide supergene zones were mined and processed, these deposits often being shallow and containing 5% or more copper.

The development of froth flotation had an enormous impact on copper mining, enabling the most abundant primary mineral, chalcopyrite, and other sulphides to be efficiently separated from ores of relatively low grade and fine grain size. Another major development was the introduction of vast tonnage open-pit mining methods to the copper industry, allowing the excavation of tens of thousands of tonnes of ore per day. This made economical the processing of huge low-grade bulk copper deposits known as *porphyries*, the most important being found in the United States and South America.

The importance of froth flotation and high-tonnage mining can be seen by considering that until 1907 practically all the copper mined in the United States was from underground vein deposits, averaging 2.5% Cu, whereas at present ore grades in the United States average only 0.6% Cu and about 50% of the world's copper is produced from porphyry deposits, the rest mainly from vein-type and bedded deposits.

The exact definition of copper porphyry has been the subject of debate amongst geologists for a long time (Lacy, 1974). They are essentially very large oval or pipe-shaped deposits containing on average 140 Mt of ore, averaging about 0.8% Cu and 0.015% Mo, and a variable amount of pyrite (Sutolov, 1974). All porphyry copper deposits contain at least traces of molybdenite (MoS_2), and in many cases molybdenum is an important by-product. Porphyry copper mineralisation is often referred to as disseminated, and although on a large scale immense volumes of ore may contain disseminated values, on a small scale the occurrence of sulphides is controlled by fractures. Even apparently disseminated sulphide minerals are often aligned with quartz micro-veinlets, or lie in a chain-like fashion (see Figure 1.2b). The chains mark early fractures, which have been sealed and camouflaged by quartz and feldspar (Edwards and Atkinson, 1986).

The first deposits of this type to be mined on a large scale were in the southwestern states of the United States. It was apparent that the deposits could be economically mined in bulk by large-scale low-cost methods such as block-caving and open-pit methods. This is because the copper minerals are distributed uniformly through large blocks of the deposit so that the expensive selective mining methods which must be used with vein or bedded deposits are not needed. The extent of the ore body is usually determined by its copper content rather than by geological structure, the copper content tending to decrease away from the core of the mass. The cut-off grade, which determines the boundary between ore and waste, varies from mine to mine and according to the prevailing economic climate.

Porphyry copper operations are very much influenced by the geology of the ore deposition. Mining necessarily starts in the upper zones of the ore body where secondary alteration has enriched the ore grade, and where the mineralogy allows the production of concentrates often grading more than 40% Cu at high recovery. High levels of output can be achieved with fairly compact mills and smelters. As the operation matures, however, lower grade primary (*hypogene*) ore is encountered, in which the mineralogy limits concentrate grades to only around 25–30% Cu, and more ore needs to be produced to realise the same net copper output, the alternative being to maintain the current plant throughput while metal output declines. Reagent use and flowsheets often have to be adapted to accommodate these changes in mineralogy. A classic case is the El Teniente mine in Chile, the world's largest underground copper mine, which was developed in one of the largest known copper porphyry deposits on earth (estimated to contain 44 Mt of copper in ore grading 0.99% Cu or more). In 1979, the ore, of grade 1.54% Cu, was being mined and processed at the rate of $57{,}500\,t\,d^{-1}$ to produce a concentrate containing 40% Cu (Dayton, 1979). By 1984, with the secondary supergene zone approaching exhaustion, the ore grade had fallen to 1.4% Cu, and the mining rate had increased to $68{,}500\,t\,d^{-1}$, with a further expansion to $90{,}000\,t\,d^{-1}$ being undertaken. It was predicted that the mined grade would fall to 1.2% by the end of the 1980s and to 1.0% by the end of the twentieth century (Burger, 1984).

Although mining and processing of copper porphyries is on a vast scale, concentration of the ore is fairly straightforward, due to the high efficiency of froth flotation, and to the fact that breakage of the ore occurs preferentially at the

fracture zones containing the copper sulphides. This means that relatively coarse grinding produces composite particles with much of the valuable mineral exposed, facilitating rougher flotation.

Copper sulphide minerals are readily floatable and respond well to anionic collectors such as xanthates, notably amyl, iso-propyl and butyl. Alkaline circuits of pH 8.5–12 are generally used, with lime controlling the pH and depressing any pyrite present. Frother usage has changed significantly in recent years, away from the natural reagents such as pine oil and cresylic acids, to the synthetic frothers such as the higher alcohols (e.g. MIBC) and polyglycol esters. Cleaning of the rougher concentrates is usually necessary to reach an economic smelter grade (25–50% Cu depending on mineralogy), and rougher concentrates as well as middlings must often be reground for maximum recovery, which is usually between 80 and 90%. Primary grinding is normally to about 50–60% −75 microns, rougher concentrates being reground to 90–100% −75 microns to promote optimum liberation of values. Reagent consumption is generally in the range 1–5 kg of lime per tonne of ore, 0.002–0.3 kg t^{-1} of xanthate, and 0.02–0.15 kg t^{-1} of frother.

One of the largest copper concentrators in the world is at the Freeport mine in the Republic of Indonesia on the island of New Guinea. The plant was progressively expanded since initial start-up in 1972 from 7500 t d^{-1} to 200,000 t d^{-1} to compensate for the lower grade ore encountered as the open pit deepened. The principal copper mineral in the porphyry deposit is chalcopyrite. Gold and silver are also present in the primary ore, which in 1997 graded 1.3% Cu, 1.32 g t^{-1} Au and 2.82 g t^{-1} Ag (Coleman and Napitupulu, 1997). The gold content is the largest known reserve of gold in the world.

The flotation circuit is large (comprising four concentrators) but fairly simple. After primary grinding to produce a flotation feed grind size of 15% passing 212 microns, the ore is conditioned with lime, frother and collector, before being fed to the rougher flotation circuit. The rougher flotation circuit consists of four parallel banks of Wemco 127 m^3 flotation cells with nine cells per bank. The cleaner circuit consists of fourteen column cells for primary and secondary cleaning and twelve 85 m^3 mechanical scavenger flotation cells. The concentrate produced from the columns report to final concentrate while the concentrate from the scavengers are recycled back to the cleaner feed. In 1996, the Freeport operation produced 526,000 t of copper and 1,760,000 troy ounces of gold (Coleman and Napitupulu, 1997). Typical copper and gold recoveries are 86 and 76%, respectively.

By-products are important to the economics of copper porphyry operations, and the most important by-product of the North and South American porphyries is molybdenum. Molybdenum occurs as the highly floatable mineral, molybdenite, which is separated from the copper minerals after regrinding and cleaning of the copper rougher concentrates. Regrinding to promote optimum liberation needs careful control, as molybdenite is a soft mineral which slimes easily and whose floatability decreases as particles become finer. Rougher concentrates are therefore classified, only coarse cyclone underflows being reground in closed circuit. Cleaned copper concentrates are thickened, after which the copper minerals are depressed allowing molybdenite to be floated into a concentrate which is further cleaned, sometimes in up to twelve stages. Cleaning is important as molybdenite concentrates are heavily penalised by the smelter if they contain copper and other impurities, and the final copper content is often adjusted by leaching in sodium cyanide, which easily dissolves chalcocite and covellite and some other secondary copper minerals. Chalcopyrite, however, does not dissolve in cyanide, and in some cases is leached with hot ferric chloride.

Copper depression is achieved by the use of a variety of reagents, sometimes in conjunction with prior heat treatment. Heat treatment is used to destroy residual flotation reagents, and is most commonly achieved by the use of steam injected into the slurry. Depression of chalcopyrite may be effectively accomplished by the use of sodium cyanide, but this reagent is not so effective when chalcocite and bornite are present, in which case depression can be completed by the use of ferro- and ferri-cyanides, or by using "Nokes Reagent", a product of the reaction of sodium hydroxide and phosphorus pentasulphide. This reagent has an instantaneous depressing action on copper minerals and is rapidly consumed, so is added to the circuit in stages. It can be an expensive depressant because of its high (2–5 k t^{-1} of concentrate)

consumption, and is sometimes used in combination with cyanide. Other copper depressants are arsenic Nokes (As_2O_3 dissolved in Na_2S), sodium sulphide, sodium hydrosulphide, and thioglycolic acid. Ye et al. (1990) have shown that ozone conditioning can also effectively depress copper minerals. The molybdenite is floated using a light fuel oil as collector.

Figure 12.65 shows the molybdenum recovery flowsheet at the Chuquicamata Mine in Chile, the world's biggest copper producer (Sisselman, 1978). The copper concentrate, containing 0.8–3% MoS_2 is floated in the rougher circuit after depressing the copper minerals with sodium hydrosulphide (Shirley and Sutolov, 1985). The first cleaner concentrate is recleaned in four to seven stages using $2.5\,kg\,t^{-1}$ of arsenic Nokes reagent, and regrinding of first and fourth cleaner concentrates, to produce a concentrate containing 55% Mo and 1–2% Cu. This product is then leached with sodium cyanide to reduce the copper content, which is predominantly as chalcopyrite, to below 0.3%. Sodium cyanide is added also to the last two cleaner stages. All flotation cells in the molybdenum plant operate with nitrogen from the smelter oxygen plant, rather than air, the reducing potential considerably lowering the consumption of depressant (Crozier, 1986).

By-products play an important role in the economics of the Palabora Mining Co. in South Africa, which treats a complex carbonatite ore to recover copper, magnetite, uranium, and zirconium values. The ore assays about 0.5% Cu, the principal copper minerals being chalcopyrite and bornite, although chalcocite, cubanite ($CuFe_2S_3$), and other copper minerals are present in minor amounts. The flotation feed is coarse (80%–300 microns) due to the high grinding resistance of the magnetite in the ore which would increase grinding costs if ground to a finer size, and due to the fact that the flotation tailings are treated by low-intensity magnetic separation to recover magnetite, and Reichert cone gravity concentration to recover uranothorite and baddeleyite.

The flotation circuit consists of eight separate sections, the last two sections being fed from an

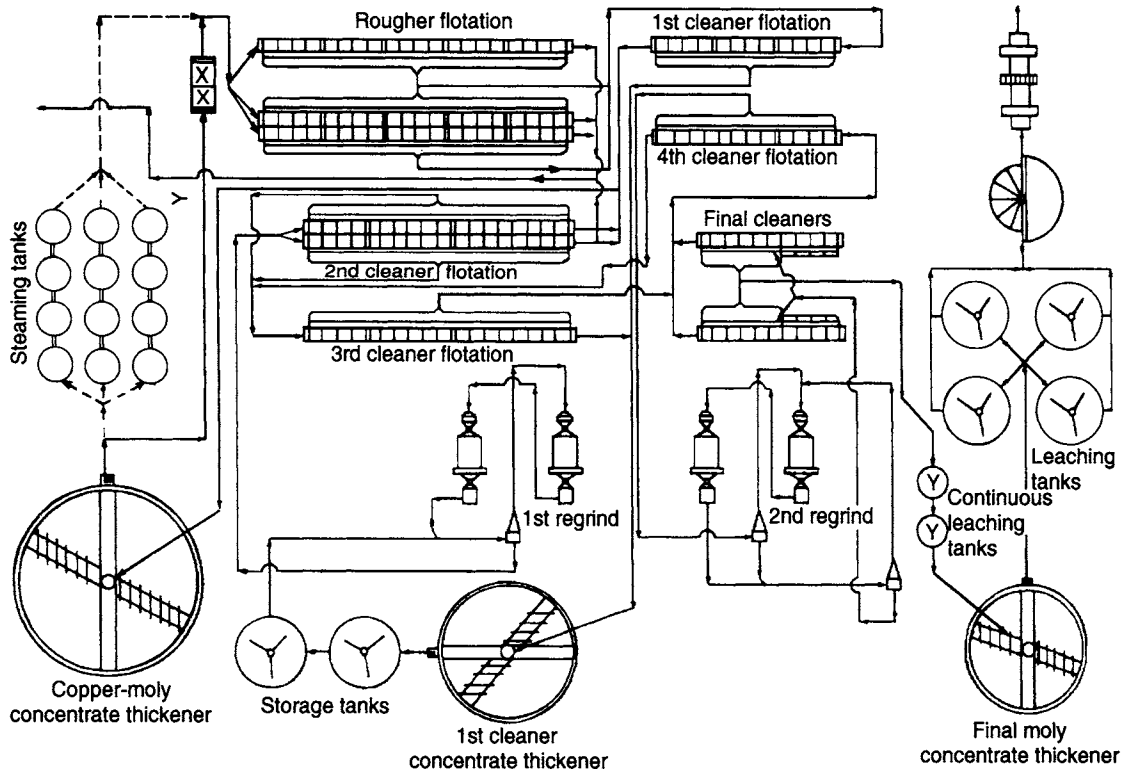


Figure 12.65 Molybdenum flotation at Chuquicamata (Sisselman, 1978)

autogenous grinding circuit. The first five parallel sections, the original Palabora flowsheet, are fed from conventional mills, each at the rate of 385 t h^{-1} (Figure 12.66). Flotation feed is conditioned with sodium isobutyl xanthate and frother before being fed to the rougher flotation banks. The more readily floatable minerals, mainly liberated chalcopyrite and bornite, float off in the first few cells, and more collector is added before the final scavenger cells, in order to float off the less floatable particles, such as cubanite, and in order to attempt to float the less responsive copper minerals, such as valleriite, a copper–iron sulphide containing Mg and Al groups in the crystal lattice. Valleriite occurs intergrown with other sulphide minerals (Figure 12.67), and due to the fact that it is a very soft mineral, it can lead to poor flotation recoveries. During comminution, breakage occurs along the soft and friable

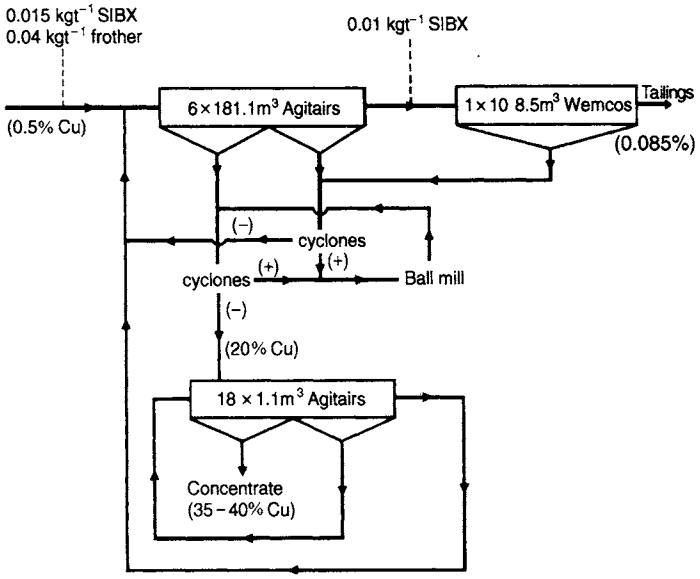


Figure 12.66 Flowsheet of original section of Palabora flotation circuit

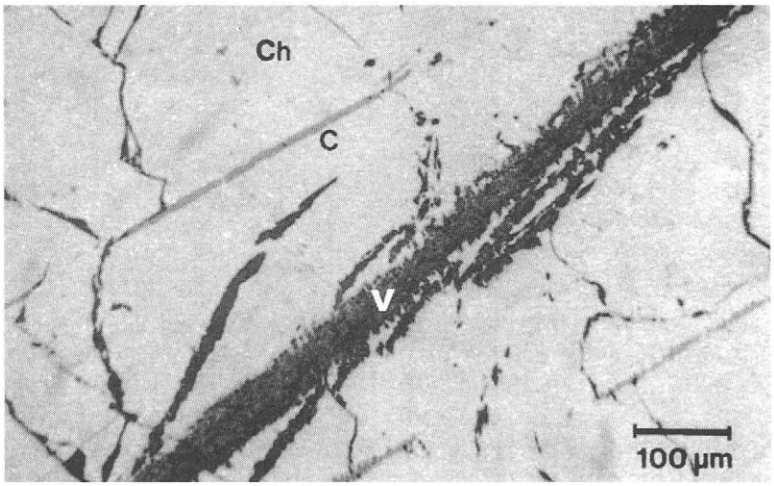


Figure 12.67 Palabora copper ore. Valleriite (V) and cubanite intergrown with chalcopyrite (Ch)

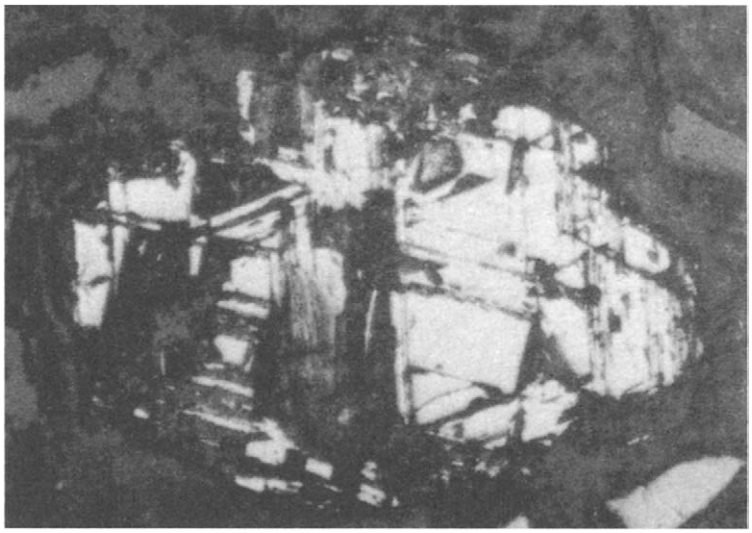


Figure 12.68 Palabora flotation tailings particle, showing valleriite (dark) forming a coating around chalcopyrite (light)

valleriite, leaving grains of other copper sulphides with a valleriite coating, preventing these grains from floating (Figure 12.68).

Rougher and scavenger concentrates are reground to 90%–45 microns, before being fed to the cleaner circuit at a pulp density of 14% solids, this dilution being possible due to the removal of magnetite and other heavy minerals into the tailings, and the fine particle size produced after grinding.

Oxidised copper ores

Due to the nature of copper deposits and mineralisation, it is sometimes possible to selectively mine and process the oxidised cap on the primary zone. Minerals such as malachite and azurite are soluble in dilute sulphuric acid and can be processed economically by acid leaching as a prelude to precipitation of the copper by electrolysis (electrowinning). Processing of such oxidised ores has become more attractive due to the availability of cheap sulphuric acid produced at smelters, as a means of reducing sulphur dioxide emissions into the atmosphere.

In Central Africa significant tonnages of oxidised ore were concentrated by flotation before being leached, ores containing a mixture of sulphide and oxidised minerals being treated by first floating off the sulphides to produce a concentrate for the smelter. A good example was the Chingola Division of Nchanga Consolidated Copper Mines in Zambia where sulphide tailings were floated in an oxide circuit using sodium hydrosulphide, sodium isopropyl xanthate and frother, with the concentrates being acid leached.

Much of the published work on oxide copper minerals is concerned with malachite, and chrysocolla, a copper silicate (Deng and Chen, 1991). The latter is one of the most widely distributed and least understood of all the major copper minerals, being a very difficult mineral to characterise and float (Laskowski et al., 1985). Malachite responded well to flotation techniques and in Central Africa flotation of malachite ores after sulphidisation is successfully practised (Fuerstenau and Raghavan, 1986). Xanthate collector coatings are loosely bound to oxide copper minerals and sulphidisation enhances the flotation process.

Today flotation is rarely used for copper oxide recovery. Such ores are generally leached with sulphuric acid, and the metal is recovered by solvent extraction and electrowinning. Low grade ores are often heap leached (Witt et al., 1999).

Flotation of lead–zinc ores

The bulk of the world's lead and zinc is supplied from deposits which often occur as finely disseminated bands of galena and sphalerite, with varying

amounts of pyrite, as replacements in various rocks, typically limestone or dolomite. This banding sometimes allows dense medium preconcentration prior to grinding (Figure 11.13).

Although galena and sphalerite usually occur together in economical quantities, there are exceptions, such as the lead ore body in S.E. Missouri, of the United States, where the galena is associated with relatively minor amounts of zinc (Watson, 1988), and the zinc-rich Appalachian Mountain region, mined in Tennessee and Pennsylvania, where lead production is very small.

Feed grades are typically 1–5% Pb and 1–10% Zn, and although relatively fine grinding is usually needed (often to well below 75 μm), fairly high flotation concentrate grades and recoveries can be achieved. In an increasing number of cases, ultrafine grinding down to 10 μm is needed to produce acceptable flotation performance from very fine grained ores such as those at the Century mine in Australia. Typically, lead concentrates of 55–70% lead are produced, containing 2–7% Zn, and zinc concentrates of 50–60% Zn, containing 1–6% Pb. Although galena and sphalerite are the major ore minerals, cerussite ($PbCO_3$), anglesite ($PbSO_4$), marmatite ((Zn,Fe)S) and smithsonite ($ZnCO_3$) can also be significant. In some deposits the value of associated metals, such as silver, cadmium, gold, and bismuth, is almost as much as that of the lead and zinc, and lead–zinc ores are the largest sources of silver and cadmium.

Several processes have been developed for the separation of galena from zinc sulphides, but by far the most widely used method is that of two-stage selective flotation, where the zinc and iron minerals are depressed, allowing the galena to float, followed by the activation of the zinc minerals in the lead tailings to allow a zinc float.

Sphalerite (and to a lesser extent pyrite) can become activated by heavy metal ions in solution, which replace metallic zinc on the mineral surfaces by a process of ion exchange (e.g. Equation 12.11). This activated surface can adsorb xanthate and produce a very insoluble heavy metal xanthate which provides the surface with a water-repellent "envelope". Clean sphalerite is not strongly hydrophobic in xanthate solutions, as zinc xanthate has a relatively high solubility, and hence a stable envelope is not formed.

Heavy metal ions are often present in the slurry water, especially if the ore is slightly oxidised. The addition of lime or soda ash to the slurry can precipitate them as relatively insoluble basic salts, thus "de-activating" the sphalerite to some extent. The alkali is usually added to the grinding mills as well as to the lead float conditioner, as it is in the grinding process that many heavy metal ions are released into solution.

Lead flotation is usually performed at a pH of between 9 and 11, lime, being cheap, often being used to control alkalinity. Not only does lime act as a strong depressant for pyrite, but it can also depress galena to some extent. Soda ash is sometimes preferred because of this, especially when the pyrite content is relatively low.

The effectiveness of alkalis as deactivators is dependent on the concentration of heavy metal ions in solution, as the basic salts which are precipitated, although of extremely limited solubility, can provide a source of heavy metal ions sufficient to cause sphalerite activation. In most cases, therefore, other depressants are required, the most widely used being sodium cyanide (up to $0.15\,kg\,t^{-1}$) and zinc sulphate (up to $0.2\,kg\,t^{-1}$), either alone or in combination. These reagents are commonly added to the grinding circuit, as well as to the lead float, and their effectiveness depends very much on pulp alkalinity.

Apart from the reactions with metal ions in solution, cyanide has long been used to dissolve surface copper from activated sphalerite, and can react with iron and zinc xanthates to form soluble complexes, eliminating xanthate from the surfaces of the minerals of these metals. Pyrite is thus depressed with the sphalerite, and cyanide is generally the preferred depressant where soda ash regulates alkalinity and pyrite presence is significant.

The effectiveness of depressants also depends on the concentration and selectivity of the collector. Xanthates are most widely used in lead–zinc flotation, and the longer the hydrocarbon chain, the greater the stability of the metal xanthate in cyanide solutions and the higher the concentration of cyanide required to depress the mineral. If the galena is readily floatable, potassium or sodium ethyl xanthate may be used, together with a "brittle" frother such as MIBC. Sodium isopropyl xanthate may be needed if the galena is tarnished, or if considerable amounts of lime are used to promote

pyrite depression. Powerful collectors such as amyl xanthate can be used if the sphalerite is clean and hydrophilic, and are needed where the galena is highly oxidised and floats poorly.

Although cyanides are widely used due to their high degree of selectivity, they do have certain disadvantages. They are toxic and expensive, and they depress and dissolve some of the gold and silver which are often present in economic amounts. For these reasons, zinc sulphate is used in many plants to supplement cyanide. This reduces cyanide consumption (usually to well below $0.1\,kg\,t^{-1}$), and a number of mines in the USA achieve depression by the use of zinc sulphate alone.

After flotation of the galena, the tailings are usually treated with between 0.3 and $1\,kg\,t^{-1}$ of copper sulphate, which reactivates the surface of the zinc minerals (Equation 12.11), allowing them to be floated. Lime ($0.5–2\,kg\,t^{-1}$) is used to depress pyrite, as it has no depressing effect on the activated zinc minerals, and a high pH (10–12) is used in the circuit. Isopropyl xanthate is perhaps the most commonly used collector, although ethyl, isobutyl, and amyl are also used, sometimes in conjunction with dithiophosphate (aerofloats), depending on conditions. As activated sphalerite behaves in a similar way to chalcopyrite, thionocarbamates such as Z-200 are also common collectors, selectively floating the zinc minerals from the pyrite.

Careful control of reagent feeding must be observed when copper sulphate is used in conjunction with xanthates, as xanthates react readily with copper ions. Ideally, the minerals should be conditioned with the activator separately, so that when the conditioned slurry enters the collector conditioner there is little residual copper sulphate in solution. Although the activation process is fairly rapid in acidic or neutral conditions, in practice it is usually carried out in an alkaline circuit in order to prevent pyrite activation, and a conditioning time of some 10–15 min is required to make full use of the reagent. This is because the alkali precipitates the copper sulphate as basic compounds which are sufficiently soluble to provide a reservoir of copper ions for the activation reaction.

The Sullivan concentrator of Cominco Ltd, British Columbia, operates an interesting flowsheet which includes de-zincing of the lead concentrates and de-leading of the zinc concentrates (Fairweather, 2005). The ore is essentially a replacement deposit in argillaceous quartzite, the ore bodies being massive, fine-grained mixtures of sulphides, sometimes interbanded with the country rock. The principal economic minerals are galena and marmatite (7ZnS:FeS), iron being present mainly as pyrrhotite, and to a lesser extent pyrite. Silver is closely associated with the galena and is an important by-product.

The flowsheet is shown in Figure 12.69. After primary grinding to 55%–74 μm with cyanide, xanthate, and lime, the ore is fed to a unit flotation cell, where a mixture of MIBC and pine oil frothers is added. The pH is maintained at 8.5, and a coarse lead concentrate is floated, and cleaned once. This concentrate, assaying about 65% lead, is used as medium in the DMS circuit preceding grinding. The tailing from the coarse lead flotation is ground to 87%–74 μm, and is conditioned with sodium isopropyl xanthate, cyanide, lime, and MIBC, before being fed to the lead roughers at a pH of 9.5. Further addition of cyanide and xanthate to the head of the scavenger cells produces a concentrate which is returned to secondary grinding. The lead rougher concentrate is cleaned, the tailings being reground and returned to the lead roughers. The pH in the cleaners is 10.0, and the cleaner concentrate is further cleaned at pH 10.5 to produce a concentrate containing 10–14% Zn. The final stage of lead flotation is the de-zincing of the second lead cleaner concentrate. After activating the zinc minerals with copper sulphate, the galena is depressed by raising the pH to 11.0 by the addition of lime, and by steam heating the slurry to 30–40 °C. A rougher de-zincer concentrate is cleaned once in the first few cells of the bank, and the dezincer tailing is the final lead concentrate, assaying about 62% Pb and 4.5% Zn. The lead scavenger tailings are conditioned with about $0.7\,kg\,t^{-1}$ of copper sulphate, prior to feeding to zinc rougher flotation where xanthate, lime and frother are added to the cells. A rougher concentrate is floated at pH 10.6, and is reground before being fed to the first stage of cleaning. The tailings from this stage, containing 2.5–4% Pb, are pumped back to the head of the lead circuit to allow a better recovery of lead in that concentrate. The cleaner concentrate is recleaned twice, the final concentrate being combined with the de-zincer concentrate to produce the final zinc concentrate containing 50% Zn and 4% Pb.

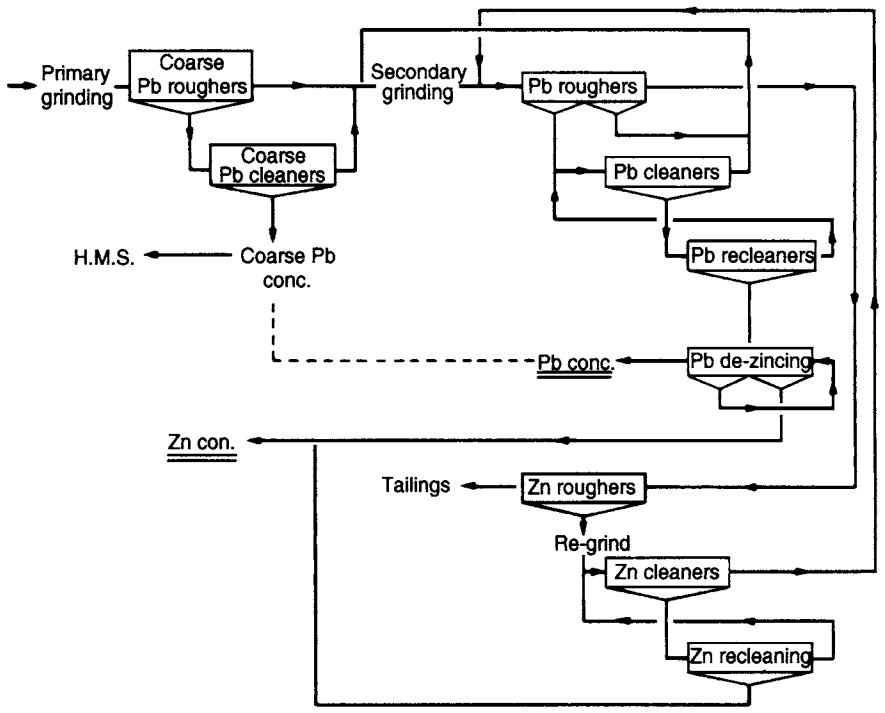


Figure 12.69 Sullivan concentrator flowsheet

The increasing fine-grained nature and complexity of lead–zinc ores has led in some cases to the need for rougher concentrates to be ground extremely finely. Flotation of a material that had been ground to an ultra-fine size was achieved at the MacArthur River Mine in Australia, where rougher concentrates are ground to 12 μm to produce a bulk lead–zinc concentrate. At Mount Isa Mines rougher concentrates of lead and zinc are ground to 10 and 15 μm respectively prior to cleaner flotation (Young and Gao, 2000). At the Century Mine, zinc concentrates are ground to below 10 μm to effectively liberate fine-grained silicates (Burgess et al., 2003). Due to the high intensity of ultra-fine grinding, inert grinding media is often used to prevent oxidation of mineral surfaces. The production of ultra-fine concentrates usually results in very tenacious froths, with pulping and material handling problems being common.

Extremely fine intergrowth between galena and sphalerite inhibits selective flotation separation, and in some cases sphalerite is activated by copper ions in the ore to such an extent that depression of sphalerite fails, even when the most powerful combinations of reagents, such as zinc sulphate and cyanide, are used. Bulk flotation of lead and zinc minerals may in such cases have a number of economical advantages. Coarse primary grinding is often sufficient with bulk flotation, as the valuable minerals need be liberated only from the gangue, not from each other. The flotation circuit design is normally relatively simple. In contrast, selective flotation calls for finer primary grinding, in order to free the valuable minerals not only from the gangue, but also from each other. This increases mill size and energy requirements; the flotation volume will increase proportionally to the number of selective concentrates.

However, the production of bulk lead–zinc concentrates is only reasonable if there are smelters which are adequately equipped for such concentrates. The only smelting process available is the *Imperial Smelting Process*, which was developed at a time when most of the lead and zinc was recovered from low-pyrite ore deposits. In recent years, however, lead and zinc are increasingly being recovered from complex and highly pyritic ores.

Bulk concentrates for smelting in the ISP should be low in iron, as iron is recovered in the smelter slag. An increase in iron content increases slag production, and correspondingly increases zinc losses, as the slag carries about 5% zinc. Furthermore, a high iron content increases smelter energy consumption. When smelter revenues are compared, the highest revenues are achieved when selective concentrates are produced. Even mixing selective concentrates into a bulk concentrate will yield higher revenues than bulk concentrates produced by direct flotation. This is because better selectivity between non-ferrous minerals and pyrite is achieved by the optimal conditions adapted to the separation of galena and pyrite in the first, and sphalerite and pyrite in the second step. The chemical conditions in a bulk flotation cannot be adjusted to meet both conditions simultaneously if a high amount of pyrite is present. It has been shown that, although selective is more expensive than bulk flotation, the increase in revenues gained is often much higher than the additional operating costs (Bergmann and Haidlen, 1985).

Bulk flotation followed by separation can sometimes be used, although in most cases the activated sphalerite and pyrite in the bulk concentrate are covered with a layer of collector, and are difficult to depress unless extremely large amounts of reagent are used. This is especially the case if copper sulphate has been used to activate the sphalerite; cyanide will react with residual copper ions in solution. Every attempt is made at plants using bulk flotation to use the minimum collector feed for the bulk flotation step, which can lead to low recoveries. Bulk flotation is performed at Zinkgruvan, Sweden's largest zinc mine (Anon., 1977). Grinding is autogenous and the lead ions released during grinding activate the sphalerite to such an extent that deactivation by alkali is not practical at this stage. The flotation plant consists of bulk flotation and lead flotation stages, each circuit consisting of rougher, scavenger, and cleaner steps. The galena and sphalerite are floated with $0.12\,kg\,t^{-1}$ of potassium ethyl xanthate, no activator being required. After five stages of cleaning, the concentrate is conditioned with $0.6\,kg\,t^{-1}$ of $ZnSO_4$ to depress the sphalerite, and the galena is floated at pH 10 with potassium ethyl xanthate. After six stages of cleaning, and further additions of $ZnSO_4$, a lead concentrate of 65% and a zinc concentrate of 55% are produced.

An interesting bulk-selective flowsheet is operated at the Tochibora mine, in Japan (Anon., 1984a), which has an annual output of 960,000 t of ore, grading 4.3% Zn, 0.3% Pb, and $22\,g\,t^{-1}$ Ag. Pyrite is not present to any extent in the ore, the principal gangue minerals being hedenbergite ($CaFeSi_2O_6$), quartz, calcite, and epidote. Crushed ore is ground to 80% passing 75 μm, and is conditioned with Na_2CO_3 and $CuSO_4$ before bulk flotation at pH 9.4. Sodium ethyl xanthate is used as collector and pine oil as frother. After cleaning the bulk flotation concentrates, the slurry is conditioned with NaCN and activated carbon, after which galena is floated, the tailings being the zinc concentrate. The lead concentrate is fed into trommels, the oversize forming a graphite by-product concentrate, while the undersize is fed to shaking tables. The table middlings and tailings are recycled to the differential flotation circuit, the cleaned concentrate being the final lead concentrate. Concentrates grading 60.7% Zn and 65.3% Pb are obtained at recoveries of 93.3% Zn and 80.2% Pb.

Flotation of copper–zinc and copper–lead–zinc ores

The production of separate concentrates from ores containing economic amounts of copper, lead, and zinc is complicated by the similar metallurgy of chalcopyrite and activated zinc minerals. The mineralogy of many of these ores is a complex assembly of finely disseminated and intimately associated chalcopyrite, galena, and sphalerite in a gangue consisting predominantly of pyrite or pyrrhotite (often 80–90%), quartz, and carbonates. Such massive sulphide ores of volcanosedimentary origin are also a valuable source of silver and gold.

The complex Cu–Pb–Zn ores represent 15% of total world production and 7.5% of the world copper reserves, these percentages being higher for zinc (Cases, 1980). Grades of ore mined 0.3–3% Cu, 0.3–3% Pb, 0.2–10% Zn, $3–100\,g\,t^{-1}$ silver, and $0–10\,g\,t^{-1}$ gold, on average.

The major processing problems encountered are related specifically to the mineralogy of the assemblies. Due to the extremely fine dissemination and interlocking of the minerals, extensive fine grinding is often needed, usually to well below

75 μm. There are notable exceptions to this such as at Bleikvassli in Norway where a primary grind of 80%–240 μm is adequate, with no regrinding (Anon., 1980). In the New Brunswick deposits in Canada, however, grinding to 80%–40 μm is required in certain areas, optimum mineral recoveries being in the range 10–25 μm. Such extensive fine grinding is extremely energy intensive (in the order of 50 kW h t^{-1}), and the large surface area produced leads to high reagent consumptions, the release of metal ions into solution, which reduces flotation selectivity, and a greater tendency for surface oxidation. Oxidation is particularly serious with galena, which is often overground in closed-circuit grinding, being the heaviest mineral in the complex ores.

In most cases, concentrates are produced at relatively poor grades and recoveries, typical grades being:

	%Cu	*%Pb*	*%Zn*
Copper concentrates	20–30	1–10	2–10
Lead concentrates	0.8–5	35–65	2–20
Zinc concentrates	0.3–2	0.4–4	45–55

Recoveries of 40–60% for copper, 50–60% for lead, and 70–80% for zinc are reported for New Brunswick deposits (Stemerowicz and Leigh, 1978). Smelting charges become excessive with contaminated concentrates, as very rarely is a metal paid for when it is not in its proper concentrate and penalties are often imposed for the presence of zinc and lead in copper concentrates. Silver and gold are well paid for in copper and lead concentrates, whereas payment in zinc concentrates is often zero. Direct sale of the concentrates to custom smelters is necessary where the size of the ore body precludes the development of a specialised smelter complex, such as that at the Ronnskar works of Boliden, Sweden, where a collection of metallurgical plants facilitates the transfer, or recycling, of residues and by-products from one process stage to another for the recovery of all metal values (Barbery et al., 1980).

The overall revenue for a mine exploiting such deposits can be very low compared to the relatively high contained value of the ore. Gray (1984) has shown the economic limitations of processing complex ores by a standard route by comparing the concentrator performance at two Australian mines: North Broken Hill and Woodlawn. The former mine realised about 56% of the potential ore value in payments received, whereas Woodlawn realised only about 27% of the ore value in payments. The disparity in the two balances is almost solely due to the differences in recovery resulting from the much greater mineralogical complexity of the Woodlawn deposits. Deposits with such complex mineralogy are to be found in many parts of the world, whereas deposits with mineralogy comparable with North Broken Hill are now rare. The metallurgist's task is to characterise each deposit quantitatively and systematically and then to select the economically optimum combination of process steps to suit the characteristics. Imre and Castle (1984) have also comprehensively reviewed the exploitation strategies for complex Cu–Pb–Zn ore bodies, discussing the interaction and optimisation of the beneficiation and extractive metallurgical flowsheets and the options for extractive metallurgy in processing complex sulphides containing pyrite. Barbery (1986) has also discussed the many potential processing options available for treating complex sulphides, concluding that it is likely, for some years, that combined processes will be developed, linking physical separation processes with hydrometallurgy for maximum efficiency in recovering values into concentrates that are well paid by conventional existing smelters. In turning such integrated treatment concepts into reality, the fundamental question will be: is one flowsheet, involving one set of processes, capital and operating costs superior to another treatment approach with a different set of costs and metallurgical performance? Further, it is necessary to assess the impact of different product grades from the integrated process on subsequent downstream processes. The answer to this question, although critical, is likely to be very complex, and McKee (1986) has analysed the role of computer analysis in answering such questions.

Flotation is, at present, the only method that can be used to beneficiate the complex sulphide ores, and a wide variety of flowsheets are in use, some involving sequential flotation, others bulk flotation

of copper and lead minerals followed by separation. Bulk flotation of all the economic sulphides from pyrite has also been studied. Although bulk flotation has certain advantages, it has been shown that the requirements for adequate galena flotation, as well as those for selective flotation of sphalerite from pyrite, are difficult to meet in a single bulk circuit, and better metallurgical efficiency can be obtained by floating, and then mixing, separate copper–lead and zinc concentrates. However, the main disadvantage is that a concentrate having no market is produced, for which new metallurgical processes have to be developed (Barbery, 1986).

In the flotation of *copper–zinc ores*, where lead is absent, or is not present in economic quantities, lime is almost universally used to control alkalinity at pH 8–12, and to deactivate the zinc minerals by precipitation of heavy metal ions. In a few cases, the addition of lime to the mills and flotation circuit is sufficient to prevent the flotation of zinc minerals, but in most cases supplementary depressants are required. Sodium cyanide is often added in small quantities ($0.01–0.05\,kg\,t^{-1}$) to the mills and cleaners; if present in large amounts chalcopyrite is also depressed. Zinc sulphate is also used in conjunction with cyanide, and in some cases sodium sulphite (or bisulphite) or sulphur dioxide depressants are used. Work in the United States (Hoyack and Raghavan, 1987) has indicated that sulphite depresses pyrite, but only has a slight effect on the flotation of sphalerite. The depression of sphalerite is probably governed by electrochemical reactions that yield a hydrophilic surface product, $Fe_2(SO_4)_3 \cdot Fe(OH)_3$.

After conditioning, the copper minerals are floated using either xanthates, or if the mineralogy allows, a selective copper collector such as isopropyl thionocarbamate. Typically, copper concentrates contain 20–30% Cu and up to 5% Zn. Copper flotation tailings are activated with copper sulphate, and zinc minerals are floated as described in the previous section.

Due to the very close control of reagent additions required in copper–zinc separations, on-stream X-ray analysis of plant flow-streams is being increasingly used, together with some form of automatic control. A good example is the Pyhasalmi concentrator in Finland (Figure 12.70), which is highly automated, and involves sequential flotation of copper, zinc, and pyrite (Wills, 1983). The copper circuit consists of conventional roughing and scavenging, followed by three cleaning stages, the tailings passing to the zinc flotation circuit. Despite the use of cyanide ($0.025\,kg\,t^{-1}$) and zinc sulphate ($1.45\,kg\,t^{-1}$), a problem in the copper circuit is the natural activation of sphalerite by copper-bearing water; because of this a flotation time of about 20 min is required for satisfactory copper recovery (about 90%) and the copper concentrate contains about 25% Cu and 3.5% Zn. Reagent additions are controlled automatically according to set-points regulated by on-stream analysis of copper, zinc, and iron contents in various flowstreams. Due to the varying quality of the ore, caused by fluctuating quantities of activated zinc minerals, cyanide addition is the most important variable affecting the economic recovery and is controlled from the set-points to keep the zinc content of the copper concentrate at a minimum while maintaining optimum copper recovery.

The method most widely used to treat ores containing economic amounts of lead, copper, and zinc is to initially float a bulk lead–copper concentrate, while depressing the zinc and iron minerals. The zinc minerals are then activated and floated, while the bulk concentrate is treated by the depression of either the copper or lead minerals to produce separate concentrates.

The bulk float is performed in an alkaline circuit, usually at pH 7.5–9.5, lime, in conjunction with depressants such as cyanide and zinc sulphate, being added to the mills and bulk circuit. Depression of zinc and iron sulphides is sometimes supplemented by the addition of small amounts of sodium bisulphite or sulphur dioxide to the cleaning stages, although these reagents should be used sparingly as they can also depress galena.

The choice and dosage of collector used for bulk flotation are critical not only for the bulk flotation stage but also for the subsequent separation. Xanthates are commonly used, and while a short-chain collector such as ethyl xanthate gives high selectivity in floating galena and chalcopyrite and permits efficient copper–lead separation, it does not allow high recoveries into the bulk concentrate, particularly of the galena. Much of the lost galena subsequently floats in the zinc circuit, contaminating the concentrate, as well as representing an economic loss. Because of this, a powerful collector such as amyl or isobutyl xanthate is commonly

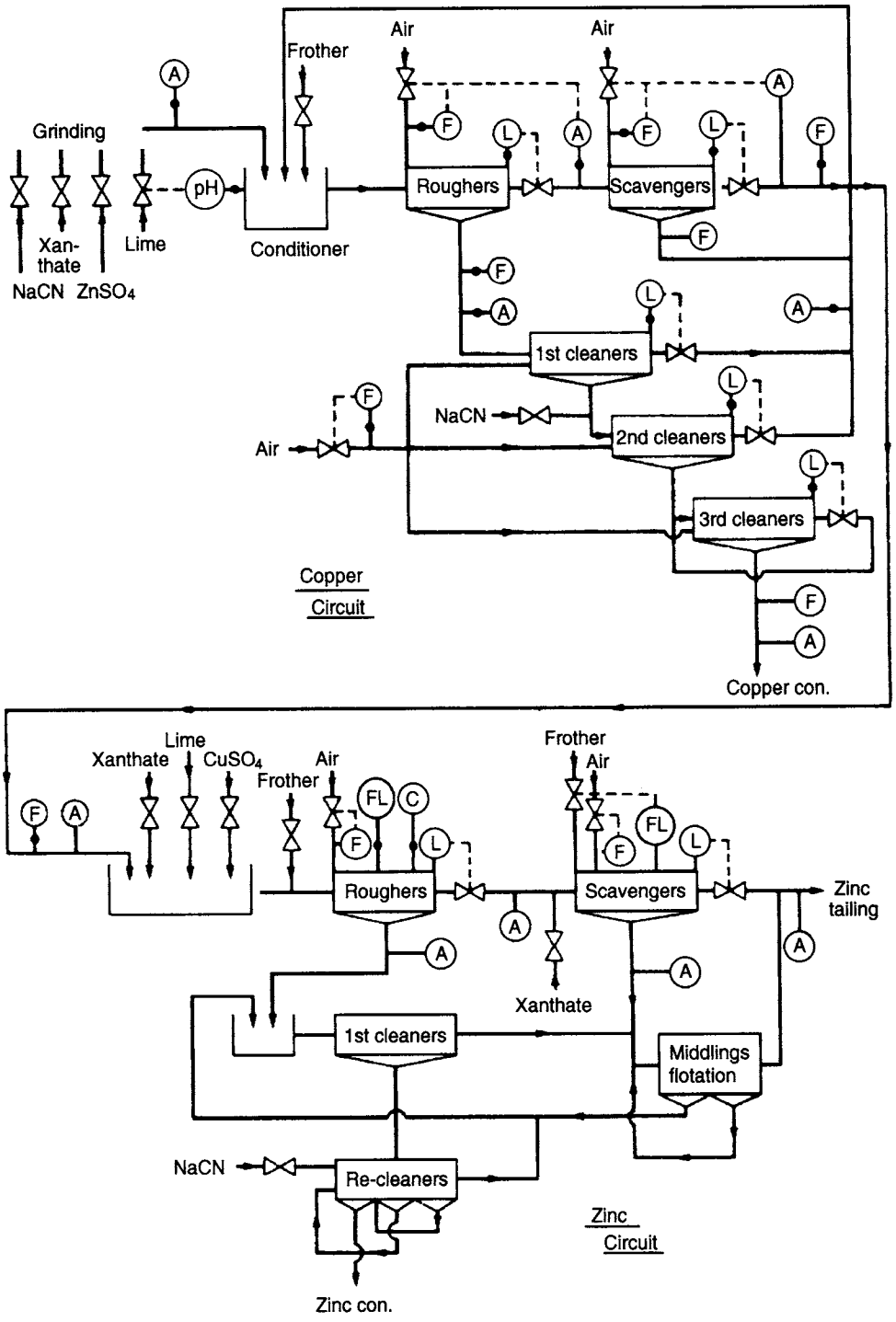


Figure 12.70 Pyhasalmi flotation circuit. F = flow rate; L = level; A = assay; FL = froth level; C = conductivity

used, and very close control of the dosage is required. Usually, fairly small amounts, of between 0.02 and 0.06 kg t^{-1}, are used, as an excess makes copper–lead separation difficult, and large amounts of depressant are required which may depress the floating mineral, contaminating lead and copper concentrates.

Although the long-chain collectors improve bulk recovery, they are not as selective in rejecting zinc, and sometimes a compromise between selectivity and recovery is needed, and a collector such as sodium isopropyl xanthate is chosen. Dithiophosphates, either alone or in conjunction with xanthates, are also used as bulk float collectors, and small amounts of thionocarbamate may be used to increase copper recovery.

The choice of the method for separating copper from the lead minerals depends on the response of the minerals and the relative abundance of the copper and lead minerals. It is preferable to float the mineral present in least abundance, and galena depression is usually performed when the ratio of lead to copper in the bulk concentrate is greater than unity.

Lead depression is also undertaken if economic amounts of chalcocite or covellite are present, as these minerals do not respond to depression by cyanide, or if the galena is oxidised or tarnished and does not float readily. It may also be necessary to depress the lead minerals if the concentration of copper ions in solution is high, due to the presence of secondary copper minerals in the bulk concentrate. The standard copper depressant, sodium cyanide, combines with these ions to form complex cuprocyanides (Equation 12.23), thus reducing free cyanide ions available for copper depression. Increase in cyanide addition only serves to accelerate the dissolution of secondary copper minerals.

Depression of galena is achieved using sodium dichromate, sulphur dioxide, and starch in various combinations, whereas copper minerals are depressed using cyanide, or cyanide–zinc complexes. Methods of depression used at various concentrators can be found elsewhere (Wills, 1984).

Depression of galena by the addition of sodium dichromate at high pH is still used in many plants. The hydrophobic character of the xanthate layer on the galena surface is inhibited by the formation of hydrated lead chromate (Cecile et al., 1980). At Vihanti (Figure 12.71), the galena is depressed by the addition of 0.01 kg t^{-1} of sodium dichromate to the bulk concentrate. After copper flotation, the separation tailings are further floated to remove residual copper, the cleaner tailings producing the final lead concentrate. Although there is no automatic control of the separation circuit, the rate of addition of dichromate is critical, as an excess is returned to the rougher feed with the cleaner tailing, which depresses lead into the zinc circuit.

Although the amount of dichromate used is only small (0.01–0.2 kg t^{-1}), chromate ions can cause environmental pollution, and other methods of depression are sometimes preferred. Depression of galena by sulphite adsorption is the most widely used method, sulphur dioxide, either as liquid or gas, being added to the bulk concentrate; sodium sulphite is less commonly used. In many cases, causticised starch is added in small amounts as an auxiliary depressant, but tends to depress the copper if insufficient sulphur dioxide is used. The sulphur dioxide reduces the pH to between 4 and 5.5, the slightly acidic conditions cleaning the surfaces of the copper minerals, thus aiding their floatability. Small amounts of dichromate may be added to the circuit to supplement lead depression.

In some plants, galena depression is aided by heating the slurry to about 40 °C by steam injection. Kubota et al. (1975) showed that galena can be completely depressed, with no reagent additions, by raising the slurry temperature above 60 °C, and this method is being used by the Dowa Mining Company in Japan (Anon., 1984b, 1984c). The xanthate adsorbed on the galena is removed, but that on the chalcopyrite surface remains. It is thought that preferential oxidation of the galena surface at high temperature is the mechanism for depression. At Woodlawn in Australia, the lead concentrate originally assayed 30% Pb, 12% Zn, 4% Cu, 300 ppm Ag, and 20% Fe, and received very unfavourable smelter terms (Burns et al., 1982). Heat treatment of the concentrate at 85 °C for 5 min, followed by reverse flotation, gave a product containing 35% Pb, 15% Zn, 2.5% Cu, 350 ppm Ag, and 15% Fe, with improved sales terms.

At the Brunswick Mining concentrator in Canada (McTavish, 1980) (Figure 12.72), the bulk copper–lead concentrate is conditioned for 20 min with 0.03 kg t^{-1} of a wheat dextrine–tannin extract

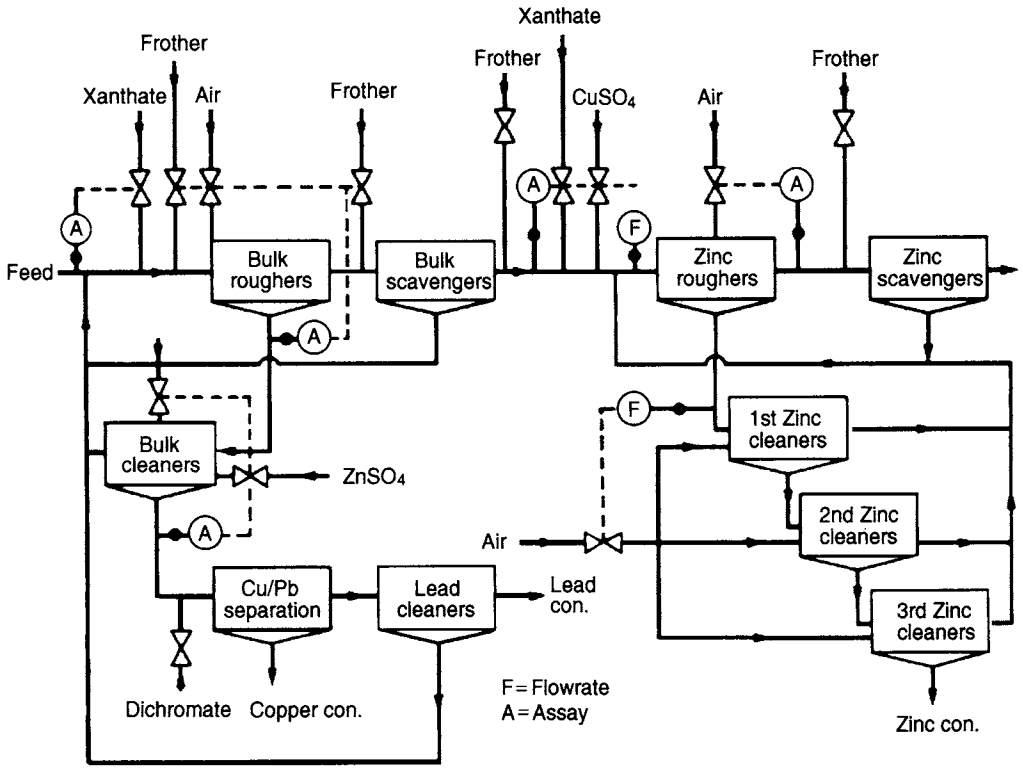


Figure 12.71 Vihanti flotation circuit

mixture to depress the galena, and $0.03\,kg\,t^{-1}$ of activated carbon to absorb excess reagents and contaminants, and then the pH is lowered to 4.8 with liquid SO_2. The slurry is further conditioned for 20 min at this low pH, then $0.005\,kg\,t^{-1}$ of thionocarbamate is added to float the copper minerals. The rougher concentrate is heated by steam injection to 40 °C, and is then cleaned three times to produce a copper concentrate containing 23% Cu, 6% Pb, and 2% Zn. The lead concentrate produced is further upgraded by regrinding the copper separation tails, and then heating the slurry with steam to 85 °C, and conditioning for 40 minutes. Xanthate and dithiophosphate collectors are then added to float pyrite. The rougher concentrate produced is reheated to 70 °C and is cleaned once. The hot slurry from the lead upgrading tailing contains about 32.5% Pb, 13% Zn, and 0.6% Cu, and, after cooling, is further treated to float a lead–zinc concentrate, leaving a final lead concentrate of 36% Pb and 8% Zn.

In general, where the ratio of lead to copper in the bulk concentrate is less than unity, depression of the copper minerals by sodium cyanide may be preferred. Where standard cyanide solution may cause unacceptable dissolution of precious metals and small amounts of secondary copper minerals, a cyanide–zinc complex can sometimes be used to reduce these losses. At Morococha in Peru (Pazour, 1979), a mixture of sodium cyanide, zinc oxide, and zinc sulphate has been used, allowing a recovery of 75% of the $120\,g\,t^{-1}$ of silver in the ore.

Close alkalinity control is necessary when using cyanides, a pH of between 7.5 and 9.5 commonly being used, although the optimum value may be higher, dependent on the ore. Cyanide depression is not used if economic quantities of chalcocite or covellite are present in the bulk concentrate, since it has little depressing action on these minerals. As cyanide is a very effective sphalerite depressant, most of the zinc reporting to the bulk concentrate is depressed into the copper concentrate, which may incur smelter penalties. Cyanide, however, has little action on galena, allowing effective flotation of the galena from the chalcopyrite, and hence a low

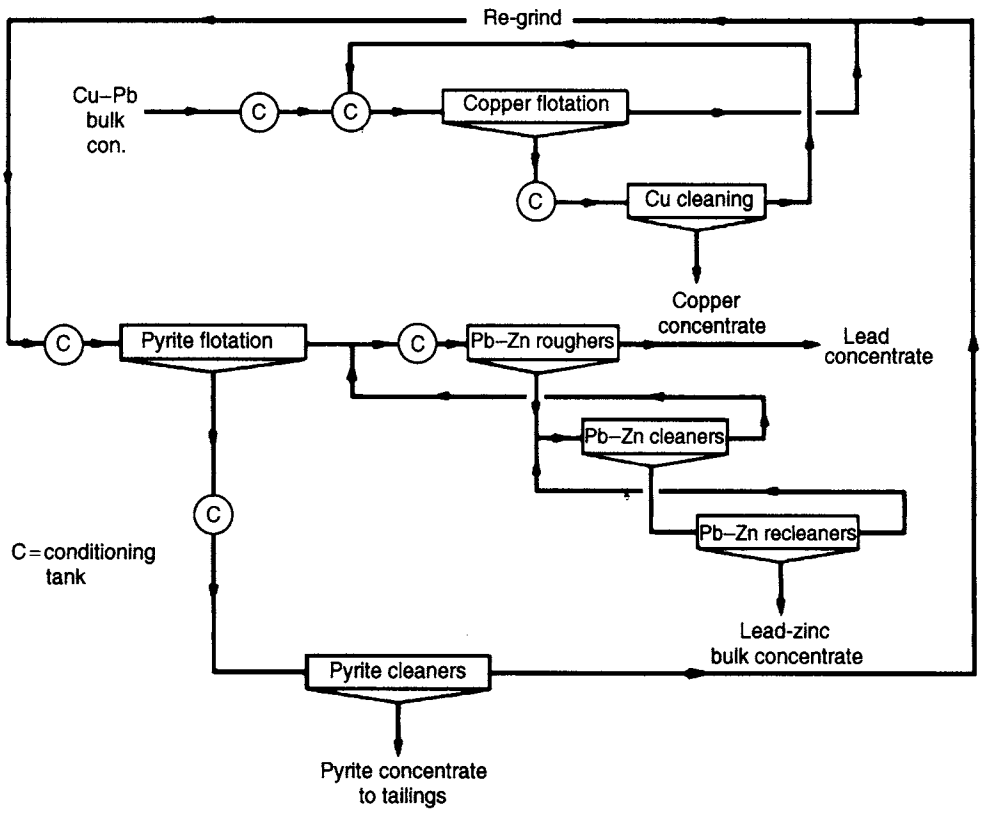


Figure 12.72 Brunswick mining flotation circuit

lead–copper concentrate. Lead is never paid for in a copper concentrate, and is often penalised.

In a few cases, adequate metallurgical performance cannot be achieved by semi-bulk flotation, and sequential selective flotation must be performed. This necessarily increases capital and operating costs, as the bulk of the ore – the gangue minerals – is present at each stage in separation, but it allows selective use of reagents to suit the mineralogy at each stage. The general flowsheet for sequential flotation involves conditioning the slurry with SO_2 at low pH (5–7), and using a selective collector such as ethyl xanthate, dithiophosphate, or thionocarbamate, which allows a copper concentrate which is relatively low in lead to be floated. The copper tailings are conditioned with lime or soda ash, xanthate, sodium cyanide, and/or zinc sulphate, after which a lead concentrate is produced, the tailings being treated with copper sulphate prior to zinc flotation.

Sequential separation is required where there is a marked difference in floatability between the copper and lead minerals, which makes bulk rougher flotation and subsequent separation of the minerals in the bulk concentrate difficult, as at the Black Mountain concentrator in South Africa (Beck and Chamart, 1980). In Australia, sequential separation was performed at Cobar Mines Ltd (Seaton, 1980). Metallurgical development at Woodlawn in Australia was an ongoing process. The original circuit, designed to depress lead with dichromate, was never effective for various reasons, and a combination of bulk and sequential flotation was then used (Roberts et al., 1980; Burns et al., 1982). The feed, containing roughly 1.3% Cu, 5.5% Pb, and 13% Zn, was conditioned with SO_2, starch, sodium metabisulphite and a dithiophosphate collector, after which a copper concentrate was produced, which was cleaned twice. The copper tailings were conditioned with lime, NaCN, starch, and sodium secondary butyl xanthate, prior to flotation of a lead concentrate which contained the less floatable copper minerals. This concentrate was reverse cleaned by steam heating to 85 °C prior

to flotation of the copper minerals with no further reagent addition. The floated copper minerals were pumped to the initial copper cleaning circuit. Lead rougher tailings fed the zinc roughing circuit.

Flotation of nickel ores

Nickel is produced from two main sources: sulphidic ores and lateritic ores. While 70% of the land-based nickel resources are contained in lateritic deposits, the majority of the world's current production of nickel still comes from sulphidic sources (Bacon et al., 2000). The dominant nickel mineral in these deposits is pentlandite – $(NiFe)_9S_8$. However, many ores also have minor amounts of millerite (NiS) and violarite (Ni_2FeS_4). Nickel can also be found within the pyrrhotite (Fe_8S_9) lattice (substitute for iron). In some cases in the Sudbury area deposits of Canada, about 10% of the nickel is in the pyrrhotite (Kerr, 2002). Depending on the downstream smelting requirements, nickel flotation can occur as two processes: bulk sulphide flotation (e.g. in Western Australia's nickel operations) or separate pyrrhotite flotation (e.g. Canada's Sudbury area). In addition to iron sulphides, nickel often occurs with economic concentrations of copper (Sudbury), cobalt (Western Australia), and precious metals such as gold, platinum, palladium, rhodium, ruthenium, iridium, and osmium (Noril'sk operation in north west Siberia, and in the Bushveld Complex in South Africa).

A good review of six of the current major nickel flotation operations is given by Kerr (2002), which covers typical Sudbury area operations as well as operations in Western Australia (Mt Keith) and Russia (Noril'sk).

Flotation of platinum ores

Platinum is one of the Platinum Group Metals (PGMs), which also include palladium, iridium, osmium, rhodium, and ruthenium. They are generally found together in economic ores, and 90% of PGM production comes from South Africa and Russia. In 2004, 44% of platinum was used in catalysts for motor vehicle emission control, and 33% in jewellery. The PGMs are classed with gold and silver as precious metals.

There are three main types of PGM deposit: PGM-dominant (e.g. the Bushveld Igneous Complex in South Africa), Ni–Cu dominant (e.g. Sudbury in Canada and Noril'sk in Russia) and miscellaneous. PGMs are usually recovered by flotation as a bulk low-grade sulphide concentrate, followed by smelting and refining.

There are over 100 known PGMs including sulphides, tellurides, antimonides, arsenides, and alloys. Each of these has a unique metallurgical behaviour, and the mode of occurrence and grain size considerably varies according to location (Corrans et al., 1982). The mineral association and gangue minerals present specific challenges to flotation that affect downstream processing, e.g. talc (Shortridge et al., 2000) and chromite (Wesseldijk, 1999). Typical reagent suites include thiol collectors (xanthate, in some cases with co-collectors dithiophosphate or dithoicarbamate); in some cases, copper sulphate is added as an activator; polymeric depressants such as guar or carboxymethyl cellulose are added to inhibit recovery of naturally floatable talcaceous gangue (Wiese et al., 2005).

The wide range of valuable mineral densities in PGM ores presents problems in conventional classification in grinding circuits, so the South African flotation concentrators sometimes employ combined milling and flotation circuits without classification (Snodgrass et al., 1994). Flash flotation and preconcentration by DMS or gravity are also used.

Flotation of iron ore

Iron ore minerals such as goethite and hematite are floated by collectors such as amines, oleates, sulphanates, or sulphates. Processing involves preconcentration by gravity or magnetic separation, followed by flotation. Iron ore flotation has increased in importance due to market requirements for higher grade products. This requires the flotation of silicate impurities from the iron ore. Amines are commercially used for the flotation of silica from magnetite ore at the Kudremukh Iron Ore Company Ltd, India, and in many other parts of the world (Das et al., 2005).

The requirement for higher grade product has seen an increase in the use of flotation columns in iron ore treatment. In Brazil, all new iron ore concentration circuits commissioned since

the 1990s have consisted of rougher–cleaner–scavenger column-only configurations (Araujo, et al. 2005).

Flotation of coal

Unlike metalliferous flotation, where all of the product is treated by flotation, in coal treatment only a portion is treated. This is typically 10 to 25% of the feed tonnage and represents the fines portion, usually below 250 μm in size, but sometimes up to 1 mm. Mining production methods, in particular the increased use of longwall mining, has resulted in an increase in fines production and made the flotation of coal fines more economically viable. In many countries environmental legislation has limited the amount of coal that can be sent to tailing ponds, with flotation being the only effective way to recover this coal.

Flotation circuits in coal processing are relatively simple with roughing and scavenging flotation used. Sometimes roughing alone is adequate. The mass recovery in coal flotation is high (up to 70%) and frother usage rates can be high to keep the froth mobile. Many flotation circuits use mechanical paddles to physically remove the heavy froth from the flotation cells. Petrochemical products are usually used as collectors with the most common used being diesel oil, liquid paraffin, and kerosene.

Coal operations can produce one of two products, depending on the quality of coal mined, these being either high value coking coal for pyrometallurgical industries or lower value thermal coal for power generation. Coking coal product demands few impurities and the ash content (non-combustible content) is typically between 5 and 8%. Often coking coals require washing and this has seen flotation machines such as the Jameson Cell and flotation columns increasingly used. Flotation concentrates for thermal coals range from 8 to 14%. Often this can be achieved without froth washing and mechanical flotation cells are still commonly used (Nicol, 2000).

References

Ackerman, P.K., et al. (1984). Effect of alkyl substituents on performance of thionocarbamates as copper sulphide and pyrite collectors, in *Reagents in the Minerals Industry*, ed. M.J. Jones and R. Oblatt, IMM, London, 69.

Ackerman, P.K., et al. (1986). Importance of reagent purity in evaluation of flotation collectors, *Trans. Instn. Min. Metall.*, **95**(Sept.), C165.

Adam, K. and Iwasaki, I. (1984). Effects of polarisation on the surface properties of pyrrhotite, *Minerals and Metallurgical Processing*, **1**(Nov.), 246.

Adkins, S.J. and Pearse, M.J. (1992). The influences of collector chemistry on kinetics and selectivity in base-metal sulphide flotation, *Minerals Engineering*, **5(3–5)**, 295.

Agar, G.E. (1984). Copper sulphide depression with thioglycollate and thiocarbonate, *CIM Bull.*, **77** (Dec.), 43.

Agar, G.E. (1985). The optimization of flotation circuit design from laboratory rate data, in *Proc. XVth Int. Min. Proc. Cong.*, 2, Cannes, 100.

Agar, G.E. and Kipkie, W.B. (1978). Predicting locked cycle flotation test results from batch data, *CIM Bull.*, **71** (Nov.), 119.

Agar, G.E., et al. (1980). Optimising the design of flotation circuits, *CIM Bull.*, **73**, 173.

Agar, G.E., et al. (eds) (1991). *Column '91* CANMET.

Ahmed, N. and Jameson, G.J. (1989). Flotation kinetics, *Mineral Processing and Extractive Metallurgy Review*, **5(1–4)**, 77.

Alexander, D.J., Runge, K.C., Franzidis, J.P., and Manlapig, E.V. (2000). The application of multi-component floatability models to full scale flotation circuits, *7th Mill Operators Conference*, Aus. IMM Kalgoorlie, Australia (Oct.), 167–178.

Andrews, P.R.A. (1990). Review of developments in cassiterite flotation in respect of physico-chemical considerations, *Minerals, Materials and Industry*, IMM, London, 345.

Anon. (1977). Swedish mills-flowsheets, operating data, *World Mining*, **30**(Oct.), 137.

Anon. (1980). Bleikvassli and Mofjell, *Mining Mag.* (Nov.), 427.

Anon. (1984a). Kamioka mine, *Mining Mag.* (Nov.), 387.

Anon. (1984b). Kosaka mine and smelter, *Mining Mag.* (Nov.), 403.

Anon. (1984c). Hanaoka mine, *Mining Mag.* (Nov.), 414.

Anon. (1986a). Phosphates-a review of processing techniques, *World Mining Equip.*, **10**(Apr.), 40.

Anon. (1986b). Flash flotation, *Int. Mining*, **3**(May), 14.

Aplan, F.F. and Chander, S. (1987). Collectors for sulphide mineral flotation, in *Reagents in Mineral Technology*, ed. P. Somasundaran and B. Moudgil, Marcel Dekker, New York, 335.

Araujo A.C., Vianna R.P.M., and Peres A.E.C. (2005). Flotation machines in Brazil – columns vs mechanical cells, in *Proc. Centenary of Flotation Symp.*, ed. Jameson G., Aus. IMM Brisbane (Jun.), 187–192.

Arbiter, N. and Harris, C.C. (1962). Flotation machines, *Froth Flotation 50th Anniversary Volume*, AIMME, New York, 347.

Arsentiev V.A., Dendyak T.V., and Korlovsky S.I. (1988). The effect of synergism to improve the efficiency of nonsulfide ores flotation, *Proc. 16th Int. Mineral Proc. Cong.*, ed. Forssberg K., Elsevier, Part B, 1439–1449.

Avotins, P.V., Wang, S.S., and Nagaraj, D.R. (1994). Recent advances in sulfide collector development, in *Reagents for Better Metallurgy*, ed. P.S. Mulukutla, SME, Inc., Littleton.

Bacon, W., Dalvi, A., and Parker, M. (2000). Nickel Outlook – 2000 to 2010, *Mining Millenium 2000.*

Baldauf, H., et al. (1985). Alkane dicarboxylic acids and aminoaphthol sulphonic acids a new reagent regime for cassiterite flotation, *Int. J. Min. Proc.*, **15**(Aug.), 117.

Barbery, G. (1986). Complex sulphide ores: Processing options, in *Mineral Processing at a Crossroads- problems and prospects*, ed. B.A. Wills and R.W. Barley, Martinus Nijoff Publishers, Dordrecht, 157.

Barbery, G., et al. (1980). Exploitation of complex sulphide deposits: A review of processing options from ore to metals, in *Complex Sulphide Ores*, ed. M.J. Jones, IMM, 135.

Barbian, N., Hadler, K., Ventura-Medina, E., and Cilliers, J.J. (2005). The froth stability column: Linking froth stability and flotation performance, *Minerals Engineering*, **18(3)**, Mar. 317–324.

Beck, R.D. and Chamart, J.J. (1980). The Broken Hill concentrator of Black Mountain Mineral Development Co. (Pty) Ltd., South Africa, in *Complex Sulphide Ores*, ed. M.J. Jones, IMM, 88.

Bergh, L.G. and Yianatos, J.B. (1993). Control alternatives for flotation columns, *Minerals Engineering*, **6(6)**, 631.

Bergmann, A. and Haidlen, U. (1985). Economical aspects of bulk and selective flotation, in *Flotation of Sulphide Minerals*, ed. K.S.E. Forssberg, Elsevier, Amsterdam.

Beyzavi, A.N. (1985). A contribution to scheelite flotation, taking particularly into account calcite-bearing scheelite ores, *Erzmetall*, **38**(Nov.), 543.

Bradshaw, D.J. (1997). *Synergistic Effect between Thiol Collectors used in the Flotation of Pyrite.* PhD Thesis, University of Cape Town, South Africa.

Bradshaw, D. and O'Connor, C. (1996). Measurement of the sub-process of bubble loading in flotation, *Minerals Engineering,* **9** (4), 443–448.

Bradshaw, D.J., Oostendorp, B., and Harris, P.J. (2005). Development of methodologies to improve the assessment of reagent behaviour in flotation with particular reference to collectors and depressants, *Minerals Engineering*, **18(2)**, 239–246.

Broekaert, E., et al. (1984). New processes for cassiterite ore flotation, in *Mineral Processing and Extractive Metallurgy*, ed. M.J. Jones and P. Gill, IMM, London, 453.

Broman, P.G., et al. (1985). Experience from the use of SO_2 to increase the selectivity in complex sulphide ore flotation, in *Flotation of Sulphide Minerals*, ed. K.S.E. Forssberg, Elsevier, Amsterdam, 277.

Buckley, A.N. and Woods, R. (1997). Chemisorption – the thermodynamically favoured process in the interaction of thiol collectors with sulphide, *International Journal of Mineral Processing*, **51**, 15–26.

Buckley, A.N., et al. (1985). Investigation of the surface oxidation of sulphide minerals by linear potential sweep voltammetry and X-ray photoelectron spectroscopy, *Flotation of Sulphide Minerals*, ed. K.S.E. Forssberg, Elsevier, Amsterdam, 41.

Burger, J.R. (1984). Chile: World's largest copper producer is expanding, *Engng. Min. J.*, **185**(Nov.), 33.

Burgess, F., Reemeyer, L., Spagnolo, M., Ashley, M., and Brennan, D. (2003). Ramp up of the Pasminco Century Concentrator to 500 000 tpa zinc metal production in concentrate, in *Proceedings of Aus. IMM Eighth Mill Operators Conference*, Aus. IMM: Melbourne Townsville, Australia, 22–23 (Jul.), 153–163.

Burns, C.J., et al. (1982). Process development and control at Woodlawn Mines, *14th Int. Min. Proc. Cong.*, Paper IV-18, CIM, Toronto, Canada, Oct.

Cases, J.M. (1980). Finely disseminated complex sulphide ores, in *Comple Sulphide Ores*, ed. M.J. Jones, IMM, 234.

Cecile, J.L., et al. (1980). Galena depression with chromate ions after flotation with xanthates: A kinetic and spectrometry study, in *Complex Sulphide Ores*, ed. M.J. Jones, IMM, 159.

Chander, S. (1985). Oxidation/reduction effects in depression of sulphides – a review, *Minerals and Metallurgical Processing*, **2**(Feb.), 26.

Chander, S. (1988a). Electrochemistry of sulfide mineral flotation, *Minerals and Metallurgical Processing*, **5**(Aug.), 104.

Chironis, N.P. (1986). Cell creates microbubbles to latch on to finer coal, *Coal Age*, **91**(Aug.), 62.

Cienski, T. and Coffin, V. (1981). Column flotation operation at Mines Gaspé molybdenum circuit, *Can. Min. J.*, **102**(Mar.), 28.

Clayton, R., Jameson, G.J., and Manlapig, E.V. (1991). The development and application of the Jameson cell, *Minerals Engineering*, **4(7–11)**, 925.

Clingan, B.V. and McGregor, D.R. (1987). Column flotation experience at Magma Copper Co. *Minerals and Metallurgical Processing*, **4**(Aug.), 121.

Coleman, R. and Napitupulu, P. (1997). Freeport's fourth concentrator – a large step towards the 21st century, *Aus. IMM 6th Mill Operators Conference*, Madang, New Guinea (Oct.), 17–21.

Collins, D.N., et al. (1984). Use of alkyl iminobis-methylene phosphonic acids as collectors for oxide and salt-type minerals, in *Reagents in the Minerals Industry*, ed. M.J. Jones and R. Oblatt, IMM, London, 1.

Corrans, I.J., Brugman, C.F., Overbeek, P.W., and McRae, L.B. (1982). The recovery of platinum group

metals from ore of the UG2 Reef in the Bushveld Complex, in *XIIth CMMI Congress*, ed. H.W. Glen, SAIMM, Johannesburg, South Africa, 629–634.

Cowburn, J.A., Stone, R., Bourke, S., and Hill, B. (2005). Design developments of the Jameson Cell, in *Proc. Centenary of Flotation Symp.*, ed. Jameson G., Aus. IMM Brisbane (Jun.), 193–200.

Crawford, R. and Ralston, J. (1988). The influence of particle size and contact angle in mineral flotation, *Int. J. Min. Proc.*, **23**, 1–24.

Crozier, R.D. (1984). Plant reagents. Part 1: Changing pattern in the supply of flotation reagents, *Mining Mag.* (Sept.), 202.

Crozier, R.D. (1986). Codelo's development plans for Chuquicamata and El Teniente, *Mining Mag.*, **155**(Nov.), 460.

Crozier, R.D. (1990). Non-metallic mineral flotation, *Industrial Minerals*, (Feb.), 55.

Crozier, R.D. (1991). Sulphide collector mineral bonding and the mechanism of flotation, *Minerals Engineering*, **4(7–11)**, 839.

Crozier, R.D. (1992). *Flotation: Theory, Reagents and Testing*, Pergamon Press, Oxford.

Crozier, R.D. and Klimpel, R.R. (1989). Frothers: plant practice. *Mineral Processing and Extractive Metallurgy Review*, **5(1–4)**, 257.

Cubillos, F.A. and Lima, E.L. (1997). Identification and optimizing control of a rougher flotation circuit using an adaptable hybrid-neural model, *Minerals Engineering.*, **10 (7)**, Jul., 707–721.

Das, B., Prakash, S., Biswal, S.K., Reddy, P.S.R., and Misra, V.N. (2005). Studies on the beneficiation of iron ore slimes using the flotation technique, *Proceedings of Centenary of Flotation Symposium*, Aus. IMM: Melbourne Brisbane, Qld, 6–9 Jun. (CD ROM) 737–742.

Dayton, S. (1979). Chile: Where major new copper output can materialise faster than any place else, *Engng. Min. J.*, **180**(Nov.), 68.

Deng, T. and Chen, J. (1991). Treatment of oxidized copper ores with emphasis on refractory ores, *Mineral Processing and Extractive Metallurgy Review*, **7(3–4)**, 175.

Dowling, E.C., et al. (1985). Model discrimination in the flotation of a porphyry copper ore, *Minerals and Metallurgical Proces*sing, **2**(May), 87.

Edwards, R. and Atkinson, K. (1986). *Ore Deposit Geology*, Chapman and Hall, London.

Fairweather, M.J. (2005). The Sullivan concentrator – the last (and best) 30 years, in *Proc. Centenary of Flotation Symp.*, ed. G. Jameson, Aus. IMM Brisbane (Jun.), 835–844.

Fee, B.S. and Klimpel, R.R. (1986). pH regulators, in *Chemical Reagents in the Minerals Industry* ed. D. Malhotra and W.F. Riggs, SME Inc., Littleton, 119.

Feteris, S.M., Frew, J.A., and Jowett, A., 1987. Modelling the effect of froth depth in flotation, *Int. J. Min. Proc.*, **20**, 121–135.

Fewings, J.H., Slaughter, P.J., Manlapig, E.V., and Lynch, A.J. (1979). The dynamic behaviour and automatic control of the chalcopyrite flotation circuit at Mount Isa Mines Ltd., *Proc. XIIIth Int. Min. Proc. Cong.*, Warsaw, 405.

Finch, E. and Riggs, W.F. (1986). Fatty acids – a selection guide, in *Chemical Reagents in the Minerals Industry*, ed. D. Malhotra and W.F. Riggs, SME Inc., Littleton, 95.

Finch, J.A. and Dobby, G.S. (1990). *Column Flotation*, Pergamon Press, Oxford.

Finch, J.A., Kitching, R., and Robertson, K.S. (1979). Laboratory simulation of a closed-circuit grind for a heterogeneous ore, *CIM Bull.*, **72**(Mar.), 198.

Firth, B.A. (1999). Australian coal flotation practices, *Advances in flotation technology*, Parekh, B. K., Miller J.D. (eds), SME.

Fuerstenau, D.W. (1988). Flotation science and engineering advances and challenges, *Proc. XVI International Mineral Processing Congress*, Stockholm, ed. K.S.E. Forssberg, Vol. A, Elsevier, Amsterdam, 63.

Fuerstenau, D.W. and Raghavan, S. (1986). Surface chemical properties of oxide copper minerals, in *Advances in Mineral Processing*, ed. P. Somasundaran, Chapter 23, SME Inc., Littleton, 395.

Fuerstenau, M.C. and Somasundaran, S. (2003). Flotation, in *Principles of Mineral Processing*, ed. M.C. Fuerstenau and K.N. Han, Soc for Mining, Metallurgy and Exploration Inc., SME, Colorado, USA.

Fuerstenau, D.W., Li, C., and Hanson, J.S. (1991). Enhancement of fine hematite flotation by shear flocculation and carrier flotation, *Proc. XVII Int. Min. Proc. Cong.*, Dresden, Vol. 2, 169.

Fuerstenau, D.W., et al. (1985). Sulphidization and flotation behaviour of anglesite, cerussite and galena, in *Proc. XVth Int. Min. Proc. Cong.*, 2, Cannes, 74.

Fuerstenau, M.C., et al. (1985). *Chemistry of Flotation*, AIMME, New York.

Fuerstenau, M.C., et al. (1986). Flotation behaviour of chromium and manganese minerals, in *Advances in Mineral Processing*, ed. P. Somasundaran, Chapter 17, SME Inc., Littleton, 289.

Gaudin, A.M. (1957). *Flotation*, McGraw-Hill, New York.

Gefvert, D.L. (1986). Cationic flotation reagents for mineral beneficiation, in *Chemical Reagents in the Minerals Industry*, ed. D. Malhotra and W.F. Riggs, SME Inc., Littleton, 85.

Glembotskii, V.A., Klassen, V.I., and Plaksin, I.N. (1972). *Flotation*, Primary Sources, New York.

Goh, S.W., Buckley, A.N., Lamb, R.N., and Woods, R. (2005). Distinguishing monolayer and multilayer adsorption of thiol collectors with ToF-SIMS and XPS, in *Proc. Centenary of Flotation Symp.*, ed. G. Jameson, Aus. IMM Brisbane (Jun.), 439–448.

Gorain, B.K., Franzidis, J.P., and Manlapig, E.V. (1996). Studies on impeller type, impeller speed and air flow

rate in an industrial flotation cell – Part 3. Effect on superficial gas velocity, *Minerals Engineering*, **9**, 639–654.

Gorain, B.K., Franzidis, J.P., and Manlapig, E.V. (1997). Studies on impeller type, impeller speed and air flow rate in an industrial flotation cell – Part 4. Effect of bubble surface area flux on flotation performance, *Minerals Engineering*, **10**, 367–379.

Gorain, B.K., Franzidis, J.P, and Manlapig, E.V. (1999). The empirical prediction of bubble surface area flux in mechanical flotation cells from cell design and operating data, *Minerals Engineering*, **12**, 309–322.

Gray, P.M.J. (1984). Metallurgy of the complex sulphide ores, *Mining Mag.* (Oct.), 315.

Greet, C.J., Kinal, J., and Steinier, P. (2005). Grinding media – its effect on pulp chemistry and flotation behaviour – fact or fiction, in *Proc. Centenary of Flotation Symp.*, ed. G. Jameson, Aus. IMM Brisbane (Jun.), 967–972.

Guy, P.J. and Trahar, W.J. (1985). The effects of oxidation and mineral interaction on sulphide flotation, in *Flotation of Sulphide Minerals*, ed. K.S.E. Forssberg, Elsevier, Amsterdam, 91.

Harbort, G.J., Manlapig, E.V., and DeBono, S.K. (2002). Particle collection within the Jameson Cell downcomer, *Trans IMM*, Sec. C 111/*Proc. Aus. IMM*, 307, Jan.–Apr., C1–C10.

Harbort, G.J., et al. (1994). Recent advances in Jameson flotation cell technology, *Minerals Engineering*, **7(2/3)**, 319.

Hardwicke, G.B., et al. (1978). Granby Mining Corporation, in *Milling Practice in Canada*, CIM Special Vol., 16.

Harris, C.C. (1976). Flotation machines, in *Flotation: A. M. Gaudin Memorial Volume*, AIMME, New York, 753.

Harris, P.J. (1982). Frothing phenomena and froths, in *Principles of Flotation*, ed. R.P. King., S. Afr. Inst. Min. Metall., Johannesburg.

Harris, M.C., Runge, K.C., Whiten, W.J., and Morrison, R.D. (2002). JKSimFloat as a practical tool for flotation process design and optimisation, *SME Mineral Processing Plant Design, Practice and Control Conference*, Vancouver, Canada (Oct.), 461–478.

Hart, B., Biesinger, M., and Smart, R. St. C. (2005). Improved statistical methods applied to surface chemistry in minerals flotation, in *Proc. Centenary of Flotation Symp.*, ed. Jameson, G., Aus. IMM Brisbane, (Jun.), 457–465.

Hartarti, F., Mular, M., Stewart, A., and Gorken, A. (1997). Increased gold recovery at PT Freeport Indonesia using Aero 7249 promoter, *Proc. Sixth Mill Operators Conference*, Aus. IMM, Madang, PNG, 165–168.

Hatfield, D., Robertson, C., Burdukova, L., Harris, P., and Bradshaw, D. (2004). Evaluation of the effect of depressants on froth structure and flotation performance of a platinum bearing ore, *2004 SME Annual Meeting*, Denver, 1, 23–25 Feb., Preprint no. 04–186.

Heimala, S., et al. (1988). Flotation control with mineral electrodes, *Proc. XVI International Mineral Processing Congress*, Stockholm, ed. K.S.E. Forssberg, Vol. B, 1713, Elsevier, Amsterdam.

Hemmings, C.E. (1980). An alternative viewpoint on flotation behaviour of ultrafine particles, *Trans. Inst. Min. Metall.*, **89**(Sept.), C113.

Herbst, J.A., et al. (1986). Strategies for the control of flotation plants, in *Design and Installation of Concentration and Dewatering Circuits*, ed. A.L.Mular and M.A. Anderson, Chapter 36, SME Inc., Littleton, 548.

Hernandez-Aguilar, J.R., Gomez, C.O., and Finch, J.A. (2002). A technique for the direct measurement of bubble size distributions in industrial flotation cells, *Proc. 34th Annual Meeting of the Canadian Mineral Processors of CIM*, Ottawa,(Jan.), 389–402.

Holme, R.N. (1986). Sulphonate-type flotation reagents. *Chemical Reagents in the Minerals Industry*, ed. D. Malhotra and W.F. Riggs, SME Inc., Littleton, 99.

Holtham, P.N. and Nguyen, K.K. (2002). On-line analysis of froth surface in coal and mineral flotation using JKFrothCam, *Int. J. Min. Proc.*, **14 (2–3)**, Mar., 163–180.

Hope, G.A., Woods, R., Parker, G.K., Watling, K.M., and Buckley, F.M. (2005). Spectroelectrochemical Raman studies of flotation-reagent – surface interaction, in *Proc. Centenary of Flotation Symp.*, ed. Jameson, G., Aus. IMM Brisbane (Jun.), 473–481.

Houot, R. (1983). Beneficiation of iron ore by flotation, *Int. J. Min. Proc.*, **10**, 183.

Houot, R., et al. (1985). Selective flotation of phosphatic ores having a siliceous and/or a carbonated gangue, *Int. J. Min. Proc.*, **14**(Jun.), 245.

Hoyack, M.E. and Raghavan, S. (1987). Interaction of aqueous sodium sulphite with pyrite and sphalerite, *Trans. Inst. Min. Metall.*, **96**(Dec.), C173.

Hsieh, S.S. and Lehr, J.R. (1985). Beneficiation of dolomitic Idaho phosphate rock by the TVA diphosphonic acid depressant process, *Minerals and Metallurgical Processing*, **2**(Feb.), 10.

Imre, U. and Castle, J.F. (1984). Exploitation strategies for complex Cu-Pb-Zn orebodies, in *Mineral Processing and Extractive Metallurgy*, ed. M.J. Jones and P. Gill, IMM, London, 473.

Ives, K.J. (ed.) (1984). *The Scientific Basis of Flotation*, Martinus Nijoff Publishers, The Hague.

Iwasaki, I. (1983). Iron ore flotation, theory and practice, *Mining Engng.*, **35**(Jun.), 622.

Iwasaki, I. (1999). Iron ore flotation – Historical perspective, in *Advances in Flotation Technology*, ed. Parekh, B.K. and Miller, J.D. SME, Littleton, Colorado, 231–243.

Jiwu, M., et al. (1984). Novel frother-collector for flotation of sulphide minerals-CEED, in *Reagents in the*

Minerals Industry, ed. M.J. Jones and R. Oblatt, IMM, London, 287.

Johnson, N.W. (1972). The flotation behaviour of some chalcopyrite ores, PhD Thesis, University of Queensland.

Johnson, N.W. and Munro, P.D. (1988). Eh-pH measurements for problem solving in a zinc reverse flotation process, *The Aus.IMM Bulletin and Proceedings*, **293**(May), 53.

Johnson, N.W. and Munro, P.D. (2002). Overview of Flotation Technology and Plant Practice for Complex Sulphide Ores, *SME Mineral Processing Plant Design, Practice and Control Conference*, Vancouver, Canada (Oct.), 1097–1123.

Jones, M.H. and Woodcock, J.T. (1983). Decomposition of alkyl dixanthogens in aqueous solutions, *Int. J. Min. Proc.*, **10**, 1.

Jones, M.H. and Woodcock, J.T. (eds) (1984). *Principles of Mineral Flotation*, Australas. Inst. Min. Metall., Victoria.

Jordan, T.S., et al. (1986). Non-sulphide flotation: Principles and practice, in *Design and Installation of Concentration and Dewatering Circuits*, ed. A.L. Mular and M.A. Anderson, Chapter 2, SME Inc., Littleton, 16.

Jowett, A. (1966). Gangue mineral contamination of froth, *Brit. Chem. Eng.*, **2**, 330–333.

Kampjarvi, P. and Jamsa-Jounela, S-L. (2002). Level control strategies for flotation cells, *Proc. 15th Triennial World Cong.*, IFAC, Barcelona.

Kaya, M. and Laplante, A.R. (1991). Froth washing technology in mechanical flotation machines, *Proc. XVII Int. Min. Proc. Cong. Dresden*, Vol. 2, 203.

Kennedy, A. (1990). The Jameson flotation cell. *Mining Mag.*, **163**(Oct.), 281.

Kerr, A. (2002). An Overview of recent developments in flotation technology and plant practice for Nickel ores, *SME Mineral Processing Plant Design, Practice and Control Conference*, Vancouver, Canada (Oct.), 1142–1158.

King, R.P. (ed.) (1982). *The Principles of Flotation*, S. Afr. I.M.M.

Kittel, S., Galleguillos, P., and Urtubia, H. (2001). Rougher automation in Escondida flotation plant, *Annual Meeting of SME*, SME Denver, Feb.

Kirjavainen, V.M. and Laapas, H.R. (1988). A study of entrainment mechanism in flotation, *Proc. XVI Int. Mineral Processing Congress, Stockholm* ed. K.S.E. Forssberg Vol. A, Elsevier, Amsterdam, 665.

Kitzinger, F., Rosenblum, F., and Spira, P. (1979). Continuous monitoring and control of froth level and pulp density, *Mining Engng.*, **31**(Apr.), 310.

Klimpel, R.R. (1986). The industrial practice of sulphide mineral collectors. *Chemical Reagents in the Minerals Industry*, ed. D. Malhotra and W.F. Riggs, SME Inc., Littleton, 73.

Konigsman, K.V. (1985). Flotation techniques for complex ores, in *Complex Sulphides*, ed. A.D. Zunkel et al., TMS-AIME, Pennslyvania, 5.

Konigsman, K.V., Hendriks, D.W., and Daoust, C. (1976). Computer control of flotation at Mattagami Lake Mines, *CIM Bull.* (Mar.), 117.

Kubota, T., et al. (1975). A new method for copper lead separation by raising pulp temperature of the bulk float, *Proc. XIth Int. Min. Proc. Cong.*, Cagliari, Istituto di Arte Mineraria, Cagliari.

Labonte, G. and Finch, J.A. (1988). Measurement of electrochemical potentials in flotation systems, *CIM Bull.*, **81**(Dec.), 78.

Lacy, W.C. (1974). *Porphyry Copper Deposits*, Australian Mineral Foundation Inc.

Lane, G., Brindley, S., Green, S., and Mcleod, D. (2005). Design and engineering of flotation circuits (in Australia), in *Proc. Centenary of Flotation Symp.*, ed. G., Jameson, Aus. IMM Brisbane (Jun.), 127–140.

Laskowski, J.S. (1986). The relationship between flotability and hydrophobicity, in *Advances in Minerals Processing*, ed. P. Somarsundaran, SME, Littleton, Colorado, 189–208.

Laskowski, J.S. and Poling, G.W. (1995). *Processing of Hydrophobic Minerals and Fine Coal,* CIM, Montreal.

Laskowski, J., et al. (1985). Studies on the flotation of chrysocolla, *Mineral Proc. & Tech. Review*, **2**, 135.

Lawver, J.E., et al. (1984). New techniques in beneficiation of the Florida phosphates of the future, *Minerals and Metallurgical Processing*, **1**(Aug.), 89.

Learmont, M.E. and Iwasaki, I. (1984). Effect of grinding media on galena flotation, *Minerals and Metallurgical Processing*, **1**(Aug.), 136.

Leja, J. (1982). *Surface Chemistry of Froth Flotation*, Plenum Press, New York.

Lekki, J. and Laskowski, J. (1975). A new concept of frothing in flotation systems and general classification of flotation frothers, *Proc. 11th Int. Min.* Proc. Cong., Cagliari, 427.

Lelinski, D., Redden, L.D., and Nelson, M.G. (2005). Important considerations in the design of mechanical flotation machines. *Proc. Centenary of Flotation Symp.*, ed. G. Jameson, Aus. IMM Brisbane (Jun.), 217–224.

Lepetic, V.M. (1986). Cassiterite flotation: A review, in *Advances in Mineral Processing*, ed. P. Somasundaran, Chapter 19, SME Inc., Littleton, 343.

Lindgren, E. and Broman, P. (1976). Aspects of flotation circuit design, *Concentrates*, **1**, 6.

Liu, Q. and Laskowski, J.S. (1989). The role of metal-hydroxides at mineral surfaces in dextrin adsorption, II. Chalcopyrite-galena separations in the presence of dextrin, *Int. J. Min. Proc,* **27**(Sept.), 147.

Liu, Q. and Laskowski, J.S. (1999). Adsorption of polysaccharides onto sulphides and their use in sulphide flotation, in Polymers in the Mineral Processing Industry, ed. J.S. Laskowski, MetSoc., Canada, 71–88.

Luttrell, G.H. and Yoon, R.H. (1984). The collectorless flotation of chalcopyrite ores using sodium sulphide, *Int. J. Min. Proc.*, **13**(Nov.), 271.

Lynch, A.J., Johnson, N.W., Manlapig, E.V., and Thorne, C.G. (1981). *Mineral and Coal Flotation Circuits*, Elsevier Scientific Publishing Co., Amsterdam.

Mackenzie, M. (1986). Organic polymers as depressants, in *Chemical Reagents in the Minerals Industry*, ed. D. Malhotra and W.F. Riggs, SME Inc., Littleton, 139.

Malghan, S.G. (1986). Role of sodium sulphide in the flotation of oxidised copper, lead, and zinc ores, *Minerals and Metallurgical Processing*, **3**(Aug.) 158.

Malhotra, D., et al. (1986). Plant practice in sulphide flotation, in *Chemical Reagents in the Minerals Industry*, ed. D. Malhotra and W.F. Riggs, SME Inc., Littleton 21.

Malinovskii, V.A., et al. (1973). Technology of froth separation and its industrial applications, *Trans. 10th Int. Min. Proc. Cong.*, Paper 43, London.

Marabini, A. (1994). Advances in synthesis and use of chelating reagents in mineral flotation, in *Reagents for Better Metallurgy*, ed. P.S. Mulukutla, SME, Inc., Littleton.

Martin, C.J., et al. (1989). Complex sulphide ore processing with pyrite flotation by nitrogen, *Int. J. Min. Proc.*, **26**(Jun.), 95.

Martin, C.J., et al. (1991). Review of the effect of grinding media on flotation of sulphide minerals, *Minerals Engineering*, **4(2)**, 121.

McKay, J.D., et al. (1986). Column flotation of Montana chromite ore, *Minerals and Metallurgical Processing*, **3**(Aug.), 170.

McKee, D.J. (1986). Future applications of computers in the design and control of mineral beneficiation circuits, *Automation for Mineral Resource Development*, Pergamon Press, Oxford, 175.

McKee, D.J. (1991). Automatic flotation control – a review of the last 20 years of effort, *Minerals Engineering*, **4(7–11)**, 653–666.

McTavish, S. (1980). Flotation practice at Brunswick Mining, *CIM Bull.* (Feb.), 115.

Meenan, G.F. (1999). Modern coal flotation practices, Advances in Flotation Technology, ed. B.K. Parekh, and J.D. Miller, SME, Littleton, Colorado, 309–316.

Melo, F. and Laskowski, J.S. (2005). Fundamental properties of flotation frothers and their effect on flotation, in *Proceedings Centenary of Flotation Symposium*, Aus. IMM, Brisbane (6–9 Jun.), 347–354.

Mielczarski, J.A. and Mielczarski, E. (2005). Surface monitoring, understanding and modification at molecular level in mineral beneficiation by infrared external reflection spectroscopy, in *Proceedings Centenary of Flotation Symposium*, Aus. IMM, Brisbane (6–9 Jun.), 515–522.

Miettunen, J. (1983). The Pyhasalmi Concentrator – 13 years of computer control, *Proc. 4th IFAC Symp. on Automation in Mining, Mineral and Metal Processing*, Finnish Soc. Aut. Control, Helsinki, 391.

Miller, G. and Readett, D.J. (1992). The Mount Isa Mines Limited copper solvent extraction and electrowinning plant, *Minerals Engineering*, **5(10–12)**.

Mingione, P.A. (1984). Use of dialkyl and diaryl dithiosulphate promotors as mineral flotation reagents, in *Reagents in the Minerals Industry*, ed. M.J. Jones and R. Oblatt, IMM, London, 19.

Mori, S., et al. (1985). Kinetic studies of fluorite flotation. *Proc. XVth Int. Min. Proc. Cong.*, 3, Cannes, 154.

Moudgil, B.M. (1986). Advances in phosphate flotation, in *Advances in Mineral Processing*, ed. P. Somasundaran, Chapter 25, SME Inc., Littleton, 426.

Moudgil, B.M. and Barnett, D.H. (1979). Agglomeration-skin flotation of coarse phosphate rock, *Mining Engng.*, Mar., 283.

Moys, M.H. and Finch, J.A. (1988). Developments in the control of flotation columns, *Int. J. Min. Proc.*, **23**(Jul.) 265.

Murdock, D.J. and Wyslouzil, H.E. (1991). Large-diameter column flotation cells take hold, *Engng. Min. J.*, **192**(Aug.), 40.

Nagaraj, D.R. (1994). A critical assessment of flotation agents, in *Reagents for Better Metallurgy*, ed. P.S. Mulukutla, SME, Inc., Littleton.

Nagaraj, D.R., et al. (1986). Structure-activity relationships for copper depressants, *Trans. Inst. Min. Metall.*, **95**(Mar.), C17.

Nakazawa, H. and Iwasaki, I. (1985). Effect of pyrite-pyrrhotite contact on their flotabilities, *Minerals and Metallurgical Processing*, **2**(Nov.), 206.

Nicol, S.K. (2000). Fine coal beneficiation, in *Advanced Coal Preparation Monograph Series*, ed. A.R. Swanson, and A.C. Partridge, Vol IV, Part 9, Australian Coal Preparation Society.

Niitti, T. and Tarvainen, M. (1982). Experiences with large Outokumpu flotation machines, *Proc. XIVth Int. Min. Cong.*, Paper No. VI-7, CIM, Toronto, Canada, Oct.

Nummela, W. and Iwasaki, I. (1986). Iron ore flotation, in *Advances in Mineral Processing*, ed. P. Somasundaran, Chapter. 18, SME Inc., Littleton, 308.

Nyamekye, G.A. and Laskowski, J.S. (1993). Adsorption and electrokinetic studies on the dextrin sulfide mineral interactions, *J. Coll. Interf. Sci.*, **157**, 160–167.

Oberg, T.G. and Deming, S.N. (2000). Find optimun operating conditions fast, *Chem. Eng. Rogrell*, **96**(4), 53–60.

O'Connor, C.T. and Dunne, R.C. (1994). The flotation of gold-bearing ores – a review, *Minerals Engineering*, **7(7)**, 839.

Osborne, D.G. (1988). *Coal Preparation Technology*, Graham and Trotman Ltd, London.

Paakkinen, E. and Cooper, H.R. (1979). Flotation process control, in *Computer Methods for the 80's in the Minerals Industry*, ed. A. Weiss, AIMME, New York.

Parsonage, P.G. (1985). Effects of slime and colloidal particles on the flotation of galena, in *Flotation of Sulphide Minerals*, ed. K.S.E. Forssberg, Elsevier, Amsterdam, 111.

Partidge, A. and Smith, G. (1971). Small-sample flotation testing: A new cell, *Transactions of the Institute of Mining and Metallurgy*, **80**, C199–C200.

Pavlica, J., et al. (1986). Industrial application of ferrosulphate and sodium cyanide in depressing zinc minerals, in *Proc. 1st Int. Min. Proc. Symp.*, 1, Izmir, 183.

Pazour, D.A. (1979). Morococha-five product mine shows no sign of dying, *World Mining*, **32**(Nov.), 56.

Piantadosi, C., Jasieniak, M., Skinner, W.M., and Smart R., St. C. (2000). Statistical comparison of surface species in flotation concentrates and tails from TOF-SIMS evidence, *Minerals Engineering*, **13(13)**, Nov., 1377–1394.

Pradip (1988). Application of chelating reagents in mineral processing, *Minerals and Metallurgical Processing* **5**(May), 80.

Pugh, R.J. (1989). Macromolecular organic depressants in sulphide flotation – a review, 1. Principles, types and applications, *Int. J. Min. Proc.*, **25**(Jan.), 101.

Rahal, K.R., Franzidis, J.P., and Manlapig, E.V. (2000). Flotation plant modelling and simulation using the floatability characterisation test rig (FCTR), *Aus.IMM 7th Mill Operators Conference*, Kalgoorlie, Australia (Oct.).

Ralston, J. (1991). E_h and its consequences in sulphide mineral flotation, *Minerals Engineering*, **4(7–11)**, 859.

Ralston, J. and Newcombe, G. (1992). Static and dynamic contact angle, in *Colloid Chemistry in Mineral Processing*, ed. J.S. Laskowski and J. Ralston, Chapter 5, Elsevier, Amsterdam.

Ralston, J., Fornasiero, D., and Mishchuk (2001). The hydrophobic force in flotation – a critique, *Colloids and Surfaces A: Physicochemical and Engineering Aspects*, **192**, 39–51.

Ranney, M.W. (ed.) (1980). *Flotation Agents and Processes – Technology and Applications*, Noyes Data Corps., New Jersey.

Rao, S.R. (1971). *Xanthates and Related Compounds*, Marcel Dekker, New York.

Rao, S.R. (2004). *Surface Chemistry of Froth Flotation*, 2nd edition, Kluwer Academic/Plenum Publishers, New York.

Rao, K.H., Kundu, T., Parker, S.C., and Forssberg, K.S.E. (2005). Molecular modelling of mineral surface structures and adsorption phenomena in flotation, *In Proceedings Centenary of Flotation Symposium*, Aus. IMM, Brisbane (6–9 Jun.), 557–572.

Redeker, I.H. and Bentzen, E.H. (1986). Plant and laboratory practice in non-metallic mineral flotation, *Chemical Reagents in the Minerals Industry*, ed. D. Malhotra and W.F. Riggs, SME Inc., Littleton, 3.

Riggs, W.F. (1986). Frothers – an operator's guide, in *Chemical Reagents in the Minerals Industry* ed. D. Malhotra and W.F. Riggs, SME Inc., Littleton, 113.

Roberts, A.N., et al. (1980). Metallurgical development at Woodlawn Mines, Australia, in *Complex Sulphide Ores*, ed. M.J. Jones, IMM, 128.

Sastry, K.V.S. (1988). *Column Flotation '88* SME Inc., Littleton.

Savassi, O.N., Alexander, D.J., Manlapig, E.V., and Franzidis, J.P. (1998). An empirical model for entrainment in industrial flotation plants, *Minerals Engineering*, **11**, 243–256.

Schulze, H.J. (1984). *Physio-chemical Elementary Processes in Flotation*, Elsevier Science Publishing Co., Amsterdam.

Seaton, N.R. (1980). Copper-lead-zinc ore concentration at Cobar Mines Pty Ltd., Cobar, N. S. W., in *Mining and Metallurgical Practices in Australasia*, ed. J.T. Woodcock, Aust. IMM.

Senior, G.D. and Poling, G.W. (1986). The chemistry of cassiterite flotation, in *Advances in Mineral Processing*, ed. P. Somasundaran, Chapter 13, SME Inc., Littleton, 229.

Ser, F. and Nieto, J.M. (1985). Sphalerite separation from Cerro Colorado copper-zinc bulk concentrate, in *Proc. XVth Int. Min. Proc. Cong.*, 3, Cannes, 247.

Shaw, D.R. (1981). Dodecyl mercaptan: A superior collector for sulphide ores, *Mining Engng*, **33**(Jun.), 686.

Shergold, H.L. (1984). Flotation in mineral processing, in *The Scientific Basis of Flotation*, ed. K.J. Ives, Martinus Nijoff Publishers, The Hague, 229.

Shortridge, P.G., Harris, P.J., Bradshaw, D.J., and Koopal, L.K. (2000). The effect of chemical composition and molecular weight of polysaccharide depressants on the flotation of talc, *International Journal of Mineral Processing*, **59**, 215–224.

Shin, B.S. and Choi, K.S. (1985). Adsorption of sodium metasilicate on calcium minerals, *Minerals and Metallurgical Processing*, **2**(Nov.), 223.

Shirley, J. and Sutolov, A. (1985). Byproduct molybdenite, in *SME Mineral Processing Handbook*, ed. N.L. Weiss, Section 16–17(2), AIMME.

Singh, A., Louw, J.J., and Hulbert, D.G. (2003). Flotation stabilization and optimization, *J. South African Inst. Mining and Met.*, **103(9)**, Nov., 581–588.

Sisselman, R. (1978). Chile's Chuquicamata: Looking to stay no. 1 in copper output, *Engng. Min. J.*, **8**(Aug.), 59.

Sivamohan, R. (1990). The problem of recovering very fine particles in mineral processing a review, *Int. J. Min. Proc.*, **28(3/4)** May, 247.

Smeink, R.G., Leerdam van, G.C., and Mahy. J.W.G. (2005). Determination of preferential adsorption of Depramin® on mineral surfaces by ToF-SIMS, *Minerals Engineering*, **18(2)** Feb., 247–255.

Smith, R.W. (1989). Structure-function relationships of long chain collectors, in *Challenges in Mineral*

Processing, ed. K.V.S. Sastry and M.C. Fuerstenau, SME, Inc., Littleton, 51.

Smith, P.G. and Warren, L.J. (1989). Entrainment of particles into flotation froths, in *Frothing in Flotation*, Gordon and Breach, New York, 123–145.

Snodgrass, R.A., Hay, M.P., and Du Preez, P.J. (1994). Process development and design of the Northam Merensky concentrator, *XVth CMMI Congress*, SAIMM, vol2, 341–357.

Somasundaran, P. and Sivakumar, A. (1988). Advances in understanding flotation mechanisms, *Minerals and Metallurgical Processing*, **5**(Aug.), 97.

Somasundaran, P., et al. (1993). Chelating agents for selective flotation of minerals, *XVIII IMPC, Sydney*, Aus. IMM, Vol. 3, 577.

Sorensen, T.C. (1982). Large Agitair flotation design and operation, *XIVth Int. Min. Proc. Cong.*, Paper No.VI–10, CIM, Toronto, Canada, Oct.

Soto, H. and Iwasaki, I. (1985). Flotation of apatite from calcareous ores with primary amines, *Minerals and Metallurgical Processing*, **2**(Aug.), 160.

Steane, H.A. (1976). Coarser grind may mean lower metal recovery but higher profits, *Can. Min. J.*, **97**(May), 44.

Steenberg, E. and Harris, P.J. (1984). Adsorption of carbomethoxycellulose, guar gum and starch onto talc, sulphides, oxides and salt-type minerals, *South African Journal of Chem.*, **37(3)**, 85–90.

Stemerowicz, A.I. and Leigh, G.W. (1978). Flotation techniques for producing high recovery bulk Zn–Pb–Cu–Ag concentrates from a New Brunswick massive sulphide ore, *CANMET Rep.* (Aug.), 79–8.

Sutherland, K.L. and Wark, I.W. (1955). *Principles of Flotation*, Australian IMM.

Sutolov, A. (1974). *Copper Porphyries*, University of Utah Printing Services.

Thompson, M.Y. (1991). Copper, *Metals and Minerals Annual Review*, **43**.

Thornton, A.J. (1991). Cautious adaptive control of an industrial flotation circuit, *Minerals Engineering*, **4(12)**, 1227–1242.

Trahar, W.J. (1981). A rational interpretation of the role of particle size in flotation, *Int. J. Min. Proc.*, **8**, 289.

Trahar, W.J. and Warren, L.J. (1976). The floatability of very fine particles – A review, *Int. J. Min. Pro.*, **3**, 103–131.

Tucker, J.P., Deglon, D.A. Franzidis, J.P. Harris, M.C. and O'Connor, C.T. (1994). An evaluation of a direct method of bubble size measurement in a laboratory batch flotation cell, *Minerals Engineering*, **7(5/6)**, 667–680.

Tuteja, R.K. and Spottiswood, D.J. (1995). Recent progress in the understanding of column flotation – a review, *The Aus.IMM Proceedings*, **300(2)**, 23.

Tveter, E.C. and McQuiston, F.W. (1962). Plant practice in sulphide mineral flotation, *Froth Flotation 50th Anniversary Volume*, AIMME, New York, 382.

Twidle, T.R., et al. (1985). Optimising control of lead flotation at Black Mountain, *Proc. XVth Int. Min. Proc. Cong.*, **3**, Cannes, 189.

Van Olst, M., Brown, N., Bourke, P., and Ronkainen, S. (2000). Improving flotation plant performance at Cadia by controlling and optimising the rate of froth recovery using Outokumpu FrothMaster™, *7th Mill Operators Conf.*, Kalgoorlie (Oct.), 127–135.

Venkatachalam,S. (1992). Electrogenerated gas bubbles in flotation, *Mineral Processing and Extractive Metallurgy Review*, **8**, 47

Vera, M.A., Manlapig, E.V., and Franzidis, J.P. (1999). Simultaneous determination of collection zone rate constant and froth zone recovery in a mechanical flotation environment, *Minerals Engineering*, **12**, 1163–1176.

Wang, D., et al. (1988). The effect of carrier-promoting aggregation of coarse particles in fine particle flotation, in *Production and Processing of Fine Particles*, ed. A.J. Plumpton, Pergamon Press, New York, 309.

Wang, X., et al. (1989a). The aqueous and surface chemistry of activation in the flotation of sulphide minerals – a review. Part I: An electrochemical model, *Mineral Processing and Extractive Metallurgy Review*, **4(3–4)**, 135.

Wang, X., et al. (1989b). The aqueous and surface chemistry of activation in the flotation of sulphide minerals – review. Part II: A surface precipitation model, *Mineral Processing and Extractive Metallurgy Review*, **4(3–4)** 167.

Wang, J., Somasundaran, P., and Nagaraj, D.R. (2005). Adsorption mechanism of guar gum at solid–liquid interfaces, *Minerals Engineering*, **18(1)**, Jan., 77–81.

Warder, J. and McQuie, J. (2005). The role of flash flotation in reducing overgrinding of nickel at WMC's Leinster Nickel Operation, in *Proc. Centenary of Flotation Symp.*, ed. G. Jameson, Aus.IMM Brisbane (Jun.), 931–938.

Watson, J.L. (1988). South East Missouri lead belt – a review 1987, *Minerals Engineering*, **1(2)**, 151.

Weber, A., Meadows, D., Villaneuva, F., Paloma, R., and Prado, S. (2005). Development of the world's largest flotation machine, *Proc. Centenary of Flotation Symp.*, ed. G. Jameson, Aus.IMM Brisbane (Jun.), 285–292.

Wesseldijk, Q.I., Bradshaw, D.J., Harris, P.J., and Reuter, M.A. (1999). The flotation behaviour of chromite with respect to the beneficiation of UG2 ore, *Minerals Engineering*, **12(10)**, 1177–1184.

Wiegel, R.L. (1999). Phosphate rock beneficiation practice, in Advances in Flotation Technology, ed. B.K. Parekh, and J.D. Miller, SME, Littleton, Colorado, 213–218.

Wiese, J., Harris, P.J., and Bradshaw, D.J. (2005). The influence of the reagent suite on the flotation of ores from the Merensky reef, *Minerals Engineering* **18(2)**, 189–198.

Williams, S.R. and Phelan, J.M. (1985). Process development at Woodlawn Mines, in *Complex Sulphides*, ed. A.D. Zunkel et al., TMS-AIME, Pennsylvania, 293.

Wills, B.A. (1983). Pyhasalmi and Vihanti concentrators, *Min. Mag.* (Sept.), 176.

Wills, B.A. (1984). The separation by flotation of copper-lead-zinc sulphides, *Mining Mag.* (Jan.), 36.

Witt, J. K., Cantrell, P.E., and Neira, M.P. (1999). Heap leaching practices at San Manuel Oxide operations, *4th International Conference COPPER 99-COBRE 99*, **4**, 41–58.

Woods, R. (1976). Electrochemistry of sulphide flotation, in Flotation: *A.M. Gaudin Memorial Volume*, ed. M.C. Fuerstenau, Vol. 1, AIMME, New York, 298.

Woods, R. (1988). Flotation of sulphide minerals: Electrochemical perspectives, *Copper '87 Volume 2 Mineral Processing and Process Control*, ed. A. Mular et al., Universidad de Chile, 121.

Woods, R. (1994). Chemisorption of thiols and its role in flotation, *Proceedings of IV Meeting of the Southern Hemisphere on Mineral Technology; and III Latin-American Congress on Froth Flotation.* Concepcion, Chile, 1–14.

Woods, R. and Richardson, P.E. (1986). The flotation of sulphide minerals – electrochemical aspects, in *Advances in Mineral Processing*, ed. P. Somasundaran, Chapter 9, SME, Colorado.

Wrobel, S.A. (1970). Economic flotation of minerals, *Min. Mag.*, **122**(Apr.), 281.

Ye, Y., et al. (1990). Molybdenite flotation from copper/molybdenum concentrates by ozone conditioning, *Minerals and Metallurgical Processing*, **7**(Nov.), 173.

Yianatos, J.B. (2003). Design, modelling and control of flotation equipment, in *XXII International Mineral Processing Congress*, ed. L. Lorenzen, et al., Cape Town, South Africa, 29 Sept.–3 Oct. SAIMM, Johannesburg, 59–68.

Yianatos, J.B., et al. (1988). Effect of column height on flotation column performance, *Minerals and Metallurgical Processing*, **5**(Feb.), 11.

Yoon, R.H. and Basilio C.I. (1993). Adsorption of thiol collectors on sulphide minerals and precious metals – a new perspective, *Proceedings of XVIII Int. Miner. Process. Cong.*, Sydney, 611–617.

Young, P. (1982). Flotation machines, *Min. Mag.*, **146**(Jan.), 35.

Young, M.F. and Gao, M. (2000). Performance of the IsaMills in the George Fisher flowsheet, in *Proceedings of Aus.IMM Seventh Mill Operators Conference*, Aus.IMM, Melbourne, Kalgoorlie, Australia (Oct.), 12–14.

Zachwieja, J.B. (1994). An overview of cationic reagents in mineral processing, In *Reagents for Better Metallurgy*, ed. P.S. Mulukutla, SME, Inc., Littleton.

Zhang, W. and Poling, G.W. (1991). Sulphidization-promoting effects of ammonium sulphate on sulphidized xanthate flotation of malachite, *Proc. XVII Int. Min. Proc. Cong.*, Dresden, Vol. IV, 187.

Zhou, R. and Chander, S. (1991). Sulfidization-flotation of malachite with sodium tetrasulfide, *Proc. XVII Int. Min. Proc. Cong.*, Dresden, Vol. IV, 47.

13

Magnetic and electrical separation

Introduction

Magnetic and electrical separators are being considered in the same chapter, as there is often a possibility of an overlap in the application of the two processes. For example, as can be seen later, there is often debate as to which form of separation is best suited at various stages to the treatment of heavy mineral sand deposits.

Magnetic separation

Magnetic separators exploit the difference in magnetic properties between the ore minerals and are used to separate either valuable minerals from non-magnetic gangue, e.g. magnetite from quartz, or magnetic contaminants or other valuable minerals from the non-magnetic values. An example of this is the tin-bearing mineral cassiterite, which is often associated with traces of magnetite or wolframite which can be removed by magnetic separators.

All materials are affected in some way when placed in a magnetic field, although with most substances the effect is too slight to be detected. Materials can be classified into two broad groups, according to whether they are attracted or repelled by a magnet:

(1) *Diamagnetics* are *repelled* along the lines of magnetic force to a point where the field intensity is smaller. The forces involved here are very small and diamagnetic substances cannot be concentrated magnetically.

(2) *Paramagnetics* are *attracted* along the lines of magnetic force to points of greater field intensity. Paramagnetic materials can be concentrated in high-intensity magnetic separators. Examples of paramagnetics which are separated in commercial magnetic separators are ilmenite ($FeTiO_3$), rutile (TiO_2), wolframite ($(Fe, Mn)WO_4$), monazite (rare earth phosphate), siderite ($FeCO_3$), pyrrhotite (FeS), chromite ($FeCr_2O_4$), hematite (Fe_2O_3), and manganese minerals.

Some elements are themselves paramagnetic, such as Ni, Co, Mn, Cr, Ce, Ti, O, and the Pt group metals, but in most cases the paramagnetic properties of minerals are due to the presence of iron in some ferromagnetic form.

Ferromagnetism can be regarded as a special case of paramagnetism, involving very high forces. Ferromagnetic materials have very high susceptibility to magnetic forces and retain some magnetism when removed from the field (*remanence*). They can be concentrated in low-intensity magnetic separators and the principal ferromagnetic mineral separated is magnetite (Fe_3O_4), although hematite (Fe_2O_3) and siderite ($FeCO_3$) can be roasted to produce magnetite and hence give good separation. The removal of "tramp" iron from ores can also be regarded as a form of low-intensity magnetic separation.

It is not intended to review the theory of magnetism in any depth, as this is amply covered elsewhere (Svoboda, 1987).

The unit of measurement of *magnetic flux* density or *magnetic induction* (B) (the number of lines of force passing through a unit area of material) is the *tesla* (T).

The magnetising force which induces the lines of force through a material is called the *field intensity* (H), and by convention has the units ampere per metre ($1\,\mathrm{A\,m^{-1}} = 4\pi \times 10^{-7}\,\mathrm{T}$).

The *intensity of magnetisation* or the *magnetisation* (M A/m) of a material relates to the magnetisation induced in the material, and:

$$B = \mu_0(H + M) \tag{13.1}$$

the constant of proportionality, μ_0 being the *permeability of free space*, and having the value of $4\pi \times 10^{-7}\,\mathrm{T \cdot m/A}$. In vacuum, $M = 0$, and it is extremely low in air, such that Equation 13.1 becomes:

$$B = \mu_0 H \tag{13.2}$$

so that the value of the field intensity is virtually the same as that of flux density, and the term *magnetic field intensity* is then often loosely used. However, when dealing with the magnetic field inside materials, particularly ferromagnetics that concentrate the lines of force, the value of the induced flux density will be much higher than the field intensity, and it must be clearly specified which term is being referred to.

Magnetic susceptibility (S) is the ratio of the intensity of magnetisation produced in the material to the magnetic field which produces the magnetisation, i.e.:

$$S = M/H \tag{13.3}$$

Combining Equations 13.1 and 13.3:

$$B = \mu_0 H(1 + S)$$

or

$$B = \mu\mu_0 H \tag{13.4}$$

where $\mu = 1 + S$, and is a dimensionless number known as the *relative permeability*.

For paramagnetic materials, S is a small positive constant, and is a negative constant for diamagnetic materials. Figure 13.1 shows plots of induced magnetisation (M) versus the strength of the external field (H), for paramagnetic (hematite) and diamagnetic (quartz) materials. Both plots show straight line relationships between M and H, in each case the slope representing the magnetic susceptibility (S) of the material, i.e. about 0.01 for hematite and around -0.001 for quartz.

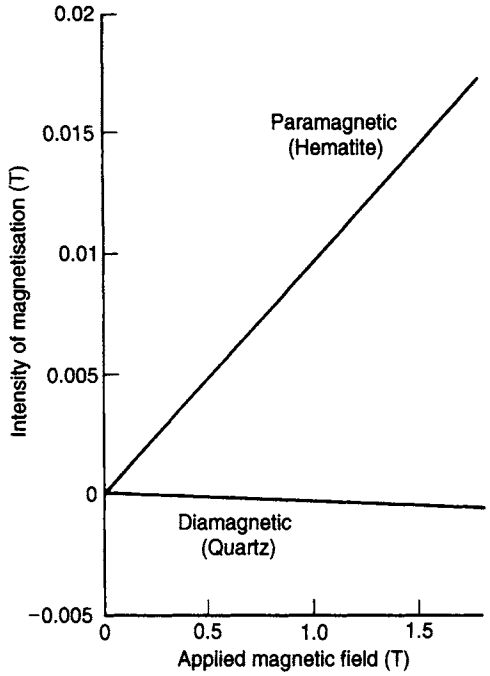


Figure 13.1 Magnetisation curves for paramagnetic and diamagnetic materials

The magnetic susceptibility of a ferromagnetic material is dependent on the magnetic field, decreasing with field strength as the material becomes *saturated*. Figure 13.2 shows a plot of M versus H for magnetite, showing that at an applied field of 1 T the magnetic susceptibility is about 0.35, and saturation occurs at about 1.5 T. Many high-intensity magnetic separators use iron cores and frames to produce the desired magnetic flux concentrations and field strengths. Iron saturates magnetically at about 2–2.5 T, and the non-linear ferromagnetic relationship between inducing field strength and magnetisation intensity necessitates the use of very large currents in the energising coils, sometimes up to hundreds of amperes.

The capacity of a magnet to lift a particular mineral is dependent not only on the value of the field intensity, but also on the *field gradient*, i.e. the rate at which the field intensity increases towards the magnet surface. Because paramagnetic minerals have higher magnetic permeabilities

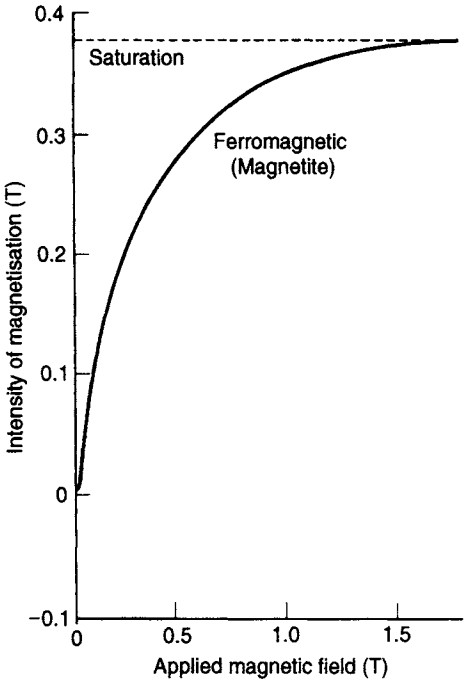


Figure 13.2 Magnetisation curve for ferromagnetic material

than the surrounding media, usually air or water, they concentrate the lines of force of an external magnetic field. The higher the magnetic susceptibility, the higher is the field density in the particle and the greater is the attraction up the field gradient towards increasing field strength. Diamagnetic minerals have lower magnetic susceptibility than their surrounding medium and hence expel the lines of force of the external field. This causes their expulsion in the direction down the gradient of the field towards the decreasing field strength. This negative diamagnetic effect is usually orders of magnitude smaller than the positive paramagnetic attraction (Cohen, 1986).
It can be shown that

$$F \propto H\frac{\mathrm{d}H}{\mathrm{d}l} \qquad (13.5)$$

where F is the force on the particle, H is the field intensity, and $\mathrm{d}H/\mathrm{d}l$ is the field gradient.

Thus in order to generate a given lifting force, there are an infinite number of combinations of field and gradient which will give the same effect. Production of a high field gradient as well as high intensity is therefore an important aspect of separator design.

Magnetic separator design

Certain elements of design are incorporated in all magnetic separators, whether they are low or high intensity, wet or dry. The prime requirement, as has already been mentioned, is the provision of a high-intensity field in which there is a steep field strength gradient. In a field of uniform flux, such as in Figure 13.3(a), magnetic particles will orient themselves, but will not move along the lines of flux. The most straightforward method for producing a converging field is by providing a V-shaped pole above a flat pole, as in Figure 13.3(b). The tapering of the upper pole concentrates the magnetic flux into a very small area giving high intensity. The lower flat pole has the same total magnetic flux distributed over a larger area. Thus there is a steep field gradient across the gap by virtue of the different intensity levels.

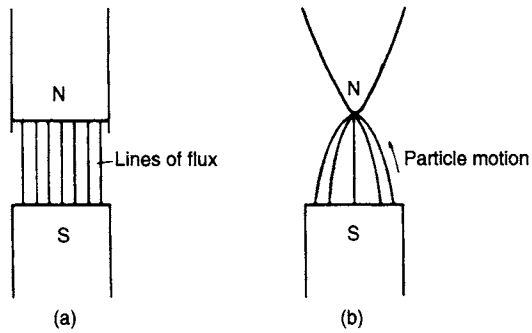


Figure 13.3 (a) Field of uniform flux, (b) converging field

Another method of producing a high field gradient is by using a pole which is constructed of alternate magnetic and non-magnetic laminations (Figure 13.4).

Provision must be incorporated in the separator for regulating the intensity of the magnetic field so as to deal with various types of material. This is easily achieved in electromagnetic separators by varying the current, while with permanent magnets the interpole distance can be varied.

Commercial magnetic separators are continuous-process machines and separation is carried out on a moving stream of particles passing into and through the magnetic field. Close control of the speed of passage of the particles through the field is essential, which rules out free fall as a means of feeding.

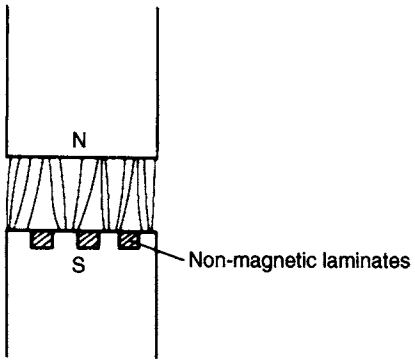


Figure 13.4 Production of field gradient by laminated pole

Belts or drums are very often used to transport the feed through the field.

The introduction into a magnetic field of particles which are highly susceptible concentrates the lines of force so that they pass through them (Figure 13.5).

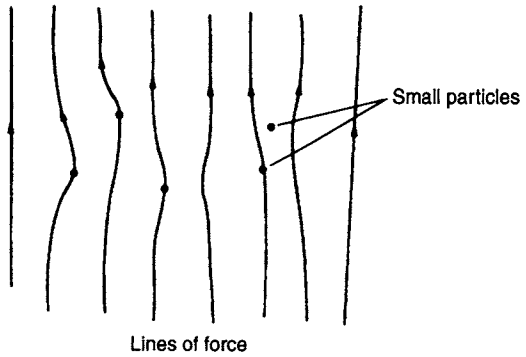


Figure 13.5 Concentration of flux on mineral particles

Since the lines of force converge to the particles, a high field gradient is produced, which causes the particles themselves to behave as magnets, thus attracting each other. Flocculation, or agglomeration, of the particles can occur if they are small and highly susceptible and if the field is intense. This has great importance as these magnetic "flocs" can entrain gangue and can bridge the gaps between magnetic poles, reducing the efficiency of separation. Flocculation is especially serious with dry separating machines operating on fine material. If the ore can be fed through the field in a monolayer, this effect is much less serious, but, of course, the capacity of the machine is drastically reduced. Flocculation is often minimised by passing the material through consecutive magnetic fields, which are usually arranged with successive reversal of the polarity. This causes the particles to turn through 180°, each reversal tending to free the entrained gangue particles. The main disadvantage of this method is that flux tends to leak from pole to pole, reducing the effective field intensity.

Provision for collection of the magnetic and non-magnetic fractions must be incorporated into the design of the separator. Rather than allow the magnetics to contact the pole-pieces, which would cause problems of detachment, most separators are designed so that the magnetics are attracted to the pole-pieces, but come into contact with some form of conveying device, which carries them out of the influence of the field, into a bin or a belt. Non-magnetic disposal presents no problems, free fall from a conveyor into a bin often being used. Middlings are readily produced by using a more intense field after the removal of the highly magnetic fraction.

Types of magnetic separator

Magnetic separators can be classified into low- and high-intensity machines, which may be further classified into dry-feed and wet-feed separators.

Low-intensity separators are used to treat ferromagnetic materials and some highly paramagnetic minerals.

Low-intensity magnetic separation

Dry low-intensity magnetic separation is confined mainly to the concentration of coarse sands which are strongly magnetic, the process being known as *cobbing*, and often being carried out in drum separators. Below the 0.5 cm size range, dry separation tends to be replaced by wet methods, which produce much less dust loss and usually a cleaner product. Low-intensity wet separation is now widely used for purifying the magnetic medium in the dense medium separation process (see Chapter 11), as well as for the concentration of ferromagnetic sands.

Drum separators are the most common machines in current use for cleaning the medium in DMS

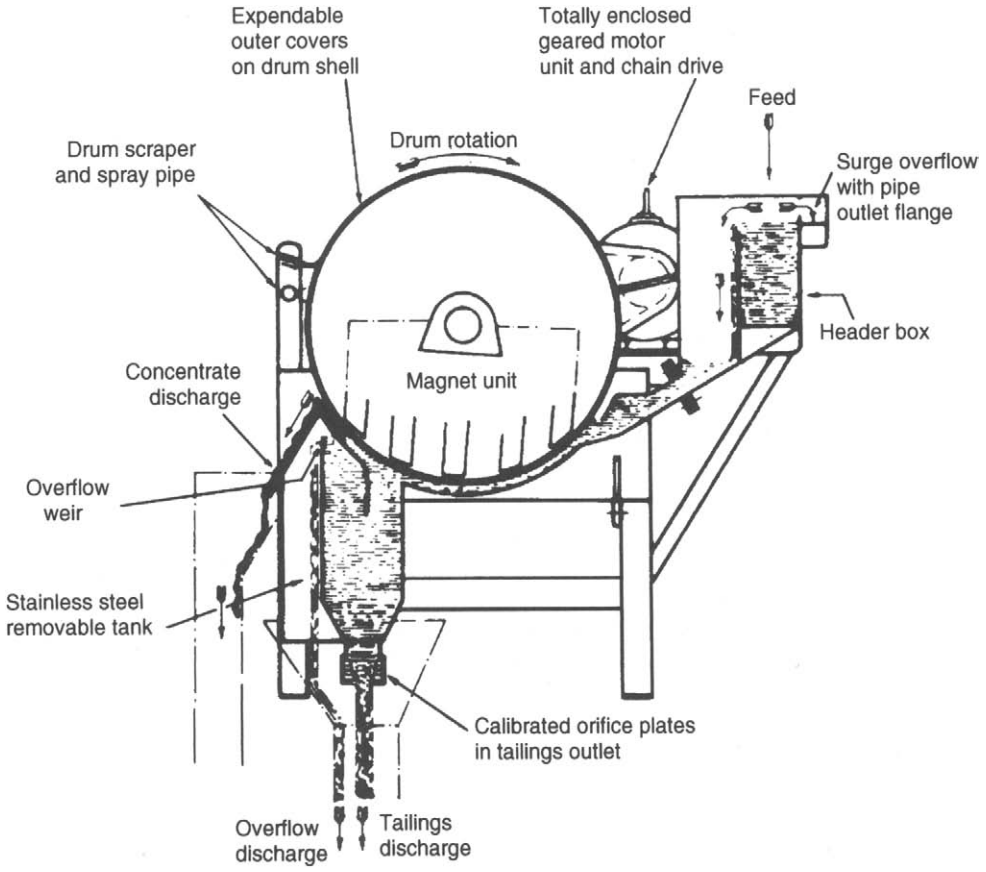


Figure 13.6 Drum separator

circuits and are widely used for concentrating finely ground iron ore. They consist essentially of a rotating non-magnetic drum (Figure 13.6) containing three to six stationary magnets of alternating polarity, although the *Permos* separator uses many small magnet blocks, whose direction of magnetisation changes in small steps. This is said to generate a very even magnetic field, requiring less magnetic material (Wasmuth and Unkelbach, 1991).

Although initially drum separators employed electromagnets, permanent magnets are used in modern devices, utilising ceramic or rare earth magnetic alloys, which retain their intensity for an indefinite period (Norrgran and Marin, 1994). Separation is by the "pick-up" principle. Magnetic particles are lifted by the magnets and pinned to the drum and are conveyed out of the field, leaving the gangue in the tailings compartment. Water is introduced into the machine to provide a current which keeps the pulp in suspension. Field intensities of up to 0.7 T at the pole surfaces can be obtained in this type of separator.

The drum separator shown in Figure 13.6 is of the *concurrent* type, whereby the concentrate is carried forward by the drum and passes through a gap, where it is compressed and dewatered before leaving the separator. This design is most effective for producing an extremely clean magnetic concentrate from relatively coarse materials and is widely used in dense medium recovery systems.

The separator shown in Figure 13.7 is of the *counter-rotation* type, where the feed flows in the opposite direction to the rotation. This type is used in roughing operations, where occasional surges in feed must be handled, where magnetic material losses are to be held to a minimum, while an extremely clean concentrate is not required, and when high solids loading is encountered.

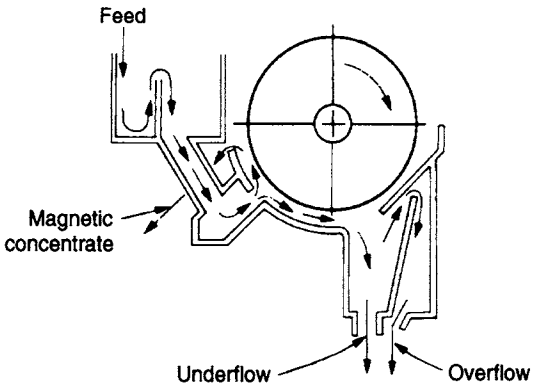


Figure 13.7 Counter-rotation drum separator

Figure 13.8 shows a *counter-current* separator, where the tailings are forced to travel in the opposite direction to the drum rotation and are discharged into the tailings chute.

This type of separator is designed for finishing operations on relatively fine material, of particle size less than about 250 μm.

Drum separators are widely used to treat low-grade taconite ores, which contain 40–50% Fe, mainly as magnetite, but in some areas with hematite, finely disseminated in bands in hard siliceous rocks. Very fine grinding is necessary to free the iron minerals that produce a concentrate that requires pelletising before being fed to the blast furnaces.

In a typical flowsheet the ore is ground progressively finer, the primary grind usually being undertaken autogenously, or by rod milling, followed by magnetic separation in drum separators. The magnetic concentrate is reground and again treated in drum separators. This concentrate may be further reground, followed by a third stage of magnetic separation. The tailings from each stage of magnetic separation are either rejected or, in some cases, treated by spiral or cone concentrators to recover hematite.

At Palabora, the tailings from copper flotation (Figure 12.66) are deslimed, after which the +105 μm material is treated by Sala drum separators to recover 95% of the magnetite at a grade of 62% Fe.

The cross-belt separator (Figure 13.9) and disc separators once widely used in the mineral sands industry, particularly for recovering ilmenite from heavy mineral concentrates, are now considered obsolete. They are being replaced with rare earth roll magnetic separators and rare earth drum magnetic separators (Arvidson, 2001).

Rare earth roll separators use alternate magnetic and non-magnetic laminations as shown in Figure 13.4. Feed is carried onto the magnetic roll by means of a thin belt as shown in Figure 13.9, hence there is no bouncing or scattering of particles as they enter the magnetic zone, and they all enter the magnetic zone with the same horizontal velocity. These factors contribute to achieving a sharp separation. Roll speed can be adjusted over a wide range, allowing the product quality to be "dialled in".

Dry rare earth drum separators provide a fan of separated particles which can often be seen as distinct streams (Figure 13.10). The fan can be separated into various grades of magnetic product and a non-magnetic tailing. In some mineral sands applications, drum separators have been integrated with one or more rare earth rolls, arranged to treat the middlings particles from the drum as shown in Figure 13.10.

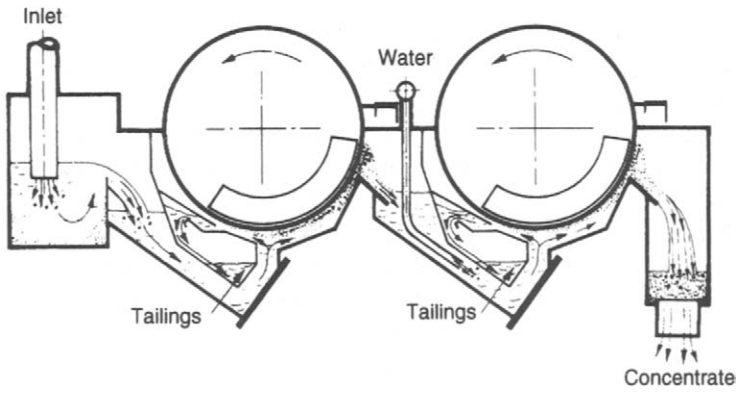


Figure 13.8 Counter-current separator

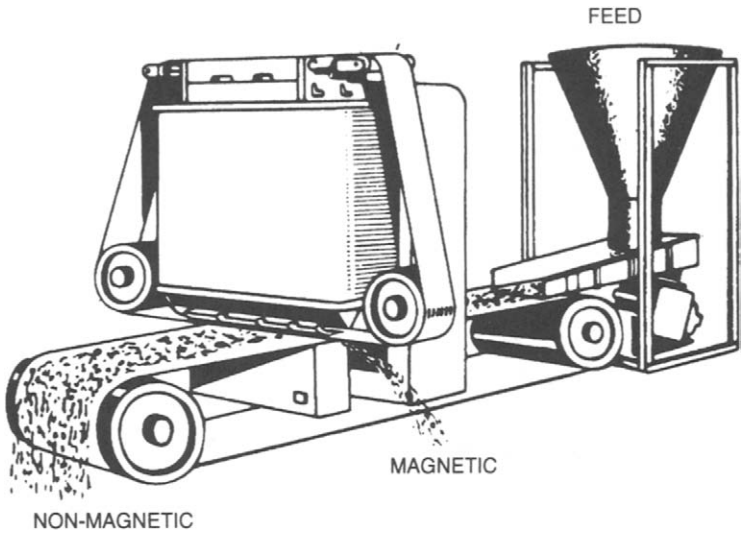


Figure 13.9 Cross-belt separator

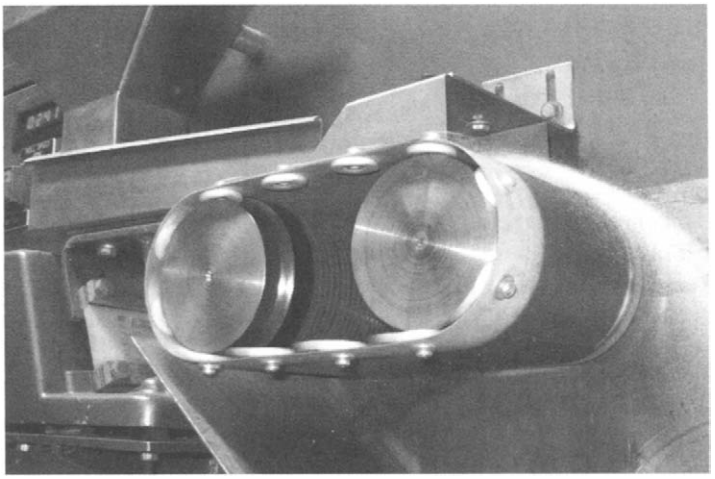


Figure 13.10 A laboratory dry rare earth drum separator (Courtesy JKMRC and JKTech Pty Ltd)

High-intensity separators

Very weakly paramagnetic minerals can only be effectively removed from an ore feed if high-intensity fields of 2 T and more can be produced (Svoboda, 1994).

Until the 1960s high-intensity separation was confined solely to dry ore, having been used commercially since about 1908.

Induced roll magnetic separators, IRMs (Figure 13.11), are widely used to treat beach sands, wolframite, tin ores, glass sands, and phosphate rock. They have also been used to treat feebly magnetic iron ores, principally in Europe. The roll, on to which the ore is fed, is composed of phosphated steel laminates compressed together on a non-magnetic stainless steel shaft. By using two sizes of lamination, differing slightly in outer diameter, the roll is given a serrated profile which promotes the high field intensity and gradient required. Field strengths of up to 2.2 T are attainable in the gap between feed pole and roll. Non-magnetic particles are thrown off the roll into the tailings compartment, whereas magnetics are gripped, carried out of the influence of the field

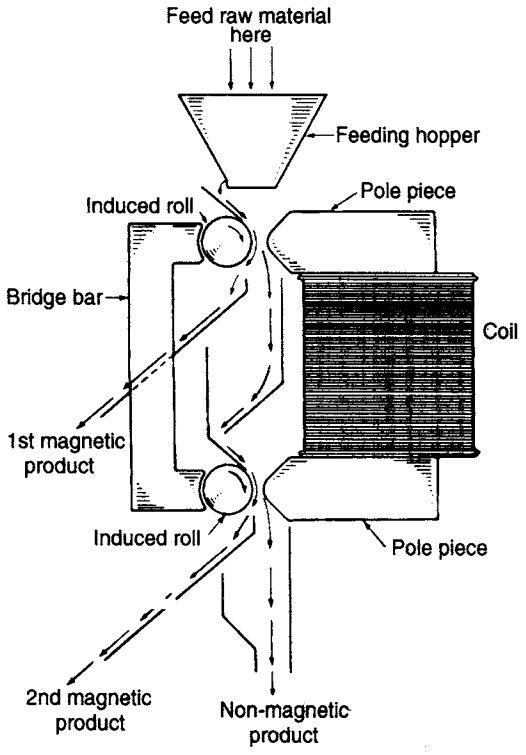


Figure 13.11 Induced roll separator

and deposited into the magnetics compartment. The gap between the feed pole and rotor is adjustable and is usually decreased from pole to pole to take off successively more weakly magnetic products.

The setting of the splitter plates cutting into the trajectory of the discharged material is obviously of great importance.

In some cases IRMs are now being displaced by the new rare earth drum and roll separators.

Dry high-intensity separation is largely limited to ores containing little, if any, material finer than about 75 μm. The effectiveness of separation on such fine material is severely reduced by the effects of air currents, particle–particle adhesion, and particle–rotor adhesion.

Without doubt the greatest advance in the field of magnetic separation was the development of continuous wet high-intensity magnetic separators, WHIMS machines (Lawver and Hopstock, 1974). These reduce the minimum particle size for efficient separation allowing ores to be concentrated magnetically that cannot be concentrated effectively by dry high-intensity methods, because of the fine grinding necessary to ensure complete liberation of the magnetic fraction. In some flowsheets, expensive drying operations can be eliminated by using a wet concentration system.

Perhaps the most well-known WHIMS machine is the *Jones separator*, the design principle of which is utilised in many other types of wet separator used today.

The machine consists of a strong main frame (Figure 13.12) made of structural steel. The magnet yokes are welded to this frame, with the electromagnetic coils enclosed in air-cooled cases. The actual separation takes place in the plate boxes which are on the periphery of the one or two rotors attached to the central roller shaft. The feed, which is thoroughly mixed slurry, flows through the separator via fitted pipes and launders into the plate boxes (Figure 13.13), which are grooved to concentrate the magnetic field at the tip of the ridges. Feeding is continuous due to the rotation of the plate boxes on the rotors and the feed points are at the leading edges of the magnetic fields. Each rotor has two symmetrically disposed feed points.

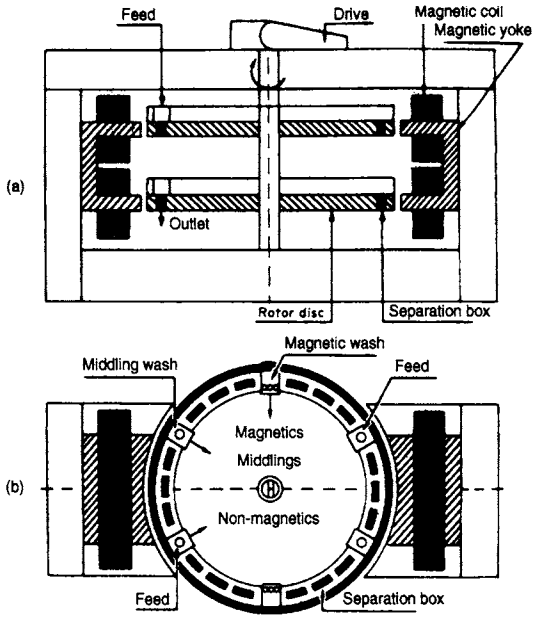


Figure 13.12 Operating principle of the Jones high-intensity wet magnetic separator in cross-section (a) plan and (b) view

The feebly magnetic particles are held by the plates, whereas the remaining non-magnetic slurry passes straight through the plate boxes and is

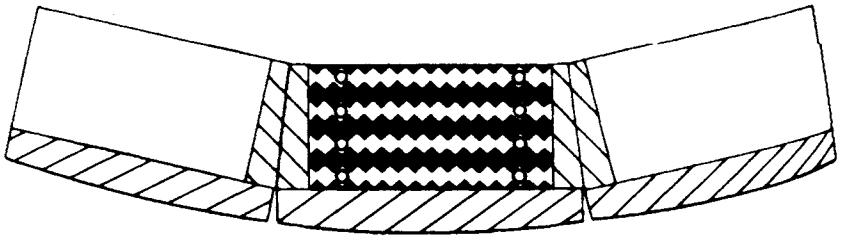


Figure 13.13 Plan of Jones plate box showing grooved plates and spacer bars

collected in a launder. Before leaving the field any entrained non-magnetics are washed out by low-pressure water and are collected as a middlings product.

When the plate boxes reach a point midway between the two magnetic poles, where the magnetic field is essentially zero, the magnetic particles are washed out with high pressure scour water sprays operating at up to 5 bar (Figure 13.14). Field intensities of over 2 T can be produced in these machines. The production of a 1.5 T field requires an electric power consumption in the coils of 16 kW per pole. Of the 4 t of water used with every tonne of solids, approximately 90% is recycled.

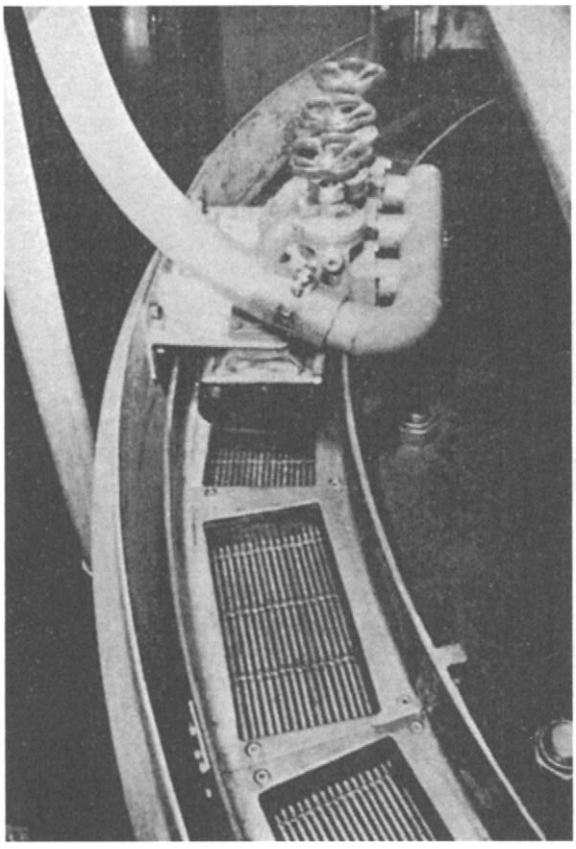


Figure 13.14 Jones separator – magnetic wash

Wet high-intensity magnetic separation has its greatest use in the concentration of low-grade iron ores containing hematite, where they frequently replace flotation methods, although the trend towards magnetic separation has been slow in North America, mainly due to the very high capital cost of such separators. It has been shown (White, 1978) that the capital cost of flotation equipment for concentrating weakly magnetic ore is about 20% that of a Jones separator installation, although flotation operating costs are about three times higher. Total cost depends on terms for capital depreciation; over 10 years or longer the high-intensity magnetic separator may be the most attractive process. Additional costs for water treatment may also boost the total for a flotation plant. Figure 13.15 shows a Jones separator in operation on a Brazilian iron ore plant.

Various other designs of wet high-intensity separator have been produced, a four-pole machine being manufactured by Boxmag-Rapid Ltd. The plate boxes in this design are an array of magnetic stainless steel "wedge-bars" similar to those used in fine screening (Figure 13.16).

In addition to their large-scale application for the recovery of hematite, wet high-intensity separators are now in operation for a wide range of duties, including removal of magnetic impurities from cassiterite concentrates, removal of fine magnetic from asbestos, removal of magnetic impurities from scheelite concentrates, purification of talc, the recovery of wolframite and non-sulphide molybdenum-bearing minerals from flotation tailings, and the treatment of heavy mineral beach sands. They have also been successfully used for the recovery of gold and uranium from cyanidation

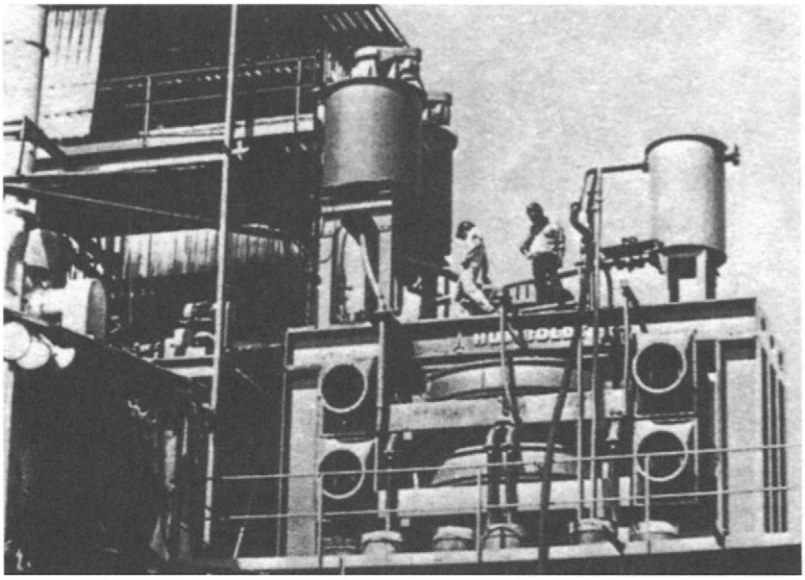


Figure 13.15 Jones separator treating Brazilian hematite ore

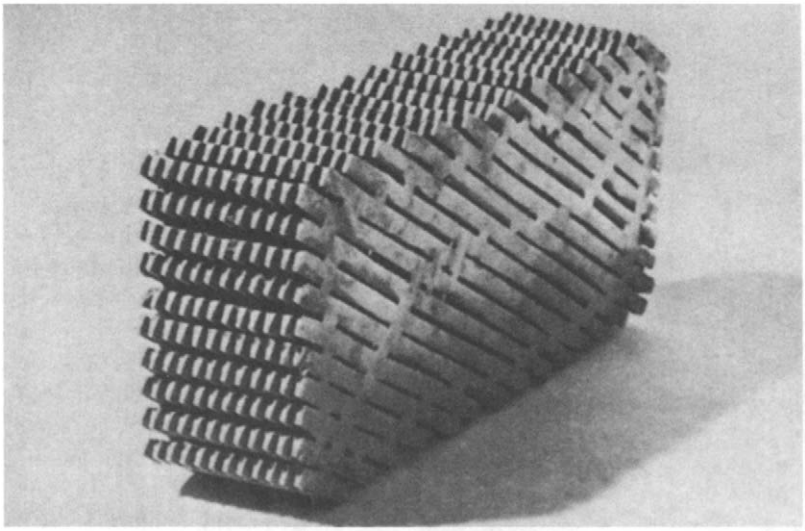


Figure 13.16 Section through Boxmag-Rapid grid assembly

residues in South Africa (Corrans, 1984). These residues contain some free gold, while some of the fine gold is locked in sulphides, mainly pyrite, and in various silicate minerals. The free gold can be recovered by further cyanidation, while flotation can recover the pyritic gold. Magnetic separation can be used to recover some of the free gold, and much of the silicate-locked gold, due to the presence of iron impurities and coatings.

The paramagnetic properties of some sulphide minerals, such as chalcopyrite and marmatite, have been exploited by applying wet high-intensity magnetic separation to augment differential flotation processes commonly used to separate these minerals from less magnetic or non-magnetic sulphides (Tawil and Morales, 1985). Testwork showed that a Chilean copper concentrate could be upgraded from 23.8 to 30.2% Cu, at 87% recovery.

This was done by separating the chalcopyrite from pyrite in a field of 2 T. In Cu–Pb separation operations, it was found that chalcopyrite and galena could be effectively separated with field strengths as low as 0.8 T. When the process was applied to the de-coppering of a molybdenite concentrate, it was possible to reduce the copper content from 0.8 to 0.5% with over 97% Mo recovery.

High-gradient magnetic separators

In order to separate paramagnetic minerals of extremely low magnetic susceptibility, high magnetic forces must be generated. These forces can be produced by increasing the magnetic field strength, and in conventional high-intensity magnetic separators use is made of the ferromagnetic properties of iron to generate a high B-field (induced field) many hundreds of times greater than the applied H-field, with a minimum consumption of electrical energy. The working field occurs in air-gaps in the magnetic circuit, the disadvantage being that the volume of iron required is many times greater than the gap volume where separation takes place. The steel plates in a Jones separator, for example, occupy up to 60% of the process volume. Thus high-intensity magnetic separators using conventional iron circuits tend to be very massive and heavy in relation to their capacity. A large separator may contain over 200 t of iron to carry the flux, hence capital and installation costs are extremely high.

As iron saturates at around 2–2.5 T, conventional iron circuits are of little value for generating fields above about 2 T. Such fields can only be generated by the use of high H-fields produced in solenoids, but the energy consumption is extremely high and there are problems in cooling the solenoid.

An alternative is to increase the magnetic force by increasing the value of the magnetic field gradient. Instead of using one large convergent field in the gap of a magnetic circuit, the uniform field of a solenoid is used (Figure 13.17). The core, or working volume, is filled with a matrix of secondary poles, such as ball bearings, or wire wool, the latter filling only about 10% of the working volume. Each secondary pole, due to its high permeability, can produce a maximum field strength of the order of 2 T, but more importantly, each pole produces, in its immediate vicinity, high

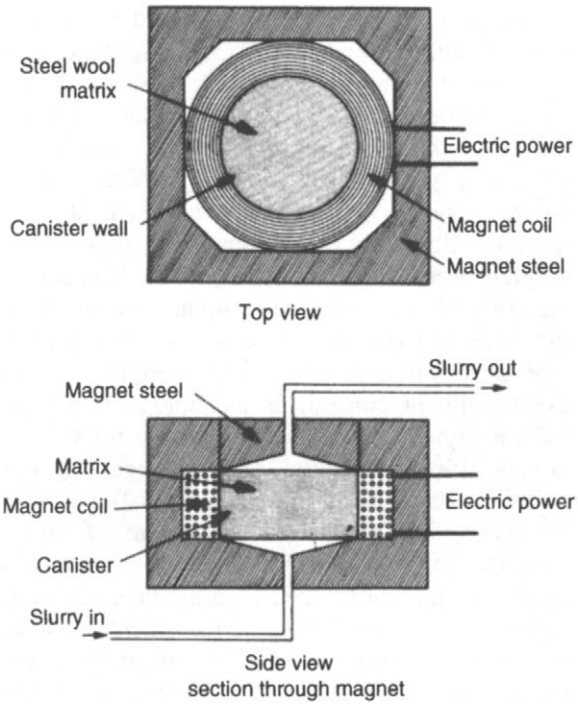


Figure 13.17 High-gradient magnetic separator

field gradients of up to 14 T mm^{-1}. Thus a multitude of high gradients across numerous small gaps, centred around each of the secondary poles, is achieved.

The solenoid can be clad externally with an iron frame to form a continuous return path for the magnetic flux, thus reducing the energy consumption for driving the coil by a factor of about 2. The matrix is held in a canister into which the slurry is fed. As particles are captured, the ability of the matrix to extract particles is reduced. Periodically the magnetic field can be removed and the matrix flushed with water to remove the captured material.

An inherent disadvantage of high gradient separators is that an increase in field gradient necessarily reduces the working gap between secondary poles, the magnetic force having only a short reach, usually not more than 1 mm. It is therefore necessary to use gaps of only about 2 mm between poles, such that the matrix separators are best suited to the treatment of very fine particles. They are used mainly in the kaolin industry for removing micron-sized particles which contain iron. Several large separators, with the ferromagnetic matrix contained in baskets approximately 2 m in diameter

are in commercial use in the United States and in Cornwall, England. They operate with fields of 2 T, and have capacities ranging between 10 and 80 $t\,h^{-1}$ depending on the final clay quality desired.

One of the most important factors which will affect coal preparation policy in the future is the environmental issue associated with acid rain and its link with sulphur emissions from fossil fuels. Sulphur occurs in coal in three forms. It is part of the coal substance (organic sulphur), or occurs as the minerals pyrite and marcasite, or as sulphates. The most important factor for the engineer is the pyritic sulphur content, as technology is not yet sufficiently developed to consider the removal of organic sulphur. If pyrite can be liberated by fine crushing to around 1 mm, then froth flotation or gravity methods can be used to remove it from the coal. However, if very fine crushing is necessary to liberate the pyrite, then high-gradient magnetic separation is a possibility. Increased international interest is at present being shown by coal preparation engineers in coal–liquid mixtures as a replacement for conventional hydrocarbon fuels such as diesel oil and natural gas. A typical coal–water mixture consists of pulverised coal of less than 50 microns particle size, and low ash content (2–6%) dispersed in an aqueous slurry, with a pulp density of between 50 and 80% solids. In order to produce these mixtures it is necessary to treat good quality coal by fine grinding and deep cleaning to remove ash and sulphur. High-gradient magnetic separation is capable of removing pyrite from pulverised coal, and much work is currently being performed on a variety of coal types (Lua and Boucher, 1990).

Superconducting separators

Undoubtedly the future developments and applications of magnetic separation in the mineral industry will lie in the use of high magnetic forces. Matrix separators with very high field gradients and multiple small working gaps can draw little advantage from field strengths above the saturation levels of the secondary poles. However, "open-gradient" separators, with large working volumes to *deflect* coarser particles at high capacity, rather than *capture* particles, as in high-gradient separators, need to use the highest possible field strengths in order to generate the high magnetic forces required to treat feebly paramagnetic particles. Field strengths in excess of 2 T can only be generated economically by the use of *superconducting magnets* (Kopp, 1991; Watson, 1994).

Certain alloys have the property of presenting no resistance to electric currents at extremely low temperatures. An example is niobium–titanium at 4.2 K, the temperature of liquid helium. Once a current commences to flow through a coil made from such a superconducting material, it will continue to flow without being connected to a power source, and the coil will become, in effect, a permanent magnet. Superconducting magnets can produce extremely intense and uniform magnetic fields, of up to 15 T. The main problem, of course, is in maintaining the extremely low temperatures, and in 1986 a Ba/La/Cu oxide composite was made superconductive at 35 K, promoting a race to prepare ceramic oxides with much higher superconducting temperatures (Malati, 1990). Unfortunately these materials are of a highly complex crystal structure, making them difficult to fabricate into wires. They also have a low current-carrying capacity, so it is likely that for the foreseeable future superconducting magnets will be made from ductile niobium alloys, embedded in a copper matrix.

In 1986 a superconducting high-gradient magnetic separator was designed and built by Eriez Magnetics to process kaolinite clay in the United States (Stefanides, 1986). This machine uses only about 0.007 kW in producing 5 T of flux, the ancillary equipment needed requiring another 20 kW. In comparison, a conventional 2 T high-gradient separator of similar throughput would need about 250 kW to produce the flux, and at least another 30 kW to cool the magnet windings.

The 5 T machine is an assembly of concentric components (Figure 13.18). A removable processing canister is installed in a processing chamber located at the centre of the assembly. This is surrounded by a double-walled, vacuum-insulated container that accommodates the superconductive magnet's niobium/titanium-tantalum winding, and the liquid helium coolant. A thermal shield, cooled with liquid nitrogen to 77 K, limits radiation into the cryostat. In operation, the supply of slurry is periodically cut off, the magnetic field is shut down, and the canister backwashed with water to clear out accumulated magnetic contaminants.

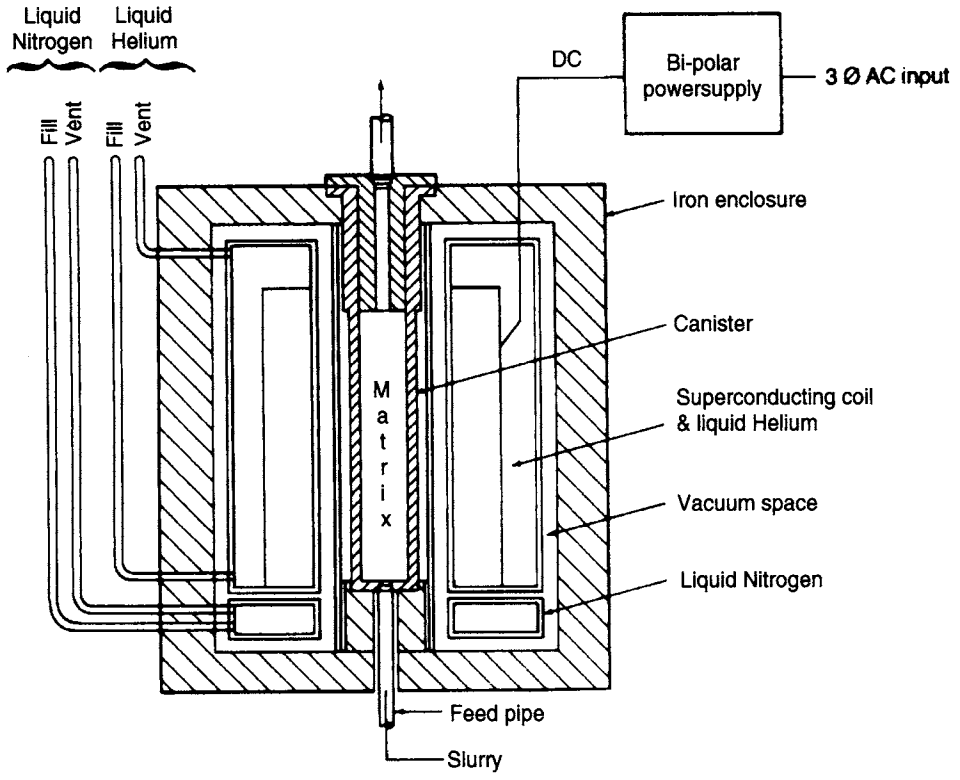


Figure 13.18 5 T superconducting magnetic separator

An open-gradient drum magnetic separator with a superconducting magnet system has been operating commercially since the late 1980s (Unkelbach and Kellerwessel, 1985; Wasmuth and Unkelbach, 1991) (Figure 13.19). Although separation is identical to that in conventional drum separators, the magnetic flux density at the drum surface can reach over 4 T, generated by the superconductive magnet assembly within the drum.

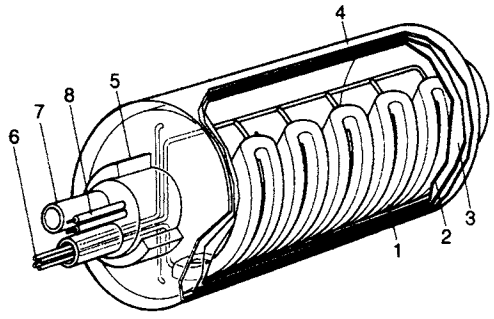


Figure 13.19 Superconducting drum separator: 1 – magnetic coils, 2 – radiation shield, 3 – vacuum tank, 4 – drum, 5 – plain bearing, 6 – helium supply, 7 – vacuum line, 8 – current supply

Electrical separation

Electrical separation utilises the difference in electrical conductivity between the various minerals in the ore feed. Since almost all minerals show some difference in conductivity it would appear to represent the universal concentrating method. In practice, however, the method has fairly limited application, and its greatest use is in separating some of the minerals found in heavy sands from beach or stream placers (Dance and Morrison, 1992). The fact that the feed must be perfectly dry imposes limitations on the process, but it also suffers from the same great disadvantage as dry magnetic separation – the capacity is very small for finely divided material. For most efficient operation, the feed should be in a layer, one particle deep, which severely restricts the throughput if the particles are as small as, say, 75 μm.

The first mineral separation processes utilising high voltage were virtually true electrostatic processes employing charged fields with little or no current flow. High-tension separation, however, makes use of a comparatively high rate of electrical discharge, with electron flow and gaseous ionisation having major importance. The theory of electrostatic and high-tension separations has been comprehensively reviewed by Kelly and Spottiswood (1989a–c) and Manouchehri et al. (2000).

The attraction of particles carrying one kind of charge towards an electrode of the opposite charge is known as the "lifting effect", as such particles are lifted from the separating surface towards the electrode. Materials which have a tendency to become charged with a definite polarity may be separated from each other by the use of the lifting effect even though their conductivities may be very similar. As an example, quartz assumes a negative charge very readily and may be separated from other poor conductors by an electrode which carries a positive charge. Pure electrostatic separation is relatively inefficient, even with very clean mineral, and is sensitive to changes of humidity and temperature.

A large percentage of the commercial applications of high-tension separation has been made using the "pinning effect", in which non-conducting mineral particles, having received a surface charge from the electrode, retain this charge and are pinned to the oppositely charged separator surface by positive–negative attraction. Figure 13.20 shows a laboratory high-tension separator, which makes use of the pinning effect to a high degree in combination with some lifting effect. Figure 13.21 shows the principle of separation diagrammatically.

The mixture of ore minerals, of varying susceptibilities to surface charge, is fed on to a rotating drum made from mild steel, or some other conducting material, which is earthed through its support bearings. An electrode assembly, comprising a brass tube in front of which is supported a length of fine wire, spans the complete length of the roll, and is supplied with a fully rectified DC supply of up to 50 kV, usually of negative polarity. The voltage supplied to the assembly should be such that ionisation of the air takes place. This can often be seen as a visible *corona discharge*. Arcing between the electrode and the roll must be avoided, as this destroys the ionisation. When ionisation occurs, the minerals receive a spray discharge of electricity which gives the poor conductors a high surface charge, causing them to be attracted to and pinned to the rotor surface. The particles of relatively high conductivity do not become charged as rapidly, as the charge rapidly dissipates through the particles to the earthed rotor. These particles of higher conductivity follow a path, when leaving the rotor, approximating to the one which they would assume if there were no charging effect at all.

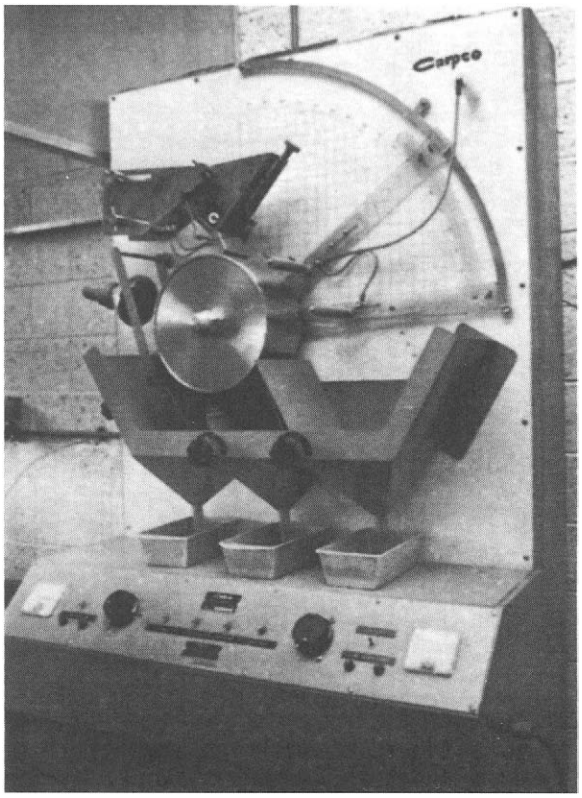


Figure 13.20 Laboratory high-tension separator

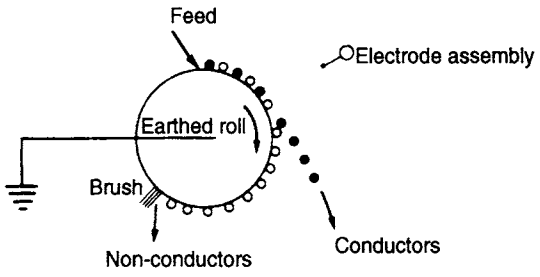


Figure 13.21 Principle of high-tension separation

The electrode assembly is designed to create a very dense high-voltage discharge. The fine wire of the assembly is placed adjacent to and parallel to the large diameter electrode and is mechanically and electrically in contact with it. This fine wire tends to discharge readily, whereas the large tube tends to have a short, dense, non-discharging field. This combination creates a very strong discharge pattern which may be "beamed" in a definite direction and concentrated to a very narrow arc. The effect on the minerals passing through the beam is very strong and is due largely to gaseous ions which are created due to the high-voltage gradient in the field of the corona.

A combination of the effects of pinning and lifting can be created by using a static electrode large enough to preclude corona discharge, following the electrode. The conducting particles, which are flung from the rotor, are attracted to this electrostatic electrode, and the compound process produces a very wide and distinct separation between the conducting and the non-conducting particles.

Table 13.1 shows typical minerals which are either pinned to or thrown from the rotor during high-tension separation.

Table 13.1 Typical behaviour of minerals in high-tension separators

Minerals pinned to rotor	*Minerals thrown from rotor*
Apatite	Cassiterite
Barite	Chromite
Calcite	Diamond
Corundum	Fluorspar
Garnet	Galena
Gypsum	Gold
Kyanite	Hematite
Monazite	Ilmenite
Quartz	Limonite
Scheelite	Magnetite
Sillimonite	Pyrite
Spinel	Rutile
Tourmaline	Sphalerite
Zircon	Stibnite
	Tantalite
	Wolframite

To cater for such an extensive range of minerals, all the parameters influencing separation must be readily adjusted while the separator is performing. These variables include the roll speed, the position of the electrode wire with respect to the electrode tube, the position of the electrode assembly with respect to the roll, variation of the DC voltage and polarity, the splitter plate position, the feed rate, and heating of the feed. Heating the feed is important, since best results are generally obtained only with very dry material. This is particularly difficult in high humidity regions. It is not often that a single pass will sufficiently enrich an ore and Figure 13.22. shows a typical flowsheet, where the falling particles are deflected to lower sets of rollers and electrodes until the required separation has taken place.

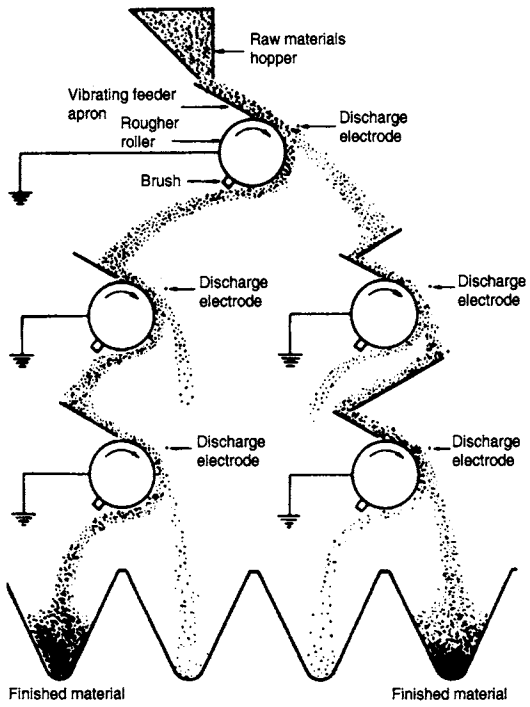


Figure 13.22 Arrangement of separators in practice

High-tension separators operate on feeds containing particles of between 60 and 500 μm in diameter. Particle size influences separation behaviour, as the surface charges on a coarse grain are lower in relation to its mass than on a fine grain. Thus a coarse grain is more readily thrown from the roll surface, and the conducting fraction often contains a small proportion of coarse non-conductors. Similarly, the finer particles are most influenced by the surface charge, and the non-conducting fraction often contains some fine conducting particles.

Final cleaning of these products is often carried out in purely electrostatic separators, which employ the "lifting effect" only. Modern electrostatic separators are of the plate or screen type, the former being used to clean small amounts of non-conductors from a predominantly conducting feed, while the screen separators remove small amounts of conductors from a mainly non-conducting feed. The principle of operation is the same for both types of separator. The feed particles gravitate down a sloping, grounded plate into an electrostatic field induced by a large, oval, high-voltage electrode (Figure 13.23).

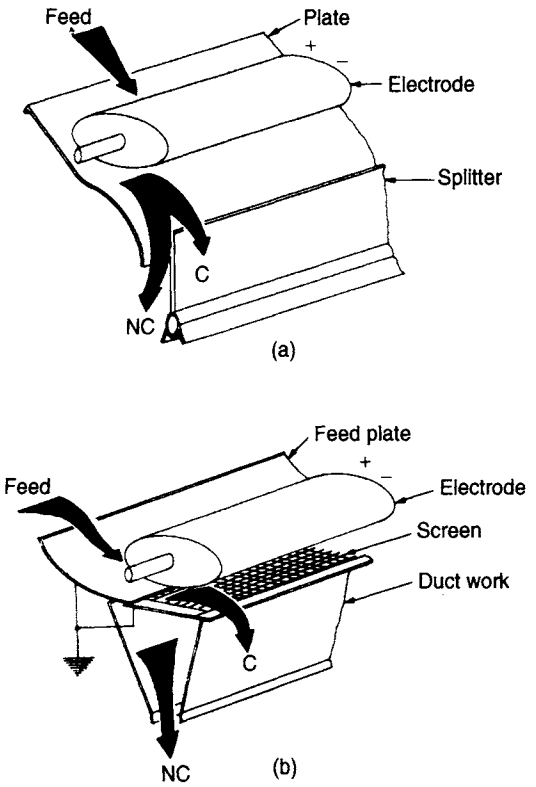


Figure 13.23 (a) Plate and (b) screen electrostatic separators

The electrostatic field is effectively shorted through the conducting particles, which are lifted towards the charged electrode in order to decrease the energy of the system. Non-conductor grains are poorly affected by the field. The fine grains are most affected by the lifting force, and so fine conductors are preferentially lifted to the electrode, whereas coarse non-conductors are most efficiently rejected. This is the converse of the separation which takes place in the high-tension separators, where most effective separation of fine non-conductors from coarse conductors takes place; a combination of high-tension separators as primary roughers, followed by final cleaning in electrostatic separators, is therefore used in many flowsheets. Since the magnitude of the forces involved in electrostatic separation is very low, the separators are designed for multiple passes of the non-conductors (Figure 13.24).

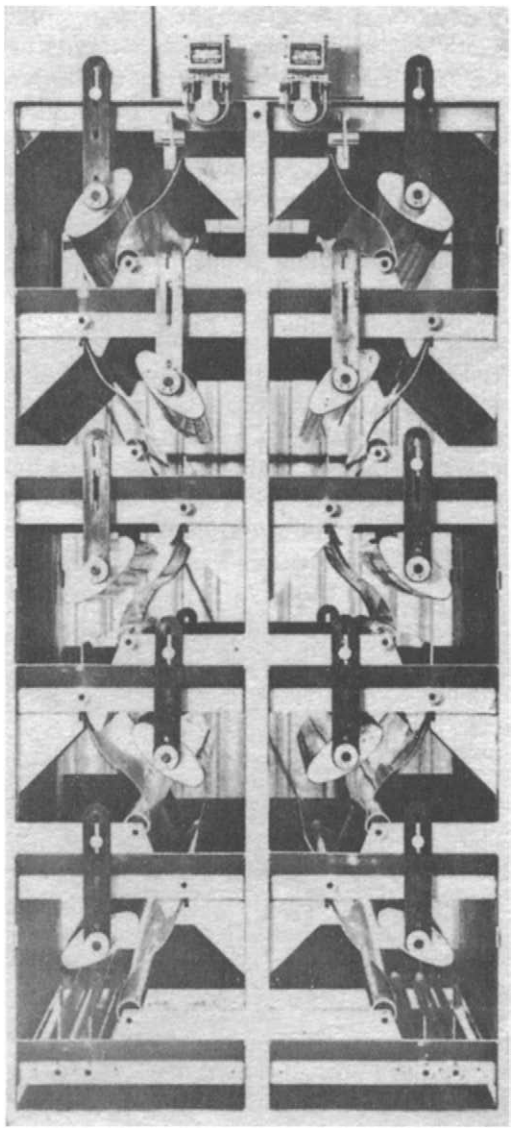


Figure 13.24 Plate electrostatic separator with two-start, ten electrodes

High tension roll (HTR) and electrostatic plate (ESP) separators have been the mainstay of the mineral sands industry for the last 50 years. Very little development of the machines has occurred in that period, their generally poor single pass separation has been tolerated, and overcome by using multiple machines and multiple recycle streams. However, in the last few years innovative new designs have started to appear, from new as well as established manufacturers. OreKinetics has introduced the new CoronaStat and UltraStat machines. These machines which are significant developments of existing HTR and ESP machines employ additional static electrodes which improve efficiency of separation. Unlike existing machines the static electrodes are not exposed, making the machines much safer to operate.

Existing manufacturers have also introduced new electrical separation machines. Roche Mining (MT) have developed the Carara HTR separator which incorporates an additional insulated plate static electrode (Germain et al., 2003). Outokumpu Technology have developed the eForce HTR separator, which also incorporates additional static electrodes, as well as an electrostatic feed classifier (Elder and Yan, 2003).

These new generation machines will change the way heavy minerals plants are designed. Their improved efficiencies will reduce the number of stages required, and hence the capital cost of the plant.

It was mentioned earlier that there is some possibility of an overlap in the application of magnetic and high-tension separators, particularly in the processing of heavy mineral sand deposits. Table 13.2. shows some of the common minerals present in such alluvial deposits, along with their properties, related to magnetic and high-tension separation. Mineral sands are commonly mined by floating dredges, feeding floating concentrators at up to $2000\,t\,h^{-1}$ or more. Figure 13.25

Table 13.2 Typical beach sand minerals

Magnetics	*Non-magnetics*
Magnetite – T	Rutile – T
Ilmenite – T	Zircon – P
Garnet – P	Quartz – P
Monazite – P	

T = thrown from high-tension separator surface.
P = pinned to high-tension separator surface.

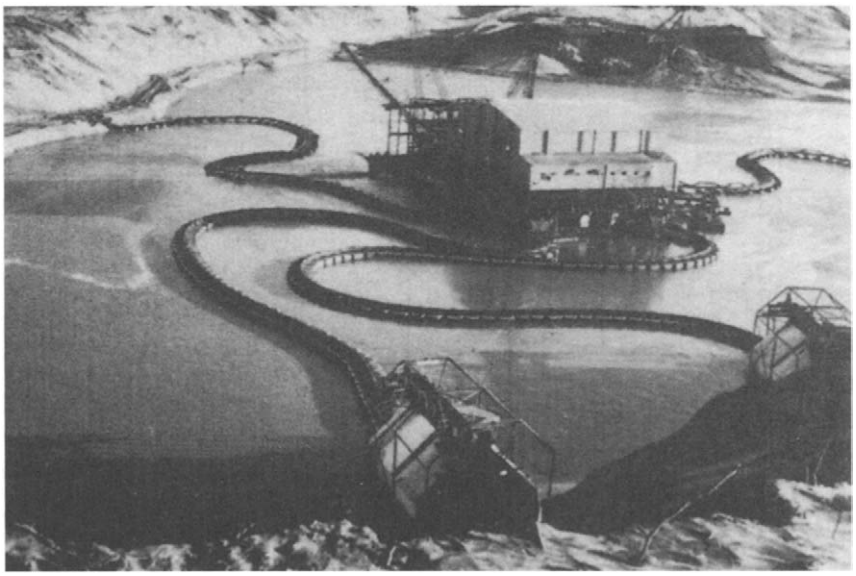


Figure 13.25 Heavy mineral sand mining and pre-concentration plant

shows a typical dredge and floating concentrator operating at Richards Bay in South Africa. Such concentrators, consisting of a complex circuit of sluices, spirals, or Reichert cones, upgrade the heavy mineral content to around 90%, the feed grades varying from less than 2%, up to 20% heavy mineral in some cases. The gravity concentrate is then transferred to the separation plant for recovery of the minerals by a combination of gravity, magnetic, and high-tension methods.

Flowsheets vary according to the properties of valuable minerals present, wet magnetic separation often preceding high-tension separation where magnetic ilmenite is the dominant mineral. A generalised flowsheet for such a separation is shown in Figure 13.26. Low-intensity drum separators remove any magnetite from the feed, after which high-intensity wet magnetic separators separate the monazite and ilmenite from the zircon and rutile. Drying of these two fractions is followed by high-tension separation to produce final separation, although further cleaning is sometimes carried out by electrostatic separators. For example, screen electrostatic separators may be used to clean the zircon and monazite concentrates, removing fine conducting particles from these fractions. Similarly, plate electrostatic separators could be used to reject coarse non-conducting particles from the rutile and ilmenite concentrates.

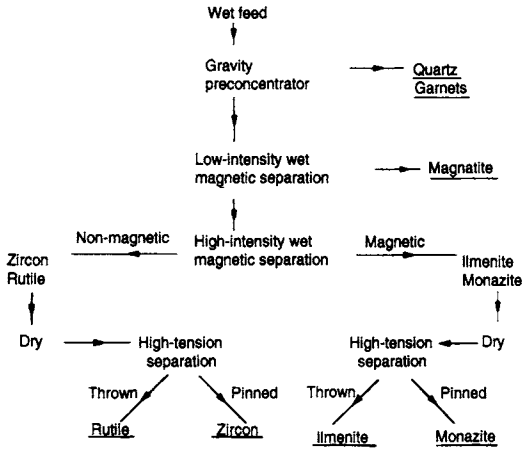


Figure 13.26 Typical beach sand treatment flowsheet

Figure 13.27 shows a simplified circuit used by Tiwest Joint Venture, on the west coast of Australia (Benson et al., 2001).

The heavy mineral concentrate is first separated into conductor and non-conductor streams using HTR separators. The conductors are treated using crossbelt and roll magnet separators to remove the ilmenite as a magnetic product. The non-magnetic stream is cleaned with high intensity roll and rare earth magnets to separate the weakly magnetic leucoxene from non-magnetic rutile. The non-conductors undergo another stage of wet gravity separation to remove quartz and other low density contaminants, before sizing and cleaning using HTR, ESP and Ultrastat separators to produce fine and coarse zircon products.

Similar flowsheets are used in South-East Asia for the treatment of alluvial cassiterite deposits, which are also sources of minerals such as ilmenite, monazite and zircon.

Magnetic separators are commonly used for upgrading low-grade iron ores, wet high-intensity separation often replacing the flotation of hematite. A combination of magnetic and high-tension separation has been used at the Scully Mine of Wabush Mines in Canada (Anon., 1974). The ore, grading about 35% Fe, is a quartz-specular hematite-magnetite schist, and after crushing and autogenous grinding to −1 mm, is fed to banks of rougher and cleaner spiral concentrators (Figure 13.28).

The spiral concentrate is filtered and dried, and cleaned in high-tension roll separators. The spiral tailings are thickened, and further treated by magnetic drum separators to remove residual magnetite, followed by Jones wet high-intensity separators, which remove any remaining hematite. The magnetic concentrates are classified and dried, and blended with the high-tension product, to give a final concentrate of about 66% Fe. Cleaning of only the gravity tailings by magnetic separation is preferred, as relatively small amounts of magnetic concentrate have to be dealt with, the bulk of the material being unaffected by the magnetic field. Similarly, relatively little material is pinned to the rotor in the high-tension treatment of the gravity concentrate, the iron minerals being unaffected by the ionic field.

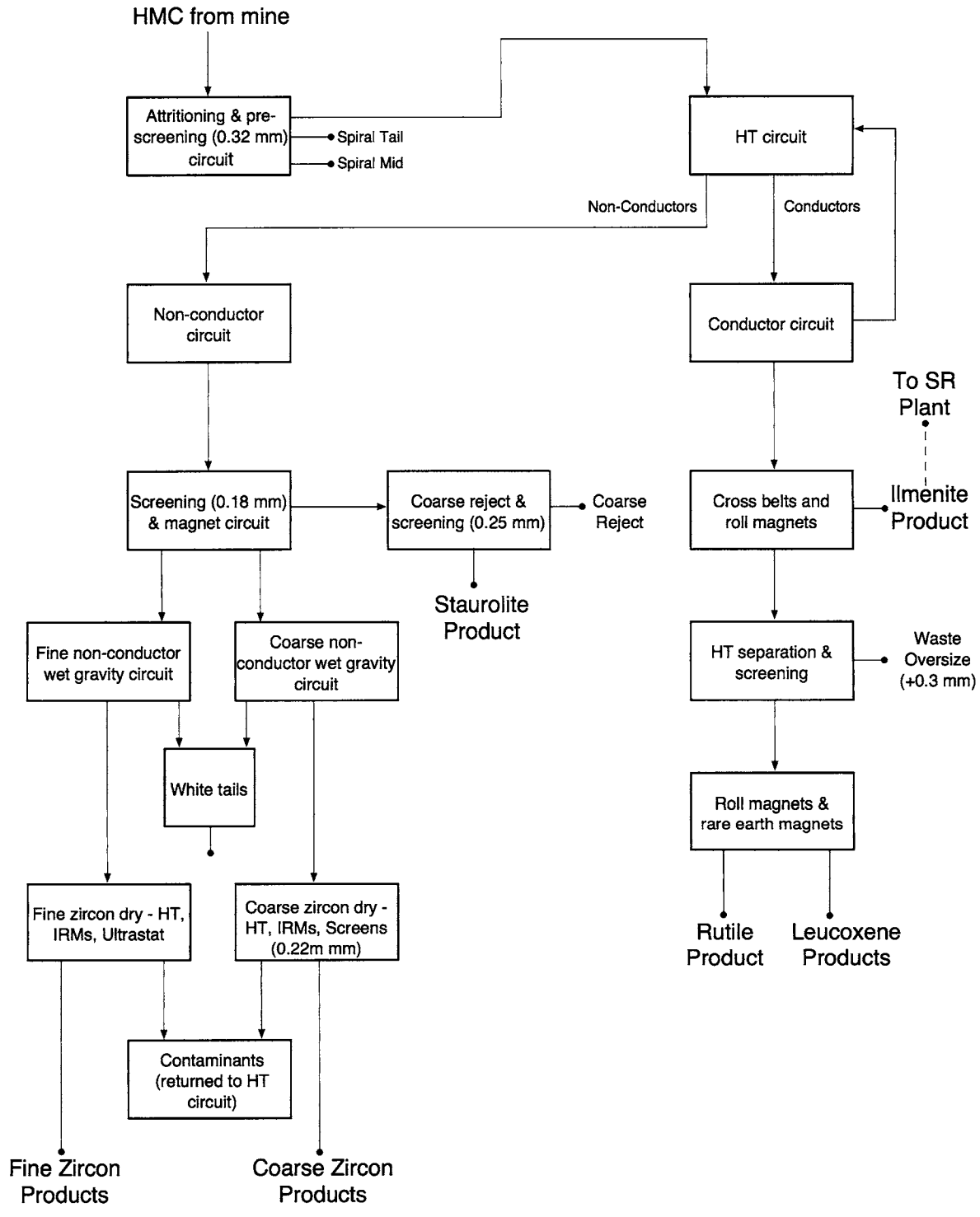


Figure 13.27 Simplified mineral sands circuit used by Tiwest Joint Venture (from Benson et al., 2001)

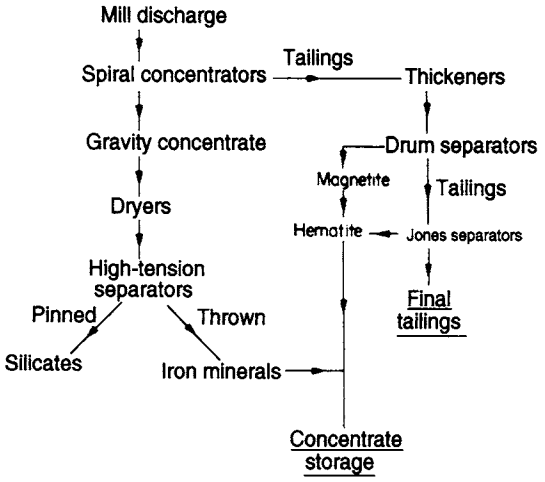


Figure 13.28 Flowsheet of Scully concentrator

References

Anon. (1974). Canadian iron mines contending with changing politics, restrictive taxes, *Engng. Min. J.* (Dec.), 72.

Arvidson, B.R. (2001). The many uses of rare-earth magnetic separators for heavy mineral sands processing, *Int. Heavy Minerals Conference*, Aust. IMM, Perth, 131.

Benson, S., Showers, G., Louden, P., and Rothnie, C. (2001). Quantitative and process mineralogy at Tiwest, *Int. Heavy Minerals Conference*, Aust. IMM, Perth, 60.

Cohen, H.E. (1986). Magnetic separation, in *Mineral Processing at a Crossroads*, ed. B.A. Wills and R.W. Barley, Martinus Nijhoff Publishers, Dordrecht, 287.

Corrans, I.J. (1984). The performance of an industrial wet high-intensity magnetic separator for the recovery of gold and uranium, *J. S. Afr. Inst. Min. Metall.*, **84**(Mar.), 57.

Dance, A.D. and Morrison, R.D. (1992). Quantifying a black art: The electrostatic separation of mineral sands, *Minerals Engng.*, **5(7)**, 751.

Elder, J. and Yan, E. (2003). eForce... Newest generation of electrostatic separator for the minerals sands industry, *Heavy Minerals 2003*, S. Afr. Inst. Min. Metall., Johannesburg, 63.

Germain, M., Lawson, T., Henderson, D.K., and MacHunter, D.M. (2003). The application of new design concepts in high tension electrostatic separation to the processing of mineral sands concentrates, *Heavy Minerals 2003*, S. Afr. Inst. Min. Metall., Johannesburg, 100.

Kelly, E.G. and Spottiswood, D.J. (1989a). The theory of electrostatic separations: A review, Part I: Fundamentals, *Minerals Engng.*, **2(1)**, 33.

Kelly, E.G. and Spottiswood, D.J. (1989b). The theory of electrostatic separations: A review, Part II: Particle charging, *Minerals Engng.*, **2(2)**, 193.

Kelly, E.G. and Spottiswood, D.J. (1989c). The theory of electrostatic separations: A review, Part III: The separation of particles, *Minerals Engng.*, **2(3)**, 337.

Kopp, J. (1991). Superconducting magnetic separators, *Magnetic and Electrical Separation*, **3(1)**, 17.

Lawver, J.E. and Hopstock, D.M. (1974). Wet magnetic separation of weakly magnetic minerals, *Minerals Sci. Engng.*, **6**, 154.

Lua, A.C. and Boucher, R.F. (1990). Sulphur and ash reduction in coal by high gradient magnetic separation, *Coal Preparation*, **8(1/2)**, 61.

Malati, M.A. (1990). Ceramic superconductors, *Mining Mag.*, **163**(Dec.), 427.

Manouchehri, H.R., Rao, K.H., and Forssberg, K.S.E. (2000). Review of electrical separation methods, Part 1: Fundamental aspects, *Minerals and Metallurgical Processing*, **17(1)**, 23.

Norrgran, D.A. and Marin, J.A. (1994). Rare earth permanent magnet separators and their applications in mineral processing, *Minerals and Metallurgical Processing*, **11(1)**, 41.

Stefanides, E.J. (1986). Superconducting magnets upgrade paramagnetic particle removal, *Design News*, May.

Svoboda, J. (1987). *Magnetic Methods for the Treatment of Minerals*, Elsevier, Amsterdam.

Svoboda, J. (1994). The effect of magnetic field strength on the efficiency of magnetic separation, *Minerals Engng.*, **7(5/6)**, 747.

Tawil, M.M.E. and Morales, M.M. (1985). Application of wet high intensity magnetic separation to sulphide mineral beneficiation, in *Complex Sulfides*, ed. A.D. Zunkel, TMS-AIME, Pennsylvania, 507.

Unkelbach, K.H. and Kellerwessel, H. (1985). A superconductive drum type magnetic separator for the beneficiation of ores and minerals, *Proc. XVth Int. Min. Proc. Cong.*, Cannes, **1**, 371.

Wasmuth, H.-D. and Unkelbach, K.-H. (1991). Recent developments in magnetic separation of feebly magnetic minerals, *Minerals Engng.*, **4(7–11)**, 825.

Watson, J.H.P. (1994). Status of superconducting magnetic separation in the minerals industry, *Minerals Engng.*, **7(5/6)**, 737.

White, L. (1978). Swedish symposium offers iron ore industry an overview of ore dressing developments, *Engng. Min. J.*, **179**(Apr.), 71.

14

Ore sorting

Introduction

Ore sorting is the original concentration process, having probably been used by the earliest metal workers several thousand years ago. It involves the appraisal of *individual* ore particles and the rejection of those particles that do not warrant further treatment.

Hand sorting has declined in importance due to the need to treat large quantities of low-grade ore which requires extremely fine grinding. Hand sorting of some kind, however, is still practised at some mines, even though it may only be the removal of large pieces of timber, tramp iron, etc. from the run-of-mine ore.

Electronic ore-sorting equipment was first produced in the late 1940s, and although its application is fairly limited, it is an important technique for the processing of certain minerals (Sassos, 1985; Salter and Wyatt, 1991; Sivamohan and Forssberg, 1991; Collins and Bonney, 1998; Arvidson, 2002).

Electronic sorting principles

Sorting can be applied to pre-concentration, in which barren waste is eliminated to reduce the tonnage reporting to the downstream concentration processes, such as in uranium or gold ore sorting, or to the production of a final product, such as in limestone or diamond sorting. The ore must be sufficiently liberated at a coarse size (greater than 5–10 mm) to allow barren waste to be discarded without significant loss of value. Preconcentration by sorting is seen as a method of improving the sustainability of mineral processing operations by reducing the consumption of energy and water in grinding and concentration, and achieving more benign tailings disposal (Cutmore and Ebehardt, 2002).

Many rock properties have been used as the basis of electronic sorting, including reflectance and colour in visible light (magnesite, limestone, base metal and gold ores, phosphates, talc, coal), ultraviolet (scheelite), natural gamma radiation (uranium ore), magnetism (iron ore), conductivity (sulphides), and X-Ray luminescence (diamonds). Infrared, Raman, microwave attenuation, and other properties have also been tested.

Electronic sorters inspect the particles to determine the value of some property (e.g. light reflectance) and then eject those particles which meet some criterion (e.g. light vs dark rocks). Either valuables or waste may be selected for ejection. It is essential, therefore, that a distinct difference in the required physical property is apparent between the valuable minerals and the gangue.

The particle surfaces must be thoroughly washed before sorting, so that blurring of the signal does not occur and, as it is not practical to attempt to feed very wide rock size ranges to a single machine, the feed must undergo preliminary sizing. The ore must be fed in a monolayer, as display of individual particles to the sorting device must be effected.

Photometric sorting is the mechanised form of hand-sorting, in which the ore is divided into components of differing value by visual examination (Arvidson, 2002).

The basis of the photometric sorter (Figure 14.1) is a laser light source and sensitive photomultiplier, used in a scanning system to detect light reflected from the surfaces of rocks passing through the sorting zone (Figure 14.2). Electronic circuitry analyses the photomultiplier signal, which changes with the intensity of the reflected light and produces control signals to actuate the appropriate valves of an air-blast rejection device to remove certain particles selected by means of the analysing process. The sorter is fully automatic and can be attended by one operator on a part-time basis. Typical throughput per machine ranges from $25\,t\,h^{-1}$ for a $-25+5$ mm feed to $300\,t\,h^{-1}$ for a $-300+80$ mm material.

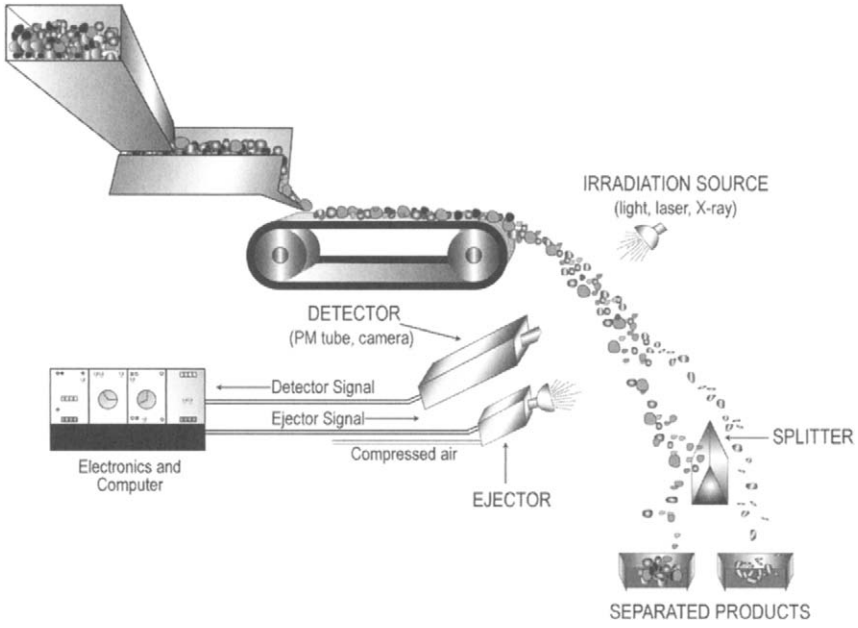


Figure 14.1 Principles of photometric sorting

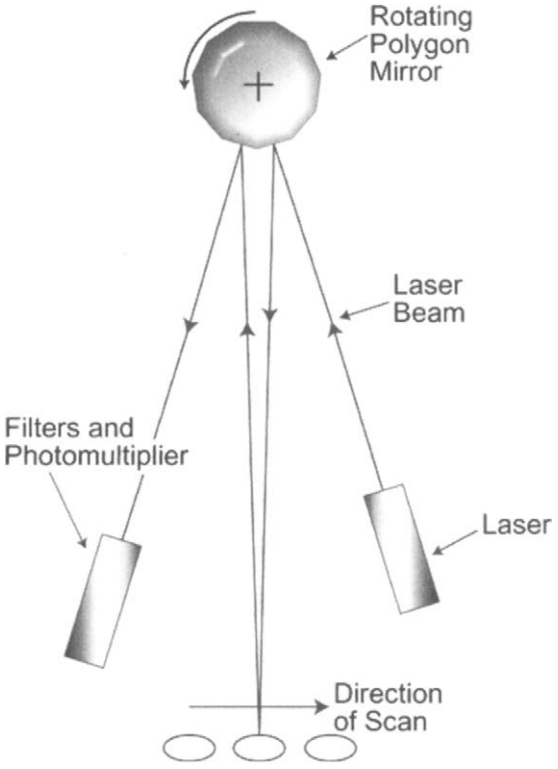


Figure 14.2 Laser beam scanning

Examples

The Gunson's Sortex MP80 machine was probably the first sorter to employ microprocessor technology (Anon., 1980). The sorter handled minerals in the size range 10–150 mm at feed rates of up to $150\,t\,h^{-1}$.

The RTZ Ore Sorters Model 16 photometric sorter has been used successfully in industry since 1976 on a wide range of ore types (Anon., 1981b).

An RTZ ore-sorting machine at the Doornfontein mine in South Africa was used for treating gold ores (Keys et al., 1974). Rocks having white or grey quartz pebbles in a darker matrix are accepted, while quartzite, ranging from light green, through olive green to black, is rejected. Most of the gold occurs in rocks in the "accept" category. Uniform distribution of the ore entering the sorter is achieved by the use of tandem vibrating feeders and the ore is washed on the second feeder to remove slimes which may affect the light-reflecting qualities.

The modern photometric sorter is typified by the UltraSort UFS120, which is used in the processing of magnesite, feldspar, limestone, and talc. Ore passes from a vibrating feeder to high pressure water sprays and counterweight feeder where water is removed and the rocks are accelerated to form a monolayer. They drop onto a short conveyor

moving at 2 m/s from where they pass via a high speed 5 m/s "slinger" conveyor into free fall, now well separated. The rock layer, 0.8–1.2 m wide, is scanned by a laser beam at up to 4000 times per second, and the reflection analysed in less than 0.25 μs by photomultiplier tubes and high speed parallel processors operating in excess of 80 MB/s. One or more of 120 air ejectors are fired to divert the value or waste past a cutter and into the accept/reject bins. As the position of the rock is accurately identified, and the ejector firing duration is less than 1 ms, the sorter can operate very selectively. A range of lasers of different wavelengths can be used, from ultraviolet to infrared, to achieve optimum discrimination.

Scanning video cameras can be used in place of the scanning laser and photomultiplier tubes, to provide more subtle discrimination of rock properties using image analysis techniques.

Electronic sorting has been employed in diamond recovery since the 1960s, initially using simple optical sorters and more recently machines based on the fact that diamonds luminesce when irradiated by X-Rays (Anon., 1971; Rylatt and Popplewell., 1999). X-Ray sorters are used in almost all diamond operations for the final stages of recovery after the ore has been concentrated by DMS (Chapter 11). They replace grease separation (Chapter 12) which is now used only in rare cases where the diamonds luminesce weakly or to audit the X-Ray tailings. Luminescence is a more consistent diamond property than oleophilicity, and sorters are more secure than grease belts or tables. Figure 14.3 shows an early dry X-Ray sorter, in which the DMS concentrates are exposed to a beam of X-Rays in free fall from a conveyor belt, the luminescence detected by photomultiplier tubes and the diamonds ejected by air ejectors. Both dry and wet X-Ray machines are now available, and the process is usually multistage to ensure efficient rejection of waste with very high diamond recoveries.

Radiometric sorting has been used to preconcentrate uranium ore in South Africa (Anon., 1981c), Namibia, Australia (Bibby, 1982), and Canada. A sorter installed at the Rossing Mine in Namibia (Gordon and Heuer, 2000) detects gamma radiation from the higher grade ore pieces using scintillation counters comprising NaI crystals and photomultiplier tubes mounted under the belt (Figure 14.4). Lead shielding is used to achieve improved resolution of detection. A laser-based optical system similar to that used in photometric sorters is used to determine rock position and size for ejection, and can be adapted to determine additional optical characteristics of the rocks.

Several other physical properties of ores and minerals have been exploited in a range of sorting machines.

Neutron absorption separation has been used for the sorting of boron minerals (Mokrousov et al., 1975). The ore is delivered by a conveyor belt between a slow neutron source and a scintillation neutron detector. The neutron flux attenuation by the ore particles is detected and used as the means of sorting. The method is most applicable in the size range 25–150 mm. Boron minerals are easy to sort by neutron absorption since the neutron capture cross-section of the boron atom is very large compared with those of common associated elements and thus the neutron absorption is almost proportional to the boron content of the particles.

Photoneutron separation is recommended for the sorting of beryllium ores, since when a beryllium isotope in the mineral is exposed to gamma radiation of a certain energy, a photoneutron is released and this may be detected by scintillation or by a gas counter.

The RTZ Ore Sorters Model 19 sorter measured conductivity and magnetic properties and had application to a wide variety of ores including sulphides, oxides, and native metals (Anon., 1981a). The machine treated 25–150 mm rocks at up to 120 t/h. Such systems employ a tuned coil under the belt which is influenced by the conductivity and/or magnetic susceptibility of the rocks in its proximity. Phase shift and amplitude are used to decide on acceptance or rejection. The radiometric sorter shown in Figure 14.4 can be adapted to conductivity and magnetic sorting by replacing the scintillometers with 40 electromagnetic sensors.

Outokumpu developed the "Precon" sorter and installed it at its Hammaslahti copper mine, now closed (Kennedy, 1985). It used gamma scattering analysis to evaluate the total metal content, and had a capacity of 7 t/h for 35 mm lumps rising to 40 t/h for 150 mm lumps. It preconcentrated primary crushed ore, rejecting about 25% as waste grading 0.2% copper, compared with an average feed grade of 1.2%.

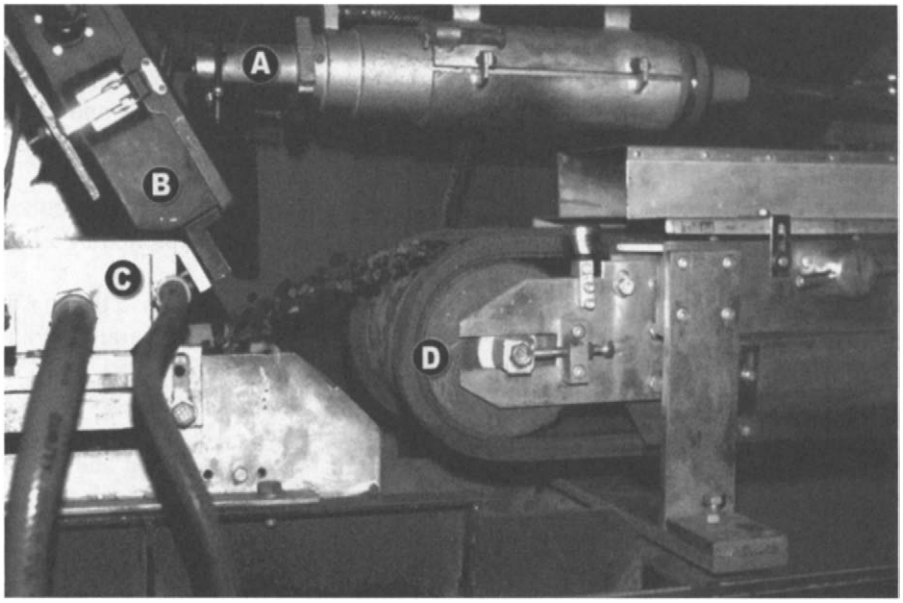


Figure 14.3 Early diamond sorter. A: X-Ray generator; B: Photomultiplier tubes; C: Air ejectors; D: Feed belt (Courtesy JKMRC and JKTech Pty Ltd)

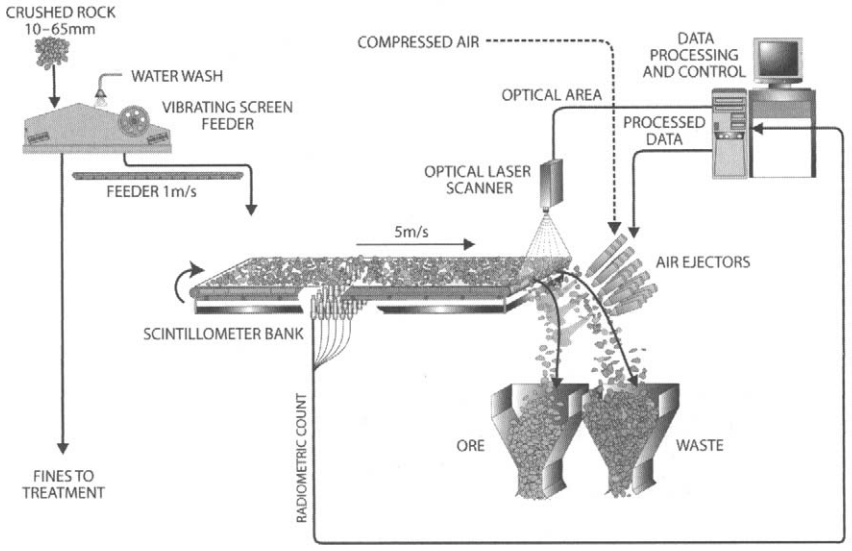


Figure 14.4 The Ultrasort radiometric sorter (Courtesy Ultrasort Pty Ltd)

Microwave attenuation has been used to sort diamond-bearing kimberlite from waste rock (Salter et al., 1989). The development was notable for the first use of high speed pulsed water ejectors.

Equipment to sort asbestos ore has been developed (Collier et al., 1973). The detection technique was based on the low thermal conductivity of asbestos fibres and used sequential heating and infra-red scanning to detect the asbestos seams. A similar machine was installed at King Island Scheelite in Tasmania, where the scheelite was sensed by its fluorescence under ultra-violet radiation.

References

Anon. (1971). New generation of diamond recovery machines developed in South Africa, *S.A. Min. Eng. J.*, May, 17.

Anon. (1980). Micro-processor speeds optical sorting of industrial minerals, *Mine and Quarry*, **9**(Mar.), 48.

Anon. (1981a). New ore sorting system, *Min. J.*, (11 Dec.), 446.

Anon. (1981b). Photometric ore sorting, *World Mining*, **34**(Apr.), 42.

Anon. (1981c). Radiometric sorters for Western Deep Levels gold mine, South Africa, *Min. J.*, Aug., 132.

Arvidson, B. (2002). Photometric ore sorting, in *Mineral Processing Plant Design, Practice and Control*, ed. A.L. Mular, D.N. Halbe, and D.J. Barratt, 1033–1048 (SME).

Bibby, P.A. (1982). Preconcentration by radiometric ore sorting, *Proc. First Mill Operators Conference, Mt. Isa*, 193–201 (Aus. IMM).

Collier, D., et al. (1973). Ore sorters for asbestos and scheelite, *Proc. 10th Int. Min. Proc. Cong.*, London.

Collins, D.N. and Bonney, C.F. (1998). Separation of coarse particles (over 1 mm), *Int. Min. Miner.*, **1, 2**(Apr.), 104–112.

Cutmore, N.G. and Ebehardt, J.E. (2002). The future of ore sorting in sustainable processing, *Proc. Green Processing, Cairns*, May, 287–289 (Aus. IMM).

Gordon, H.P. and Heuer, T. (2000). New age radiometric sorting – the elegant solution, in *Proc. Uranium 2000, Saskatoon*, ed. E. Ozberk, and A.J. Oliver, 323–337 (Can. Inst. Min. Met.).

Kennedy, A. (1985). Mineral processing developments at Hammaslahti, Finland, *Mining Mag.* (Feb.), 122.

Keys, N.J., et al. (1974). Photometric sorting of ore on a South African gold mine, *J. S. Afr. IMM*, **75** (Sept.), 13.

Mokrousov, V.A., et al. (1975). Neutron-radiometric processes for ore beneficiation, *Proc. XIth Int. Min. Proc. Cong*, Cagliari, 1249.

Rylatt, M.G. and Popplewell, G.M. (1999). The BHP NWT diamonds project: Diamond processing in the Canadian Arctic, *Min. Engng.*, **51, 1(37–43)** and **2 (19–25)**, Jan. and Feb.

Salter, J.D. and Wyatt, N.P.G. (1991). Sorting in the minerals industry: Past, present and future, *Minerals Engng.*, **4(7–11)**, 779.

Salter, J.D. et al. (1989). Kimberlite-gabbro sorting by use of microwave attenuation: Development from the laboratory to a 100 t/h pilot plant, *Proc. Mat. Min. Inst. Japan – Inst. Min. Met. Symp. "Today's Technology for the Mining and Metallurgical Industries"*, Kyoto (Oct.), 347–358 (Inst. Min. Met.).

Sassos, M.P. (1985). Mineral sorters, *Engng. Min. J.*, **185**(Jun.), 68.

Sivamohan, R. and Forssberg, E. (1991). Electronic sorting and other preconcentration methods, *Minerals Engng.*, **4(7–11)**, 797.

15

Dewatering

Introduction

With few exceptions, most mineral-separation processes involve the use of substantial quantities of water and the final concentrate has to be separated from a pulp in which the water–solids ratio may be high.

Dewatering, or solid–liquid separation, produces a relatively dry concentrate for shipment. Partial dewatering is also performed at various stages in the treatment, so as to prepare the feed for subsequent processes.

Dewatering methods can be broadly classified into three groups:

(1) sedimentation;
(2) filtration;
(3) thermal drying.

Sedimentation is most efficient when there is a large density difference between liquid and solid. This is always the case in mineral processing where the carrier liquid is water. Sedimentation cannot always be applied in hydrometallurgical processes, however, because in some cases the carrier liquid may be a high-grade leach liquor having a density approaching that of the solids. In some cases, filtration may be necessary.

Dewatering in mineral processing is normally a combination of the above methods. The bulk of the water is first removed by sedimentation, or thickening, which produces a thickened pulp of perhaps 55–65% solids by weight. Up to 80% of the water can be separated at this stage. Filtration of the thick pulp then produces a moist filter cake of between 80 and 90% solids, which may require thermal drying to produce a final product of about 95% solids by weight.

Sedimentation

Rapid settling of solid particles in a liquid produces a clarified liquid which can be decanted, leaving a thickened slurry, which may require further dewatering by filtration.

The settling rates of particles in a fluid are governed by Stokes' or Newton's laws, depending on the particle size (Chapter 9). Very fine particles, of only a few microns diameter, settle extremely slowly by gravity alone, and centrifugal sedimentation may have to be performed. Alternatively, the particles may be agglomerated, or *flocculated*, into relatively large lumps, called *flocs*, that settle out more rapidly.

Coagulation and flocculation

Coagulation causes extremely fine colloidal particles to adhere directly to each other. All particles exert mutual attraction forces, known as *London-Van der Waals' forces*, which are effective only at very close range. Normally, the adhesion due to these forces is prevented by the presence around each particle of an electrically charged atmosphere, which generates repulsion forces between particles approaching each other. There is, therefore, in any given system a balance between the attractive forces and the electrical repulsion forces present at the solid–liquid interface (Figure 15.1).

In any given system the electrical charges on the particle surfaces will be of the same sign, aqueous suspensions of pH 4 and above generally being negative. Positively charged surfaces occur mainly in strong acid solutions.

The repulsion forces not only prevent coagulation of the particles, but also retard their settlement by keeping them in constant motion, this effect being more pronounced the smaller the particle.

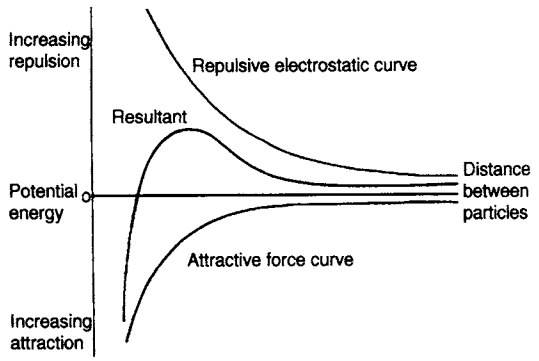


Figure 15.1 Potential energy curves for two particles approaching each other

Coagulants are electrolytes having an opposite charge to the particles, thus causing charge neutralisation when dispersed in the system, allowing the particles to come into contact and adhere as a result of molecular forces. Inorganic salts have long been used for this purpose, and as counter-ions in aqueous systems are most frequently positively charged, salts containing highly charged cations, such as Al+++, Fe+++, and Ca++, are mainly used. Lime, or sulphuric acid, depending on the surface charge of the particles, can also be used to cause coagulation. Most pronounced coagulation occurs when the particles have zero charge in relation to the suspending medium, this occurring when the *zeta potential* is zero. The nature of the zeta potential can be seen from Figure 15.2, which shows a model of the *electrical double layer* at the surface of a particle (Moss, 1978). The surface shown has a negative charge, such that positive ions from solution will be attracted to it, forming a bound layer of positive ions, known as the *Stern layer* and a *diffuse layer* of counter ions decaying in concentration with increasing distance until the solution equilibrium concentration is attained. These layers of ions close to the surface constitute the electrical double layer. When a particle moves in the liquid, shear takes place between the bound layer, which moves with the particle, and the diffuse layer, the potential at the plane of shear being known as the zeta potential. The magnitude of the zeta potential depends on the surface potential and the concentration and charge of the counter-ions. In general, the greater the counter-ion charge and counter-ion concentration, the lower is the zeta potential, although ions

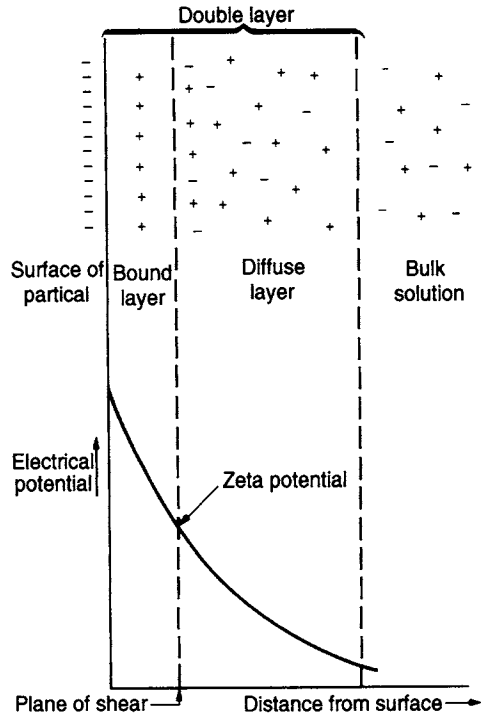


Figure 15.2 The electrical double layer

of high charge may cause complete charge reversal; therefore optimum doses of electrolyte are critical.

Flocculation involves the formation of much more open agglomerates than those resulting from coagulation and relies upon molecules of reagent acting as bridges between separate suspended particles (Hunter and Pearse, 1982; Pearse, 1984; Hogg, 2000). The reagents used to form the "bridges" are long-chain organic polymers, which were formerly natural minerals, such as starch, glue, gelatine, and guar gum, but which are now increasingly synthetic materials, loosely termed polyelectrolytes. The majority of these are anionic in character but some of them are non-ionic, and some cationic, but these form a minor proportion of the commercially available products of today's flocculant market. Inorganic salts are not able to perform this bridging function, but they are sometimes used in conjunction with an organic reagent as a cheaper means of charge neutralisation, although an ionic polyelectrolyte can and often does perform both functions.

The polyacrylamides, which vary widely in molecular weight and charge density, are extensively used as flocculants (Mortimer, 1991). The charge density refers to the percentage of the acrylic

monomer segments which carry a charge. For instance, if the polymer is uncharged it comprises n similar segments of the acrylic monomer. The polymer is thus a homopolymer polyacrylamide.

Chemical formula

If the acrylic monomer is completely hydrolysed with NaOH, the product comprises n segments of sodium acrylate – an anionic polyelectrolyte, having a charge density of 100%.

Charge density may be controlled in manufacture between the limits 0 and 100%, to produce a polyacrylamide of anionic character, weak or strong, depending on the degree of hydrolysis.

By similar chemical reactions, polymers of cationic character can be produced. Much of the development, to date, of the polyacrylamide family of products has been directed towards providing products of increasingly higher molecular weight, whilst maintaining the high degree of water solubility required for use in solid–liquid separation. It is now possible to obtain water soluble products with a wide range of ionic character varying from 100% cationic content through non-ionic to 100% anionic content and with molecular weights from several thousand to over 10 million (Moody, 1992).

It would be expected that, since most suspensions encountered in the minerals industry contain negatively charged particles, cationic polyelectrolyes, where the cation adsorbs to the particles, would be most suitable. Although this is true for charge neutralisation purposes, and attraction of the polymer to the particle surface, it is not necessarily true for the "bridging" role of the flocculant. For bridging, the polymer must be strongly adsorbed, and this is promoted by chemical groups having good adsorption characteristics, such as amide groups. The majority of commercially available polyelectrolytes are anionic, since these tend to be of higher molecular weight than the cationics, and are less expensive.

The mode of action of the anionic polyacrylamide depends on a segment of the very long molecule being adsorbed on the surface of a particle, leaving a large proportion of the molecule free to be adsorbed on another particle, so forming an actual molecular linkage, or bridge, between particles (Figure 15.3).

While only one linkage is shown in Figure 15.3, in practice many such interparticle bridges are formed, linking a number of particles together. The factors influencing the degree of flocculation are the efficiency or strength of adsorption of the polymer on the surface, the degree of agitation during flocculation and the subsequent agitation, which can result in breakdown of flocs (Lightfoot, 1981; Owen et al., 2002).

Although the addition of flocculants to a slurry can lead to significant improvements in sedimentation characteristics, it also affects dewatering behaviour, flocculation generally being detrimental to final consolidation of the sediment. It is usually beneficial, however, to filtration processes, and flocculants are widely used as filter aids. However, the specific requirements of a flocculant used to promote sedimentation are not necessarily the same as for one used as a filter aid. The behaviour of the flocculated suspension and the performance of solid–liquid separations are determined by the size of the flocs and by their structure. Large flocs promote settling and are desirable for clarification and thickening. Floc density is of secondary importance in these processes. Conversely, dense flocs

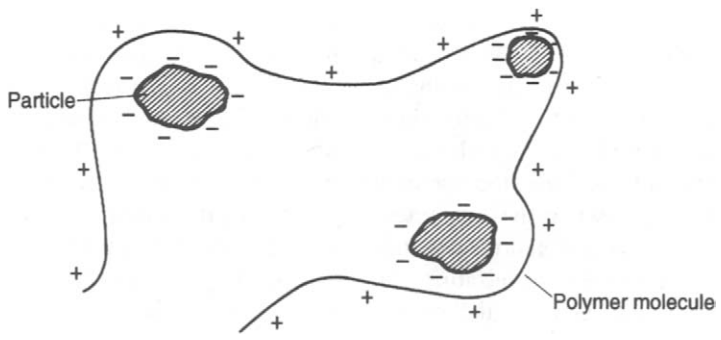


Figure 15.3 Action of an anionic polyelectrolyte

are most appropriate for consolidation of the sediment, and size is of lesser importance in this stage. Therefore the optimisation of solid–liquid separation processes requires careful control of floc size and structure. The maximum effect of a flocculant is achieved at an optimum dosage rate and pH; excess polymer can cause dispersion of the particles due to floc breakdown. Physical factors are also of great importance, growth and development of the flocs being affected by particle–particle collisions and hydrodynamic interactions (Hogg et al., 1987). Laboratory batch cylinder tests are commonly used to assess the effectiveness of flocculants to enhance the settling rate of suspensions. Reproducibility of such tests is often poor, depending on factors such as number of cylinder inversions and cylinder diameter. A new method using vertically mounted concentric rotating cylinders (Couette geometry) has been found to overcome these problems and give highly reproducible results (Farrow and Swift, 1996).

Due to the fragile nature of the flocs, flocculating agents are not successful with hydrocyclones, while success with centrifuges can only be achieved with special techniques for a limited range of applications. Even pumping of the flocculated slurry may destroy the flocs due to rupture of the long-chain molecules.

Polyelectrolytes are normally made up of stock solutions of about 0.5–1%, which are diluted to about 0.01% before adding to the slurry. The diluted solution must be added at enough points in the stream to ensure its contact with every portion of the system. A shower pipe is frequently used for this purpose (Figure 15.4). Recent work has shown that the age of the stock solution can have a significant effect on flocculant performance. Dosage decreased with solution age, the optimum age being 72 h (Owen et al., 2002).

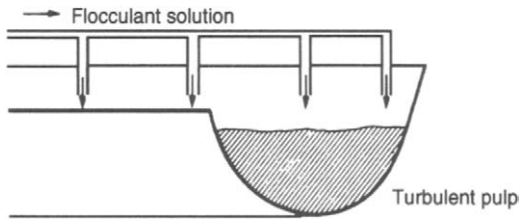


Figure 15.4 Typical method of flocculant addition

Mild agitation is essential at the addition points, and shortly thereafter, to assist in flocculant dispersion in the process stream. Care should be taken to avoid severe agitation after the flocs have been formed.

Selective flocculation

The treatment of finely disseminated ores often results in the production of ultra-fine particles, or slimes, which respond poorly to conventional separation techniques, and are often lost in the process tailings. *Selective* flocculation of the desired minerals in the pulp, followed by separation of the aggregates from the dispersed material, is a potentially important technique, although plant applications are at present rare (Attia, 1992). Although attempts have been made to apply selective flocculation to a wide range of ore types, the bulk of the work has been concerned with its application to the treatment of clays, iron, phosphate, and potash ores. A prerequisite for the process is that the mineral mixture must be stably dispersed prior to the addition of a high molecular weight polymer, which selectively adsorbs on only one of the constituents of the mixture. Selective flocculation is then followed by removal of the flocs of one component from the dispersion.

The greatest amount of work on selective flocculation has been concerned with the treatment of fine-grained non-magnetic oxidised taconites, which has led to the development of Cleveland Cliffs Iron Company's 10 Mt/yr operation in the United States. The finely intergrown ore is autogenously ground to 85%–25 μm with caustic soda and sodium silicate, which act as dispersants for the fine silica. The ground pulp is then conditioned with a corn-starch flocculant which selectively flocculates the hematite. About one-third of the fine silica is removed in a de-slime thickener, together with a loss of about 10% of the iron values. Most of the remaining coarse silica is removed from the flocculated underflow by reverse flotation, using an amine collector (Paananen and Turcotte, 1980; Siirak and Hancock, 1988).

Gravity sedimentation

Gravity sedimentation or *thickening* is the most widely applied dewatering technique in mineral

processing, and it is a relatively cheap, high-capacity process, which involves very low shear forces, thus providing good conditions for flocculation of fine particles.

The *thickener* is used to increase the concentration of the suspension by sedimentation, accompanied by the formation of a clear liquid. In most cases the concentration of the suspension is high and hindered settling takes place. Thickeners may be batch or continuous units, and consist of relatively shallow tanks from which the clear liquid is taken off at the top, and the thickened suspension at the bottom (Suttill, 1991; Schoenbrunn and Laros, 2002). The *clarifier* is similar in design, but is less robust, handling suspensions of much lower solid content than the thickener (Seifert and Bowersox, 1990).

The continuous thickener consists of a cylindrical tank, the diameter ranging from about 2 to 200 m in diameter, and of depth 1–7 m. Pulp is fed into the centre via a *feed-well* placed up to 1 m below the surface, in order to cause as little disturbance as possible (Figure 15.5). The clarified liquid overflows a peripheral launder, while the solids which settle over the entire bottom of the tank are withdrawn as a thickened pulp from an outlet at the centre. Within the tank are one or more rotating radial arms, from each of which are suspended a series of blades, shaped so as to rake the settled solids towards the central outlet. On most modern thickeners these arms rise automatically if the torque exceeds a certain value, thus preventing damage due to overloading. The blades also assist the compaction of the settled particles and produce a thicker underflow than can be achieved by simple settling. The solids in the thickener move continuously downwards, and then inwards towards the thickened underflow outlet, while the liquid moves upwards and radially outwards. In general, there is no region of constant composition in the thickener.

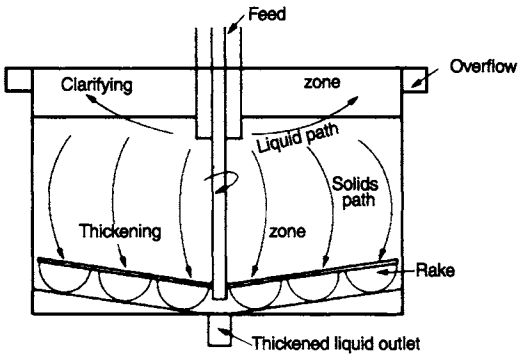


Figure 15.5 Flow in a continuous thickener

Thickener tanks are constructed of steel, concrete, or a combination of both, steel being most economical in sizes of less than 25 m in diameter. The tank bottom is often flat, while the mechanism arms are sloped towards the central discharge. With this design, settled solids must "bed-in" to form a false sloping floor. Steel floors are rarely sloped to conform with the arms because of expense. Concrete bases and sides become more common in the larger-sized tanks. In many cases the settled solids, because of particle size, tend to slump and will not form a false bottom. In these cases the floor should be concrete and poured to match the slope of the arms. Tanks may also be constructed with sloping concrete floors and steel sides, and earth bottom thickeners are in use, which are generally considered to be the lowest cost solution for thickener bottom construction (Hsia and Reinmiller, 1977).

The method of supporting the mechanism depends primarily on the tank diameter. In relatively small thickeners, of diameter less than about 45 m, the drive head is usually supported on a superstructure spanning the tank, with the arms being attached to the drive shaft. Such machines are referred to as *bridge* or *beam* thickeners (Figure 15.6). The underflow is usually drawn from the apex of a cone located at the centre of the sloping bottom.

A common arrangement for larger thickeners, of up to about 180 m in diameter, is to support the drive mechanism on a stationary steel or concrete centre column. In most cases, the rake arms are attached to a drive cage, surrounding the central column, which is connected to the drive mechanism. The thickened solids are discharged through an annular trench encircling the centre column (Figure 15.7). Figure 15.8 shows an 80 m diameter thickener of this type.

In the *traction thickener*, a single long arm is mounted with one end on the central support column while to the other are fixed traction wheels that run on a rail on top of the tank wall. The wheels are driven by motors which are mounted on the end of the arm and which therefore travel around with it. This is an efficient and economical design

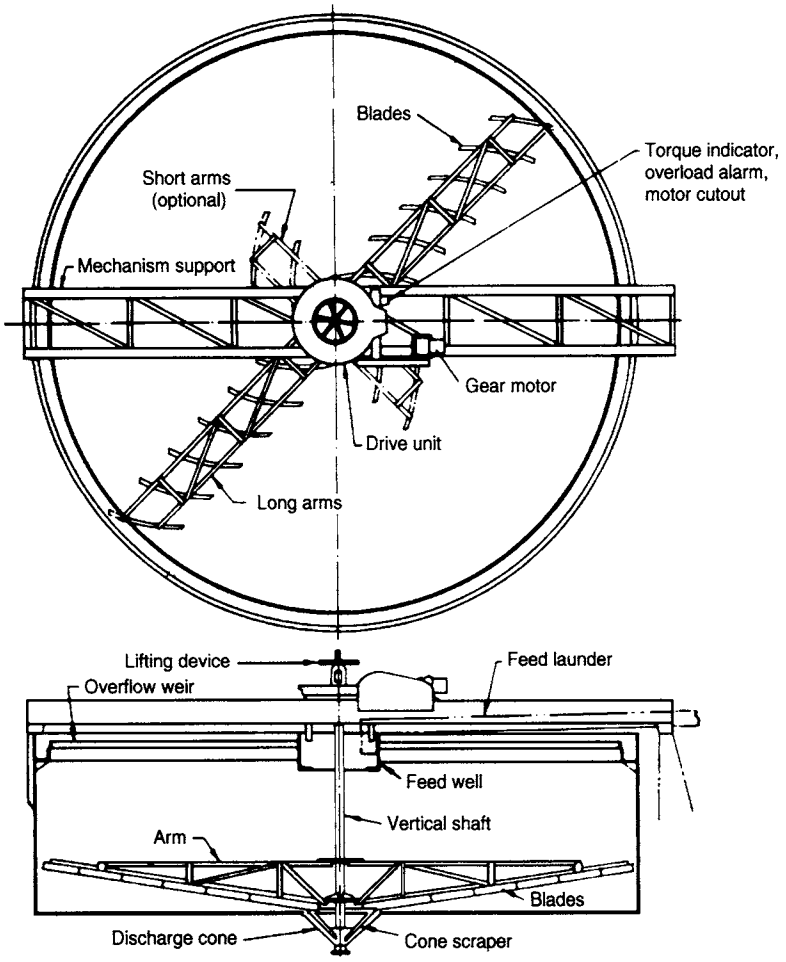


Figure 15.6 Thickener with mechanism supported by superstructure

since the torque is transmitted through a long lever arm by a simple drive. They are manufactured in sizes ranging from 60 m to approximately 120 m in diameter.

Cable thickeners have a hinged rake arm fastened to the bottom of the drive cage or centre shaft. The hinge is designed to give simultaneous vertical and horizontal movement of the rake arm. The rake arm is *pulled* by cables connected to a torque or drive arm structure, which is rigidly connected to the centre shaft at a point just below the liquid level. The rake is designed to automatically lift when the torque developed due to its motion through the sludge rises. This design allows the rake arm to find its own efficient working level in the sludge, where the torque balances the rake weight.

In all thickeners the speed of the raking mechanism is normally about 8 m min^{-1} at the perimeter, which corresponds to about 10 rev h^{-1} for a 15 m diameter thickener. Energy consumption is thus extremely low, such that even a 60 m unit may require only a 10 kW motor. Wear and maintenance costs are correspondingly low.

The underflow is usually withdrawn from the central discharge by pumping, although in clarifiers the material may be discharged under the hydrostatic head in the tank. The underflow is usually collected in a sludge-well in the centre of the tank bottom, from where it is removed via piping through an underflow tunnel. The underflow lines should be as short and as straight as possible to reduce the risk of choking, and this can be achieved, with large tanks, by taking them up

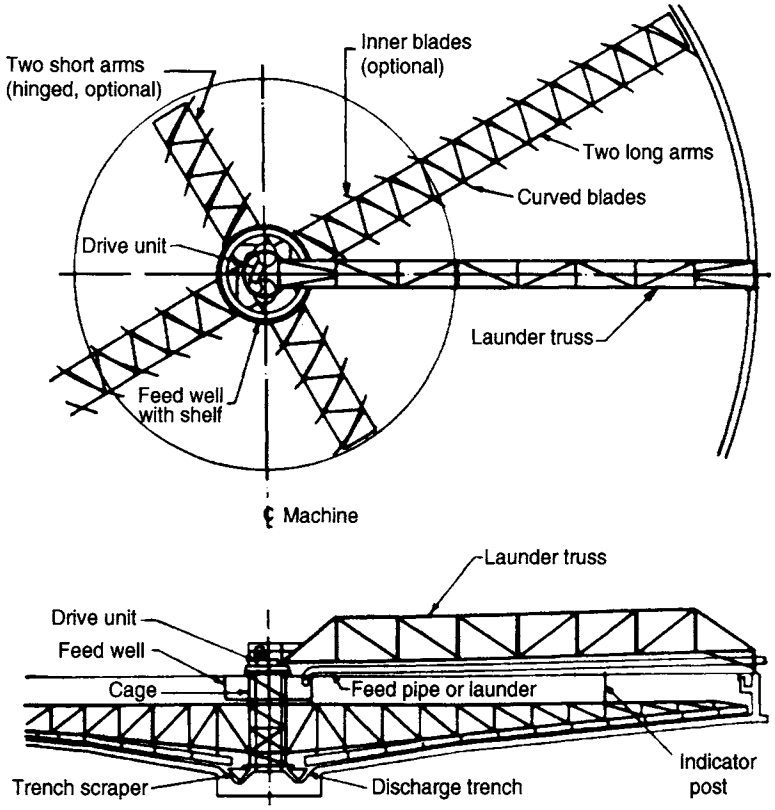


Figure 15.7 Thickener with column supported by centre column

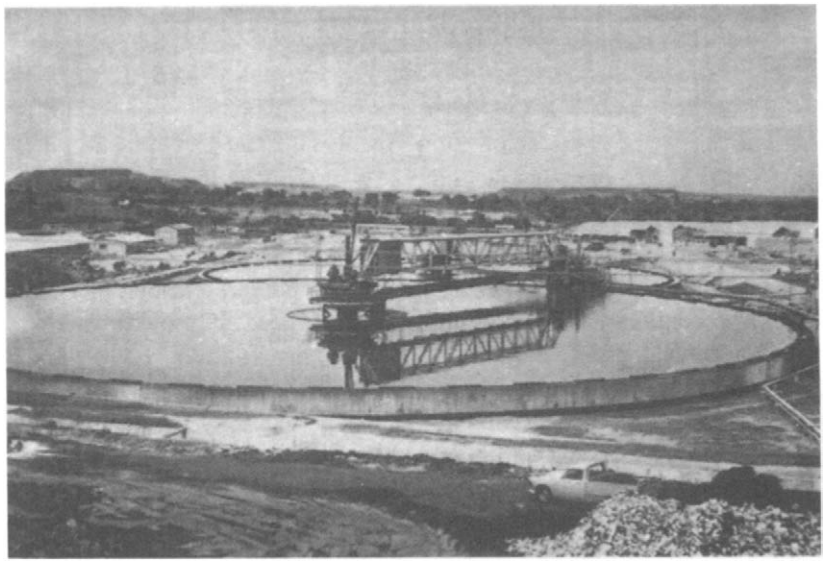


Figure 15.8 80 m diameter centre-column-supported thickener

from the sludge-well through the centre column to pumps placed on top, or by placing the pumps in the base of the column and pumping up from the bottom. This has the advantage of dispensing with the expensive underflow tunnel. A development of this is the *caisson thickener*, in which the centre column is enlarged sufficiently to house a central control room; the pumps are located in the bottom of the column, which also contains the mechanism drive heads, motors, control panel, underflow suction, and discharge lines. The interior of the caisson can be a large heated room. The caisson concept has lifted the possible ceiling on thickener sizes; at present they are manufactured in sizes up to 180 m in diameter.

Underflow pumps are often of the *diaphragm* type (Anon., 1978). These are positive action pumps for medium heads and volumes, and are suited to the handling of thick viscous fluids. They can be driven by electric motor through a crank mechanism, or by directly acting compressed air. A flexible diaphragm is oscillated to provide suction and discharge through non-return valves, and variable speed can be achieved by changing either the oscillating frequency or the stroke. In some plants, variable-speed pumps are connected to nucleonic density gauges on the thickener underflow lines, which control the rate of pumping to maintain a constant underflow density. The thickened underflow is pumped to filters for further dewatering.

Thickeners often incorporate substantial storage capacity so that, for instance, if the filtration section is shut down for maintenance, the concentrator can continue to feed material to the dewatering section. During such periods the thickened underflow should be recirculated into the thickener feedwell. At no time should the underflow cease to be pumped, as chokage of the discharge cone rapidly occurs.

Since capital is the major cost of thickening, selection of the correct size of thickener for a particular application is important.

The two primary functions of the thickener are the production of a clarified overflow and a thickened underflow of the required concentration.

For a given throughput the clarifying capacity is determined by the thickener diameter, since the surface area must be large enough so that the upward velocity of liquid is at all times lower than the settling velocity of the slowest-settling particle which is to be recovered. The degree of thickening produced is controlled by the residence time of the particles and hence by the thickener depth.

The solids concentration in a thickener varies from that of the clear overflow to that of the thickened underflow being discharged. Although the variation in concentration is continuous, the concentrations at various depths may be grouped into four zones, as shown in Figure 15.9.

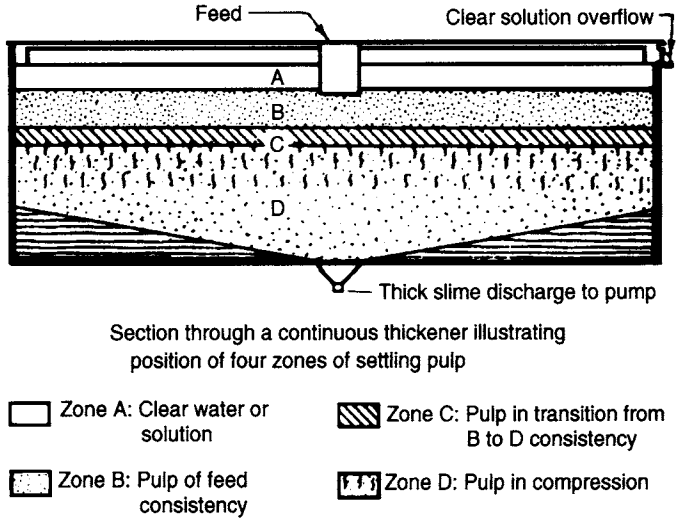


Figure 15.9 Concentration zones in a thickener (From *Chemical Engineers' Handbook* by J.H. Perry., McGraw-Hill, 1963)

When materials settle with a definite interface between the suspension and the clear liquid, as is the case with most flocculated mineral pulps, the solids-handling capacity determines the surface area. Solids-handling capacity is defined as the capacity of a material of given dilution to reach a condition such that the mass rate of solids leaving a region is equal to or greater than the mass rate of solids entering the region. The attainment of this condition with a specific dilution depends on the mass subsidence rate being equal to or greater than the corresponding rise rate of displaced liquid. A properly sized thickener containing material of many different dilutions, ranging from the feed to the underflow solids contents, has adequate area such that the rise rate of displaced liquid at any region never exceeds the subsidence rate.

The satisfactory operation of the thickener as a clarifier depends upon the existence of a clear-liquid overflow at the top. If the clarification zone is too shallow, some of the smaller particles may escape in the overflow. The volumetric rate of flow upwards is equal to the difference between the rate of feed of liquid and the rate of removal in the underflow. Hence the required concentration of solids in the underflow, as well as the throughput, determines the conditions in the clarification zone.

The method developed by Coe and Clevenger (1916) is commonly employed to determine surface area when the material settles with a definite interface.

If F is the liquid-to-solids ratio by weight at any region within the thickener, D is the liquid-to-solids ratio of the thickener discharge, and $W\,\mathrm{t\,h^{-1}}$ of dry solids are fed to the thickener, then $(F-D)W\,\mathrm{t\,h^{-1}}$ of liquid moves upwards to the region from the discharge.

The velocity of this liquid current is thus

$$\frac{(F-D)W}{A-S} \tag{15.1}$$

where A is the thickener area ($\mathrm{m^2}$) and S is the specific gravity of the liquid ($\mathrm{kg\,l^{-1}}$).

Because this upward velocity must not exceed the settling rate of the solids in this region, at equilibrium

$$\frac{(F-D)W}{A-S} = R \tag{15.2}$$

where R is the settling rate ($\mathrm{m\,h^{-1}}$).

The required thickener area is therefore

$$A = \frac{(F-D)W}{RS} \tag{15.3}$$

From a complete set of R and F values the area required for various dilutions may be found by recording the initial settling rate of materials with dilutions ranging from that of the feed to the discharge. The dilution corresponding to the maximum value of A represents the minimum solids-handling capacity and is the critical dilution.

In using this method the initial constant sedimentation rate is found through tests in graduated cylinders using dilutions ranging from the feed dilution to the underflow dilution, the rate of fall of the interface between the thickened pulp and clarified solution being timed.

Once the required surface area is established, it is necessary to apply a safety factor to the calculated area. This should be at least two.

The Coe and Clevenger method requires multiple batch tests at different arbitrary pulp densities before an acceptable unit area can be selected. The Kynch model (1952) offers a way of obtaining the required area from a single batch-settling curve, and is the basis of several thickening theories, which have been comprehensively reviewed by Pearse (1977).

The Talmage and Fitch method (1955) applies Kynch's mathematical model to the problem of thickener design. The results of a batch-settling test are plotted linearly as mudline (interface between settled pulp and clear water) height against time (Figure 15.10).

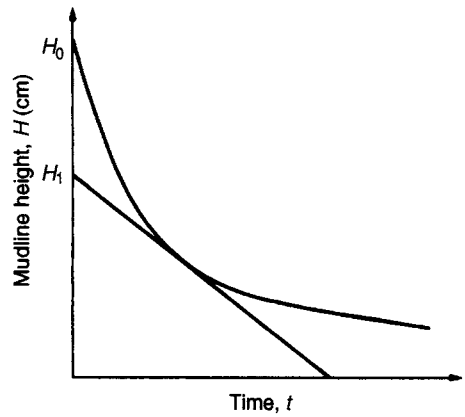


Figure 15.10 Batch-settling curve

Talmage and Fitch showed that by constructing a tangent to the curve at any point, then if H is the intercept of the tangent on the ordinate,

$$CH = C_0H_0 \qquad (15.4)$$

where $C_0\,\mathrm{kg}\,l^{-1}$ is the original feed *solids concentration*, H_0 cm is the original mudline height, and H is the mudline height corresponding to a uniform slurry of concentration $C\,\mathrm{kg}\,l^{-1}$, at the point where the tangent was taken. Therefore, for any selected point on the settling curve, the local concentration can be obtained from Equation 15.4, and the settling rate from the gradient of the tangent at that point. Thus a set of data of concentration against settling rate can be obtained from the single batch-settling curve.

For a pulp of solids concentration $C\,\mathrm{kg}\,l^{-1}$, the volume occupied by the solids in 1 litre of pulp is C/d, where $d\,\mathrm{kg}\,l^{-1}$ is the specific gravity of dry solids.

Therefore the weight of water in 1 litre of pulp

$$= 1 - \frac{C}{d} = \frac{d-C}{d}$$

Therefore the water–solids ratio by weight

$$= \frac{d-C}{dC}$$

For pulps of concentrations $C\,\mathrm{kg}\,l^{-1}$ of solids, and $C_u\,\mathrm{kg}\,l^{-1}$ of solids, the difference in water–solids ratio

$$= \frac{d-C}{dC} - \frac{d-C_u}{dC_u}$$

$$= \frac{1}{C} - \frac{1}{C_u}$$

Therefore the values of concentration obtained, C, and the settling rates, R, can be substituted in the Coe and Clevenger Equation 15.3, i.e.

$$A = \left(\frac{1}{C} - \frac{1}{C_u}\right)\frac{W}{RS} \qquad (15.5)$$

where C_u is the underflow solids concentration.

A simplified version of the Talmage and Fitch method is offered by determining the point on the settling curve where the solids go into compression. This point corresponds to the limiting settling conditions and controls the area of thickener required. In Figure 15.11, C is the compression point, and a tangent is drawn to the curve at this point, intersecting the ordinate at H. A line is drawn parallel to the abscissa, cutting the ordinate of a tangent from a point C_u on the curve, where C_u is the solids concentration of the thickener underflow. The tangent from C intersects this line at a time corresponding to t_u. H_u can be calculated from Equation 15.4.

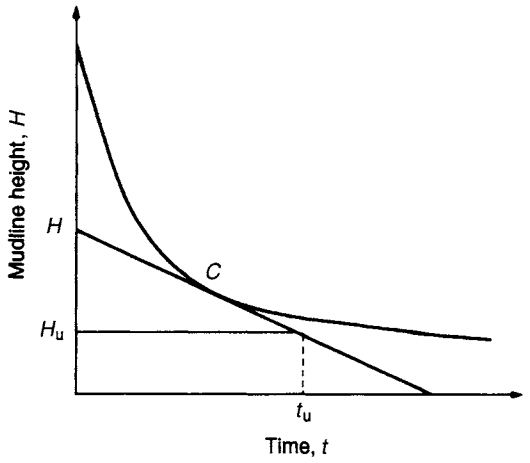


Figure 15.11 Modified Talmage and Fitch construction

The required thickener area (Equation 15.5).

$$= \frac{W(1/C - 1/C_u)}{(H - H_u)/t_u}$$

where $(H - H_u)/t_u$ is the gradient of the tangent at point C, i.e. the settling rate of the particles at the compression point concentration. Since $CH = C_0H_0$,

$$A = \frac{W[(H/C_0H_0) - (H_u/C_0H_0)]}{(H - H_u)/t_u}$$

$$= W\frac{t_u}{C_0H_0} \qquad (15.6)$$

In most cases, the compression point concentration will be less than that of the underflow concentration. In cases where this is not so, then the tangent construction is not necessary, and t_u is the point where the underflow line crosses the settling curve. In many cases, the point of compression on the curve is clear, but when this is not so, a variety of methods have been suggested for its determination (Fitch, 1977; Pearse, 1978).

The Coe and Clevenger and modified Talmage and Fitch methods are the most widely used

in the metallurgical industry to predict thickener area requirements. Both methods have limitations (Waters and Galvin, 1991), the Talmage and Fitch technique relying critically on identifying a compression point, and both must be used in conjunction with empirical safety factors. Generally, the Coe and Clevenger method tends to underestimate the thickener area requirement, whilst the Talmage and Fitch method tends to overestimate. It is usually better to overestimate in design to allow for feed fluctuations and increase in production, and because of this, and its relative experimental simplicity, the Talmage and Fitch method is often preferred, providing that a compression point is readily identifiable.

Recent work has described software for the prediction of continuous thickener area based on a phenomenological model of particle settling. The model is similar in form to the equation of Coe and Clevenger (Garridon et al., 2003). The development of thickener models over the last 100 years is reviewed by Concha and Burger (2003).

The mechanism of thickening has been far less well expressed in mathematical terms than the corresponding clarifying mechanisms. The depth of the thickener is therefore usually determined by experience. The diameter is usually large compared with the depth, and therefore a large ground area is required. *Tray thickeners* (Figure 15.12) are sometimes installed to save space. In essence, a tray thickener is a series of unit thickeners mounted vertically above one another. They operate as separate units, but a common central shaft is utilised to drive the sets of rakes.

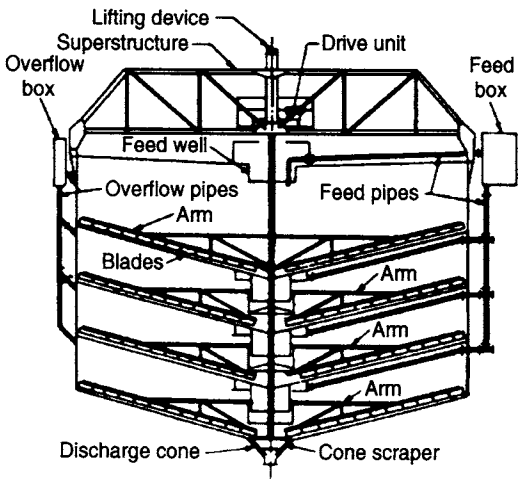


Figure 15.12 Tray thickener

High-capacity thickeners

Conventional thickeners suffer from the disadvantage that large floor areas are required, since the throughput depends above all on the area, while depth is of minor importance.

In recent years, machines known as "high-capacity" or "high rate" thickeners have been introduced by various manufacturers. Many varieties exist, and the machines are typified by a reduction in unit area requirement from conventional installations (Keane, 1982; Green, 1995).

The "Enviro-Clear" thickener developed by Envirotech Corporation is typical (Emmett and Klepper, 1980) (Figure 15.13).

The feed enters via a hollow drive shaft where flocculant is added and is rapidly dispersed by staged mechanical mixing. This staged mixing action is said to improve thickening since it makes most effective use of the flocculant. The flocculated feed leaves the mixing chambers and is injected into a blanket of slurry where the feed solids are further flocculated by contacting previously flocculated material. Direct contact between rising fluid and settling solids, which is common to most thickeners, is averted with slurry blanket injection. Radially mounted inclined plates are partially submerged in the slurry blanket; the settling solids in the slurry blanket slide downwards along the inclined plates, producing faster and more effective thickening than vertical descent. The height of the slurry blanket is automated through the use of a level sensor.

High density thickeners (or high compression thickeners) are an extension of high capacity thickening utilising a deeper mud bed to increase capacity and underflow density. High rate rakeless thickeners use a deep tank and a steep bottom cone to maximise underflow density while eliminating the rake and rake drive. In some applications underflow with the consistency of paste can be produced from high density and rakeless thickeners. However for consistent paste underflow several manufacturers offer deep cone thickeners in applications where surface tailings

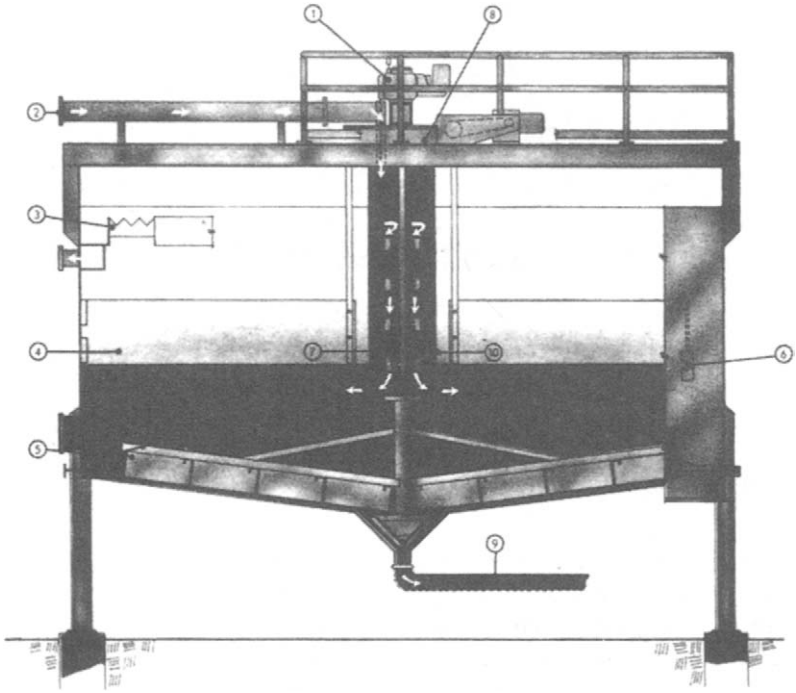


Figure 15.13 Enviro-Clear high-capacity thickener. 1 – mixer drive; 2 – feed pipe; 3 – overflow launder; 4 – inclined settling plates; 5 – rake arm; 6 – level sensor; 7 – flocculant feed pipe; 8 – drive unit with overload control; 9 – sludge discharge; 10 – mixing chamber

disposal by wet stacking or underground paste backfill is required. The tank height to diameter ratio is often 1:1 or greater (Schoenbrunn and Laros, 2002).

Centrifugal sedimentation

Centrifugal separation can be regarded as an extension of gravity separation, as the settling rates of particles are increased under the influence of centrifugal force. It can, however, be used to separate emulsions which are normally stable in a gravity field.

Centrifugal separation can be performed either by hydrocyclones or centrifuges.

The simplicity and cheapness of the hydrocyclone (Chapter 9) make it very attractive, although it suffers from restrictions with respect to the solids concentration which can be achieved and the relative proportions of overflow and underflow into which the feed may be split. Generally the efficiency of even a small-diameter cyclone falls off rapidly at very fine particle sizes and particles smaller than about 10 μm in diameter will invariably appear in the overflow, unless they are very heavy. Flocculation of such particles is not possible, since the high shear forces within a cyclone rapidly break up any agglomerates. The cyclone is therefore inherently better suited to classification rather than thickening.

By comparison, centrifuges are much more costly and complex, but have a much greater clarifying power and are generally more flexible. Much greater solids concentrations can be obtained than with the cyclone.

Various types of centrifuge are used industrially (Bragg, 1983; Bershad et al., 1990; Leung, 2002), *the solid bowl scroll centrifuge* having widest use in the minerals industry due to its ability to discharge the solids continuously.

The basic principles of a typical machine are shown in Figure 15.14. It consists essentially of a horizontal revolving shell or bowl, cylindroconical in form, inside which a screw conveyor of similar section rotates in the same direction at a slightly higher or lower speed. The feed pulp is admitted to the bowl through the centre tube of

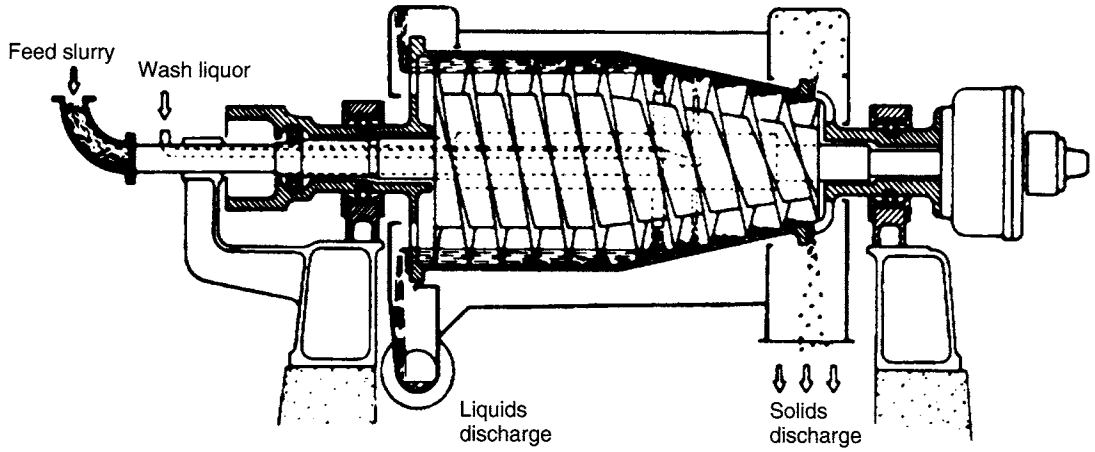


Figure 15.14 Continuous solid bowl scroll centrifuge

the revolving-screw conveyor. On leaving the feed pipe the slurry is immediately subjected to a high centrifugal force causing the solids to settle on the inner surface of the bowl at a rate which depends on the rotational speed employed, this normally being between 1600 and 8500 rev min^{-1}. The separated solids are conveyed by the scroll out of the liquid and discharged through outlets at the smaller end of the bowl. The solids are continuously dewatered by centrifugal force as they proceed from the liquid zone to the discharge. Excess entrained liquor drains away to the pond circumferentially through the particle bed.

When the liquid reaches a predetermined level it overflows through the discharge ports at the larger end of the bowl.

The actual size and geometry of these centrifuges vary according to the throughput required and the application. The length of the cylindrical section largely determines the clarifying power and is thus made a maximum where overflow clarity is of prime importance. The length of the conical section, or "beach", decides the residual moisture content of the solids, so that a long shallow cone is used where maximum dryness is required.

Centrifuges are manufactured with bowl diameters ranging from 15 to 150 cm, the length generally being about twice the diameter. Throughputs vary from about 0.5 to 50 $m^3 h^{-1}$ of liquid and from about 0.25 to 100 $t h^{-1}$ of solids depending on the feed concentration, which may vary widely from 0.5 to 70% solids, and on the particle size, which may range from about 12 mm to as fine as 2 μm, or even less when flocculation is used. The wide application of flocculation is limited by the tendency of the scroll action to damage the flocs and thus redisperse the fine particles. The moisture content in the product varies widely, typically being in the range 5–20%.

Filtration

Filtration is the process of separating solids from liquid by means of a porous medium which retains the solid but allows the liquid to pass. The theory of filtration has been comprehensively reviewed mathematically elsewhere (Coulson and Richardson, 1968; Cain, 1990) and will not be covered here.

The conditions under which filtration are carried out are many and varied and the choice of the most suitable type of equipment will depend on a large number of factors. Whatever type of equipment is used, a *filter cake* gradually builds up on the medium and the resistance to flow progressively increases throughout the operation. Factors affecting the rate of filtration include:

(a) The pressure drop from the feed to the far side of the filter medium. This is achieved in pressure filters by applying a positive pressure at the feed end and in vacuum filters by applying a vacuum to the far side of the medium, the feed side being at atmospheric pressure.
(b) The area of the filtering surface.
(c) The viscosity of the filtrate.

(d) The resistance of the filter cake.
(e) The resistance of the filter medium and initial layers of cake.

Filtration in mineral processing applications normally follows thickening. The thickened pulp may be fed to storage agitators from where it is drawn off at uniform rate to the filters. Flocculants are sometimes added to the agitators in order to aid filtration. Slimes have an adverse effect on filtration, as they tend to "blind" the filter medium; flocculation reduces this and increases the voidage between particles, making filtrate flow easier. The lower molecular weight flocculants tend to be used in filtration, as the flocs formed by high molecular weight products are relatively large, and entrain water within the structure, increasing the moisture content of the cake, even with the lower molecular weight flocculants, which have a higher shear-resistance, and the resultant filter cake is a uniform porous structure which allows rapid dewatering, yet prevents migration of the finer particles through the cake to the medium (Moss, 1978). Other filter aids are used to reduce the liquid surface tension, thus assisting flow through the medium.

The filter medium

The choice of the filter medium is often the most important consideration in assuring efficient operation of a filter. Its function is generally to act as a support for the filter cake, while the initial layers of cake provide the true filter. The filter medium should be selected primarily for its ability to retain solids without blinding. It should be mechanically strong, corrosion resistant, and offer as little resistance to flow of filtrate as possible. Relatively coarse materials are normally used and clear filtrate is not obtained until the initial layers of cake are formed, the initial cloudy filtrate being recycled.

Filter media are manufactured from cotton, wool, linen, jute, nylon, silk, glass fibre, porous carbon, metals, rayon and other synthetics, and miscellaneous materials such as porous rubber. Cotton fabrics are by far the most common type of medium, primarily because of their low initial cost and availability in a wide variety of weaves. They can be used to filter solids as fine as 10 μm.

Filtration tests

It is not normally possible to forecast what may be accomplished in the filtration of an untested product, therefore preliminary tests have to be made on representative samples of the pulp before the large-scale plant is designed. Tests are also commonly carried out on pulps from existing plants, to assess the effect of changing operating conditions, filter aids, etc. A simple vacuum *filter leaf* test circuit is shown in Figure 15.15.

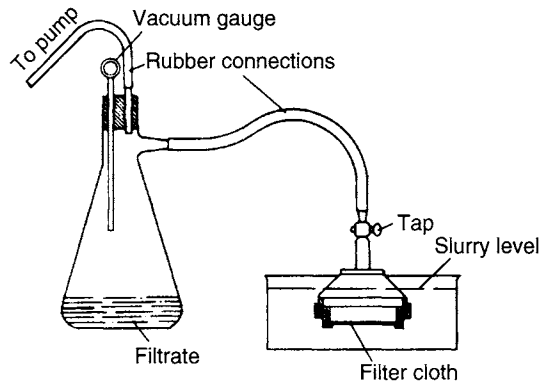


Figure 15.15 Laboratory test filter

The filter leaf, consisting of a section of the industrial filter medium, is connected to a filtrate receiver equipped with a vacuum gauge. The receiver is connected to a vacuum pump. If the industrial filter is to be a continuous vacuum filter, this operation must be simulated in the test. The cycle is divided into three sections – cake formation (or "pick-up"), drying, and discharge. Sometimes pick-up is followed by a period of washing and the cake may also be subjected to compression during drying. While under vacuum, the test leaf is submerged for the pick-up period in the agitated pulp to be tested. The leaf is then removed and held with the drainpipe down for the allotted drying time. The cake can then be removed, weighed, and dried. The daily filter capacity can then be determined by the dry weight of cake per unit area of test leaf multiplied by the daily number of cycles and the filter area.

Bench scale testing of samples for specification of filtration equipment is described by Smith and Townsend (2002).

Types of filter

Cake filters are the type most frequently used in mineral processing, where the recovery of large amounts of solids from fairly concentrated slurries is the main requirement. Those where the main requirement is the removal of small amounts of solid from relatively dilute suspensions are known as screening or clarification filters.

Cake filters may be pressure, vacuum, batch, or continuous types. The various types are reviewed by Cox and Traczyk (2002).

Pressure filters

Because of the virtual incompressibility of solids, filtration under pressure has certain advantages over vacuum. Higher flow rates and better washing and drying may result from the higher pressures that can be used. However, the continuous removal of solids from the pressure-filter chamber can be extremely difficult and consequently, although continuous pressure filters do exist, the vast majority operate as batch units.

Filter presses are the most frequently used type of pressure filter. They are made in two forms – the plate and frame press and the recessed plate or chamber press.

The *plate and frame press* (Figure 15.16) consists of plates and frames arranged alternately. The hollow frame is separated from the plate by the filter cloth. The filter press is closed by means of a screw or hydraulic piston device and compression of the filter cloth between plates and frames helps to prevent leakages. A tight chamber is therefore formed between each pair of plates. The slurry is introduced to the empty frames of the press through a continuous channel formed by the holes in the corners of the plates and frames. The filtrate passes through the cloth and runs down the grooved surfaces of the plates and is removed through a continuous channel. The cake remains in the frame and, when the frame is full, the filter cake can be washed, after which the pressure is released and the plates and frames separated one by one. The filter cake in the frames can then be discharged, the filter press closed again and the cycle repeated.

The *chamber press* (Figure 15.17) is similar to the plate and frame type except for the fact that the filter elements consist solely of the recessed filter plates. The individual filter chambers are therefore formed between successive plates. All the chambers are connected by means of a comparatively large hole in the centre of each plate. The filter cloth with a central hole covers the plate and slurry is led through the inlet channel. The clear filtrate passing through the cloth is removed by means of smaller holes in the plate, the cake gradually depositing in the chambers.

Automatic pressure filters are now widely used in most new flotation plants. Automatic means a

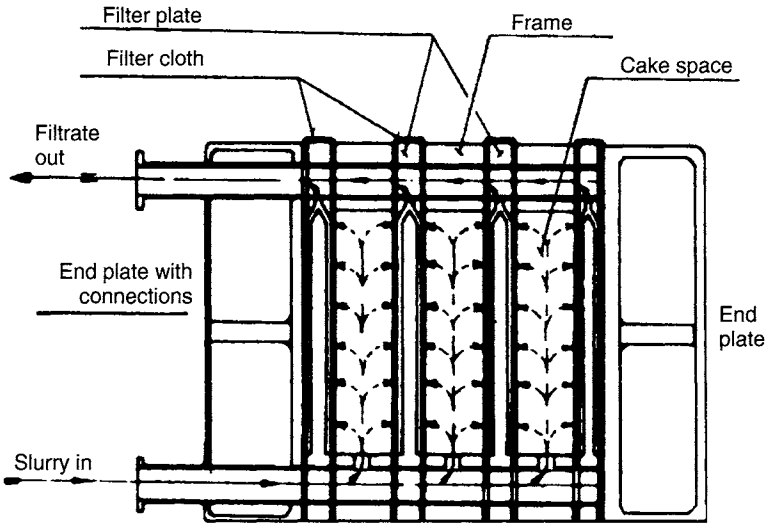


Figure 15.16 Plate and frame filter press

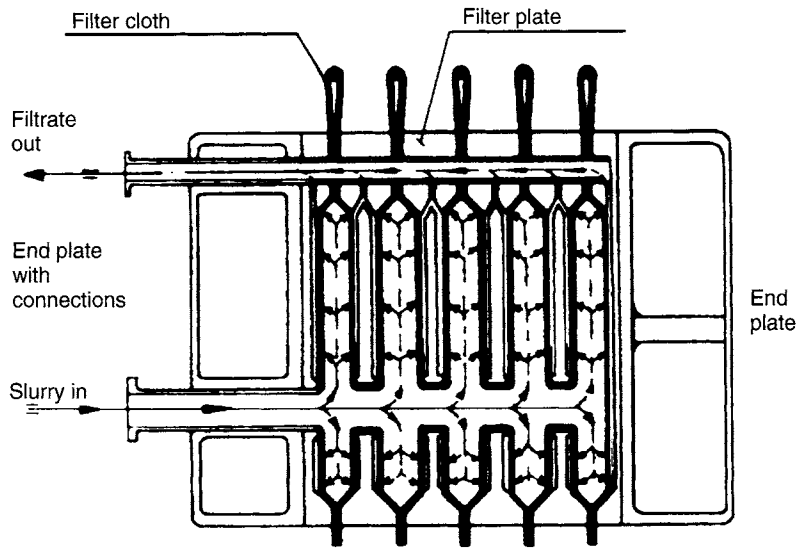


Figure 15.17 Chamber or recessed plate filter press

filter in which plate pack opening, pump and ancillary equipment starting, and valve operation as well as cake discharge are all automatically controlled (Townsend, 2003). Modern pressure filters can process up to 150 t/h dry solids per unit of copper concentrate in filters with filtration areas of up to 144 m^2. Even higher throughputs can be achieved in iron ore applications. Residual cake moisture depends on the material being filtered but values in the range 7.5–12.5% are typical.

Vacuum filters

There are many different types of vacuum filter, but they all incorporate filter media suitably supported on a drainage system, beneath which the pressure is reduced by connection to a vacuum system. Vacuum filters may be batch or continuous (Keleghan, 1986a,b).

Batch vacuum filters The *leaf filter* has a number of leaves, each consisting of a metal framework or a grooved plate over which the filter cloth is fixed (Figure 15.18).

Numerous holes are drilled in the pipe framework, so that when a vacuum is applied, a filter cake builds up on both sides of the leaf. A number of leaves are generally connected and are first immersed in slurry held in a filter feed tank and then to a cake-receiving vessel where the cake is removed by replacing the vacuum by air pressure (Figure 15.19).

Although simple to operate, these filters require considerable floor space and suffer from the possibility of sections of cake dropping from the leaves during transport from tank to tank. They are now used only for clarification, i.e. the removal of small amounts of suspended solids from liquors.

Horizontal leaf, or *tray filters*, work in much the same manner as a laboratory Buchner filter and consist of rectangular pans having a false bottom of filter medium. They are filled with pulp, the vacuum is applied until the cake is dry, when the pan is inverted, being supported on pivots, the vacuum is disconnected and low-pressure air is introduced under the filter medium to remove the cake.

Continuous vacuum filters These are the most widely used filters in mineral processing applications and fall into three classes – drums, discs, and horizontal filters.

The *rotary-drum filter* (Figure 15.20) is the most widely used type in industry, finding application both where cake washing is required and where it is unnecessary.

The drum is mounted horizontally and is partially submerged in the filter trough, into which the feed slurry is fed and maintained in suspension by agitators. The periphery of the drum is divided into compartments, each of which is provided with a number of drain lines, which pass through the inside of the drum, terminating at one end as a ring of

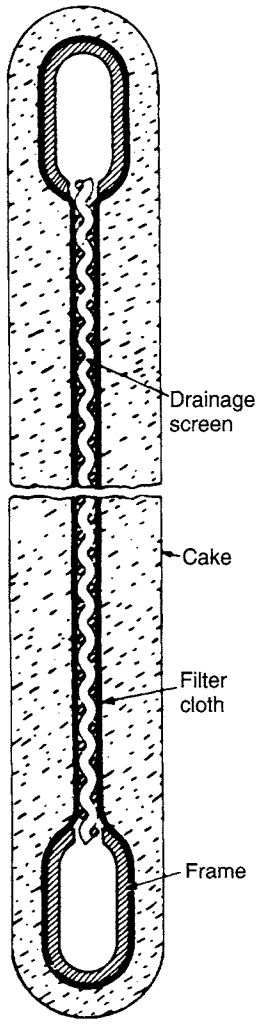


Figure 15.18 Cross-section of typical leaf filter

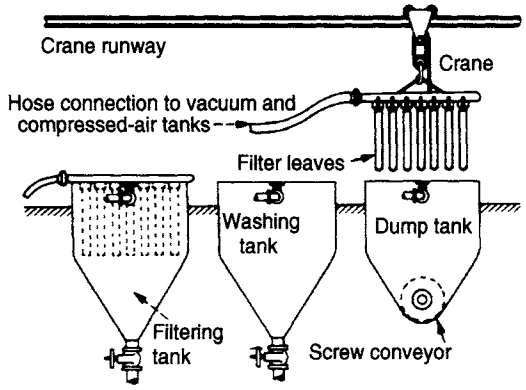


Figure 15.19 Typical leaf filter circuit (From *Chemical Engineers' Handbook* by J.H. Perry, McGraw-Hill, 1963)

ports which are covered by a rotary valve to which vacuum is applied. The filter medium is wrapped tightly around the drum surface which is rotated at low speed, usually in the range 0.1–0.3 rev min^{-1}, but up to 3 rev min^{-1} for very free-filtering materials.

As the drum rotates, each compartment goes through the same cycle of operations, the duration of each being determined by the drum speed, the depth of submergence of the drum, and the arrangement of the valve. The normal cycle of operations consists of filtration, drying, and discharge, but it is possible to introduce other operations into the basic cycle, such as cake washing and cloth cleaning.

Various methods are used for discharging the solids from the drum, depending on the material being filtered. The most common form makes use of a reversed blast of air, which lifts the cake so that it can be removed by a knife, without the latter actually contacting the medium. Another method is string discharge, where the filter cake is formed on an open conveyor – the strings – which are in contact with the filter cloth in the filtration, washing, and drying zones. A further advance on this method is belt discharge, as shown in Figure 15.20, where the filter medium itself leaves the filter and passes over the external roller, before returning to the drum. This has a number of advantages in that very much thinner cakes can be handled, with consequently increased filtration and draining rates and hence better washing and dryer products. At the same time, the cloth can be washed on both sides by means of sprays before it returns to the drum (Figure 15.21), thus minimising the extent of blinding. Cake washing is usually carried out by means of sprays or weirs, which cover a fairly limited area at the top of the drum.

The capacity of the vacuum pump will be determined mainly by the amount of air sucked through the cake during the washing and drying periods when, in most cases, there will be a simultaneous flow of both liquid and air. A typical layout is shown in Figure 15.22, from which it is seen that the air and liquid are removed separately.

The barometric leg should be at least 10 m high to prevent liquid being sucked into the vacuum pump.

Variations on standard drum filters to enable them to handle coarse, free-draining, quick-settling

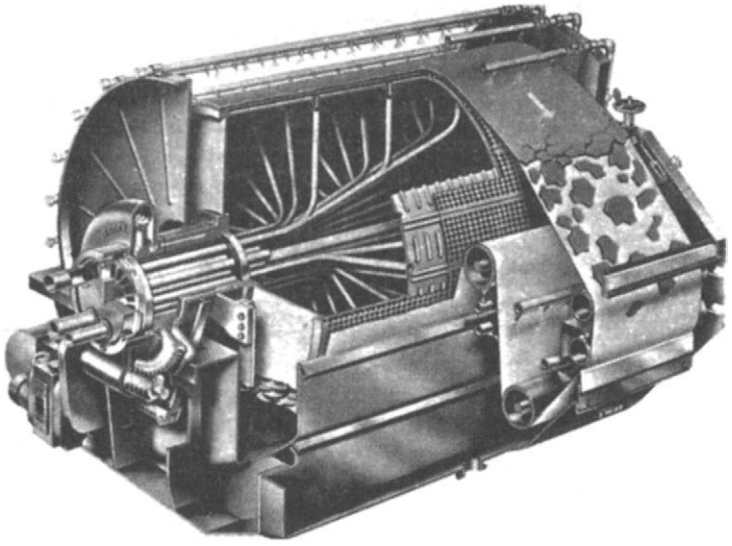


Figure 15.20 Rotary-drum filter with belt discharge

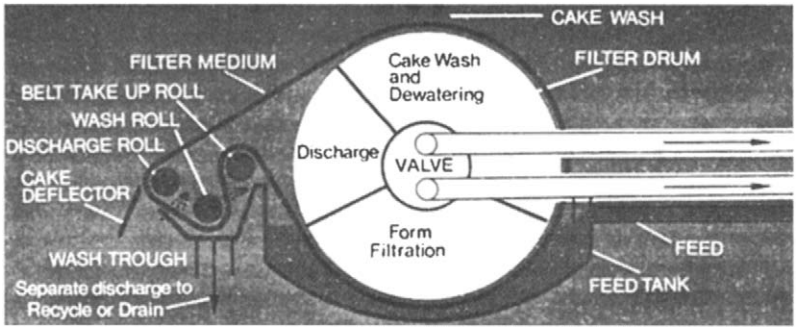


Figure 15.21 Belt discharge filter with cloth washing

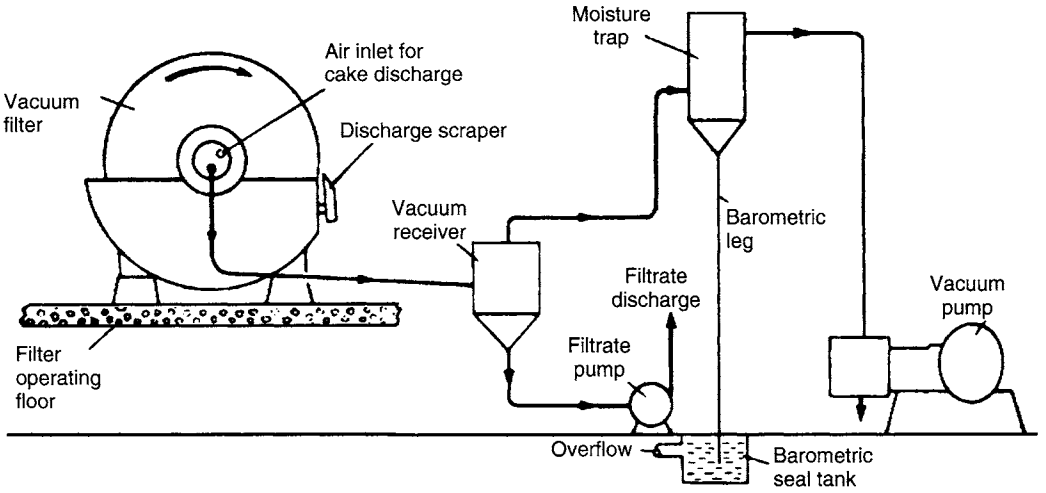


Figure 15.22 Typical rotary-drum filter system

materials include top feed units where the material is distributed at between 90 and 180° from the feed point. *Hyperbaric filters* have been developed to satisfy the need for pressure filtration (to give high filtration rates and dry cakes) and continuous operation. Some of these contain a conventional drum filter operating inside a large pressure vessel (Anlauf, 1991; Bott et al., 2003).

The principle of operation of *disc filters* (Figure 15.23), is similar to that of rotary drum filters. The solids cake is formed on both sides of the circular discs, which are connected to the horizontal shaft of the machine. The discs rotate and lift the cake above the level of the slurry in the trough, whereupon the cake is suction-dried and is then removed by a pulsating air blow with the assistance of a scraper. The discs can be located along the shaft at about 30 cm centres and consequently a large filtration area can be accommodated in a small floor space. Cost per unit area is thus lower than for drum filters, but cake washing is virtually impossible and the disc filter is not as adaptable as a drum filter.

The *horizontal belt filter* (Figure 15.24), consists of an endless perforated rubber drainage deck supporting a separate belt made from a suitable filter cloth. At the start of the horizontal travel, slurry flows by gravity on to the belt. Filtration immediately commences, due partly to gravity and partly to the vacuum applied to the suction boxes which are in contact with the underside of the drainage deck during the coarse of its travel.

The cake which forms is dewatered, dried by drawing air through it, and then discharged as the belt reverses over a small-diameter roller. If required, one or more washes can be incorporated.

The applications for horizontal belt filters are increasing. They are particularly suited to hydrometallurgical circuits where metal values are dissolved in alkali or acid. These values can be recovered from waste solids by filtration of the leached slurry and countercurrent washing (Bragg, 1983). Large belt filters are in operation on cyanide-leached gold ore and acid-leached uranium ore. Belt filters are also suited for concentrated slurries of fast settling products, where efficient washing is required. In addition to their low installed capital cost when compared with disc, drum, and press-type filters, relatively low operating costs mean that these filters offer a particularly cost-effective and reliable solution to filtration problems, especially with low-value material such as mine tailings. Work on coal slurries has shown that horizontal belt vacuum filtration should produce lower cake

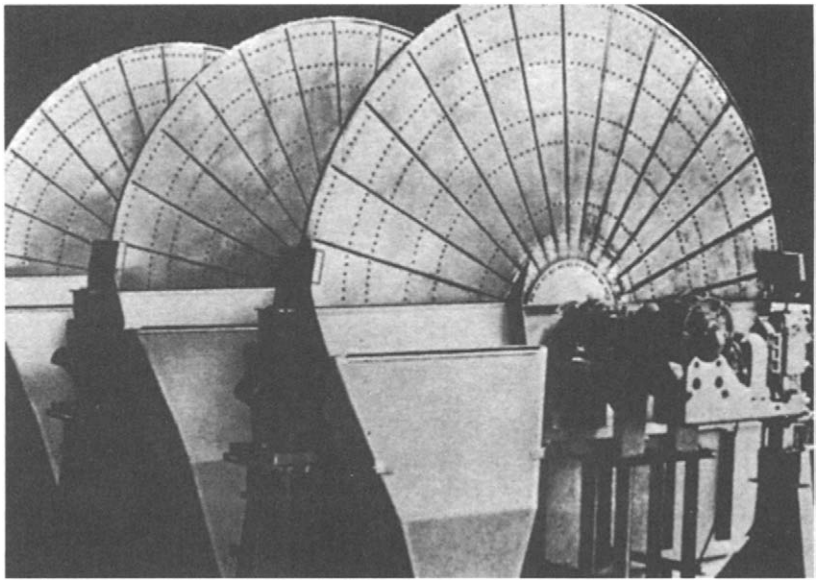


Figure 15.23 Rotary-disc filters

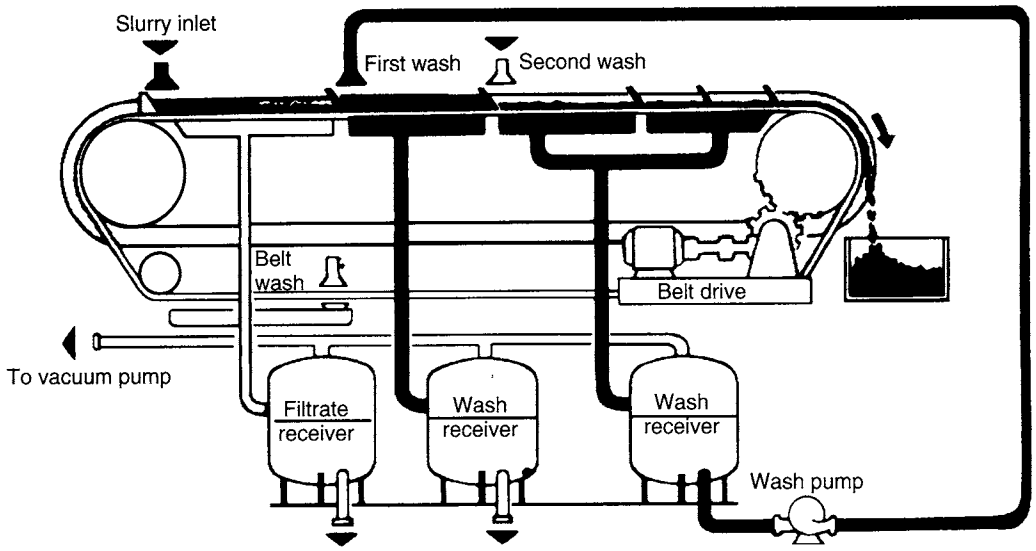


Figure 15.24 Horizontal belt filter

moistures than those from rotary vacuum filtration and at a reduced cost per tonne (Vickers et al., 1985).

Drying

The drying of concentrates prior to shipping is the last operation performed in the mineral-processing plant. It reduces the cost of transport and is usually aimed at reducing the moisture content to about 5% by weight. Dust losses are often a problem if the moisture content is lower.

Rotary thermal dryers are often used. These consist of a relatively long cylindrical shell mounted on rollers and driven at a speed of up to 25 rev min^{-1}. The shell is at a slight slope, so that material moves from the feed to discharge end under gravity. Hot gases, or air, are fed in either at the feed end to give parallel flow or at the discharge to give counter-current flow.

The method of heating may be either direct, in which case the hot gases pass through the material in the dryer, or indirect, where the material is in an inner shell, heated externally by hot gases. The direct-fired is the dryer most commonly used in the minerals industry, the indirect-fired type being used when the material must not contact the hot combustion gases. Parallel flow dryers (Figure 15.25) are used in the majority of current operations because they are more fuel efficient and have greater capacity than counterflow types (Kram, 1980). Since heat is applied at the feed end,

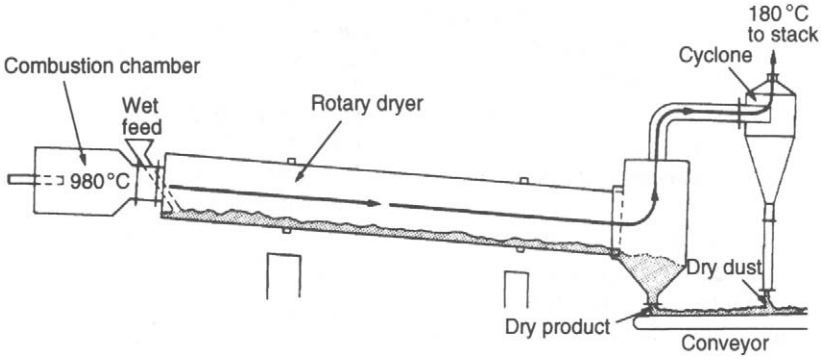


Figure 15.25 Direct fired, parallel flow rotary dryer (after Kram (1980))

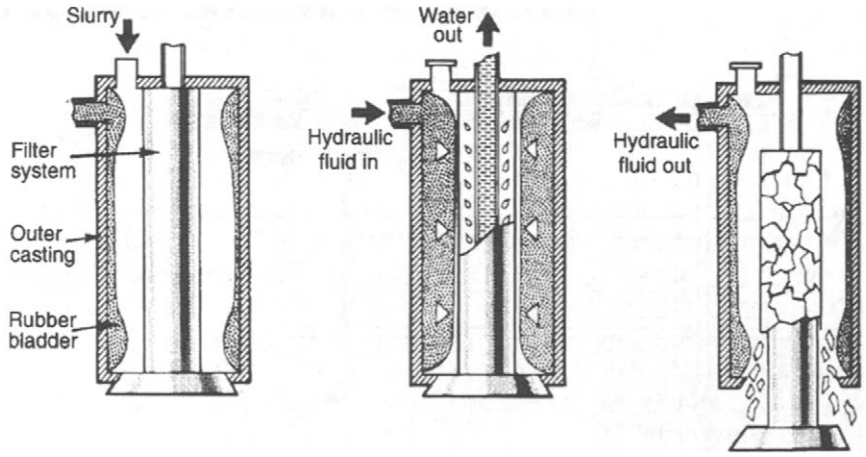


Figure 15.26 Operation of tube press

build-up of wet feed is avoided, and in general these units are designed to dry material to not less than 1% moisture. Since counter-flow dryers apply heat at the discharge end, a completely dry product can be achieved, but its use with heat-sensitive materials is limited because the dried material comes into direct contact with the heating medium at its highest temperature.

Prokesch (2002) reviews the various types of drying equipment available and describes dryer selection based on the required duty.

An alternative to direct-fired drying of slurries is the *tube press*, which uses hydraulic pressure at 100 bars to squeeze water from the slurry that enters the annular space between the filter tube and an outer tube (Figure 15.26). The outer tube contains the filtration pressure that is applied hydraulically by a tubular membrane and squeezes the water from the slurry through perforations in the filter tube. This is a perforated steel tube covered with a fine wire mesh backing and a filter cloth, known as a candle. The filtrate which collects in the central well of the candle is discharged from the press cloth by compressed air. It is reported that the tube press can save up to 80% of the energy required by comparable capacity thermal dryers (Anon., 1987).

The product from the dryers is often stockpiled, before being loaded on to trucks or rail-cars as required for shipment. The containers may be closed, or the surface of the contents sprayed with a skin-forming solution, in order to eliminate dust losses (Kolthammer, 1978).

References

Anlauf, H. (1991). Development trends and new concepts for the improved solid–liquid separation of superfine suspensions in the mineral dressing industry, *Proc. XVII Int. Min. Proc. Cong. Dresden*, **3**, 219.

Anon. (1978). Pumps for the mining industry, *Min. Mag.* (Jun.), 569.

Anon. (1987). Tube press saves on drying costs, *Mining J.* (17 Apr.), 296.

Attia, Y.A. (1992). Flocculation, in *Colloid Chemistry in Mineral Processing*, ed. J.S. Laskowski and J. Ralston, Elsevier, Amsterdam, Chapter 9.

Bershad, B.C., Chaffiotte, R.M., and Woon-Fong, L. (1990). Making centrifugation work for you, *Chemical Engng.*, **97**(Aug.), 84.

Bott, R., Langeloh, T., and Meck, F. (2003). Recent developments and results in continuous pressure and steam-pressure filtration, *Aufbereitungs Technik*, **44(5)**, 5.

Bragg, R. (1983). Filters and centrifuges, *Min. Mag.* (Aug.), 90.

Cain, C.W. (1990). Filter-cake filtration, *Chemical Engng.*, **97**(Aug.), 72.

Coe, H.S. and Clevenger, G.H. (1916). Methods for determining the capacities of slime-settling tanks, *Trans. AIMME*, **55**, 356.

Concha, F. and Burger, R. (2003). Thickening in the 20th century: A historical perspective, *Minerals & Metallurgical Processing*, **20(2)**, 57.

Coulson, J.M. and Richardson, J.F. (1968). *Chemical Engng.*, vol. 2, Pergamon Press, Oxford.

Cox, C. and Traczyk, F. (2002). Design features and types of filtration equipment, in *Mineral Processing Plant Design, Practice and Control*, ed. A.L. Mular, D. Halbe, and D.J. Barrratt, SME, Littleton, Colorado, 1343.

Emmett, R.C. and Klepper, R.P. (1980). Technology and performance of the hi-capacity thickener, *Mining Engng.*, **32**(Aug.), 1264.

Farrow, J.B. and Swift, J.D. (1996). A new procedure for assessing the performance of flocculants, *Int. J. Min. Proc.*, **46**, 263.

Fitch, E.B. (1977). Gravity separation equipment – clarification and thickening, in *Solid-Liquid Separation Equipment Scale-up*, ed. D.B. Purchas, Uplands Press, Croydon.

Green, D. (1995). High compression thickeners are gaining wider acceptance in minerals processing, *Filtration & Separation* (Nov./Dec.), 947.

Hogg, R. (1987). Agglomerate structure in flocculated suspensions and its effect on sedimentation and dewatering, *Minerals and Metallurgical Processing*, **4**(May), 108.

Hogg, R. (2000). Flocculation and dewatering, *Int. J. Min. Proc.*, **58**, 223.

Hsia, E.S. and Reinmiller, F.W. (1977). How to design and construct earth bottom thickeners, *Trans. Soc. Min. Engrs.* (Aug.), 36.

Hunter, T.K. and Pearse, M.J. (1982). The use of flocculants and surfactants for dewatering in the mineral processing industry, *Proc. IVth Int. Min. Proc. Cong.*, CIM, Toronto, Paper IX–11.

Keane, J.M. (1982). Recent developments in solids/liquid separation, *World Mining* (Oct.), 110.

Keleghan, W.T.H. (1986a). Vacuum filtration: Part 1, *Mine and Quarry*, **15**(Jan./Feb.), 51.

Keleghan, W.T.H. (1986b). The practice of vacuum filtration, *Mine and Quarry*, **15**(Mar.), 38.

Kolthammer, K.W. (1978). Concentrate drying, handling and storage, in *Mineral Processing Plant Design*, ed. A.L. Mular and R.B. Bhappu, AIMME, New York, 601.

Kram, D.J. (1980). Drying, calcining, and agglomeration, *Engng. Min. J.*, **181**(Jun.), 134.

Kynch, C.J. (1952). A theory of sedimentation, *Trans. Faraday Soc.*, **48**, 166.

Leung, W. (2002). Centrifugal sedimentation and filtering for mineral processing, in *Mineral Processing Plant Design, Practice and Control*, ed. A.L. Mular, D. Halbe, and D.J. Barrratt, SME, Littleton, Colorado, 1262.

Lightfoot, J. (1981). Practical aspects of flocculation, *Mine and Quarry*, **10**(Jan./Feb.), 51.

Moody, G. (1992). The use of polyacrylamides in mineral processing, *Minerals Engng.*, **5(3–5)**, 479.

Mortimer, D.A. (1991). Synthetic polyelectrolytes – A review, *Polym. Int.*, **25**, 29.

Moss, N. (1978). Theory of flocculation, *Mine and Quarry*, **7**(May), 57.

Owen, A.T., Fawell, P.D., Swift, J.D., and Farrow, J.B. (2002). The impact of polyacrylamide flocculant solution age on flocculation performance, *Int. J. Min. Proc.*, **67**, 123.

Paananen, A.D. and Turcotte, W.A. (1980). Factors influencing selective flocculation-desliming practice at the Tilden Mine, *Mining Engng.*, **32**(Aug.), 1244.

Pearse, M.J. (1977). *Gravity Thickening Theories: A Review*, Warren Springs Lab. Report LR 261 (MP).

Pearse, M.J. (1978). *Laboratory Procedures for the Choice and Sizing of Dewatering Equipment in the Mineral Processing Industry*, Warren Springs Lab. Report LR 281 (MP).

Pearse, M.J. (1984). Synthetic flocculants in the mineral industry – types available, their uses and disadvantages, in *Reagents in the Minerals Industry*, ed. M.J. Jones and R. Oblatt, IMM, London, 101.

Prokesch, M.E. (2002). Selection and sizing of concentrate drying, handling and storage equipment, in *Mineral Processing Plant Design, Practice and Control*, ed. A.L. Mular, D. Halbe, and D.J. Barrratt, SME, Littleton, Colorado, 1463.

Schoenbrunn, F. and Laros, T. (2002). Design features and types of sedimentation equipment, in *Mineral Processing Plant Design, Practice and Control*, ed. A.L. Mular, D. Halbe, and D.J. Barrratt, *SME, Littleton, Colorado* 1331.

Seifert, J.A. and Bowersox, J.P. (1990). Getting the most out of thickeners and clarifiers, *Chemical Engng.*, **97**(Aug.), 80.

Siirak, J. and Hancock, B.A. (1988). Progress in developing a flotation phosphorous reduction process at the Tilden iron ore mine, *Proc. XVI Int. Min. Proc. Cong., Stockholm*, ed. K.S.E. Forssberg, Elsevier, Amsterdam, **B** 1393.

Smith, C.B. and Townsend, I.G. (2002). Testing, sizing and specifying of filtration equipment, in *Mineral Processing Plant Design, Practice and Control*, ed. A.L. Mular, D. Halbe, and D.J. Barrratt, SME, Littleton, Colorado, 1313.

Suttill, K.R. (1991). The ubiquitous thickener, *Engng. Min. J.*, **192**(Feb.), 20.

Talmage, W.P. and Fitch, E.B. (1955). Determining thickener unit areas, *Ind. Engng. Chem.*, **47**(Jan.), 38.

Townsend, I. (2003). Automatic pressure filtration in mining and metallurgy, *Minerals Engng.*, **16**, 165.

Vickers, F., et al. (1985). An alternative to rotary vacuum filtration for fine coal dewatering, *Mine and Quarry*, **14**(Oct.), 25.

Waters, A.G. and Galvin, K.P. (1991). Theory and application of thickener design, *Filtration and Separation*, **28**(Mar./Apr.), 110.

16

Tailings disposal

Introduction

The disposal of mill tailings is a major environmental problem, which is becoming more serious with the increasing exploration for metals and the working of lower-grade deposits. Apart from the visual effect on the landscape of tailings disposal, the major ecological effect is usually water pollution, arising from the discharge of water contaminated with solids, heavy metals, mill reagents, sulphur compounds, etc. (Chalkley et al., 1989). Waste must therefore be disposed of in both an environmentally acceptable and, if possible, economically viable manner (Sofrá and Boger, 2002). Disposal is governed by legislation and may involve long-term rehabilitation of the site.

The nature of tailings varies widely; they are usually transported and disposed of as a slurry of high water content, but they may be composed of very coarse dry material, such as the float fraction from dense medium plants. Due to the lower costs of mining from open pits, ore from such locations is often of very low grade, resulting in the production of large amounts of very fine tailings.

Methods of disposal of tailings

The methods used to dispose of tailings have developed due to environmental pressures, changing milling practice, and realisation of profitable applications. Early methods included discharge of tailings into rivers and streams, which is still practised at some mines, and the dumping of coarse dewatered tailings on to land. The many nineteenth-century tips seen in Cornwall and other parts of Britain are evidence of this method. Due to the damage caused by such methods, and the much finer grinding necessary on most modern ores, other techniques have been developed. The most satisfactory way of dealing with tailings is to make positive use of them, such as reprocessing in order to recover additional values (see Chapter 1), or to use them as a useful product in their own right, e.g. the use of coarse (20–30 mm) DMS float as railway ballast and aggregate.

It is common practice in underground mines, in which the method of working requires the filling of mined-out areas, to return the coarser fraction of the mill tailings underground. This method has been used since the beginning of the century in South Africa's gold mines (Stradling, 1988). Back-filling worked-out stopes reduces the volume of tailings which must be impounded on the surface, but not all tailings are suited as back-fill material. It is invariably necessary to de-slime the tailings, the resultant slimes, which may account for up to 50% of the total weight, requiring surface disposal (Down and Stocks, 1977a). Some tailings swell or shrink after the fill has been placed, and some have the useful property of being self-cementing, which removes the necessity of adding cement to the back-fill, which is common practice prior to placement underground. The use of back-fill can cause surface disposal problems, in that borrowed fill may have to be used to construct the tailings impoundment, as the coarse fraction of the tailings, which is often used for construction, has been removed.

Back-fill methods have not been applied to the large amounts of tailings produced by open-pit mining methods, as this would entail temporary storage during the life of the mine prior to disposal in the worked-out pit and the most widely used method is to contain the tailings within a purpose built dam. The impoundment must provide safe and

economical storage for the required volume of tailings and permit the construction and operation of pollution control facilities.

For operations that are close to the sea, submarine tailings disposal is an alternative to conventional tailings disposal provided the governmental regulations permit disposal in such a manner. The basic submarine tailings disposal design comprises a tailings line to a de-aeration/mixing chamber, with a seawater intake line, and discharge to location and depth allowing gravity flow of a coherent density to the final sedimentation area. Such systems can place mine tailings at locations and depths constraining environmental impact to restricted areas of the seabed and deep water turbidity (Ellis et al., 1995). This form of tailings disposal attracts considerable attention from environmental groups as the final disposal of the tailings is not in a controlled impoundment but is released directly into the lower levels of the ocean and can therefore affect the deep sea ecosystem. The process is increasingly used in the Asia-Pacific region where on-land disposal options are problematic. In comparison to tailing retentions on land, the mining industry has argued that submarine tailings disposal in the Asia-Pacific region is safer for the local people and the environment as the land is unsuited to the construction of tailings dams due to the natural topography, regular seismic activity, and high rainfall (McKinnon, 2002). Due to the complexity of the decision-making process for the viability of submarine tailings disposal, tools such as an expert system have been developed to assist mining project planners explore the feasibility of this method of tailings disposal (Ganguli et al., 2002).

Tailings dams

The design, construction, and operation of tailings dams is a major consideration for most new mining developments, as well as for many existing operations (Klohn, 1981; Vick, 1981).

It is economically advantageous to site the impoundment close to the mine, but this imposes limits on site selection. The type of tailings embankment is generally determined by the local seismic activity, water clarification, tailings properties and stability, tailings distribution, foundation and hydrological conditions, and environmental conditions (Mohd. Azizli et al., 1995). The ground underlying the dam must be structurally sound and able to bear the weight of the impoundment. If such a site cannot be found close to the mine, it may be necessary to pump the tailings, at a high slurry density, to a suitable location.

Tailings dams may be built across river valleys, or as curved or multi-sided dam walls on valley sides, this latter design facilitating drainage. On flat, or gently sloping ground, lagoons are built with walls on all sides of the impoundment.

The disposal of tailings adds to the production costs, so it is essential to make disposal as cheap as possible. This requirement led initially to the development of the once commonly used *upstream method* of tailings-dam construction, so named because the centre line of the dam moves upstream into the pond.

In this method, a small starter dam is placed at the extreme downstream point (Figure 16.1) and the dam wall is progressively raised on the upstream side. The tailings are discharged by spigoting off the top of the starter dyke and, when the initial pond is nearly filled, the dyke is raised and the cycle

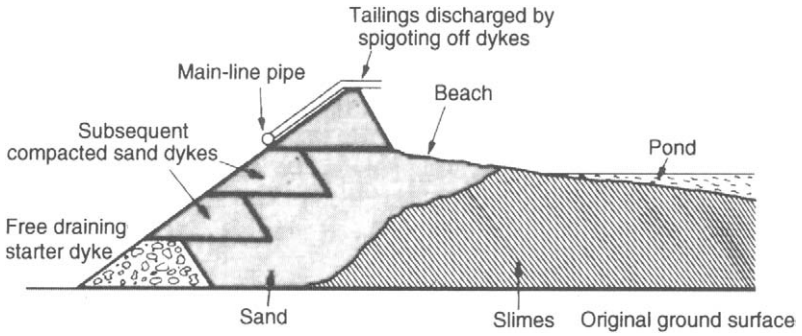


Figure 16.1 Upstream tailings darm

repeated. Various methods are used to raise the dam; material may be taken from the dried surface of the previously deposited tailings and the cycle repeated, or more commonly the wall may be built from the coarse fraction of the tailings, separated out by cyclones, or spigots, the fines being directed into the pond (Figures 16.2 and 16.3).

The main advantages of the upstream construction are the low cost and the speed with which the dam can be raised by each successive dyke increment.

The method suffers from the disadvantage that the dam wall is built on the top of previously deposited unconsolidated slimes retained behind the wall. There is a limiting height to which this type of dam can be built before failure occurs and the tailings flow out and, because of this, the upstream method of construction is now less commonly used.

The *downstream method* has evolved as a result of efforts to devise methods for constructing larger and safer tailings dams. This method produces safer

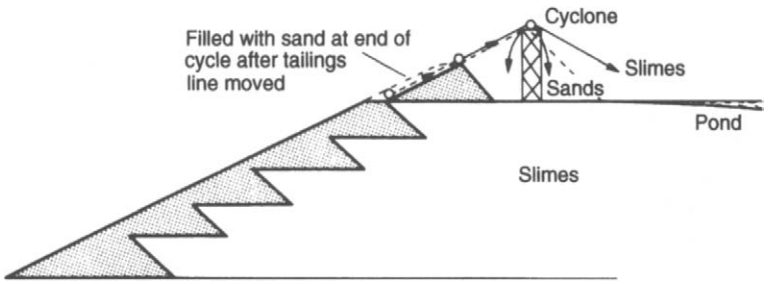


Figure 16.2 Construction of upstream tailings dam using cyclones

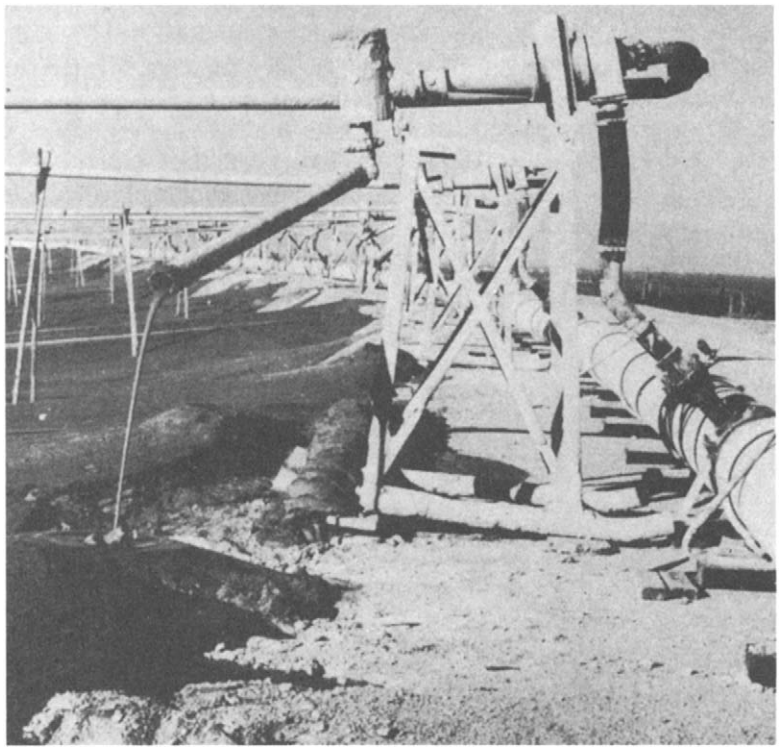


Figure 16.3 Construction of tailings dam wall utilising cyclone underflows

dams both in terms of static and seismic loading (Mohd. Azizli et al., 1995). It is essentially the reverse of the upstream method, in that as the dam wall is raised, the centreline shifts downstream and the dam remains founded on coarse tailings (Figure 16.4). Most procedures involve the use of cyclones to produce sand for the dam construction.

Downstream dam building is the only method that permits design and construction of tailings dams to acceptable engineering standards. All tailings dams in seismic areas, and all major dams, regardless of their location, should be constructed using some form of the downstream method. The major disadvantage of the technique is the large amount of sand required to raise the dam wall. It may not be possible, especially in the early stages of operation, to produce sufficient sand volumes to maintain the crest of the tailings dam above the rising pond levels. In such cases, either a higher starter dam is required or the sand supply must be augmented with borrowed fill, such procedures increasing the cost of tailings disposal.

The *centre-line method* (Figure 16.5) is a variation of that used to construct the downstream dam and the crest remains in the same horizontal position as the dam wall is raised. It has the advantage of requiring smaller volumes of sand-fill to raise the crest to any given height. The dam can thus be raised more quickly and there is less trouble keeping it ahead of the tailings pond during the early stages of construction. Care, however, must be exercised in raising the upstream face of the dam to ensure that unstable slopes do not develop temporarily.

Very stable tailings dams can be constructed from open-pit over-burden, or waste rock, according to the local circumstances. An example is shown in Figure 16.6. Since the tailings are not required for the dam construction, they may be fed into the pool without separation of the sands from the slimes. In some cases the output of overburden may not be sufficient to keep the dam crest above the tailings pond, and it may be necessary to combine waste rock and tailings sand-fills to produce a safe economical dam.

An interesting method of disposal has been used at the Ecstall (Kidd Creek) operation at Texasgulf Canada Ltd. (Amsden, 1974). The tailings disposal area consists of 3000 acres enclosed by a gravel dyke. Mill tailings are thickened and pumped to a central spigoting location inside the dam. The system is designed to build a mountain of tailings in the central area and thus keep the height of the perimeter dyke to a minimum.

Erosion of dams due to wind and rain can affect the stability and produce environmental problems. Many methods are used to combat this, such as vegetation of the dam banks (Hill and Nothard,

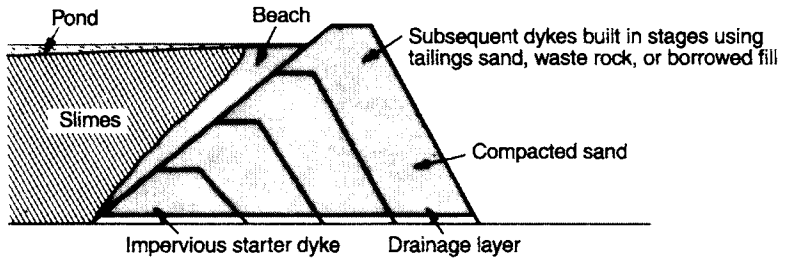


Figure 16.4 Downstream tailings dam

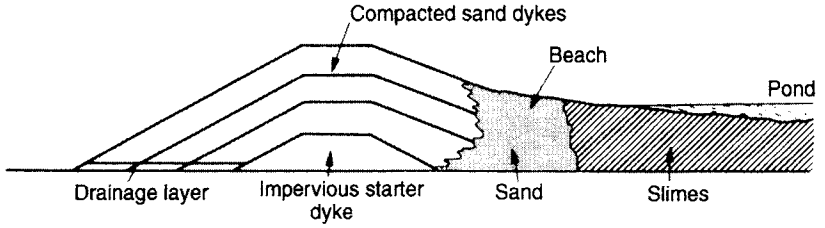


Figure 16.5 Centre-line tailings dam

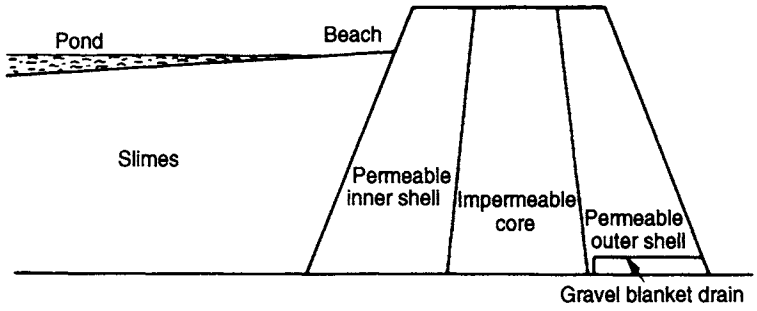


Figure 16.6 Dam constructed from overburden

1973) and chemical stabilisation to form an air and water-resistant crust.

There is little doubt that tailings dams have a visual impact on the environment due to their regular geometric shape. Perhaps the most conspicuous is the downstream type, whose outer wall is continually being extended, and cannot be re-vegetated until closure. There are, however, few reasons why dam walls should not be landscaped at some stage in their life, and many dams have been designed to permit early visual integration with the environment (Down and Stocks, 1977b). An example is the impoundment at Flambeau, North Wisconsin, USA (Shilling and May, 1977), where a rock-fill dam wall 18 m high, 24 m wide at the crest, and 111 m wide at the base was designed to minimise both visual and pollution effects (Figure 16.7). The wall consists of a clay core, with the downstream side faced with non-pyrite rock and covered with top-soil, permitting re-vegetation and consequently reduced visual impact.

The most serious problem associated with the disposal of tailings is the release of polluted water, and this has been extensively investigated (Anon., 1980). The main effects of pollution are due to the effluent pH, which may cause ecological changes; dissolved heavy metals, such as copper, lead, zinc, etc., which can be lethal to fish-life if allowed to enter local water-courses; mill reagents, which are usually present in only very small quantities, but, nevertheless, may be harmful; and suspended solids, which should be minimal if the tailings have spent long residence times in the dam, thus allowing the solids to settle and produce a clear decant. The potential effect of submarine tailings on fish-life and their prey either from altered physical habitat or from possible exposure to contaminants such as heavy metals or milling reagents is of major concern (Johnson et al., 1998). In these cases the environment is exposed to all of the tailings, not just the clear decant.

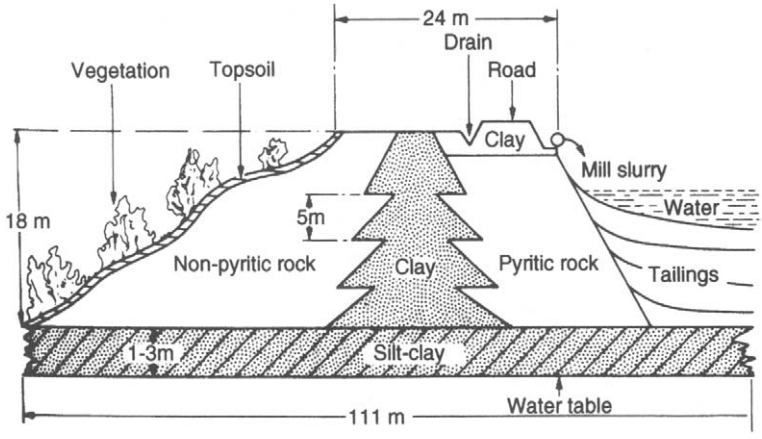


Figure 16.7 Flambeau impoundment

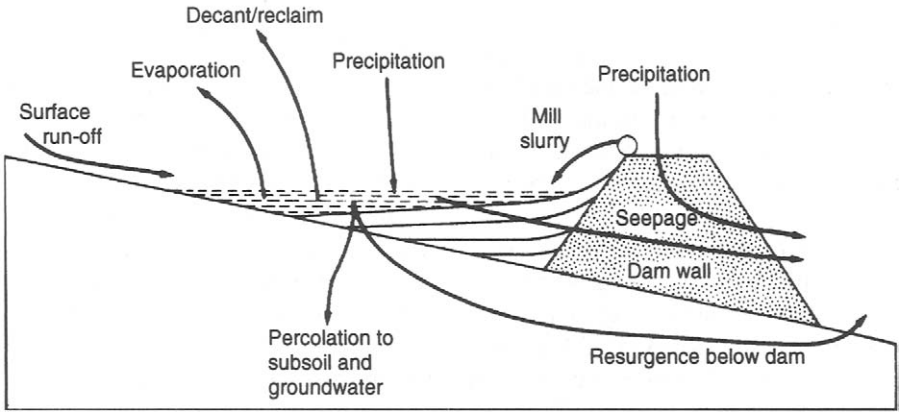


Figure 16.8 Water gain and loss in a typical tailings dam

Figure 16.8 shows a generalised representation of water gain and loss at a tailings impoundment (Down and Stocks, 1977b). With the exception of precipitation and evaporation, the rates and volumes of the water can be controlled to a large extent. It is more satisfactory to attempt to prevent the contamination of natural waters rather than to purify them afterwards, and if surface run-off to the dam is substantial, then interception ditches should be installed. It is difficult to quantify the amount of water lost to groundwater, but this can be minimised by selecting a site with impervious foundations, or by sealing with an artificial layer of clay. Seepage through the dam wall is often minimised by an impervious slimes layer on the upstream face of the dam, but this is expensive, and many mines prefer to encourage free-drainage of the dam through pervious, chemically barren material. In the case of upstream dams, this can be a barren starter dyke, while with downstream and centre-line constructions, a free-draining gravel blanket can be used. A small seepage pond with impervious walls and floors situated below the main dam can collect this water, from where it can be pumped back into the tailings pond. If the dam wall is composed of metal-bearing rock, or sulphide tailings, the seepage is often highly contaminated due to its contact with the solid tailings, and may have to be treated separately.

The tailings are often treated with lime in order to neutralise acids and precipitate heavy metals as insoluble hydroxides before pumping to the dam. Such treated tailings may be thickened and the overflow, free of heavy metals, returned to the mill (Figure 16.9), thus reducing the water and pollutant input to the tailings dam.

Assuming good control of the above inputs and outputs of dam water, the most important factor in achieving pollution control is the method used to remove surplus water from the dam. Decant facilities are required on all dams, to allow excess free water to be removed. Inadequate decant design has caused many major dam failures. Many older dams used decant towers with discharge lines running

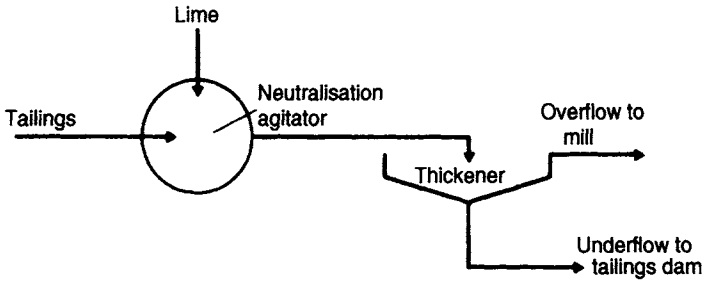


Figure 16.9 Treatment of tailings with lime

through the base of the dam to a downstream pumphouse. Failures of such structures were common due to the high pressures exerted on the pipelines, leading to uncontrolled losses of fluids and tailings downstream. Floating, or movable, pumphouses situated close to the tailings pond are now in common use.

Recycling of water from the decant is becoming more important due to pressures from governments and environmentalists. As much water as possible must be reclaimed from the tailings pond for re-use in the mill and the volume of fresh make-up water used must be kept to a minimum. The difference between the total volume of water entering the tailings pond and the volume of water reclaimed plus evaporation losses must be stored with the tailings in the dam. If that difference exceeds the volume of the voids in the stored tailings, there becomes a surplus of free water that can build up to tremendous quantities over the life of a mine. A typical dam-reclaim system is shown in Figure 16.10.

The main disadvantage of water reclamation is the recirculation of pollutants to the mill, which can interfere with processes such as flotation. Water treatment may overcome this, at little or no extra cost, as similar treatment would be required for the effluent discharge in any case. A number of wastewater treatment techniques are available, such as physical adsorption methods using active carbon, coal or bentonite clay or mineral slimes, biological oxidation of organics, removal of ionic species by ion exchange resins, and relatively new techniques such as reverse osmosis and atmospheric freezing (Rao and Finch, 1989).

Advances in the disposal of tailings using semi-dry or dry techniques offer a number of advantages over the wet disposal techniques. Dry disposal techniques require that tailings be thickened or dewatered prior to disposal. The dried tailings can then be disposed by dry stacking, thickened tailings disposal or paste fill for back-filling underground mines. These are all schemes that improve water and reagent recovery and decrease tailings volumes and footprint, which greatly assists site rehabilitation (Sofrá and Boger, 2002). Although semi-dry or dry disposal of tailings has benefits these techniques are not as capital cost–effective as the more traditional wet disposal of tailings and require a detailed understanding of the rheology and transport of the dried tailings (Nguyen and Boger, 1998).

Complexes of metals with cyanide and ammonia are especially prone to stabilisation and solubilisation in caustic solution and may require special treatment other than straightforward neutralisation by lime. Although natural degradation occurs to some extent, this is of little value in many cases

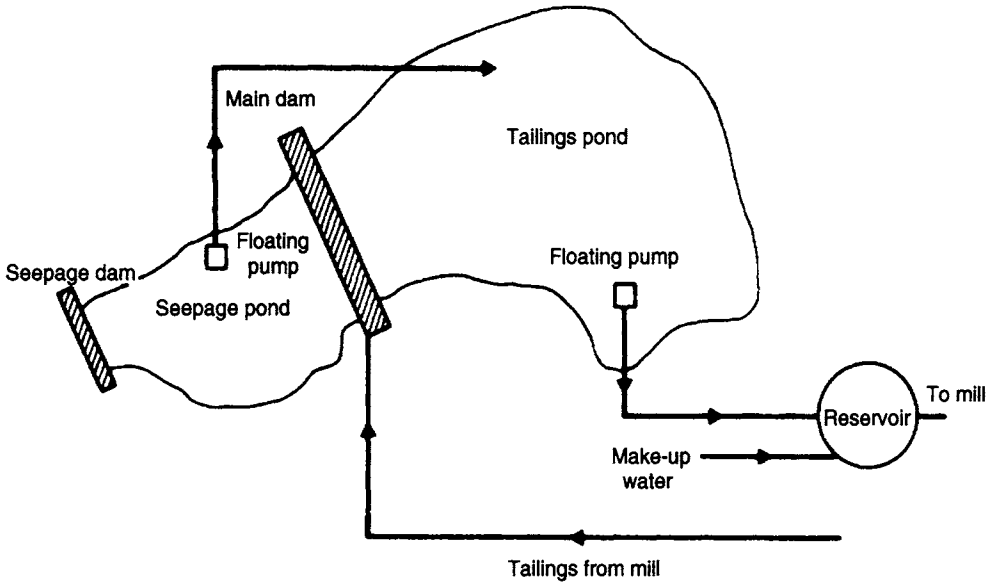


Figure 16.10 Water-reclamation system

during the winter months, when the tailings ponds may be ice-covered, and several processes have been developed to treat cyanide-bearing effluent (Scott and Ingles, 1981). Alkaline chlorination, whereby cyanide is oxidised to cyanate, has perhaps received the greatest attention (Eccles, 1977), but cyanides can also be effectively destroyed by oxidation with ozone (Jeffries and Tczap, 1978) or hydrogen peroxide, by reactions with sulphur dioxide and air (Lewis, 1984), and by electrochemical treatment, ion-exchange, and volatilisation of hydrogen cyanide. In the latter method, which has been proved full-scale in the mining industry, the tailings are acidified to produce hydrogen cyanide. This is volatilised by intensive air-sparging, while simultaneously recovering the evolved gas in a lime solution for recycling. The aerated, acidified barren solution is then reneutralised to precipitate the metal ions.

The mineralogical nature of the tailings often provides natural pollution control. For instance, the presence of alkaline gangue minerals such as limestone can render metals less soluble and neutralise oxidation products. Such ores thus present less problems than sulphide ores associated with neutral-acid gangues, which oxidise to produce sulphuric acid, and apart from acidifying the water, consume dissolved oxygen as well (Down and Stocks, 1977c). Chemical treatment of such acid effluents is essential, neutralisation by lime usually being performed, which precipitates the heavy metals, and promotes flocculation as well as reducing acidity.

There is a continuing need for the development of new, more economical methods for the removal of heavy metals from dilute acid effluents, and much research is being carried out worldwide by environmental and minerals engineers. Apart from chemical techniques such as oxidation and reduction, ion-exchange and electrochemical treatment, biological methods are also being researched and developed. For instance, it has been established that various fresh water and marine microalgae species are able to abstract heavy metal ions from aqueous solutions, thus making it possible not only to solve some industrial environmental problems, but also to recover a currently wasted product (Golab and Smith, 1992).

It has been shown by Rao et al. (1992) that acid mine drainage has potential as a coagulant for municipal waste-water, although the resultant heavy metal contamination of the discharge precludes its general use without pretreatment. It is evident that there is much research potential in these areas and that the methods used by the minerals engineer are set to play an increasingly important role in reducing the environmental impact of modern industry. Particular attention is being given to the modification of mineral processing operations to mitigate environmental impact (Feasby et al., 1995), and work has been done on incorporating the management of acid mine drainage into the block model of the mine for production planning purposes (Bennett et al., 1997). The ultimate way of avoiding water-based environmental impact is to operate dry mineral processes and consideration is being given to such options, particularly in arid areas (Napier-Munn and Morrison, 2002).

References

Amsden, M.P. (1974). The Ecstall concentrator, *CIM Bull*, **67**(May), 105.

Anon. (1980). Air and water pollution controls, *Engng. Min. J.*, **181**(Jun.), 156.

Bennett, M.W., Kempton, H.J. and Maley, J.P. (1997). Applications of geological block models to environmental management. *Proc. 4th Int. Conf. on Acid Rock Drainage (ICARD)*, Vancouver (June), 293–303.

Chalkley, M.E., et al. (eds) (1989). *Tailings and Effluent Management*, Pergamon Press, New York.

Down, C.G. and Stocks, J. (1977a). Methods of tailings disposal, *Min. Mag.* (May), 345.

Down, C.G. and Stocks, J. (1977b). Environmental problems of tailings disposal, *Min. Mag.* (Jul.), 25.

Down, C.G. and Stocks, J. (1977c). *Environmental Impact of Mining*, Applied Science Publishers, London.

Eccles, A.G. (1977). Pollution control at Western Mines Myra Falls operations, *CIM Bull.* (Sept.), 141.

Ellis, D.V., Poling, G.W., and Baer, R.L. (1995). Submarine tailings disposal (STD) for mines: An introduction, *Int. J. Rock Mech. Min. Sci. & Geomech. Abstr.*, **33(6)**, 284A.

Feasby, D.G. and Tremblay, G.A. (1995). Role of mineral processing in reducing environmental liability of mine wastes. *Proc. 27th Ann. Meet Can. Mineral Processors*, Ottawa, January (CIM), 217–234.

Ganguli, R., Wilson, T.E., and Bandopadhyay, S. (2002) STADES: An expert system for marine disposal of mine tailings, *Min. Engng.* (Apr.), 29.

Golab, Z. and Smith, R.W. (1992). Accumulation of lead in two fresh water algae, *Minerals Engng.*, **5(9)**.

Hill, J.R.C. and Nothard, W.F. (1973). The Rhodesian approach to the vegetating of slimes dams, *J. S. Afr. IMM*, **74**, 197.

Jeffries, L.F. and Tczap, A. (1978). Homestake's Grizzly Gulch tailings disposal project, *Min. Cong. J.* (Nov.), 23.

Johnson, S.W., Rice, S.D., and Moles, D.A. (1998). Effects of submarine mine tailings disposal on juvenile Yellonfin Sole (*Pleuronectes asper*): A laboratory study, *Marine Pollution Bulletin*, **36(4)**, 278.

Klohn, E.J. (1981). Current tailings dam design and construction methods, *Min. Engng.*, **33**(Jul.), 798.

Lewis, A. (1984). New Inco Tech process attacks toxic cyanides, *Engng. Min. J.*, **185**(Jul.), 52.

McKinnon, E. (2002). The environmental effects of mining waste disposal at Lihir Gold Mine, Papua New Guinea, *Journal of Rural and Remote Environmental Health*, **1(2)**, 40.

Mohd. Azizli, K., Tan Chee Yau, and Birrel, J. (1995). Technical note design of the Lohan tailings dam, Mamut Copper Mining Sdn. Bhd., Malaysia, *Minerals Engng.*, **8(6)**, 705.

Napier-Munn, T.J. and Morrison, R.D. (2003). The potential for the dry processing of ores. *Proc. Conf. on Water in Mining*, AusIMM, Brisbane (Oct.), 247–250.

Nguyen, Q.D., and Boger, D.V. (1998). Application of rheology to solve tailings disposal problems, *Int. J. Min. Proc.*, **54**, 217.

Rao, S.R. (1992). Acid mine drainage as a coagulant, *Minerals Engng.*, **5(9)**.

Rao, S.R. and Finch, J.A. (1989). A review of water re-use in flotation. *Minerals Engng.*, **2(1)**, 65.

Scott, J.S. and Ingles, J.C. (1981). Removal of cyanide from gold mill effluents, *Can. Min. J.*, **102**(Mar.), 57.

Shilling, R.W. and May, E.R. (1977). Case study of environmental Impact – Flambeau project, *Min. Cong. J.*, **63**, 39.

Sofrá, F. and Boger, D.V. (2002). Environmental rheology for waste minimisation in the minerals industry, *Chemical Engineering Journal*, **86**, 319.

Stradling, A.W. (1988). Backfill in South Africa: Developments to classification systems for plant residues, *Minerals Engng.*, **1(1)**, 31.

Vick, S.G. (1981). Siting and design of tailings impoundments, *Min. Engng.*, **33**(Jun.), 653.

Waters, J.C., Santomartino, S., Cramer, M., Murphy, N. and Taylor, J.R. (2003). Acid rock drainage treatment technologies – Identifying appropriate solutions, in *Proc. 6th ICARD*, AusIMM, Cairns (July), 831–843.

Appendix I

Metallic ore minerals

Metal	*Main applications*	*Ore minerals*	*Formula*	*% metal*	*Sp. gr.*	*Occurrence/associations*
ALUMINIUM	Where requirements are lightness, high electrical and thermal conductivity, corrosion resistance, ease of fabrication. Forms high tensile strength alloys	BAUXITE Diaspore Gibbsite Boehmite	AlO(OH) $Al(OH)_3$ AlO(OH)	–	3.2–3.5 2.3–2.4 3.0–3.1	Bauxite, which occurs massive, is a mixture of minerals such as diaspore, gibbsite, and boehmite with iron oxides and silica. Occurs as residual earth from weathering and leaching of rocks in tropical climates
ANTIMONY	Flame-resistant properties of oxide used in textiles, fibres, and other materials. Alloyed with lead to increase strength for accumulator plates, sheet, and pipe. Important alloying element for bearing and type metals	STIBNITE	Sb_2S_3	71.8	4.5–4.6	Main ore mineral. Commonly in quartz grains and in limestone replacements. Associates with galena, pyrite, realgar, orpiment, and cinnabar
ARSENIC	Limited use in industry. Small amounts alloyed with copper and lead to toughen the metals. In oxide form, used as insecticide	Arsenopyrite	FeAsS	46.0	5.9–6.2	Widely distributed in mineral veins, with tin ores, tungsten, gold, and silver, sphalerite and pyrite. Since production of metal is in excess of demand, it is commonly regarded as gangue
		Realgar Orpiment	AsS As_2S_3	70.1 61	3.5 3.4–3.5	Often associate in mineral veins in minor amounts
BERYLLIUM	Up to 4% Be alloyed with copper to produce high tensile alloys with high fatigue, wear, and corrosion resistance, which are used to make springs, bearings, and valves, and spark-proof tools. Used for neutron absorption in nuclear industry. Used in electronics for speakers and styluses	BERYL	$Be_3Al_2Si_6O_{18}$	5	2.6–2.8	Only source of the metal. Often mined as gemstone – emerald, aquamarine. Commonly occurs as accessory mineral in coarse-grained granites (pegmatites) and other similar rocks. Also in calcite veins and mica schists. As similar density to gangue minerals; difficult to separate other than by hand-sorting

(continued)

Metal	*Main applications*	*Ore minerals*	*Formula*	*%metal*	*Sp. gr.*	*Occurrence/associations*
BISMUTH	Pharmaceuticals; low melting point alloys for automatic safety devices, such as fire-sprinklers. Improves casting properties when alloyed with tin and lead	Native	Bi	100	9.7–9.8	Minor amounts in veins associated with silver, lead, zinc, and tin ores.
		Bismuthinite	Bi_2S_3	81.2	6.8	Occurs in association with magnetite, pyrite, chalcopyrite, galena, and sphalerite, and with tin and tungsten ores. Majority of bismuth produced as by-product from smelting and refining of lead and copper
CADMIUM	Rust-proofing of steel, copper, and brass by electroplating and spraying; production of pigments; negative plate in alkali accumulators; plastic stabilisers	Greenockite	CdS	77.7	4.9–5.0	Found in association with lead and zinc ores, and in very small quantities with many other minerals. Due to volatility of the metal, mainly produced during smelting and refining of zinc, as a by-product
CAESIUM	Low ionisation potential utilised in photoelectric cells, photomultiplier tubes, spectro-photometers, infra-red detectors. Minor pharmaceutical use	POLLUCITE	$Cs_4Al_4Si_9O_{26} \cdot H_2O$	10.0	2.9	Occurs in pegmatites of complex mineralogical character. Rare mineral.
		Lepidolite (Lithium mica)	$K(Li, Al)_3(Si, Al)_4O_{10}(OH, F)_2$	–	2.8–2.9	Occurs in pegmatites, often in association with tourmaline and spodumene. Often carries traces of rubidium and caesium
CHROMIUM	Used mainly as alloying element in steels to give resistance to wear, corrosion, heat, and to increase hardness and toughness. Used for electroplating iron and steel. Chromite used as refractory with neutral characteristics. Used in production of bichromates and other salts in tanning, dyeing, and pigments	CHROMITE	$FeCr_2O_4$	46.2	4.1–5.1	Occurs in olivine and serpentine rocks, often concentrated sufficiently into layers or lenses to be worked. Due to its durability, it is sometimes found in alluvial sands and gravels
COBALT	Used as alloying element for production of high-temperature steels and magnetic alloys. Used as catalyst in chemical industry. Cobalt powder used as cement in sintered carbide cutting tools	Smaltite	$CoAs_2$	28.2	5.7–6.8	Smaltite and cobaltite occur in veins, often together with arsenopyrite, silver, calcite, and nickel minerals
		Cobaltite	CoAsS	35.5	6.0–6.3	
		Carrolite	$CuCo_2S_4$	20.5	4.8–5.0	Carrolite and linnaeite sometimes occur in small amounts in copper ores. Cobalt is usually only a minor constituent in ores such as lead, copper, and nickel and extracted as by-product
		Linnaeite	Co_3S_4	58	4.8–5.0	

COPPER	Used where high electrical or thermal conductivity is important. High corrosion resistance and easy to fabricate. Used in variety of alloys – brasses, bronzes, aluminium bronzes, etc.	CHALCOPYRITE	$CuFeS_2$	34.6	4.1–4.3	Main ore mineral. Most often in veins with other sulphides, such as galena, sphalerite, pyrrhotite, pyrite, and also cassiterite. Common gangue minerals quartz, calcite, dolomite. Disseminated with bornite and pyrite in porphyry copper deposits
		CHALCOCITE	Cu_2S	79.8	5.5–5.8	Often associated with cuprite and native copper
		BORNITE	Cu_5FeS_4	63.3	4.9–5.4	Associates with chalcopyrite and chalcocite in veins
		COVELLITE	CuS	66.5	4.6	Sometimes as primary sulphide in veins, but more commonly as secondary sulphide with chalcopyrite, chalcocite, and bornite
		CUPRITE	Cu_2O	88.8	5.9–6.2	Found in oxidised zone of deposits, with malachite, azurite, and chalcocite
		MALACHITE	$CuCo_3 \cdot Cu(OH)_2$	57.5	4.0	Frequently associated with azurite, native copper, and cuprite in oxidised zone
		Native	Cu	100	8.9	Occurs in small amounts with other copper minerals
		Tennantite	$Cu_8As_2S_7$ (variable)	57.5 (variable)	4.4–4.5	Tennantite and tetrahedrite found in veins with silver, copper, lead, and zinc minerals.
		Tetrahedrite	$4Cu_2S \cdot Sb_2S_3$	52.1	4.4–5.1	Tetrahedrite more widespread and common in lead–silver veins
		Azurite	$2CuCO_3 \cdot Cu(OH)_2$	55	3.8–3.9	Occurs in oxidised zone. Not as widespread as malachite
		Enargite	$Cu_3A_5S_4$	48.4	4.4	Associates with chalcocite, bornite, covellite, pyrite, sphalerite, tetrahedrite, baryte, and quartz in near-surface deposits

(continued)

Metal	*Main applications*	*Ore minerals*	*Formula*	*% metal*	*Sp. gr.*	*Occurrence/associations*
GALLIUM	Electronics industry for production of light-emitting diodes. Used in electronic memories for computers	Occurs in some zinc ores, but no important ore minerals	–	–	–	About 90% of production is a direct by-product of alumina output. Also found in coal ash and flue dusts
GERMANIUM	Electronics industry	Argyrodite	$3Ag_2S \cdot GeS_2$	8.3	6.1	Occurs with sphalerite, siderite, and marcasite. No important ore minerals. Chief source is cadmium fume from sintering zinc concentrates
GOLD	Jewellery, monetary use, electronics, dentistry, decorative plating	NATIVE	Au	85–100 (invariably alloyed with silver and copper, and other metals)	12–20	Disseminated in quartz grains, often with pyrite, chalcopyrite, galena, stibnite, and arsenopyrite. Also found alluvially in stream or other sediments. South African "banket" is consolidated alluvial deposit
		Sylvanite	$(AuAg)Te_2$	24.5	7.9–8.3	Tellurides occurring in Kalgoorlie gold ores of Western Australia
		Calaverite	$AuTe_2$	43.6	9.0	
HAFNIUM	Naval nuclear reactors, flashbulbs, ceramics, refractory alloys, and enamels	No ore minerals	–	–	–	Produced as co-product of zirconium sponge
INDIUM	Electronics, component of low-melting-point alloys and solders, protective coating on silverware and jewellery	Occurs as trace element in many ores	–	–	–	Recovered from residues and flue dusts from some zinc smelters
IRON	Iron and steel industry	HEMATITE	Fe_2O_3	70	5–6	Most important iron ore. Occurs in igneous rocks and veins. Also as ooliths or cementing material in sedimentary rocks
		MAGNETITE	Fe_3O_4	72.4	5.5–6.5	The only ferromagnetic mineral. Widely distributed in several environments, including igneous and metamorphic rocks; and beach-sand deposits

		Goethite	$Fe_2O_3 \cdot H_2O$	62.9	4.0–4.4	Widespread occurrence, associated with hematite and limonite
		Limonite	Hydrous ferric oxides	Variable 48–63	3.6–4.0	Natural rust, chief constituent being goethite. Often associates with hematite in weathered deposits
		Siderite	$FeCO_3$	48.3	3.7–3.9	Occurs massive in sedimentary rocks and as gangue mineral in veins carrying pyrite, chalcopyrite, galena
		Pyrrhotite	FeS	61.5 (variable)	4.6	The only magnetic sulphide mineral. Occurs disseminated in igneous rocks, commonly with pyrite, chalcopyrite, and pentlandite
		Pyrite	FeS_2	46.7	4.9–5.2	One of most widely distributed sulphide minerals. Used for production of sulphuric acid, but often regarded as gangue
LEAD	Batteries, corrosion resistant pipes and linings, alloys, pigments, radiation shielding	GALENA	PbS	86.6	7.4–7.6	Very widely distributed, and most important lead ore. Occurs in veins, often with sphalerite, pyrite, chalcopyrite, tetrahedrite, and gangue minerals such as quartz, calcite, dolomite, baryte, and fluoride. Also in pegmatites, and as replacement bodies in limestone and dolomite rocks, with garnets, feldspar, diopside, rhodonite, and biotite. Often contains up to 0.5% Ag, and is important source of this metal
		Cerussite	$PbCO_3$	77.5	6.5–6.6	In oxidised zone of lead veins, associated with galena, anglesite, smithsonite, and sphalerite
		Anglesite	$PbSO_4$	68.3	6.1–6.4	Occurs in oxidation zone of lead veins
		Jamesonite	$Pb_4FeSb_6S_{14}$	50.8	5.5–6.0	Occurs in veins with galena, sphalerite, pyrite, stibnite
LITHIUM	Lightest metal. Lithium carbide used in production of aluminium. Used as base in multipurpose greases; used in manufacture of lithium batteries. Large application in ceramics industry. Very little use in metallic form	SPODUMENE	$LiAlSi_2O_6$	3.7	3.0–3.2	Occurs in pegmatites with lepidolite, tourmaline, and beryl
		Amblygonite	$2LiF \cdot Al_2O_3 \cdot P_2O_5$	4.7	3.0–3.1	Rare mineral occurring in pegmatites with other lithium minerals
		Lepidolite	$LiF \cdot KF \cdot Al_2O_3 \cdot 3SiO_2$	1.9	2.8–3.3	Mica occurring in pegmatites with other lithium minerals
		Tourmaline	Complex borosilicate of Al, Na, Mg, Fe, Li, Mn	–	3.0–3.2	Not a commercial source of metal. Some crystals used as gems. Occurs in granite pegmatites, schists, and gneisses

(continued)

Metal	*Main applications*	*Ore minerals*	*Formula*	*% metal*	*Sp. gr.*	*Occurrence/associations*
MAGNESIUM	Small amounts used in aluminium alloys to increase strength and corrosion resistance. Used to desulphur blast-furnace iron. Added to cast-iron to produce nodular iron. Used in cathodic protection, as a reagent in petrol processing and as reducing agent in titanium, and zirconium production. Structural uses where lightness required – magnesium die castings					Most magnesium extracted from brine, rather than ore minerals
		Dolomite	$MgCa(CO_3)_2$	13	2.8–2.9	Mineral used in manufacture of refractories. Occurs as gangue mineral in veins with galena and sphalerite. Also occurs widely as rock-forming mineral.
		Magnesite	$MgCO_3$	29	3.0–3.2	Used mainly for cement and refractory bricks. Often associates with serpentine
		Carnallite	$KMgCl_3 \cdot 6H_2O$	9	1.6	Occurs with halite and sylvine
		Brucite	$Mg(OH)_2$	42	2.4	Occurs in dolomitic limestones and veins with talc, calcite, and in serpentine
MANGANESE	Very important ferro-alloy. About 95% of output used in steel and foundry industry. Balance mainly in manufacture of dry cells and chemicals	PYROLUSITE	MnO_2	63.2	4.5–5.0	Often found in oxidised zone of ore deposits containing manganese. Also in quartz veins and manganese nodules
		Manganite	Mn_2O_3	62.5	4.2–4.4	Occurs in association with baryte, pyrolusite, and goethite and in veins in granite
		Braunite	$3Mn_2O_3 \cdot MnSiO_3$	78.3	4.7–4.8	Occurs in veins with other manganese minerals
		Psilomelane	Mixture of Mn oxides	–	3.3–4.7	Found with pyrolusite oxides and limonite in sediments or quartz veins
MERCURY	Electrical apparatus, scientific instruments, manufacture of paint, electrolytic cells, solvent for gold, manufacture of drugs and chemicals	CINNABAR	HgS	86.2	8.0–8.2	Only important mercury mineral. Occurs in fractures in sedimentary rocks with pyrite, stibnite, and realgar. Common gangue minerals are quartz, calcite, baryte, and chalcedony
MOLYBDENUM	Main use as ferro-alloy. Metal also used in manufacture of electrodes and furnace parts. Also used as catalyst corrosion inhibitor, additive to lubricants	MOLYBDENITE	MoS_2	60	4.7–4.8	Widely distributed in small quantities. Occurs in granites and pegmatites with wolfram and cassiterite
		Wulfenite	$PbMoO_4$	26.2	6.5–7.0	Found in oxidised zone of lead and molybdenum ores. Commonly with anglesite, cerrusite, and vanadinite

NICKEL	Very important ferro-alloy due to its high corrosion resistance (stainless steels). Also alloyed with many non-ferrous metals – chromium, aluminium, manganese. Used for electroplating steels, as base for chromium plate. Pure metal corrosion resistant, and resists alkali attack. Is non-toxic and used for food handling and pharmaceutical equipment	PENTLANDITE	(FeNi)S	22.0	4.6–5.0	Occurs invariably with chalcopyrite, and often intergrown with pyrrhotite, millerite, cobalt, selenium, silver, and platinum metals
		GARNIERITE	Hydrated Ni-Mg silicate	25–30	2.4	Often occurs massive or earthy, in decomposed serpentines, often with chromium ores, deposits being known as "lateritic"
		Niccolite	NiAs	44.1	7.3–7.7	Occurs in igneous rocks with chalcopyrite, pyrrhotite, and nickel sulphides. Also in veins with silver, silver-arsenic, and cobalt minerals
		Millerite	NiS	64.8	5.3–5.7	Occurs as needle-like radiating crystals in cavities and as replacement of other nickel minerals. Also in veins with other nickel minerals and sulphides
NIOBIUM (Columbium)	Important ferro-alloy. Added to austenitic stainless steels to inhibit intergranular corrosion at high temperatures	PYROCHLORE (Microlite)	$(Ca, Na)_2(Nb, Ta)_2O_6(O, OH, F)$	–	4.2–6.4	Occurs in pegmatites associated with zircon and apatite. Pyrochlore is the name given to niobium-rich minerals, and microlite to tantalum-rich minerals
		COLUMBITE (Tantalite)	$(Fe, Mn)(Nb, Ta)_2O_6$	–	5.0–8.0	In granite pegmatites with cassiterite wolframite, spodumene tourmaline, feldspar, and quartz. Columbite is name given to niobium-rich, and tantalite to tantalum rich-minerals in series
PLATINUM GROUP (Platinum Palladium Osmium Iridium Rhodium Ruthenium)	Platinum and palladium have wide use in jewellery and dentistry. Platinum, due to its high melting point and corrosion resistance, is widely used for electrical contact material and in manufacture of chemical					Platinum group metals occur together in nature as native metals or alloys
		NATIVE PLATINUM	Pt	45–86	21.5 (pure)	Platinum alloyed with other platinum group metals, iron, and copper. Occurs disseminated in igneous rocks, associates with chromite and copper ores. Found in lode and alluvial deposits

(continued)

Metal	*Main applications*	*Ore minerals*	*Formula*	*% metal*	*Sp. gr.*	*Occurrence/associations*
	crucibles, etc. Also widely used as a catalyst. Iridium is also used in jewellery and in dental alloys and in electrical industry. Long life platinum–iridium electrodes used in helicopter spark-plugs. Rhodium used in thermocouples, and platinum–palladium–rhodium catalysts are used in control of automobile emissions.	SPERRYLITE	$PtAs_2$	56.6	10.6	Occurs in pyrrhotite deposits and in gold-quartz veins. Also with covellite and limonite
		Osmiridium	Alloy of Os–Ir	–	19.3–21.1	Found in small amounts in some gold and platinum ores, where it is recovered as by-product
	Osmium, the heaviest metal known, with a melting point of 2200 °C, and ruthenium have little commercial importance					
RADIUM	Industrial radiography, treatment of cancer, and production of luminous paint	*See* URANIUM MINERALS	–	–	–	Constituent of uranium minerals
RARE EARTHS	The cerium subgroup is the most important industrially. Rare earths used as catalysts in petroleum refining, iron–cerium alloys used as cigarette-lighter flints. Used in ceramics and glass industry and in production of colour televisions	MONAZITE	Rare earth and thorium phosphate			*See* Thorium
		BASTNAESITE	$(Ce, La)(CO_3)F$	–	4.9–5.2	Often found in pegmatites, veins, and carbonatite plutons
		Xenotime	YPO_4	48.4 (Y)	4.4–5.1	Source of yttrium. Wide occurrence as accessory mineral, often in pegmatites, and alluvial deposits, associated with monazite, zircon, rutile, ilmenite, and feldspars

RHENIUM	Used as catalyst in production of low-lead petrol. Used as catalyst with platinum. Used extensively in thermocouples, temperature controls, and heating elements. Also used as filaments in electronic apparatus	Molybdenite	MoS_2	–	4.7–4.8	Rhenium occurs associated with molybdenite in porphyry copper deposits, and is recovered as by-product
RUBIDIUM	Rubidium and caesium largely interchangeable in properties and uses, although latter usually preferred to meet present small industrial demand	*See* CAESIUM				Rubidium widely dispersed as minor constituent in major caesium minerals
SILICON	Used in steel industry and as heavy medium alloy as ferro-silicon. Also used to de-oxidise steels. Metal used as semi-conductor	QUARTZ	SiO_2	46.9	2.65	Commonest mineral, forming 12% of earth's crust. Essential constituent of many rocks, such as granite and sandstone, and virtually sole constituent of quartzite rock
SELENIUM	Used in manufacture of fade-resistant pigments, photo-electric apparatus, in glass production, and various chemical applications. Alloyed with copper and steel to improve machineability	Naumanite	Ag_2Se	26.8	8.0	Selenides occur associated with sulphides, and bulk of selenium recovered as by-product from copper sulphide ores
		Clausthalite	PbSe	27.6	8.0	
		Eurcairite	$(AgCu)_2Se$	18.7	7.5	
		Berzelianite	Cu_2Se	38.3	6.7	
SILVER	Sterling ware, jewellery, coinage, photographic and electronic products, mirrors, electroplate, and batteries	ARGENTITE	Ag_2S	87.1	7.2–7.4	Closely associated with lead, zinc, and copper ores, and bulk of silver produced as by-product from smelting such ores
		Native	Ag	100 (max.)	10.1–11.1	Usually alloyed with copper, gold, etc., and occurs in upper part of silver sulphide deposits
		Cerargyrite	AgCl	75.3	5.8	Occurs in upper parts of silver veins together with native silver and cerussite
TANTALUM	Used in certain chemical and electrical processes due to extremely high corrosion resistance. Used in production of special steels used for medical instruments. Used for electrodes, and tantalum carbide used for cutting tools. Used in manufacture of capacitors	PYROCHLORE TANTALITE	*See* NIOBIUM			As well as ore minerals, certain tin slags are becoming important source of tantalum

(continued)

Metal	*Main applications*	*Ore minerals*	*Formula*	*% metal*	*Sp. gr.*	*Occurrence/associations*
TELLURIUM	Used in production of free machining steels, in copper alloys, rubber production, and as catalyst in synthetic fibre production	Sylvanite Calaverite	} *See* GOLD			Produced with selenium as by-product of copper refining These metal tellurides, which are important gold ores, and other tellurides of bismuth and lead, are most important sources of tellurium
THALLIUM	Very poisonous, and finds limited outlet as fungicide and rat poison. Thallium salts used in Clerici solution, an important heavy liquid	Occurs in some zinc ores, but no ore minerals	–	–	–	By-product of zinc refining
THORIUM	Radioactive metal. Used in electrical apparatus, and in magnesium–thorium and other thorium alloys. Oxide of importance in manufacture of gas-mantles, and used in medicine	MONAZITE	$(Ce, La, Th)PO_4$	–	4.9–5.4	Although occurring in lode deposits in igneous rocks such as granites, the main granites, deposits are alluvial, beach-sand deposits being most prolific source. Occurs associated with ilmenite, rutile, zircon, garnets, etc.
		Thorianite	$ThO_2 \cdot U_3O_8$	21	9.3	Occurs in some beach-sand deposits
TIN	Main use in manufacture of tin-plate, for production of cans, etc. Important alloy in production of solders, bearing-metals, bronze, type-metal, pewter, etc.	CASSITERITE	SnO_2	78.6	6.8–7.1	Found in lode and alluvial deposits. Lode deposits in association with wolfram, arsenopyrite, copper, and iron minerals. Alluvially, often associated with ilmenite, monazite, zircon, etc.
TITANIUM	Due to its high strength and corrosion resistance, about 80% of titanium produced were used in aircraft and aerospace industries. Also used in power-station heat-exchanger tubing and in chemical and desalination plants	ILMENITE	$FeTiO_3$	31.6	4.5–5.0	Accessory mineral in igneous rocks especially gabbros and norites. Economically concentrated into alluvial sands, together with rutile, monazite zircon
		RUTILE	TiO_2	60	4.2	Accessory mineral in igneous rocks, but economic deposits found in alluvial beach-sand deposits

TUNGSTEN	Production of tungsten carbide for cutting, drilling, and wear-resistant applications. Used in lamp filaments, electronic parts, electrical contacts, etc. Important ferro-alloy, producing tool and high-speed steels	WOLFRAM	$(Fe, Mn)WO_4$	50	7.1–7.9	Occurs in veins in granite rocks, with minerals such as cassiterite, arsenopyrite, tourmaline, galena, sphalerite, scheelite, and quartz. Also found in some alluvial deposits
		SCHEELITE	$CaWO_4$	63.9	5.9–6.1	Occurs under same conditions as wolfram. Also occurs in contact with metamorphic deposits
URANIUM	Nuclear fuel	PITCHBLENDE (URANINITE)	UO_2 (variable – partly oxidised to U_3O_8)	80–90	8–10	Most important uranium and radium ore. Occurs in veins with tin, copper, lead, and arsenic sulphides, and radium
		Carnotite	$K_2(UO_2)_2 (VO_4)_2 \cdot 3H_2O$ (approx.)	Variable	4–5	Secondary mineral found in sedimentary rocks, also in pitchblende deposits. Source of radium
		Autunite	$Ca(UO_2)_2(PO_4)_2 \cdot 10–12H_2O$	49	3.1	Occur together in oxidised zones as
URANIUM		Torbernite	$Cu(UO_2)_2(PO_4)_2 \cdot 12H_2O$	48	3.5	secondary products from other uranium minerals
VANADIUM	Important ferro-alloy. Vanadium used in manufacture of special steels, such as high-speed tool steels. Increases strength of structural steels – used for oil and gas pipelines. Vanadium – aluminium master alloys used in preparation of some titanium-based alloys. Vanadium compounds used in chemical and oil industries as catalysts. Also used as glass-colouring agent and in ceramics	PATRONITE	VS_4 (approx.)	28.5	–	Ocurs with nickel and molybdenum sulphides and asphaltic material
		CARNOTITE	*See* URANIUM	Variable	4–5	*See* URANIUM Frequently with carnotite
		Roscoelite (Vanadium mica)	$H_8K(MgFe)(AlV)_4(SiO_3)_{12}$	Variable	2.9	
		Vanadinite	$(PbCl)\ Pb_4(PO_4)_3$	Variable	6.6–7.1	Occurs in oxidation zone of lead, and lead–zinc deposits. Also with other vanadium minerals in sediments

(continued)

Metal	*Main applications*	*Ore minerals*	*Formula*	*% metal*	*Sp. gr.*	*Occurrence/associations*
ZINC	Corrosion protective coatings on iron and steel ("galvanising"). Important alloying metal in brasses and zinc die-castings. Used to manufacture corrosion-resistant paints, pigments, fillers, etc.	SPHALERITE	ZnS	67.1	3.9–4.1	Most common zinc ore mineral, frequently associated with galena, and copper sulphides in vein deposits. Also occurs in limestone replacements, with pyrite, pyrrhotite, and magnetite
		Smithsonite (Calamine)	$ZnCO_3$	52	4.3–4.5	Mainly occurs in oxidised zone of ore deposits carrying zinc minerals. Commonly associated with sphalerite, galena, and calcite
		Hemimorphite (Calamine)	$Zn_4Si_2O_7(OH)_2 \cdot H_2O$	54.3	3.4–3.5	Found associated with smithsonite accompanying the sulphides of zinc, iron, and lead
		Marmatite	(Zn, Fe)S	46.5–56.9	3.9–4.2	Found in close association with galena
		Franklinite	Oxide of Fe, Zn, Mn	Variable	5.0–5.2	Franklinite, zincite, and willemite occur together in a contact metamorphic deposit at Franklin, New Jersey, in a crystallite limestone, where the deposit is worked for zinc and manganese
		Zincite	ZnO	80.3	5.4–5.7	
		Willemite	Zn_2SiO_4	58.5	4.0–4.1	
ZIRCONIUM	Used, alloyed with iron, silicon, and tungsten, in nuclear reactors, and for removing oxides and nitrides from steel. Used in corrosion-resistant equipment in chemical plants	ZIRCON	$ZrSiO_4$	49.8	4.6–4.7	Widely distributed in igneous rocks, such as granites. Common constituent of residues of various sedimentary rocks, and occurs in beach sands associated with ilmenite, rutile, and monazite

APPENDIX II

Common non-metallic ores

Material	*Uses*	*Main ore minerals*	*Formula*	*Sp. gr.*	*Occurrence*
ANHYDRITE	Increasing importance as a fertiliser, and in manufacture of plasters, cements, sulphates, and sulphuric acid	ANHYDRITE	$CaSO_4$	2.95	Occurs with gypsum and halite as a saline residue. Occurs also in "cap rock" above salt domes, and as minor gangue mineral in hydrothermal metallic ore veins
APATITE	*See* PHOSPHATES				
ASBESTOS	Heat-resistant materials, such as fire-proof fabrics and brake-linings. Also asbestos cement products, sheets for roofing and cladding, fire-proof paints, etc.	CHRYSOTILE (Serpentised asbestos)	$Mg_3Si_2O_5(OH)_4$	2.5–2.6	Fibrous serpentine occurring as small veins in massive serpentine
		CROCIDOLITE	$Na_2(Mg, Fe, Al)_5 Si_8O_{22}(OH)_2$	3.4	Fibrous riebeckite, or blue asbestos, occurring as veins in bedded ironstones
		AMOSITE	$(Mg, Fe)_7Si_8O_{22} (OH)_2$	3.2	Fibrous anthophyllite, occurring as long fibres in certain metamorphic rocks
		ACTINOLITE	$Ca_2(Mg, Fe)_5Si_8 O_{22}(OH)_2$	3.0–3.4	True asbestos, occurring in schists and in some igneous rocks as alteration product of pyroxene
BADDELEYITE	Ceramics, abrasives, refractories, polishing powders, and manufacture of zirconium chemicals	BADDELEYITE	ZrO_2	5.4–6.0	Mainly found in gravels with zircon, tourmaline, corundum, ilmenite, and rare-earth minerals

(continued)

Material	*Uses*	*Main ore minerals*	*Formula*	*Sp. gr.*	*Occurrence*
BARYTES	Main use in oil- and gas-well drilling industry in finely ground state as weighting agent in drilling muds. Also in manufacture of barium chemicals, and as filler and extender in paint and rubber industries	BARYTE	$BaSO_4$	4.5	Most common barium mineral, occurring in vein deposits as gangue mineral with ores of lead, copper, zinc, together with fluorite, calcite, and quartz. Also as replacement deposit of limestone and in sedimentary deposits
BORATES	Used in manufacture of insulating fibreglass, as fluxes for manufacture of glasses and enamels. Borax used in soap and glue industries, in cloth manufacture and tanning. Also used as preservatives, antiseptics, and in paint driers	BORAX	$Na_2B_4O_7 \cdot 10H_2O$	1.7	An evaporate mineral, precipitated by the evaporation of water in saline lakes, together with halite, sulphates, carbonates, and other borates in arid regions
		KERNITE	$Na_2B_4O_7 \cdot 4H_2O$	1.95	Very important source of borates. Occurrence as borax
		COLEMANITE	$Ca_2B_6O_{11} \cdot 5H_2O$	2.4	In association with borax, but principally as a lining to cavities in sedimentary rocks
		ULEXITE	$NaCaB_5O_9 \cdot 8H_2O$	1.9	Occurs with borax in lake deposits. Also with gypsum and rock salt
		SASSOLINE	H_3BO_3	1.48	Occurs with sulphur in volcanoes and in hot lakes and lagoons
		BORACITE	$Mg_3B_7O_{13}Cl$	2.95	Occurs in saline deposits with rock-salt, gypsum, and anhydrite
CALCIUM CARBONATE	Many uses according to purity and character. Clayey variety used for cement, purer variety for lime. Marble for building and ornamental stones. Used as smelting flux, and in printing processes. Chalk and lime applied to soil as dressing. Transparent calcite (Iceland spar), used in construction of optical apparatus	CALCITE	$CaCO_3$	2.7	Calcite is a common and widely distributed mineral, often occurring in veins, either as main constituent, or as gangue mineral with metallic ores. It is a rock-forming mineral, which is mainly quarried as the sedimentary rocks limestone and chalk, and metamorphic rock marble

CHINA CLAY	Manufacture of porcelain and china. Used as filler in manufacture of paper, rubber, and paint	KAOLINITE	$Al_2Si_2O_5(OH)_4$	2.6	A secondary mineral produced by the alteration of aluminous silicates, and particularly of alkali feldspars
CHROMITE	Used as refractory in steel-making furnaces	CHROMITE	*See* CHROMIUM MINERALS (Appendix 1)		
CORUNDUM	Abrasive. Next to diamond, is hardest known mineral. Coloured variety used as gemstones	CORUNDUM (Emery)	Al_2O_3	3.9–4.1	Occurs in several ways. Original constituent of various igneous rocks, such as syenite. Also in metamorphic rocks such as marble, gneiss, and schist. Occurs also in pegmatites and in alluvial deposits. Impure form is emery, containing much magnetic and hematite
CRYOLITE	Used as flux in manufacture of aluminium by electrolysis	CRYOLITE	Na_3AlF_6	3.0	Occurs in pegmatite veins in granite with siderite, quartz, galena, sphalerite, chalcopyrite, fluorite cassiterite, and other minerals. Only real deposit in Greenland
DIAMOND	Gemstone. Used extensively in industry for abrasive and cutting purposes – hardest known mineral. Used for tipping drills in mining and oil industry	DIAMOND (Bort)	C	3.5	Distributed sporadically in kimberlite pipes. Also in alluvial beach and river deposits. Bort is grey to black and opaque, and is used industrially
DOLOMITE	Important building material. Also used for furnace linings and as flux in steel-making	DOLOMITE	$CaMg(CO_{3)_2}$	2.8–2.9	Rock-forming mineral. Occurs as gangue mineral in veins containing galena and sphalerite
EMERY	*See* CORUNDUM				
EPSOM SALTS	Medicine and tanning	EPSOMITE	$MgSO_4 \cdot 7H_2O$	1.7	Usually as encrusting masses on walls of caves or mine workings. Also in oxidised zone of pyrite deposits in arid regions

(continued)

Material	*Uses*	*Main ore minerals*	*Formula*	*Sp. gr.*	*Occurrence*
FELDSPAR	Used in manufacture of porcelain, pottery, and glass. Used in production of glazes on earthware, etc., and as mild abrasive	ORTHOCLASE (Isomorphous forms – Microline, Sanidine, and Adularia – the *potassic* feldspars)	$KAlSi_3O_8$	2.6	Most abundant of all minerals, and most important rock-forming mineral. Widely distributed, mainly in igneous, but also in metamorphic and sedimentary rocks
		ALBITE	$NaAlSi_3O_8$	2.6	
		ANORTHITE	$CaAl_2Si_2O_8$	2.74	
		(*Plagioclase* feldspars form series having formulae ranging from $NaAlSi_3O_8$ to $CaAl_2Si_2O_8$, changing progressively from albite, through oligoclase, andesine, labradorite, and bytownite to anorthite)			
FLUORSPAR	Mainly as flux in steelmaking. Also for manufacture of specialised optical equipment, production of hydrofluoric acid, and fluorocarbons for aerosols. Colour-banded variety known as *Blue-John* used as semi-precious stone	FLUORITE	CaF_2	3.2	Widely distributed, hydrothermal veins and replacement deposits, either alone, or with galena, sphalerite, barytes, calcite, and other minerals
GARNET	Mainly as abrasive for sandblasting of aircraft components, and for wood polishing. Also certain varieties used as gemstones	PYROPE	$Mg_3Al_2(SiO_4)_3$	3.7	Widely distributed in metamorphic and some igneous rocks. Also commonly found as constituent of beach and river deposits
		ALMANDINE	$Fe_3Al_2(SiO_4)_3$	4.0	
		GROSSULAR	$Ca_3Al_2(SiO_4)_3$	3.5	
		ANDRADITE	$Ca_3Fe_2(SiO_4)_3$	3.8	
		SPESSARTITE	$Mn_3Al_2(SiO_4)_3$	4.2	
		UVAROVITE	$Ca_3Cr_2(SiO_4)_3$	3.4	
GRAPHITE (Plumbago)	Manufacture of foundry moulds, crucibles, and paint; used as lubricant and as electric furnace electrodes	GRAPHITE	C	2.1–2.3	Occurs as disseminated flakes in metamorphic rocks derived from rocks with appreciable carbon content. Also as veins in igneous rocks and pegmatites

GYPSUM	Used in cement manufacture, as a fertiliser, and as filler in various materials such as paper, rubber, etc. Used to produce *plaster of Paris*	GYPSUM	$CaSO_4 \cdot 2H_2O$	2.3	Evaporate mineral, occurring with halite and anhydrite in bedded deposits
ILMENITE	About 90% of ilmenite produced is used for manufacture of titanium dioxide, a pigment used in pottery manufacture	ILMENITE	*See* TITANIUM MINERALS (Appendix 1)		
MAGNESITE	Used as refractory for steel furnace linings, and in production of carbon dioxide and magnesium salts	MAGNESITE	*See* MAGNESIUM MINERALS (Appendix 1)		
MICA	Used for insulating purposes in electrical apparatus. Ground mica used in production of roofing material, and in lubricants, wall-finishes artificial stone, etc. Powdered mica gives "frost" effect on Christmas cards and decorations	MUSCOVITE	$KAl_2(AlSi_3O_{10})(OH, F)_2$	2.8–2.9	Widely distributed in igneous rocks, such as granite and pegmatites. Also in metamorphic rocks – gneisses and schists. Also in sedimentary sandstones, clays, etc.
		PHLOGOPITE	$KMg_3(AlSi_3O_{10})(OH, F)_2$	2.8–2.85	Most commonly in metamorphosed limestones, also in igneous rocks rich in magnesia
		BIOTITE	$K(Mg, Fe)_3(AlSi_3O_{10})(OH, F)_2$	2.7–3.3	Widely distributed in granite, syenite and diorite. Common constituent of schists and gneisses and of contact metamorphic rocks
PHOSPHATES	Main use as fertilisers. Small amounts used in production of phosphorous chemicals	APATITE	$Ca_5(PO_4)_3(F, Cl, OH)$	3.1–3.3	Occurs as accessory mineral in wide range of igneous rocks, such as pegmatites. Also in metamorphic rocks, especially metamorphosed limestones and skarns. Principal constituent of fossil bones in sedimentary rocks
		PHOSPHATE ROCK	Complex phosphates of Ca, Fe, Al		Most extensive phosphate rock deposits associated with marine sediments, typically glauconite-bearing sandstones, limestones, and shales. *Guano* is an accumulation of excrement of sea-birds, found mainly on oceanic islands

(continued)

Material	*Uses*	*Main ore minerals*	*Formula*	*Sp. gr.*	*Occurrence*
POTASH	Used as fertilisers, and source of potassium salts. Nitre also used in explosives manufacture (*saltpetre*)	SYLVINE	KCl	2.0	Occurs in bedded evaporate deposits with halite and carnallite
		CARNALLITE	$KMgCl_3 \cdot 6H_2O$	1.6	In evaporate deposits with sylvine and halite
		ALUNITE	$KAl_3(SO_4)_2(OH)_6$	2.6	Secondary mineral found in areas where volcanic rocks containing potassic feldspars have been altered by acid solutions
		NITRE	KNO_3	2.1	Occurs in soils in arid regions, associated with gypsum, halite, and nitratine
QUARTZ	Building materials, glass making, pottery, silica bricks, ferro-silicon, etc. Used as abrasive in scouring soaps, sandpaper, toothpaste, etc. Due to its piezo-electric properties, quartz crystals widely used in electronics	*See* SILICON MINERALS (Appendix 1)			
ROCK SALT	Culinary and preserving uses. Wide use in chemical manufacturing processes	HALITE	NaCl	2.2	Occurs in extensive stratified evaporate deposits, formed by evaporation of land-locked seas in geological past. Associates with other water soluble minerals, such as sylvine, gypsum, and anhydrite
RUTILE	Production of welding rod coatings, and titanium dioxide, a pigment used in pottery manufacture	*See* TITANIUM MINERALS (Appendix 1)			
SERPENTINE	Used as building stone and other ornamental work. Fibrous varieties source of asbestos (*See* ASBESTOS)	SERPENTINE	$Mg_3Si_2O_5(OH)_4$	2.5–2.6	Secondary mineral formed from minerals such as olivine and orthopyroxene. Occurs in igneous rocks containing these minerals, but typically in serpentines, formed by alteration of olivine-bearing rocks

SILLIMANITE MINERALS (Aluminium silicates)	Raw material for high-alumina refractories, for iron and steel industry, and other metal smelters. Also used in glass industry, and as insulating porcelains for spark-plugs, etc.	KYANITE (Disthene)	Al_2SiO_5	3.5–3.7	Typically in regionally metamorphosed schists and gneisses, together with garnet, mica, and quartz. Also in pegmatites and quartz veins associated with schists and gneisses
		ANDALUSITE	Al_2SiO_5	3.1–3.2	In metamorphosed rocks of clayey composition. Also as accessory mineral in some pegmatites, with corundum, tourmaline, and topaz
		SILLIMANITE	Al_2SiO_5	3.2–3.3	Typically in schists and gneisses produced by high-grade regional metamorphism
		MULLITE	$Al_6Si_2O_{13}$	3.2	Rarely found in nature, but synthetic mullite produced in many countries
SULPHUR	Production of fertilisers, sulphuric acid, insecticides, gunpowder, sulphur dioxide, etc.	NATIVE SULPHUR	S	2.0–2.1	In craters and crevices of extinct volcanoes. In sedimentary rocks, mainly limestone in association with gypsum. Also in cap rock of salt domes, with anhydrite, gypsum, and calcite
		PYRITE	*See* IRON MINERALS (Appendix 1)		
TALC	As filler for paints, paper, rubber, etc. Used in plasters, lubricants, toilet powder, French chalk. Massive varieties used for sinks, laboratory tabletops, acid tanks, etc.	TALC	$Mg_3Si_4O_{10}(OH)_2$	2.6–2.8	Secondary mineral formed by alteration of olivine, pyroxene, and amphibole, and occurs along faults in magnesium rich rocks. Also occurs in schists, in association with actinolite. Massive talc known as *soapstone* or *stealite*
VERMICULITE	Outstanding thermal and sound insulating properties, light, fire-resistant, and inert – used principally in building industry	VERMICULITE	$Mg_3(Al, Si)_4O_{10}(OH)_2 \cdot 4H_2O$	2.3–2.4	Occurs as an alteration product of magnesian micas, in association with carbonatites
WITHERITE	Source of barium salts. Small quantities used in pottery industry	WITHERITE	$BaCO_3$	4.3	Not of wide occurrence. Sometimes accompanies galena in hydrothermal veins, together with anglesite and baryte
ZIRCON SAND	Used in foundries, refractories, ceramics, and abrasives, and in chemical production	ZIRCON	*See* ZIRCONIUM MINERALS (Appendix 1)		

Appendix III

Excel Spreadsheets for formulae in chapter 3

These spreadsheets are accessible by going to the Minerals Engineering International website at http://www.min-eng.com and following the prompts. The following notes describe the functionality of each spreadsheet. The spreadsheet names are the same as those used for the equivalent basic computer programs in previous editions of the book.

Gy: Sample size by Gy Formula
The function GYMass() calculates the minimum practical sampling weights required at each stage of sampling. The mass given is that obtained by Gy's formula multiplied by a safety factor of 2. For routine sampling, a confidence interval of 95% in the results would be acceptable; but for research purposes, or where greater sampling accuracy is required, 99% level of confidence would be required.

Gy: Sample error by Gy Formula
The function GYError() will calculate the maximum relative error for a sample mass from each stage of sampling, ie the fundamental errors incurred after a sample has been taken. The calculated relative error is that obtained by Gy's formula.

RecVar: Estimation of errors in recovery calculations
RecVar calculates the error associated with the two-product recovery formula for the assay recovery. Enter the Feed, Concentrate, and Tail assays and the relative error for the Feed, Concentrate, and Tail assays in the highlighted cells. The spreadsheet returns the calculated assay recovery, and the variance and standard deviation of the calculated assay recovery.

MassVar: Estimation of errors in two-product mass flow rate
MassVar calculates the error associated with the two-product recovery formula for the mass recovery. Enter the Feed, Concentrate, and Tail assays and the relative error for the Feed, Concentrate, and Tail assays in the highlighted cells. The spreadsheet returns the calculated mass recovery and the variance and standard deviation of the mass recovery.

Lagran: Reconciliation of excess data by non-weighted least squares
Lagran uses a simple node adjustment by least squares followed by Lagrangian multipliers. Enter the assay names into column B. Enter the Feed, Concentrate, and Tail assay values for each assay. The spreadsheet returns the balanced feed, concentrate, and tail assays and the balanced assay and mass recoveries.

WeightRe: Reconciliation of excess data by weighted least squares

WeightRe estimates the best mass rate by using weighted residuals least squares followed by Lagrangian multipliers. Enter the assay names and the Feed, Concentrate, and Tail assay values for each assay. Enter the relative standard deviations associated with the Feed, Concentrate and Tail assay values for each assay. The spreadsheet returns the balanced assays for the Feed, Concentrate, and Tail and the balanced assay and mass recoveries.

Wilman: Reconciliation of excess data by variances in mass equations

Wilman estimates the best mass rate by using variances in the component equations. Data adjustment is by Lagrangian multipliers. Enter the assay names and the Feed, Concentrate, and Tail assay values for each assay. Enter the relative standard deviations associated with the Feed, Concentrate, and Tail assay values for each assay. The spreadsheet returns the balanced assays for the Feed, Concentrate, and Tail and the balanced assay and mass recoveries.

Wilman : Reconciliation of excess data by variances in mass equations

B.A.Wills (1985)

Updated to MS Excel, JKTech Pty Ltd (2005)

Assay Data Ranges:	
Feed/Conc/Tail	C16:E25

SDs Data Ranges:	
Feed/Conc/Tail	F16:H25

Balance Data Ranges:	
Feed/Conc/Tail	I16:L25

Click to Calculate the Weighted Recovery Balance

Mass Recovery: 42.2 %

	Measured Data			SDs Data (Relative %)			Balanced Data			
	Feed	Conc	Tail	Feed	Conc	Tail	Feed	Conc	Tail	Recovery
Tin	21.90	43.00	6.77	1	1	1	22.00	42.84	6.76	82.24
Iron	3.46	5.50	1.76	1	1	1	3.38	5.58	1.77	69.74
Silica	58.00	25.10	75.30	1	1	1	55.55	25.29	77.68	19.23
Sulphur	0.11	0.12	0.09	1	1	1	0.10	0.12	0.09	49.35
Arsenic	0.36	0.38	0.34	1	1	1	0.36	0.38	0.34	44.96
TiO2	4.91	9.24	2.07	1	1	1	5.02	9.07	2.06	76.32

Wilman estimates the best mass rate by using variances in the component equations. Data adjustment is by Lagrangian multipliers.

Enter the assay names into column B.

Enter the Feed, Concentrate, and Tail assay values for each assay (columns C to E).

Enter the relative standard deviations associated with the Feed, Concentrate, and Tail assay values for each assay (columns F to H).

The balanced assays for the Feed, Concentrate, and Tail are reported in columns I to K.

The balanced assay recovery is reported in column L.

The balanced mass recovery is reported in cell K12.

The number of assays can be extended beyond 10 by adjusting the maximum data ranges in cells C6, C9, and C12.

e : Reconciliation of excess data by weighted least squares
(1985)
to MS Excel, JKTech Pty Ltd (2005)

ence:	0.001	5.1E-04	actual convergence
tions:	100	2	number of iterations required

ata Ranges:	
nc/Tail	C19:E28

Ranges:	
nc/Tail	F19:H28

Data Ranges:	
nc/Tail	I19:L28

Click to Calculate the Weighted Recovery Balance

Mass Recovery: 41.3 %

	Measured Data			SDs Data (Relative %)			Balanced Data			
	Feed	Conc	Tail	Feed	Conc	Tail	Feed	Conc	Tail	Recovery
	21.90	43.00	6.77	1	1	1	21.80	43.16	6.78	81.75
n	3.46	5.50	1.76	1	1	1	3.36	5.61	1.78	68.96
ca	58.00	25.10	75.30	1	1	1	55.87	25.26	77.40	18.67
lphur	0.11	0.12	0.09	1	1	1	0.10	0.12	0.09	48.36
senic	0.36	0.38	0.34	1	1	1	0.36	0.38	0.34	44.00
02	4.91	9.24	2.07	1	1	1	4.98	9.13	2.06	75.70

WeightRe estimates the best mass rate by using weighted residuals least squares followed by Lagrangian multipliers.

Enter the assay names into column B.

Enter the Feed, Concentrate, and Tail assay values for each assay (columns C to E).

Enter the relative standard deviations associated with the Feed, Concentrate, and Tail assay values for each assay (columns F to H).

The balanced assays for the Feed, Concentrate, and Tail are reported in columns I to K.

The balanced assay recovery is reported in column L.

The balanced mass recovery is reported in cell K15.

The number of assays can be extended beyond 10 by adjusting the maximum data ranges in cells C9, C12, and C15.

Lagran : Reconciliation of excess data by non-weighted least squares
B.A.Wills (1984)
Updated to MS Excel, JKTech Pty Ltd (2005)

Assay Data Ranges:	
Feed/Conc/Tail	C13:E23

Balance Data Ranges:	
Feed/Conc/Tail	F13:I23

Click to Calculate the Non-Weighted Recovery Balance

Mass Recovery: 37.0 %

	Measured Data			Balanced Data			
	Feed	Conc	Tail	Feed	Conc	Tail	Recovery
Tin	21.90	43.00	6.77	20.78	43.41	7.47	77.4
Iron	3.46	5.50	1.76	3.25	5.58	1.89	63.4
Silica	58.00	25.10	75.30	57.16	25.41	75.83	16.5
Sulphur	0.11	0.12	0.09	0.10	0.12	0.09	43.4
Arsenic	0.36	0.38	0.34	0.36	0.38	0.34	39.6
TiO2	4.91	9.24	2.07	4.79	9.28	2.15	71.8

Lagran uses a simple node adjustment by least squares followed by Lagrangian multipliers.

Enter the assay names into column B.

Enter the Feed, Concentrate, and Tail assay values for each assay (columns C to E).

The balanced assays for the Feed, Concentrate, and Tail are reported in columns F to H.

The balanced assay recovery is reported in column I.

The balanced mass recovery is reported in cell H9.

The number of assays can be extended beyond 10 by adjusting the maximum data ranges in cells C6 and C9.

RecVar : Estimation of errors in recovery calculations

B.A.Wills (1984)

Updated to MS Excel, JKTech Pty Ltd (2005)

RecVar calculates the error associated with the two-product recovery formula for the ***assay recovery***

Assay:		
Feed	3.5	%
Conc	18	%
Tail	1	%

Enter the Feed, Concentrate, and Tail assays in the highlighted cells.

SDs:	**Relative %**		Absolute
Feed	4	%	0.14
Conc	2	%	0.36
Tail	8	%	0.08

Enter the relative error for the Feed, Concentrate, and Tail assays in the highlighted cells.

Calculation	
A	3
B	26
C	0
D	236

Recovery:	75.6	%
Variance:	5.7	
SDs:	2.4	%

Calculated assay recovery

Variance of the assay recovery

Standard deviation of the assay recovery

MassVar : Estimation of errors in two-product mass flowrate

B.A.Wills (1984)

Updated to MS Excel, JKTech Pty Ltd (2005)

MassVar calculates the error associated with the two-product recovery formula for the ***mass recovery***

Assay:		
Feed	0.92	%
Conc	0.99	%
Tail	0.69	%

Enter the Feed, Concentrate, and Tail assays in the highlighted cells.

SDs:	**Relative %**		Absolute
Feed	1	%	0.0092
Conc	1	%	0.0099
Tail	1.5	%	0.01035

Enter the relative error for the Feed, Concentrate, and Tail assays in the highlighted cells.

Calculation	
A	333
B	256
C	
D	78

Yield:	76.7	%
Variance:	16.5	
SDs:	4.1	%

Calculated mass recovery

Variance of the recovery

Standard deviation of the recovery

Gy : Sample error by Gy Formula
B.Wills (1982)
Updated to MS Excel, JKTech Pty Ltd (2005)

Confidence Level	%	95%	95%, 97.5%, 99%, 99.5%, 99.9%			
Elemental Assay of Ore	%	5%	e.g. %Cu in Ore			
Elemental Assay of Mineral	%	86.6%	e.g. %Cu in Chalcopyrite			
Liberation Size	cm	0.015	Grain size of valuable mineral			
Alluvial Gold	y/n	N	Is the sample alluvial gold ore			
Mineral Density	t/m^3	7.5				
Gangue Density	t/m^3	2.65				
Number of Sampling Stages		4				
Top Size Of Ore	cm	2.5	0.5	0.1	0.004	
F95 / F5 Ratio		5	5	5	5	
Sample Mass	g	5000	500	100	10.00	
GYError	%	23.4%	9.9%	3.0%	0.1%	

The function GYError() will calculate the maximum relative error for a sample mass from each stage of sampling. The calculated relative error is that obtained by Gy's formula.

Gy : Sample size by Gy Formula
B.Wills (1982)
Updated to MS Excel, JKTech Pty Ltd (2005)

Confidence Level	%	95%	95%, 97.5%, 99%, 99.5%, 99.9%		
Elemental Assay of Ore	%	5%	e.g. %Cu in Ore		
Elemental Assay of Mineral	%	86.6%	e.g. %Cu in Chalcopyrite		
Assay Relative Error	%	2%	Maximum acceptable relative error		
Liberation Size	cm	0.015	Grain size of valuable mineral		
Alluvial Gold	y/n	N	Is the sample alluvial gold ore		
Mineral Density	t/m^3	7.5			
Gangue Density	t/m^3	2.65			
Number of Sampling Stages		4			
Top Size Of Ore	cm	2.5	0.5	0.1	0.004
F95 / F5 Ratio		5	5	5	5
GYMass	g	1369632	24501	438	0.07
GYError	%	1.4%	1.4%	1.4%	1.4%

The function GYMass() will calculate the minimum practical sampling weights required at each stage of sampling. The mass given is that obtained by Gy's formula multiplied by a safety factor of 2. For routine sampling, a confidence interval of 95% in the results would be acceptable, but for research purposes, or where greater sampling accuracy is required, 99% level of confidence would be required.

The function GYError() will calculate the maximum relative error for a sample mass from each stage of sampling. The calculated relative error is that obtained by Gy's formula.

Index

Activators, 278–9
Aerophilic, 11, 269
Aerophobic, 11
Agglomeration-skin flotation, 316
Alluvial deposits, 369
Andreasen pipette technique, 100
Anionic collectors, 272–6
  dithiophosphates, 272–3
  mercaptans, 272
  oxyhydryl, 272
  sulphydryl, 272
  xanthogenates, 272
Arrested/free crushing, 121
Augering, 51
Autogenous mills, 161–9

Ball mills, 158–61
Batac jig, 233
Batch flotation tests, 290–1
Baum jig, 232, 233
Blake crusher, 120
Bromoform, 247
Bubble generation, 285–6

Calcareous (basic) ores, 4
Canica Vetical Shaft Impact
    Crusher, 138
Carats, 17
Cationic collectors, 276
Centre peripheral discharge mills, 156
Centrifugal concentrators, 242–3
Centrifugal mills, 166
Centrifugal sedimentation, 389–90
  solid bowl scroll centrifuge, 389
Centrifugal separators, 251–4
Check in–check out method, 66
Chelating reagents, 276
Choked crushing, 121
Circuit design/optimisation, 63–4
Classification, 203–23
  horizontal current, 208–12
  hydraulic, 206–8
  hydrocyclone, 212–23
  mechanical, 208–12
  principles, 203–6
  rake classifier, 210
  spiral, 210–11
  types of classifier, 206–23
Clerici solution, 247
Closure errors, 66
Coagulation, 378–9
  chemical formula, 380–1
  diffuse layer, 379
  electrical double layer, 379
  Stern layer, 379
  zeta potential, 379
Coal, 1
  flotation, 344
  jigs, 232–3
  rank, 1
Collectors, 269, 270–6
  amphoteric, 271
  anionic, 272–6
  cationic, 276
  ionising, 170
Comminution, 108–17
  crushing, 108, 109, 110, 111
  grindability, 111–15
  grinding, 108
  interparticle, 121, 130
  method, 111
  mills, 112
  principles, 109
  simulation of processes/circuits, 112–15
  theory, 110–11
Complex circuits
  mass balancing of, 75–86
  minimisation of sum of squares of closure residuals, 81–4
  minimisation of sum of squares of component
      adjustments, 84
  reconciliation of excess data, 80–1
  weighting adjustments, 85–6
Complex ores, 7
Computer simulation, 63–4
  empirical, 63
  steady state, 63
  theoretical, 63
Concentrate, 10
Concentration, 10, 11–12, 15–20
Conditioning, 319–20
Cone crusher, 126–35
Connection matrix, 76, 78–80

Consolidation trickling, 228
Contained value, 6
Control
  adaptive, 59
  coupling behaviour, 59
  derivative action, 57
  direct digital, 57
  feed-back loops, 57
  feed-forward, 58
  integral, 57
  offset, 56, 57
  parameter estimation, 60
  single-variable, 59
  statistical process, 61
  supervisory/cascade, 57
  see also Process control
Conveyor belts, 30–1
  centrifugal pumps, 34
  feed chutes, 33
  hydraulic systems, 34
  pipelines, 34
  sandwich systems, 34
  screw systems, 34
  shuttle belts, 33
  tripper, 33
Copper, 2
  processing, 23–6
Copper–lead–zinc flotation, 336–43
Copper ore, 4
  by-products, 329–30
  flotation of, 327–32
  oxidised, 332–4
Copper–zinc flotation, 336–43
Coulter counter, 104
Crushers, 108, 118–43
  open/closed circuits, 118–19, 139–43
  primary, 118, 119–26
  secondary, 118, 126–39

Dense medium separation (DMS), 11, 226, 246–7
  application, 244
  centrifugal separators, 251–4
  circuits, 254–5
  construction of partition curves, 261–4
  efficiency of, 260–1
  gravitational vessels, 248–51
  laboratory heavy liquid tests, 257–60
  liquids, 247
  organic efficiency, 264–5
  separating vessels, 248
  suspensions, 247–8
  typical, 255–7
Denver machines, 230, 308–10
Depressants, 279–81
  inorganic, 279–81
  polymeric, 281
Derrick repulp screen, 196
Dewatering, 377–97
  drying, 396–7
  filtration, 390–7
  sedimentation, 378–89
Discrete Element Method (DEM), 114–15
Dodge crusher, 120
Drewboy bath, 250
Drum separators, 248–50
  two-compartment, 249–50
Drying, 397–8
  rotary thermal, 397–8
Duplex concentrator, 241–2
Dyna Whirlpool, 253–4

Ecart probable (probable error of separation), 261
Economic efficiency, 26–8, 59
Economic recovery, 294
Effective density, 204
Elastic behaviour, 109
Electrical separation, 365–71
Electroflotation, 315–16
Elutriation, 101–3
Empirical models, 190–1
End peripheral discharge mills, 156–8
End product, 17
Enrichment ratio, 17, 65
Entrainment, 286
Evolutionary optimisation (EVOP), 59, 325
Experiment design, 86
Expert systems, 62–3

Falcon SB concentrator, 242–3
Feeders
  apron, 37
  belt, 37
  chain, 36
  drum, 154
  grizzly, 37
  mill, 154
  scoop, 154
  spout, 154
  types, 36–7
Ferromagnetism, 353
Field gradient, 354
Field intensity, 354
Filtration, 390–7
  filter cake, 390
  medium, 390
  pressure, 390–2
  tests, 391

types, 392–7
vacuum, 392–7
Floatability, 269
Flocculation, 378–9
chemical formula, 380–1
selective, 381
Flotation, 11, 267
agglomeration-skin, 316
classification of minerals, 269–70
collectors, 270–6
control of plants, 320–7
copper ores, 327–32
direct/reverse, 268
electroflotation, 315–16
entrainment, 286
frothers, 269, 276–7
importance of pH, 282–3
importance of pulp potential, 283–5
oxidised copper ores, 332–6
plant practice, 316–19
principles, 267–9
reagents, 268
reagents and conditioning, 319–20
regulators, 269, 277–81
role of bubble generation/froth performance, 285–6
Flotation engineering, 287–315
basic circuits, 292–3
circuit flexibility, 302–4
comparison of machines, 312–15
flotation machines, 304–12
flowsheet design, 293–302
laboratory testing, 257, 260
pilot plant testwork, 291–2
Flotation plant practice
carrier flotation, 318
flash flotation, 317
multi-feed circuits, 318
ore and pulp preparation, 316–19
skim-air, 317
slimes, 318
Flowsheet, 13
design, 293–302
Free-settling ratio, 204–5
Froth flotation *see* Flotation
Froth separators, 307
Frothers, 269, 276–7
Fuzzy logic, 62

Galigher Agitair machine, 310
Garridon, 388
Gold, 1, 6
Gold ore concentrators, 243–4
Gossan, 327
Grate discharge, 158
Graticules, 103
Gravitational vessels, 248–51
Gravity bucket elevators, 33–4
Gravity circuit tailings, 10
Gravity concentration, 11, 225–44
centrifugal concentrators, 242–3
duplex concentrator, 241–2
gold ore, 243–4
jigs, 227–33
Mozley Laboratory Separator, 242
pneumatic tables, 241
principles, 225–6
separators, 226–7
shaking tables, 238–41
sluices and cones, 233–6
spirals, 236–8
Gravity sedimentation, 381
Grease tabling, 256
Grinding circuits, 170–82
AG/SAG operations, 173–5
classification, 171–2
closed-circuit, 170
gravity concentrator, 171–2
multi-stage, 173
open-circuit, 170–1
overgrinding, 171
parallel, 172–3
selective, 171
two-stage, 173
wet, 170
Grinding mills, 146–82
degree of liberation, 146–7
grinding circuits, 170–82
leaching, 147
motion of charge in tumbling mill, 147–9
tumbling, 149–70
Grizzlies, 37
Gyradisc crusher, 130–1
Gyratory crusher, 123–6
concaves, 124
construction, 124–6
mantle, 125
staves, 124

Hallimond tube, 289–90
Hammer mill, 136–7
Hardinge mill, 160
Harz jig, 230
Heavy liquids, 247
laboratory tests, 257–60
Heavy medium separation (HMS) *see* Dense medium separation (DMS)
Heteropolar, 270

Heuristics, 62
High-Compression Roller Mill, 135
High-gradient magnetic separators, 363–4
High-intensity separators, 359–63
  induced roll magnetic separators, 359–60
  wet, 360–3
High pressure grinding rolls (HPGR), 108
High-tension separation, 11
Hindered settling, 205–6
Hum-mer screen, 195–6
Hutch water, 229
Hydrocyclone, 171, 176, 212–23
  cyclone efficiency, 213–15
  factors affecting performance, 218–23
  mathematical models, 215–17
  scale-up/design of, 217–18
  vortex finder, 212
Hydrophobic, 268, 269

Igneous rocks, 1
IHC Radial Jigs, 230
Impact crushers, 135–8
Imperial Smelting Process, 335–6
Induced roll magnetic separators (IRMs), 359–60
InLine Pressure Jig (IPJ), 230, 232
Interparticle comminution, 121
Iron ore flotation, 343–4
Isomorphism, 1

Jameson cell, 306–7
Jaw crushers, 120–3
  arrested/free, 121
  choked, 121
  construction, 122–3
  double-toggle Blake crushers, 120–1
  gape, 120
  interparticle comminution, 121
  single-toggle, 121–2
Jigs, 227–32
  circular/radial, 230
  coal, 232–3
  Denver mineral, 230
  Harz, 230
  InLine Pressure Jig, 230–1
  jigging action, 227–9
  types, 229–32
Jones riffle, 46
Julius Kruttschnitt Mineral Research Centre (JKMRC), 114

Kalman filtering, 60–1
Kelsey Centrifugal Jig (KCJ), 232
Knelson concentrator, 242

Laboratory flotation testing, 287–91
  batch tests, 290–1
  contact angle measurement, 288
  microflotation tests, 289–90
  mineral surface analysis, 288–9
  predictions, 288
  representational samples, 287
  storage, 287
  wet grinding, 287
LARCODEMS (Large Coal Dense Medium Separator), 252–3
Laser diffraction instruments, 104–5
Leach-Precipitation-Flotation process, 12
Lead–zinc ore flotation, 332–6
Liberation, 9, 14–15
Liners, 152–4
  angular spiral lining, 153–4
  cast iron/alloyed steel, 152–3
  cost, 153
  magnetic metal, 154
  rubber, 153–4
London-Van der Waals' forces, 378
Low-intensity magnetic separation, 356–8
  cobbing, 356
  concurrent type, 357
  counter-current, 358
  counter-rotation type, 357
  drum separators, 356–7

Magnetic flux/magnetic induction, 354
Magnetic separation, 353–65
  design, 355–6
  diamagnetics, 353
  high-gradient, 363–4
  high-intensity, 359–63
  low-intensity, 356–8
  paramagnetics, 353
  superconducting, 364–5
  types, 356
Magnetic susceptibility, 354
Magnetisation, 354
Magnetohydrostatics, 247
Mass balancing
  and complex circuits, 75–86
  dilution ratios, 68–71
  limitations of two-product formula, 71
  maximising accuracy of two-product recovery computations, 74–5
  metallurgical accounting, 65–7
  methods, 64–75
  sensitivity of mass equation, 73
  sensitivity of recovery equation, 71–3
  size analyses, 67–8
Mass-flow integration, 54–5

Mechanical flotation machines, 307
Metallic ore minerals, 409–20
Metallic ore processing, 2–9
Metallurgical accounting, 39, 65–7
  automatic control, 55–62
  computer simulation, 63–4
  design of experiments/plant trials, 86
  mass balances on complex circuits, 75–86
  mass balancing methods, 64–75
  neural networks, 62–3
  sampling/weighing, 39–51
  slurry streams, 51–5
Metallurgical efficiency, 17
Metals
  classification, 6
  distribution, 6–7
  mining, 7
  production/processing, 7–9
  supply and demand, 2, 6
Metamorphosis, 1
Microflotation tests, 289–90
Mill construction, 149–55
  combination drum-scoop feeders, 154
  drive, 151–2
  drum feeders, 154
  ends, 150
  liners, 152–4
  shell, 149–50
  spout feeders, 154
  trunnions and bearings, 150–1
Milling, 10–13
  costs, 13–14
Mineral processing, 10–13
  automatic control, 55–62
  biotechnological methods, 12
  chemical methods, 12
  comminution, 9
  concentration, 10, 11–12, 16–20
  efficiency, 14–15
  liberation, 10
  minimizing losses, 12–13
  texture, 12
Mineral surface analysis, 288–9
Minerals, 1
  classification, 269–70
  polar/non-polar, 269
Misplaced particles, 16
Mogensen screens, 194, 196
Multi-Gravity Separator (MGS), 243

Native ores, 4
Net return from smelter (NSR), 19, 26
Neural networks, 62–3
Newton's law, 204
Nickel ore flotation, 343
Non-metallic ores, 6
  types, 421–7
Norwalt washer, 250–1
Nucleonic density gauges, 226

Oil, 2
Oil agglomeration, 13
OK machines, 311–12
On-line analysis, 46–9
  centralised, 47
  on-stream, 47–9
On-line size analysis, 50–4
On-stream ash analysis, 49–50
Optimum grind size, 15
Ore dressing, 7
Ore handling, 30
  feeding, 36–7
  removal of harmful materials, 30–2
  storage, 34–6
  transportation, 32–4
Ore sorting, 373–6
  electronic principles, 373
  photometric, 373
Organic efficiency, 264–5
Organisation of Petroleum Exporting Countries (OPEC), 2
Oxidised copper ores, 332–44
Oxidised ores, 7

Particle size, 90
  and shape, 90–1
  sieve analysis, 91–7
  sub-sieve techniques, 97–106
Partition coefficient (partition number), 260
Partition curves, 261–4
Partition (Tromp) curve, 260
Peat, 1
Pebble mills, 158
Pendulum roller mills, 169
Performance/partition curve, 213–16
Phenomenological models, 190
Pilot plant testwork, 291–2
Pinched sluices and cones, 233–6
Plant trial design, 86
Platinum, 1
Platinum ore flotation, 343
Pneumatic tables, 241
Polymorphism, 1
Poppet valves, 44
Porphyries, 328
Pressure filters, 392–3
  automatic, 392–3
  chamber, 392
  plate and frame, 392

Primary crushers, 118, 119–26
  gyratory crushers, 123–6
  jaw crushers, 120–3
Process control, 55–62
  basic function, 56
  direct digital control, 57
  evolutionary optimisation, 59
  feed-back/closed loop, 56–8
  feed-forward loops, 58–9
  financial models, 56
  Kalman filtering, 60–1
  offset, 56–7
  statistical, 61–2
  supervisory/cascade, 57
Product array, 113
Pulp potential, 283–5

Quicksand, 206

Ratio of concentration, 17
Reagents, 319–20
Recovery, 16
Recovery-grade curve, 17
Refractory, 12
Regulators, 269, 277–81
  activators, 278–9
  depressants, 279–81
Relative permeability, 354
Rhodax crusher, 131–5
Riffles, 239
Rocks, 1
Rod mills, 155–6
Roll crushers, 132–5
Roller mills, 169
Rotary coal breakers, 138–9
Rougher concentrates, 292–3
Run-of-mine ore, 30

Sala AS machines, 312
Sample division
  coning/quartering, 46
  Jones riffle, 46
Sampling/weighing, 39–51
  assay sampling, 40–3
  automatic, 44
  bulk sample, 45
  cutters, 43–4
  division methods, 46
  moisture sampling, 40
  on-line analysis, 46–9
  on-line size analysis, 50
  on-stream ash analysis, 49–50
  systems, 43–6
  weighing the ore, 50–1
Scavengers, 292
Screen types, 191–9
  banana/multi-shape, 192
  Bradford Breaker, 197
  circular, 198
  dewatering, 192
  flip-flow, 197
  grizzly, 192
  high frequency, 195–6
  horizontal, low-head, linear, 192
  inclined, 191
  inclined flat screens, 198
  linear, 199
  modular, 193–4
  Mogensen divergators, 196
  Mogensen Sizers, 194
  Pansep, 199
  resonance, 192
  roller, 197
  Rotaspiral, 196–7
  sieve bend, 198–9
  static/static grizzlies, 196
  trommels, 196
  vibrating, 191–6
Screen vibrations
  circular motion, 193
  linear, 193
  oval motion, 193
  types, 191–6
Screening, 186–202
  desliming/de-dusting, 186
  dewatering, 186
  grading, 186
  mathematical models, 190–1
  media recovery, 186
  scalping, 186
  sizing/classifying, 186
  trash removal, 186
Screening performance, 186–91
  cut point, 187
  efficiency/partition curve, 187
  factors affecting, 188–91
  feed rate, 188–9
  moisture, 189–90
  near-mesh particles, 188
  open area, 189
  particle shape, 189
  particle size, 188
  same feed, 187
  screen angle, 189
  vibration, 189
Screening surfaces, 199–202
  bolt-in, 199–200
  modular, 201
  modular wire, 202

self-cleaning, 200
tensioned, 200
tensioned rubber/polyurethane mats, 200–1
wedge wire panels, 202
Secondary crushers, 118, 126–39
cone, 126–35
impact, 135–8
rotary coal breakers, 138–9
Sedimentary rocks, 4
Sedimentation, 378–89
centrifugal sedimentation, 389–90
coagulation and flocculation, 378–81
gravity, 381–8
high-capacity thickeners, 388–9
selective flocculation, 381
Selective flocculation, 13
Settling cones, 208
Shaking tables, 238–41
Shear flocculation, 13
Sieve analysis, 91–7
application, 91
choice of sizes, 93
effectiveness, 91
presentation of results, 94–7
process, 91
techniques, 91–2
test sieves, 92–3
testing methods, 93–4
Siliceous (acidic) ores, 4
Silver, 1
Sink-and-float process *see* Dense medium separation (DMS)
Slimes, 31, 226, 318
Slurry streams, 51–5
Smelter contracts, 19
Söderlund, 164
Sorting, 8
Spirals, 236–8
Statistical process control, 61–2
Stirred media detritors, 168–9
Stirred mills, 167–8
Stokes' law, 204
Sub-sieve techniques, 97–107
conversion factors, 97–8
elutriation techniques, 101–3
laser diffraction instruments, 104–5
microscopic/image analysis, 103–4
on-line particle size analysis, 105–6
sedimentation methods, 98–101
Stokes' equivalent diameter, 98
Sulphide ores, 4
Superconducting separators, 364–5
Suspensions, 247–8

Table mills, 169
Tailings disposal, 400–7
back-filling, 406
centre-line method, 403
dams, 400–6
downstream method, 401–2
upstream method, 400–1
Tailings retreatment, 6–7
Teeter chambers, 206
Terminal velocity, 203
Teska Bath, 251
Tetrabromoethane (TBE), 247
Thickener, 32, 380–1
cable, 383
caisson, 385
clarifier, 382
high-capacity, 388–9
operation, 386–7
pumps, 385
raking mechanism, 383
size/function, 385
traction, 38
tray, 388
Tidco Barmac Crusher, 137–8
Tin processing, 20–3
Tower mills, 166–7
Tri-Flo separator, 254
Tromp (Partition) curve, 260
Trunnions, 149, 150–1
overflow, 156–7
Tube press, 398
Tumbling mill
autogenous, 161–9
cascading, 148
cataracting, 148, 149
centrifuging, 148
construction, 149–55
critical speed, 148
motion of charge, 147–9
types, 155–61
wastefulness of, 146
Turbulent resistance, 203, 204
Two-product formula, 65
Tyler H-series screen, 195–6

Universal crusher, 120

Vacuum filters, 393–7
batch, 392
continuous, 393
horizontal belt, 396
hyperbaric, 396
leaf, 393

Vacuum filters (*Continued*)
rotary-drum, 393–5
tray, 393
Vezin sample cutter, 44
Vibratory mills, 165–6
Viscous resistance, 203
Vorsyl separator, 252

Washability curves, 259
Water Flush technology, 130
Water-only-cyclone, 212
Weightometers, 50
Wemco cone separator, 248
Wet high-intensity magnetic separators (WHIMS), 360–3
Work of adhesion, 268–9

Xanthates, 272

Zone of supergene enrichment, 327